Iron Melt Flow in Thin Walled Sections Cast in Vertically Parted Green Sand Moulds

Larsen, Per; Tiedje, Niels Skat; Andersen, Uffa; Rasmussen, Niels

Publication date:
2004

Document Version
Publisher's PDF, also known as Version of record

Iron Melt Flow in Thin Walled Sections Cast in Vertically Parted Green Sand Moulds

Per Larsen

Ph.D. Thesis

Iron Melt Flow in Thin Walled Sections Cast in Vertically Parted Green Sand Moulds

Ph.D. Thesis

by

Per Larsen

Supervisors
Niels Tiedje, Associate Professor — DTU
Niels Rasmussen, Department manager — DISA Industries A/S

Publication numbers
TM-02-04
IPL-117-04
EF-841

Content

Preface

The present work is the final thesis of an industrial research project at DISA Industries. The project is part of fulfilling the requirements for a Ph.D degree from the Technical University of Denmark and an Industrial Ph.D. degree within the Academy of Technical Science of Denmark.

I would like to use this opportunity to show my gratitude to all the people, who have helped me during the project and from whom I have learned so many things both practically and theoretically.

First of all I would like to thank the Academy of Technical Science of Denmark. Without their financial support of the project, it would not have been possible to conduct it. The work in connection with preparing the commercial report and the courses to be followed for fulfilling the requirements for an industrial researcher have added a valuable commercial aspect to the project. And this is certainly knowledge I can use in my future career.

It would not have been possible to upgrade the test foundry at the Technical University of Denmark without large donations from several sides. The heart of the upgraded test foundry, a DISAMATIC 2110 moulding machine, has kindly been placed at the disposal for the test foundry by DISA Industries. Without large donations from both the Valdemar Birn Foundation and the A.P. Moller Foundation the establishment of the test foundry would not have been possible.

The foundry industry in Denmark has shown a large interest in the project and the rebuilding of the test foundry at DTU. Many donations from foundries in Denmark and suppliers to the foundry industry have helped to rebuild the test foundry and to conduct the trials. I would like to mention Dania Iron Foundry for practical support; Elkem for supplying materials for melt treatment and especially Henning Kjær from Elkem for sharing his experience in melt treatment with me. MagmaSoft has during the project kindly given me access to their newest versions of their simulation software, which has been a great help.

My colleagues in the Application department at DISA Industries have all been of big help to me both in solving theoretical problems, practical foundry problems and producing drawings etc. for the equipment needed for the trials. In connection with the trials I would like to thank the people in the machine and pattern shops at DISA and DTU for good cooperation during the project. The people in the test foundry at DTU have been a great help in conducting the many trials during the project.

My supervisors, Niels Tiedje, DTU, Uffe Andersen, DISA, and later in the project Niels Rasmussen, DISA, have been a big help in both the theoretical and practical matters.

And least but not least I would like to thank my family and friends for putting up with so many never returned calls during the project.

Per Larsen

1 April 2004

Abstract

Shortage of resources can be expected to become more wide spread in the future. Furthermore the focus on the environmental aspects will also be intensified. Today the clearest example is the large attention on the fuel consumption of cars. Many different approaches can be made to reduce the fuel consumption and pollution of passenger cars, trucks etc. The engine design can be optimized for higher efficiency, the wind resistance can be reduced, combinations of combustion engines and electrical power can be used etc. But no matter which approach is taken, parts have to be used for building the vehicles. I.e. reducing the weight of the needed parts is a general way of saving fuel, applicable together with all other means of saving fuel.

Even though iron castings have been used in cars from the first car ever build, a big potential still exists for optimizing iron cast parts from a weight-saving point of view. This can be done by designing parts with thin walled sections and building stiffness into the parts via ribs, hollow section etc. Processing of parts with thin walled sections becomes hence important.

Detailed analysis of melt flow in a conventional bottom filling gating system and in thin sections have been made via videos of the metal flow. Conventional bottom filling gating systems are shown to give relatively low control over the melt flow. The result is flow patterns being able to change radically from mould to mould due to minor fluctuations in the pouring conditions. At this type of gating system it is very difficult to avoid pressure shock waves. The pressure shock waves can be initiated at two different stages of the filling. If the gating system contains a dead end and the cross sections are completely filled behind the melt front, a pressure shock wave will be initiated by the hammer effect when the melt reaches the dead end of the runner. Pressure shock waves can also be initiated when the last air pocket in a partly filled runner is closed. The pressure shock waves result in disintegrating melt surfaces.

Flow in thin walled sections is not only important when casting thin walled parts, as thin plate shaped ingates are used for casting many parts. This is illustrated with a brake disc. 6 layouts have been made. The filling sequences have been recorded on video. The trials show the difficult task to design a bottom filling system generating no splash during the initial filling and obtaining a balanced filling. When calm flow is wanted, normally the runners are designed to give low velocities. But to secure calm flow, pressure shock waves also have to be avoided. When pressure shocks are avoided and runners with good control over the melt are used, relatively high velocities can still result in calm flow with coherent melt fronts. Conventional types of gating systems have been used for 5 of the 6 layouts. The flow patterns in these systems are to a large degree controlled by the relative sizes of the dynamic and braking forces acting on the melt and not solely by the geometry of the runners. A non-conventional gating system has also been tested. The system gives a high degree of control over the flow, the balance between the dynamic and braking forces have only little influence on the flow patterns.

An exhaust manifold with 2 mm wall thickness has been cast utilising a developed stream lined gating system. The manifold is cast with no visible defects coming from the filling. The very stream-lined gating system gives uniform flow patterns from mould to mould compared to what is seen for conventional gating systems. This means, the conventional types of gating systems investigated in this work, cannot be recommended for castings with high demands to the quality, as the variation in the filling patterns can be very large from mould to mould and hence the stability of the quality will be affected.

Danish abstract

Knaphed på ressourcer kan forventes at blive mere udbredt i fremtiden. Der vil ydermere også være øget opmærksomhed på de miljømæssige aspekter. Den store fokus på bilernes brændstofforbrug er i dag det tydeligste eksempel på dette. Der kan vælges mange indgangsvinkler til at reducere brændstofforbrug og forurening for biler, lastbiler etc. Motordesignet kan optimeres for højere effektivitet, vindmodstanden kan reduceres, kombinationer af forbrændingsmotorer og elektriske motorer kan benyttes osv. Men lige meget hvilken indgangsvinkel, der vælges, der skal bruges dele til at bygge køretøjerne af. Dvs. reduktion af vægten af de nødvendige indgående dele er en general måde at spare brændstof på, da den er anvendelig sammen med alle andre brændstofbesparende tiltag.

Selvom jernstøbegods har været brugt i biler, siden den første bil blev bygget, eksisterer der stadigvæk et stort potentiale for optimering af jernstøbegods med henblik på vægtbesparelse. Dette kan gøres ved at designe emner med små godstykkelser og bygge stivhed ind i emnerne v.hj.a. ribber, hule sektioner osv. Fremstilling af tyndvæggede emner bliver dermed vigtig.

Strømning af smelte i konventionelle indløbssystemer med bundfyldning og i tynde sektioner er detaljeret analyseret v.hj.a. videooptagelser af det strømmende metal. Konventionelle indløbssystemer med bundfyldning er vist at give relativ lille kontrol over den strømmende smelte. Resultatet er strømningsmønstre, der kan ændre sig væsentligt fra form til form pga. mindre uundgåelige fluktuationer i istøbningsforholdene. Ved de konventionelle typer indløb er det meget svært at undgå trykbølger. Trykbølgerne kan blive dannet på to forskellige tidspunkter i fyldningsforløbet. Hvis indløbssystemet indeholde blinde ender og tværsnittet af løbet er helt fyldt med smelte bag smeltefronten, vil en trykbølge blive dannet af hammereffekten, idet smelten rammer den blinde ende. Trykbølger kan også bliver dannet, når den sidste luftlomme i et delvist fyldt indløb lukkes. Trykbølgerne bryder smelteoverfladerne op.

Strømning i tyndvæggede sektioner er ikke kun vigtig for støbning af tyndvæggede emner, da tynde pladeformede indløb bruges ved støbning af mange forskellige emner. Dette er illustreret med en bremseskive. 6 forskellige layouts er lavet. Fyldesekvenserne er optaget på video. Forsøgene viser, hvor svært det er at designe indløb med bundfyldning, som ikke giver sprøjt ved begyndelsen af fyldningen og som giver en balanceret fyldning. Indløbene designes normalt til at give lave hastigheder, hvis der ønskes en rolig strømning. Men for at sikre en rolig strømning, skal trykbølger også undgås. Når der ikke opstår trykbølger og løbene giver god kontrol over smelten, kan en rolig strømning med sammenhængende smeltefronter opnås ved relativt høje hastigheder. Ved 5 af de 6 layouts er der brugt konventionelle typer indløb. I disse indløb er strømningsmønstrene i stor udstrækning styret af forholdet mellem de dynamiske og bremsende kræfter, som virker på smelten. Et ikke konventionelt indløb er også blevet testet. Dette indløb giver en stor grad af kontrol over strømningen; balancen mellem de dynamiske og bremsende kræfter har derfor kun en lille indflydelse på strømningsmønstrene.

En udstødningsmanifold med 2 mm vægtykkelse er blevet støbt ved anvendelse af et nyudviklet strømlinet indløbssystem. Manifolden er støbt uden nogen synlige defekter fra fyldningen. Det strømlinede indløbssystem giver meget ensartede strømningsmønstre fra form til form sammenlignet med, hvad der er set for konventionelle indløbssystemer. Dette betyder, at de konventionelle typer af indløbssystemer, der er undersøgt i dette arbejde, ikke kan anbefales til dele, som stiller store krav til kvaliteten, da strømningsmønstrene kan variere meget fra form til form, hvorfor ensartetheden af kvaliteten vil blive påvirket.

1 Introduction

1.1 Background

Shortage of resources can be expected to become more widespread in the near future. Even more focus will be put on how much energy and raw material etc. is used under both production and daily use of all kinds of things. The shortage of resources is already seen on the prices for pig iron and steel scrap. The U.S. steel scrap prices have increased from approximately 70 US$ per ton in January 2002 to 302 US$ in February 2004 [Ref. 1.1]. The prices for pig iron follow the prices for scrap. Due to the more controlled quality of pig iron are the pig iron prices a little higher than the scrap prices. The pig iron prices have reached 335 US$ per ton in 2004 [Ref. 1.2]. The heavy increase in the prices is mainly due to a fast growing Chinese demand.

The automotive sector has until now been the sector leading in the development to minimize the amount of resources being used. Both during production and use of vehicles a lot of attention is on the resources consumed, most clearly seen on the demands for low fuel consumption figures. The need for lower fuel consumption figures is not only driven by the need to reduce the resources used, it is also driven by the need to reduce the impact on the environment.

The automotive sector will be the pilot through this work. The need to minimize the consumption of resources is generally valid for all sectors. Maybe not so pronounced now but it will come in a foreseeable future. In addition to being the sector with until now the most pronounced focus on consumption of resources, the automotive sector is also a very large sector. In 2003 the world wide production of vehicles was 59 million including commercial vehicles [Ref. 1.3]. Out of this figure 50 million were passenger cars. This makes of course also the automotive sector very interesting. Besides from being a very interesting sector from an economical point of view, the automotive sector is also interesting from a technically point of view due to the focus on development of new materials and processes.

Different approaches can be made to reduce the consumption of resources in the automotive sector. Focusing for instance on the fuel consumption and pollution from passenger cars, trucks etc. the engine design can be optimized for higher efficiency, the wind resistance can be reduced for lower fuel consumption, combinations of combustion engines and electrical power can be used etc. But no matter which approach is taken; parts have to be used for building the vehicles. Hence reducing the weight of the needed parts is the most general way of saving fuel, as it is applicable together with all other means of saving fuel.

Reducing the weight of the needed parts can be achieved in many different ways. One way is to change the used material to one having a higher strength / weight ratio. This is mainly the reason for substituting iron parts with parts of aluminium, magnesium, carbon, fibre composites etc. Another way is to keep iron as the base material and optimize the design of the parts making it possible to utilize the material better.

Iron castings have been used in cars from the first car ever build. However a big potential still exists for optimizing cast iron parts. Even though cast iron parts have been used in cars for many years not much have been done until recently to optimize the design of the parts with

the aim to get an optimum utilisation of the amount of material used, i.e. to save weight. This is for instance reflected in the fact that the basic design of many cast iron parts seen in cars are several decades old [Ref. 1.4].

Different other things make it interesting to keep iron as the base material. Compared to other materials iron is very competitive on the price. This is the case even though the prices for scrap and pig iron are very high at the moment. Iron is a well-known material. Foundries producing iron parts are found all over the world. For parts with very high mechanical and / or thermal loads, materials used for substituting iron such as aluminium and magnesium have problems. Some parts have to have wear resistant inserts when produced in aluminium. When producing the part in iron no inserts are needed [Ref. 1.5]. Even though inserts are needed, it can still be the most feasible way to produce the part as for instance is seen with the huge amount of blocks produced in aluminium.

Looking at parts for engines the light weight alloys seem to get bigger and bigger problems with supplying the needed mechanical and thermal properties. The needed properties constantly increase due to the wish to raise the efficiency and the performance to weight ratio of the engines. Raising the efficiency and performance to weight ratio of a combustion engine normally includes raising the working temperature and mean pressures. This makes it more and more difficult to use aluminium etc. as substitute for iron. For instance for cylinder heads is work going on to develop processes making it possible to combine different aluminium alloys in the same cast part by casting them together. This makes it possible to combine high temperature resistant alloys with alloys having good flowability making it possible to cast the channels for the cooling water area [Ref. 1.6]. Without such measures it is not possible to meet the property requirements of very high performing engines with aluminium as base material. The technology with casting several alloys together seems to be quite complicated compared to casting the parts in one material. Furthermore if it is needed to cast alloys together with different base materials the recycling aspect is getting complicated.

With a performance to weight ratio increasing faster and faster the light weight materials are having larger and larger problems with providing the needed properties. This indicates a possible renaissance for some cast iron parts as for instance the crankcase [Ref. 1.7] and the heads as mentioned above. With the constantly increasing efficiency and weight to performance ratio even iron based materials have problems with supplying the needed properties for some parts. For instance highly alloyed materials like Ni-Resist have to be used for the exhaust manifold for high performance engines where the working temperature of the manifold now approaches 1100 °C [Ref. 1.8].

The result is that no clear indications show a future market for castings without iron playing a major role. The wish for higher efficiency and performance to weight ratios results in a constant optimization of the parts demanding for more dedicated solutions. This can very easily mean that small changes in the demand to a specific part can mean that it is more feasible to change to another base material. In the end the result is a casting market with very dedicated solutions utilizing a wide mix of different base materials.

In the cases where it turns out to be more feasible to use iron as the base material may it be due to the fact that iron is able to cope with higher mechanical and thermal loads or other reasons it is necessary to reduce the weight of the parts. Using iron as the base material and reducing the weight and in some cases even raising the design load of a part means optimizing the

design utilizing the potential of the material better. This is done by designing parts with thinner wall thicknesses and building stiffness into the parts via ribs, hollow sections etc. Due to the fact that not much have been done until recently to optimize the design of iron casting with the aim to save weight a big weight saving potential is still present in iron castings [Ref. 1.4].

This leads to a need for production of parts with very small wall thicknesses in iron. Knowledge about flow in thin sections becomes hence import.

Not only flow in thin sections has to be mastered also the metallurgy in connection with thin walled parts puts new demands on the foundries. Furthermore means reducing the wall thickness of the parts to an absolute minimum that the dimensional capabilities of the casting process used is getting relatively more important.

Apart from reducing the fuel consumption of the vehicle makes lowering the weight it also possible to reduce the resources used for producing the part. This is most clearly seen if iron is kept as the base material, but it is also valid in the cases where the base material is changed. This is due to the fact that the base material will not be changed if the change means higher consumption of resources for production. Hence it has a double effect to reduce the weight of the parts needed, as both the resources used under production and daily use are reduced.

Many different parts are used for producing vehicles. A substantial portion of the parts needed are most feasible produced with the help of casting processes, as a large part of the final geometry can be produced in one process. Some parts will be difficult maybe even impossible to produce without some sort of casting process. For instance cylinder blocks and heads will virtually be impossible to produce with the present design without casting them.

The DISAMATIC process utilizing vertically parted flaskless moulds has over the last 30 years proven to be very cost effective for the production of cast iron parts. About half the production of cast iron parts used in the automotive sector is produced on DISAMATIC's [Ref. 1.9]. As a consequence of this it seems to be reasonable to develop the DISAMATIC process to be able to cope with the demands from the future iron castings.

1.2 Main tasks

The main task of this project is to investigate iron melt flow in thin walled sections in vertically parted green sand moulds. The present work aims at building up knowledge making it possible to produce parts with extremely small wall thicknesses. The successful production of thin walled parts can be seen as a chain consisting of many links. Two of the basic links in the chain are to produce suitable moulds and to get the metal into the mould cavity. The focus will be on these two aspects, well knowing the chain contains many other links.

This objective will be achieved by a literature review of commonly used theory for designing gating systems for parts cast in green sand moulds. To compliment the theory and due to the fact that the theory for gating thin walled iron parts is not so comprehensive three different series of trials will be conducted.

The first series of trials will concern plates with thicknesses in the range 2 - 4 mm. The aim with this series of trials is to investigate the flow in thin sections with a simple geometry easy to overlook. Furthermore the simple geometry makes it possible to record the flow patterns on video for closer examination. Even when talking about parts with normal section thicknesses, flow in thin walled sections can play an important role. This is due to the fact that thin plate shaped ingates are used for casting many different parts. This will be illustrated with the second series of trials, using a brake disc as example. The third series of trials is with an exhaust manifold with very small wall thicknesses, demonstrating the possibilities of the process on a realistic geometry. Both the second and third series of trials also include capturing the real metal flow on video as done at the first serials of trials.

To be able to conduct the trials under controlled conditions, it has been necessary to upgrade the test foundry at The Technical University of Denmark to establish up to date test facilities.

References:

Ref. 1.1 Emergency Steel Scrap Coalition Http://www.scrapemergency.com/crisis.html (2004)

Ref. 1.2 Ryan's Notes 629 Fifth Avenue Pelham, New York 10803. Weekly news letters 2002-2004

Ref. 1.3 Marktberichte / Marktstudien 30.01.04-6.02.04 (KW 6) VDMA

Ref. 1.4 Journalen: Det kører i olie. Television program broadcasted on DR1 20.30 o'clock October 26 1998.

Ref. 1.5 Dünnwandiger Zylinderblöcke aus Gusseisen, Giesserei-Praxis 2003 4

Ref. 1.6 Serienreife Lösung zur Fertigung von Zylinderköpfen aus Gradientenguss, Gießerei-Erfahrungsaustausch, 05/2003 p. 177-180

Ref. 1.7 Casting doubt on the new. European Automotive Design May 2003 p 24-26

Ref. 1.8 Hochleistungsfähige Gußwerkstoffe für Abgaskrümmer und Turbolader - Turbinengehäuse. Wilhelm Kallen, Klaus Röhrig. Konstruieren + gießen 26 (2001) Nr. 4

Ref. 1.9 Aluminium Castings made in Vertically Parted Green Sand Moulds. Ph.D. Thesis by Niels Winther Rasmussen. The Technical University of Denmark 1998

2 Gating Technology

The gating system has to transport the melt from the mould surface to the casting cavity in a suitable way, i.e. without lowering the melt quality; some times the gating system even has to raise the melt quality. Secondly the gating system has to secure an appropriate heat distribution in the casting and feeders. In some cases the gating system also acts as a feeder. Thirdly the gating system has to connect to the casting in acceptable places and it has to be easily removable. Last but certainly not least in a time with very low casting prices; the gating system has to be as small as possible to raise the yield and hence make the foundry more competitive.

Even though the gating system has a lot of functions, some of them putting contradicting demands on the design, most gating systems are designed using rather simple equations and practical experience. Detailed methods generally applicable do not exist. This means that if a detailed study of a gating system is to be made, it is a rather time consuming job and hence also quite expensive.

When talking about iron castings made in green sand moulds, the filling is in practice always driven by gravity, i.e. the melt is poured from somewhere above the mould and enters the top of the mould with a velocity given by the set up of the pouring device. Some of the dynamic energy from the pouring stream can be transferred to the gating system. For green sand iron castings newly developed systems [Ref. 2.2] where metal is pumped into the bottom or the side of the mould, have been introduced to the market, but no system is yet running in production. Hence the focus will be on gravity driven filling in this section.

Even though no system with filling through the side or bottom of the mould is yet in production for iron, different aspect of this process should be mentioned. First of all with a system not depending on gravity as driving force the flow velocities can be controlled to a much higher degree. When relying on gravity and using a bottom gated layout, high velocities will be seen at the beginning of the filling sequence where the gating system is not filled and no back pressure exists. At the end of the filling low velocities will be seen due to a small driving metallostatic pressure. The opposite is more feasible; at the beginning of the filling the gating system is empty and no back pressure exists hence a slow filling is desirable, when the gating system is filled higher flow velocities can be accepted without harming the metal, i.e. without excessive oxide formation etc. The filling profile can be controlled with a bottom or side filling system. With a suitable control system and knowledge about the areas of the horizontal cross sections of the parts to be cast, the melt front velocity can be controlled in all parts of the casting. This is especially interesting for thin walled castings, where the heat content is relatively low. Seen from a yield point of view a side or bottom filling pouring device will also be feasible, the pouring cup and down runner will not any longer be necessary, raising the yield and leaving extra space on the pattern plate, in some case making it possible to get more castings in the mould.

In total many positive things seen from a process point of view can be found for pouring devices filling through the bottom or side of the mould. But the big drawback of such systems is reliability. It is difficult to find materials suitable for the manufacturing of the parts needed for such pouring devices. When producing castings on vertically parted moulding lines with conventional pouring devices; relative high up times are seen to day. A new system has to be able to match these up times. With production speeds for vertically parted moulding machines up

to over 500 moulds pr. hour high demands are put on the equipment. The result is that until now it has not been feasible to go for bottom or side filling pouring devices for iron.

Gravity driven filling is hence still the way iron is poured when cast in green sand moulds. Due to this and as mentioned above will the focus in the rest of this section be on gravity driving filling.

In contrast to what is the case for iron poured in green sand moulds, are side filling pouring devices successfully running in production for casting high quality aluminium parts in green sand. In the case of aluminium significantly lower temperatures are seen than when casting iron. And generally aluminium is seen to demand very calm flow patterns when compared to iron. Hence it makes it feasible to run with side filling pouring devices when casting high quality aluminium parts in green sand moulds.

2.1 Fluid flow

Designing gating systems is basically seen working with fluid flow. To give a full description of flowing fluids Navier-Stokes equations can be used. The pressure and velocities as a function of time and position are described with Navier-Stokes equations. Navier-Stokes equations are valid for viscous flow of a Newtonian fluid. Fluids in which shear stress is directly proportional to the rate of deformation are called Newtonian fluids. The Navier-Stokes equations in a Cartesian coordinate system can be seen below [Ref. 2.1]:

$$\rho\cdot\frac{Du_1}{Dt}=\rho\cdot g_1-\frac{\partial p}{\partial x_1}+\frac{\partial}{\partial x_1}\left[2\cdot\mu\cdot\frac{\partial u_1}{\partial x_1}+(\zeta-\frac{2}{3}\cdot\mu)\cdot(\frac{\partial u_1}{\partial x_1}+\frac{\partial u_2}{\partial x_2}+\frac{\partial u_3}{\partial x_3})\right]$$
$$+\frac{\partial}{\partial x_2}\left[\mu\cdot(\frac{\partial u_1}{\partial x_2}+\frac{\partial u_2}{\partial x_1})\right]+\frac{\partial}{\partial x_3}\left[\mu\cdot(\frac{\partial u_3}{\partial x_1}+\frac{\partial u_1}{\partial x_3})\right]$$

$$\rho\cdot\frac{Du_2}{Dt}=\rho\cdot g_2-\frac{\partial p}{\partial x_2}+\frac{\partial}{\partial x_2}\left[2\cdot\mu\cdot\frac{\partial u_2}{\partial x_2}+(\zeta-\frac{2}{3}\cdot\mu)\cdot(\frac{\partial u_1}{\partial x_1}+\frac{\partial u_2}{\partial x_2}+\frac{\partial u_3}{\partial x_3})\right]$$
$$+\frac{\partial}{\partial x_3}\left[\mu\cdot(\frac{\partial u_2}{\partial x_3}+\frac{\partial u_3}{\partial x_2})\right]+\frac{\partial}{\partial x_1}\left[\mu\cdot(\frac{\partial u_1}{\partial x_2}+\frac{\partial u_2}{\partial x_1})\right] \qquad \textbf{[Eq. 2.1]}$$

$$\rho\cdot\frac{Du_3}{Dt}=\rho\cdot g_3-\frac{\partial p}{\partial x_3}+\frac{\partial}{\partial x_3}\left[2\cdot\mu\cdot\frac{\partial u_3}{\partial x_3}+(\zeta-\frac{2}{3}\cdot\mu)\cdot(\frac{\partial u_1}{\partial x_1}+\frac{\partial u_2}{\partial x_2}+\frac{\partial u_3}{\partial x_3})\right]$$
$$+\frac{\partial}{\partial x_1}\left[\mu\cdot(\frac{\partial u_3}{\partial x_1}+\frac{\partial u_1}{\partial x_3})\right]+\frac{\partial}{\partial x_2}\left[\mu\cdot(\frac{\partial u_2}{\partial x_3}+\frac{\partial u_3}{\partial x_2})\right]$$

Where:
ρ Density [kg/m^3]
u Velocity [m/s]
t Time [s]
g Gravity constant [m/s^2]
p Pressure [Pa]
x Position [m]
μ Dynamic viscosity [Pa·s]
ζ Volume viscosity coefficient [Pa·s]

The indices 1, 2 and 3 indicate that the parameter is to be taken in the corresponding main direction in the Cartesian coordinate system.

Unfortunately Navier-Stokes equations can only be solved analytically in very few simple cases. Hence numerical methods have to be used to solve it. This means the equations can not be used for doing manual calculations of gating systems. Much simpler equations have to be used. These equations will be described in the following sections.

On the other hand, when doing simulations of flow problems is it possible to solve the Navier-Stokes equations numerically and in that way they come in handy for treating the fluid flow problems when designing gating systems.

2.2 Basic equations

As mentioned above the focus will be on gating system where the flow is driven by gravity. One of the basic equations for dimensioning gravity driven gating systems builds on energy conservation, if there are no losses, the following equation is valid [Ref. 2.3]:

$$\text{Kinetic energy} = \text{Potential energy}$$
$$1/2 \cdot M \cdot v^2 = M \cdot g \cdot H \qquad \textbf{[Eq. 2.2]}$$
$$v = \sqrt{2 \cdot g \cdot H}$$

Where:
M Mass [kg]
v Velocity [m/s]
g Gravity constant [m/s^2]
H Height [m]

This equation yields the metal velocity after a free fall of height H, for an ideal flow, i.e. a flow with no losses. Metal flow in gating systems is not ideal due to wall friction, pressure drops in directional changes etc, hence a loss coefficient m (less than 1) is added leading to:

$$v = m \cdot \sqrt{2 \cdot g \cdot H} \qquad \textbf{[Eq. 2.3]}$$

This equation is also known as Torricelli's law. In some of the literature references the loss coefficient is called the discharge coefficient. In this work the term "loss coefficient" will be used as it is found more descriptive for the physical phenomenon. The loss coefficient incorporates all kinds of energy losses in the gating system. This makes it complicated to calculate a theoretical value for the loss coefficient. Different places in the literature values for loss coefficients can be found, for instance [Ref. 2.3] and [Ref. 2.4]. When designing gating systems in practice, the actual used value for the loss coefficient depends much on the foundry engineer's personal experience. Good practice is to dimension the gating system with the best available value for the loss coefficient. Then measure the actual pouring time and back calculate the loss coefficient, making it possible to use a more qualified value next time a similar gating system has to be designed. The empirical nature of the loss coefficient is also reflected in the different approaches to the loss coefficient seen in the literature. In [Ref. 2.3] the loss coefficient is described with the numbers of 90 degree turns the melt undergoes in the gating system. In [Ref. 2.4] the loss coefficient is described by the shapes of the cross sections the melt has to pass. In [Ref. 2.5] and [Ref. 2.13] a more scientific approach to determine the losses has been taken. The contributions to the losses from friction and directional changes have been calculated. This approach will be discussed in section 2.7.

The flow rate W [mass/time] through a cross section with area F, can be written as:

$$W = \rho \cdot F \cdot v \qquad \textbf{[Eq. 2.4]}$$

Where ρ is the density of the material, and v is the mean velocity over the cross section in question. Inserting Eq. 2.3 and writing mass flow as total mass, G, divided by flow time, t, one yields:

$$\frac{G}{t} = \rho \cdot F \cdot m \cdot \sqrt{2 \cdot g \cdot H} \qquad \textbf{[Eq. 2.5]}$$

Isolating the area i.e. the cross section area of the runner yields:

$$F = \frac{G}{t \cdot \rho \cdot m \cdot \sqrt{2 \cdot g \cdot H}} \qquad \textbf{[Eq. 2.6]}$$

Focusing on iron and inserting a mean value of 6890 kg/m^3 for the temperature and composition depending density, and 9.81 m/s^2 for the gravity constant and converting to units normally used when designing gating systems, one can rewrite the equation to:

$$F = \frac{1036 \cdot G}{t \cdot m \cdot \sqrt{H}} \qquad \textbf{[Eq. 2.7]}$$

Where:
F Cross sectional area [mm^2]
G Weight of metal flowing through the cross section [kg]
t Time for the metal to flow through the cross section [s]
H Metallostatic pressure height [mm]
m Loss coefficient

With the help of this very simple equation or variations of it and practical experience, a large part of all gating systems used in practice is designed. Different variants of this equation can be found many places in the literature for instance in [Ref. 2.3], [Ref. 2.4], [Ref. 2.6].

In this equation the needed cross sectional area follows $1/\sqrt{H}$. In practice almost all gating systems are made with a straight taper of the down runner from one calculated cross section area to the next. This yields too large areas. I.e. the basis for getting partly filled down runners exists. This will be discussed more closely in the experimental section with the exhaust manifold. On the other hand the flow rate at bottom filling gating systems will fall as the filling proceeds, due to the back pressure build up. This means that the problem with partly filled runners due to straight tapers will get less pronounced at the filling proceeds.

2.3 Reynolds number

When designing gating systems for sensitive alloys demanding a calm flow in the runners and mould cavity a laminar flow is preferable to a turbulent flow. Different aspects make a calm flow preferable. For instance the formation of oxides and sand erosion will be minimized, and the ability to get slag particles to settle on the walls of the runners will be better. When the flow takes place in a closed channel i.e. when the fluid is completely bounded by solid faces and the flow is incompressible, the Reynolds number can be used to describe the flow. The Reynolds number is the ratio between the inertia forces and the viscous forces. The inertia forces is a measure for the tendency of the flow to move in the direction of the momentum in the flow, the viscous forces are trying to counteract this motion, due to viscous drag from the side walls of the channel containing the flow. I.e. it is a balance between dynamic forces and braking shear forces from viscosity. Reynolds number is given by [Ref. 2.7]:

$$\mathrm{Re} = \frac{\text{Inertia forces}}{\text{Viscous forces}}$$

[Eq. 2.8]

$$\mathrm{Re} = \frac{\rho \cdot V \cdot D}{\mu}$$

Where:
ρ Density [kg/m^3]
V Flow velocity [m/s]
D Characteristic distance [m]
μ Dynamic viscosity [Pa·s]

The characteristic distance is a distance describing the size of the cross section in which the flow takes place. For circular channels this is the diameter. For other shapes the hydraulic dia-

meter is used. For rectangular shaped cross sections the hydraulic diameter is given by [Ref. 2.7]:

$$D_h = \frac{4 \cdot A}{P} \qquad \textbf{[Eq. 2.9]}$$

Where A is the cross section area and P the perimeter.

When the flow takes place in a plate shaped channel i.e. when the width (w) is much larger than the height (h) one gets:

$$\begin{aligned} D_h &= \frac{4 \cdot w \cdot h}{2 \cdot (w + h)} \\ D_h &= \frac{2 \cdot w \cdot h}{w + h} \\ D_h &= \frac{2 \cdot h}{1 + h/w} \\ D_h &\approx 2 \cdot h \end{aligned} \qquad \textbf{[Eq. 2.10]}$$

I.e. twice the plate thickness [Ref. 2.1] has to be used in plate shaped cross sections. The viscous drag from a plate shaped channel is smaller than the drag from a tube with the plate thickness as diameter. This seems also fair because the flow in a tube is surrounded by walls in all directions giving viscous drag, while the flow in a plate only has walls in two directions giving viscous drag.

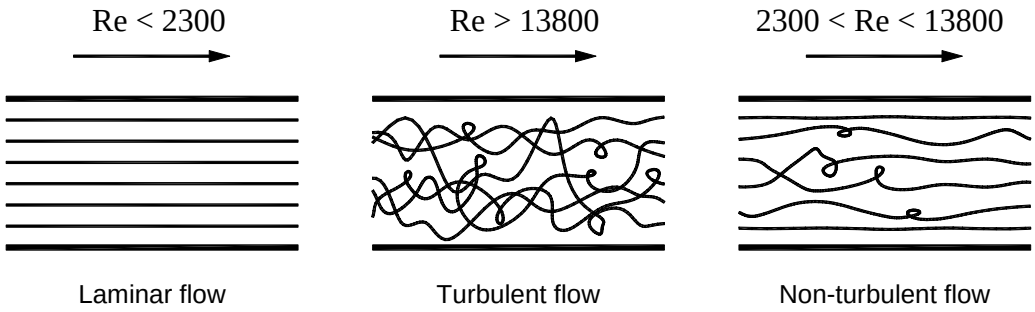

Figure 2.1 Flow pattern depending on Reynolds number [Ref. 2.25].

When Re < 2300 the flow will normally be laminar. When the Reynolds number is in the range 2300 < Re < 13800 the flow is in a transition zone with a mixed turbulent and laminar flow. For Re > 13800 the flow can be expected to be fully turbulent [Ref. 2.13]. The flow patterns are illustrated on Figure 2.1 [Ref. 2.25]. The values given for the transitions are the normally used values. They depend on the conditions for the flow. Under special condition laminar flow can be maintained at Reynolds numbers as high as 40000 [Ref. 2.1].

The Reynolds number is only applicable in the case where the cross section of the runner is completely filled. Otherwise the flow has to be dealt with as an open channel flow. When the cross sections of the runners are completely filled the possible turbulence takes place underneath the melt surface, i.e. it is bulk turbulence. The Reynolds number cannot be used to describe the turbulence taken place on the melt surface when the melt front passes through the gating system.

In general internal flows may be laminar, turbulent or a combination of the two. For some simple laminar internal flows, analytical expressions to describe the flow i.e. pressure and velocity can be made. When the flow is turbulent analytical solutions can not be found in any case, and the expressions used for describing the flow builds on semi-empirical theories and experimental data [Ref. 2.7].

To illustrate the use of the Reynolds calculation, a layout used in the experimental section will be taken as an example. The layout can be seen on Figure 2.2. It is for casting of a solid brake disc of 245 mm diameter in a vertically parted mould. The disc is cast in grey iron.

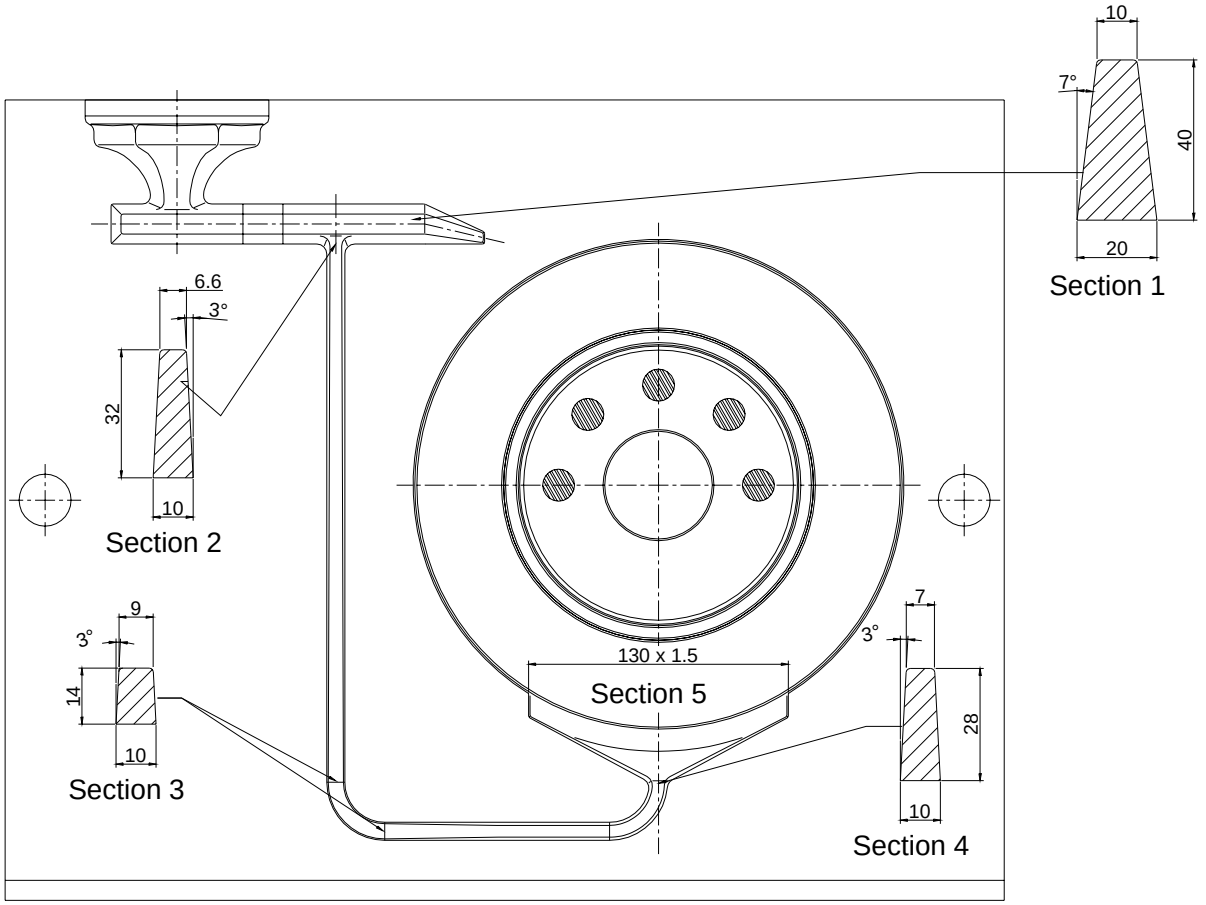

Figure 2.2 Layout used for example with Reynolds number.

For a grey iron at 1350 °C is the dynamic viscosity μ 4.52 mPa·s, and the density ρ is 6436 kg/m^3 [Ref. 2.20].

From trials discussed in section 5, the flow rates at different stages of the filling sequence are known. They can be seen in Table 2.1.

Melt level in the disc	Flow rate [cm^3/s]
Bottom	178
Middle	145
Top	102

Table 2.1 Filling rates found experimentally.

The Reynolds numbers for the marked sections on Figure 2.2 at different stages in the filling sequence can be seen in Table 2.2.

Section no.	Area [mm^2]	D_h [mm]	Re Bottom	Re Middle	Re Top
1	600	21.7	9167	7472	5253
2	266	13.2	12574	10250	7205
3	133	11.3	21500	17526	12320
4	239	13.1	13893	11325	7961
5	195	3.0	3899	3179	2234

Table 2.2 Reynolds numbers at different sections at different stages of the filling sequence.

All Reynolds numbers are seen to be below 13800, except for cross section 3 at the bottom of the down runner. Only at this cross section fully developed turbulent flow can be expected. At cross section 5, the plate shaped ingate, the Reynolds numbers are below 2300 or only a little larger at all stages of the filling sequence, and hence the flow can be expected to be laminar or close to laminar when it enters the casting cavity.

When designing the layout shown on Figure 2.2 care has been taken to obtain low Reynolds numbers and uniform melt velocities over the plate shaped ingate. Hence the found Reynolds numbers are somewhat on the lower side of what is normally seen in gating systems. The obtainable Reynolds numbers are of course very dependent on the mould size. Higher moulds lead to higher velocities at the bottom of the mould and hence higher Reynolds numbers. The highest vertically parted moulds are at present time 850 mm’s, a free fall of this height results in a velocity of 4 m/s !

In general the practical use of the Reynolds number is often complicated because of uneven melt velocities over the cross sections. Take for instance a wide plate shaped ingate connected to a horizontal runner, which is often used when casting brake disc's in vertically parted moulds. A mean velocity for the melt passing through the ingate can be calculated if the appropriate loss coefficient is known or experimental data exists. But in most cases the melt flow is not uniform over the cross section of the ingate. This means that the melt will pass through the gate at high velocities at some parts of the ingate and in other parts the velocities will be much lower or even zero. As the melt velocity is in the numerator of the equation for the Reynolds number, a large range of Reynolds numbers in practice exist for the same cross section. Hence the practical use of the Reynolds number is difficult. Figure 2.3 shows an example of a brake disc cast with a wide plate shaped ingate connected to a horizontal runner. The temperature distribution in the plate shaped ingate and the disc shows the unbalanced flow through the ingate.

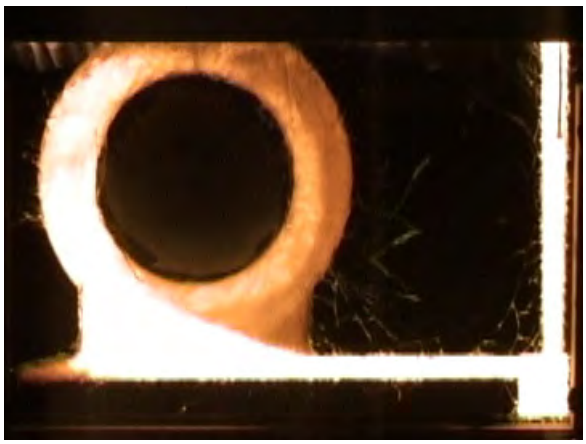

Figure 2.3 Flow distribution in plate shaped ingate. The top of the disc and the pouring cup is cover by a core making it possible to record the filling on video through glass plates.

Another aspect which needs attention when describing internal flow is the entrance length.

When flow enters a channel the flow pattern develops over a distance before stationery or fully developed flow exists. The development of the flow pattern in a tube with laminar flow at the entrance and a turbulent fully developed flow is shown on Figure 2.4. The boundary layer is laminar close to the entrance, when it becomes turbulent the growth velocity of it increases due to the enhanced mixing in turbulent flows. X_L is the point where the flow becomes fully developed, i.e. where the flow pattern does not change further down the flow. The relatively flat velocity profile of the fully developed flow indicates turbulent flow.

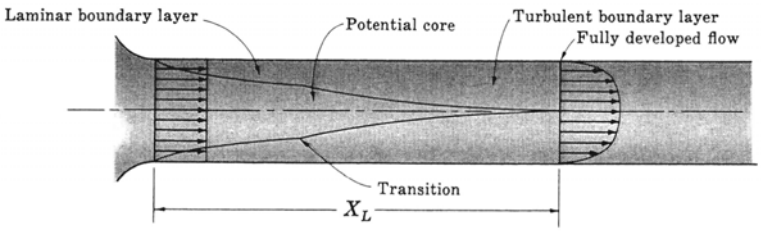

Figure 2.4 Development of boundary layers in a tube when the flow is laminar at the entrance [Ref. 2.8].

The shape of the transition zone from the entrance to the point where fully developed flow exists depends on several factors. First of all the flow at the entrance to the tube is important. Only in rare cases is the flow laminar at the entrance to a runner section. Due to the complexity of the flow no exact solutions exists for describing the development of the flow. The boundary conditions at the entrance to the channel are often not known, which makes it even more difficult. As a result approximate estimates have to be used. If the flow at the entrance to the channel is laminar, and the Reynolds number is low resulting in a fully developed laminar flow, the entrance length can be estimated using [Ref. 2.7]:

$$X_f \cong 0.06 \cdot Re \cdot D \qquad \textbf{[Eq. 2.11]}$$

If the flow in the channel is turbulent, enhanced mixing between the layers takes place making the entrance length shorter. From experimental data, turbulent flow is known to be fully developed within 25 to 40 pipe diameters from the entrance [Ref. 2.7]. Runners used in vertically parted moulds have very different dimensions. A typical hydraulic diameter is 1 cm; turbulent flow in such a channel will be fully developed after 25 - 40 cm.

The Reynolds number can tell whether the flow is laminar or turbulent. But the flow pattern is heavily influenced by the entrance of the channel a significant distance from the channel entrance. In general, flow in runners has often Reynolds numbers making them turbulent, and often the flow at the entrance to the runners is not laminar enhancing the development of turbulent flow.

2.4 Weber number

The Reynolds number can only be used to describe the amount of turbulence in the bulk of the flow taken place in filled runner cross sections. Turbulence at the melt front is in many cases more harmful. At the melt to air interface it is possible for new oxides to be formed and to be swirled into the melt. The surface turbulence can be described as the ratio between the inertia forces from melt velocity trying to break the surface up and the surface tension forces trying to keep the surface together. The dimensionless ratio between these two forces is called the Weber number. It is given by [Ref. 2.10]:

$$We = \frac{\text{Inertia forces}}{\text{Surface tension forces}}$$

[Eq. 2.12]

$$We = \frac{\rho \cdot V^2 \cdot r}{\sigma}$$

Where:

ρ	Density [kg/m^3]
V	Flow velocity [m/s]
r	Radius of curvature [m]
σ	Surface tension [N/m]

The radius of curvature is given by:

$$\frac{1}{r} = \frac{1}{r_1} + \frac{1}{r_2}$$

[Eq. 2.13]

Where the two radii are measured in two planes at right angles.

When the Weber number is 1, the inertia forces and the surface tension forces balance. No work has been done closely investigating if this can be used as the threshold value to describe when the melt surface starts to break up; the little work done suggests a value between 0.2 and 0.8 [Ref. 2.6].

Due to the fact that the square of the velocity is in the numerator in the equation for the Weber number, the Weber number is quite sensitive to velocity. In most gating systems an uneven melt velocity distribution is seen over the cross sections. The high sensitivity to velocity makes the practical use of the Weber number even more difficult than the use of the Reynolds number.

Or the other way around; the high sensitivity to velocity, puts focus on the importance of having uniform melt velocities over the cross sections, keeping the maximum velocity as low as possible. If the velocities are uniform, higher mean velocities can be used while still obtaining a coherent melt front. This is seen in [Ref. 2.11] where flow with uniform velocities at high Weber numbers leads to coherent melt fronts.

The layout on Figure 2.2 used to illustrate the use of the Reynolds number is designed to give very good control over the melt securing uniform melt flow velocity across the plate shaped ingate, hence it makes sense to use the Weber calculations on this section.

The surface tension for grey iron at 1350 ° C can be expressed as [Ref. 2.14]:

$$\sigma = 1913 - 195 \cdot \ln(1 + 365 \cdot a_s) + 30 \cdot (\text{wt\%C}) \qquad \textbf{[Eq. 2.14]}$$

Where:

σ	Surface tension [mN/m]
a_s	Activity of S, can be taken as the weight % of S
wt%C	Weight % C

With 0.06 wt% S and 3.4 wt% C the surface tension is calculated to 1.4 N/m. The temperature used for calculation of the surface tension could be argued to be lower as this is a property found at the melt front. The influence from temperature on surface tension can be seen in section 2.8.1.1.

From Table 2.1 and Table 2.2, the initial melt front velocity in the plate shaped ingate can be calculated to 0.91 m/s. Due to the plate shaped design of the ingate, the radius of curvature is half the thickness i.e. 0.75 mm. Using 6436 kg/m^3 for the density as with the Reynolds calculations, the Weber number for the plate shaped ingate is found to be 2.9. And hence inertia forces are stronger than the surface tension forces. A snapshot from the actual filling when the melt front passes through the plate shaped ingate is seen on Figure 2.5. The melt front is not planar but on the other hand no droplets have yet left the main melt front. The two melt tongues at the sides have entered the disc cavity.

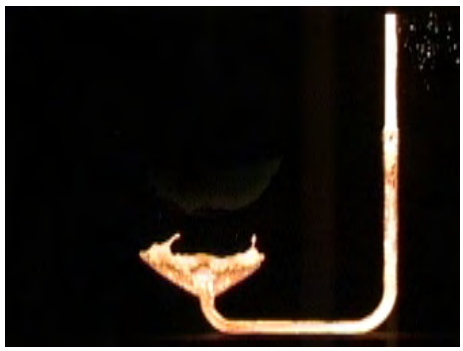

Figure 2.5 Flow through plate shaped ingate.

2.5 Froude number

When casting parts with demands to the quality, bottom filling gating system are often used. This means a large part of the flow is going in the opposite direction of gravity; gravity will hence help to keep the surface together in the same way as the surface tension. I.e. a dimensionless number describing the balance between inertia and gravity can be used here in the same way as the Weber number describes the balance between inertia and surface tension. The ratio between inertia and gravity is called the Froude number [Ref. 2.10] Figure 2.6 shows the dimensions needed for the calculation of the Froude number, the number is given by:

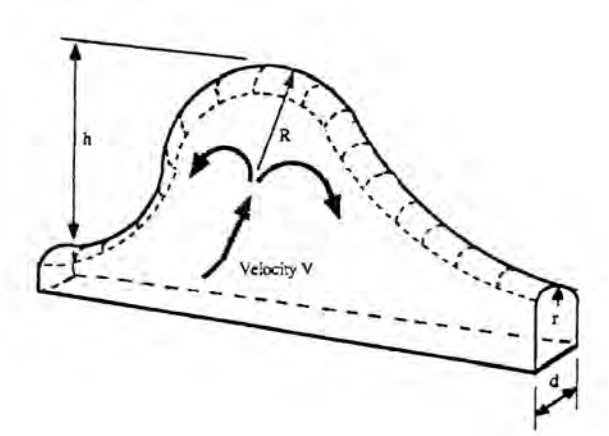

Figure 2.6 Dimensions needed for calculation of the Froude number [Ref. 2.10].

$$Fr = \frac{\text{Inertia forces}}{\text{Gravity forces}}$$

[Eq. 2.15]

$$Fr = \frac{V^2}{g \cdot h}$$

Reusing the data for the flow in the ingate of the brake disc layout used in the example for the Weber calculations i.e. V = 0.91 m/s, a surface wave of 0.01 m will give a Froude number of 9.3. This means the inertia forces will be much stronger than the gravity forces. And hence inertia is controlling the development of surface waves when comparing to gravity forces.

It has to be mentioned that in fluid flow the application of the Froude number is normally a little different. It is often used to describe waves on fluid surfaces, like a wave on a river moving up or down stream i.e. parallel to the surface and not perpendicular to the surface as is the case here.

2.6 Surface tension

The surface tension used in the Weber number is in it self a useful parameter. When the metal is flowing in a non-wetting mould, the surface tension will generate a back pressure. This can be expressed as the pressure difference over the melt to air interface. The pressure difference due to surface tension is given by [Ref. 2.6]:

$$P_{\text{Surface tension}} = P_i - P_e = \sigma \cdot \left(\frac{1}{r_1} + \frac{1}{r_2} \right)$$

[Eq. 2.16]

Where:
P_i Pressure inside the metal [Pa]
P_e Pressure outside the metal acting on the melt front [Pa]
σ Surface tension [N/m]
r_1 and r_2 Two radii defining the curvature of the melt front, the two radii are measured in two planes at right angles [m]

For a thin plate shaped casting with planar melt front r_2 is much larger than r_1 i.e. only the curvature of the melt front in the thickness direction of the plate is significant. For small wall thicknesses i.e. below approximately 7 mm, the curvature of the melt front in the thickness direction will be equal to half the plate thickness T. The pressure from the surface tension is then given by:

$$P_{\text{Surface tension plate}} = \frac{\sigma}{r}$$

$$P_{\text{Surface tension plate}} = \frac{2 \cdot \sigma}{T} \qquad \textbf{[Eq. 2.17]}$$

For flow in a thin cylindrical tube the melt front will have a sphere shaped front with $r_1 = r_2$. If the diameter is equal to the plate thickness used above, then T = 2r. Hence:

$$P_{\text{Surface tension tube}} = \sigma \cdot \left(\frac{1}{r} + \frac{1}{r} \right)$$

$$P_{\text{Surface tension tube}} = \frac{2 \cdot \sigma}{r}$$

$$P_{\text{Surface tension tube}} = \frac{4 \cdot \sigma}{T} \qquad \textbf{[Eq. 2.18]}$$

I.e. due to curvature in 3 dimensions compared to curvature in 2 dimensions the pressure from the surface tension has been doubled. Using the plate thickness T or the diameter r of the cylinder as the describing parameter, these two values for the back pressure from surface tension is the minimum and maximum values obtainable for all other geometries with the same wall thickness.

The pressure from surface tension can be converted to an equivalent metallostatic height given by:

$$P_{\text{Metal}} = \rho \cdot g \cdot h$$

$$h = \frac{P_{\text{Metal}}}{\rho \cdot g} \qquad \textbf{[Eq. 2.19]}$$

Where:
ρ Density [kg/m^3]
g Gravity constant [m/s^2]
h Height of metal [m]

This gives the following equation for the height of metal corresponding to the back pressure generated by the surface tension for a plate:

$$h_{Plate} = \frac{2 \cdot \sigma}{\rho \cdot g \cdot T} \quad \textbf{[Eq. 2.20]}$$

The equation for a cylinder is:

$$h_{Cylinder} = \frac{4 \cdot \sigma}{\rho \cdot g \cdot T} = \frac{2 \cdot \sigma}{\rho \cdot g \cdot r} \quad \textbf{[Eq. 2.21]}$$

Where the thickness of the plate T equals 2 times the radius r of the cylinder.

For a ductile iron at 1350 °C is the density 6260 kg/m^3 [Ref. 2.19]. The surface tension at 1350 °C is given by [Ref. 2.14]:

$$\sigma = 1913 - 195 \cdot \ln(1 + 365 \cdot a_s) + 30 \cdot (wt\%C) \quad \textbf{[Eq. 2.22]}$$

Where:
σ Surface tension [mN/m]
a_s Activity of S and can be taken as the weight % of S
wt%C Weight % C

With 3.6 wt% C and 0.01 wt% S the surface tension is calculated to 1.72 N/m.

Eq. 2.22 for the surface tension of ductile iron is seen to be the same as Eq. 2.14 for the surface tension of grey iron. The quite different values of the surface tension for grey iron and ductile iron can be obtained with the same equation due to the relative large difference in sulphur content. Going into more detailed studies of the size of the surface tension and hence taking more parameters into account will end op with different equations for describing the surface tension of grey and ductile iron.

The back pressures generated by the surface tension as a function of size (wall thickness for the plate and diameter for the cylinder) is given in Table 2.3. Values for grey iron have also been added. They are based on σ = 1.4 N/m and ρ = 6436 kg/m^3 as found in section 2.4

	Ductile Iron				Grey Iron			
	Plate		Cylinder		Plate		Cylinder	
Size	Pres.	Fe H.	Pres.	Fe H.	Pres.	Fe H.	Pres.	Fe H.
mm	Pa	mm	Pa	mm	Pa	mm	Pa	mm
0.5	6884	112	13768	224	5600	89	11200	177
1.0	3442	56	6884	112	2800	44	5600	89
1.5	2295	37	4589	75	1867	30	3733	59
2.0	1721	28	3442	56	1400	22	2800	44
2.5	1377	22	2754	45	1120	18	2240	35
3.0	1147	19	2295	37	933	15	1867	30
3.5	983	16	1967	32	800	13	1600	25
4.0	861	14	1721	28	700	11	1400	22
4.5	765	12	1530	25	622	10	1244	20
5.0	688	11	1377	22	560	9	1120	18
5.5	626	10	1252	20	509	8	1018	16
6.0	574	9	1147	19	467	7	933	15

Table 2.3 Back pressure due to surface tension in plates and cylinders.

I.e. in a plate shaped casting in ductile iron with a wall thickness of more than 4-5 mm, the back pressure due to surface tension will not be significant. The surface tension in grey iron is for this example 20 % lower than for ductile iron, hence the thickness where surface tension becomes insignificant is somewhat smaller.

2.7 Bernoulli equation

When dimensioning pipe systems etc. different versions of the Bernoulli equation are often used. The most basic one is shown below [Ref. 2.7]:

$$\frac{V_2^2 - V_1^2}{2} + g \cdot \left[x_2 - x_1 \right] + \frac{p_2 - p_1}{\rho} = 0 \qquad \textbf{[Eq. 2.23]}$$

Where:
V Velocities [m/s]
g Gravity constant [m/s^2]
x Height [m]
p Pressure [Pa]
ρ Density [kg/m^3]

This equation yields a relation between the conditions (pressure, velocity and height) at two points in the fluid system. Even though the equation is used in many connections, quite strict conditions exist for the exact validity of it. They are:

1. Steady flow
2. No friction

3. Incompressible flow
4. Gravity is the only body force
5. Flow along a stream line

When looking at gating systems is condition 1 rarely 100 % fulfilled. On the other hand, when the gating system is completely filled in bottom filling gating systems, are the changes in flow due to growing back pressure relatively slow and steady flow can be assumed. In top filling systems a steady state will exist during the filling of the casting. Condition 2 is not fulfilled in any case. Sand moulds have rough surfaces that results in friction; directional changes in the flow will also mean losses. The losses will be discussed later in this section. With the pressures seen in gating systems, incompressibility is fulfilled. Unless centrifugal castings or electromagnetic pumps are in the picture, gravity is the only body force and condition 4 is fulfilled. Flow along a stream line means the calculations are valid for flow connecting the two points in question which follow a line where the flow direction at any point is tangent to the line.

When working with metal flow in green sand moulds, the flow is incompressible. When assuming completely filled runners, the continuity equation can be used with the cross sectional areas of the runners. The continuity equation is given by:

$$A_1 \cdot V_1 = A_2 \cdot V_2$$

$$V_1 = V_2 \cdot \frac{A_2}{A_1}$$

[Eq. 2.24]

Inserting this into the Bernoulli equation and rearranging it yields:

$$\frac{V_2^2 - V_2^2 \cdot \frac{A_2^2}{A_1^2}}{2} + g \cdot \left[x_2 - x_1 \right] + \frac{p_2 - p_1}{\rho} = 0$$

$$\frac{V_2^2 \cdot \left(1 - \frac{A_2^2}{A_1^2} \right)}{2} = g \cdot \left[x_1 - x_2 \right] + \frac{p_1 - p_2}{\rho}$$

[Eq. 2.25]

$$V_2^2 = \frac{2 \cdot g \cdot \left[x_1 - x_2 \right] + \frac{2 \cdot (p_1 - p_2)}{\rho}}{1 - \frac{A_2^2}{A_1^2}}$$

Eq. 2.25 can be used to calculate the melt front velocity V_2 if the pressures, the heights and the cross sectional areas are known at position 1 and 2. This can be a little difficult but for castings with simple geometries the areas are easily found and the pressure can also be found if

well known pouring conditions exists. In this way the velocity as a function of the height can be calculated.

Using the Bernoulli equation gives the same velocity as using Eq. 2.2 with $x_1 - x_2$ as the pressure height. Rearranging Eq. 2.23 makes it possible to add terms of pressure losses in the flow:

$$\frac{\rho \cdot \left(V_2^2 - V_1^2\right)}{2} + \rho \cdot g \cdot \left[x_2 - x_1\right] = p_1 - p_2 \qquad \textbf{[Eq. 2.26]}$$

When adding loss terms to the Bernoulli equation, it is called the energy equation in stead of the Bernoulli equation. I.e.:

$$\frac{\rho \cdot \left(V_2^2 - V_1^2\right)}{2} + \rho \cdot g \cdot \left[x_2 - x_1\right] = p_1 - p_2 - \Delta p_{Loss} \qquad \textbf{[Eq. 2.27]}$$

Adding the loss term to Eq. 2.25 where the continuity equation has been applied yields:

$$V_2^2 = \frac{2 \cdot g \cdot \left[x_1 - x_2\right] + \frac{2 \cdot \left(p_1 - p_2 - \Delta p_{Loss}\right)}{\rho}}{1 - \frac{A_2^2}{A_1^2}} \qquad \textbf{[Eq. 2.28]}$$

When using Eq. 2.27 and Eq. 2.28, it is convenient to have position 1 to be at the melt level in the pouring cup and position 2 to be just beneath the melt front in the mould cavity. The pressure at position 1 is the ambient pressure. Assuming no velocity is transferred from the pouring stream to the gating system, the velocity at position 1 is zero. This is reasonable to assume if the pouring cup is not too small and a constant melt level is maintained in the pouring cup and if it is not possible for the pouring stream to enter directly into the gating system and hence transfer momentum from the pouring stream into the gating system. The pressure at position 2 is the ambient pressure plus the pressure in the mould cavity due to mould and core gasses, plus the back pressure generated by the surface tension. Assuming sufficient venting, back pressure due to mould and core gasses can be ignored. In section 2.6 the back pressure due to surface tension has been found to:

$$\Delta P_{Surface\ tension} = P_i - P_e = \sigma \cdot \left(\frac{1}{r_1} + \frac{1}{r_2}\right) \qquad \textbf{[Eq. 2.29]}$$

The total loss in a gating system is made up of contributions from directional changes, friction, resistance to flow at entrances into sections, etc. Hence it is depending on the geometry of the actual gating system in question. To illustrate the contributions to the total pressure loss in a gating system, the layout showed on Figure 2.7 will be used.

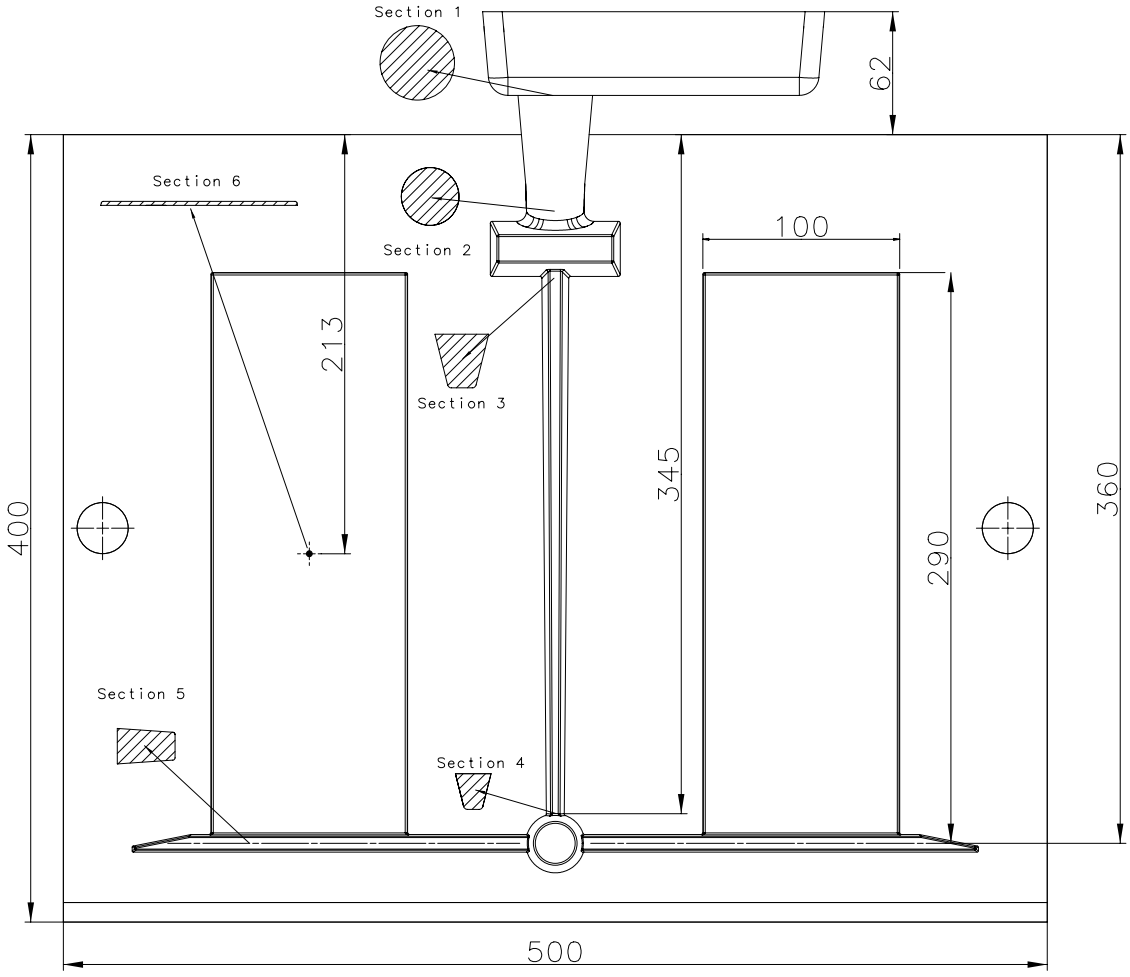

Figure 2.7 Layout for calculating pressure losses.

A pouring basin is used for securing consistent boundary conditions. The expressions available for calculating the different contributions to the total loss are empirical expressions containing constants found through trials. Due to the 3 dimensional nature of flow it is only in special cases for laminar flow possible to derive analytical expressions for the losses. For turbulent flow one has to rely on empirical expression [Ref. 2.7]. These expressions are hence not exact expressions for the losses, but they can give good estimates. Furthermore does some of the expressions demand fully developed stationary flow in circular sections to be valid. As those expressions are the only available they will be used as approximations.

The losses identified in the gating system on Figure 2.7 are discussed below:

1. **Outlet of the pouring basin.**

The flow through the outlet of the basin into the circular section beneath it, results in a loss given by the empirical found relation [Ref. 2.7]:

$$\Delta P_{Outlet} = C_{Outlet} \cdot \frac{\rho \cdot V^2}{2} \qquad \textbf{[Eq. 2.30]}$$

C_{Outlet} is a constant found through trials. V is the mean velocity in the circular section beneath the basin.

2. Friction in the circular section below the basin

Friction against the walls of the gating system will result in a pressure drop. The pressure drop due to friction for turbulent flow in channels with rough surfaces can be expressed as [Ref. 2.1]:

$$\Delta P_{Friction} = \lambda \cdot \frac{l}{D_h} \cdot \frac{\rho \cdot V^2}{2} \qquad \textbf{[Eq. 2.31]}$$

Where l is the length the friction takes place over, D_h is the hydraulic diameter. λ is a friction coefficient depending on Reynolds number. [Ref. 2.1] gives the following expression for λ:

$$\frac{1}{\sqrt{\lambda}} = -0.87 \cdot \ln\left(\frac{2.51}{Re \cdot \sqrt{\lambda}} + \frac{0.27 \cdot K_s}{D_h} \right) \qquad \textbf{[Eq. 2.32]}$$

λ has to be found iteratively. K_s is the surface roughness. The equation is strictly seen only valid for fully developed stationary flow. But it will be used as an approximation here.

3. Reduction of the cross section of the circular runner below the basin

The reduction of the cross section area of the circular section is also introducing a loss into the system, although probably relatively small. It is given by [Ref. 2.7]

$$\Delta P_{Reduction} = C_{Reduction} \cdot \frac{\rho \cdot V^2}{2} \qquad \textbf{[Eq. 2.33]}$$

V is the velocity at the outlet of the reduction i.e. at section 2. $C_{Reduction}$ is a constant depending on the area ratio between inlet and outlet, and the length the reduction takes place over.

4. Transition from circular section to rectangular at the top of the down runner

The geometry makes it difficult to find an expression for the loss through this section. Due to the area ratio between the rectangular down runner and the section above it, the loss will be handled as flow through the inlet to a section, i.e. in the same way as under point 1.

5. Friction in the down runner

The losses due to friction in the down runner can be estimated by Eq. 2.31 and Eq. 2.32.

6. Reduction of the cross section of the down runner

The losses due to reduction of the area of the down runner can be estimated by Eq. 2.33.

7. Directional change at the down runner well

Directional changes in the flow result in pressure drops [Ref. 2.1] gives the following expression for the pressure drop in connection with a directional change:

$$\Delta P_{\text{Directinoal change}} = C_{\text{Directinoal change}} \cdot \frac{\rho \cdot V^2}{2} \qquad \textbf{[Eq. 2.34]}$$

Where $C_{\text{Directional change}}$ is a constant determined empirical. This has been done in [Ref. 2.13] for different types of runner cross sections in connection with different designs of the directional change.

8. Friction in the horizontal runner

The losses due to friction in the horizontal runner can be determined by Eq. 2.31 and Eq. 2.32.

9. The directional change from the horizontal runner into the plates

This is a combination of a directional change and entrance to a new section. As an approximation it will be handled as flow through an entrance to a new section, i.e. as under point 1.

10. Friction in the plates

The friction losses in the plates are by nature the same as under the points 2, 5 and 6. From trials the flow velocity is known to result in a Reynolds number lower than 2300, i.e. the flow is expected to be laminar. Turbulent flow is expected in the horizontal runner, i.e. the starting condition for the flow in the plates is turbulent, meaning it is hard to say precisely whether the turbulence will die out or continue in the plates. Losses in laminar flows are smaller than in turbulent flows due to changed velocity profiles at the walls [Ref. 2.7] and the dissipation of energy in turbulent flows, and of course also due to the generally lower velocities in laminar flows compared to turbulent flows. The pressure loss in a laminar fully developed flow in a circular section is given by [Ref. 2.1]:

$$\Delta P_{\text{Friction}} = \frac{64}{\text{Re}} \cdot \frac{L}{D} \cdot \frac{\rho \cdot V^2}{2} \qquad \textbf{[Eq. 2.35]}$$

The equation will be used as an approximation. The hydraulic diameter of the plates will be used instead of D.

The losses described here are specific for the gating system seen on Figure 2.7. However most of them will be found in other gating systems. Using the approach with the Energy equation makes it necessary to identify the single contributions to the total loss for the gating system in question.

Using the Energy equation to dimension a gating system is normally seen as a more scientific way to do it compared to using Eq. 2.7 where a more or less well known loss coefficient has to be used. But when it comes to calculating the losses needed for using the Energy equation, one has to use empiric equations with constants found experimentally. I.e. basically both methods build on empiric knowledge.

The advantage of the Energy approach is the possibility of estimating the size of the contributions to the total loss coming from the different parts of the gating system. And hence it is possible to use this knowledge to control the flow better.

The loss coefficients found in the literature for use in Eq. 2.7 are normally independent of velocity. This is for instance the case for the loss coefficients found in [Ref. 2.3] and [Ref. 2.4]. When using the Energy equation with the loss terms given above is the influence from velocity incorporated. Even though the loss coefficients found in the literature for use in Eq. 2.7 are independent of velocity, are they giving good results, this is because they are found for typical velocities seen in gating systems.

The velocity is in the expressions for the different losses needed for the energy equation. It is also in the friction coefficient given by Eq. 2.32. The velocity is an important factor when deciding if the flow is turbulent or laminar and hence which expression should be used for the friction losses. In total this complexity makes it impossible to rearrange Eq. 2.28 and isolate the velocity when the different contributions to the losses have been incorporated. Hence the solution has to be found iteratively. I.e. one has to estimate a flow rate. Then the losses generated from the corresponding flow velocities in the different sections have to be calculated and finally inserted into Eq. 2.28 to check whether the losses and the velocity together give a solution for Eq. 2.28. If this is not the case a new estimate for the flow rate has to be found, of course on the basis of the results from the first estimate and a new calculation has to be made. This has to be repeated until a reasonable accurate solution to Eq. 2.28 has been found. I.e. it is a quite time consuming task to solve the Energy equation, the help of computer are needed.

The results from the equations available for describing the single loss terms are encumbered with some degree of uncertainty due to the empirical nature of the equations and the conditions the equations are found under, i.e. as for instance fully developed flow in circular channels. Expressions for losses connected to flow through different geometries can be found many places in the literature; see for instance [Ref. 2.1] and [Ref. 2.7]. A very comprehensive work and one of the main references within flow science is [Ref. 2.9]. It gives a large number of empirical found constants for equations describing losses in different sections. As mentioned above, the exact use of these equations often require conditions such as fully developed stationary flow in circular channels to be fulfilled, which in practice never is the case for gating systems. The lack of experimental data directly aimed at calculating liquid metal flow in gating systems in green sand moulds together with the quite comprehensive calculations needed makes the use of Eq. 2.7 more feasible.

One also has to bear in mind that when dimensioning a gating system the main concern is not to get the flow rate exactly right in the first trial but to secure the desired quality of the casting. Of course there is a connection here. The main concern is first to get the needed quality and then to get the filling time right i.e. in practice to fit it into the available time in the machine cycle for pouring. Making small adjustments to the flow rate is relatively easy compared to removing quality problems introduced by the filling. Or said with other words the design is important, the dimensioning is easier to adjust.

Even though the use of the energy equation is quite cumbersome as discussed above the use of it will be illustrated on the following pages. This is interesting because it can show the relative sizes of the contributions to the total loss coming from the different parts of the gating system.

The loss terms will be found when the melt fronts have reached the middle of the plates. For the layout as shown on Figure 2.7 for casting 2 mm plates the dimensions of the cross sections are given in Table 2.4. The melt flow rate is from experiments described in section 4 known to be 110 cm^3/s at this stage of the filling sequence. The velocities and the Reynolds numbers are also listed in Table 2.4.

Section	Dimension	Area	D_h	Velocity	Re
	mm	mm^2	mm	m/s	
1	Ø37.9	1128	37.9	0.096	6499
2	Ø29.3	674	29.3	0.163	8409
3	13.8/13.8/6.9	143	11.6	0.770	15713
4	8.8/8.8/4.4	58	7.4	1.893	24636
5	9/14.7/7 (*2)	118 (*2)	10.3	0.468	8471
6	2/100	200 (*2)	4	0.275	1934

Table 2.4 Dimensions of the gating system shown on Figure 2.7 and velocities when the melt front has reached the middle of the plates found experimentally.

The different contributions to pressure losses in the system can now be calculated. The example is calculated for ductile iron at 1350 °C with $\rho = 6260$ kg/m^3, $\mu = 3.56$ mPa·s [Ref. 2.19] and $\sigma = 1.721$ N/m [Ref. 2.14].

The contribution from surface tension is not depending on velocity. With a planar melt front in the plates, only the curvature in the thickness direction of the plates is significant. I.e. $r_1 = 1$ mm and r_2 is much larger than r_1 giving:

$$\Delta P_{\text{Surface tension}} = \frac{\sigma}{r}$$

$$\Delta P_{\text{Surface tension}} = \frac{1{,}721}{0{,}001} \qquad \textbf{[Eq. 2.36]}$$

$$\Delta P_{\text{Surface tension}} = 1721\text{Pa}$$

This value is not directly a pressure loss in the system but the pressure just beneath the melt surface in the plates, i.e.:

$$P_2 = \Delta P_{\text{Surface tension}} \qquad \textbf{[Eq. 2.37]}$$

1. Outlet of the pouring basin.

The constant in Eq. 2.30 can be taken as 0.5 for a sharp edge at the outlet [Ref. 2.7]. Table 2.4 gives the velocity at Section 1 to 0.096 m/s. The pressure loss is calculated to:

$$\Delta P_1 = C_{\text{Outlet}} \cdot \frac{\rho \cdot V^2}{2}$$

$$\Delta P_1 = 0.5 \cdot \frac{6260 \cdot 0.096^2}{2} \qquad \textbf{[Eq. 2.38]}$$

$$\Delta P_1 = 14\,\text{Pa}$$

I.e. this contribution is insignificant.

2. Friction in the circular section below the basin

The size of the cross section is not constant; mean values for section 1 and 2 are hence used. I.e. V = 0.130 m/s D_h = 33.6 mm. K_s, the surface roughness used for the determination of the friction coefficient λ with Eq. 2.32 is set to 0.2 mm equal to the average grain size of the sand. For a mean Reynolds number of 7454 is λ found iteratively to 0.040 via Eq. 2.32. Eq. 2.31 gives the pressure loss:

$$\Delta P_2 = \lambda \cdot \frac{l}{D_h} \cdot \frac{\rho \cdot V^2}{2}$$

$$\Delta P_2 = 0.040 \cdot \frac{0.060}{0.0336} \cdot \frac{6260 \cdot 0.130^2}{2} \qquad \textbf{[Eq. 2.39]}$$

$$\Delta P_2 = 4\,\text{Pa}$$

I.e. this contribution is insignificant.

3. Reduction of the cross section of the circular runner below the basin

The constant in Eq. 2.33 is 0.05 [Ref. 2.7] resulting in a pressure loss of:

$$\Delta P_3 = C_{Reduction} \cdot \frac{\rho \cdot V^2}{2}$$

$$\Delta P_3 = 0.05 \cdot \frac{6260 \cdot 0.163^2}{2} \qquad \textbf{[Eq. 2.40]}$$

$$\Delta P_3 = 4\,Pa$$

I.e. this contribution is insignificant.

4. Transition from circular section to rectangular at the top of the down runner

With 0.5 [Ref. 2.7] as the constant gives Eq. 2.30 the loss:

$$\Delta P_4 = C_{Outlet} \cdot \frac{\rho \cdot V^2}{2}$$

$$\Delta P_4 = 0.5 \cdot \frac{6260 \cdot 0.770^2}{2} \qquad \textbf{[Eq. 2.41]}$$

$$\Delta P_4 = 928\,Pa$$

5. Friction in the down runner

The friction loss in the down runner will be calculated on the basis of mean values between top and bottom, i.e. Re_{mean} = 20175, $D_{h\ mean}$ = 9.5 mm and V_{mean} = 1.332 m/s K_s the surface roughness is again taken as 0.2 mm. Solving Eq. 2.32 iteratively for λ gives λ = 0.051. With a flow length of 0.272 m Eq. 2.31 yields the pressure drop in the down runner:

$$\Delta P_5 = \lambda \cdot \frac{l}{D_h} \cdot \frac{\rho \cdot V^2}{2}$$

$$\Delta P_5 = 0.051 \cdot \frac{0.272}{0.0095} \cdot \frac{6260 \cdot 1.332^2}{2} \qquad \textbf{[Eq. 2.42]}$$

$$\Delta P_5 = 8109\,Pa$$

6. Reduction of the cross section of the down runner

The constant in Eq. 2.33 is 0.05 [Ref. 2.7] resulting in a pressure loss of:

$$\Delta P_6 = C_{Reduction} \cdot \frac{\rho \cdot V^2}{2}$$

$$\Delta P_6 = 0.05 \cdot \frac{6260 \cdot 1.893^2}{2} \qquad \textbf{[Eq. 2.43]}$$

$$\Delta P_6 = 561 Pa$$

7. Directional change at the down runner well

The constant in Eq. 2.34 is in [Ref. 2.13] found to 1.8 for a block shaped and a disc shaped transition. This is independent of the runner geometry. In this case, two exits from the well exist and the area ratio between the horizontal runner and the down runner is quite large. With the lack of influence from the runner geometry on the loss coefficient, it is reasonable to assume the same friction factor here. With the big area ratio between inlet and outlet of the well, the well also becomes relative large when comparing to the cross section of the down runner, hence the significant velocity becomes the velocity at the outlet. This is used to calculate the pressure drop:

$$\Delta P_7 = C_{Directional\ change} \cdot \frac{\rho \cdot V^2}{2}$$

$$\Delta P_7 = 1.8 \cdot \frac{6260 \cdot 0.468^2}{2} \qquad \textbf{[Eq. 2.44]}$$

$$\Delta P_7 = 1234 Pa$$

It has to be mentioned that this value is connected with some uncertainty due to the geometry which combine flow through a T junction, area expansion and flow through a small reservoir.

8. Friction in the horizontal runner

With Re = 8471, D_h = 10.3 and K_s = 0.2 mm is the friction coefficient λ found to 0.052 iteratively via Eq. 2.32. The flow length is chosen to be to the middle of the plates. Eq. 2.31 yields:

$$\Delta P_8 = \lambda \cdot \frac{l}{D_h} \cdot \frac{\rho \cdot V^2}{2}$$

$$\Delta P_8 = 0{,}052 \cdot \frac{0{,}125}{0{,}0103} \cdot \frac{6260 \cdot 0{,}468^2}{2} \qquad \textbf{[Eq. 2.45]}$$

$$\Delta P_8 = 433 Pa$$

9. The directional change from the horizontal runner into the plates

The constant in Eq. 2.30 can be taken as 0.5 [Ref. 2.7]. Table 2.4 gives the velocity at Section 6 to 0.275 m/s. The pressure loss is calculated to:

$$\Delta P_9 = C_{\text{Directional change}} \cdot \frac{\rho \cdot V^2}{2}$$

$$\Delta P_9 = 0.5 \cdot \frac{6260 \cdot 0.275^2}{2} \qquad \textbf{[Eq. 2.46]}$$

$$\Delta P_9 = 118\,\text{Pa}$$

10. Friction in the plates

Assuming laminar flow in the plates the pressure loss can be estimated from Eq. 2.35:

$$\Delta P_{10} = \frac{64}{Re} \cdot \frac{L}{D} \cdot \frac{\rho \cdot V^2}{2}$$

$$\Delta P_{10} = \frac{64}{1934} \cdot \frac{0.140}{0.004} \cdot \frac{6260 \cdot 0.275^2}{2} \qquad \textbf{[Eq. 2.47]}$$

$$\Delta P_{10} = 274\,\text{Pa}$$

If the flow is assumed to be turbulent, Eq. 2.31 and Eq. 2.32 would have to be used, they result in a pressure loss of 679 Pa. I.e. at the same velocity turbulent flow results in higher losses than laminar flow.

With these contributions is the total pressure loss found to:

$$\Delta P_{\text{Loss Total}} = \Delta P_1 + \Delta P_2 + \Delta P_3 + \Delta P_4 + \Delta P_5 + \Delta P_6 + \Delta P_7 + \Delta P_8 + \Delta P_9 + \Delta P_{10}$$

$$\Delta P_{\text{Loss Total}} = 14 + 4 + 4 + 928 + 8109 + 561 + 1234 + 433 + 118 + 274$$

$$\Delta P_{\text{Loss Total}} = 11.7\,\text{kPa}$$

Some of the contributions to the total loss are insignificant and can hence be excluded form further iterations.

In our case the velocities are known, hence rearranging Eq. 2.28 makes it possible to calculate the total pressure loss:

$$V_2^2 = \frac{2 \cdot g \cdot \left[x_1 - x_2 \right] + \frac{2 \cdot \left(p_1 - p_2 - \Delta p_{Loss} \right)}{\rho}}{1 - \frac{A_2^2}{A_1^2}}$$

[Eq. 2.48]

$$\Delta p_{Loss} = \rho \cdot g \cdot \left[x_1 - x_2 \right] - \left(1 - \frac{A_2^2}{A_1^2} \right) \cdot \frac{\rho \cdot V_2^2}{2} + p_1 - p_2$$

With position 1 as the melt level in the pouring basin and position 2 as the melt front when it has reached the middle of the plates, the following conditions exist:

Position 1 - Basin		Position 2 - Plate	
x_1	: 0.062 m	x_2	: - 0.213 m
A_1	: $111.36 \cdot 10^{-4}$ m^2	A_2	: $200 \cdot 10^{-6}$ m^2
p_1	: 0 Pa	p_2	: 1721 Pa

Eq. 2.48 yields a total pressure loss of 14.9 kPa. The total loss in the system was calculated to 11.7 kPa, i.e. around 20 % from the actual loss in the system. With all the approximations done during the calculations of the total pressure loss a deviation of 20 % is acceptable. Unfortunately does the structure of Eq. 2.28 make the calculated velocity very sensitive to the calculated loss especially when the velocity is below 1 m/s. This means a deviation in the calculated losses of 20 % results in a substantially larger deviation in the calculated velocity.

The above showed calculations illustrate one iteration with the Energy equation. Several iterations are necessary in the normal case where the velocities are unknown. When compared to the use Eq. 2.7 the use of the Energy equation is very complicated and time consuming. Furthermore the use of the Energy equation is difficult due to lack of empirical data directly aimed at liquid metal flow in green sand moulds. But the very rough calculation of the pressure loss made here resulting in 20 % deviation from the real loss also shows the possibilities in the Energy equation.

With empirically found equations and loss constants, for the different contributions to the total loss, determined via trials with liquid metal flowing through sand moulds would it probably be possible to obtain very accurate results. The extra calculation work needed when using the Energy equation compared to the simple equation Eq. 2.7 will computers be able to do in no time.

2.8 Material data in general

In general the material data found in the literature vary somewhat. This is especially the case for the surface tension and the viscosity. Unfortunately often the references do not give the exact conditions under which the values have been found; i.e. exact temperature, chemical composition, melt treatment etc. One also has to bear in mind the practical difficulties with measuring high temperature data; due to this some variation in the results can be expected. If one needs to do precise calculations, material data for the specific alloy has to be established.

When discussing the precision of the physical data, especially surface tension and viscosity, one has to bear in mind that the melt velocity often also is part of the equations where the physical data are used. Even when the exact (mean) velocity at a cross section is known, a velocity distribution over the cross section with a relatively large difference between minimum and maximum velocity very often exist. This variation in velocity will mean a larger variation in the calculated parameters as for instance the Reynolds number and the Weber number than the seen variation in the physical data will result in.

An overview of the effects of temperature and the most common alloying elements on surface tension, viscosity and density will be given here.

2.8.1 Surface tension

Detailed information on the effect of different alloying elements can be found in [Ref. 2.15], [Ref. 2.16], [Ref. 2.17]. As mentioned above the values from the different sources differ some.

2.8.1.1 Temperature

From 1300 °C to 1400 °C the surface tension increases approximately 0.07 N/m. Above 1500 °C the surface tension starts to decrease [Ref. 2.15].

2.8.1.2 Sulphur

Sulphur is having a heavy impact on surface tension. Going from 0.04 % to 0.2 % sulphur can reduce the surface tension with 0.4 N/m. This is valid in the temperature range 1300 to 1400 °C [Ref. 2.15].

2.8.1.3 Phosphorous

Phosphorous decreases the surface tension by 0.03 N/m for each % added [Ref. 2.15].

2.8.1.4 Aluminium

The effect of aluminium on grey and ductile iron can be seen on Figure 2.8. Conversion between N/m and dynes/cm is done via 1000 dynes/cm = 1 N/m. In this case the connection between changes in surface tension due to aluminium content and the susceptibility to pinholes has been established. Aluminium is seen to reduce the surface tension between 0.05 and 0.2 % for ductile iron and between 0.008 and 0.30 % for grey iron. I.e. in this interval is the susceptibility for pinholes highest.

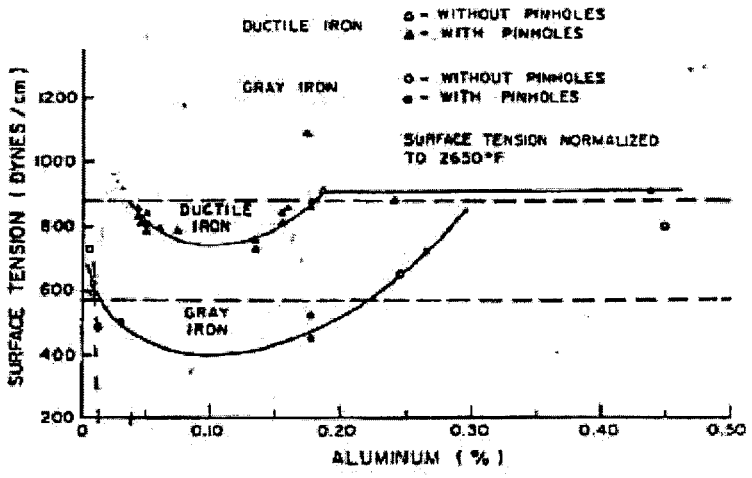

Figure 2.8 Surface tension as a function of aluminium content [Ref. 2.16].

2.8.1.5 Magnesium and Cerium

Both appear to increase the surface tension. But if their effects at constant levels of sulphur and oxygen are studied, they are seen to reduce the surface tension markedly. I.e. the effect seen in ductile iron is the effect of removing sulphur from the melt and not the direct influence of magnesium [Ref. 2.15].

2.8.1.6 Others

Carbon, Silicon and Manganese have only minor effects on the surface tension [Ref. 2.15]. The surface tension decreases with increasing carbon content in the hypoeutectic range. In the hypereutectic range increases the surface tension with increasing carbon content.

2.8.1.7 Estimating the surface tension

When pouring metal on a horizontal mould surface the thickness h of the metal pool is given by [Ref. 2.3]:

$$h = \sqrt{\frac{2 \cdot \sigma}{\rho \cdot g} \cdot \left(1 - \cos\theta\right)} \qquad \textbf{[Eq. 2.49]}$$

Where θ is the wetting angle showed on Figure 2.9. Non-wetting conditions mean θ = 180° and a droplet is balancing on the mould face. This leads to the maximum thickness of the metal pool. When the metal front moves over a horizontal mould surface, for instance when the horizontal parts of the gating system is filled; Eq. 2.49 can be used to check if completely filled runner cross sections can be expected right from the first melt passing through the system. This calculated height is the maximum thickness of the advancing melt front. When the melt front is moving over a horizontal surface, the inertia forces of the melt will try to flatten out the melt pool, while the surface tension forces and friction forces tries to keep it together.

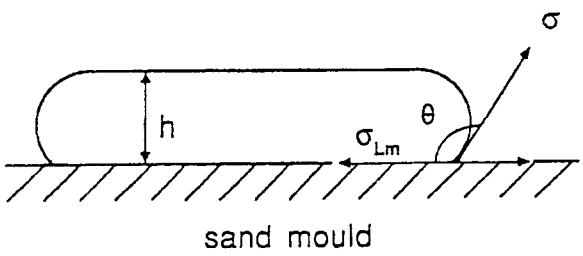

Figure 2.9 Wetting angle θ **[**Ref. 2.3**].**

Eq. 2.49 can also be used to find a rough estimate of the surface tension by measuring the height and wetting angle of a plate cast on top of a mould. One could argue that a value found this way is more usable for foundry applications as the atmosphere is more like the one present in the mould cavity. When doing this test with grey iron, the height of the plate is found to be 8.8 mm. The height is very equal over the plate. The wetting angle is a little more difficult to measure. A picture of a section cut through the metal is showed on Figure 2.10. With a relatively precise value for the height of the metal, the surface tension can be plotted as a function of wetting angle, see Figure 2.11. To estimate the sensitivity of surface tension to the measured thickness, curves showing the surface tension for a thickness

Figure 2.10 Cross section of plate cast on top of the mould.

variation of ±0.2 mm have also been shown. The variation in the calculated surface tension due to the variation of ±0.2 mm in measured thickness is also plotted; the curve is labelled Max deviation. The angle is measured to be approximately 140° giving a surface tension of 1.38 N/m. In section 2.4 a value of 1.4 N/m has been calculated for at similar grey iron with the help of equations given in the literature.

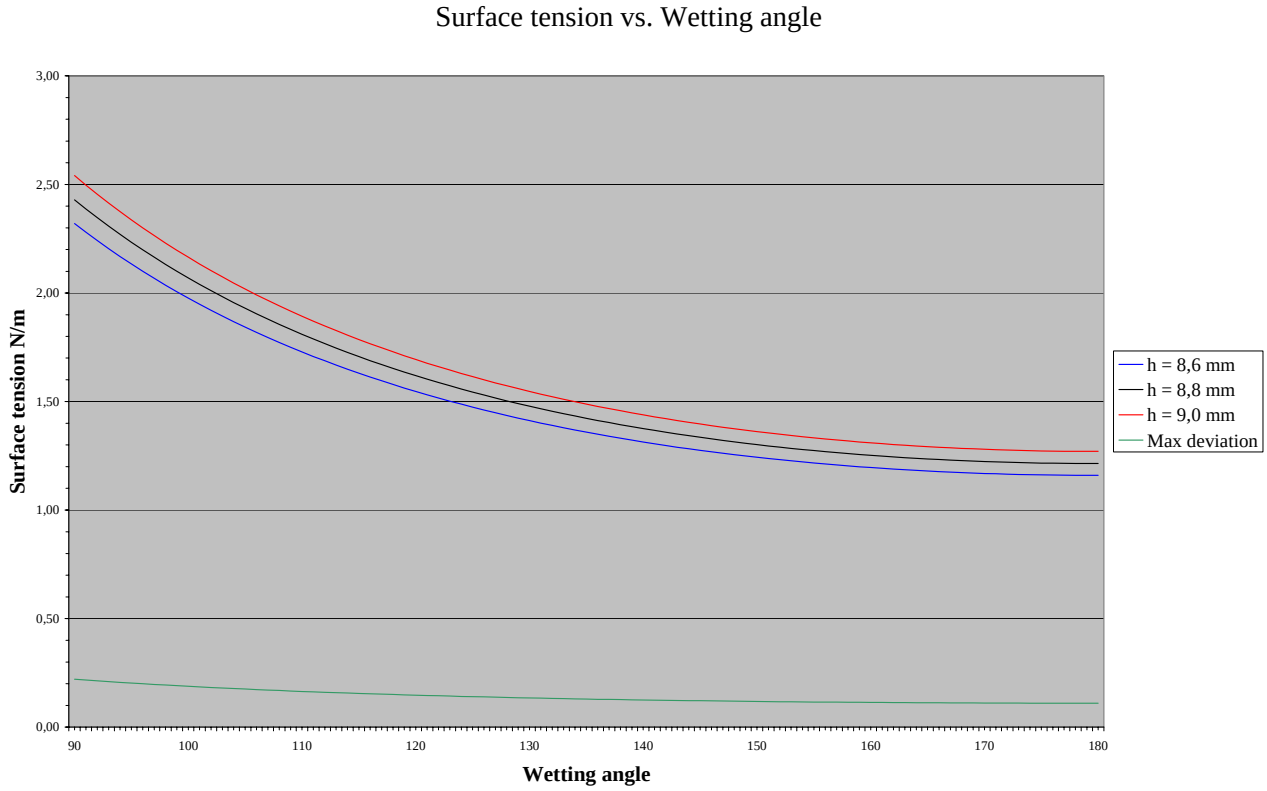

Figure 2.11 Surface tension as a function of wetting angle and metal height for grey iron.

The surface tension can also be calculated with the use of equations like [Ref. 2.14]:

$$\sigma = 1913 - 195 \cdot \ln(1+365 \cdot a_s) + 30 \cdot (wt\%C) \qquad \textbf{[Eq. 2.50]}$$

Unfortunately only a limited number of parameters are included in such equations, and not all parameters influencing the surface tension like temperature, the exact composition, melt treatment, atmosphere etc.

2.8.2 Viscosity

Detailed information on viscosity can be found in [Ref. 2.15], [Ref. 2.18], [Ref. 2.19], [Ref. 2.20]. The most common alloying elements and temperature have the following influence on viscosity:

2.8.2.1 Temperature

The viscosity is decreasing with temperature. The influence of temperature is not linear. The largest influence is seen just above the liquidus temperature after the metal has become liquid [Ref. 2.15].

2.8.2.2 Carbon

At constant temperature the viscosity as a function of carbon content will have a minimum at around 2 wt % C [Ref. 2.15]. On the other hand reports [Ref. 2.21] an increase in viscosity with increasing carbon content for a binary iron carbon alloy at 20 °C above the liquidus. This is illustrated on Figure 2.12. I.e. the sources do not agree on the effect of carbon on viscosity. This disagreement can be due to the alloys used for the investigations. In [Ref. 2.21] has a binary iron carbon alloy been used, in [Ref. 2.15] a foundry grade iron carbon alloy has probably been used. It is important to check whether material data are found for technical alloys or real foundry alloys with the alloying elements and impurities seen in foundry grades.

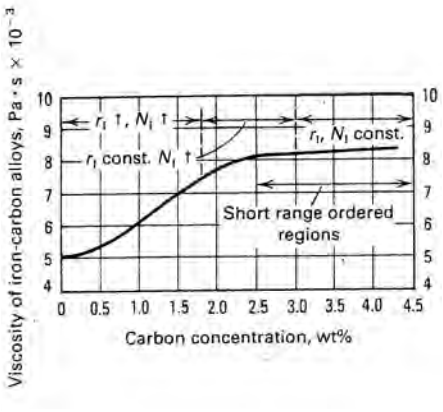

Figure 2.12 Viscosity as a function of carbon content [Ref. 2.21].

2.8.2.3 Silicon

Adding silicon decreases viscosity [Ref. 2.15].

2.8.2.4 Manganese

Adding manganese decreases viscosity. The effect depends on carbon content and is not linear [Ref. 2.15].

2.8.2.5 Phosphorous

Adding phosphorous will decrease viscosity [Ref. 2.15].

2.8.2.6 Sulphur

Adding sulphur will increase viscosity [Ref. 2.15].

2.8.2.7 General

Ductile iron is having a lower viscosity than grey iron [Ref. 2.19], [Ref. 2.20]. This is due to the lower sulphur levels in ductile iron than in grey iron. Different equations for calculating the viscosity can be found as for instance [Ref. 2.14]:

$$\log_{10} \mu = -0{,}721 + \frac{2747}{T} \qquad \textbf{[Eq. 2.51]}$$

Where:

μ Dynamic viscosity [mPa·s]
T Temperature [K]

Again only a limited number of parameters are taken into account. In this case only the temperature is in the equation.

2.8.3 Density

The density is also in a large part of the equations used to describe flow phenomena. The relative variation in density is generally smaller than what is seen for surface tension and viscosity

2.8.3.1 Temperature

Raising the temperature lowers the density by 0.5 kg/m^3/°C [Ref. 2.14]

2.8.3.2 Carbon

Raising the carbon content will lower the density [Ref. 2.15].

2.8.3.3 Silicon

Raising the silicon content will lower the density with 130 kg/m^3 pr. wt % silicon added [Ref. 2.15].

2.8.3.4 General

Equations for calculating the density can be found such as [Ref. 2.14]:

Error! Objects cannot be created from editing field codes. **[Eq. 2.52]**

Where:

T	Temperature [°C]
% Si	wt % Si

This is valid for 3.7 wt % C. As with the other parameters, specific data for the actual alloy has to be found if exact calculations are going to be made.

2.8.4 Summing up on material data

Values reported for the material properties vary some; also their dependence on composition, temperature etc. is not clear in all cases. Often the exact conditions under which the values are found are not reported. The equations established to describe the properties only include a limited number of variables, limiting their applicability.

One also has to bear in mind the differences between technical alloys seen in laboratories and the ones used in practise in the foundries. Hence if precise material data is needed, the establishment of them has to be done on the specific alloy and not a technical composition, and it has to be done under the same conditions as they are to be used under.

2.9 Influence of the material properties on filling behaviour

Although the material data can be difficult to measure and they are dependent on the actual circumstances they are found under, they have a heavy impact on the flow properties. This will be illustrated with an example from [Ref. 2.22]. In this work a V pulley with three spokes was cast with top filling using two different iron compositions, one with low sulphur content and one with 0.3 % sulphur. The filling sequences were recorded with a high-speed camera through Pyrex glass plates. The layout can be seen on Figure 2.13. The diameter of the pulley is 180 mm.

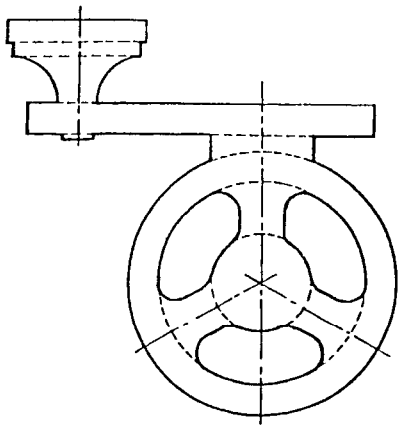

Figure 2.13 Lay out for pulley [Ref. 2.22].

Snap shots grabbed from the original movies showing the initial filling of the gating system can be seen below:

Figure 2.14 Filling of the horizontal runner. Alloy with 0.3 % sulphur [Ref. 2.22]. Melt entering into the plate shaped ingate before the horizontal runner is filled is marked on the picture to the right.

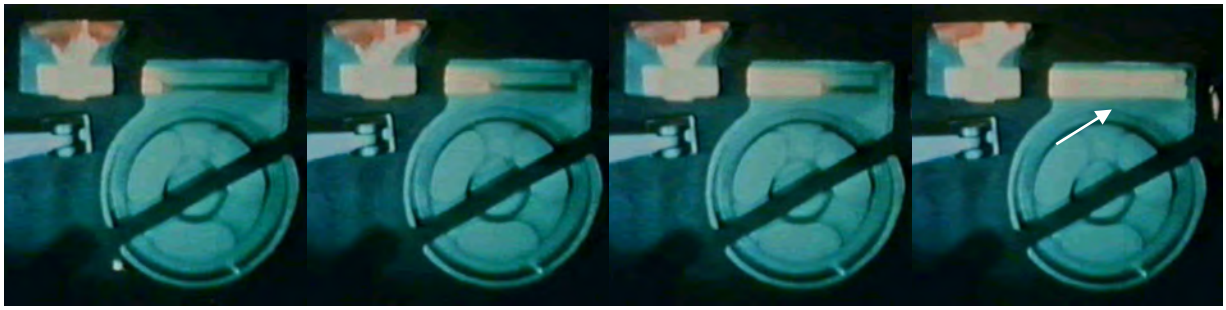

Figure 2.15 Filling of the horizontal runner. Alloy with low sulphur level [Ref. 2.22]. The melt not entering the plate shaped ingate before the horizontal runner is completely full is marked on the picture to the right.

The differences in colour are due to different settings on the camera, the pouring temperature was in both cases 1350 °C. The thickness of the plate shaped ingate is 1.8 mm

When the sulphur level is low, the surface tension is able to prevent the melt from entering into the plate shaped ingate to the pulley while the horizontal runner fills up. The cross section of the horizontal runner looks to be almost completely filled behind the melt front.

In the case with 0.3 % sulphur the melt enters into the plate shaped ingate long before the horizontal runner is filled. The cross section of the horizontal runner is far from completely filled behind the melt front.

This corresponds well with the higher sulphur level giving lower surface tension. From Table 2.3 the back pressure from surface tension from a 1.8 mm thick plate shaped geometry is seen to be equal to approximately 32 mm for a ductile iron, i.e. a low sulphur composition. This is a little more than the height of the horizontal runner in the pulley trials.

This big difference in the way the initial filling takes place is reflected in the rest of the filling sequence by a more splashing flow for the high sulphur alloy. This can be seen below:

Figure 2.16 Initial filling of the pulley. Alloy with 0.3 % sulphur [Ref. 2.22].

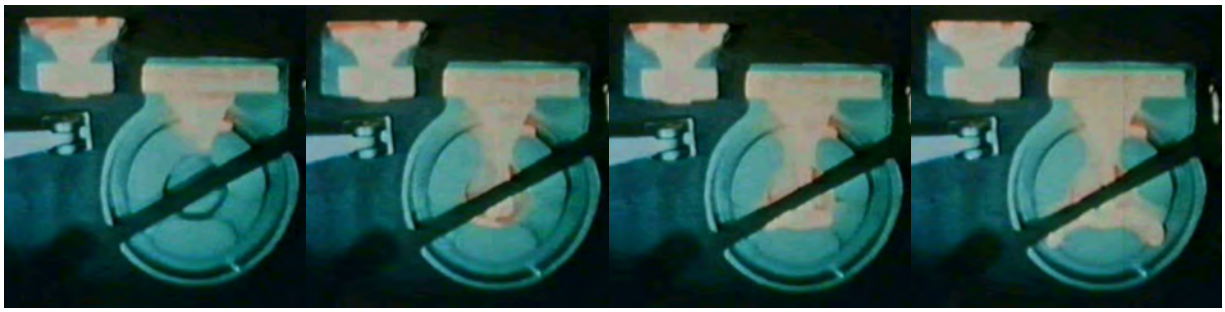

Figure 2.17 Initial filling of the pulley. Alloy with low sulphur level [Ref. 2.22].

The melt fronts are kept more together at the low sulphur alloy; the melt fronts are also having bigger curvatures.

2.9.1 Water analogy models

To get a better understanding of what is going on inside the mould during filling, many experiments with water models have been carried out. Some examples can be seen in [Ref. 2.23] for simulating iron melt flows in green sand moulds. A lot of interesting information can be extracted from such trials. But with the example shown in section 2.9, the difficulties of such work are also highlighted. A relatively small change in the melt composition, in this case the sulphur level, changes the behaviour of the melt radically. Changes like this are very difficult to incorporate into water models. In this case the ratio between surface tension and density has to be kept the same in the water model as in the real casting to be simulated.

The trials with the V pulley described in the previous section have also been carried out with water. The results can be found in [Ref. 2.22]. Unfortunately it is not possible to grab usable pictures from the original material due to very low contrast between the coloured water used and the mould. In line with the conclusions in the original work, it can be said that the iron with low sulphur level is giving the most coherent melt fronts, then comes the iron with high sulphur levels, and finally the water is giving the highest degree of splitting up of the liquid fronts. I.e. a rather big span of flow behaviours is seen going from water to iron with low sulphur. Apart from problems with getting similarity between the water model and the real pouring process, another aspect has to be remembered as reported in [Ref. 2.24]. This is varying material parameters with changing temperature. When casting thin walled parts, the flowing metal will undergo relatively large changes in temperature during filling, hence the problem with temperature depending data is relatively more important when casting thin walled parts, than when casting chunky parts.

2.10 Different categories of vertical gating systems

Different ways of classifying gating systems for vertically parted moulds can be used. Here the terminology from [Ref. 2.25] is used. Distinguishing between pressurized, depressurized, non-pressurized and mixed system will be used here. The difference is in the position of the flow restricting area i.e. the area determining the filling time. This can be seen on Figure 2.18, showing how 12 circular castings can be made with the different types of gating systems. All examples are using bottom or side gated systems. In principle combinations where the ingates were positioned at the top of the castings could also have been used. The trend is though today to go to bottom or in some cases side filling systems to secure the quality of the casting; hence this is what is used here.

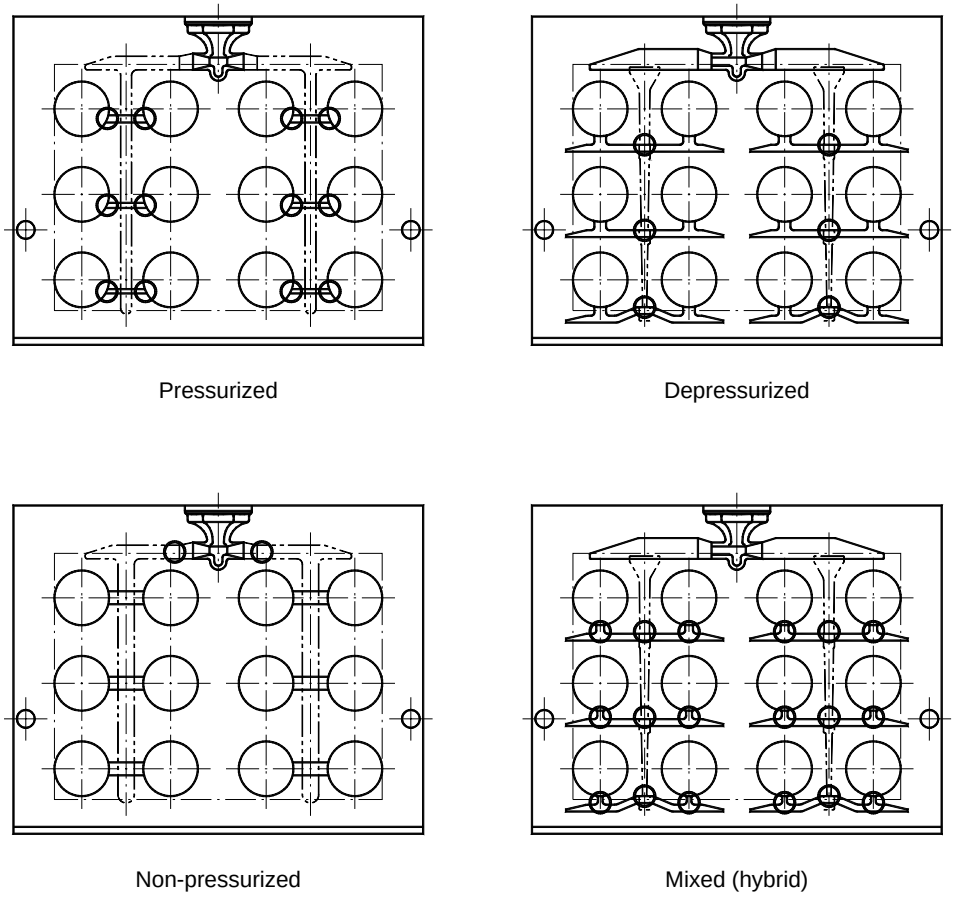

Figure 2.18 4 different types of gating system. Flow restricting areas are marked with circles [Ref. 2.25].

The pressurized gating system has the flow restricting area at the ingate to the casting, marked with circles on the figure. On the way through the gating system, the metal going into each cavity will have the highest velocity when it passes through the ingate. At least at the beginning of the filling where no back pressure exists, this system gives a fountain like filling of the part, which can cause many sorts of casting defects. The pressurized gating system is the smallest of the 4 types, giving the highest yield. This is because no part of the system has to be opened up to depressurize it; only the size needed for getting the wanted amount of iron through is used.

The depressurized gating system has the flow restricting area somewhere between the ingate to the casting and the pouring cup. Normally the restricting area is placed at the bottom of the down runner, or when castings are placed at several levels in the mould, at the connection to the common down runner. Variations of the depressurized gating system are the most used in vertically parted moulds, when quality demands exist for the casting. With this type of system it is possible to obtain a relatively low velocity in the ingates to the casting. The depressurized system gives a medium yield.

The non-pressurized gating system has the flow restricting area close to the pouring cup. The non-pressurized gating system is the biggest of the 3 types giving the lowest yield. The non-pressurized system can give metal flow with low velocities in the inlets to the casting cavity.

In a non-pressurized system the runners are not completely filled during the filling sequence. This is the case for the other systems. Working with partly filled runners can lead to different kinds of defects.

The mixed system is a mixture of at least two of the above mentioned systems. The one illustrated is a depressurized system with pressurized ingates. The idea with a mixed system is to make a compromise between two or more systems and hence getting parts of the benefits from the systems used, such as getting relative good yield and relative low velocities. The mixed system gives a yield in the middle range depending on the actual design.

The flow restricting area can in all systems be calculated with Eq. 2.7. The depressurized areas are calculated from different rules of thumbs defining how much the areas should be opened up relative to the restricting area. Detailed information about this for the different systems can be found in [Ref. 2.25]. For the opening of areas, more rough rules of thumb based on area ratios are given many places in the literature. For instance [Ref. 2.21] recommend a slightly pressurized system for ductile iron designed on the basis of the ratio 4:8:3 for the down runner – runner – ingate areas. Gating systems designed with such rules seems to be rather heavy, and less sophisticated with respect to the design. On the other hand one has to bear in mind, that such rules in most cases are developed in connection with horizontal flask lines, giving lower ferrostatic highs and hence lower velocities to be handled.

2.11 Transition from down runner to horizontal runner

The Weber calculations can be used to describe the tendency of the melt front to split up. But it can only be used for describing flow in continuous cross sections. When an abrupt directional change in the melt flow takes place, the Weber number cannot be calculated due to large local variations in the size of the melt velocity and the direction of it.

When using vertically parted moulds and producing parts with high quality demands, bottom filling gating systems are often used. This means that the melt has to be transferred to the bottom of the mould, a directional change has to be made to get the metal underneath the casting cavity, and often another directional change is made to get the metal into the casting cavity. The first directional change is the most difficult, because the highest velocities are normally found here. One could imagine some sort of zigzag shaped design of the down runner giving a high loss coefficient resulting in reduction of the velocity. Gating systems with zigzag shapes or similar designs for reducing the melt velocity take up extra space on the pattern plate and they lower the yield. Such or similar designs are only rarely used.

The directional change at the bottom of the down runner is prone to break up the melt surface and new oxides are formed. Droplets shooting into the continuation of the gating system in front of the main melt front are also often seen at the transition from the vertical down runner to the horizontal runner. In some cases these droplets will have time to partly solidify. When they are not completely remelted, the basis for a casting defect has been established.

Due to the relatively large mould heights in vertically parted moulds, the melt front velocity at the bottom of the vertical down runner is high. In section 2.2 the velocity of free falling metal is found to be given by:

$$v = \sqrt{2 \cdot g \cdot H} \qquad \textbf{[Eq. 2.53]}$$

A free fall of 51 mm results in a velocity of 1 m/s. A free fall of 350 mm results in a velocity of 2.6 m/s. The square root in Eq. 2.53 reduces the growth rate of the velocity after it has passed 1 m/s. The friction in the system is proportional to the square of the velocity i.e. the losses will grow relatively faster when 1 m/s is exceeded. Still even though the square root in Eq. 2.53 reduces the growth rate of the velocity and the losses follow the square of the velocity, high velocities are seen at the bottom of the down runner and they increase with larger mould heights.

This makes the transition between the down runner and the horizontal runner critical. The transition has to:

1. Hold the melt back until the down runner has been filled completely.
2. Catch the first melt, letting no melt droplets enter the horizontal runner before the main melt front. This should be done as gentle as possible generating as little splash as possible in the transition zone.
3. Secure a coherent melt front in the horizontal runner and a completely filled cross section of it.
4. Give room for the flow to find a natural flow path around the corner, when the runners are filled completely, not resulting in (to much) turbulence, sand erosion etc.
5. Often the flow restriction area is right above the transition, hence the melt enters the transition with a high velocity and have to leave it with a low velocity.

The transition from down runner to the horizontal runner can be designed in many different ways. A lot of work has been done on investigating how this is done in the most feasible way for horizontally parted moulds, see for instance [Ref. 2.6], [Ref. 2.12]. Not so much work has been done for vertically parted moulds. Different types of bends combined with different runner shapes applicable in vertically parted mould have been analyzed quite comprehensive in [Ref. 2.13]. Trials were made determining the loss coefficients for different combinations of runners and bends. The trials also show how well the runner after a 90 degree bend is filled. The different types of bends used can be seen on Figure 2.20. The cylinder shaped transition was only used in the theoretical part of the work. The different runner cross sections can be seen on Figure 2.19. The area of the different cross sections was in all cases 110 mm^2. The gating systems were designed to give an iron flow rate of 1 kg/s.

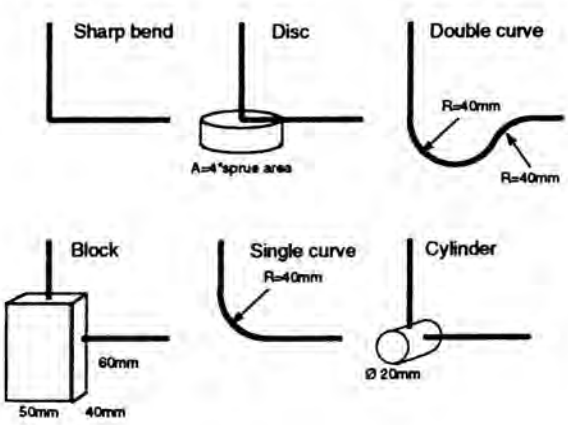

Figure 2.20 Different types of bends [Ref. 2.13].

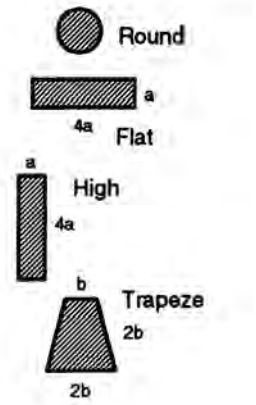

Figure 2.19 Different types of cross sections [Ref. 2.13].

The average flow rates as a function of geometry is showed on Figure 2.21 The flow in the flat runner is significantly lower on a 90 % level than in the other geometries. This indicates a higher loss coefficient for this runner type. This higher loss coefficient can be useful when velocity needs to be taken out of the melt.

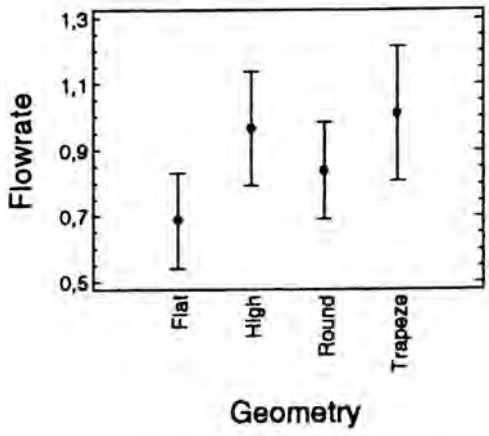

Figure 2.21 Flow rate as a function of runner geometry [Ref. 2.13].

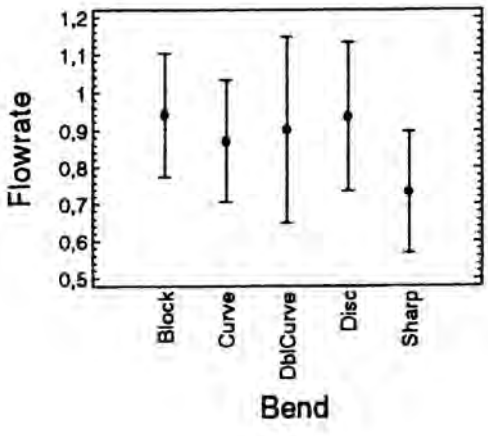

Figure 2.22 Flow rate as a function of bend design [Ref. 2.13].

The average flow rates as a function of the design of the bend can be seen on Figure 2.22. All though no significant difference in the flow rates on a 90 % level can be found, the flow rate in the sharp bend looks to be smaller than in the other. This also sounds reasonable as an artificial choke will be formed at the sharp bend, reducing the active cross sectional area the flow takes place in. This vena contracta is illustrated on Figure 2.23 together with the passing of the first melt trough the system.

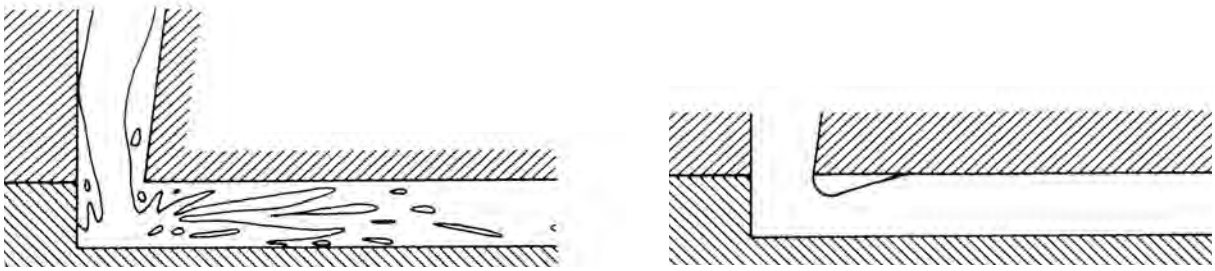

Figure 2.23 Flow in a sharp bend. Initial flow and stationary flow with a vena contracta [Ref. 2.6].

Figure 2.23 illustrate how the initial melt passes through a sharp bend resulting in a lot of splashes. The trial setups used in [Ref. 2.13] does not make it possible to give detailed information about how the different transitions handle the first melt passing through, i.e. whether splashes occur as seen on Figure 2.23 or whether the performance of directional transition is better. In the chapters of this report concerning trials, snapshots from videos of the real metal flow through bends of the block, single curve and cylinder type will be shown. Hence the functioning of the different transitions from vertical to horizontal runner will be discussed more closely in these chapters. Only the principal function of a well shall here be illustrated with Figure 2.24, showing no melt splashes going into the horizontal runner. Figure 2.24 illustrates how it can be done in horizontally parted mould; it can easily be converted into a transition usable in vertically parted moulds.

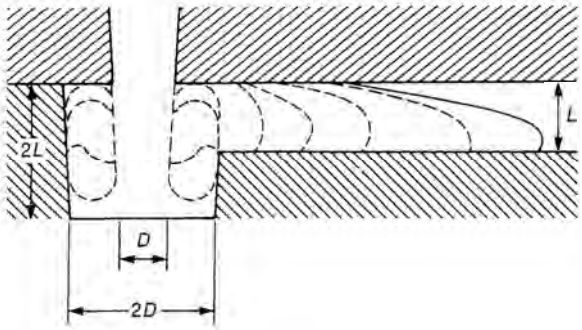

Figure 2.24 Basic idea behind a well as transition from vertical down runner to horizontal runner [Ref. 2.6].

Another important feature of the transition from vertical runner to horizontal runner is the ability to keep the horizontal runner filled. [Ref. 2.13] reports the block type and the disc type to give the best results. Only the high runner with the biggest dimension on the parting line was not possible to keep full with these two transitions.

2.12 Pouring time

When discussing the optimum pouring time, it is reasonable to distinguish between gating systems for conventional section thicknesses and gating systems for thinner section thicknesses; as the deciding parameters for calculating the optimum pouring time are different.

2.12.1 Conventional sections

Many different more or less empiric rules have been developed to estimate the optimal pouring time; some of them are listed in [Ref. 2.25], [Ref. 2.26] and [Ref. 2.30]. Most of them are based on the weight of the casting and the thinnest section. An example is [Ref. 2.25]:

$$t_{max} = B \cdot \sqrt{G} \qquad \textbf{[Eq. 2.54]}$$

The equation gives the maximum filling time in seconds of the casting cavity, i.e. filling time exclusive time for filling the gating system. G is the casting weight in kg and B is a constant given by:

Thinnest Wall thickness mm	Factor B
3-5	3 for $G \leq 1$ kg and 1.5 for $G \geq 4$ kg
5-10	4 for $G \leq 1$ kg and 2.0 for $G \geq 4$ kg
10-20	5 for $G \leq 1$ kg and 2.5 for $G \geq 4$ kg
>20	6 for $G \leq 1$ kg and 3.0 for $G \geq 4$ kg

Table 2.5 Factors for estimating the maximum filling time of a casting cavity.

Such rules have to be seen as rules of thumb. On the other hand many of them combined with experience are used with good success.

Another factor deciding the pouring time is the speed of the moulding machine. With the ever-growing demands for productivity, the upper limit for the pouring time is in many cases the time available in the machine cycle for pouring. The lower limit for the pouring time is the in practice maximum possible pouring rate in kg/s not reducing the quality of the casting by giving sand erosion, gas inclusion etc. When high capacity moulding machines and a wish to have as many castings in the mould as the size of the mould face allows; the upper and lower values mentioned above for the pouring time often overlap. In most cases the moulding machine is slowed down to prevent an excess scrap level.

2.12.2 Thin sections

When casting thin walled parts avoidance of cold shots puts special demands on the pouring time. Hence the maximum flow length becomes interesting, i.e. the length a given alloy under given circumstances can flow in a small section before cold run occurs. When talking about maximum flow lengths, a parameter called fluidity has to be introduced. In flow engineering fluidity is the reciprocal value of viscosity. But in the foundry language it refers to the length the metal can flow in a mould. This is normally tested with the spiral test. Different variations are used; one example can be seen on Figure 2.25. The idea is to fill a long channel with a rather small cross section, provoking a cold run after some part of the channel has been filled. To be able to compare the results, it is of course very important to have good control over the boundary conditions i.e. temperature, driving metal head etc. from test to test. The fluidity is simply measured as the length of the filled channel. Even though this test can seem a little old fashioned, it is very powerful and easy to conduct in practice. It is still in industrial use as can be seen in [Ref. 2.28].

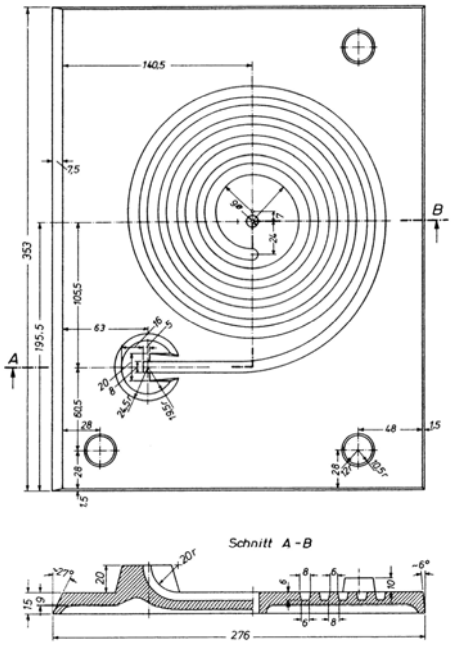

Figure 2.25 Drag part for spiral test, the cope part is flat [Ref. 2.27].

2.12.3 Fluidity

When a combination of flow and solidification takes place in a thin section the solidification morphology of the material controls how the melt front comes to a stop [Ref. 2.6], [Ref. 2.30]. One has to distinguish between pure metals, alloys solidifying over a temperature range and eutectics solidifying at a single temperature as pure metals.

2.12.3.1 Fluidity of pure metals

Flow and solidification of a pure metal in a thin section can be seen on Figure 2.26. The metal solidifies at a single temperature, i.e. solidification takes place from the walls of the channel with columnar grains. The solid-liquid interface is smooth. The single temperature solidification morphology makes it possible for flow to take place in the centre of the section as long as a free passage exists. At some point down stream, the solid fronts meet and the flow stops. The liquid in front of the choke solidifies creating a shrinkage pipe. Due to the smooth surfaces of the solid on the channel walls and the single solidification temperature, the flow continues until the channel is completely blocked; hence pure metals have a high fluidity.

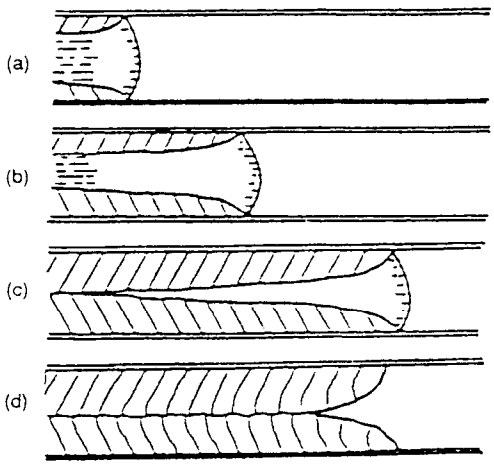

Figure 2.26 Solidification of a pure metal [Ref. 2.30].

2.12.3.2 Fluidity of alloys with a solidification interval

Flow and solidification in a thin section of a metal with a low addition of alloying element resulting in a solidification interval can be seen on Figure 2.27. Solidification again starts to take place from the channel walls. But with the small alloy additions, the smooth solid liquid interface is transformed in to a rough interface. Later fine grains starts to nucleate at the melt front. At some point the flow is choked and the remaining liquid solidifies equiaxed. The rough solid-liquid interface is giving a significant resistance to flow and hence also a significant decrease in fluidity. This significant change in fluidity is caused by very small additions of alloying elements, levels normally seen as impurities are in some cases enough. [Ref. 2.6] Shrinkage porosities are seen a little behind the melt front.

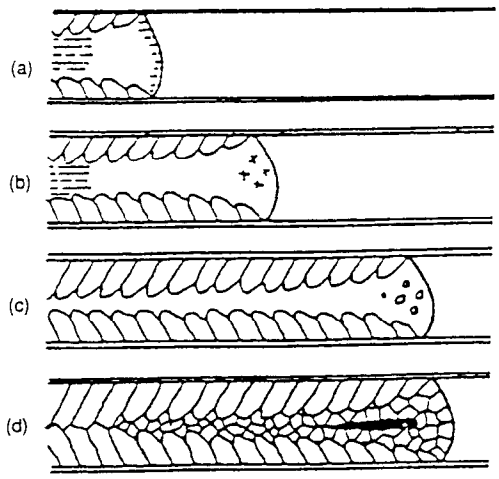

Figure 2.27 Solidification of a metal with low addition of alloying element giving a solidification range [Ref. 2.30].

At higher additions of alloying elements columnar grains still form at the channel walls, but the main mode of solidification changes to formation of equaixed grains in the flow. This is for instance the case for modified hypoeutectic aluminium alloys and well inoculated ductile irons. These grains will travel with the stream. The flowing metal is transformed into a mushy substance. When a critical concentration of the flowing grains is reached the flow stops. This happens at a significantly higher mean temperature than the solidus temperature. The fluidity of alloys with a solidification interval is therefore relatively low compared to the pure metals. The remaining melt solidifies with equiaxed grains. Shrinkage is distributed over the last melt to solidify.

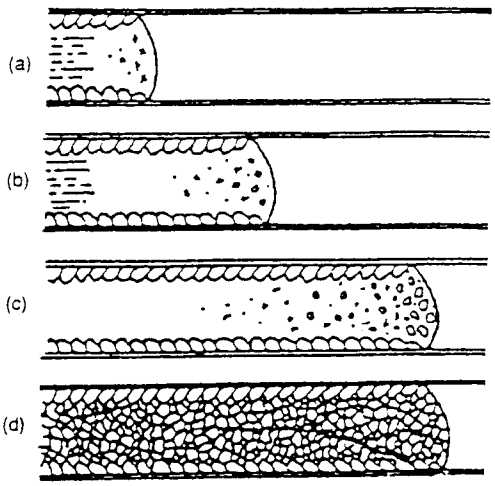

Figure 2.28 Solidification of a metal with a solidification interval [Ref. 2.30].

In this case small changes in the amounts of alloying elements or addition of other elements do not change the mode of solidification; hence such small changes in the composition have only little influence on the fluidity as long as the effective super heat is the same. This is in contrast to the big changes in fluidity taken place when going from a pure metal to a composition with low additions of alloying elements.

2.12.3.3 Fluidity of eutectic alloys

When working with eutectic alloys, solidification takes place at a single temperature. Hence in that sense it is similar to pure metals. This means that the fluidity of eutectic alloys is normally in the same size as the fluidity for the pure metals. I.e. the maximum fluidity for an alloy is often found at the eutectic composition. Exceptions to this rule however exist. For instance, in the Al-Si system the maximum fluidity is found at around 25 wt % Si, while the eutectic composition has 12.5 wt % Si [Ref. 2.30]. The reason for this exception is the large difference in the heat of fusion for silicon and aluminium. Silicon has around 4 time higher heat of fusion than aluminium; hence the hypereutectic compositions releases more heat during solidification and the alloy can flow longer before freezing. It has to be mentioned that the difference in fluidity from the eutectic composition to 25 wt % Si is relatively small when comparing for instance to the difference seen when going from 5 wt % Si to the eutectic composition.

As a general rule the popular casting alloys are alloys with good fluidity. For instance near eutectic grey irons in the iron carbon group, and not steel. Steel gives of course some other problems due to the high pouring temperature needed. In the aluminium group, eutectic or near eutectic Al-Si alloys and not Al-Cu are used. This is the case even though the Al-Cu alloys give good strength values after a heat treatment [Ref. 2.6].

2.12.3.4 Fluidity of the Iron Carbon system

Changes in fluidity due to changes in the chemical composition and hence the solidification morphology for the iron carbon system can be seen on Figure 2.29. Fluidity as a function of carbon content is plotted. The fluidity is seen to be high both for the pure iron and for the eutectic composition. In the middle range the fluidity is seen to be at a relatively low but approximately constant level. This is in good agreement with the above described connection between fluidity and position in the phase diagram.

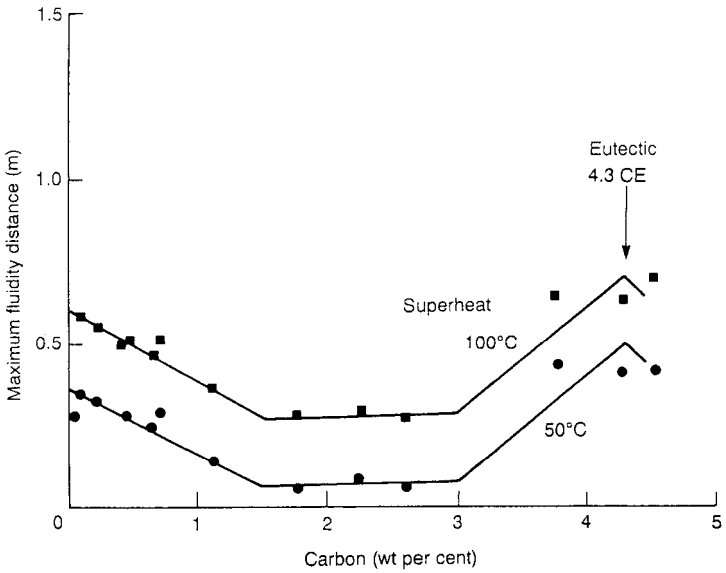

Figure 2.29 Fluidity versus carbon content and super heat [Ref. 2.6].

On Figure 2.29 the fluidity is plotted at two different levels of superheat. Raising the superheat from 50 to 100 °C is seen to give an almost constant increase in fluidity. This sounds reasonable, as the heat capacity is not changed much by the carbon level. The increase in fluidity due to 50 °C extra superheat is around half the increase gained in fluidity by going to a eutectic or near eutectic composition from an intermediate composition. Also notable is the change in fluidity at the low superheat; going from an intermediate composition to a near eutectic or eutectic composition gives around 5 times better fluidity for 50 °C superheat.

2.12.3.5 Fluidity of the Iron Phosphorus system

When talking about flow length and fluidity one has to mention the classical example of adding phosphorus to an iron melt. Doing so, it is possible to pour large thin very complicated castings with very fine details. From section 2.8.1.3 and 2.8.2.5 phosphorus is seen to decrease the surface tension a little and to decrease the viscosity. The main effect of adding phosphorus is though connected to its ability to reduce the freezing point of the alloy, i.e. the effective superheat is increased to a degree difficult to obtain otherwise.

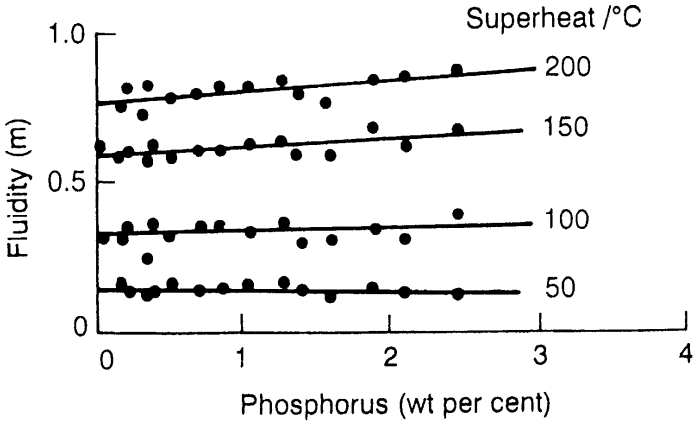

Figure 2.30 Fluidity as a function of phosphorus content and superheat. [Ref. 2.6].

This is clearly seen from Figure 2.30 where the fluidity lengths have been plotted as a function of the effective superheat taken the lowered freezing point into account and the phosphorus content.

2.12.3.6 Calculation of the fluidity

As discussed above the solidification morphology controls how the metal front is brought to a stand still when cold run occurs. From the connection between the fluidity and the chemical composition of the iron carbon system seen on Figure 2.29, it is also expected that no simple exact equation connecting chemical composition, temperature etc. and fluidity can be established. Approximate relations can although be established when dividing the task into two; one for metals solidifying at a fixed temperature i.e. pure metals and eutectics and one for alloys solidifying over a temperature range.

For pure metals and eutectic alloys both solidifying at a single temperature, the fluidity can be approximated to [Ref. 2.6]:

$$L_f = v \cdot t_f \qquad \textbf{[Eq. 2.55]}$$

v is the velocity of the metal and t_f is the freezing time for the cross section.

For alloys solidifying with a freezing range the flow is assumed to stop when 50 % has solidified, i.e. the approximated equation for the fluidity changes to [Ref. 2.6]:

$$L_f = \frac{v \cdot t_f}{2} \qquad \textbf{[Eq. 2.56]}$$

Note that t_f is the freezing time when the alloy is not superheated. If the metal is superheated as in almost all practical cases, the time for removing the superheat has to be added to t_f. In the case of alloys with a freezing range, the contribution to freezing time from superheat shall not be divided by 2.

For sand moulds, where the mould material is the restricting factor in the cooling of the casting, the freezing time t_f is approximated to [Ref. 2.6]

$$t_f = k \cdot m^2 \qquad \textbf{[Eq. 2.57]}$$

Where m is the modulus of the casting i.e. the volume divided by the cooling surface area, k is a constant. This equation is known as Chvorinov's rule.

For metal dies and other cases where the restricting factor in the heat flow is the heat transfer from the solidifying metal to the mould, the equation for the freezing time is:

$$t_f = \frac{k' \cdot m}{h} \qquad \textbf{[Eq. 2.58]}$$

Where k' is a different constant and h is the heat transfer coefficient between mould and metal. Focusing on eutectic and near eutectic compositions solidifying at single temperature, inserting Eq. 2.58 for the freezing time in Eq. 2.55 yields:

$$L_f = \frac{v \cdot k' \cdot m}{h} \qquad \textbf{[Eq. 2.59]}$$

According to the conditions for the use of Eq. 2.58 this should not be valid for sand castings as the sand has low heat conductivity. But experimental data referred in [Ref. 2.6] show a linear relation between casting module and fluidity for sand cast parts with section thicknesses in the range 1.4-4 mm. The reason for this could be the relative small amount of heat to be removed through the sand. With a small amount of heat to be removed, the thermal signal will only have to travel a relatively short distance in the mould before the casting is solidified compared to what is the case when heavier sections are cast. Hence thermal conductivity of the mould becomes less important and the heat transfer coefficient becomes more important when small amounts of heat have to be removed as is the case with parts with thin sections.

This means that the heat transfer coefficient is the controlling parameter. When this is the case and assuming that the metal is poured at the melting point T_m and that the heat input into the mould is so small, that the mould at the metal mould interface reasonable can be set to a constant temperature T_o, can the freezing time be expressed as [Ref. 2.6]:

$$t_f = \frac{\rho_s \cdot H}{h \cdot (T_m - T_0)} \cdot \frac{V}{A} \qquad \textbf{[Eq. 2.60]}$$

Where:

ρ_s Density of the solid [kg/m^3]
H Latent heat of solidification [J/kg]
h Heat transfer coefficient between mould and casting [W/m·K]
T_m Pouring temperature equal to melting temperature [°C]
T_0 Constant mould temperature [°C]
V Volume of the casting [m^3]
A Cooling area of the casting [m^2]

Inserting this into Eq. 2.55 gives an estimate of the possible flow length in thin walled sections where the heat transfer coefficient is the controlling factor:

$$L_f = v \cdot \frac{\rho_s \cdot H}{h \cdot (T_m - T_0)} \cdot \frac{V}{A} \qquad \textbf{[Eq. 2.61]}$$

For thin walled castings the module V/A is approximately half the thickness i.e. t/2, hence the fluidity or maximum flow length for thin sections can be written as:

$$L_f = v \cdot \frac{\rho_s \cdot H}{h \cdot (T_m - T_0)} \cdot \frac{t}{2} \qquad \textbf{[Eq. 2.62]}$$

This is for parts cast without any superheat. The equation can be adjusted to also take a superheat into account. The term H is the energy to be removed pr. mass casting. The energy from a superheating of the metal is given by ($T_{superheat}$ - T_m) · C_p. Keeping $T_m - T_0$ as the driving potential for the removal of the superheat, gives the following estimate for the flow length when the superheat is incorporated:

$$L_f = v \cdot \frac{\rho_s \cdot (H + (C_p \cdot (T_{Super\ heat} - T_m)))}{h \cdot (T_m - T_0)} \cdot \frac{t}{2} \qquad \textbf{[Eq. 2.63]}$$

For calculating the fluidity of alloys solidifying over a temperature range, H/2 can be used in stead of H according to Eq. 2.56. When substituting H with H/2 Eq. 2.63 is transformed to:

$$L_f = v \cdot \frac{\rho_s \cdot (H/2 + (C_p \cdot (T_{Super\ heat} - T_m)))}{h \cdot (T_m - T_0)} \cdot \frac{t}{2} \qquad \textbf{[Eq. 2.64]}$$

The equation is valid for alloys solidifying over a temperature interval.

When using ductile iron as an example and calculating the fluidity for a eutectic composition, the following values can be used: H = 220 KJ/kg [Ref. 2.14] and [Ref. 2.15], ρ_s = 7051 kg/m^3 [Ref. 2.14], T_m = 1134 °C, T_0 = 20 °C, h = 1000 W/m^2 ·K. With a section thickness of 3 mm one gets:

ΔT superheat	0	50	100	150	200	250
T superheat	1134	1184	1234	1284	1334	1384
Velocity m/s	Fluidity in m					
0.05	0.10	0.12	0.14	0.16	0.18	0.20
0.10	0.21	0.25	0.29	0.33	0.37	0.41
0.15	0.31	0.37	0.43	0.49	0.55	0.61
0.20	0.42	0.50	0.56	0.65	0.73	0.81
0.25	0.52	0.62	0.72	0.82	0.92	1.02
0.30	0.63	0.75	0.86	0.98	1.10	1.22
0.35	0.73	0.87	1.01	1.15	1.28	1.42
0.40	0.84	0.99	1.15	1.31	1.47	1.62
0.45	0.94	1.12	1.30	1.47	1.65	1.83
0.50	1.04	1.24	1.44	1.64	1.83	2.03
0.55	1.15	1.37	1.58	1.80	2.02	2.23
0.60	1.25	1.49	1.73	1.96	2.20	2.43

Table 2.6 Fluidity as a function of velocity and superheat.

The percentage of the total flow length coming from the contribution from the super heat can be seen below:

ΔT superheat	0	50	100	150	200	250
T superheat	1134	1184	1234	1284	1334	1384
% flow length from superheat	0	16	27	36	43	49

Table 2.7 Percent of total fluidity coming from superheat.

The percentage of the total fluidity coming from superheat is independent of the flow velocity. To get a significant impact on the fluidity superheats of 100 °C or higher have to be used.

The values given above are for a melt solidifying at a single temperature i.e. a pure metal or eutectic composition. This gives the highest values for the fluidity. The lowest values for fluidity is gained at intermediate compositions where according to Eq. 2.56 only approximately 50 % of the heat of fusion is effective in keeping the metal flowing. To compare the change in fluidity, data for selected flow velocities are plotted below both for alloys with and without a solidification range.

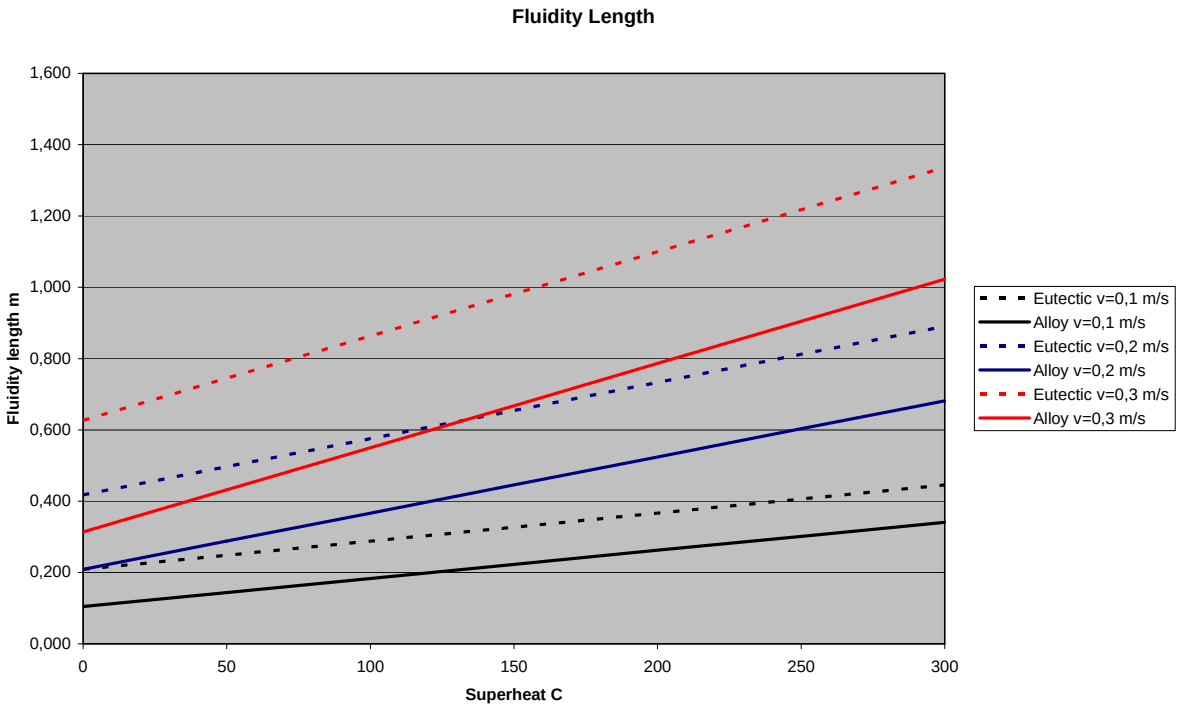

Figure 2.31 Fluidity lengths as a function of superheat and alloy composition.

I.e. at a 100 °C superheat and a flow velocity of 0.3 m/s the fluidity changes from 1.1 m to 0.69 m when changing from a eutectic composition to a non-eutectic. This is the expected minimum and maximum limits for the fluidity.

With the equations for the fluidity i.e. the possible flow length, the maximum possible filling time without getting a cold run can be calculated from knowledge about the geometry of the casting, i.e. the distance the metal has to flow in the thin sections. The equations for calcula-

ting the fluidity are of course not exact equations due to the assumptions made during deducing them, but they give the basic connection between the important parameters.

More complex equations for the fluidity and possible pouring times can be found in [Ref. 2.30] but unfortunately they contain different constants and loss coefficients making them hard to use in practice.

One has to bear in mind that the fluidity is calculated for a flow balanced perfectly. In the spiral test the freedom of the flow is very little in the sense that it is a very compact and constrained cross section giving no room for the melt to choose different paths. In real thin walled castings the geometry makes it difficult to have the same control over the melt flow, making it possible for the melt to split up in to different flows. This has of course to be avoided as much as possible.

2.12.3.7 Parameters influencing the fluidity

From Eq. 2.63 the influence of the different parameters on fluidity can be seen. Under normal conditions when producing green sand castings, the changeable parameters are the velocity and the superheat of the metal. The wall thickness can in some cases be changed after permission from the user of the casting, but this has to be seen as a fall back solution and it is normally not possible. The fluidity is seen to be reversed proportional with the heat transfer coefficient. In other casting processes like for instance die casting, it is normal practice to change the heat transfer coefficient with different kinds of die coatings. In connection with green sand castings normally no measures are taken to change the given heat transfer coefficient.

A lot of work has been done on determining material data for green sand moulds and heat transfer coefficients between mould and casting. A literature review can be found in [Ref. 2.29]. Determining the heat transfer coefficient is quite complicated due to the many factors influencing it. [Ref. 2.31] and [Ref. 2.32] highlights the important aspects. A few will be mentioned here. A significant influence from interfacial temperature is seen. Effects coming from gap formation between metal and mould reported in [Ref. 2.32] have also significant influence on the heat transfer coefficient. The gab formation is a combined effect of mould dilation and metal contraction and expansion in connection with graphite precipitation for cast irons. Effects from water vaporizing in the mould at the mould – metal interface enhance the heat transfer until the vapour is driven into the mould and hence this also plays a role.

To sum up: determining the heat transfer coefficient is very complicated as many factors influence it. If exact calculations are to be made incorporating the heat transfer coefficient, a constant value of the coefficient cannot be used as it changes during the cooling sequence. For rough estimates like the one done with Eq. 2.63 it is however reasonable to use a constant value.

The reduction in fluidity due to solidification morphology can in some cases be influenced by melt treatment [Ref. 2.30]. If the precipitation of grains in the early phase of the solidification is encouraged the fluidity is lowered. If it is possible to change the alloy to a eutectic composition or near eutectic this of course is giving a relative large improvement in fluidity.

Parameters not included in Eq. 2.63 and Eq. 2.64 having some effect on the fluidity in thin walled green sand castings can be found; they include for instance the mould material and the pressure head. [Ref. 2.30] reports a slight dependence of pressure head. The higher pressure will be able to force the metal through small cross sections, hence the flow will continue for a longer time. Even though the cooling power of the sand, given by a combination of the heat conductivity and the heat capacity of the moulding sand, is not a part in the equation for fluidity some effect from this must be expected. Under normal conditions the variation in cooling power from a green sand mould can be expected to be 15 % [Ref. 2.5] for the DISAMATIC process. This variation is due to variation in density. I.e. the effect from the sand can be estimated to be fairly constant for standard silica based green sand. This combined with an expectation of only a minor influence from the sand on the fluidity makes it reasonable not to include it in the equation.

2.13 Discussion

Most gating systems used for production of iron parts in green sand moulds are dimensioned with the help of rather simple equations like Eq. 2.7 and practical experience. Different dimensionless numbers used in flow engineering can be used to support the dimensioning of the gating system. The most used are the Reynolds number and the Weber number. The Reynolds number is a measure for the turbulence in the bulk flow. The Weber number is a measure for the turbulence at the melt to air interface at the melt front. The melt velocity is in the numerator in the equation for the Reynolds number and the velocity squared is in the numerator in the equation for the Weber number, i.e. both numbers are sensitive to the velocity.

This makes the practical use of the two numbers problematic. When fluid flow takes place in channels a natural velocity profile will exist at every cross section as for instance is seen on Figure 2.4. In reality is the velocity profile often much more uneven than the natural velocity profile indicates as for instance is seen in a plate shaped ingate showed on Figure 2.3. Very different local values for the dimensionless numbers can be found due to the large variations in the local velocities. This is illustrated with a conventional layout for casting a brake disc as an example.

To be able to calculate the different dimensionless numbers physical data for the alloy has to be known. The values found in the literature vary somewhat; the sources do not give detailed information about the circumstances the values have been found under. On the other hand variations in material data of say 20 % are overridden by variations in the local velocity in addition to the variations coming from the natural velocity profile over the cross section.

A more scientific approach to the dimensioning of gating systems can be made with the use of the Energy equation, which is normally used in fluid flow engineering. Unfortunately the calculation of the pressure losses in the gating system is based on some more or less empiric equations including constants found experimentally. To get accurate results, the equations and constants for calculating the contributions to the total loss from the different parts of the gating system need to be found through trials directly aimed at trimming them to be used for dimensioning gating systems. The very rough calculations made in section 2.7 giving a reasonable realistic value for the total loss in a gating system show the potential of the Energy equation. If the expressions for the losses coming from the different parts of the gating system are trimmed to foundry use accurate results can be expected. This means trials have to be done

with families of parts of the gating system like for instance the down runner to establish a correlation between the loss in the part and the geometry and melt velocity. This has to be done for the different design features commonly used in gating systems. This is necessary if accurate results are wanted

The advantage of this approach is the possibility to estimate the size of the contributions to the total loss coming from different parts of the gating system; hence it is possible to identify which parts of the system are giving significant contributions to the total loss. This can be used to build in extra losses for reducing the melt velocity at different points of the gating system. Or it can be used to estimate the effect on the losses coming from often used design features such as overlaps between different parts of the gating system.

One has to keep in mind that the Energy equation and the simple Eq. 2.7 and the dimensionless numbers can only be used to dimension gating systems. They cannot directly be used for designing gating systems; they can only support the designing. I.e. the actual design of the gating system depends very much on the foundry engineer's personal experience.

For iron melts the chemical composition has a large influence on the flow properties. This is illustrated with an example from the literature concerning the casting of a V pulley. The same example is used to show the difficulties in using water models for the prediction of the flow patterns.

When producing castings in vertically parted moulds the transition from the vertical down runner to the horizontal runner is important due to the relatively large pressure heights giving relatively large velocities in this area. The transition can be done in several ways; the choice of transition type will affect the pressure loss in the system and the quality of the melt.

Many different rules exist for determining the optimum pouring time. For normal section thicknesses, the optimum pouring time is often found from a combination of casting weight and the thinnest section. More and more often, practical considerations including the maximum time available for pouring in the machine cycle time and the maximum amount of iron in kg/s it is possible to pour without increasing the scrap level, have large influence on the chosen pouring time. For thin walled castings the fluidity of the metal plays an important rule when determining the optimum pouring time. For thin sections is a simple approximated expression for the fluidity of iron cast in green sand moulds given. Under normal condition the superheat and the pouring rate are the parameters the foundry engineer uses to change the fluidity. Although seldom changed in practice, when talking about iron cast in green sand moulds, the heat transfer coefficient has a significant impact on the fluidity when casting thin walled sections. When casting thin walled sections is the fluidity approximately proportional to the heat transfer coefficient.

References

Ref. 2.1 Strømningslære Leif Bjørnø. Arne Hartig Polyteknisk forlag 1984

Ref. 2.2 Casting iron using Lorapour technology. Foundry Trade Journal September 2002

Ref. 2.3 Mould filling experiments on mould flow in thin wall castings. Nieswaag, H. ; Denn, H.J.J. 1990, 57th World foundry congress Exchange paper 10

Ref. 2.4 DISA Industries Application manual Reg. No. 9152H2111 Edition 09/95 p. 3.5

Ref. 2.5 Aluminium Castings made in Vertically Parted Green Sand Moulds. Ph.D Thesis by Niels Winther Rasmussen. The Technical University of Denmark 1998

Ref. 2.6 Castings. John Campbell. Butterworth Heinemann 2002

Ref. 2.7 Introduction to fluid mechanics. 3rd Edition. Robert W Fox, Alan T. McDonald. John Wiley & Sons 1985

Ref. 2.8 Theory and Problems of Fluid Dynamics 2nd Edition. Schaum's Outline Series. William F. Huges and John A. Brighton. McGraw-Hill International Editions 1991

Ref. 2.9 Handbook of Hydraulic Resistance. 3rd Edition. I.E.Idelchik. CRC Press Begell House 1994

Ref. 2.10 Critical Gate Velocities for Film-Forming Casing Alloys: A Basis for Process Specification J. Runyoro, S.M.A. Boutorabi. J. Campbell University of Birmingham AFS Transactions 100 p. 225-234

Ref. 2.11 Formfyldning af meget tyndvægget støbegods The Technical University of Denmark IPL-070-03 Søren Skov Hansen 2003

Ref. 2.12 A study of the principles of gating as applied to sprue base design. K. Grube, J.G. Kura and J.H. Jackson. AFS transactions 60 p. 125-136 1952

Ref. 2.13 Flow through bends in gating systems. Final report for EDP 005MUP2 Niels Tiedje 1997

Ref. 2.14 Recommended Thermophysical properties for selected commercial allows. Kenneth C. Mills Woddhead Publishing Limited 2002

Ref. 2.15 Cast Iron: Physical and Engineering Properties H.T. Angus Butterworths 1978

Ref. 2.16 Elkem Technical Information sheet 19 Elkem ASA, Silicon Division 2003

Ref. 2.17 Surface tension measurements of high temperature metallic melts I. Egry, S. Schneider, I. Seyhan and T. Volkmann Institute für Raumsimulation, DLR, Cologne, Germany

Ref. 2.18 Thermophysical Properties of 201 Aluminum, Ductile Iron and Sebiloy II. R.A. Overfelt, R.E. Tayler, S.I. Bakhtiyarov, S. Wang AFS Transactions 02-146

Ref. 2.19 Ductile Iron http://metalcasting.auburn.edu/data/Ductile_Cast_Iron/Ductile.html

Ref. 2.20 Class 40 Gray Iron http://metalcasting.auburn.edu/data/Class_40_Iron/Class40Iron.html

Ref. 2.21 ASM Handbook. Volume 15 Casting. ASM International Second Printing 1992

Ref. 2.22 Flow Analysis of mould filling using high speed motion pictures of the metal. Water modeling and numerical calculations. Preben Ingerslev and Svend Thorhauge Andersen Technical University of Denmark Institute of Manufacturing Materials 1987

Ref. 2.23 A Water Analog Study of the Effects of Gating Designs on Inclusion Separation and Mold Filling Control. X. Xue, S. Feldager Hansen and Preben N. Hansen Laboratoury of Thermal Processing of Materials Technical University of Denmark 1992.

Ref. 2.24 Afprøvning af modelteknik til studium af fyldningsforløb ved støbning af symmetriske emner ved anvendelse af transparente modeller. Svend Thorhauge Andersen og Preben Ingerslev Laboratoriet for Termiske Materialseprocesser TM 82.19 The Technical University of Denmark 1982

Ref. 2.25 DISA Industries Application manual Re 9155D7010 2003

Ref. 2.26 Indløbssystemer til vertikal støbning af tynde plader i støbejern. Erik Møller, Asger Sturlason AMT-publikation 81.08-B Technical University of Denmark Institute of Manufacturing Materials 1981

Ref. 2.27 Maskenspiralform zur Prüfung des Fließvermögen VDG – Merkblatt P 120 Dezember 1972 Verein Deutscher Giessereifachleute

Ref. 2.28 Gießspirale – Zurück in die Zukunft. Gießerei-Erfahrungsaustausch, 11-12 p 518 2003

Ref. 2.29 Wärmetransport in Formen bei der Erstarrung und Abkühlung von Mittel- und Großguß aus Gußeisen. Giessereiforschung 54 2002 Nr. 4 Horst Wolff, Siegfried Engler, Alexander Schrey, Gotthard Wolf.

Ref. 2.30 Relationship Between Metal Fluidity and Optimum Pouring Time: A Literature Review. M. Tiryakioglu, D.R. Askeland, C.W. Ramsey. AFS Transactions, 101 p. 685-691

Ref. 2.31 Thermophysical Properties of Mold Materials. Horst Wolff, Siegfried Engler, Alexander Schrey, Gotthard Wolf. Advanced Engineering Materials 2003, 5, No. 1-2

Ref. 2.32 Assessment of Metal/Mould Interfacial Heat Transfer during Solidification of Cast Iron. K.N. Prabhu and W.D. Griffiths. Materials Science Forum Vols. 329-330 p 455-460 (2000)

3 Test Facilities

To give the reader a clear picture of the conditions the trials have been conducted under, a description of the established test facilities will here be given.

3.1 Framework for the test facilities

The project is a co-operation between The Institute for Manufacturing and Management at The Technical University of Denmark (DTU) and DISA Industries. Part of the co-operation agreement between the two partners was upgrading the test foundry at DTU. At the starting point of the project, DISA Industries put a DISAMATIC 2110 moulding machine at disposal for the test foundry. The A.P. Moller foundation and The Valdemar Birn foundation donated 1.000.000 dkr. each to the upgrading of the test foundry. This together with some other smaller but still important donations made up the economic framework for upgrading the test foundry.

3.2 Sand plant

The original sand plant consisted of a Webac speedmullor sand mixer with a capacity of 100 kg pr batch and a Samum aerator. Not much has been done to the mixer besides mounting new blades and adjusting them to give optimum mixing efficiency. The water addition to the mixer was previously done by a manual controlled water meter. This has been changed to a digitally one, giving better control over the added amount of water. No moisture measuring device for online determination of the water content has been available. Hence the addition of water is based on the water used in the previous batch mixed. As long as the moisture content of the old sand is reasonable homogeneous this way of running can be practised with only minor variations in the compactability from batch to batch. After mounting a new sling wheel in the aerator, its function was irreproachable despite its age.

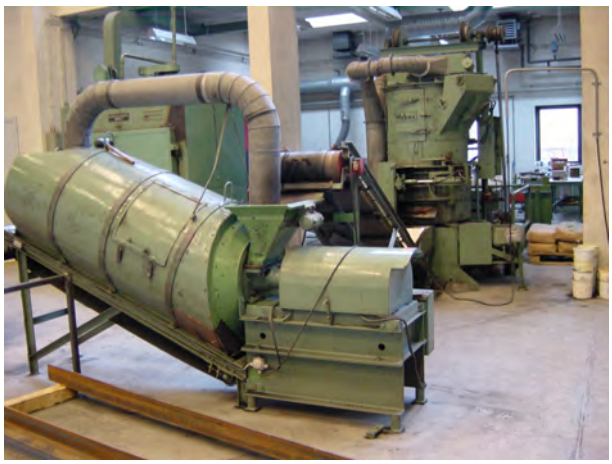

Figure 3.1 Mixer and aerator.

In general the quality of the sand after the aerator is very good. It is what normally is called “silk sand”. I.e. sand with absolutely no lumps. The set up can be seen on Figure 3.1.

In DISAMATIC foundries the sand is transported from the mixer to the moulding machine on conveyers. Unfortunately this was not economically possible. Therefore a rather special solution for sand transport has been chosen. A crane operated SSU (Sand Supply Unit) was designed. The size of the SSU was determined by the lifting capacity of the crane in the foundry. This resulted in a capacity equal to 5 meters of moulds i.e. half the installed mould string

length. A platform above the DISAMATIC was designed to carry the SSU when it delivers sand to the DISAMATIC. The setup can be seen on Figure 3.2. The dimensioning of the steel construction was done based on the norms given in [Ref. 3.1].

Figure 3.2 Filling of SSU and SSU ready to deliver sand to moulding machine.

This setup means the sand has to travel a very short distance on conveyers giving a minimum loss of moisture. On the other hand the “silk sand” coming out of the aerator is compacted to some extend in the SSU. It is though a very small SSU giving a relative small compaction compared to what normally is seen in DISAMATIC foundries. The optimum from a moulding point of view had of course been to have the aerator installed between the SSU and the moulding machine. Still, comparing to what is seen in production foundries, well aerated sand is available at the moulding machine.

A frequent point of discussion, when talking optimal moulding capability of vertical moulding machines, is asymmetrical filling of the sand hopper. To handle this discussion point, a stainless steel funnel ending in an Ø130 mm tube was mounted at the outlet of the SSU. The SSU was aligned on the platform positioning the centre of the tube within 1-2 mm of the centreline of the sand hopper on the DISAMATIC. The setup can be seen on Figure 3.3. The funnel is mounted with rubber scrappers to prevent damage of the conveyor band and to reduce sand spillage. The size of the outlet of the SSU was adjusted to a capacity making it able to keep up with the sand usage of the DISAMATIC and not over filling the funnel.

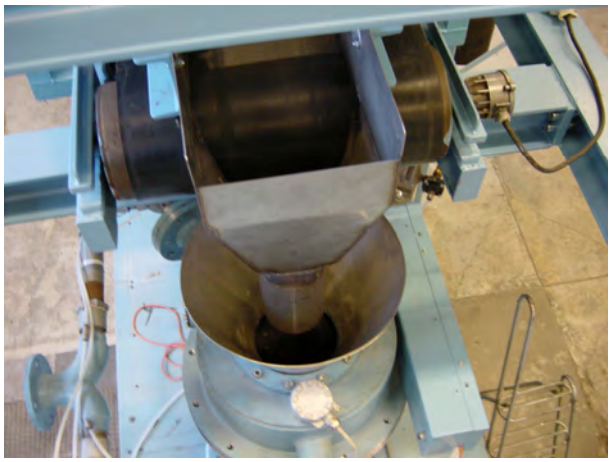

Figure 3.3 Funnel on the outlet of SSU giving symmetrical filling of the sand hopper.

3.3 DISAMATIC Moulding machine

The DISAMATIC moulding machine produces flaskless horizontally parted green sand moulds. The DISAMATIC moulding machines are high speed moulding machines, the newest models being capable of producing up to 500 moulds per hour. The working principle of a DISAMATIC can be seen on Figure 3.4.

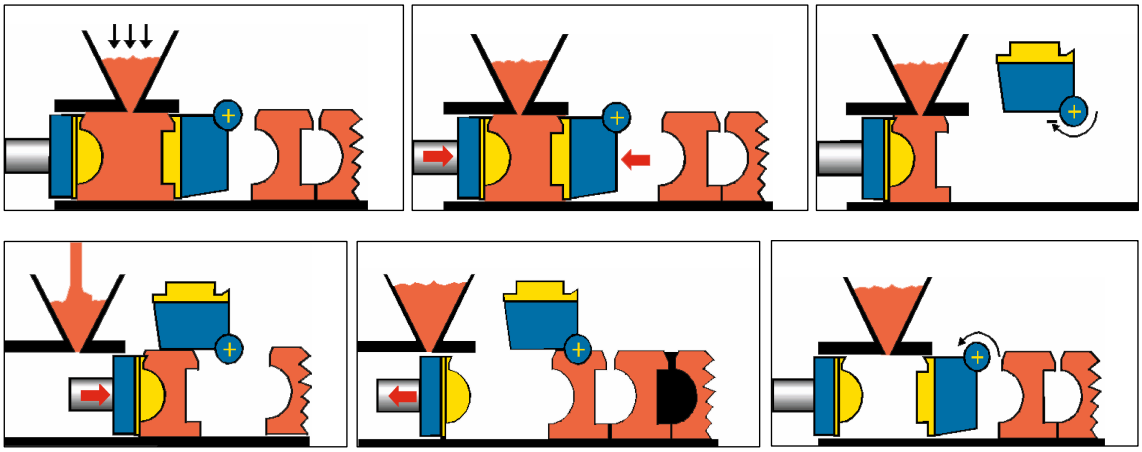

Figure 3.4 DISAMATIC working principle, yellow parts are the pattern plates [Ref. 3.2].

In the first frame the sand is blown into the mould chamber with the aid of compressed air. The mould is squeezed on the second frame. On the third frame the swing plate moves to the right and swings up opening the right side of the chamber. On the next frame the mould is moved out of the chamber with the press plate and pushed against the last produced mould and the mould string consisting of the previously produced moulds is moved one mould thickness forward. On the last two frames the machine moves back to the starting position ready for producing the next mould. In this way a long string of moulds pushed against each other is produced. In the interfaces between each mould a cavity exists given by the impression of the two pattern plates, marked with yellow on Figure 3.4. I.e. both sides of the mould is utilized. The pouring takes place down the mould string, and can be done during the operations where the string is not moved. At the end of the mould string a shake out is installed for separating the castings from the sand.

The moulding machine installed in the test foundry is a DISAMATIC 2110. The moulds produced are 500 mm wide and 400 mm high, the thickness can be varied from 100 to 315 mm. 10 meters of pouring / cooling string is installed. The 10 meters pouring / cooling length is made with an AMC (Automatic Mould Conveyor). The AMC assists the moulding machine in moving the mould string forward, preventing the moulds close to the machine from being squeezed together during mould transport. This would mean dimensional problems perpendicular to the parting line. With the installed sand plant and pouring device available, the moulding machine cannot run continually, all moulds are produced before the pouring starts.

The machine has produced more than 5.000.000 moulds, but all wear parts, i.e. bearings etc. have been changed making the machine mechanically as good as new. Furthermore different kits have been installed, up dating it to the newest design. I.e. the parameters influencing the process are up to date with the newest knowledge.

3.4 Green sand

The DISAMATIC operates with green sand, i.e. sand bonded without drying or chemical reactions. The strength is given only by blowing and squeezing of the moulding sand. The absence of a curing time makes the process highly productive compared to other mould production methods; as mentioned up to 500 moulds pr hour can be produced.

The green sand can either be a natural mix of sand and clay found many places in the world, or it can be what is called synthetic sand, where the composition is controlled [Ref. 3.3]. Only in very seldom cases natural sand is used on DISAMATIC's. The main components of synthetic moulding sand are beside sand, clay, water and coal dust. Bentonite clay is normally used for flaskless moulding to assure adequate strength. In most cases the base sand is silica, making the mould material relatively cheap. Another very attractive feature of the clay bound sands is the easy reuse. After pouring and shake out; the sand can be reconditioned in a mixer with small additions of water, clay etc. and then reused.

Many different properties can be used to describe the quality of green sand. Table 3.1 gives recommended values for the most commonly used properties. The given values are for green sand suitable for iron production on a DISAMATIC 2110.

2110		
Average sand grain size (washed)	0.14-0.28 DIN	AFS 110-60
Grain size distribution (washed)	3-4 sieves for 90% grains	
Green compression strength	1500-2100 p/cm^2	21-30 psi
Green tensile strength	>200p/cm^2	>2.9 psi
Spalling strength	>300p/cm^2	>4.3 psi
Wet tensile strength	>20p/cm^2	>0.3 psi
Permeability	>50	>50
Compactability	40% ± 2%	40% ± 2%
Moisture content	adjusted until a compactability of 40% ± 2% is obtained	
Active clay content (MB)	>7%	>7%
AFS clay content	active clay +3 to 4.5%	
Loss on ignition	3.5-5%	3.5-5%

Table 3.1 Recommend properties for green sand suitable for iron production on a DISAMATIC 2110 [Ref. 3.4].

Due to the relative small amount of iron poured in each mould when conducting trials with thin walled geometries, the iron to sand ratio is very good, meaning low impact on the sand. Because of this, reconditioning of the sand has consisted of adding water to obtain the wanted compactability of 40 % ± 2 %. Valdemar Birns Iron foundry has kindly sponsored used and reconditioned sand, making it possible to maintain the needed amount of system sand, which is around 4 tons in total.

3.5 Data acquisition on the DISAMATIC

The control system on the installed DISAMATIC 2110 is relay based. Because of this it is not possible to read out the process parameters, as it would be on a PLC controlled machine. The hydraulic system is pneumatic controlled via proportional valves. The control of the movements of the swing and press plate is done by limit switches. This means that it is not possible to record the mould thickness before and after squeezing and hence the compressibility of the sand. The value and the consistency of the compressibility are good indications of the sand quality. The quality of the mixed sand, mainly the compactability, is quite sensitive to variations in the moisture content of the old sand, due to the simple way the water addition to the sand in the mixer is controlled. For this reason a need for a final check of the sand quality exists. This can conveniently be done with the help of the compressibility. It is of course only a check which can not be used to control the sand quality.

When running trials, and of course also when running production, constant process parameters are very important. To be able to verify the stability of the process variables, the machine was equipped with an external data acquisition system. This is due to the comments about the control system given above and the need for a final check of the quality of the sand. The data acquisition system makes it possible to record a variety of pneumatic and hydraulic pressures and positions. The recorded parameters are:

Pneumatic pressures:

Main Air supply
Air for the pneumatic control system of the machine
Pressure controlling hydraulic pressure via proportional valve
Pressure for adjusting the squeeze pressure
Pressure for the AMC thrust bars
Pressure in the blow tank
Pressure over the sand during the blow

Hydraulic pressures:
Hydraulic pump
Press plate squeeze operation
Swing plate squeeze operation
AMC forward movement

Positions:
Horizontal position of the press plate
Horizontal position of the swing plate
Vertical position of press plate relative to bottom wear plate
Vertical position of swing plate relative to bottom wear plate

Velocities:
Horizontal velocity of swing plate yoke

All the data were captured using pc based equipment. The software used is DasyLab. All data were recorded to the hard disc making it possible to process the data at a later stage and to compare to data from different test days. Sampling rates between 200 and 500 Hz were used. A typical screen picture is seen below with graphs and digital readings of the measured parameters:

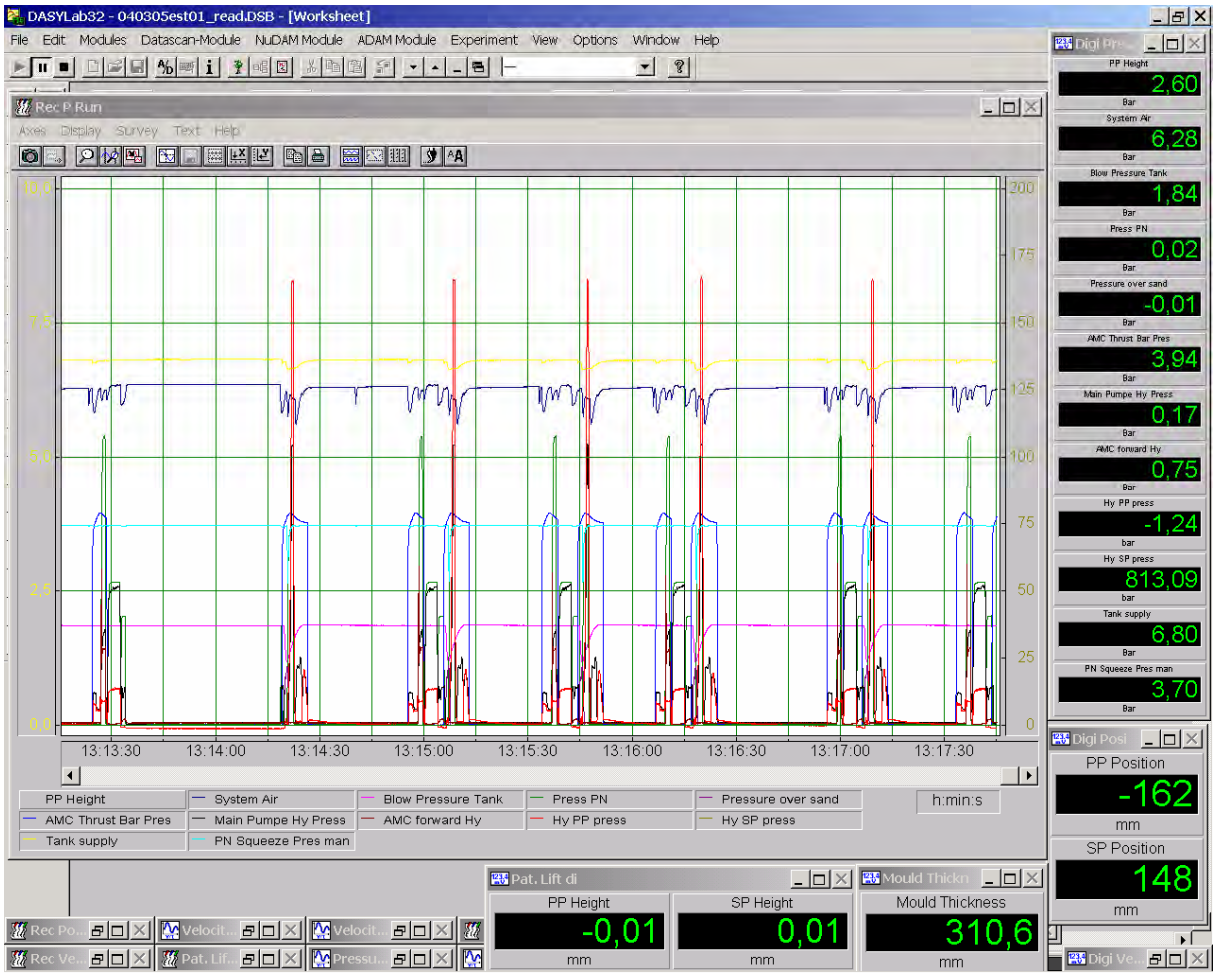

Figure 3.5 Screen dump from data acquisition system.

For measuring pneumatic pressures, standard pressure transducers with an output of 4-16 mA for 0-10 bar reading were used. The pneumatic transducers have mainly been mounted because of known problems with the main air supply in the building. The hydraulic system is pneumatic controlled via proportional valves. Because of this, consistent running of the hydraulic system can only be obtained if enough pneumatic system pressure is available to maintain a stable minimum pressure, in this case 5.5 bars. With the aid of the data recording equipment, it was possible to make the necessary changes to the main air supply in the building and to verify stable conditions exists during the trials assuring very constant process parameters. The tank pressure giving the blow pressure has also been monitored; again stable values could be verified.

For measuring hydraulic pressures, standard pressure transducers with an output of 4-16 mA for 0-250 bar and 0-400 bar reading were used. The hydraulic pressure transducers were mainly mounted to check the final pressure in the cylinders for the press plate and the swing

plate squeeze operation. The obtained hydraulic squeeze pressures vary less than ± 0.5 bar from mould to mould corresponding to less than 1 %. I.e. the compression of the moulds is very uniform giving constant moulding conditions.

The positions of the swing and pressure plates were recorded with linear position sensors. The sensors can be seen on Figure 3.6. The positions are recorded with a precision of 0.2 mm. The position system is mainly used for recording the compressibility of the sand, as this parameter tells a lot about the quality of the sand, but of course not every thing. Normally sand is tested with a compactability test, for instance the "three ram test". [Ref. 3.4] recommends a compactability of 40 % ± 2 % for sand suitable for a DISAMATIC 2110. Depending on machine settings and patterns used, this corresponds to a compressibility of 22-25 %. Making compactability tests for every batch mixed, is quite time consuming; hence it is more practical to use the compressibility as a final test. As mentioned above this is of course only a verification of the process stability; it does not give possibilities for controlling the process.

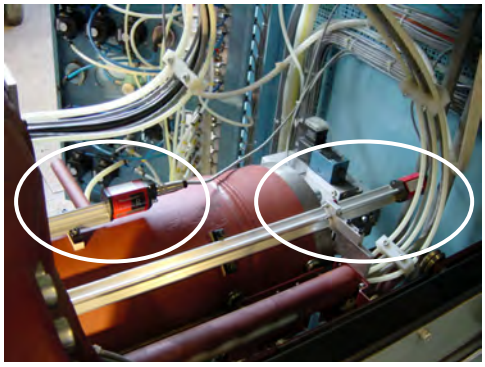

Figure 3.6 Linear position sensors for press and swing plate.

Apart from depending on the sand, the compressibility is depending on squeeze pressure and blow pressure and the patterns used, but as long as these parameters are kept constant the compressibility also has to be constant, if the sand is homogeneous. The compressibility is calculated from:

$$\text{Compressibility} = 1 - \frac{\text{Mould thickness after squeezing}}{\text{Mould thickness before squeezing}} \qquad \textbf{[Eq. 3.1]}$$

The results from a test day can be seen on Figure 3.7.

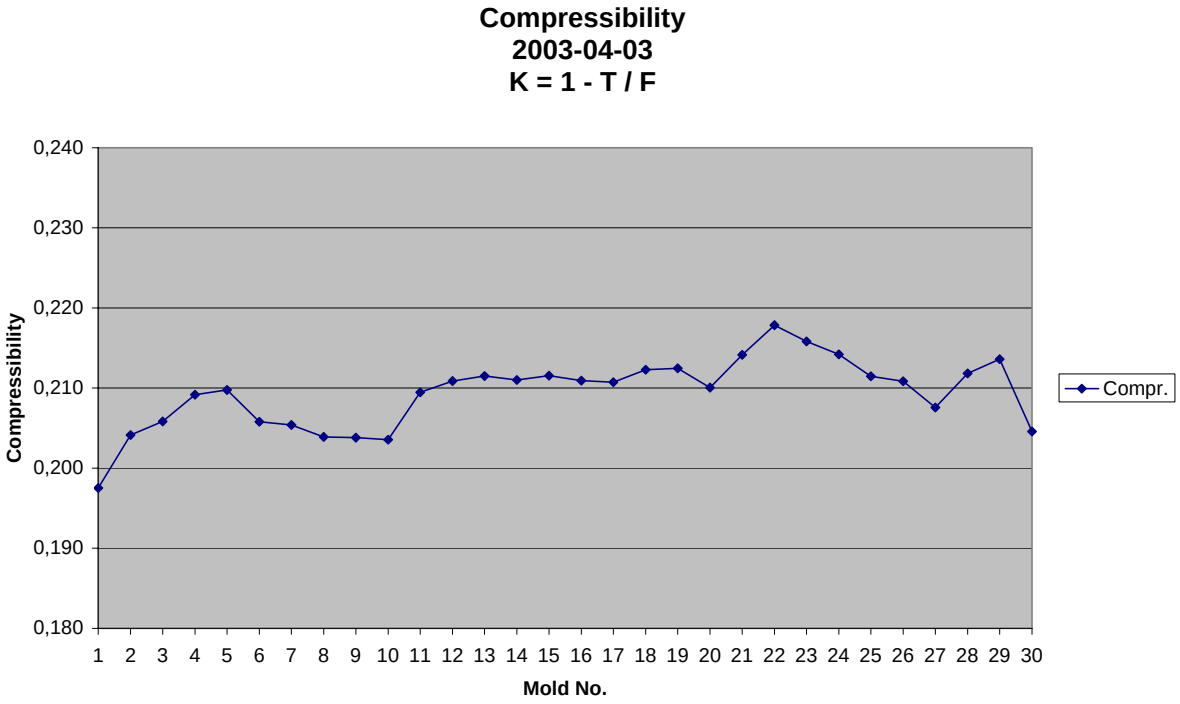

Figure 3.7 Compressibility for the single moulds.

I.e. quite uniform results can be obtained. Unfortunately this varies some from day to day, probably due to non uniform moisture content in the old sand.

For measuring the vertical positions of the swing and press plates relative to the bottom wear plate, analogue limit switches were used. The output depends linearly on the distance to the metal in front of them. The limit switches have been mounted on the back sides of the swing and press plates. The precision of limit switches connected to the measuring setup is within 0.02 mm. The relative vertical positions of the swing and press plates during the operation of the machine are used to get an overview of the machine related contribution to the vertical mismatch. The setup can be seen on Figure 3.8.

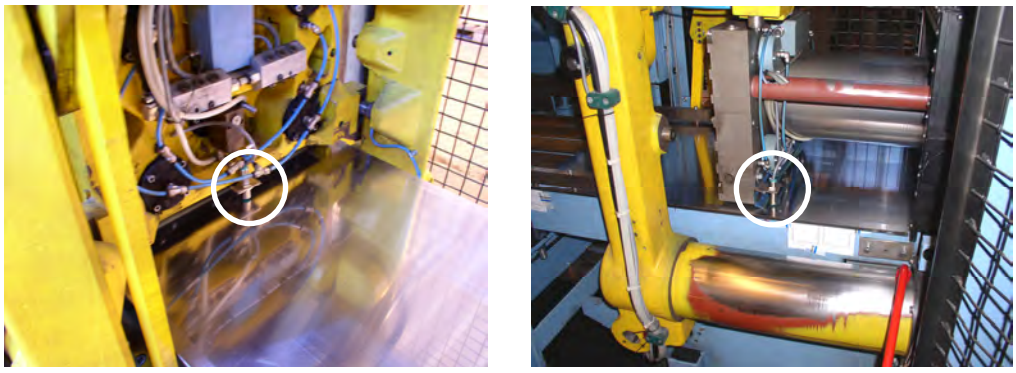

Figure 3.8 Limit switches for monitoring the vertical movement of swing and pressure plate relative to the bottom wear plate.

3.6 Melting furnaces

The melting furnace is a high frequency furnace (3830 Hz) with 100 kW power. Very little was done to the melting furnace. The refractory lining was changed in order not to risk accidents with metal penetrating through the lining. With the new lining the capacity of the furnace is around 140 kg. The furnace can be seen on Figure 3.9.

The high frequency means a minimum of melt bath agitation during melting. This makes it difficult to get alloying material dissolved into the melt. The added material has a tendency to float on top of the melt bath, and hence a relative large part of it is lost with the slag.

Figure 3.9 Furnace for cast iron.

3.7 Temperature control

The largest problem with the furnace was controlling the temperature. During some of the trials, the melt had to be kept in the furnace preferably at a constant temperature for at longer time. Due to the relatively small amount of iron even in a completely full furnace, the temperature changes fast. Hence a system for continuous temperature measurement in the furnace was needed. Handheld pyrometers give good measurements, but they are not well suitable if many measurements at short time intervals are needed. Different systems with thermocouples shielded in ceramic and quartz tubes were tested. But none of them could with stand the temperature shocks when inserted into the melt and taken out repeatedly.

An infrared device for measuring temperature was installed. The installed device is a 2-beam system from the Marathon series produced by Raytek. After trimming the infrared device to the actual conditions, the deviation between the infrared measurements and the pyrometer measurements was maximum 5 ºC. For achieving good measurements with the infrared device, it is crucial to have a clean melt surface. Even though using a high frequency furnace giving a minimum of agitation, it was possible to maintain a clean melt surface with no oxides when the temperature was above 1400-1420 ºC and the power was switched on. The device can be connected to a pc for recording the measured data and for setting up of the device.

With this device the temperature could be held at a fairly constant temperature for a long period of time without overheating at any time.

3.8 Magnesium treatment ladle

For making the magnesium treatment when producing ductile iron a treatment ladle was made according to the tundish cover principle. See Figure 3.10. Several different methods for making the magnesium treatment are used commercially. The tundish ladle is under most conditions convenient, effective, reliable and also economical. The process is very consistent and gives high recovery of magnesium. The carbon and temperature losses encountered during the treatment are relative low. The levels of fume and flare are also low compared to other processes [Ref. 3.5]. And last but not least, the simplicity of the treatment ladle makes is suitable for single runs in a test foundry. The ladle was designed to be able to treat 120 kg iron. To get maximum recovery of magnesium, the height to diameter ratio was chosen to be 2:1. The dish on top of the ladle was designed to be able to accommodate 100 kg iron to make it possible to fill it fast and hence not loose to much temperature when emptying the furnace. The size of the hole in the dish was dimensioned with the help of [Ref. 3.4]:

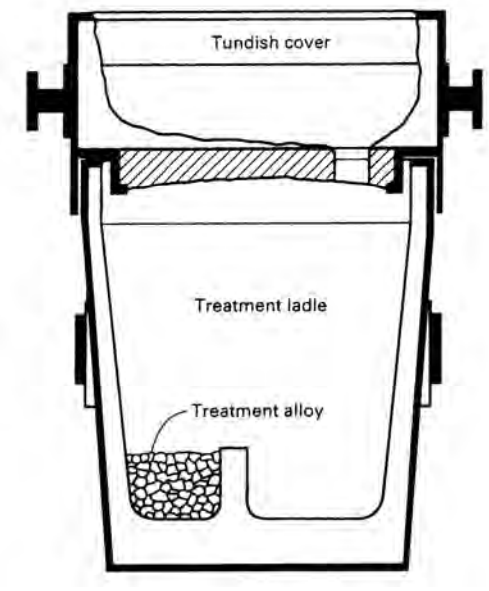

Figure 3.10 Treatment ladle according to the tundish cover principle [Ref. 3.6].

$$F = \frac{W}{t \cdot \rho \cdot m \cdot \sqrt{2 \cdot g \cdot h}} \qquad \textbf{[Eq. 3.2]}$$

Where:

F	Area [m^2]
W	Weight of metal [kg]
t	Time [s]
ρ	density [kg/m^3]
m	Dimensionless loss coefficient
g	Gravity [m/s^2]
h	Average pressure height [m]

The hole was designed to give a filling time of 10 seconds of the ladle.

The treatment ladle is preheated over a gas jet for several hours until it is red hot inside. The temperature was measured in the stone in the bottom of the ladle separating the two chambers. After 4 hours of heating the temperature was around 930 °C. To reduce the temperature loss of the metal, the lining of the ladle was made of 2 layers. The outside layer being an in-

Figure 3.11 Magnesium treatment ladle.

sulating layer, the total lining thickness is 60 mm. With the same total thickness, this gives a substantial reduction in heat loss compared to making the lining solely of high alumina refractory [Ref. 3.8]. To further reduce the heat loss of the treatment ladle, the outside of it was covered with 50 mm hard rock wool. The sprout of the ladle was kept at a minimum length to reduce the heat loss of the metal flowing over a cold sprout. With longer sprouts, the velocity of the metal will also be higher when it leaves the sprout, which makes pouring less controllable. The ladle can be seen on Figure 3.11.

3.9 Core shooter

DISA Industries put a 10 L core shooter at disposal for the test foundry. A lot of cores had to be used during the project. To secure a good and uniform quality of them, it was important to have a well functioning and stable machine to produce them on. The core shooter can be seen on Figure 3.12. The core shooter is PLC controlled. All the process parameters normally involved in core making can be regulated on the machine. The core shooter is running automatically but with manual core box handling. It is equipped with gassing plate etc. for automatic curing with gas. An automatic core box clamping system for vertically parted core boxes is also incorporated. The maximum core box dimensions are: height 325 mm, width 600 mm and depth 400 mm. The blow area is 275 x 230 mm. The closing force of the core shooter is 39.000 N. It was not possible to run with the cold box process due to the environmental limitations i.e. a scrubber etc. was not available. Hence a CO_2 curing binder was used.

Figure 3.12 Core shooter.

All the cores blown have been made with Novanol 180 from Ashland. This is a CO_2 curing phenol-resol based binder. When using this binder as a substitute for a standard cold box binder, one has to keep several things in mind. First of all the strength is generally lower and especially the edges are weak compared to a cold box binder. Binder levels of 2.5 – 3.5 wt % have to be used meaning reduced flowability of the sand when compared to using a cold box binder, where the total addition of binder normally is in the range of 1.0 – 1.2 wt %. Cores made with Novanol are not suited for long storage times as they deteriorate.

3.10 Spectrometer

For testing the chemical composition a spectrometer was installed. The installed spectrometer is a Spectromax from Spectro being able to test for all common elements in iron melts. The Spectromax is a simultaneous measuring optical emission spectrometer with argon flushed spark stand for quantitative spectrochemical analysis of metal samples [Ref. 3.7]. To be able to measure the carbon content in cast iron the specimens for testing have to solidify with a white structure, i.e. with rapid cooling. Copper chills were made giving specimens with 3 mm

thickness. With the spectrometer, fast and accurate information about the melt composition can be found, making it possible to adjust the melt to the wanted composition before making the magnesium treatment and before pouring. With the small amounts of iron to be handled and the high frequency furnace making it difficult to get alloying elements dissolved into the melt, some process variation must be expected; hence the importance of being able to check and adjust the composition is highlighted.

3.11 Miscellaneous

Several other things more or less process related had to be done to assure a functional and safe running of the trials.

To assure safe handling of the melt, a small traverse crane was installed in the pouring zone covering the area from the furnace to the pouring position. An installation with minimum height was chosen to give as short wires as possible hence obtaining maximum control over the load. Apart from adding safety to the melt handling, this setup also means minimum time for melt handling, and hence minimizing the temperature loss.

The original shake out was not able to brake down the rather strong DISAMATIC moulds. Due to the fact that it is a test foundry, many unpoured moulds can be expected, this makes it even harder for the shake out. The castings to be produced are thin walled and hence quite delicate, meaning it is not possible to leave them in the shake out to assist braking down the moulds. A new shake out was installed. The distance between the grids of the shake out is 50 mm. Because of the relative large amount of unpoured moulds a lot of hard lumps of this size can be found in the old sand hopper. A lot of hard lumps in the old sand put extra demands on the performance of the mixer.

To be able to pour the moulds it was necessary to build a platform along the pouring / cooling line. This assured a good working height giving good control over the melt when pouring.

Even through the amount of iron which is to be poured is very limited compared to what is poured in real foundries the internal environment in the foundry hall has to be acceptable. Hence an exhaust system had to be installed over the mould string. A system with movable hoods was made giving good access to the moulds for installing thermocouples, external cores on the top of the moulds etc. and for the pouring of the moulds. The system is seen on Figure 3.13.

Figure 3.13 Exhaust hoods.

3.12 Summing up on test facilities

In general a well functioning test foundry has been established with good possibilities to make trials under reproducible conditions. Both the mould and melt production capabilities are absolutely up to data. This combined with CAD CAM facilities and milling machines, situated in the same building, usable for the production of patterns and core boxes, gives the basis for a very powerful setup for making practical research and development in the foundry field.

References

Ref. 3.1 Norm Tabeller over Stålbjælker og Stålsøjler m.m. Lemvig-Müller & Munck A/S, (1979)

Ref. 3.2 DISA Industries, presentation material, (2003)

Ref. 3.3 Aluminium Castings made in Vertically Parted Green Sand Moulds. Ph.D Thesis by Niels Winther Rasmussen. The Technical University of Denmark, (1998)

Ref. 3.4 DISA Industries Application manual Re 9155D7010 (2003)

Ref. 3.5 Elkem technical information sheet No. 10. Tundish Cover Ladle Nodularization Elkem ASA, Silicon Division, (2002)

Ref. 3.6 Cast Irons ASM Speciality Handbook ASM International J.R. Davis, (1996)

Ref. 3.7 SPECTROMAX User manual Rev 0 Spectro, (2002)

Ref. 3.8 Elkem technical information sheet No. 21. Heat Conservation in Liquid Iron. Elkem ASA, Silicon Division, (2002)

4 Casting of Plates

A plate was chosen as the first simple test geometry. There are several reasons for that. It is ideal for fundamental studies of flow. Due to the simple geometry it is possible to capture the real filling sequences on video; this makes it possible to track the movement of free surfaces. Even though it is a very simple geometry, it is normally seen as a quite difficult geometry to cast. When working with thin walled parts the significant dimension is the wall thickness, because the curvatures of the surfaces normally are relative small compared to the wall thickness. Hence a thin plate is a good approximation to even rather complicated thin walled geometries.

A basic layout with two symmetrical plates was chosen. The layout can be seen on Figure 4.1. Two symmetrical plates were chosen in order to be able to compare two flows, which in theory should be exactly the same. The aim with this layout is not to cast a plate in the most feasible way, but to make a study of metal flow in very thin walled sections. To investigate the differences in flow behaviour depending on wall thickness, pattern plates were made for casting 2, 3 and 4 mm thick plates. The pattern plates were made according to [Ref. 4.1] to fit on the DISAMATIC 2110 moulding machine in the test foundry at DTU.

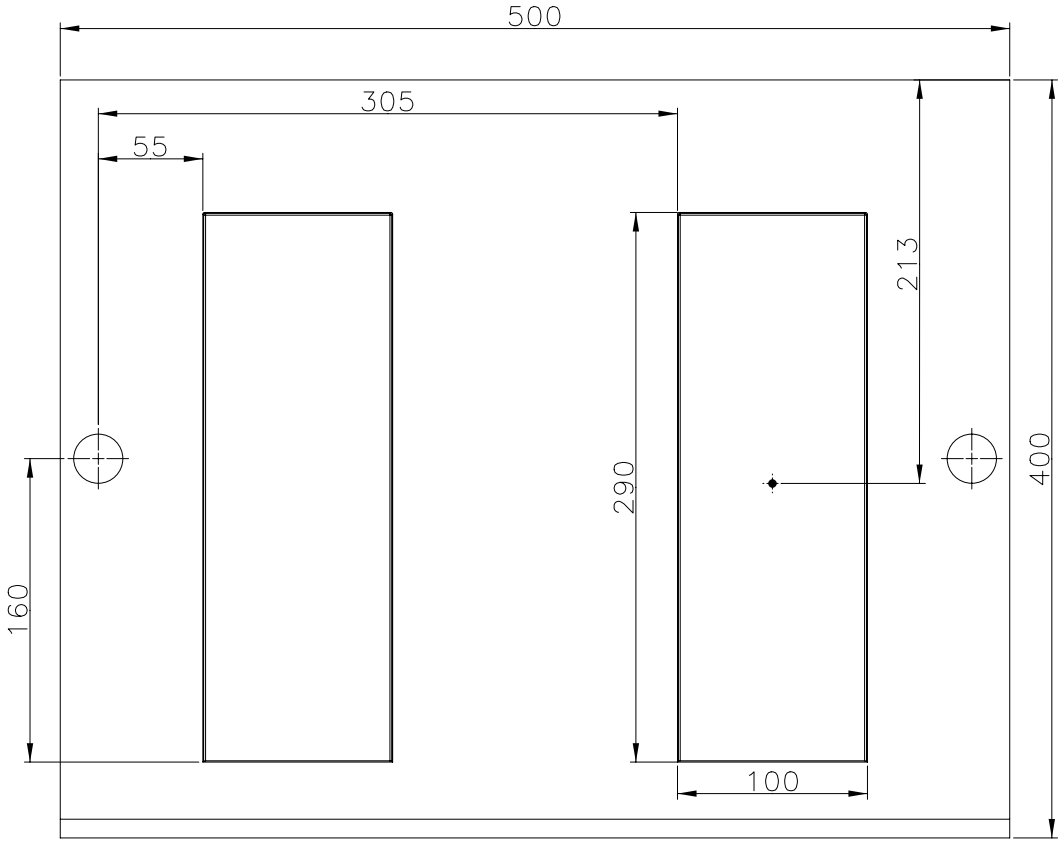

Figure 4.1 Basic layout for plate castings. Pattern plate made for a DISMATIC 2110.

4.1 Gating system

A conventional bottom filling gating system is chosen, as most parts with quality demands are cast with bottom filling gating systems. The calculations of the important cross sections are made with the following equation [Ref. 4.2] as discussed in section 2.1:

$$F = \frac{G}{\rho \cdot \sqrt{2 \cdot g} \cdot T \cdot m \cdot \sqrt{H}} \qquad \textbf{[Eq. 4.1]}$$

Where:
F Cross section area [m^2]
G Weight of iron flowing through the cross section [kg]
T Flow time [s]
m Loss coefficient
H Ferrostatic pressure height [m]
g Acceleration due to gravity [m/s^2]

Different runs of the plate trials have been made. In each run the gating systems were designed to give the same average melt front velocity in the plates independent of the plate thickness. The first layout is showed on Figure 4.2.

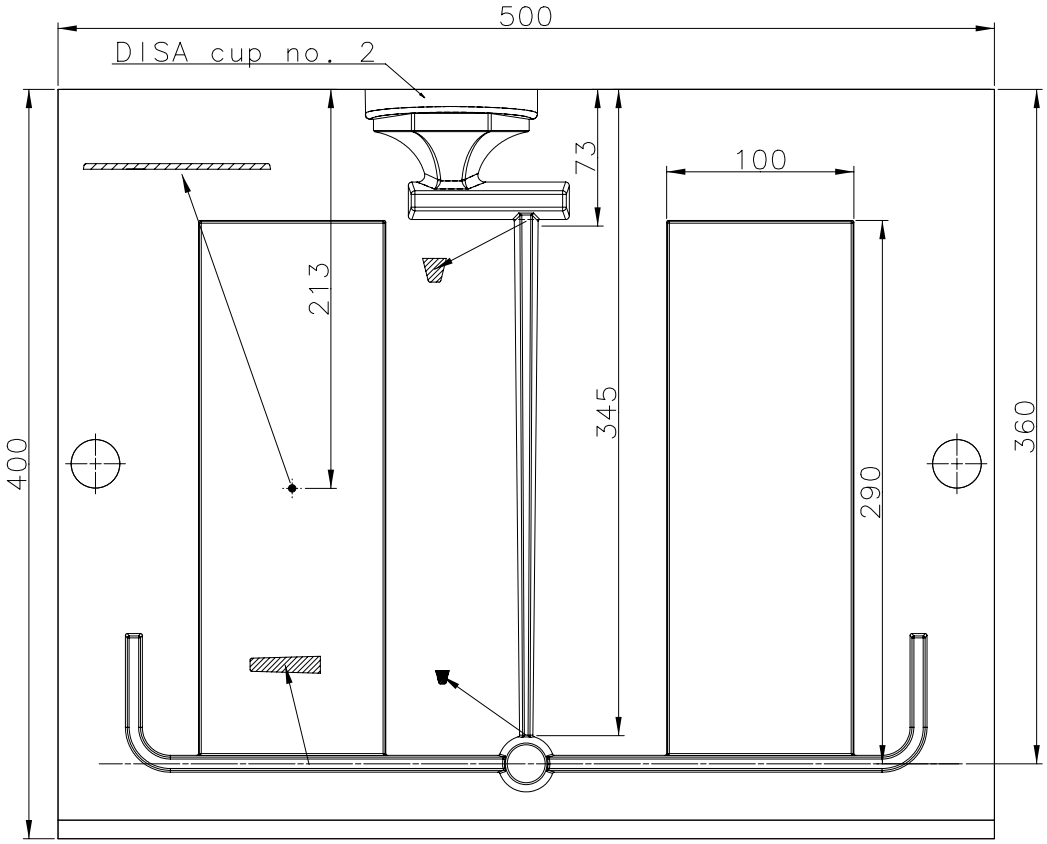

Figure 4.2 First basic layout. 120 mm/s melt front velocity.

Many different values for the loss coefficient can be found in the literature. See for instance [Ref. 4.2] and [Ref. 4.3]. In the present study it was planned to make videos of the filling sequences making it possible to measure the exact melt front velocities. I.e. the actual loss coefficient can be back calculated. To be able to easily estimate the losses in the gating system it was chosen to use a loss coefficient of 1 (i.e. no losses) when designing the gating systems.

4.2 Experimental setup

The plates and the gating system were all placed in the same mould half, making it possible to use glass plates as the other mould half. Normally heat resistant glass types, for instance Pyrex are used for this kind of trials. Heat resistant glass is unfortunately quite expensive. It was tried to use normal window glass instead. 3 layers of plain 3 mm window glass were used. The main purpose with the trials was to investigate the filling sequence. If the glass could withstand the heat for the relative short time the filling takes, it would be enough. The extra layers were added to give extra strength. The wall thicknesses to be cast are also relative small giving a low heat impact on the glass. Due to the small thickness of the single glass plates the temperature difference across a single glass plate will be relatively small resulting in relatively small temperature introduced stresses.

The first trials were made with moulds from a jolt squeeze machine, because it was easier to handle the moulds with flasks. An adapter made it possible to run the 2110 pattern plates on the jolt squeeze machine. A system for taken the flaskless moulds out of the DISAMATIC moulding machine was later developed giving substantially better moulds for the trials. See Figure 4.3. A green sand suitable for producing moulds on a DISAMATIC 2110 for casting iron was used, as described in section 3.4.

Figure 4.3 Handling of the flaskless moulds and mounting of glass.

After the glass plates were mounted with clamps, the tray with the mould could easily be handled.

The moulds were placed on a stand with adjustment possibilities securing that the moulds were positioned in level, see Figure 4.4.

The filling sequences were recorded with an S-VHS camera and later a digital video camera, both cameras giving 25 frames pr. s. Both formats were edited on a PC using a video capture card. With the setup it is possible to produce slow motion versions of the videos and grab single frames for close studies of the flow patterns. 25 pictures pr. second were adequate for the filling velocities investigated in this work.

Figure 4.4 Mould mounted with glass ready for pouring.

4.2.1 Measuring the melt front velocity

For measuring the melt front velocities in the plates and the gating system, pictures from the filling sequences were grabbed with suitable time intervals, intervals down to 0.04 s were used. The positions of the melt fronts on the pictures were found and converted into positions on the real layout. From this data, the melt front positions can be plotted as a function of time and compared to theoretical values found for different loss coefficients. Various other things can be examined in this way, for instance where the main melt flow takes place and how well the transition from the vertical down runner to the horizontal runner performs.

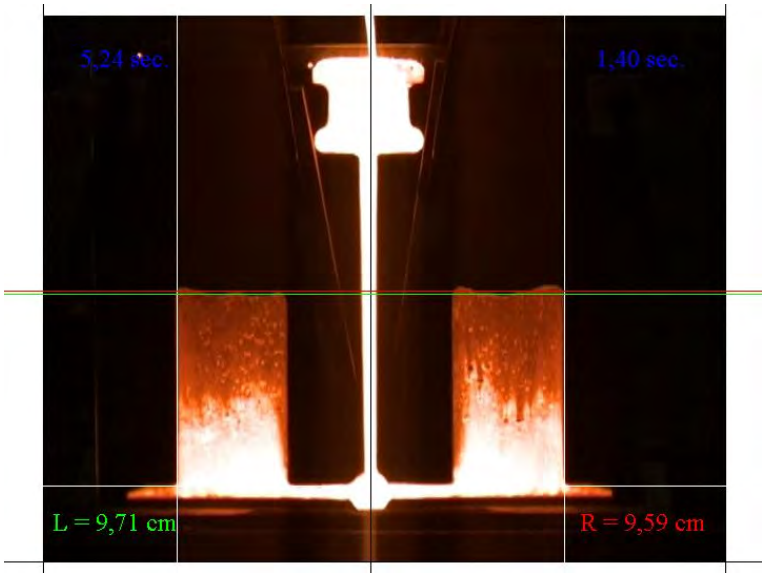

Figure 4.5 Measuring the melt front levels.

4.2.2 Alloy used for the trials and melt treatment

The tests have been made with ductile iron. The normative minimum and maximum values and the wanted values for the content of the important elements are seen below:

	C	Si	Mn	P	S	Mg
Min %	3.2	2.8	-	-	-	0.02
Max %	3.8	3.4	0.5	0.05	0.02	0.08
Wanted %	3.6	3.0	0.06	0.02	0.01	0.06

Table 4.1 Chemical analysis of the melt

The magnesium treatment was at the first trials made with a 10 % MgFeSi from Elkem. In the later trials the treatment was done with Remag, a 3.2 % MgFeSi also from Elkem especially suitable for treating iron for thin walled castings. The treatment was done in a tundish ladle with a capacity of 120 kg. The temperature loss in the ladle was significant, even though the ladle was preheated over gas jet until it was red-hot, see Figure 4.6.

Figure 4.6 Treatment ladle after preheating.

When running the trials where the filling sequences were captured on video, the handling of each mould took around 2 minutes. With at least 9 moulds to be poured from each melt batch, the melt would solidify in the treatment ladle. In order to prevent this, the melt was poured back into the furnace after the magnesium treatment. This made it possible to maintain the temperature of the melt at a very constant level and to get very good control over the finial pouring temperature. It was controlled with in +/- 5 ºC.

The pouring was done with a hand ladle made of ceramic fibres; the same material is often used for sleeves for insulated feeders. This fibre ladles were used to minimize the temperature losses. The inside of the ladle was coated with aluminium silicate based core paint. The light hand ladle gave good control over the pouring. The melt was tapped directly from the furnace into the ladle. The temperature loss for this operation was measured to be 50 ºC. The ladle could contain 7 kg.

Figure 4.7 Fibre pouring ladle.

The inoculation was done with Ultraseed from Elkem at the first trials. Later Alinoc, also from Elkem, was used. 0.2 % was added in both cases to the fibre ladle before tapping the melt from the furnace. To secure a complete melting of the inoculant, a 0-1 mm grain size was used. The melt swirls around in the ladle when tapped from the furnace giving good mixing.

At each trial run 3 moulds with each plate thickness were cast from the same batch of melt. This gave a good understanding of the consistency of the results. The glass did break from time to time, but the 3 repetitions made it possible to obtain results for all plate thicknesses at each trial run. The moulds were poured in random order.

4.3 1. Series of Trials. Melt velocity 120 mm/s

The melt front velocity in the plates was chosen to be 120 mm/s in this run of the trials. The 120 mm/s is the velocity of the melt when it passes the middle of the plates. The velocity of the melt when it enters the plates is 153 mm/s. No losses have been used when calculating the two velocities. The important cross sections of the gating systems were calculated with the aid of Eq. 4.1. The basic layout is seen on Figure 4.2. Complete drawings of the layouts for the 2, 3 and 4 mm plates can be seen in Appendix 4.1. The important dimensions are listed in Table 4.2. Both the calculated dimensions and the measured dimensions of the gating systems are listed.

The cross section under the pouring cup is calculated on the basis of the maximum flow through the choke before backpressure is build up. 10 % extra area is added for safety. The 90 degree bends at the ends of the horizontal runner were added for reducing the melt velocity gradually, and hence reducing the risk of a shock wave due to the hammer effect when the melt reaches the end of the runner and comes to an abrupt stand still.

The relatively big cross section of the horizontal runners was chosen on the basis of some (later shown) faulty simulations giving a lot of splash in the horizontal runners for smaller cross sections.

The pouring temperature, i.e. the temperature in the fibre ladle, was chosen to be 1370 °C.

Plate thickness		2 mm	3 mm	4 mm
Drawing number		26D0010	26D0020	26D0020
Choke area (Design)	mm^2	24	35	47
Choke area (Real)	mm^2	25	41	56
Initial speed at choke	mm/s	2595	2595	2595
Area under cup (Design)	mm^2	57	86	115
Area of the horizontal runner (Design)	mm^2	200	300	300
Section size of horizontal runner (Design)	mm	9/7/25	9/7/37.5	9/7/37.5
Area of the horizontal runner (Real)	mm^2	205	314	307
Area ratio Runner/Choke (Design)		8.5	8.5	6.4
Initial melt front speed in the horizontal runner (Design)	mm/s	153	153	204
Initial melt front speed in the horizontal runner (Real)	mm/s	162	177	243
Initial melt front speed in the plates (Design)	mm/s	153	153	153
Initial melt front speed in the plates (Real)	mm/s	162	177	182
Mean melt front speed in the plates (Design)	mm/s	120	120	120
Mean melt front speed in the plates (Real)	mm/s	127	139	143
Final melt front speed in the plates (Design)	mm/s	69	69	69
Final melt front speed in the plates (Real)	mm/s	73	80	82
Theoretical filling time of the plates (Design)	s	2.4	2.4	2.4
Theoretical filling time of the plates (Real)	s	2.2	2.0	2.0

Table 4.2 Important dimensions for the 3 layouts.

As seen from Table 4.2 some deviations between the nominal dimensions and the real dimensions of the gating systems were found. In the calculations made later in this section for determining the loss coefficients, the real dimensions of the gating systems have been used.

4.3.1 3 mm Plates

The filling of the 3 mm plates has been examined more closely. The temperature distribution at the end of the filling is seen on Figure 4.8.

The melt front positions in the plates have been extracted from the videos. The mean value of the melt front levels in the two plates has been plotted as a function of time on Figure 4.9. The time given is from the melt enters the plates.

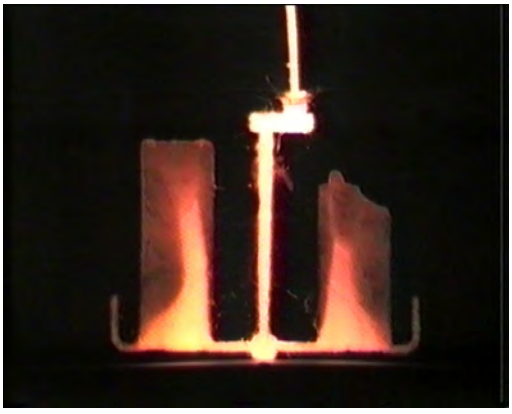

Figure 4.8 Temperature distribution at the end of filling.

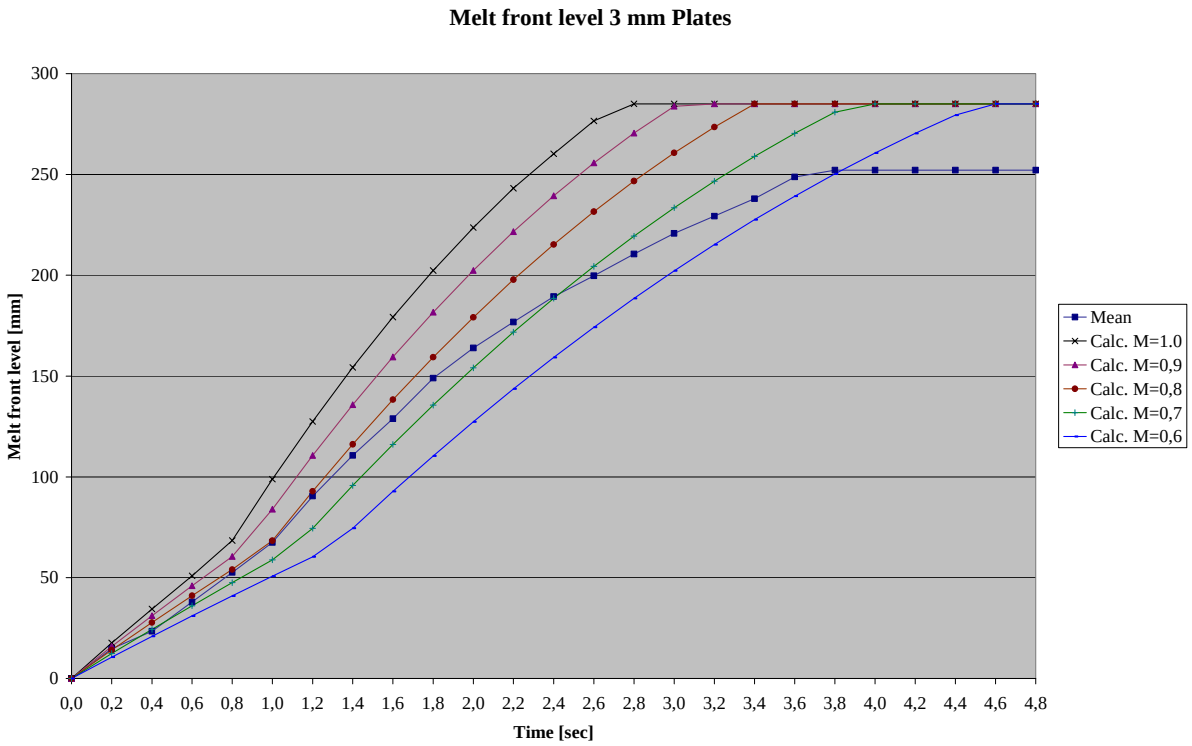

Figure 4.9 Measured and theoretical melt front levels as a function of time.

Theoretical curves for the melt front level found for different values of the total loss coefficient i.e. the loss coefficient used for dimensioning the choke are also plotted on Figure 4.9. Comparing the measured and the theoretical curves makes it possible to estimate the total loss coefficient.

The change in slope at around 0.8 s on Figure 4.9 is due to the bend at the ends of the horizontal runner. The bends take quite a large volume of the melt compared to the plates, giving a rather slow filling of the plates until the bends have been completely filled.

Before estimating the loss coefficient a few considerations have to be made. First of all, Eq. 4.1 cannot give the melt front level as a function of time directly. Rearranging Eq. 4.1 to express the melt flow rate in kg/s gives:

$$\frac{G}{T} = F \cdot \rho \cdot \sqrt{2 \cdot g} \cdot m \cdot \sqrt{H} \qquad \textbf{[Eq. 4.2]}$$

The theoretical melt front levels have been calculated with a discretisation of Eq. 4.2 with time steps of 0.005 s. The measured area of the chokes has been used for the calculations.

Several contributions to the total loss in a gating system can be identified as discussed in section 2.7. One of them is the back pressure due to surface tension. The back pressure generated by surface tension can be equalled to a metallostatic height. This height for a plate geometry is in section 2.6 found to be given by:

$$h = \frac{2 \cdot \gamma}{\rho \cdot g \cdot T} \qquad \textbf{[Eq. 4.3]}$$

The values for different alloys and plate thicknesses were calculated in section 2.6. Extracting the values for 2, 3 and 4 mm plates cast in ductile iron gives:

Plate thickness	Back pressure	Back pressure
mm	mm Fe	Pa
2	28	1721
3	19	1147
4	14	861

Table 4.3 Back pressure from surface tension.

The effect from surface tension can be taken into account by reducing the effective driving pressure with the values given in Table 4.3. The effect from the surface tension can in this way be extracted from the loss coefficient.

When including the effect from surface tension in the calculations of the theoretical melt front levels are the curves showing the melt front levels as a function of time getting a more realistic shape especially towards the end of the filling sequence. Hence it makes it easier to compare theoretical and measured curves.

Before this is done, the relative size of the back pressure compared to the total driving pressure has to be calculated. The driving pressure varies from 345 mm when the melt enters the plates, to 70 mm when the metal reaches the top of the plates. I.e. in the 2 mm plates the relative influence of the back pressure from surface tension is in the range 8 % to 40 %. 40 % is a significant number. But one has to remember; it is only valid in the last part of the filling. The influence of the back pressure on the flow is better illustrated with curves showing the melt front levels as a function of time with and without surface tension taken into account. This can be seen for the 2 mm plates on Figure 4.10. Results have been plotted for calculations done without losses and with 0.9 as the loss coefficient.

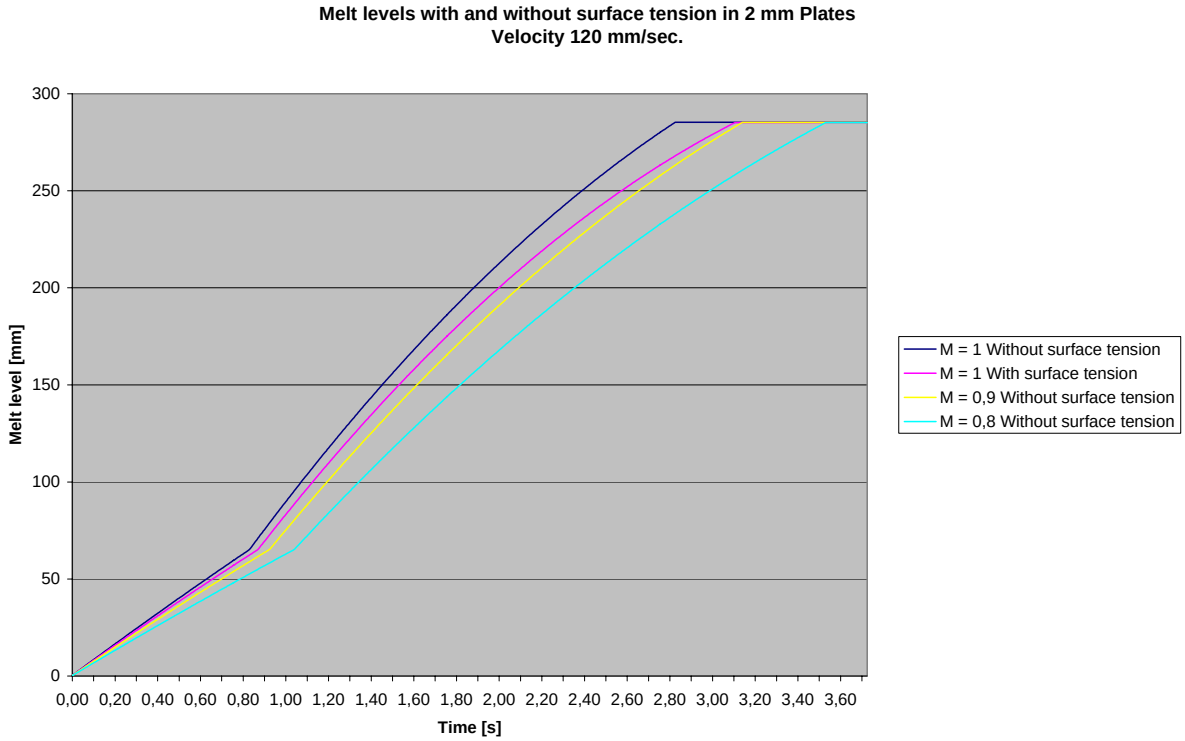

Figure 4.10 Calculated melt front levels found both with and without the influence of the surface tension at different values of the loss coefficient M.

The relative impact on driving pressure from back pressure generated by surface tension is large at the end of the filling. But the impact from surface tension on the total filling time of the plates is seen to be similar to lowering the loss coefficient from 1 to 0.9.

The influence from surface tension in the 3 and 4 mm plates is relatively smaller due to the correlation between the back pressure from surface tension and the plate thickness reducing the back pressure with increasing thickness. This can be seen in Appendix 4.2. For the 3 mm plates the impact from surface tension on filling time is equal to a reduction in the loss coefficient from 1 to 0.95. For the 4 mm plates the impact from surface tension on filling time is equal to a reduction in the loss coefficient from 1 to 0.97 i.e. an insignificant impact. The reductions of the loss coefficients have to be seen as mean values based on complete filling of the plates.

The theoretical curves for the melt front levels have been calculated with a reduction in active driving pressure according to the values given in Table 4.3. I.e. the loss coefficients found are without the effect from surface tension. If the effect from surface tension has to be included in the loss coefficient, it can be adjusted according to the reductions given above.

Looking at Figure 4.9 the best fit between measured and calculated melt front levels is found for a total loss coefficient of 0.8. The fit at the start of the filling is very good, later in the filling it looks like if the loss coefficient is smaller. During the last part of the filling the pouring cup was only partly filled reducing the effective driving pressure. Taking this into account and comparing the theoretical and measured curves at Figure 4.9 a good estimate for the total

loss coefficient is 0.8. When partly filled pouring cups are seen in the next trials is the melt level used for calculating the theoretical melt front levels reduced accordingly.

One could expect a reduction in the loss coefficient (i.e. higher losses) towards the end of the filling, as a relatively larger part of the flow takes place in the plates. The trials to be discussed in the next sections do not clearly show this effect.

[Ref. 4.2] recommends a loss coefficient of around 0.4 for flow in 3 mm sections. But this value is intended for flow in plate shaped ingates where the velocities normally are significantly higher than the nominal 120 mm/s seen here. The impact from velocity on losses is known from section 2.7 where the pressure loss in turbulent flow due to friction is estimated to:

$$\Delta P_{Friction} = \lambda \cdot \frac{l}{D_h} \cdot \frac{\rho \cdot V^2}{2} \qquad \textbf{[Eq. 4.4]}$$

I.e. one has to expect a dependence on velocity and the length of the flow taken place in the plates. This will be discussed more closely in section 4.5.2.2.

4.3.1.1 Melt flow pattern

From Figure 4.8 the melt flow is seen to take place at the edges of the plates turning towards the down runner. I.e. the braking forces in the system are larger than the dynamic forces. The braking forces are mainly the friction coming from viscous drag at the walls of the mould cavity and losses due to directional changes. In section 2.7 is a complete list of the losses in this gating system given. At the melt front a contribution to the braking forces is also coming from the back pressure generated by surface tension. The dynamic forces are inertia forces coming from the velocity of the melt.

The flow pattern with flow at the inside edges of the plates is a self-reinforcing mechanism. When less flow takes place at the outside edges, the temperature drops and the viscosity gets bigger making it even less feasible for the flow to take place at the outside edges.

The melt front levels get asymmetric quite early in the filling sequence. This happens even though the layout is symmetric apart from the pouring cup. The layout puts very little restriction on the melt flow. I.e. the balance between dynamic and braking forces decides whether the flow takes place at the inside or the outside edges of the plates. If for instance the viscosity of the melt was significantly lower then the braking forces from the viscous drag at the walls of the mould cavity would be smaller. The smaller drag forces mean the flow can possible be shifted towards the outside edge of the plates. In that sense the flow pattern is not controlled completely by the geometry of the gating system but to a large extend by the balance between the dynamic and braking forces. If the gating system had 100 % control over the melt flow pattern changes in the viscosity etc. would not change the flow pattern. This is desirable as the balance between braking and dynamic forces is hard to predict.

Some influence on the flow from the asymmetry at the pouring cup could not be excluded. This together with simulations also showing asymmetrical filling, made it reasonable to change to a symmetric layout.

4.4 2. Series of Trials. Melt velocity 120 mm/s symmetrical layout

Due to the final remarks in the previous section it was decided to change to a symmetrical layout. Hence the pouring cup was positioned at the centre of the pattern plate, with the down runner directly beneath it. This was done well aware of the drawbacks when the pouring stream has direct access to the down runner. When this is the case the amount of dynamic energy transferred to the gating system from the pouring stream is very dependent on the direction of the pouring stream, i.e. whether it hits directly into the down runner or the walls of the pouring cup. Slag and other impurities will also have direct access to the gating system. The trials with making videos of the filling demanded the complete gating system to be on the same pattern plate. This makes it impossible to make an overlap at the bottom of the pouring cup, as shown in Figure 4.11. This would have kept the symmetry of the layout and at the same time have prevented to pouring stream from having direct access to the down runner. The basic layout can be seen on Figure 4.12.

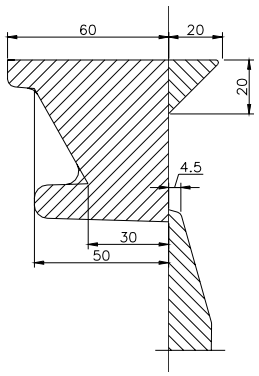

Figure 4.11 Pouring cup with overlap at the bottom.

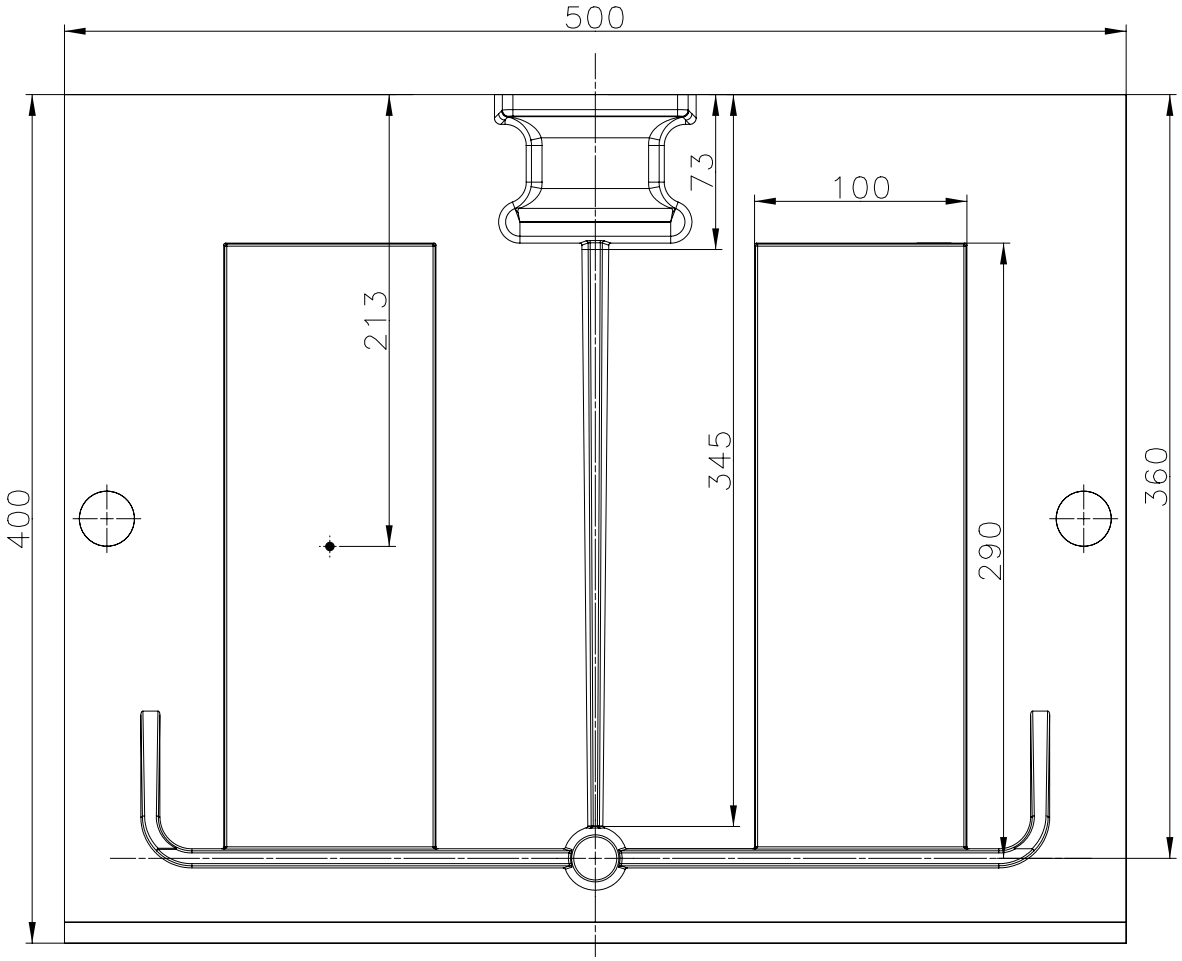

Figure 4.12 Second basic layout. 120 mm/s melt front velocity.

The pouring cup has also been changed to a square shaped one. This type is more suitable for hand pouring, because it reflects the melt less back towards the pourer. The cross section of the bend at the ends of the horizontal runner has furthermore been gradually reduced. This has been done for two reasons. First it reduces the volume of the bend lowering the impact on the melt front velocity in the initial filling of the plates. Second it helps to reduce the risk of getting a shock wave in the melt due to the hammer effect, when it comes to an abrupt stand still at the end of the runner. Otherwise the data for the layout are the same as in the previous section. I.e. the velocity of the melt front when it passes the middle of the plates is designed to be 120 mm/s when calculated without losses.

The plates were cast under the same conditions as the first layout, i.e. in ductile iron with a pouring temperature of 1370 ºC.

4.4.1 4 mm Plates

A snapshot from the end of the filling of the 4 mm plates is shown in Figure 4.13. The flow takes place at the outside edges of the plates. The flow stops before the top of the plates is reached, i.e. the flow length is shorter than at the 3 mm plate. This is due to pouring temperature fluctuations. The trial was made before the infrared temperature device was installed. Thus the temperature measurement was less precise and efficient. The two other runs with this set up unfortunately ended up with broken glass during the filling. However both of them filled completely.

Figure 4.13 Snapshot from the end of the filling of the 4 mm plates.

The possible lower pouring temperature means lower viscosity for the initial part of the flow taken place until the solidification starts. It is a near eutectic alloy. The percentage of the total flow length coming from superheat for near eutectic alloys is in section 2.12.3.6 shown to be relatively small unless very high superheats are utilized. Hence only a small influence from temperature fluctuations on the loss coefficient can be expected. But on the other hand this also means that unless running with rather high superheats small fluctuations in the pouring temperature only changes the flow length marginally. Hence the differences in the flow length before cold shot occurs it probably due to other reasons than the pouring temperature. This will be discussed more closely in section 4.7.2.2.

The measured and theoretical melt front levels are plotted on Figure 4.14 in the same way as done in the previous section. The data for the layout for the 4 mm plates have been used for calculating the theoretical curves.

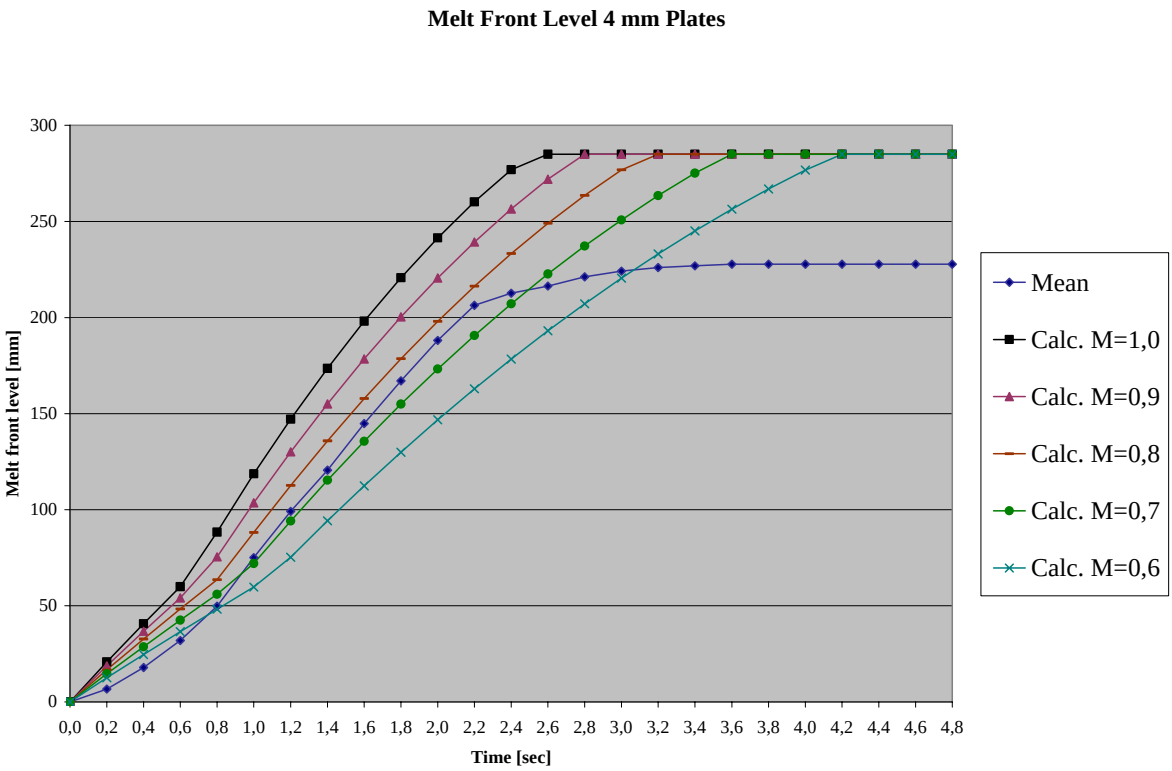

Figure 4.14 Measured and theoretical melt front levels as a function of time.

Finding the best fit between measured and theoretical data points gives a total loss coefficient between 0.7 and 0.8.

4.4.2 3 mm Plates

The layout for the 3 mm plates resulted in an almost complete filling. Figure 4.15 shows a snapshot towards the end of the filling. The melt flow is seen to take place at the inside edges of the plates. The melt levels are plotted as a function of time on Figure 4.16. Theoretical melt levels calculated for different values of the loss coefficient are also plotted.

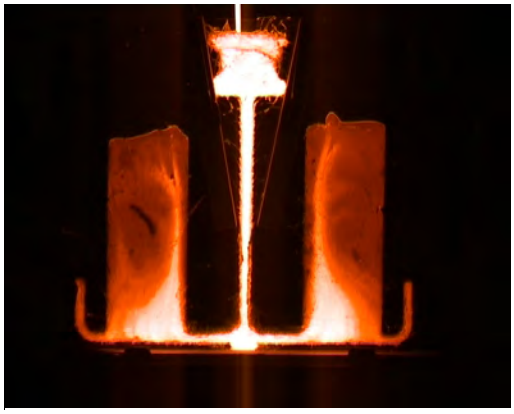

Figure 4.15 End of filling of 3 mm plates.

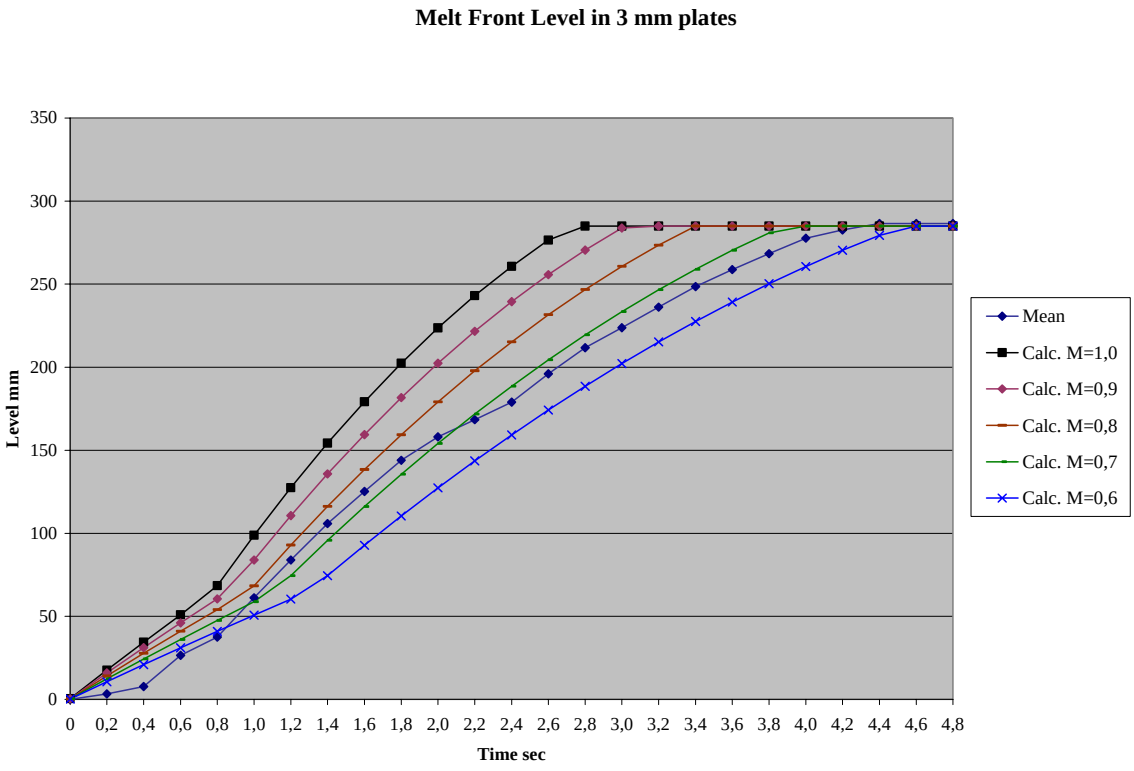

Figure 4.16 Measured and theoretical melt front levels as a function of time.

The best fit between measured and theoretical data points is for a total loss coefficient of 0.7. The off set of the measured curve around 2.2 s is caused by the inner layer of glass breaking giving a small shift in time. Removing this shift would move the last part of the curve very close to the theoretical curve for a loss coefficient of 0.7.

4.4.2.1 Comparison of flow with and without glass plates

The plates have also been cast in moulds with both sides made of green sand. The available sand gives unfortunately some sand burn on. The burn on is where the largest heat impact has been on the sand. I.e. the sand burn on is a picture of where the main flow has taken place. The flow patterns can be compared on Figure 4.17.

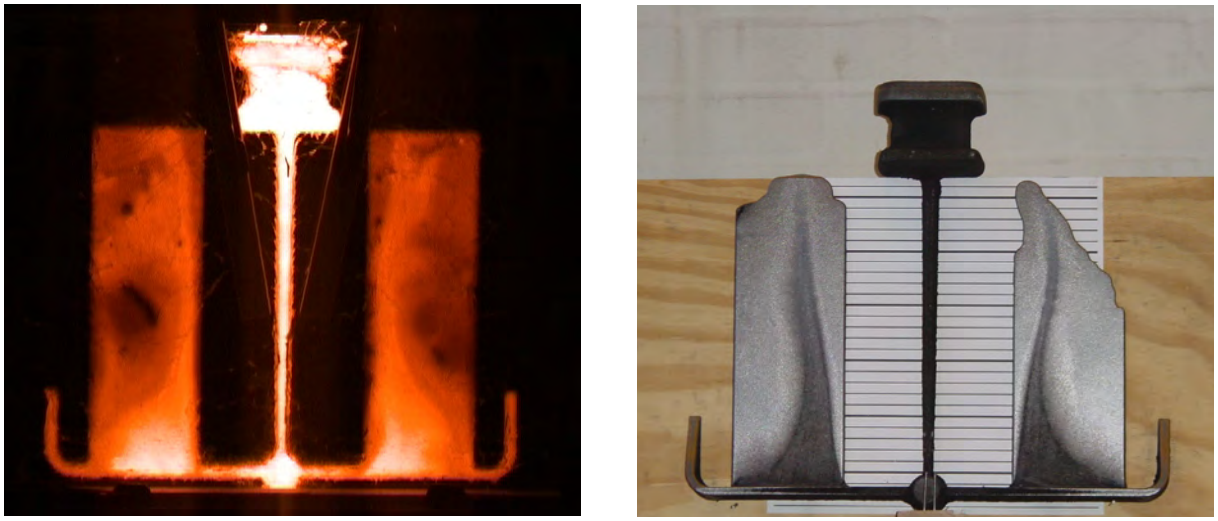

Figure 4.17 Flow patterns in 3 mm plates cast with and without glass as one mould half.

In both cases the flow is seen to take place at the inside edge of the plates. The flow in the part cast without glass is moved a little away from the edge of the plate compared to the flow in the trials with glass. In both cases the flow path is shifted towards the middle of the plates in the upper part of the plates. At all test days the trials have been repeated in moulds where both sides have been made of green sand, and the same agreement between the flow patterns is seen. I.e. the flow patterns are very similar when running with or without glass as one mould half. The flow patterns seen in the trials with glass plates instead of a green sand mould half can therefore be seen as a good approximation to the flow taken place in moulds completely made of green sand. The differences in flow length before cold shot occurs in the two cases will be discussed in section 4.7.2.2.

4.4.3 2 mm Plates

It was not possible to fill the 2 mm thick plates with a mean front velocity of 120 mm/s. During the filing of the horizontal runner the melt tongues going into the plates solidified and blocked the flow. The little flow that took place is on the inside edges of the plates. This can be seen on Figure 4.18.

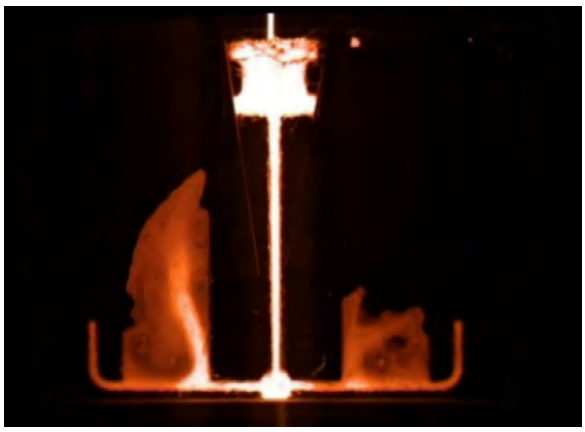

Figure 4.18 Flow in the in 2 mm plates.

4.4.3.1 Cold shots in the 2 mm plates

The trials were repeated in green sand moulds to a have a closer look at the cold shots. 20 moulds were poured to investigate the flow lengths before cold shots occur and the consistency of the cold shots. A pouring basin was used to get consistent mould filling conditions. The setup with the basins can be seen on Figure 4.19. The basins will be described in section 4.7.

Figure 4.19 Setup with pouring basins.

A picture of the first casting made is shown on Figure 4.20. Pictures of the first 12 castings made can be seen in Appendix 4.3.

As described in section 4.4.3 the flow has taken place at the inside edge of the plates. This is also reflected in the cold shot patterns seen in Appendix 4.3. The cold shot patterns are to some extend different from mould to mould. This is connected to the very non-uniform flow across the section of the plates. The flow takes place in channels in the plates as seen on Figure 4.18 in stead of in the complete cross section.

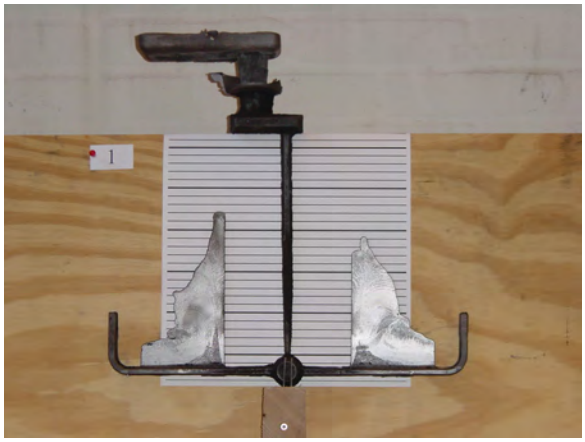

Figure 4.20 Cold shot in 2 mm plate.

The flow lengths before cold shots occur seen in Appendix 4.3 are similar to the ones seen in the trials with the glass plates. I.e. the cooling conditions are similar when running with and without glass as one mould half.

An expression for the fluidity of the metal has been derived in section 2.12.3.6. Using this together with the material data also used in the section yields the graph shown on Figure 4.21 for a 2 mm plate when the melt front velocity is 120 mm/s.

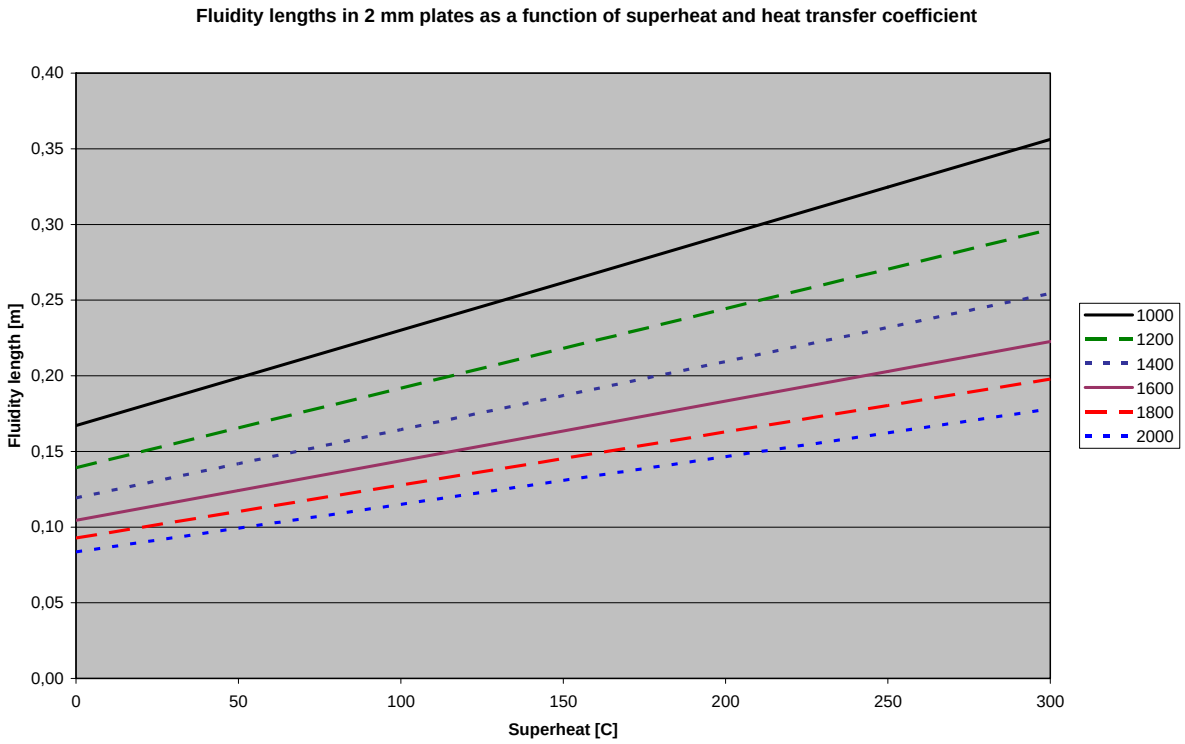

Figure 4.21 Fluidity as a function of superheat and heat transfer coefficient for 2 mm plates.

As discussed in section 2.12.3.6 the heat transfer coefficient is not well known. Furthermore the coefficient is most likely not constant over time. The fluidity has been plotted for heat transfer coefficients in the range 1000 - 2000 W/m^3K which should cover the values normally seen as realistic. The pouring temperature was 1370 °C. The temperature of the metal when it enters the plates has not been measured. A significant temperature drop caused by the flow through the gating system must be expected due to the relatively low flow rates and the shape of the horizontal runner. The superheat when the metal enters the plates is estimated to around 100 °C.

For a superheat of 100 °C the calculated fluidity is in the range from 110 mm to 220 mm for heat transfer coefficients between 1000 and 2000 W/m^2K. Comparing this to the pictures in Appendix 4.3 shows some agreement, the magnitude is clearly right. The flow in the plates is quite chaotic. It takes place in channels and not in the complete cross section of the plates. With this and the approximations done when deducing the equation in mind the agreement between calculated and experimental found fluidity is surprisingly good.

Designing a gating system securing uniform flow across the complete section of the plates, as for instance done in [Ref. 4.4], would probably give longer flow distances and also more uniform fluidity lengths. This combined with measuring the temperature of the metal when it enters the plates would probably make it possible to estimate the heat transfer coefficient.

4.4.4 Summing up on the loss coefficients

For the 3 mm plates the total loss coefficient for the layout shown on Figure 4.12 was found to be 0.7, for the 4 mm plates it was found to be 0.7 - 0.8 i.e. a tendency to a decreasing loss with increasing wall thickness. With the equations from section 2.7 in mind, this also sounds reasonable. These values have been found after excluding the effect from surface tension. The effect from surface tension on the loss coefficient is found in section 4.3. Including the effect from surface tension in the loss coefficient gives 0.65 for the 3 mm plate. The effect from surface tension on the loss coefficient for the 4 mm plate is in practice insignificant.

Before concluding on these values for the loss coefficient one has to take the actual boundary conditions into consideration. The calculations have been made with the top of the mould giving the pressure height. Snapshots from the filling sequence show a well filled pouring cup during the complete filling. But the down runner is located at the centre of the bottom of the pouring cup, giving direct access for the pouring stream into the gating system. There are no direction changes or other measures for taken some of the momentum out of the pouring stream. Hence momentum from the pouring stream can, in theory, be transferred into the gating system. This influence of the boundary conditions will be discussed more closely in section 4.8. In this section a pouring basin has been used to prevent the possible transfer of momentum from the pouring stream to the gating system.

4.4.5 Summing up on the flow patterns in the plates

The flow pattern in the 3 mm plates is showed on Figure 4.15. This flow pattern is descriptive for the flow through the complete filling sequence, i.e. the preferred flow path is at the inside edges of the plates. The flow pattern for the 4 mm plates is showed on Figure 4.13. The initial flow takes place at the centre of the plates, shifting to the outside edges later in the filling. I.e. for the 4 mm plates the preferred flow path is shifted to the centre/outside edges of the plates compared to what is seen in the 3 mm plates. The reduction in thickness from 4 to 3 mm causes this difference. For the same melt front velocity means a reduction in wall thickness increasing braking forces from surface tension and friction against the mould walls. The sizes of the braking forces will be discussed more closely in section 4.5.2.2. Due to the larger braking forces the flow pattern is shifted towards the inside edge of the plates when going from 4 to 3 mm wall thickness. The flow patterns are summarized in Table 4.4.

Test day	Mean velocity mm/s	Size of horizontal runner	4 mm	3 mm	2 mm
2	120	Big	Centre → Outside	Inside	Inside

Table 4.4 Main flow paths.

The velocities of the melt in the horizontal runner are showed in Table 4.2. The initial velocity in the horizontal runner for the 3 mm setup is 153 mm/s while it is 204 mm/s for the 4 mm setup. This difference also promotes the shifting of the preferred flow path towards the out-

side edges of the plates. But the velocities in the horizontal runners are in both cases relatively low, reducing the influence on the flow paths in the plates.

The velocity of the melt front is relatively slow in the initial filling of the plates. This is due to the bend at the ends of the horizontal runners. They were meant for gradually reducing the velocity of the melt, and hence reducing the risk of getting a pressure shock wave in the melt due to the hammer effect when it hits the end of the runner. But they do more harm than they do benefit, especially in the 2 mm plates. The melt front solidifies partly during the initial filling of the plates due to the low velocity of the melt front, which leaves only a small channel open for melt transport. Hence they have been almost completely removed in the next trial. One could also have chosen to reduce the cross sectional areas even more of the bends, and hence reduce the influence on the melt velocity in the plates. Basically seen it is a good idea to go against gravity if a gradually reduction in the melt velocity is wanted.

4.5 3. Series of Trials. Melt velocity 300 mm/s

The mean melt front velocity in the plates has now been raised to 300 mm/s when calculated without losses. This is done by enlarging the down runners. The velocities of the melt in the horizontal runners have also been raised to prevent the problems with partly solidification during filling of the horizontal runner. The bend at the ends of the horizontal runners is almost removed. The transition from vertical down runner to horizontal runner is the same, i.e. an Ø30 mm cylinder, 45 mm high with 5 degrees draft. The melt front velocity has been raised to get a more complete filling of the 2 mm plates, and to investigate how the flow patterns change with velocity. The melt front velocity in the plates has also been raised to investigate when the melt fronts starts to break up. A snapshot from the filling of the 4 mm plates is showed on Figure 4.22. The basic layout is shown below:

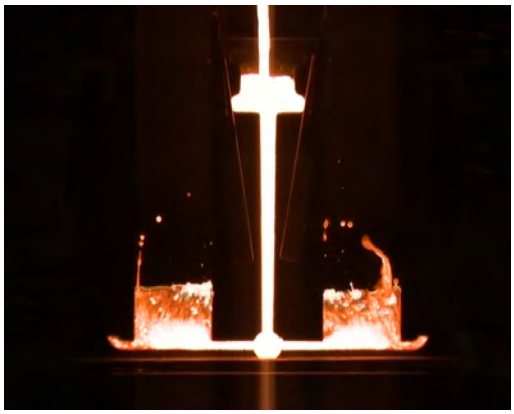

Figure 4.22 300 mm/sec melt front velocity. 4 mm plate thickness.

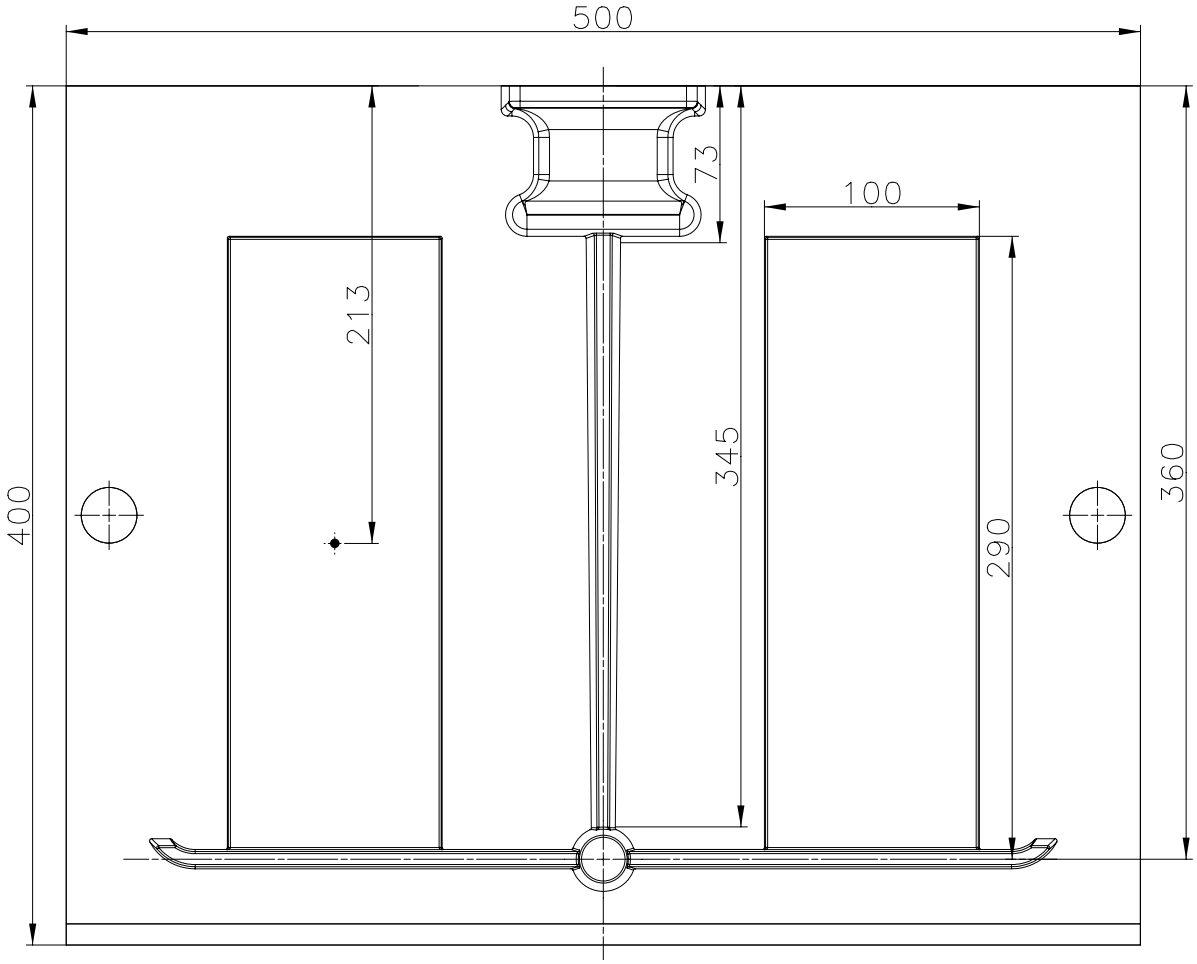

Figure 4.23 Third basic layout. 300 mm/s melt front velocity.

The important values for the gating system are shown below:

Plate thickness		2 mm	3 mm	4 mm
Drawing number		26D0180	26D0190	26D0200
Choke area (Design)	mm^2	59	88	118
Choke area (Real)	mm^2	63	91	120
Initial speed at choke	mm/s	2595	2595	2595
Area under cup (Design)	mm^2	157	235	313
Area of the horizontal runner (Design)	mm^2	200	300	300
Section size of the horizontal runner (Design)	mm	9/7/25	9/7/37.5	9/7/37.5
Area of the horizontal runner (Real)	mm^2	205	314	307
Area ratio Runner/Choke (Design)		3,4	3,4	2,5
Initial melt front speed in the horizontal runner (Design)	mm/s	382	382	509
Initial melt front speed in the horizontal runner (Real)	mm/s	398	376	505
Initial melt front speed in the plates (Design)	mm/s	382	382	382
Initial melt front speed in the plates (Real)	mm/s	408	394	388
Mean melt front speed in the plates (Design)	mm/s	300	300	300
Mean melt front speed in the plates (Real)	mm/s	321	310	305
Final melt front speed in the plates (Design)	mm/s	172	172	172
Final melt front speed in the plates (Real)	mm/s	184	178	175
Theoretical filling time of the plates (Design)	s	0.95	0.95	0.95
Theoretical filling time of the plates (Real)	s	0.89	0.92	0.94

Table 4.5 Important dimensions of the 3 layout.

Some deviations between the calculated dimensions and the real dimensions of the gating systems are seen. Making gating systems in wood is not an exact science; one always has to check the actual dimensions before proceeding. The real dimensions have been used in the calculations for determining the loss coefficients.

The trials were made under the same conditions as the previous trials, i.e. with ductile iron and with a pouring temperature of 1370 °C.

As in the previous sections the effect from surface tension is extracted from the results before the loss coefficient is found. This is done to get a better fit between the shapes of the measured and theoretical curves showing the melt front level as a function of time. The impact from surface tension on the loss coefficient for the complete filling of the plates is found in section 4.3.1 for a mean melt front velocity of 120 mm/s. The effect from surface tension can be seen as a constant reduction in driving pressure through the complete filling sequence of the plates. This means that the influence from surface tension is independent of melt front velocity. That can also be seen in Appendix 4.4 where the melt front levels in the plates calculated with and without the effect from surface tension are plotted for a mean melt front velocity of 300 mm/s.

4.5.1 4 mm Plates

A snapshot from the filling of the 4 mm plates can be seen on Figure 4.24. The pouring cup was unfortunately not kept completely full during the filling of the plates. It gets more difficult to keep the pouring cup completely filled as the pouring rate is increased. The melt front levels in the plates have been plotted as a function of time on Figure 4.25. Theoretical levels for different loss coefficients are also shown.

The driving pressure used in the calculations of the theoretical melt levels has been reduced according to the real melt level in the pouring cup.

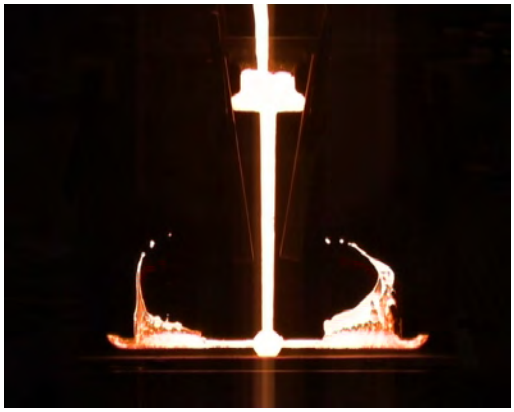

Figure 4.24 Snapshot from the initial filling of the 4 mm plates.

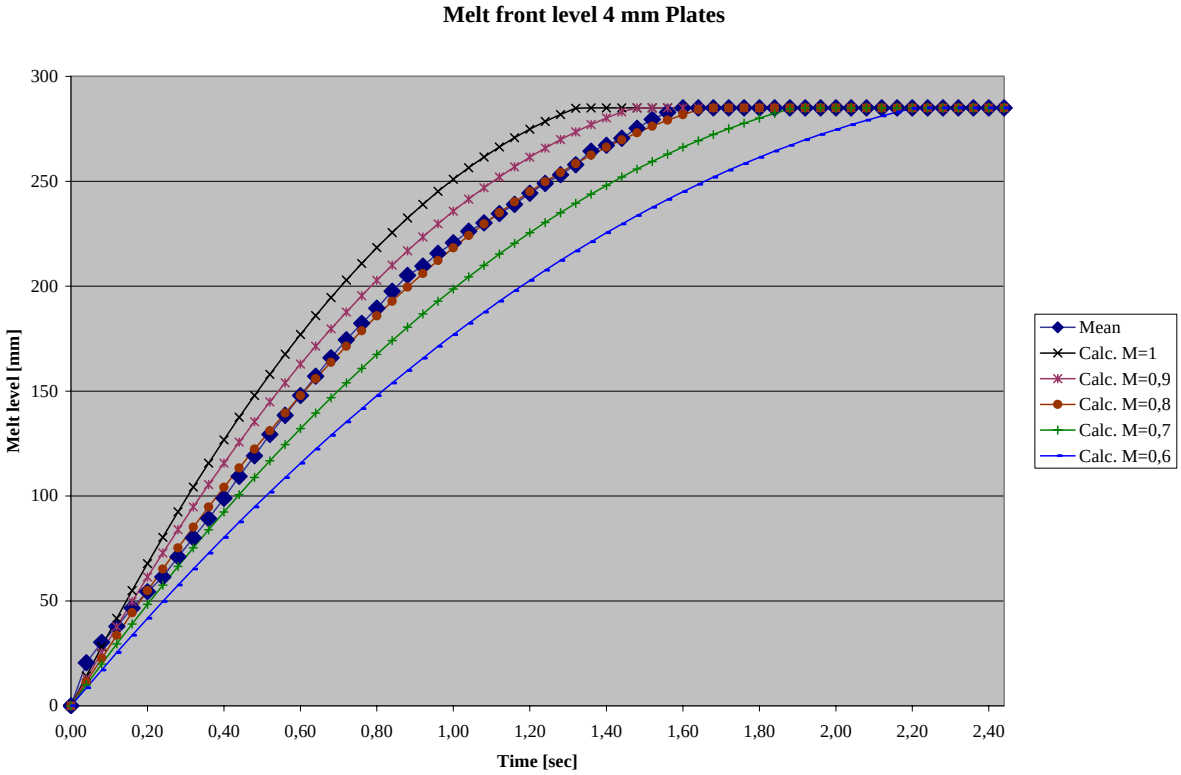

Figure 4.25 Measured and theoretical melt front levels as a function of time.

The measured melt front level is a little ahead of the theoretical melt front level during the first 0.2 s. This is caused by difficulties in determining the melt front levels right at the beginning where melt is blown into the plates; this can be seen on Figure 4.24. For the rest of the filling sequence the fit between measured data and theoretical data for a total loss coefficient of 0.8 is very good. The effect from surface tension has been extracted from the loss coefficient as described in section 4.3.1. The influence from surface tension is very small for the 4 mm plates. The loss coefficient has to be reduced with approximately 0.03 if the influence from surface tensions has to be included.

4.5.1.1 Filling of the down runner well and the horizontal runner

Besides giving data for determining the loss coefficient, the videos of the filling sequences contain other interesting information. Snapshots showing the initial filling of down runner well and the horizontal runner of the 4 mm plates are shown below:

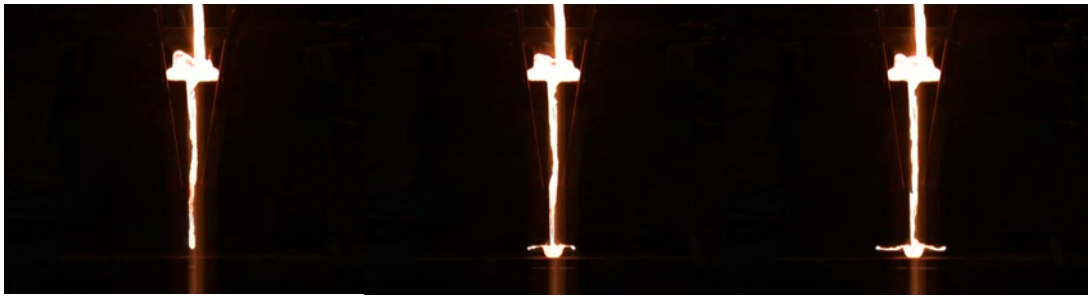

Time 0.36 s Time 0.40 s Time 0.44 s

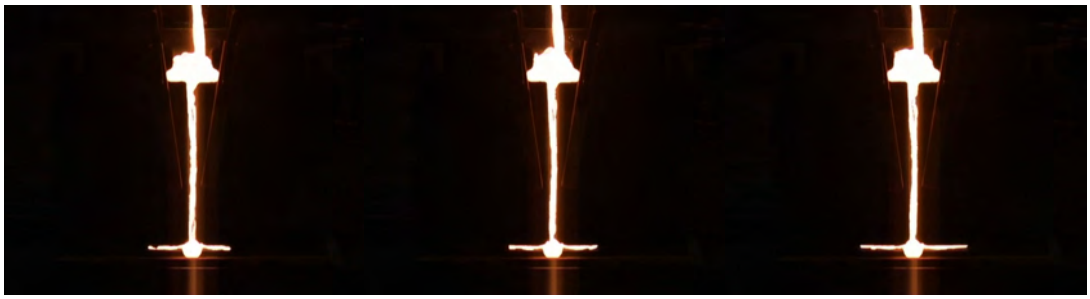

Time 0.48 s Time 0.52 s Time 0.56 s

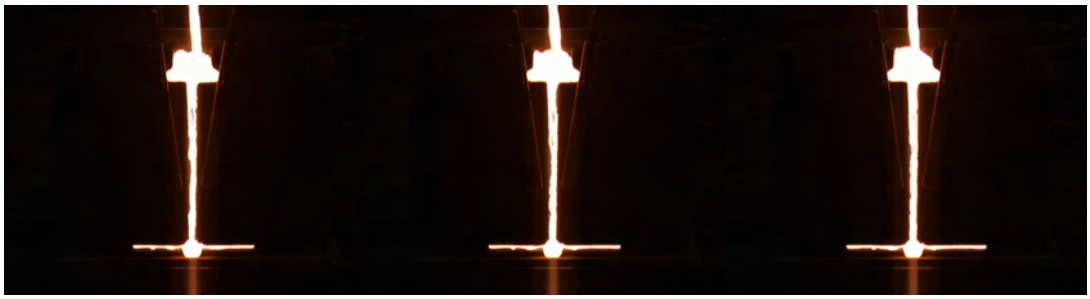

Time 0.60 s Time 0.64 s Time 0.68 s

Time 0.72 s Time 0.76 s Time 0.80 s

Figure 4.26 Snapshots showing the initial filling of the down runner well and the horizontal runner. Times given are from the first melt enters the pouring cup.

The initial melt flow through the down runner well and the horizontal runner is showed on the enlargements below:

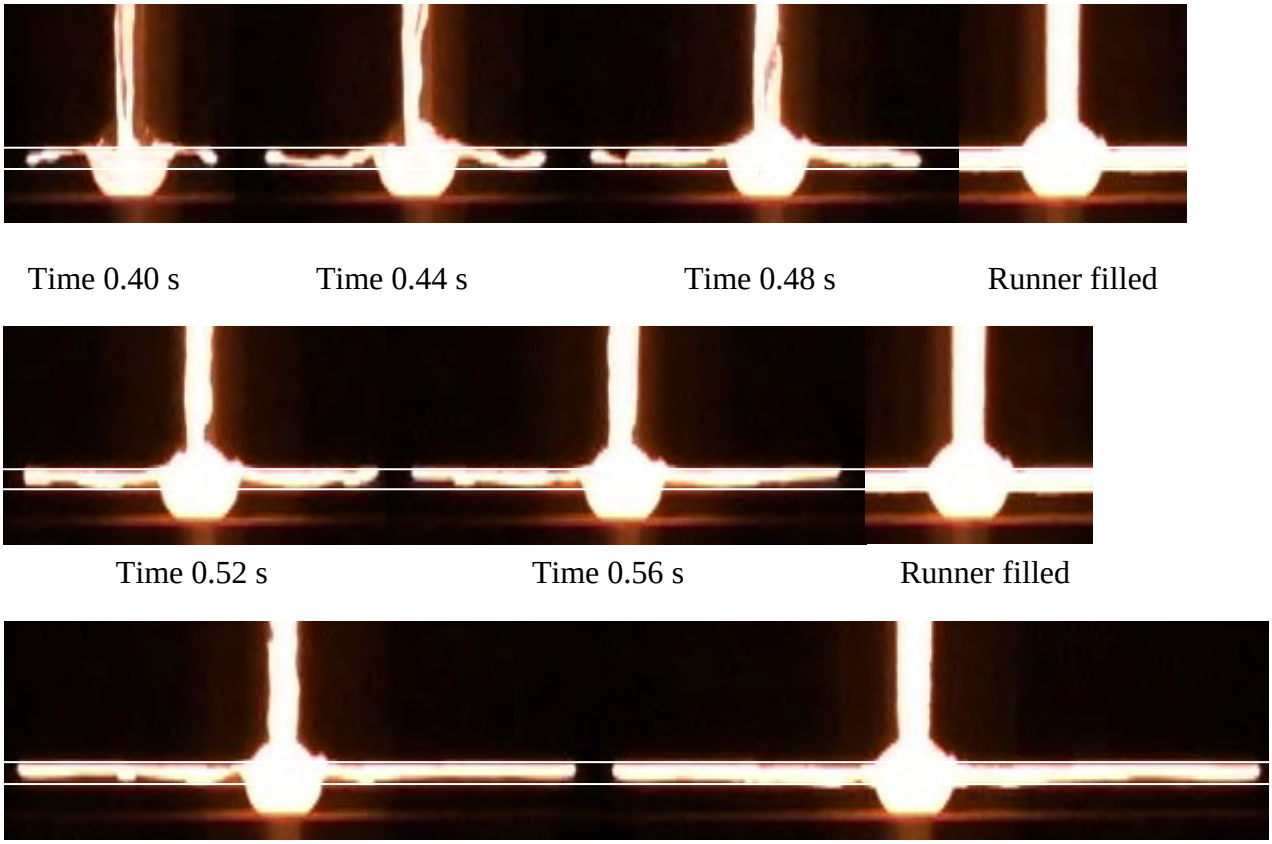

Figure 4.27 Enlargements of the down runner well. Times given are from the melt enters the pouring cup. The white lines indicate top and bottom of the horizontal runner.

Pictures of the completely filled runner are also shown on Figure 4.27 for comparison.

The cross section of the horizontal runner is not completely filled when the first melt passes through it. But what is more surprising; the initial flow takes place at the top of the horizontal runner, and not along the bottom surface as expected. This is due to the shape of the transition from vertical to horizontal runner and the velocity of the metal. The metal is reflected from the bottom of the well ending up at the top of the horizontal runner.

For maintaining a high melt quality the cross sections of the runners have to be completely filled when the first melt passes through. Partly filled runner cross sections can lead to many different problems as for instance excessive oxide formation.

The well is a cylinder Ø30 mm, 45 mm deep with 5 degree draft. The vertical dimension of the horizontal runner is 9 mm. The well has to handle a melt flow rate of 248 cm^3/s in the initial phase when calculated without losses.

4.5.1.2 Melt flow pattern in the plates

Snapshots from the initial filling of the 4 mm plates can be seen below. They are from the same filling sequence as discussed above.

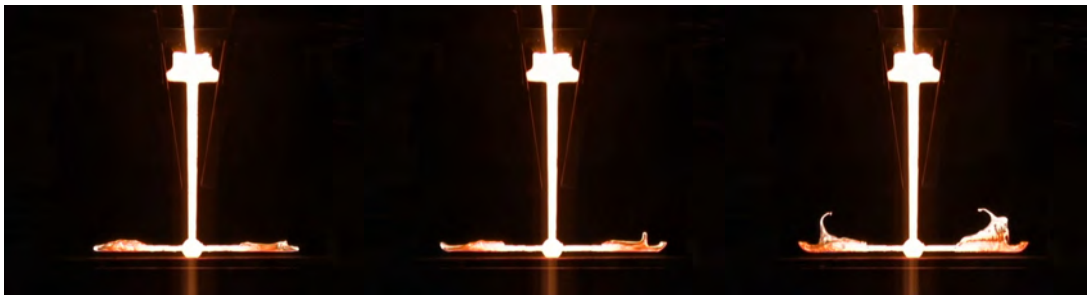

Time 0.96 s Time 1.00 s Time 1.04 s

Time 1.08 s Time 1.12 s Time 1.16 s

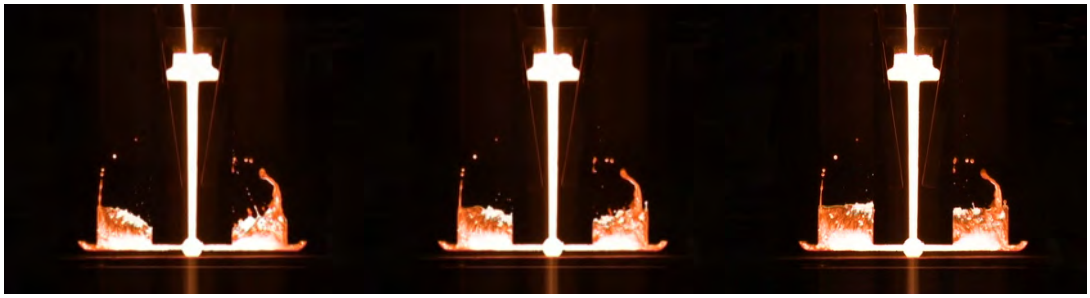

Time 1.20 s Time 1.24 s Time 1.28 s

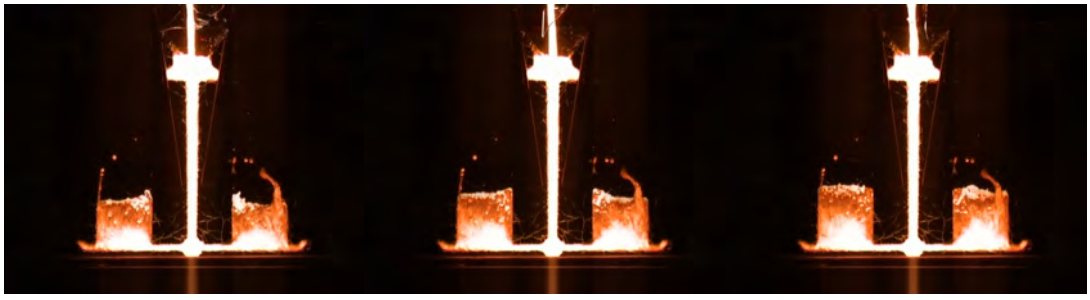

Time 1.32 s Time 1.36 s Time 1.40 s

Figure 4.28 Snapshots from the initial filling of the 4 mm plates. Times given are from the first melt enters the pouring cup.

The melt fronts are very unstable in the initial part of the filling. Melt splashes are shot more than 150 mm into the plates ahead of the main melt front. When looking at the casting after it is taken out of the mould is it seen that the melt jets are not remelted and they would have given problems if this had been a real casting. I.e. in this case the braking forces in the system are not strong enough to keep the melt fronts together. The velocity of the melt shooting into the plates between 1.00 and 1.08 s is found from the snapshots to be approximately 1500 mm/s. This even though the melt front velocity in the horizontal runner is approximately 500 mm/s. I.e. very high local velocities can be found.

The cross section of the horizontal runner is almost, if not completely, filled when the melt fronts reach the ends of the runner. Hence no buffers exist when the melt fronts hit the ends of the runner. The melt comes to an abrupt stand still and the dynamic energy is converted into static pressure resulting in a pressure shock wave in the melt. The shock wave shoots the metal into the plate cavities.

In section 2 some of the dimensionless numbers used to describe flow have been discussed. The velocity can be found in the equations for most of these numbers. The use of the dimensionless numbers is difficult when large variations in local velocities can be found. From section 2.4 the Weber number can be calculated for the 4 mm plates discussed here. The physical data found for a ductile iron in section 2.7 is used for the calculations. With a melt front velocity of 1500 mm/s it is found to 16.4. When calculating the Weber number with the mean velocity of the melt when entering the plates given in Table 4.5, i.e. 388 mm/s the Weber number is 1.1.

The melt flow in the initial phase takes place at the outside edge of the plates. On the picture sequence on Figure 4.28 it looks as if the preferred flow path is moving towards the middle of the plates. The flow is taken place at the outside edge of the plates later in the filling sequence. This can be seen on Figure 4.29.

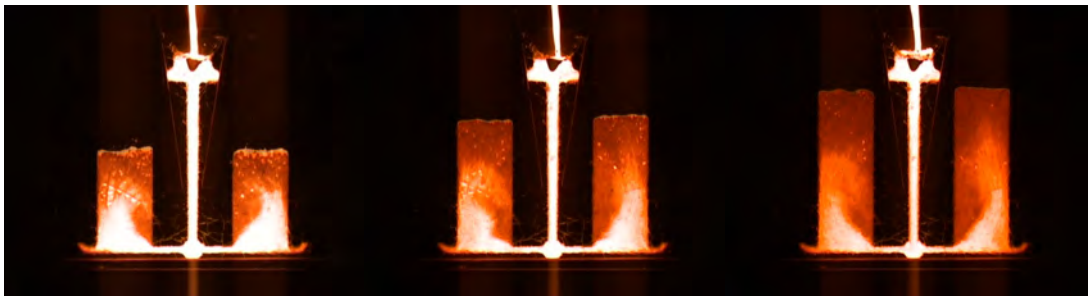

Time 1.68 s Time 2.00 s Time 2.44 s

Figure 4.29 Snapshots from the last part of the filling of the 4 mm plates. Times given are from the first melt enters the pouring cup.

The shift from flow at the outside edges to the middle of the plates and then back again to the outside edges is controlled by the balance between dynamic and braking forces in the system. The shock wave initiated when the horizontal runner is filled has also an influence on the flow pattern. This will be showed with an example in section 4.7.2.2.

The first melt is blown to the ends of the horizontal runner by inertia forces resulting in early melt flow at the outside edges of the plates. The melt at the ends of the horizontal runner is re-

latively cold, making it more feasible for flow to take place at the middle of the plates. At some stage the melt flow at the ends of the horizontal runner, although it is low, is together with heat conduction able to heat the ends up; again making it more feasible for the flow to take place here.

The flow is shifted towards the outside edge of the plates in the later stages of the filling sequence even though the dynamic forces are getting smaller due to decreasing melt flow velocity as the filling proceeds.

I.e. very delicate balances decide where the main flow takes place. This makes it very difficult to predict the flow pattern and hence the temperature distribution. This will be showed more detailed with the 3 mm plates. As mentioned the shock wave has also an influence on the flow pattern; making it even more difficult to predict the flow within this type of gating system.

4.5.2 3 mm Plates

A snapshot from the filling of the 3 mm plates is shown in Figure 4.30. The melt front level in the trials and the theoretical melt level can be seen on Figure 4.31. It has not been possible to keep the pouring cup completely full during the filling sequence. The driving pressure used for the calculations of the theoretical curves on Figure 4.31 has been reduced according to the real melt level in the pouring cup.

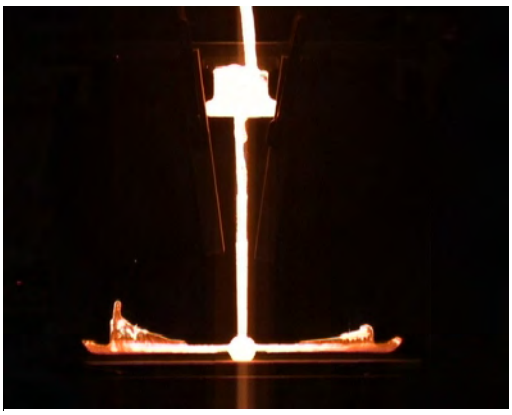

Figure 4.30 Snapshot from the initial filling of the 3 mm plates.

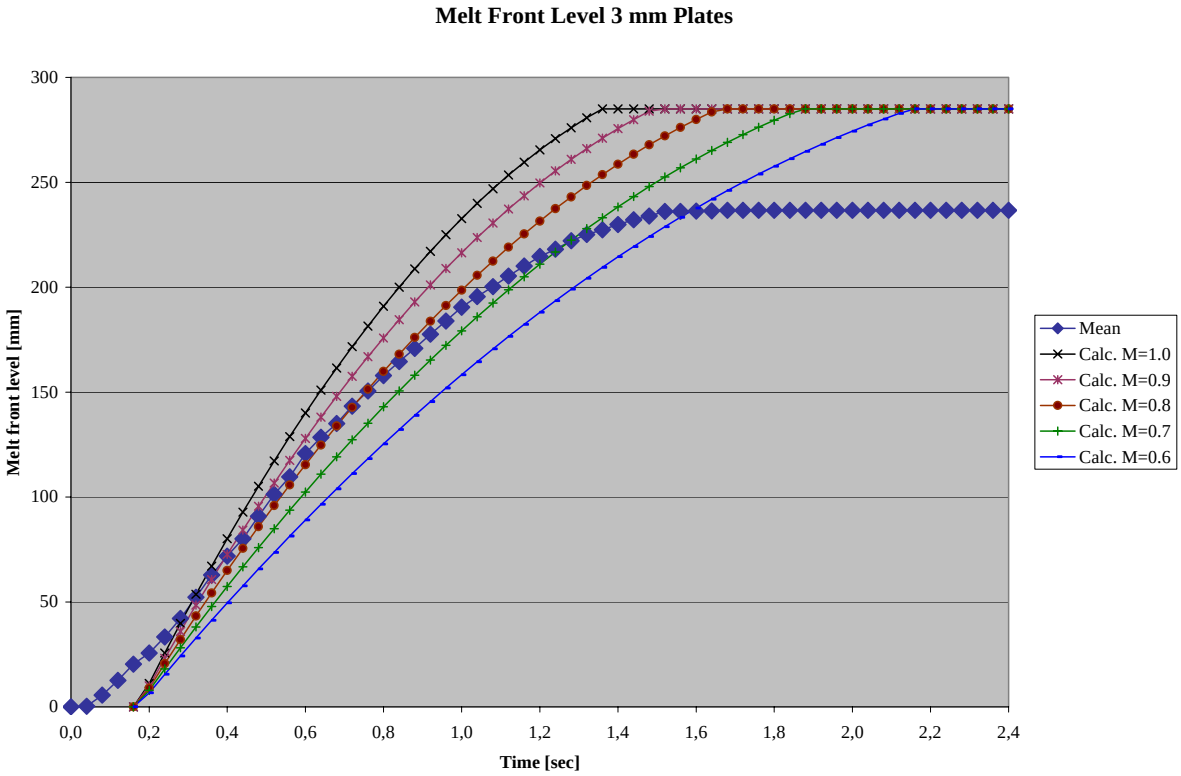

Figure 4.31 Measured and theoretical melt front levels as a function of time.

The melt fronts are seen to move very slowly compared to the theoretical curves in the first 0.2 s of the filling sequence. This is due to an air pocket in the down runner, which will be discussed later. When shifting the theoretical curves parallel to the time axis and comparing slopes, the best fit between theoretical and measured data is found for a loss coefficient of 0.8 for the complete layout. The effect from surface tension has been extracted from the loss coefficient as described in section 4.3.1. The total loss coefficient has to be reduced to 0.75 if the influence from surface tension has to be included.

4.5.2.1 Filling of the down runner well and the horizontal runner

Snapshots showing the initial melt passing through the down runner well and the horizontal runner of the 3 mm plate layout are shown below:

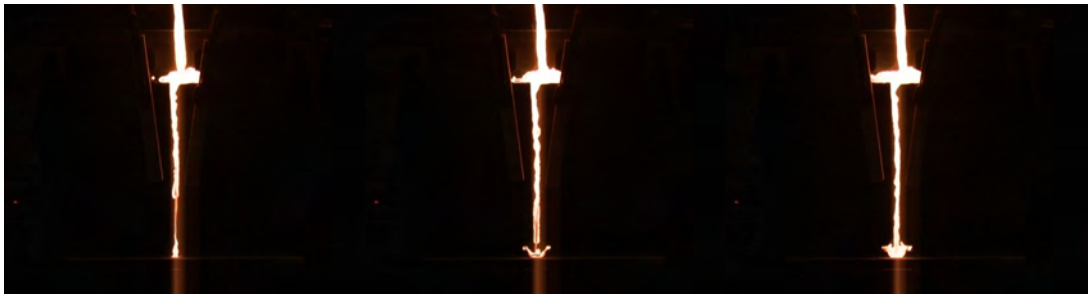

Time 0.36 s Time 0.40 s Time 0.44 s

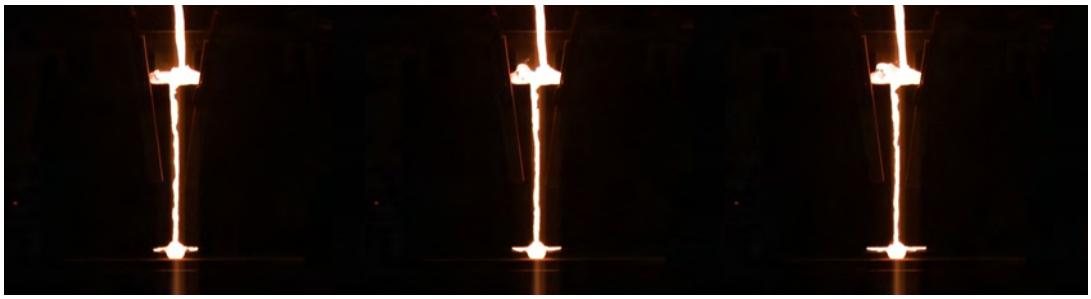

Time 0.48 s Time 0.52 s Time 0.56 s

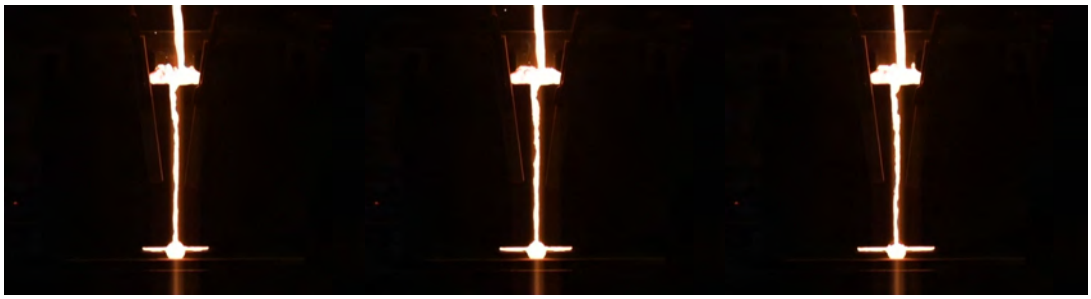

Time 0.60 s Time 0.64 s Time 0.68 s

Time 0.72 s Time 0.76 s Time 0.80 s

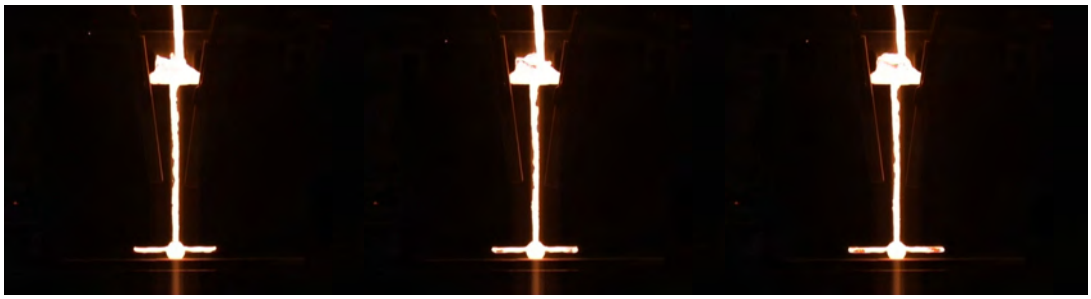

Time 0.84 s Time 0.88 s Time 0.92 s

Figure 4.32 Snapshots showing the initial filling of the down runner well and the horizontal runner. Times given are from the first melt enters the pouring cup.

The filling of the gating system for the 3 mm plates can be compared to the filling of the gating system for the 4 mm plates by comparing Figure 4.32 and Figure 4.26. The melt fronts are seen to proceed at close to the same rate in the two different gating systems.

Enlargements of the transition from vertical to horizontal runner can be seen on Figure 4.33.

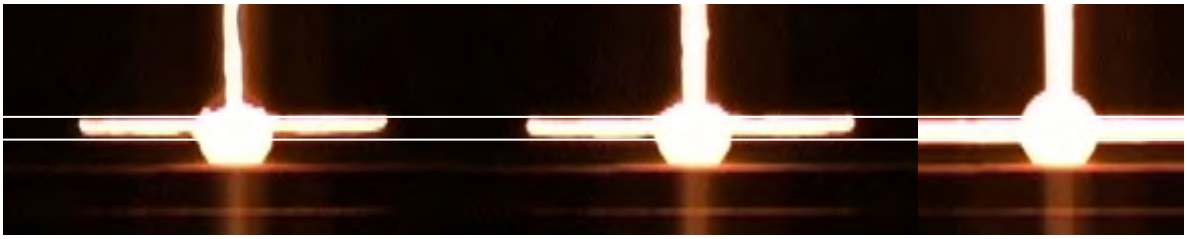

Time 0.68 s Time 0.80 s Runner filled

Figure 4.33 Enlargements of the transition from vertical to horizontal runner.

As with the 4 mm plates the initial melt flow takes place at the top of the horizontal runner with no contact to the bottom surface. This is less pronounced at the 3 mm plate than at the 4 mm plates. The reason for this better performance is the size of the cylinder giving the transition from vertical to horizontal runner. The same size has been used for all 3 plate thicknesses. I.e. the cylinder has to handle a smaller melt flow rate at the 3 mm plate than at the 4 mm plate and hence it is able to perform better.

No melt droplets are blown into the horizontal runner in front of the main melt front; only problems with a partly filled cross section are seen. The small amount of melt reaching the well after 0.36 s acts as a cushion for the main melt flow. The cross section of the down runner is not completely filled on the snapshots shown on Figure 4.32. This together with the small amount of melt going into the well at 0.36 s makes it easier for the well to prevent droplets.

The well is the same as in the previous trials, i.e. a cylinder Ø30 mm, 45 mm deep with 5 degree draft. The vertical dimension of the horizontal runner is 9 mm. The well has to handle a melt flow rate of 177 cm^3/s in the initial phase when calculated with no losses.

4.5.2.2 Melt flow pattern in the plates

Snapshots showing the initial melt flow patterns in the 3 mm plates are showed below. The snapshots are from the same filling sequence as discussed above:

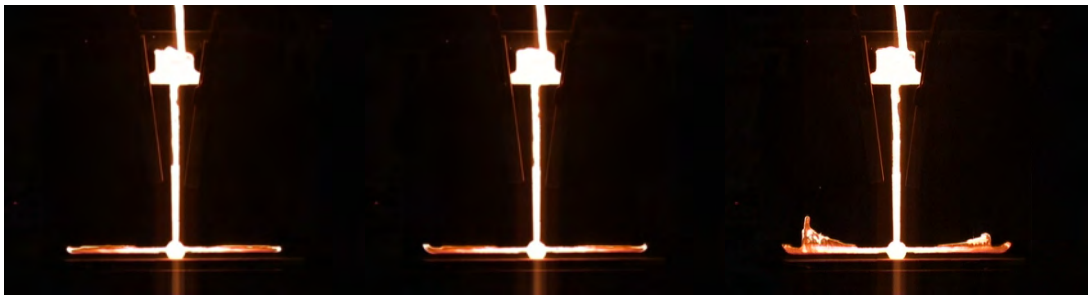

Time 1.40 s Time 1.44 s Time 1.48 s

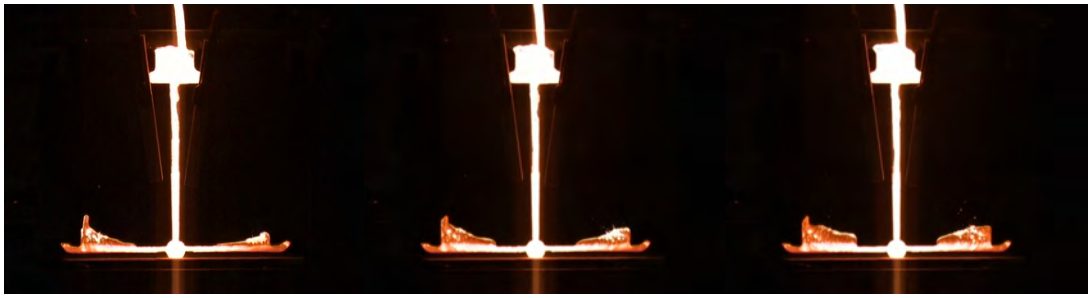

Time 1.52 s Time 1.56 s Time 1.60 s

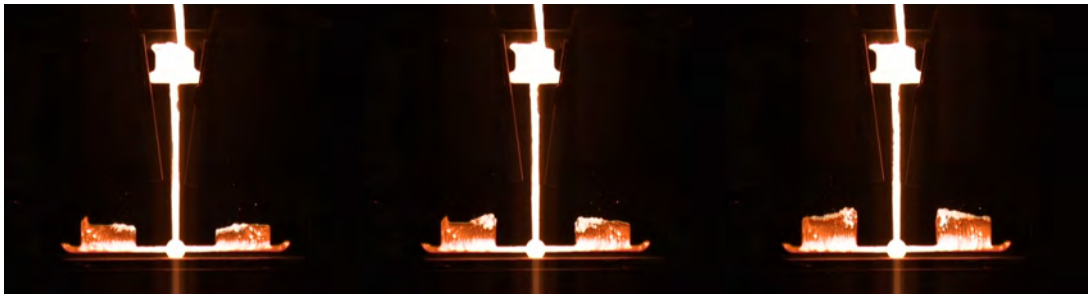

Time 1.64 s Time 1.68 s Time 1.72 s

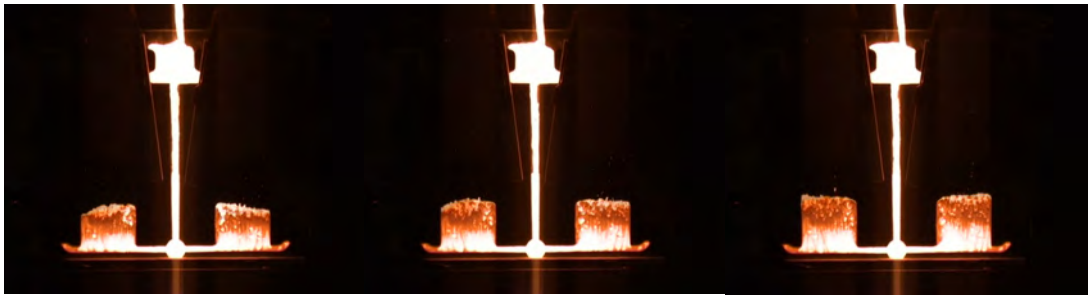

Time 1.76 s Time 1.80 s Time 1.84 s

Figure 4.34 Snapshots from the initial filling of the 3 mm plates. Times given are from the first melt enters the pouring cup.

Compared to the initial filling of the 4 mm plates, the flow is seen to be much more controlled. Only small melt tongues shoot into the plate cavity at 1.48 and 1.52 s. This is partly caused by the smaller plate thickness leading to larger back pressure due to surface tension. The back pressure due to surface tension is known from section 2.5:

$$P_{Surface\ tension} = \frac{2 \cdot \gamma}{T} \qquad \textbf{[Eq. 4.5]}$$

I.e. when reducing the thickness from 4 to 3 mm the back pressure from surface tension will be raised with 1/3.

The back pressure from wall friction in the plates will also increase when the plate thickness is reduced. An estimate for the back pressure from wall friction in the plates assuming laminar flow is found in section 2.7:

$$\Delta P_{Friction\ Laminar} = \frac{64}{Re} \cdot \frac{L}{D_h} \cdot \frac{\rho \cdot V^2}{2} \qquad Re = \frac{\rho \cdot V \cdot D_h}{\mu} \qquad \textbf{[Eq. 4.6]}$$

An estimate for the back pressure from wall friction in the plates assuming turbulent flow is also found in section 2.7:

$$\Delta P_{Friction\ Turbulent} = \lambda \cdot \frac{L}{D_h} \cdot \frac{\rho \cdot V^2}{2} \qquad \frac{1}{\sqrt{\lambda}} = -0{,}87 \cdot \ln\left(\frac{2{,}51}{Re \cdot \sqrt{\lambda}} + \frac{0{,}27 \cdot K_s}{D_h} \right) \qquad \textbf{[Eq. 4.7]}$$

Using the same material parameters as used in section 2.7 for flow of ductile iron in green sand moulds, and calculating the back pressure when the melt front has reached the middle of the plates, i.e. with L = 0.140 m and 275 mm/s as the melt front velocity yields the following pressure losses in the 3 different plate thicknesses:

Plate Thickness	Re	ΔP friction Turbulent		ΔP friction Laminar	
mm		Pa	mm Fe	Pa	mm Fe
2	1934	679	11	274	4
3	2901	376	6	122	2
4	3869	253	4	69	1

Table 4.6 Back pressure from friction when the melt front level has reached the middle of the plates.

The Reynolds number for the 2 mm plates is below 2300 indicating laminar flow, while it is above 2300 for the 3 and 4 mm plates indicating turbulent flow. Weather the flow is laminar or turbulent especially in the 2 mm plates is hard to say exactly as the value of 2300 for the transition from laminar to turbulent is depending on the actual circumstances the flow takes place under.

As mentioned in section 2.7 this is not exact calculations, strictly seen Eq. 4.6 and Eq. 4.7 are only valid for fully developed flow. But the relative sizes of the back pressures as a function

of plate thickness are probably valid, giving a good indication of what happens when changing the wall thicknesses. The back pressure from surface tension is given in Table 4.3. The calculated back pressure from friction in turbulent flow is approximately a third of the back pressure from surface tension and the ratio is even smaller when comparing laminar flow to surface tension. Hence the back pressure from surface tension is the significant in this comparison.

Both for turbulent and laminar flow is the size of the friction proportional to the length the metal has travelled in the section. Friction in laminar flow depends linearly on the velocity since the Reynolds number contains the velocity and hence reduces V^2 in the expression for the friction given by Eq. 4.6. As the filling progresses the flow length growths but on the other hand the velocity decreases at the same time. Hence the two factors work against each other. The friction when the melt reaches the top of the plates is given in Table 4.7. The velocity is approximately 158 mm/s, and the flow length is 0.280 m.

Plate Thickness	Re	ΔP friction Turbulent		ΔP friction Laminar	
mm		Pa	mm Fe	Pa	mm Fe
2	1111	487	8	315	5
3	1667	270	4	140	2
4	2223	178	3	79	1

Table 4.7 Back pressure from friction when the melt front level reaches the top of the plates.

I.e. if assuming turbulent flow the losses decrease while the losses increase if assuming laminar flow compared to the losses found when the melt level has reached the middle of the plates. The difference is due to the fact that the losses from turbulent flow follow the velocity squared, while the losses from laminar flow follow the velocity.

During the filling of the last half of the plates, is the contribution to the total loss from friction in the plates relatively constant for both laminar and turbulent flow. The driving pressure when the plates are completely filled is 70 mm. When comparing this to the back pressures from friction given in Table 4.7 are the back pressures from friction in the plates relatively small.

The mass flow in a 3 mm plate is ¾ of the mass flow in a 4 mm plate when the velocities are the same; this means the momentum is reduced with ¼. I.e. at the same time as the back pressure from surface tension and friction increases with decreasing wall thickness, is the momentum decreasing. All three parameters make it hence easier maintain coherent melt fronts when the wall thickness is reduced.

The melt flow velocity in the horizontal runner in the 3 mm plates is lower than in the 4 mm plates; this also helps to reduce the amount of splashes shooting into the 3 mm plates. In both cases the ratio between the area of the horizontal runner and the choke is relatively big. For the 3 mm plates is the ratio 3.4 and for the 4 mm plates is it 2.5. At these high ratios a relatively small change in ratio will not change the flow pattern; hence the influence from the different relative sizes of the horizontal runner compared to the choke is insignificant. This lack of influence from the horizontal runner on the flow at the conditions investigated here is sup-

ported by trials described in section 4.6. At these trials the horizontal runner has been reduced significantly without having influence on the flow pattern.

The preferred flow path seems to shift to the middle of the plates at 1.80 s, see Figure 4.34. But this changes later in the filling sequence. The preferred flow path at the end of the filling is at the outside edge of the plates as seen below:

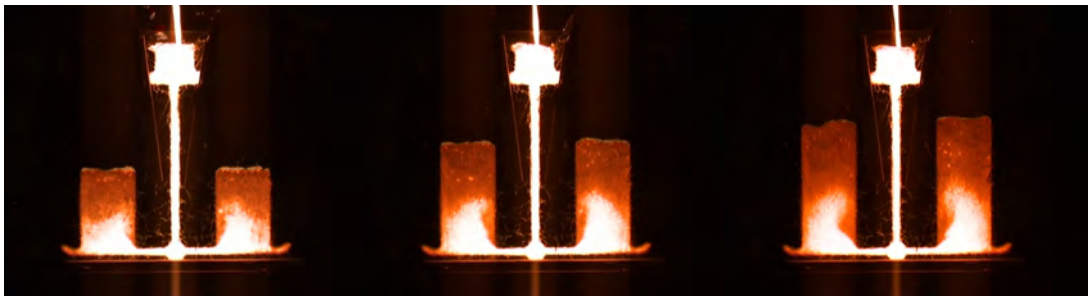

Time 2.12 s Time 2.36 s Time 2.60 s

Figure 4.35 Snapshots from the last part of the filling of the 3 mm plates. Times given are from the first melt enters the pouring cup.

One could expect the opposite as the back pressure from the growing melt level in the plates becomes larger as the filling proceeds meaning lower flow velocities resulting in lower momentum, which again should make the flow more prone to take a path up the inside edges of the plates. But this is not the case. When taking a closer look at the temperature distribution in the horizontal runner the explanation can be found. Enlargements of the horizontal runner are showed on Figure 4.36.

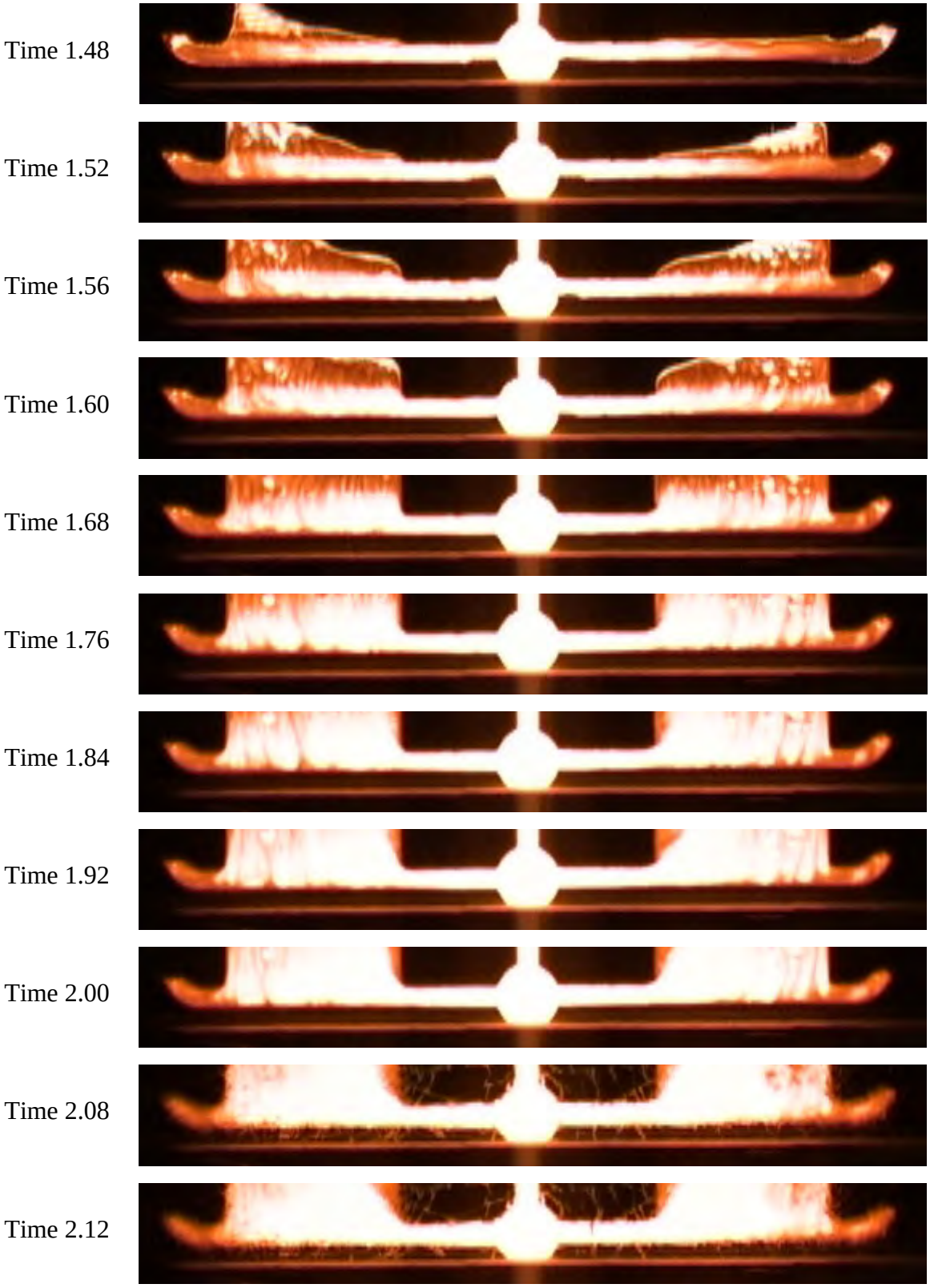

Figure 4.36 Temperature distribution in the horizontal runner of the 3 mm plate. Times given are from the melt enters the pouring cup.

The relative temperatures in the horizontal runner can be seen from the colours on the pictures. The first cold metal ends up at the far ends of the horizontal runner. During the remaining filling sequence, the ends are reheated lowering the viscosity in this area. This changes the balance between dynamic and braking forces, making it more feasible for the flow to take place at the outside edge of the plates. The change in the balance between braking and dynamic forces takes place to the advantage of the dynamic forces even though the dynamic forces get smaller due to the bigger back pressure. I.e. as mentioned in section 4.5.1.2; the balance between dynamic and braking forces is very delicate.

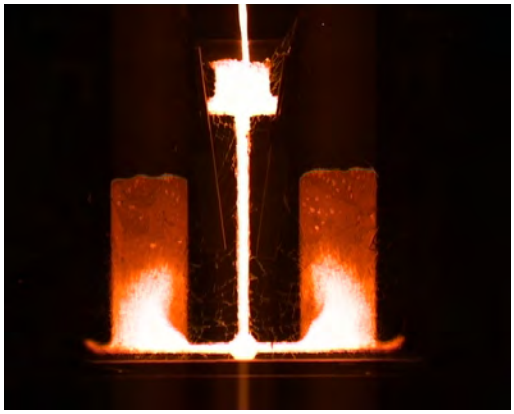

Figure 4.37 The flow does not make a sharp bend around the corner

The metal flow will not make a sharp bend, i.e. for instance make a sharp bend at the corner where the plate attaches to the horizontal runner, see Figure 4.37. This effect gets more pronounced with higher velocities.

The initial melt front velocity in the plates is relative slow compared to the theoretical values. This can be seen on Figure 4.31. The reason for this difference between measured and theoretical values is seen on Figure 4.38. A 100 mm deep air pocket exists in the down runner. Apart from influencing the flow rate it is also the basis for aspiration. Air pockets at the top of the down runner will be discussed more closely in section 4.6.2.3.

Figure 4.38 Down runner at 1.48 s.

4.5.3 2 mm Plates

A snapshot from the filling of the 2 mm plates can be seen on Figure 4.39. The mean melt front level in the left and right plate from the trials and the theoretical melt front levels found for different loss coefficients can be seen in Figure 4.40 below:

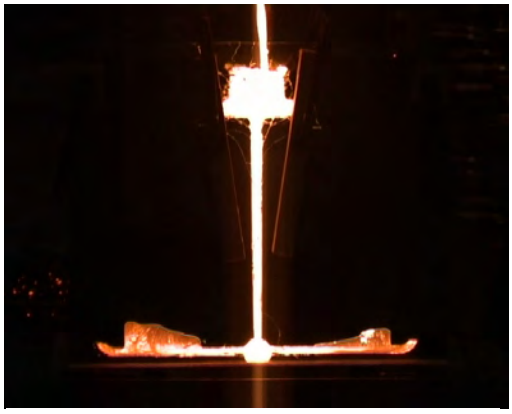

Figure 4.39 Snapshot from initial filling of the 2 mm plates.

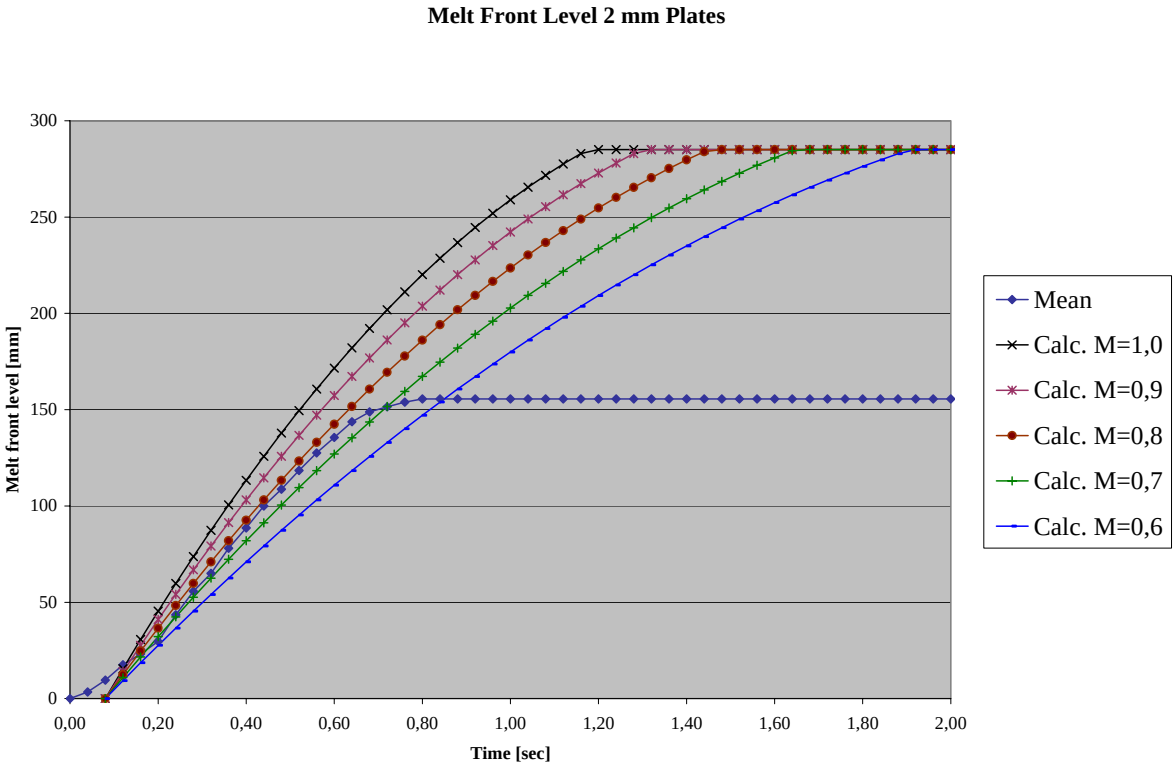

Figure 4.40 Measured and theoretical melt front levels

The melt fronts move relatively slow in the beginning compared to the theoretical curves. The curves have been shifted parallel with the time axis to find the best fit between the slopes of the measured data and the theoretical data. The best fit is found for a loss coefficient between 0.7 and 0.8. The effect from surface tension has been extracted from the loss coefficient as described in section 4.3.1. The loss coefficient has to be reduced to 0.6-0.7 if the influence from surface tensions has to be included.

4.5.3.1 Filling of the down runner well and the horizontal runner

Snapshots showing the initial melt passing through the down runner well and the horizontal runner are shown below:

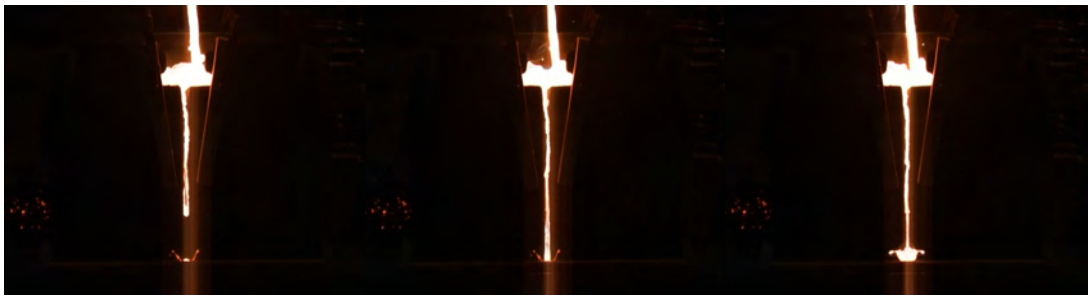

Time 0.40 Time 0.44 Time 0.48

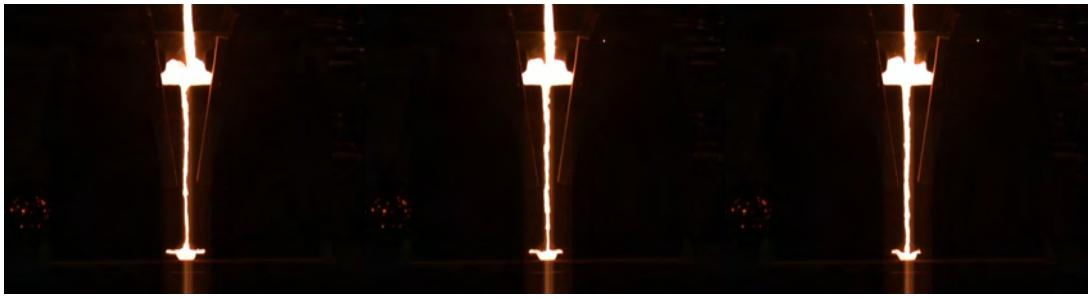

Time 0.52 Time 0.56 Time 0.60

Time 0.64 Time 0.68 Time 0.72

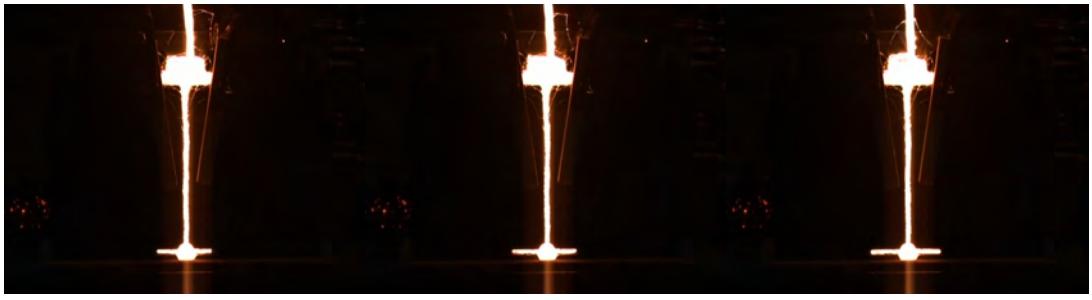

Time 0.76 Time 0.80 Time 0.84

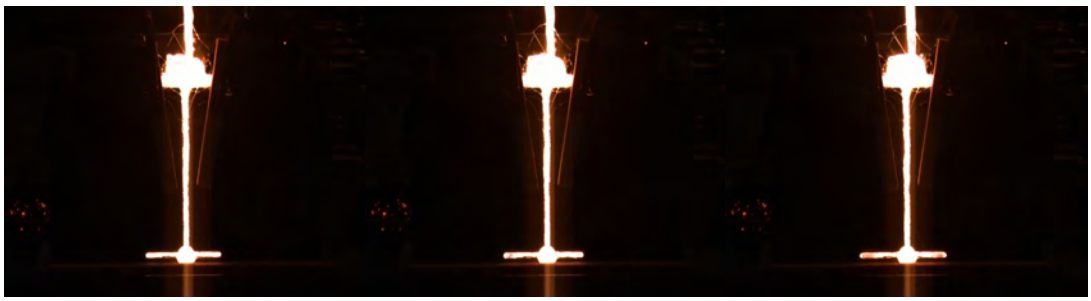

Time 0.88 Time 0.92 Time 0.96

Figure 4.41 Snapshots showing the initial filling of the down runner well and the horizontal runner.

Enlargements of the transition from vertical down runner to horizontal runner can be seen below:

Time 0.68 s Time 0.72 s Time 0.76 s Runner filled

Figure 4.42 Transition from vertical down runner to horizontal runner.

The directional change of the melt is seen to take place in a very controlled manner, with no melt droplets entering the horizontal runner before the main melt front. The cross section of the horizontal runner is almost completely filled right from the first melt enters it. The down runner is not completely filled after 0.96 s. This makes it easier for the down runner well to perform as intended, as the melt flow rate is reduced. A small amount of melt arrives in the well before the main melt stream. This acts as a cushion for the main melt stream, also enhancing the performance of the well.

The well is the same as in the previous trials, i.e. a cylinder Ø30 mm, 45 mm deep with 5 degree draft. The vertical dimension of the horizontal runner is 9 mm. The well has to handle a melt flow rate of 106 cm^3/s in the initial phase when calculated without losses.

4.5.3.2 Melt flow pattern in the plates

Snapshots from the filling of the 2 mm plates can be seen below. The snapshots are from the same filling sequence as discussed above:

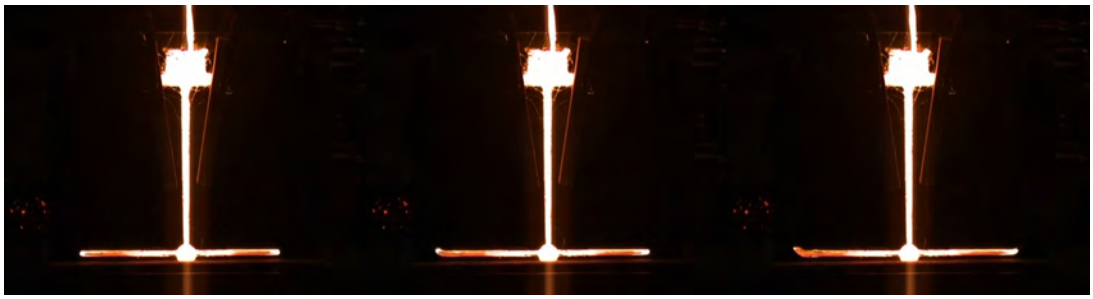

Time 1.36 Time 1.40 Time 1.44

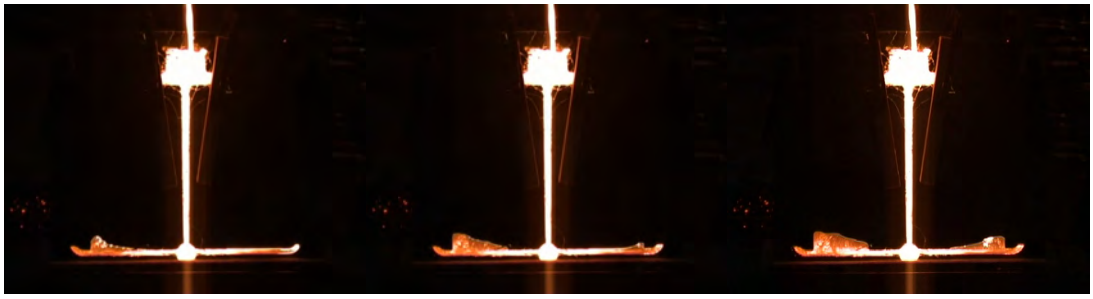

Time 1.48 Time 1.52 Time 1.56

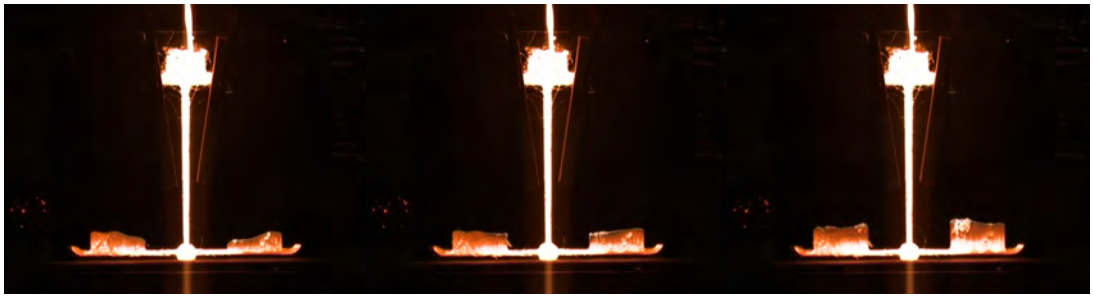

Time 1.60 Time 1.64 Time 1.68

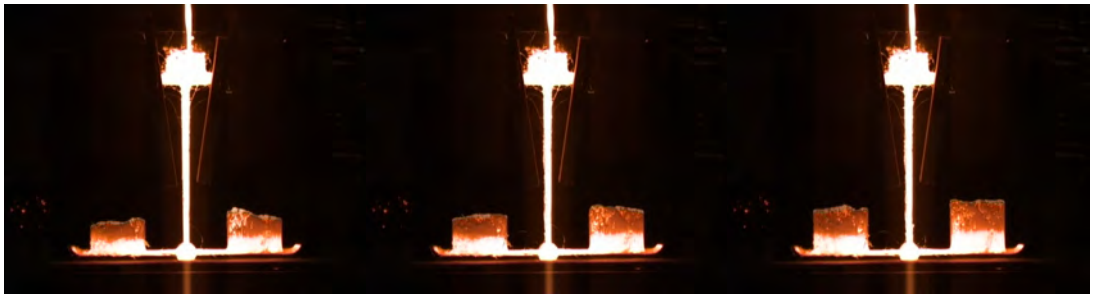

Time 1.72 Time 1.76 Time 1.80

Figure 4.43 Snapshots showing the initial filling of the 2 mm plates. Times given are from the first melt enters the pouring cup.

In this case the initial filling of the plates is seen to be very controlled; no melt is blown into the plate cavities ahead of the main melt front. Both the back pressure from surface tension and the back pressure caused by friction seen in Table 4.6 are getting significant larger when going down in wall thickness. At the 2 mm plates they are able to prevent disintegration of the melt fronts. The melt front velocity in the horizontal runner is the same in the layouts for the 2 mm and 3 mm plates making it possible to compare the two directly.

The preferred melt flow path is in the middle of the plates during the complete filling sequence, see Figure 4.43 and Figure 4.44.

When comparing the flow patterns for the 3 mm plates seen on Figure 4.34 and Figure 4.35 with the flow patterns for the 2 mm plates seen on Figure 4.43 and Figure 4.44 a clear change in preferred flow path is seen. The flow is not shifted to the outside edge of the plates; it takes place at the middle of the plates. I.e. the balance between dynamic and braking forces has shifted to the advantage of the braking forces moving the flow pattern towards the middle of the plates.

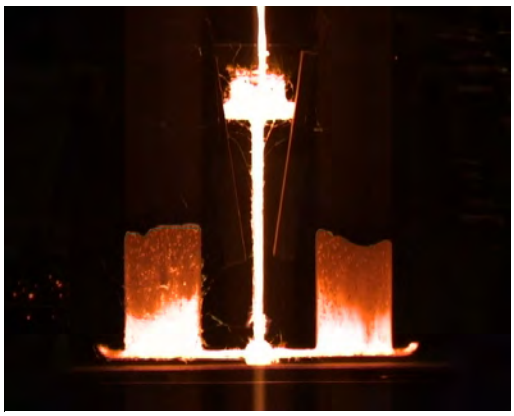

Figure 4.44 Preferred melt flow pattern during the filling sequence.

4.5.4 Summing up on the loss coefficients

The loss coefficients for the 3 and 4 mm plates are found to be 0.8. For the 2 mm plate it is found to be 0.7-0.8. The loss coefficients are without the effect from surface tension. The effect from surface tension lowers the loss coefficient for the 2 mm plate with 0.1 giving a total loss coefficient for the layout for the 2 mm plates of 0.6-0.7. When the surface tension is included in the loss coefficient for the layout for the 3 mm plate it changes to 0.75. The effect from surface tension on the loss coefficients for the layout for the 4 mm plates is very small and can be neglected.

The wall friction in the plates is estimated. The effect from wall friction follows the same trend as the surface tension. I.e. decreasing the wall thickness increases the resistance to flow generated by wall friction.

The losses are found for mean melt velocities of approximately 240 mm/s in the plates. When comparing to the loss coefficients found in section 4.4 no significant differences can be seen. The mean melt velocities in section 4.4 were approximately 100 mm/s in the plates. One has to remember that the investigated velocities are relatively low and hence the direct influence from velocity is small. This is illustrated with the friction losses in the plates given in Table 4.6. The values found are small when comparing to the driving pressure even at the end of the filling where the minimum driving pressure is seen. The expressions for the losses in turbulent and laminar flow follow respectively the square of the velocity and the velocity, i.e. the influence from velocity is quite strong. At higher velocities one can expect the found loss coefficients to depend significantly on the velocity as the absolute values of the losses due to friction grow fast with the velocity.

4.5.5 Summing up on the filling of the down runner well and the horizontal runner

The cylindrical down runner well is not performing as intended at the 3 and 4 mm plates. The first melt is reflected from the bottom of the well and enters the horizontal runner at the top surface of the runner. The melt is able to travel quite a distance before it touches the bottom surface of the runner. For the 3 and 4 mm plates no melt droplets are blown into the horizontal runner in front of the main melt front. The down runner is in both cases not completely filled. The result is reduced melt flow making it possible for the well to prevent droplets being blown into the horizontal runner.

The well performs as intended for the 2 mm plates. No melt droplets enter the horizontal runner before the main melt front, and the cross section of the runner is almost completely filled when the first melt enters. The down runner is again not completely filled, resulting in reduced melt flow through the well, hence making it easier for the well to perform as intended.

The partly filled down runners are caused by partly filled pouring cups. The cross sectional area at the top of the down runner is dimensioned assuming the pressure height from a completely filled pouring cup plus an addition to the cross sectional area of 10 % as a safety margin. If the melt level in the pouring cup is too low it is not possible to maintain the flow necessary to keep the down runner completely filled. Hence one has to use a larger safety margin when dimensioning the cross section at the top of the down runner if partly filled pouring cups are likely to appear. This is especially valid for hand pouring, as partly filled pouring cups is more likely to be seen here compared to when using a automatic pouring device. The direction of the pouring stream will also have some influence on the presence of partly filled down runners. This will be shown with an example in section 4.6.2.3.

The performance of the well cannot be compared to the trials in section 4.4, due to the partly filled down runners. The partly filled down runners make it easier for the well to perform as intended.

The well is in all 3 cases a cylinder Ø30 mm, 45 mm deep with 5 degree draft. The vertical dimension of the horizontal runners is in all 3 cases 9 mm. The theoretical initial melt flow rate is 248 cm^3/s for the 4 mm plates, 177 cm^3/s for the 3 mm plates and 106 cm^3/s for the 2 mm plates. The real melt flow rates are significantly smaller due to the partly filled down runners.

In general the cylindrical well does not perform as intended especially at the higher flow rates. If the well had been enlarged enough it would be able to perform as intended. This has not been done because trials with square shaped wells described in section 6 show much better performance at approximately the same size as utilized here for the cylindrical shaped one.

4.5.6 Summing up on the flow patterns in the plates

The preferred flow paths in the 3 and 4 mm plates are seen to change during the filling sequence. The preferred flow path is at the outside edge of the plates in the beginning, and then it moves towards the middle. Finally it ends up at the outside edge again. I.e. the dynamic forces end up being larger than the braking forces. The balance deciding the flow path is delicate, making it difficult to predict the flow paths.

The main flow path in the 2 mm plates is in the middle of the plates, i.e. in this case the dynamic and braking forces are balanced giving a close to symmetrical heat distribution in the plates. The initial melt flow velocity in the horizontal runner of the 2 and 3 mm plates is designed to be the same, making it possible to compare the two flows directly. The reduction in plate thickness from 3 to 2 mm increases the braking forces, making the preferred flow path shift from the outside edges of the 3 mm plates to the centre of the 2 mm plates.

Below the flow patterns in the plates are compared to the one found in section 4.4. The mean flow velocity in section 4.4 was 120 mm/s here it is 300 mm/s. Both velocities are found when calculating without losses.

Test day	Mean velocity mm/s	Size of horizontal runner	4 mm	3 mm	2 mm
2	120	Big	Centre→Outside	Inside	Inside
3	300	Big	Outside→Centre→Outside	Outside→Centre→Outside	Centre

Table 4.8 Comparison of melt flow paths as a function of melt velocity.

Higher melt velocities mean bigger dynamic forces and an enhanced tendency for the flow to take place towards the outside edge of the plates. This change in flow pattern is for the 3 mm plates shown on Figure 4.45.

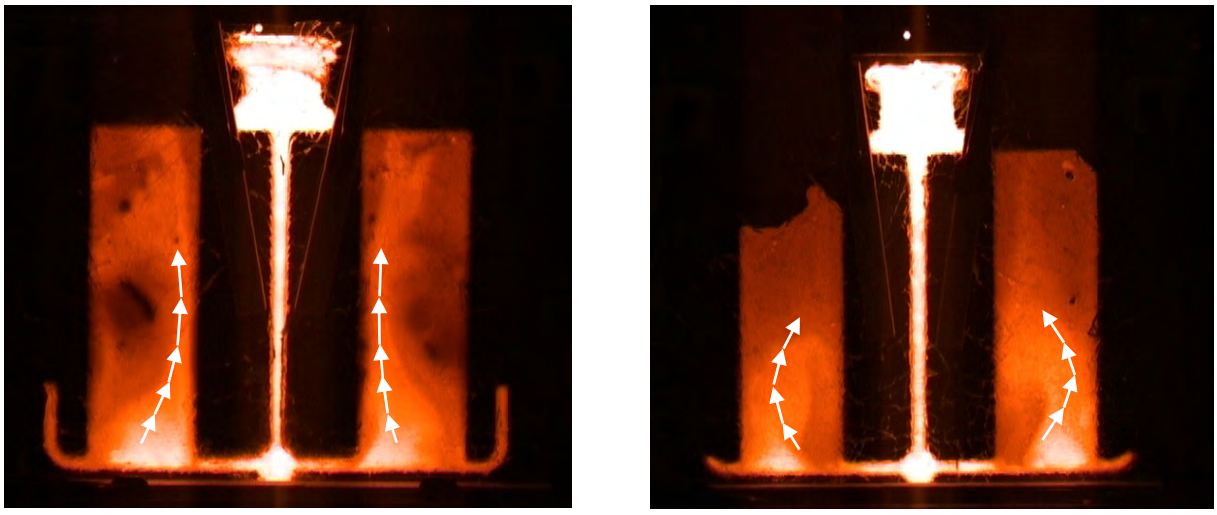

Figure 4.45 Flow patterns in 3 mm plates at 120 and 300 mm/s mean flow velocity.

I.e. even in very thin sections is it possible to change the temperature distribution by varying the flow velocity. This comes in handy if heavier sections are connected to the thin sections. Changing the temperature distribution enhancing high temperatures at the heavier sections makes it possible to get directional solidification towards the heavier sections where a feeder for instance could be connected to the casting.

If an even temperature distribution a cross the plates is wanted, it is in theory possible to choose a design somewhere between the two shown on Figure 4.45 and get the flow to take place through the middle of the plates. With this conventional type of gating system it is hard to control, as the balance between braking and dynamic forces to a large degree controls the flow patterns. If an even temperature distribution is wanted in the plates, it would be much better to design a gating system where the geometry of the runners has 100 % control over the flow pattern. This has been done in [Ref. 4.4], where a fan shaped ingate to the plates has been used. This can be seen on Figure 4.46. The concept can be developed even further. An example of this can be seen in the section 5 with the brake discs.

Figure 4.46 Fan shaped ingate giving good control over the melt flow pattern [Ref. 4.4].

4.6 4. Series of Trials. Melt velocity 300 mm/s. Reduced horizontal runner

In this trial all the parameters have been kept constant compared to the last trial except for the area of the horizontal runner and the design of the ends of the horizontal runner. The area of the horizontal runner has been changed to give an area ratio between the total area of the horizontal runner and the area of the choke of 4. This ratio is still relative large compared to what normally is used [Ref. 4.2], [Ref. 4.5]. The previous trials have shown a tendency for the flow to take place at the outside edge of the plates. Reducing the horizontal runner even more is expected to result in a very unbalanced filling sidewise due to the higher melt velocities gained in the horizontal runner.

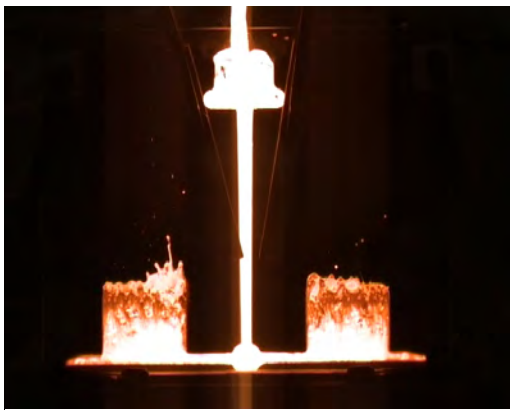

Figure 4.47 300 mm/s melt front velocity, reduced horizontal runner. 3 mm plate thickness.

In the previous trials a 90 degree bend has been added to the ends of the horizontal runner to gradually reduce the velocity of the melt. Unfortunately this design results in a relatively slow initial filling making it possible for the solidification to start before the melt starts to enter the plate cavities. The bends have now been completely removed. The ends of the horizontal runner have been tapered down according to the recommendations in [Ref. 4.2]. The basic layout can be seen on Figure 4.48.

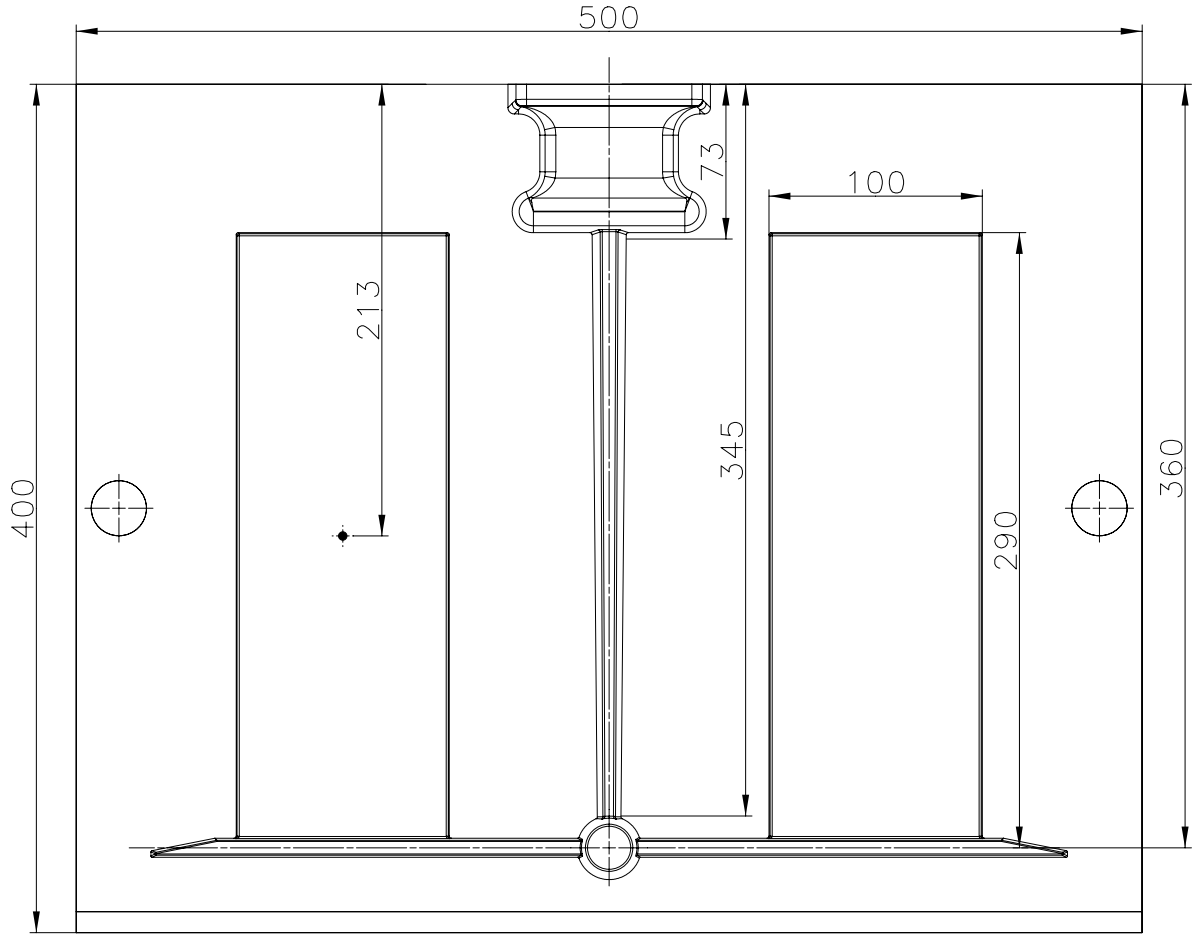

Figure 4.48 Fourth basic layout. 300 mm/sec melt front velocity. Reduced horizontal runner

The important values for the gating systems can be seen in Table 4.9.

Plate thickness		2 mm	3 mm	4 mm
Drawing number		26D0210	26D0220	26D0230
Choke area (Design value)	mm^2	59	88	118
Choke area (Real value)	mm^2	63	91	120
Initial speed at choke	mm/s	2595	2595	2595
Area under cup	mm^2	156	235	313
Area of the horizontal runner (Design)	mm^2	118	177	235
Section size of the horizontal runner (Design)	mm	9/7/14.7	9/7/22.1	9/7/29.4
Area ratio Runner/Choke (Design)		4	4	4
Initial melt front speed in the horizontal runner (Design)	mm/s	649	649	649
Initial melt front speed in the plates (Design)	mm/s	382	382	382
Initial melt front speed in the plates (Real)	mm/s	408	394	388
Mean melt front speed in the plates (Design)	mm/s	300	300	300
Mean melt front speed in the plates (Real)	mm/s	321	310	305
Final melt front speed in the plates (Design)	mm/s	172	172	172
Final melt front speed in the plates (Real)	mm/s	184	178	175
Theoretical filling time of the plates (Design)	s	0.95	0.95	0.95
Theoretical filling time of the plates (Real)	s	0.89	0.92	0.94

Table 4.9 Design and real dimensions of the gating systems.

In this series of trials the effect from surface tension on the loss coefficient has been extracted in the same way as in the previous trials.

4.6.1 4 mm Plates

A snapshot from the filling of the 4 mm plates is shown on Figure 4.49. The pouring cup has not been completely filled during the filling sequence. This can be seen Figure 4.55 and Figure 4.58. The driving pressure used when calculating the theoretical melt front levels has been reduced according to the actual level measured on the snapshots. The measured and theoretical melt front levels are plotted on Figure 4.50.

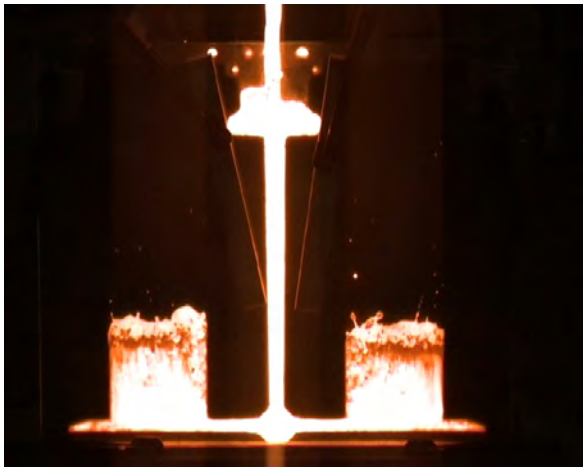

Figure 4.49 Melt stream entering directly into the down runner.

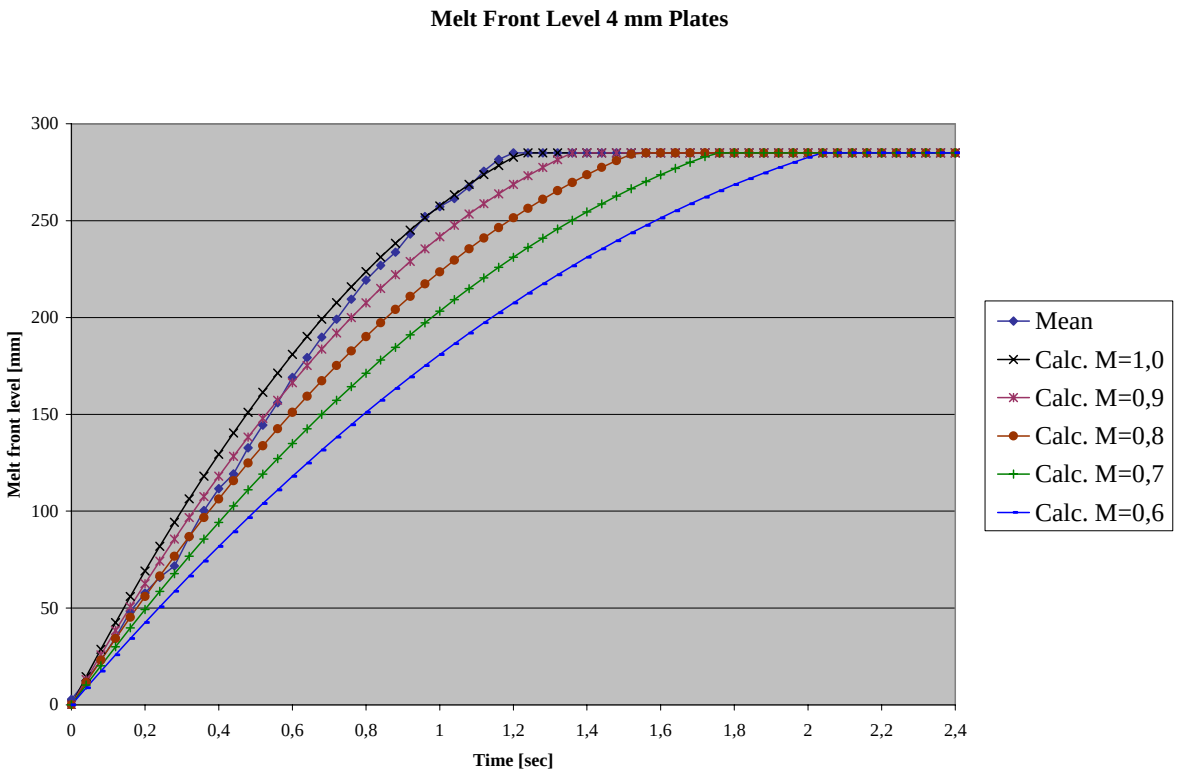

Figure 4.50 Measured and theoretical melt front levels as a function of time.

When looking on the total filling time a loss coefficient of 1, i.e. no losses, seems to be appropriate. The explanation for the apparently loss free system is to be found in the direction of the pouring stream. Snapshots from the filling of the plates are shown on Figure 4.55 and Figure 4.58. The pouring stream goes directly into the down runner on all the pictures. This together with a very low melt level in the pouring cup makes it possible to transfer momen-

tum from the pouring stream into the gating system. This observation is supported by a completely filled down runner during the initial filling of the plates (after 0.64 s), i.e. before back pressure is build up. With a relatively low melt level in the pouring cup, one would expect a partly filled down runner due to the lack of driving pressure. This reason for this is showed in Appendix 4.5. The runner is filled; hence some momentum must be transferred from the pouring stream into the gating system.

The driving pressure used for calculating the theoretical melt front levels on Figure 4.50 has been reduced 22 mm according to the actual melt level in the pouring cup. Making the calculations without a reduction in the driving pressure gives the results shown below:

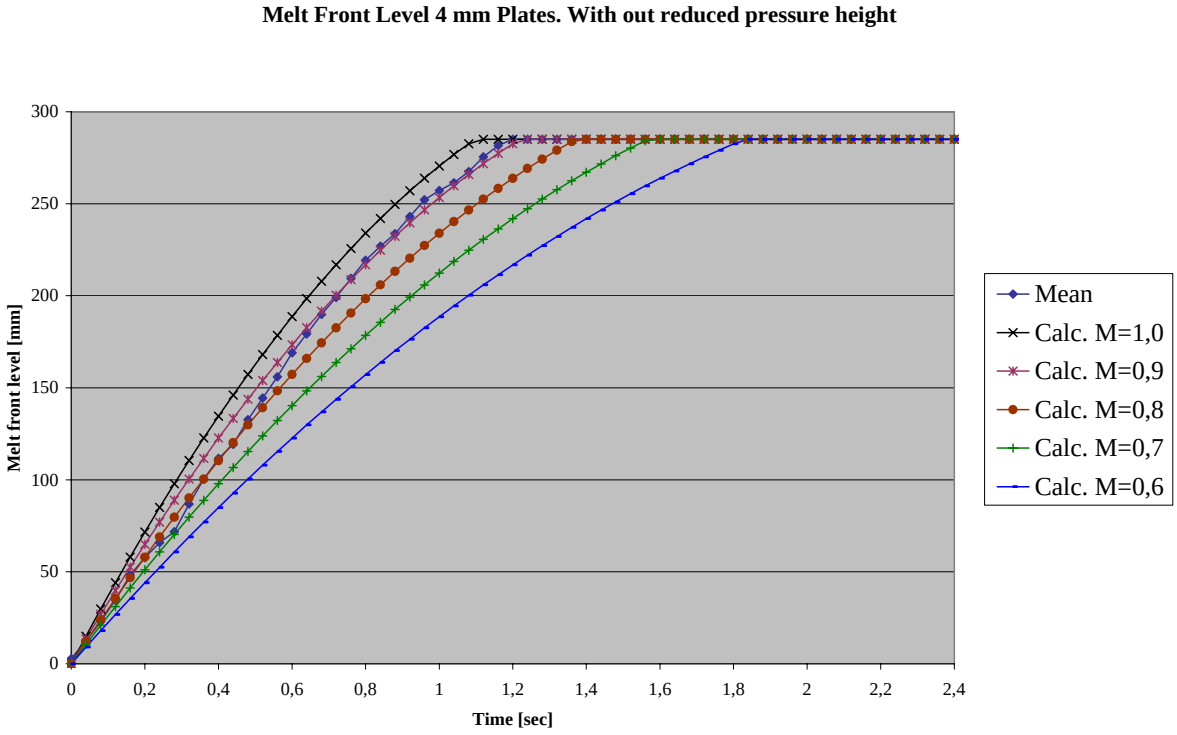

Figure 4.51 Measured and theoretical melt front levels as a function of time. Without reduced pressure height.

I.e. if dynamic pressure equal to about 22 mm ferrostatic height can be transferred into the gating system a loss coefficient of 0.9 is found, which is in line with the values found for the 4 mm plates in the other trials. The effect from transfer of momentum into the gating system on the melt front level is relative large at the end of the filling due to the low driving pressure in the final stage.

A pouring basin will be used in the next trial run to secure better boundary conditions; it will prevent possible transfer of momentum from the pouring stream to the gating system. The pouring basin will also give a well defined driving pressure during the mould filling.

4.6.1.1 Filling of the down runner well and the horizontal runner

Snapshots showing the initial melt passing through the down runner well and the horizontal runner are shown below:

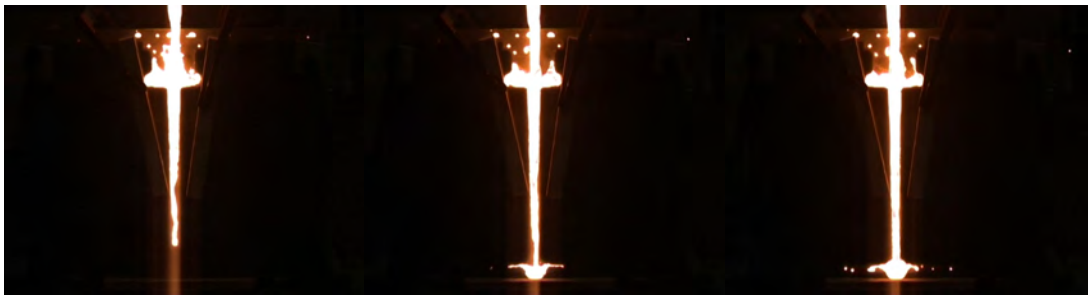

Time 0.20 Time 0.24 Time 0.28

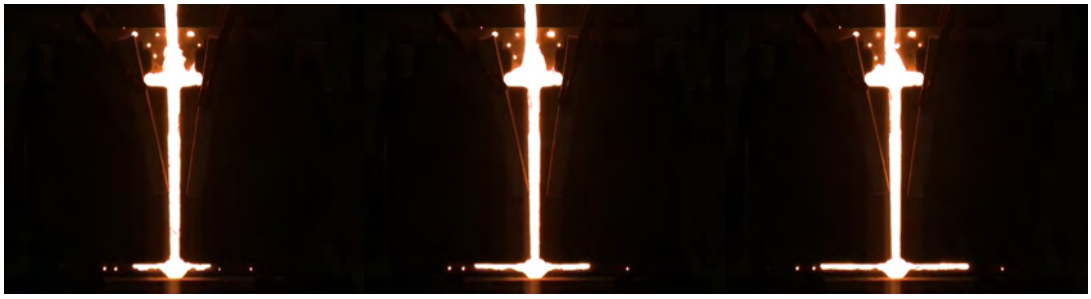

Time 0.32 Time 0.36 Time 0.40

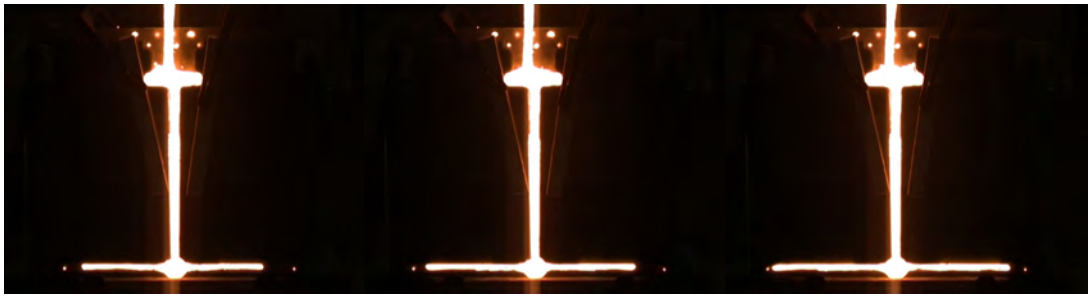

Time 0.44 Time 0.48 Time 0.52

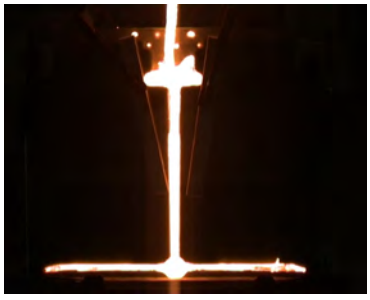

Time 0.56

Figure 4.52 Snapshots showing the initial melt passing through the down runner well and the horizontal runner.

Enlargements of the down runner well can be seen on Figure 4.53.

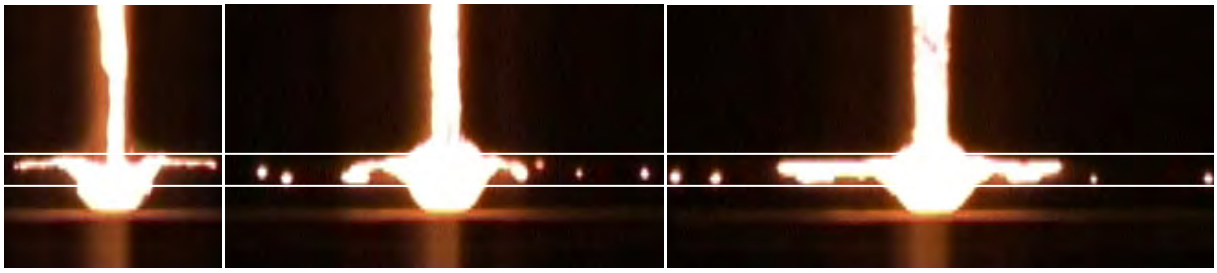

Time 0.24 Time 0.28 Time 0.32

Figure 4.53 Enlargements of the down runner well at the 4 mm plates. The white lines indicate top and bottom of the horizontal runner.

The completely filled runners and well is for comparison shown on Figure 4.54. The well is seen not to perform as intended. The melt is reflected from the bottom of the cylinder, resulting in droplets shooting into the horizontal runner. Again the initial melt flow takes place at the top of the horizontal runner.

The well is the same as in the previous trials, i.e. a cylinder Ø30 mm, 45 mm deep with 5 degree draft. The vertical dimension of the horizontal runner is 9 mm. The well has to handle a melt flow rate of 290 cm^3/s in the initial phase when calculated without losses.

Figure 4.54 Completely filled transition from vertical to horizontal runner

4.6.1.2 Melt flow pattern in the plates

Snapshots from the initial filling of the 4 mm plates are shown below:

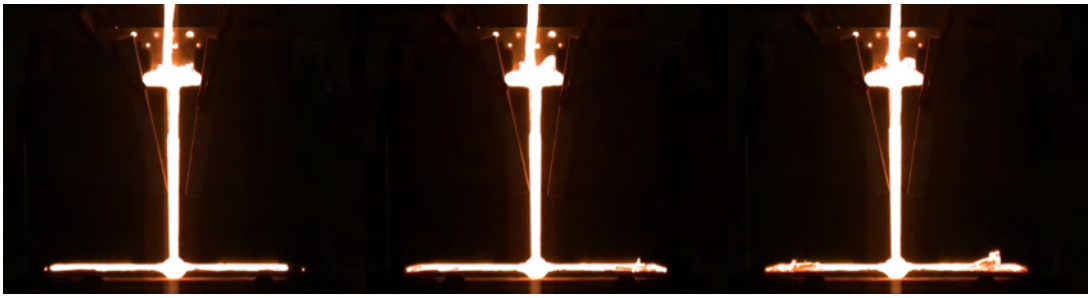

Time 0.52 Time 0.56 Time 0.60

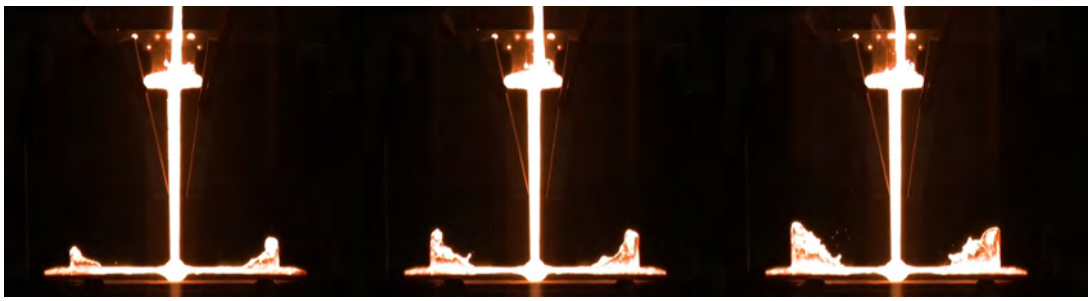

Time 0.64 Time 0.68 Time 0.72

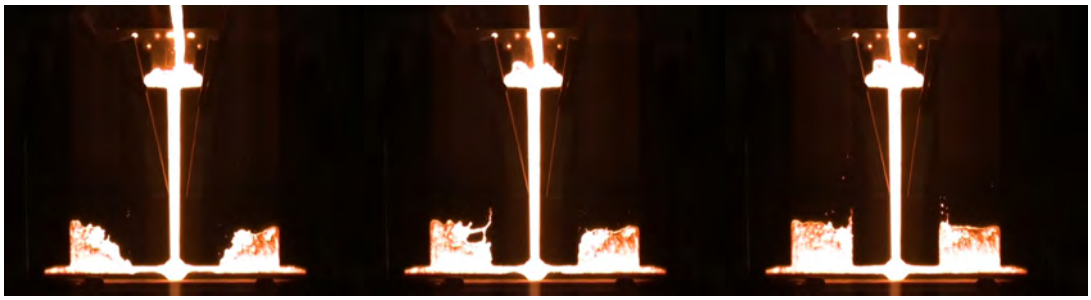

Time 0.76 Time 0.80 Time 0.84

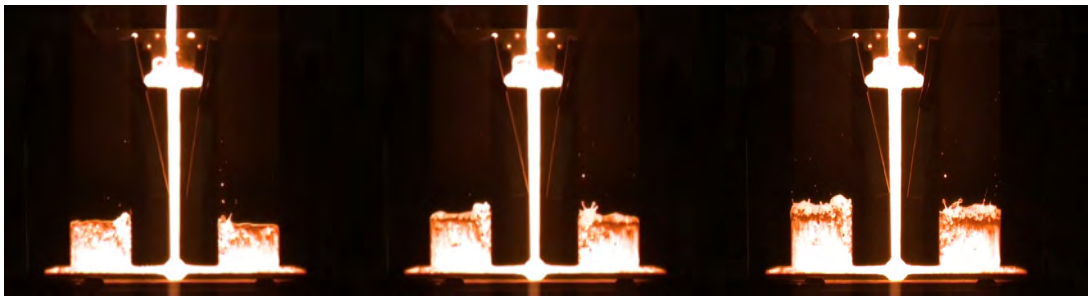

Time 0.88 Time 0.92 Time 0.96

Figure 4.55 Snapshots showing the initial filling of the 4 mm plates.

The initial filling of the plates from 0.52 to 0.80 s takes place without large splashes shooting into the plate cavity. Large splashed were seen at the 4 mm plates in the previous trial, see Figure 4.24.

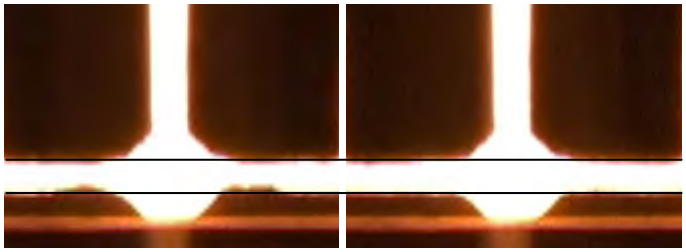

Time 0.80 Time 0.84

Figure 4.56 Air pockets at the down runner well.

Small “explosions” at the melt surface is seen after 0.80 s on Figure 4.55. They shoot melt droplets ahead of the main melt front. The reason for this is a partly filled horizontal runner. Until 0.80 s cavities exist at the sides of the down runner well. See Figure 4.56. The air pockets in the horizontal runner are caused by a vena contracta when the melt leaves the well. I.e. a region with low pressure exists at the sides of the well. The air pockets act as buffers for the hammer effect, when the melt hits the end of the horizontal runner. When the air pockets are closed the dynamic pressure is converted into static pressure.

When talking about pressures in a flowing media a more detailed definition is needed. This is illustrated on Figure 4.57. When measuring the pressure with the tube in the middle of the flow parallel to the stream the effect from the velocity of the flowing media is included in the recorded pressure. And hence the pressure recorded is referred to as the total pressure. On the other hand when measuring the pressure at the wall of the flowing media the effect from the velocity is not included in the recorded pressure. Hence the pressure recorded is called the static pressure. The difference between the total pressure and the static pressure is called the dynamic pressure. It is given by [Ref. 4.6]:

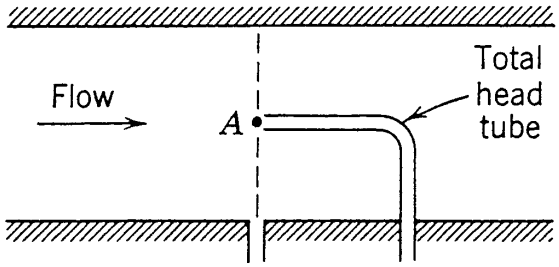

Figure 4.57 Measuring pressure in a flowing media [Ref. 4.6].

$$P_{Dynamic} = 1/2 \cdot \rho \cdot v^2 \qquad \textbf{[Eq. 4.8]}$$

The dynamic pressure can also be seen as the kinetic energy of the flowing media. The kinetic energy is given by:

$$E_{Kinetic} = 1/2 \cdot m \cdot v^2 \qquad \textbf{[Eq. 4.9]}$$

If converting to specific energy by dividing with the volume one yields a pressure equal to the one given by Eq. 4.8. No matter which approach is taking it seems intuitive right that some energy or pressure has to be relieved when the melt comes to an abrupt stand still. It is also important to note that the size of this effect is proportional to the velocity squared. Hence it is quite sensitive to the velocity.

As mentioned above the dynamic pressure has to be relieved after 0.80 s as the last air pockets are closed at this point. At 0.80 s a melt level of 65 mm has been reached in the plates, resulting in a significant back pressure. The back pressure prevents large melt tongues to be blown

ahead of the main melt front as for instance is seen on Figure 4.24. Instead the small “explosions” take place at the melt front. The pressure shock wave is relaxed through the plates and not through the down runner, due to the significantly higher metal head in the down runner than in the plates at 0.80 s.

I.e. because the down runner well has problems with performing as intended, the horizontal runner is not completely filled until rather late in the filling sequence. This delays the pressure shock wave coming from the hammer effect. The result is a change in the timing and appearance of the seen splashed.

The last stages of the filling sequence are seen below:

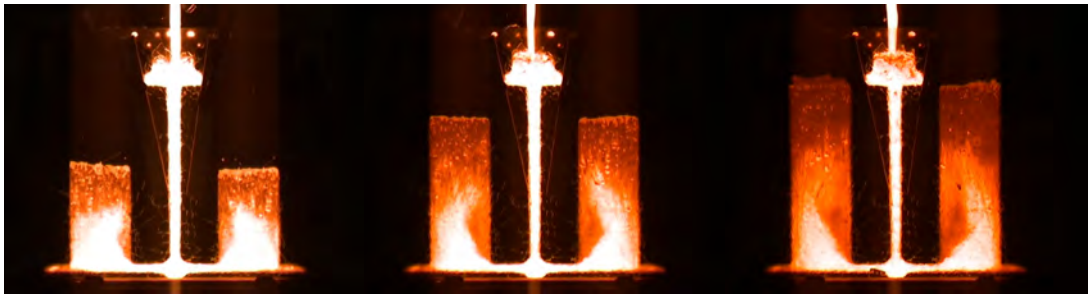

Time 1.16 Time 1.48 Time 1.80

Figure 4.58 Snapshots showing the preferred flow path in the last part of the filling.

The flow has a tendency to go through the middle of the plates in the early stages as shown on Figure 4.55. The flow is shifted towards the outside edge of the plates at the end of the filling.

The only significant difference between the filling of the plates seen here and the one seen in section 4.5.1.1 is the appearance of the splashes; otherwise the main flow patterns are the same. The flow velocity in the plates is the same, but the initial velocity of the melt in the horizontal runner is raised from 509 to 649 mm/s. Small variations in the filling of the gating system control when the pressure shock wave is initiated. This means small variations decide whether a melt tongue is blown into the plate cavity ahead of the main melt front or whether a small explosion takes place at the melt front resulting in small droplets being blown ahead of the main melt front.

4.6.2 3 mm Plates

A snapshot from the filling of the 3 mm plate is shown on Figure 4.59. As with the other trials the measured and the theoretical melt front levels have been plotted. They can be seen on Figure 4.60.

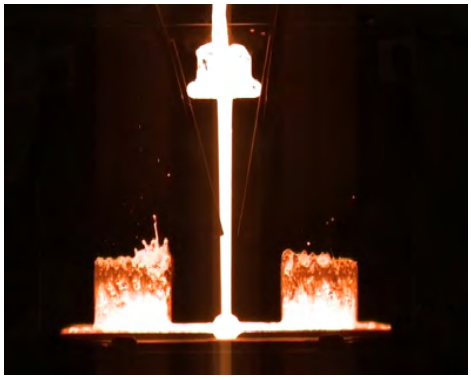

Figure 4.59 Snapshot from the initial filling of the 3 mm plates.

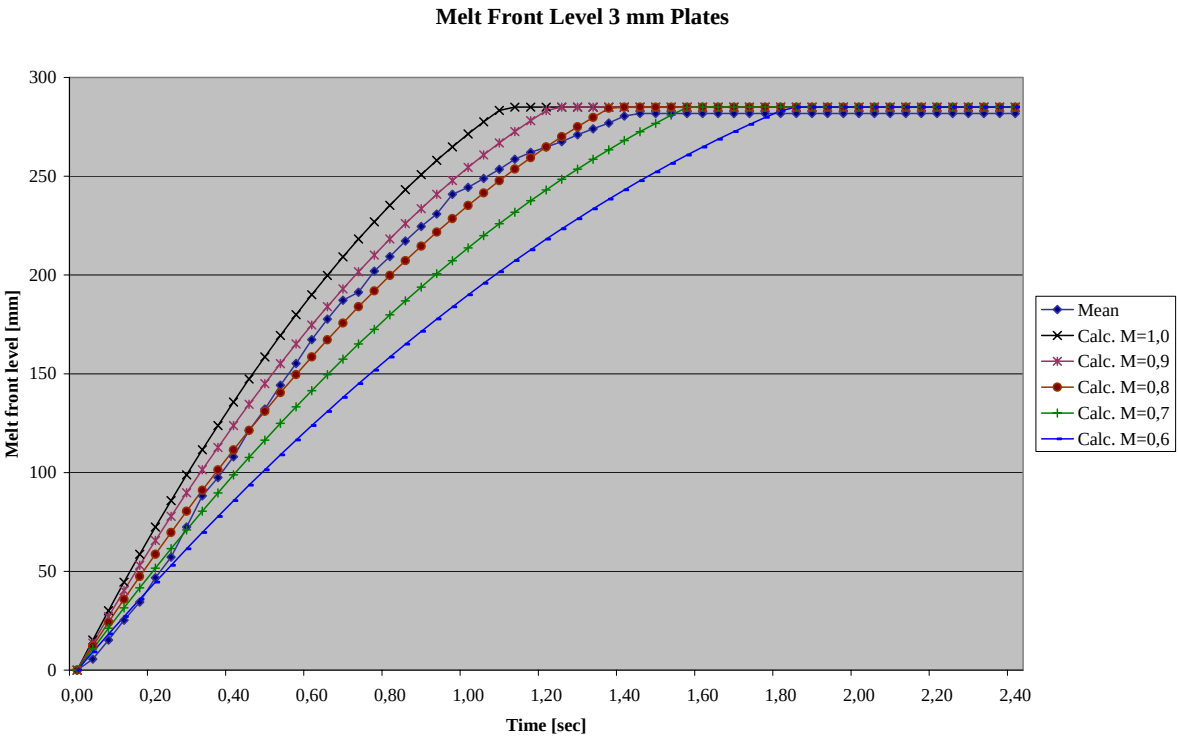

Figure 4.60 Measured and theoretical melt front levels as a function of time.

The best fit between measured data and theoretical data is for a total loss coefficient of 0.8-0.9.

4.6.2.1 Melt flow pattern in the plates

Snapshots of the initial melt flow pattern in the 3 mm plates are shown below:

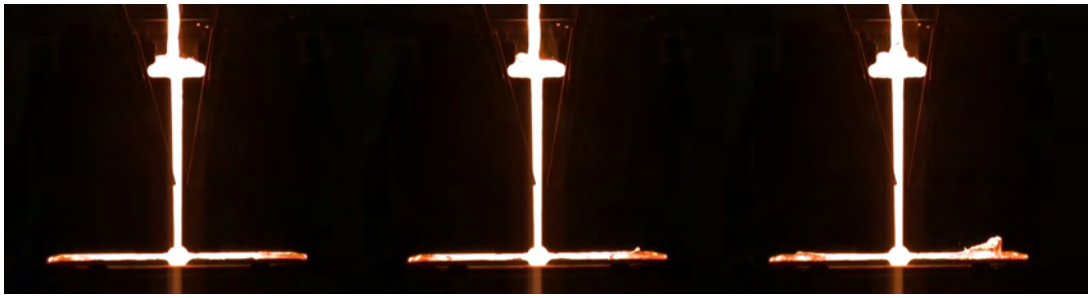

Time 0.60 Time 0.64 Time 0.68

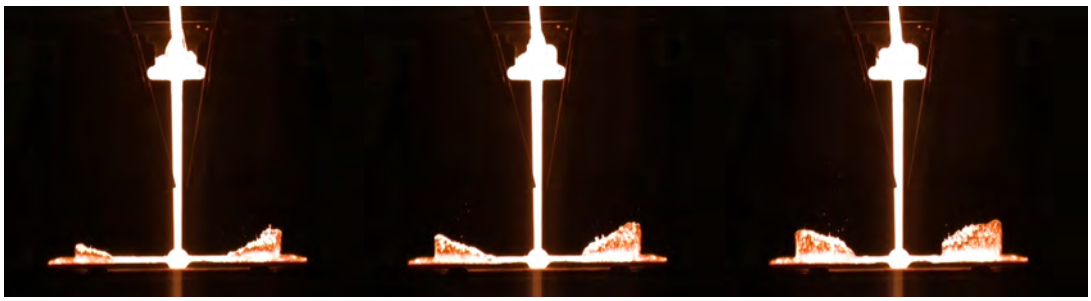

Time 0.72 Time 0.76 Time 0.80

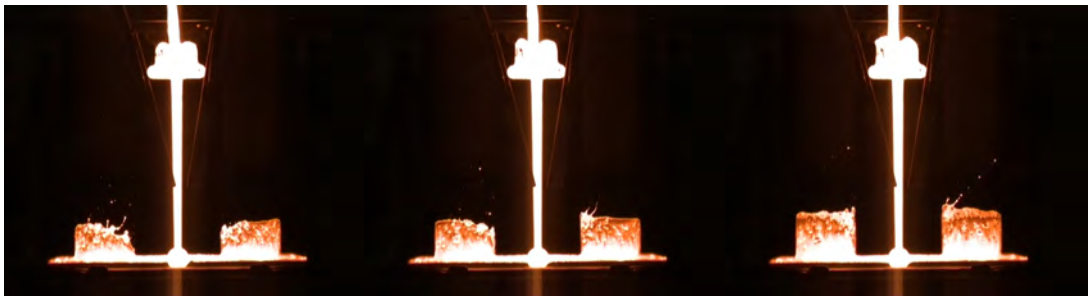

Time 0.84 Time 0.88 Time 0.92

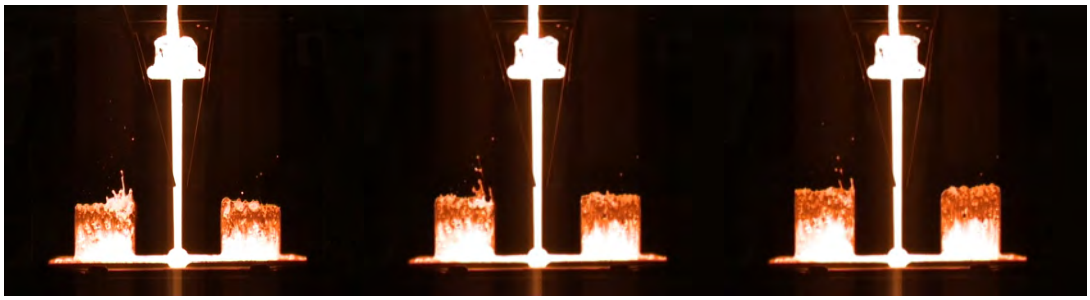

Time 0.96 Time 1.00 Time 1.04

Figure 4.61 Snapshots showing the initial filling of the 3 mm plates.

From 0.60 – 0.80 s the initial filling of the plates is relatively calm. This was also the case for the 4 mm plates. The melt front at the inside edge of the plates splits up after 0.80 s and droplets are blown around 100 mm in front of the main melt front. This happens even though

the melt level in the plates is 70 mm. The reason for this is, as with the 4 mm plates, a partly filled horizontal runner. Air pockets exist in the horizontal runner close to the down runner well. This can be seen on the enlargements on Figure 4.62.

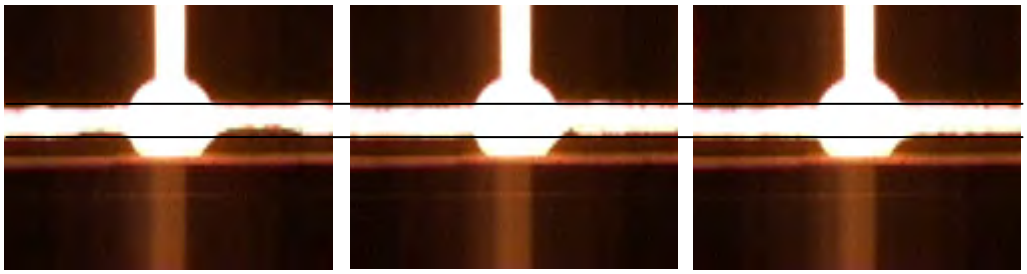

Time 0.80 Time 0.84 Time 0.88

Figure 4.62 Air pockets at the down runner well. The lines indicate the positions of the top and bottom of the horizontal runner.

The air pockets at the well are closed after 0.84 s, i.e. at the same time as the melt front in the plates starts to splits up. When the voids around the well are closed, a pressure shock wave is initiated in the melt, resulting in the melt surface splitting up. I.e. partly filled runners can delay the appearance of pressure shock waves and cause the melt surface to break up even though a relatively large part of the casting already is filled.

Snapshots from the last part of the filling are shown below:

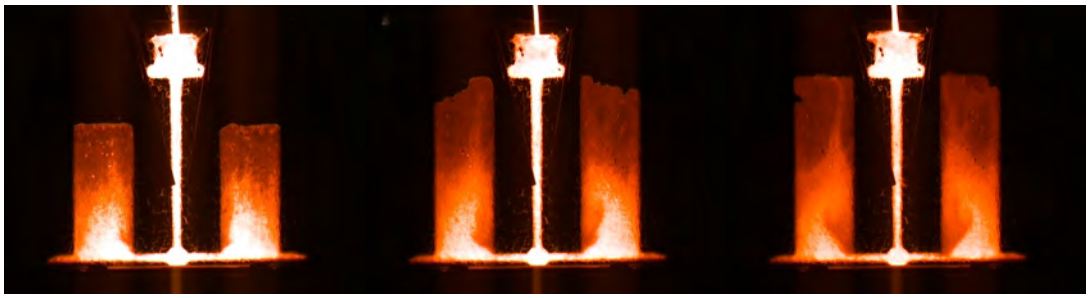

Time 1.52 Time 2.00 Time 2.48

Figure 4.63 Snapshots from the last part of the filling of the 3 mm plates.

Compared to the previous trial with the 3 mm plates, the velocity of the melt in the horizontal runner has been raised from 382 to 649 mm/s when calculated with no losses. When comparing the flow patterns in the plates no significant differences between the two runs can be found. I.e. in this velocity range the size of the horizontal runner is not affecting the flow patterns in the plates.

Making the horizontal runner bigger will not improve anything. It will maybe even on the contrary harm in the sense that it gets more difficult to get the runner completely filled when the first melt passes through it.

4.6.2.2 Anti roll pouring cup

The function of the anti roll cup [Ref. 4.2] is seen on Figure 4.64. Instead of reflecting the melt back towards the pourer, it reflects the melt horizontally towards the centre of the cup. This makes the cup suitable for hand pouring. The disadvantage of the cup is the relative big mass of it, compared to the amount of melt pr second it can handle.

Figure 4.64 Function of anti roll pouring cup.

4.6.2.3 Vena contracta at the pouring cup

Vena contractas are not only seen at the bottom of the down runner. When designing the rest of the gating system care has to be taken not to create the basis for vena contractas at other places. Snapshots showing the transition from the cup to the down runner can be seen on Figure 4.65.

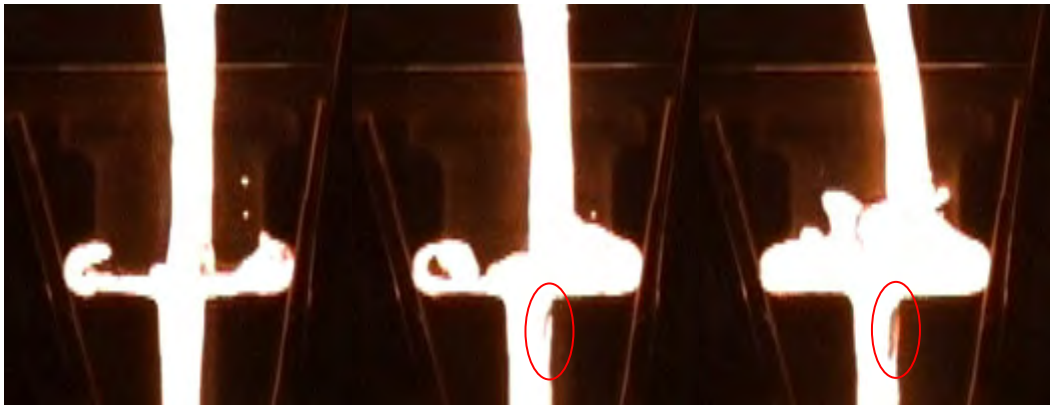

Time 0.28 Time 0.32 Time 0.36

Time 0.40 Time 0.44 Time 0.48

Figure 4.65 Vena contracta under the pouring cup.

The direction of the pouring stream together with a low melt level in the pouring cup is seen to have a large influence on the formation of a vena contracta in the top of the down runner.

It is possible to improve the design making it less prone to give a vena contracta at the top of the down runner. A design with an overlap at the top of the down runner combined with a spout shaped top of the down runner, which is normally used, would reduce the problem. In this case the design was chosen because a symmetrical layout was wanted, and because the complete gating system had to be on the same pattern plate. Sometimes the down runner has to be positioned directly under the pouring cup in practice, for instance to get extra cavities in the mould and to optimize the yield. In such cases the design shown on Figure 4.11 comes in handy. But even with such designs vena contractas can be imagined as indicated on Figure 4.66 this time is it across the parting line. If one want to avoid vena contractas very stream lined designs have to be utilized, i.e. designs where the melt flow does not pass sharp corners.

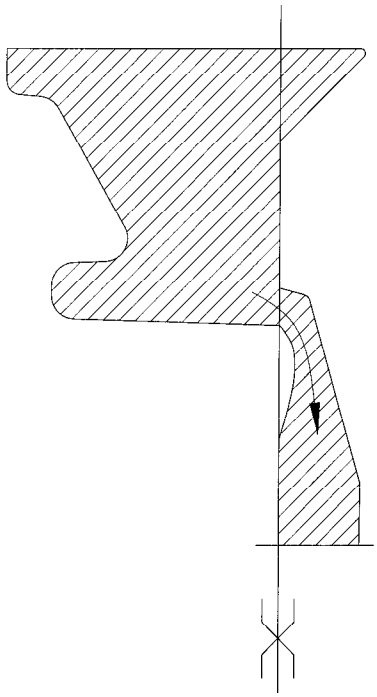

Figure 4.66 Possible vena contracta across the parting line

4.6.3 2 mm Plates

A snapshot from the filling of the 2 mm plates is seen on Figure 4.67. The measured and theoretical melt front levels are plotted on Figure 4.68.

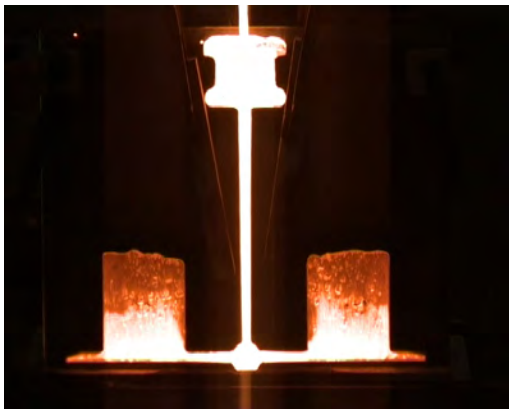

Figure 4.67 Snapshot from the filling of the 2 mm plates.

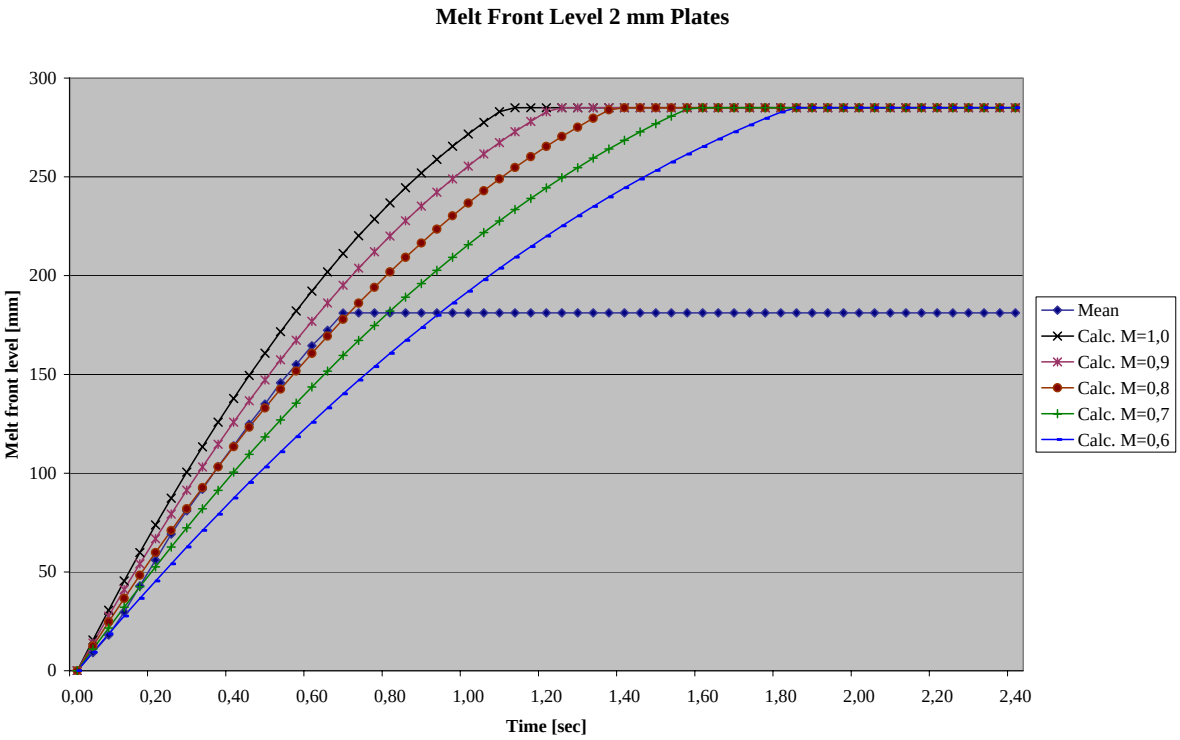

Figure 4.68 Measured and theoretical melt front levels as a function of time.

When comparing measured data and theoretical data the best fit is found for a total loss coefficient of 0.8.

4.6.3.1 Filling of the down runner well and the horizontal runner

Snapshots showing the initial melt passing through the down runner well and the horizontal runner can be seen below:

Time 0.20 Time 0.24 Time 0.28

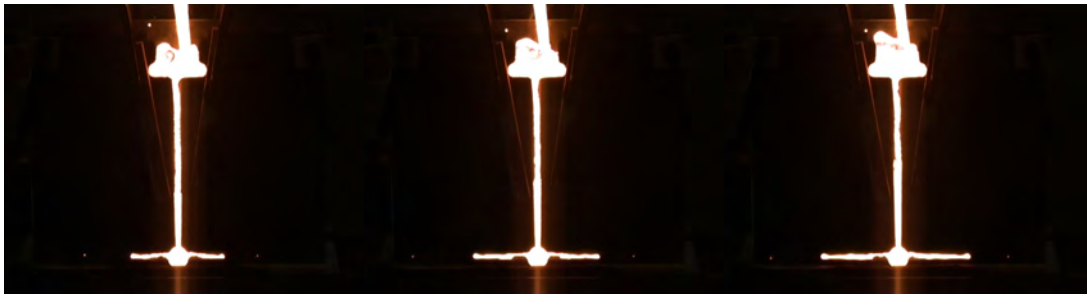

Time 0.32 Time 0.36 Time 0.40

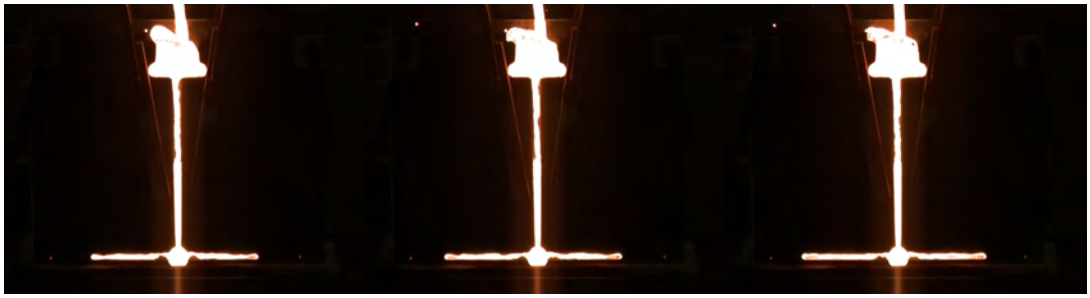

Time 0.44 Time 0.48 Time 0.52

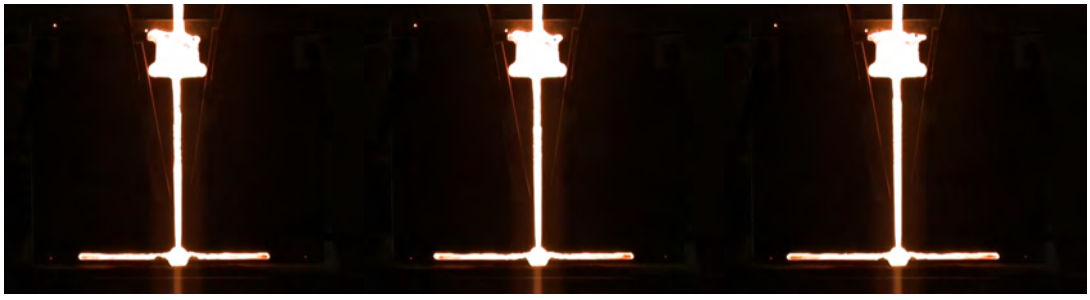

Time 0.56 Time 0.60 Time 0.64

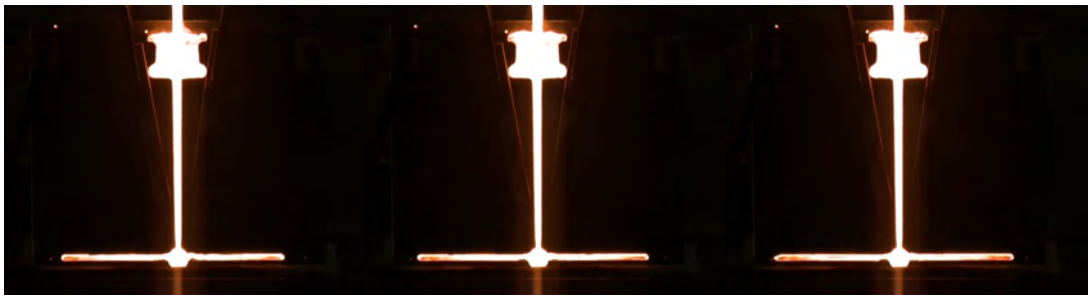

Time 0.68 Time 0.72 Time 0.76

Figure 4.69 Snapshots showing the initial melt passing through the down runner well and the horizontal runner.

The section of the horizontal runner close to the down runner well is again not completely filled. This can be seen on the enlargements below:

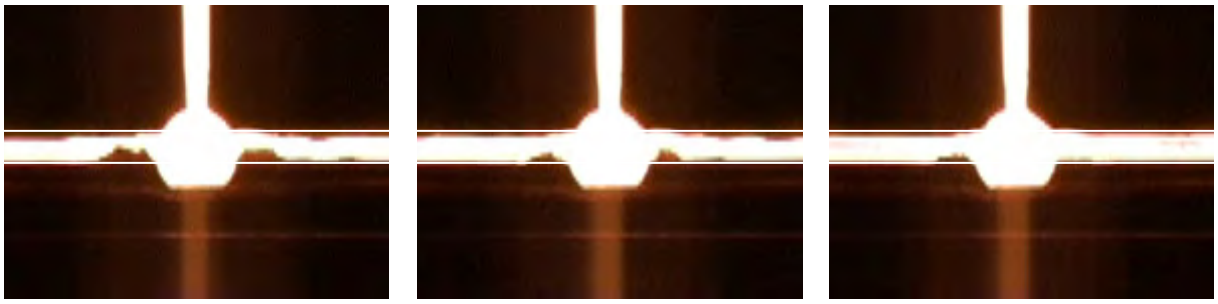

Time 0.52 Time 0.64 Time 0.76

Figure 4.70 Air pockets at the down runner well.

The well is not doing a good job; even when the melt has reached the ends of the horizontal runner air pockets exist at the well. The well is the same as in the previous trials, i.e. a cylinder Ø30 mm, 45 mm deep with 5 degree draft. The vertical dimension of the horizontal runner is 9 mm. The well has to handle a melt flow rate of 125 cm^3/s in the initial phase when calculated without losses.

4.6.3.2 Melt flow pattern in the plates

Snapshots from the initial filling of the 2 mm plates can be seen below:

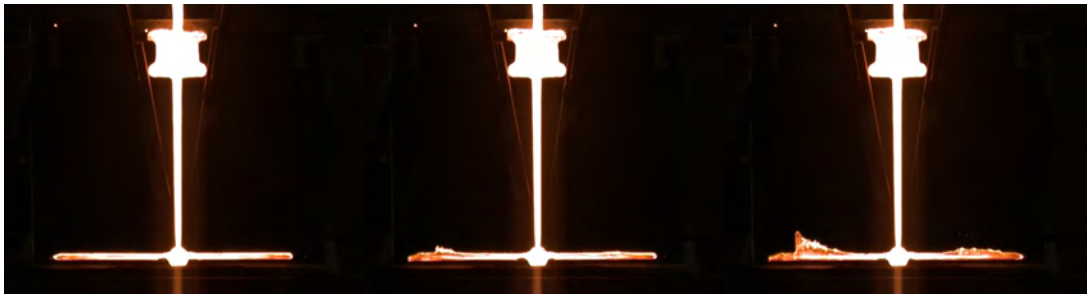

Time 0.76 Time 0.80 Time 0.84

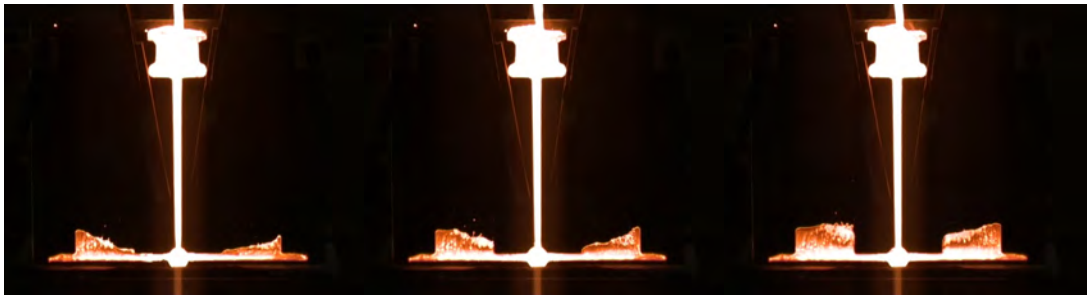

Time 0.88 Time 0.92 Time 0.96

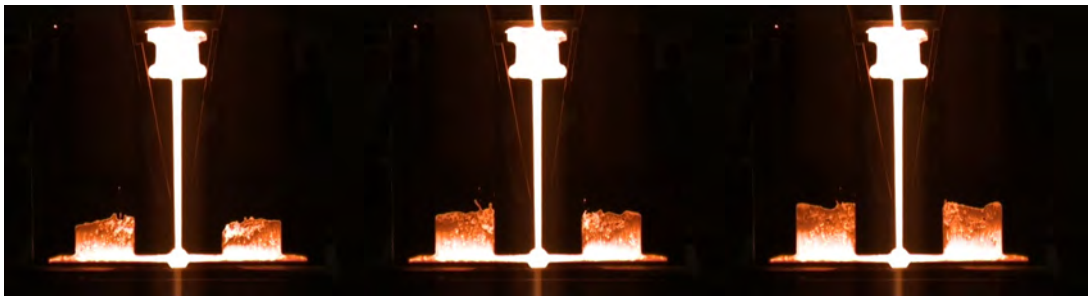

Time 1.00 Time 1.04 Time 1.08

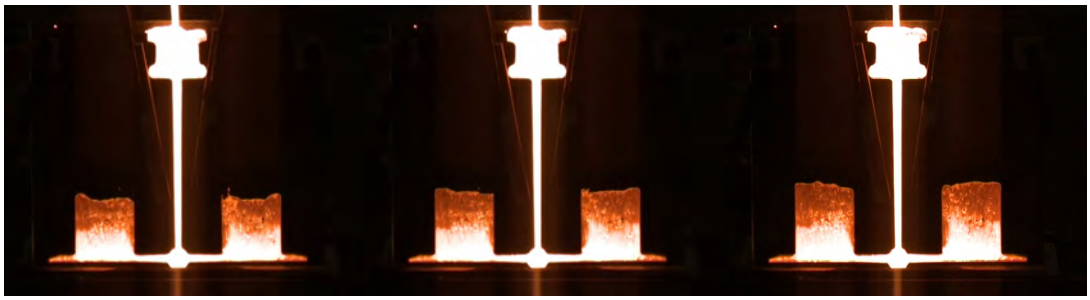

Time 1.12 Time 1.16 Time 1.20

Figure 4.71 Snapshots showing the initial filling of the 2 mm plates.

Moderate breaking up of the melt front is seen in the left plate at 1.04 s. This indicates an air pocket in the gating system being closed. I.e. even at 2 mm wall thickness small amounts of splashes can occur.

The initial melt velocity in the horizontal runner has been raised from 381 to 649 mm/s when comparing to the previous trials with the 2 mm plates described in section 4.5.3. But comparing the flow patterns on Figure 4.43 and Figure 4.71 reveals not significant difference. I.e. in this range of melt velocities the flow patterns in the plates are not controlled by the flow velocity in the horizontal runner

The flow pattern in the last part of the filling is showed on Figure 4.72. The heat distribution in the plates is seen to be very symmetrical both with respect to the two plates and with respect to the sides of the single plates. I.e. the preferred flow path is in the middle of the plates with a little tendency to shift towards the outside edge. As mentioned above the flow patterns are not changed compared to the previous trial where the melt velocity in the horizontal runner was significantly lower.

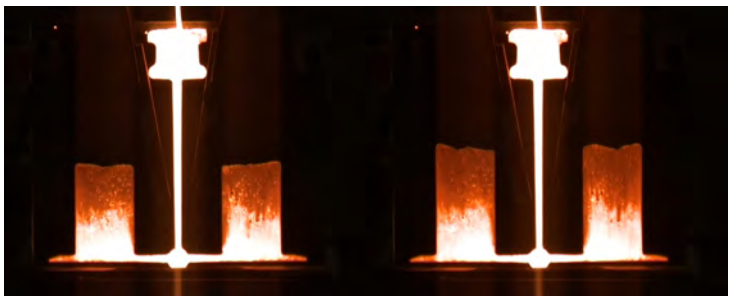

Time 1.32 Time 1.44

Figure 4.72 Flow pattern in the last part of the filling.

4.6.4 Summing up on the loss coefficients

It has not been possible to determine the loss coefficient for the 4 mm plates due to transfer of momentum from the pouring stream to the gating system. The loss coefficient for the 3 mm plates is found to 0.8-0.9 and 0.8 for the 2 mm plates. The effect from surface tension has been extracted. The total loss coefficient including the surface tension is for the 3 mm plates 0.75-0.85 and 0.7 for the 2 mm plates. The effect from surface tension is not depending on the melt front velocity as it can be seen as a constant reduction in driving pressure.

The driving pressure gets smaller and smaller towards the end of the filling when using bottom filling systems. The effect from surface tension is equal to a constant reduction of the driving pressure, i.e. the influence from surface tension relatively seen gets larger toward the end of the filling.

When determining the loss coefficients the effect from partly filled pouring cups has been taken into account. The results from the 4 mm plates show the possibility of getting momentum transferred from the pouring stream into the gating system. It is not possible to determine how much momentum has been transferred at the 2 and 3 mm plates. A pouring basin will be used in the next trials to prevent transfer of momentum and to get a well defined metal head.

4.6.5 Summing up on the filling of the down runner well and the horizontal runner

The down runner well does not perform as intended at any of the plate thicknesses. In all cases air pockets exist in the horizontal runner at the outlet of the down runner well. The air pockets are closed after a significant part of the plates is filled. A shock wave is initiated in the melt when this happens. The result is small “explosions” on the melt surface shooting droplets ahead of the main melt front. I.e. partly filled runners can delay the appearance of shock waves, and cause the melt surface to break up even though a relatively large part of the casting is filled. Moderate breaking up of the melt surface is even seen at the 2 mm thick plates where the back pressure from surface tension and friction is relative large.

This shows the importance of several things. First of all it is important to have completely filled runners right from the first melt passes through the runners. When this is fulfilled, it is important to utilize a runner design gradually reducing the melt velocity to prohibit a pressure shock wave from the hammer effect, when the melt front reaches the end of the runner.

The conventional design used here is not able to secure completely filled cross sections of the horizontal runner, and it is not able to gradually reduce the melt velocity to prevent the pressure shock wave from the hammer effect when the runner is completely filled.

In stead of using designs with dead ends, one can use stream lined designs without dead ends. Dead ends and partly filled runners are the two reasons seen for getting pressure shock waves. Unfortunately the dead ends come in handy for collecting the first cold and dirty melt. Different designs combining dead ends with stream lined designs can be imagined, one possibility is shown on Figure 4.73 It would be interesting to investigate whether such designs are able to prevent the pressure shock waves.

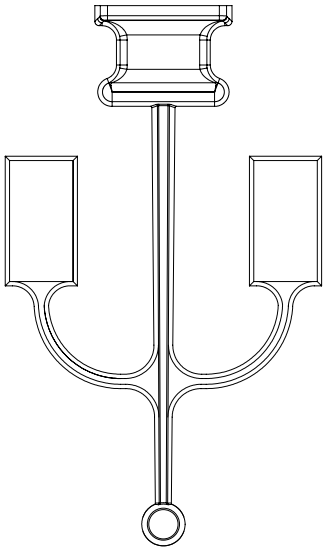

Figure 4.73 Design combining dead ends with stream lined runners.

4.6.6 Summing up on the flow patterns

The velocity of the melt in the horizontal runner is raised compared to the last trial. This change does not affect the flow patterns in the plates for any of the plate thicknesses. The main flow path in the 3 and 4 mm plates is at the outside edge of the plates in the beginning of the filling, and then it shifts a little towards the middle of the plates. In the last part of the filling it is at the outside edge again. For the 2 mm plates the main flow path is in the middle of the plates. The flow patterns are summarized in the Table 4.10.

Test day	Mean velocity mm/s	Size of horizontal runner	4 mm	3 mm	2 mm
4	300	Small	Outside→Centre→Outside	Outside→Centre→Outside	Centre

Table 4.10 Comparison of the main flow paths.

The absence of changes in the flow patterns in the plates due to the changed velocity in the horizontal runner can have different explanations. One explanation can be that the changes in the flow velocities are not large enough to affect the flow patterns. Another explanation can be due to the area ratio between the choke and the horizontal runner. Enlarging the area of the horizontal runner compared to the choke does not necessarily mean a corresponding change in the velocity profile over the cross section. The flow will follow a preferred stream lined path through the gating system, if the areas are too large the flow will take place in only a part of the complete cross section of the runner, while the metal is almost standing still in the rest of the cross section. Hence in this way the real velocities can be close to unchanged even though the areas are changed.

Surface “explosions” are seen at all 3 wall thicknesses. They are caused by pressure shock waves initiated when the last part of the gating system is filled. Hence it is not the melt velocity itself that causes the melt surface to become unstable but the pressure shock waves. If the pressure shock waves can be avoided, significantly higher velocities can probably be utilized without the melt surface breaking up. I.e. it is a question of having good control over the melt in the gating system. As clearly is seen, the conventional type of gating system used here has problems with avoiding the pressure shock waves.

4.7 5. Series of Trials. Melt velocity 300 mm/s. Filling made with pouring basin

Manual pouring is not giving consistent boundary conditions, as mentioned in the previous section. To secure consistent boundary conditions an extra core was made, making it possible to run the trials with a pouring basin. The set up can be seen on Figure 4.74. A thermocouple was mounted in the basin for recording the actual pouring temperature. Details of the pouring basin can be seen in Appendix 4.6. The temperature loss in the basin is found to be 30 ºC. The furnace temperature is raised according to this extra temperature loss to end up with the same pouring temperature as in the previous trials. The fibre pouring ladle was also equipped with a thermocouple.

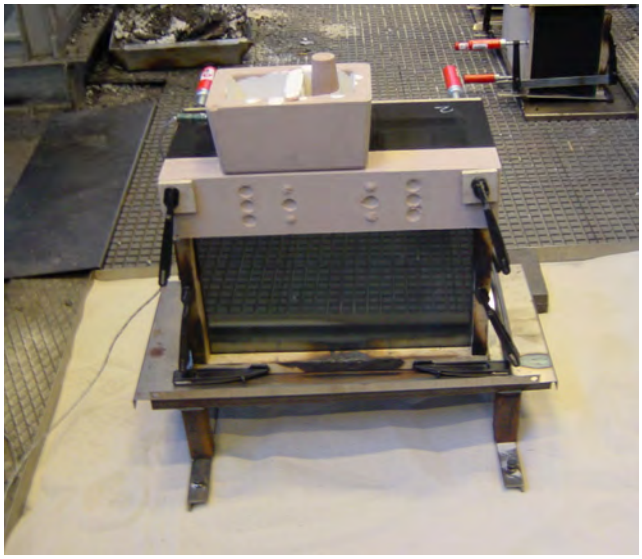

Figure 4.74 Setup with pouring basin.

The pouring basin is not to be seen as a device used in production foundries, it is only to be seen as a device giving consistent boundary conditions from mould to mould under laboratory conditions. It is a substitute for an automatic pouring device. The core was coated with aluminium silicate based core paint to prevent loose sand from the core getting into the mould cavity especially from where the stopper core seals in the base core.

The gating systems used for the trials discussed in section 4.6, are reused here. Only the pouring cups are changed. They are changed to a type fitting the outlet of the basin. The melt front velocities are slightly higher compared to what is seen in the previous trial, due to the extra ferrostatic height from the pouring basin. The basin makes it possible to investigate the performance of the gating systems under very stable pouring conditions. For instance can the consistency of the flow patterns from mould to mould be analysed. The basin also effectively removes the possibility of getting momentum transferred from the pouring stream to the gating system. Hence better estimates for the loss coefficient can be found.

The pouring basin was filled to a level 90 mm’s above the top of the green sand mould. The melt level in the basin is lowered by 3 factors: 1) Removing the stopper core, 2) Filling of the gating system, 3) Filling of the plates. All 3 factors have been taken into account when calculating the driving pressure used for determining the theoretical melt front levels in the plates. The driving pressure has been reduced as the filling of the plate’s proceeds and the melt level in the basin is decreasing. I.e. the continuity equation has been used. This can be done when completely filled cross sections of the runners are assumed. As mentioned is the gating system reused from section 4.6. The flow velocities etc. changes slightly when the effect from the basin is taken into account. The new velocities can be seen in Table 4.11.

Plate thickness		2 mm	3 mm	4 mm
Drawing number		26D0310	26D0320	26D0330
Choke area (Design value)	mm^2	59	88	118
a (Design value)	mm	4.4	5.4	6.3
Choke area (Measured value)	mm^2	63	91	120
Initial speed at choke	mm/s	2853	2851	2847
Area under cup	mm^2	157	235	313
A	mm	6.9	8.1	9.3
Area of the horizontal runner (Design)	mm^2	118	177	235
Section size of the horizontal runner (Design)	mm	9/7/14.7	9/7/22,1	9/7/29.4
Area ratio Runner/Choke (Design)		4	4	4
Initial melt front speed in the horizontal runner (Design)	mm/s	709	707	705
Initial melt front speed in the plates (Design)	mm/s	417	415	414
Initial melt front speed in the plates (Real)	mm/s	445	429	421
Mean melt front speed in the plates (Design)	mm/s	341	338	335
Mean melt front speed in the plates (Real)	mm/s	364	349	341
Final melt front speed in the plates (Design)	mm/s	233	227	220
Final melt front speed in the plates (Real)	mm/s	249	234	224
Theoretical filling time of the plates (Design)	s	0.83	0.84	0.85
Theoretical filling time of the plates (Real)	s	0.78	0.82	0.84

Table 4.11 Design and real dimensions for the gating systems.

The extra metal head coming from the pouring basin increases the melt front velocities in the plates compared to the previous trials made with the same gating systems but without the basin. The mean melt front velocities are increased with approximately 13 % compared to the previous trial. The final melt front velocities are increased with approximately 32 % compared to the previous trial without the basin. The contribution from the basin to the total driving pressure in the last part of the filling is relatively large; hence a large change in velocity is seen at the end of the filling.

In the previous sections the effect from surface tension is extracted from the results, before the loss coefficients are found. It was shown in section 4.5 that changes in the melt front velocity will not change the impact from surface tension on the loss coefficient, because the effect from surface tension can be seen as a constant reduction in driving pressure through the complete filling sequence of the plates. But in this row of trials the increase in velocity is due to an increase in the pressure head, because the pouring basin is used. As discussed in the previous sections is the influence from back pressure generated by surface tension having a relatively large influence on the flow at the end of the filling due to the small driving pressures. The larger pressure head from the pouring basin which is having a relatively large influence on the total pressure head towards the end of the filling reduces the effect from surface tension compared to the previous trials.

Graphs showing the melt front levels with and without surface tension for the 3 plate thicknesses can be seen in Appendix 4.7. The effect from surface tension on the loss coefficient is now reduced to 0.06 for the 2 mm plates, 0.04 for the 3 mm plates and 0.03 for the 4 mm plates.

4.7.1 4 mm Plates

A snapshot from the filling of the 4 mm plates can be seen on Figure 4.75. All 3 runs of the trial were successful. When comparing the videos of the flow patterns from the 3 runs no significant differences could be found. The melt front levels have been plotted on Figure 4.76. The decreasing melt level in the pouring cup has been taken into account when calculating the driving pressure used for determining the theoretical melt front levels in the plates. The top core used for connecting to the pouring basin covers the upper part of the plates; hence the measured data for the melt level stops at a 245 mm.

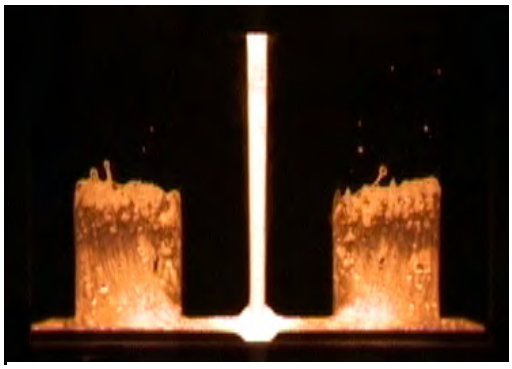

Figure 4.75 Snapshot from the filling of the 4 mm plates.

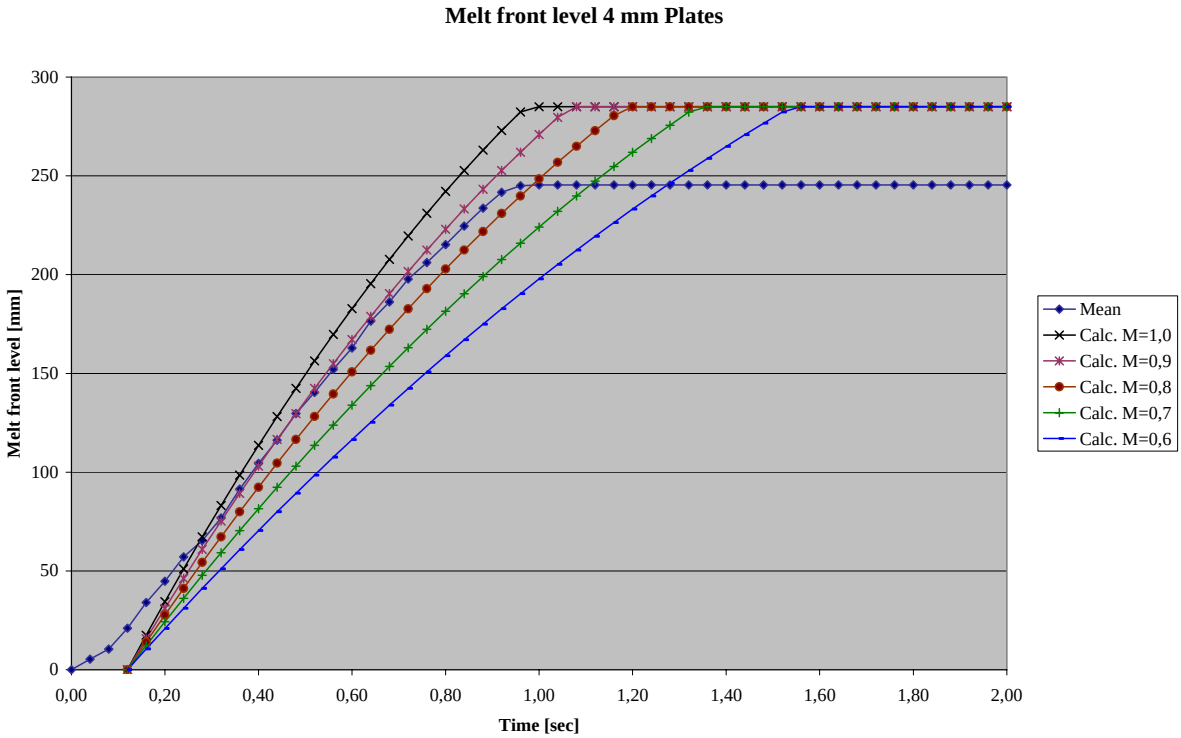

Figure 4.76 Measured and theoretical melt front levels as a function of time.

The measured melt front level is a little behind the theoretical values in the beginning. The horizontal runner is not completely filled when the melt enters the plate cavities. This makes the initial filling of the plates relatively slow. The curves have been shifted parallel to the time axis to find the best fit between the slopes of the measured and theoretical data. A total loss coefficient of 0.9 gives the best fit.

4.7.1.1 Filling of the horizontal runner

Snapshots showing the initial melt passing through the down runner well and the horizontal runner are shown below:

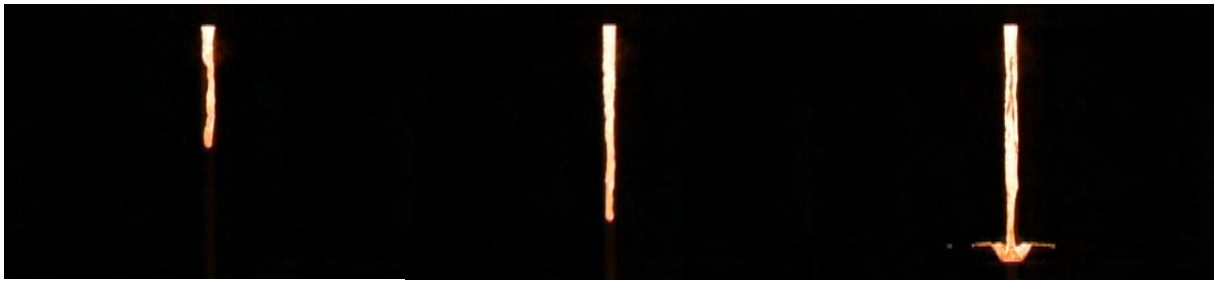

Time 0.08 Time 0.12 Time 0.16

Time 0.20 Time 0.24 Time 0.28

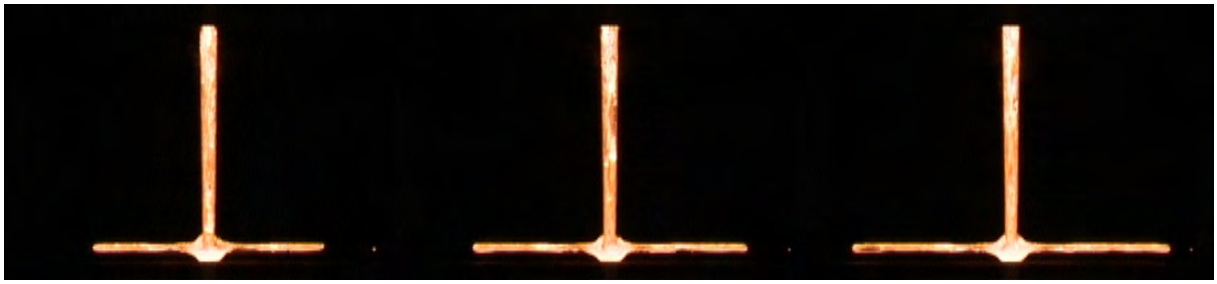

Time 0.32 Time 0.36 Time 0.40

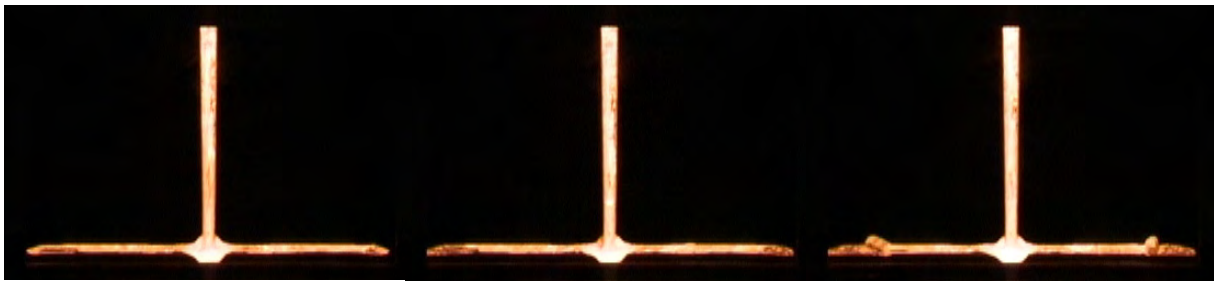

Time 0.44 Time 0.48 Time 0.52

Figure 4.77 Snapshots showing the initial melt passing through the down runner well and the horizontal runner at the 4 mm plates.

The well under the down runner gives minor problems. When the melt hits the bottom of the well a few droplets are blown into the horizontal runner; this starts at 0.16 s. When comparing to the trials with the 3 mm plates described in the next section relatively few droplets are seen in the horizontal runner. The reason for the relatively good performance of the well is the partly filled down runner. A relatively thin melt jet reaches the bottom of the well after 0.16 s, and a layer of melt is build up in the well. The main melt stream filling the complete cross section of the down runner reaches the well a little later. The first melt acts as a cushion for the main melt stream preventing a hard impact at the bottom of the well. Hence only a few droplets are blown into the horizontal runner.

The snapshots at 0.44 and 0.48 s are very much the same. The theoretical melt front velocity in the horizontal runner is approximately 700 mm/s. The melt front should hence advance 28 mm in 0.04 s. This is not the case. The trial has been made with the pouring basin giving good boundary conditions. The very little movement of the melt front must be due to a partly filled cross section of the horizontal runner. The melt flow fills up the cross section of the horizontal runner instead of moving the melt front ahead. I.e. the well is not able to secure a completely filled cross section of the horizontal runner. The theoretical melt flow rate calculated without losses is 298 cm^3/s during the filling of horizontal runner.

4.7.1.2 Melt flow pattern in the plates

Snapshots showing the initial filling of the 4 mm plates can be seen on the pictures below:

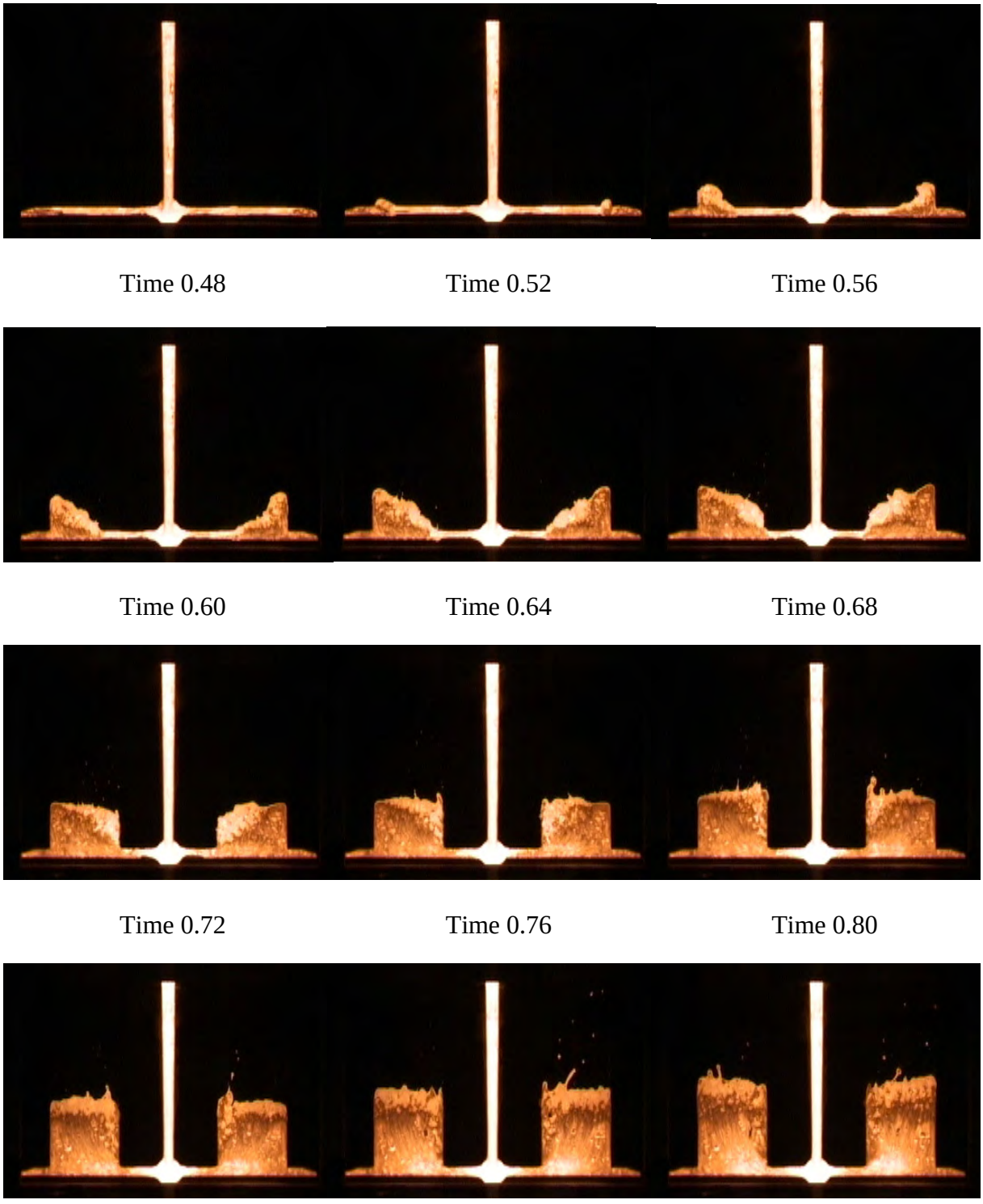

Figure 4.78 Snapshots showing the initial filling of the 4 mm plates.

The initial filling of the plates from 0.48 to 0.72 s is taking place with coherent melt fronts. Air pockets exist in the horizontal runner at the well until 0.72 s. Enlargements of the area at the well at 0.72 and 0.76 s can be seen on Figure 4.79. The bottom of the well is hidden behind the clamping for the glass. The air pockets are closed at 0.76 s. A pressure shock wave due to the hammer effect is initiated when the last air pockets are closed. This results in braking up of the melt fronts giving splashes culminating at 0.88 s. The splashes occur at the inside edges of the plates. The last air pockets in the gating system are at the well. The pressure shock wave is initiated here and spreads out from here. Hence the effect of it is seen at the inside of the plates which is at the shortest distance to the origin of the pressure shock wave.

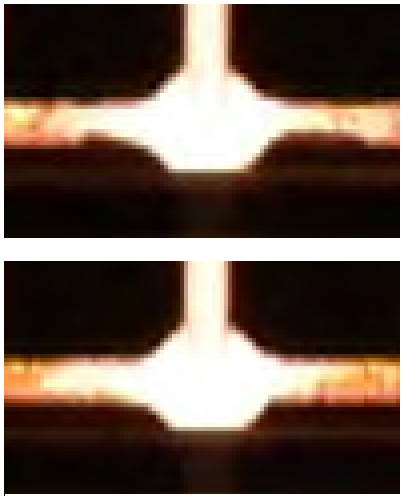

Figure 4.79 Down runner well at 0.72 and 0.76 s.

The dynamic pressure is given by [Ref. 4.6]:

$$P_{Dynamic} = 1/2 \cdot \rho \cdot v^2 \qquad \textbf{[Eq. 4.10]}$$

The initial melt front velocity in the horizontal runner can be seen in Table 4.11, it is 0.709 m/s. With ρ = 6260 kg/m^3 is the dynamic pressure found to 1570 Pa. This pressure can be converted to a height through [Ref. 4.6]:

$$H = \frac{P}{\rho \cdot g} \qquad \textbf{[Eq. 4.11]}$$

This result in a height of 25 mm. I.e. the metal splashes can be blown 25 mm ahead of the main melt front. When looking at Figure 4.78 at 0.88 s the droplets are blown approximately 120 mm ahead of the main melt front. Combining Eq. 4.10 and Eq. 4.11 gives the height as a function of the velocity:

$$H = \frac{1/2 \cdot v^2}{g} \qquad \textbf{[Eq. 4.12]}$$

The height is seen to follow the square of the velocity. If the local velocity is 1.53 m/s i.e. approximately twice the mean velocity, when the air pocket is closed, the dynamic pressure is able to lift the metal droplets 120 mm. The corresponding dynamic pressure is 7370 Pa. In section 4.5.1.2 the velocity of the droplets was found to 1.5 m/s. This corresponds very well to a local velocity in the runner of 1.53 m/s seen from an energy conservation point of view.

I.e. splashes do not occur when the melt enters the plates; they occur when the last air pockets in the gating system are closed. This shows the importance of having filled runner cross sec-

tions, and the possibility of getting melt splashes very late in the filling sequence if this is not fulfilled.

The flow pattern in the last part of the filling sequence is seen below:

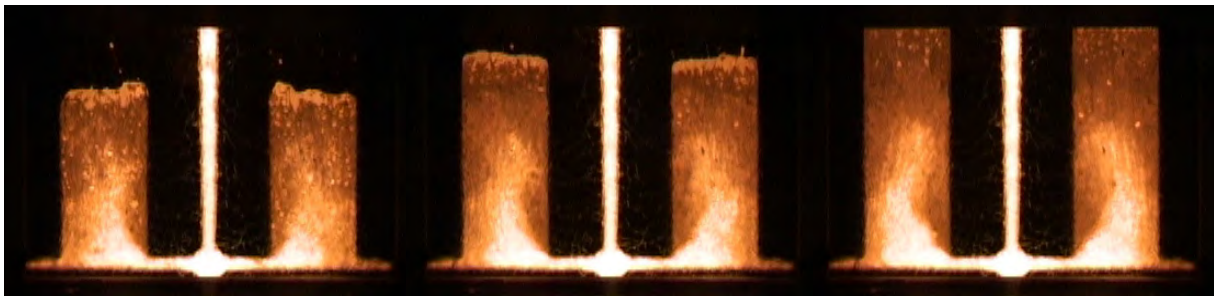

Time 1.16 Time 1.36 Time 1.56

Figure 4.80 Flow pattern in the last part of the filling of the 4 mm plates.

Comparing this flow pattern with the pattern seen in the previous trial without the pouring basin shows no significant difference.

4.7.2 3 mm Plates

The filling patterns seen in the 3 runs with the 3 mm plates are quite different. Snapshots illustrating the difference between the 3 runs can be seen below:

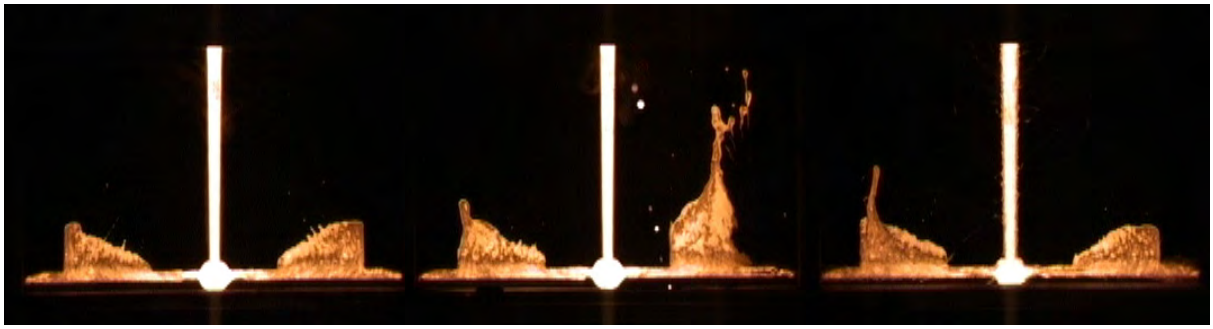

1. Run time 0.76 s 2. Run time 0.76 s 3. Run time 0.76 s

Figure 4.81 Initial filling of the plates in the 3 runs.

Run number 1 will be used for determination of the loss coefficient. A detailed analysis of the differences between run no. 1 and 2 will be made in the following sections.

The melt front levels found at run number 1 has been plotted on Figure 4.82.

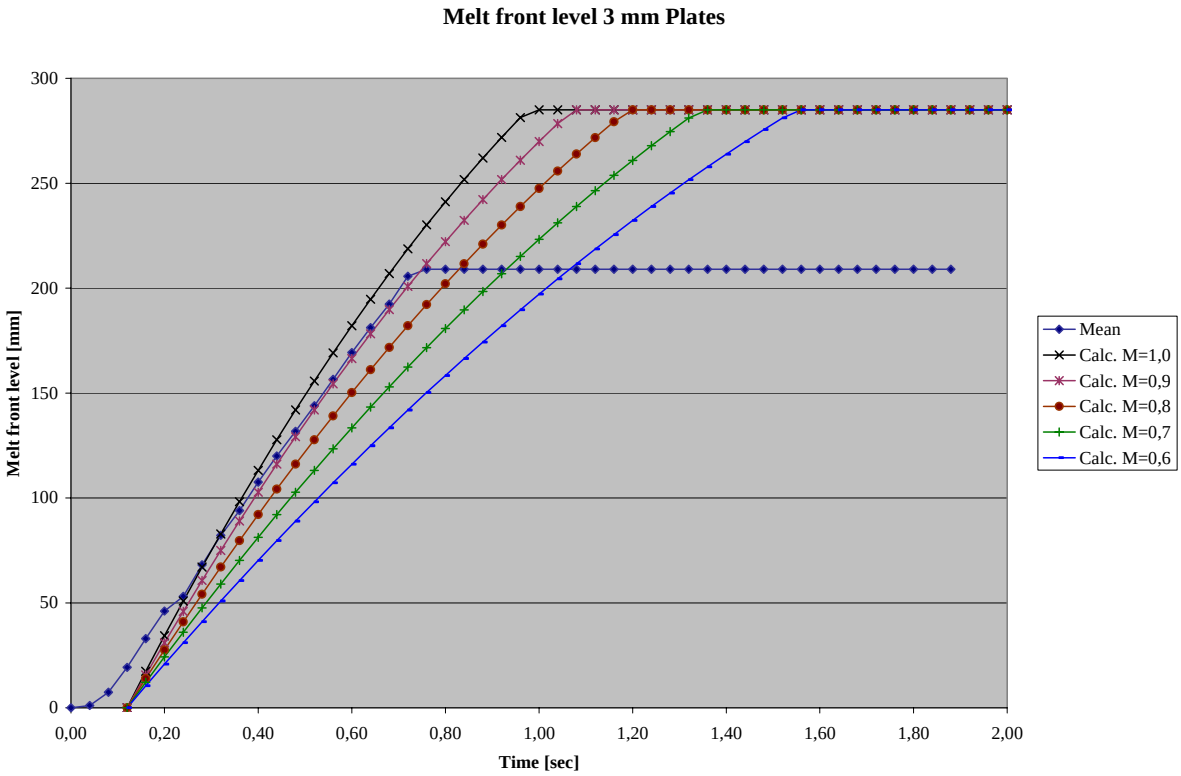

Figure 4.82 Measured and theoretical melt front levels as a function of time.

The measured melt front level is a little behind the theoretical values in the beginning. The horizontal runner is not completely filled when the melt enters the plate cavities. This results in a relatively slow initial filling of the plates. The curves have been shifted parallel to the time axis to find the best fit between the slopes of the measured and theoretical data. The best fit is found for a loss coefficient of 0.9. The glass breaks when the melt level is 209 mm. The plates in the other two runs were filled completely.

4.7.2.1 Filling of the down runner

The filling sequences of run 1 and 2 were very different. In the following the 2 filling sequences will be compared and analysed in detail. Snapshots from the 2 filling sequences can be seen on Figure 4.83. The times given are from the stopper cores are removed.

The melt flow in the down runners is seen to be a little different when comparing the two runs. Only a small droplet is a little ahead of the main melt front in run 2. This can be seen at 0.12 s. The main melt front fills otherwise the complete cross section of the down runner.

In run 1 on the other hand a thin melt jet is approximately 70 mm ahead of the main melt stream. The thin melt stream hits the bottom of the well before the main stream arrives.

This makes a big difference. The thin melt jet in run 1 fills the bottom of the well and acts as a cushion for the main flow, when it hits the bottom. The cushion prevents droplets from being shot into the horizontal runner.

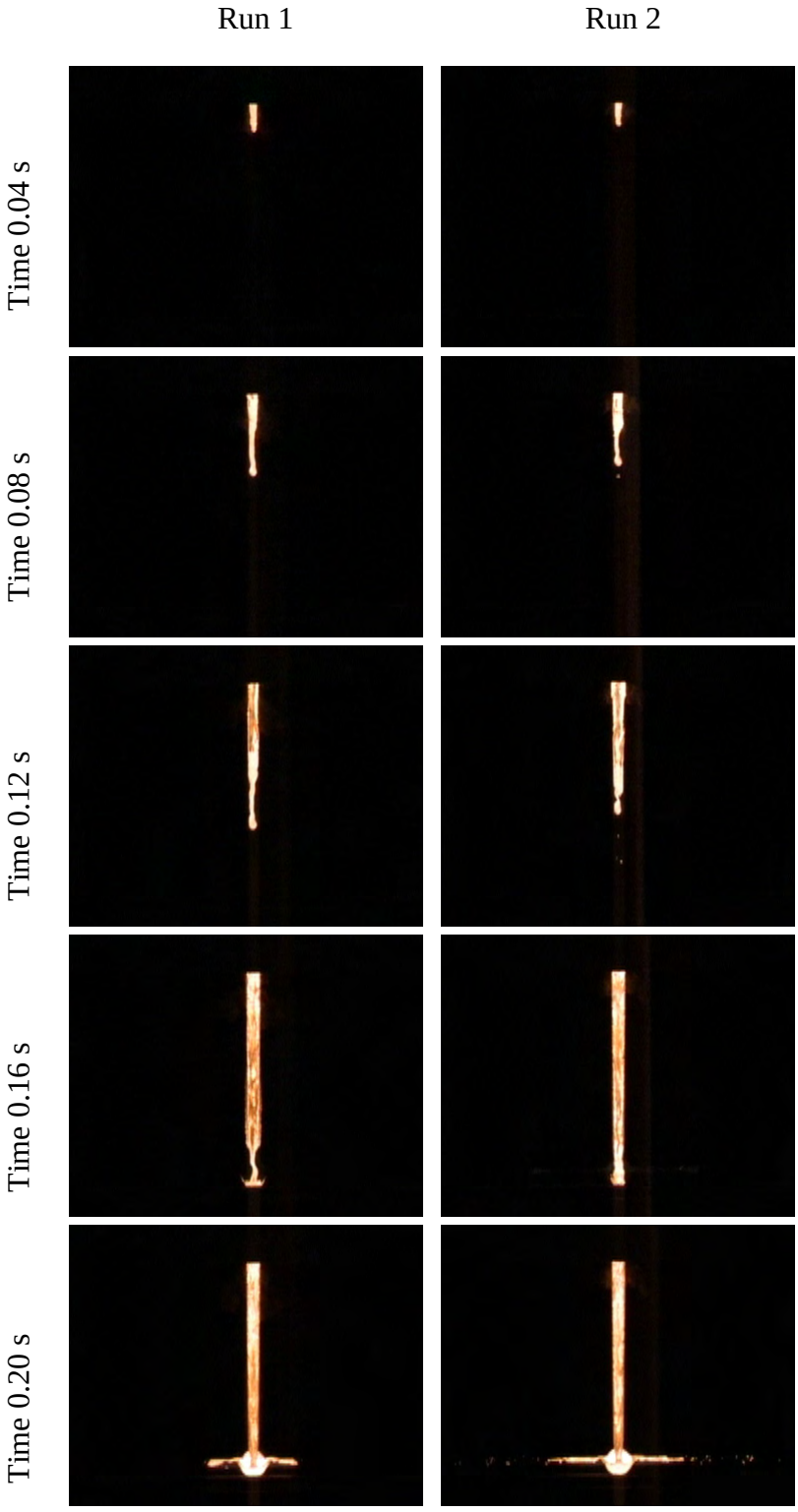

Figure 4.83 Filling of down runner and well.

The main melt stream in run 2 hits the bottom of the well directly, with no cushion of melt to soften the impact. The result is a lot of droplets blown into the horizontal runner. The difference can be seen very clearly on the snapshot at 0.20 s.

The filling has been done with the pouring basin. This can of course not secure 100 % equal pouring conditions from mould to mould, but the variations in the pouring conditions are very limited. The setup with a basin compared to real production leads to very reproducible pouring conditions.

The down runner well has to handle 226 cm^3/s melt during the filling of the horizontal runner, when calculated without losses.

The amount of droplets in the horizontal runner is very different. This big difference is caused by a very small difference in the behaviour of the melt when it flows through the down runner. When a few cm^3 melt arrives at the well before the main melt stream a hard impact is prevented and no droplets are blown into the horizontal runner.

Knowing the disadvantages an only partly filled runner cross section can lead to, the above shows the advantage of an only partly filled cross section in connection with a directional change. The advantage of a partly filled runner only exists when the transition giving the directional change doesn't perform as intended.

I.e. when having 100 % filled cross sections it is even more important to optimize the design of the transition giving the directional change.

The droplets seen can lead to inclusions in the casting. With this sort of gating system only minor changes in the boundary conditions can either lead to droplets or prevent them. An example of a gating system giving better control over the melt can be seen in section 5 where a non conventional gating system for a brake discs is shown. In section 6 different gating systems for a thin walled manifold are investigated, they are all designed to strictly control the melt flow.

4.7.2.2 Filling of the horizontal runner and the plates

The filling of the horizontal runners is also very different.

The white lines indicate the position of the main melt front. A green line indicates no movement of the main melt front compared to the previous snapshot. A red line indicates a withdrawal of the main melt front compared to the previous snapshot. A blue line indicates the end of the gating system.

The melt front advances with a reasonable constant velocity in run 1. The cross section of the horizontal runner is not filled. The cross section fills up after the melt fronts have reached the ends of the horizontal runner, i.e. at 0.36 s.

In run 2 the melt front comes to an almost complete stand still after 0.32 s. The melt fronts hardly advance until 0.52 s. The cross section of the horizontal runner is being filled up in stead. The melt reaches the ends of the horizontal runner at 0.64 s in run 2.

With only a small void close to the well and else wise a completely filled horizontal runner no buffers exist to soften the hammer effect coming

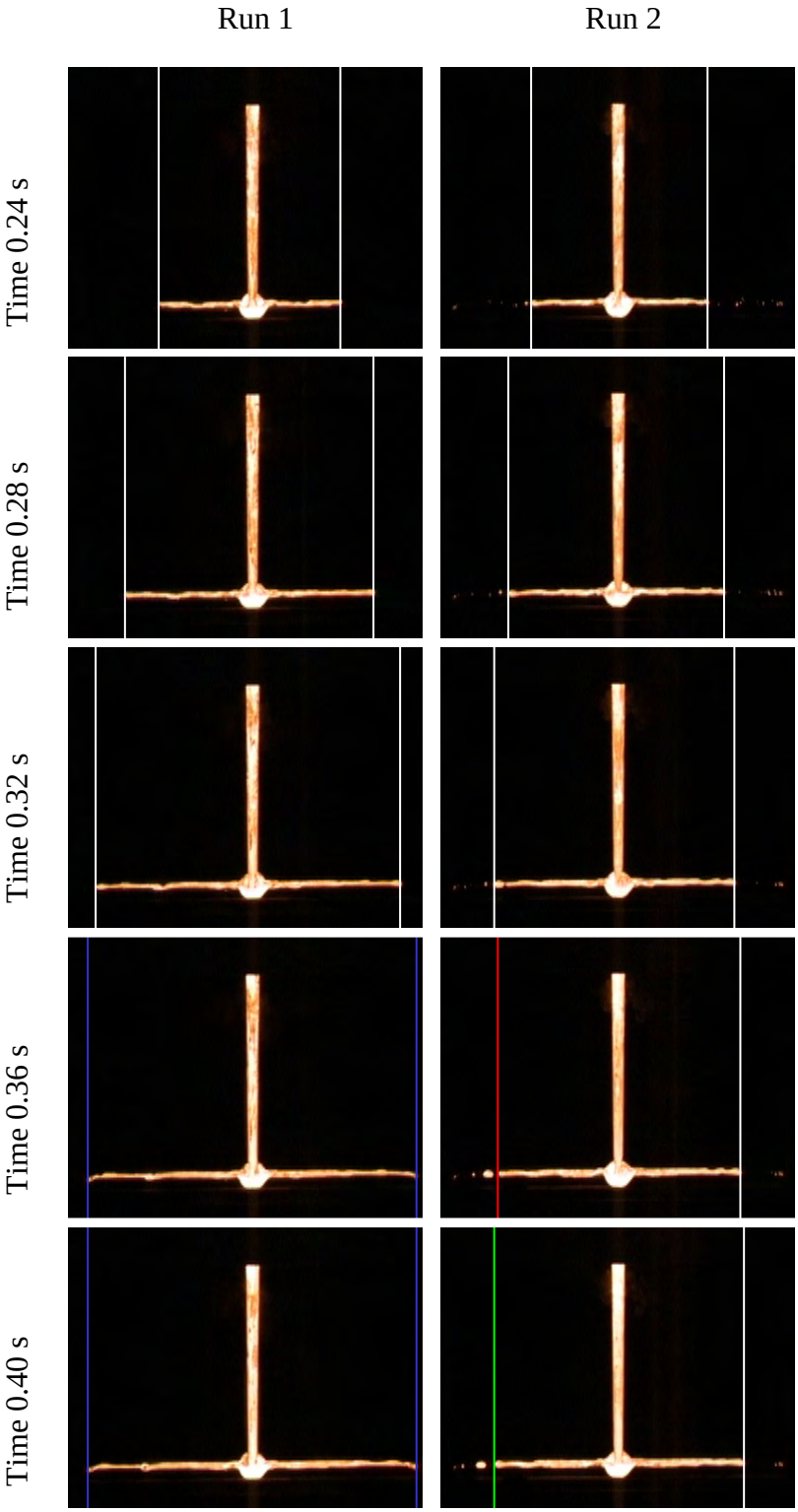

Figure 4.84 Initial filling of the horizontal runner.

from the melt hitting the ends of the horizontal runner. This results in a pressure shock wave giving a fountain shooting into the right plate after 0.64 s in run 2.

The large differences between the filling patterns of the plates in the two runs are seen from 0.64 – 0.84 s.

The reason for the large difference in the filling of the plates is small differences in the melt flow in the horizontal runner.

At 0.20 s a very thin melt jet is blown into the horizontal runner in run 2. This melt is being cooled very fast meaning loss of viscosity and hence resulting in larger resistance to flow. This makes it more feasible for the melt to fill up the cross section in stead of moving the melt front ahead.

Other scenarios can be imagined. But no matter what the exact reason is, the result is very clearly seen. The cross section of the horizontal runner is completely filled and when the melt reaches the ends of the runner the dynamic pressure is directly converted into static pressure blowing the melt into one of the cavities.

The melt is only blown into the right cavity in run 2.

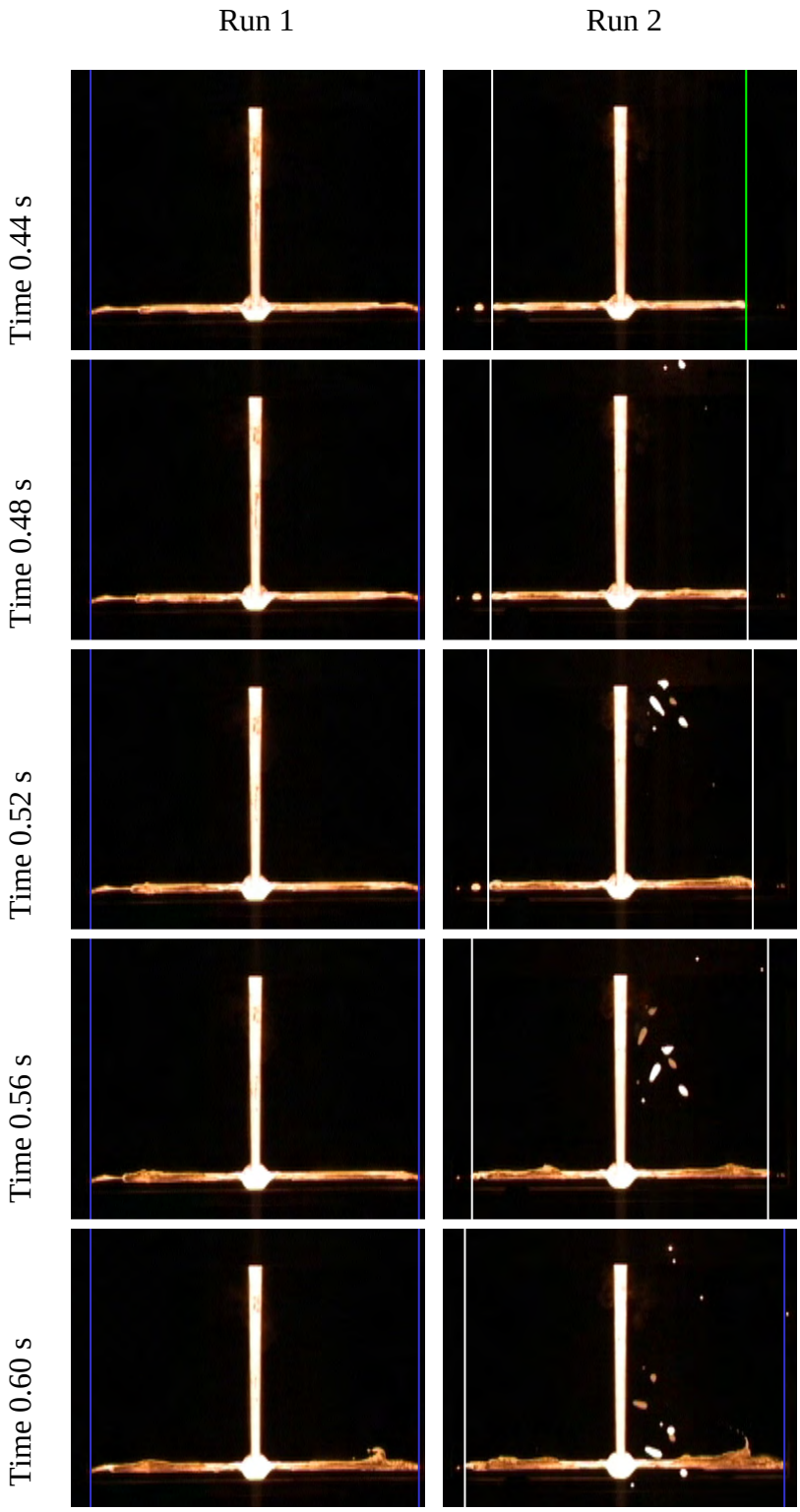

Figure 4.85 Filling of the horizontal runner. The big droplets falling down on the right hand side in run 2 from 0.48 s to 0.76 s are coming from the removal of the shutter core in the pouring basin.

This is due to the fact that the pressure will only be relaxed in the direction where the back pressure is smallest. The reason for the back pressure being smaller in the right side is difficult to find. It could be connected to the larger amount of droplets being blown into the right side of the horizontal runner when the well is being filled, as is seen on the right side of Figure 4.83 at 0.20 s.

I.e. an advantage of a partly filled cross section of the horizontal runner can be seen when comparing the flow patterns in run 1 and run 2. As with the case of the directional change the reason for seeing an advantage of a partly filled cross section is problems with another part of the gating system. In this case it is partly a consequence of the well, and mainly a consequence of the dead ends of the horizontal runner. If one works with completely filled runner cross sections it is very important to design the dead ends correct, securing a gradually reduction in melt velocity. This is not fulfilled here.

The same layout with very similar pouring conditions can give very different flow patterns both in the gating system and in the casting. I.e. a gating system like this is very sensitive to small changes in the boundary conditions. Even in

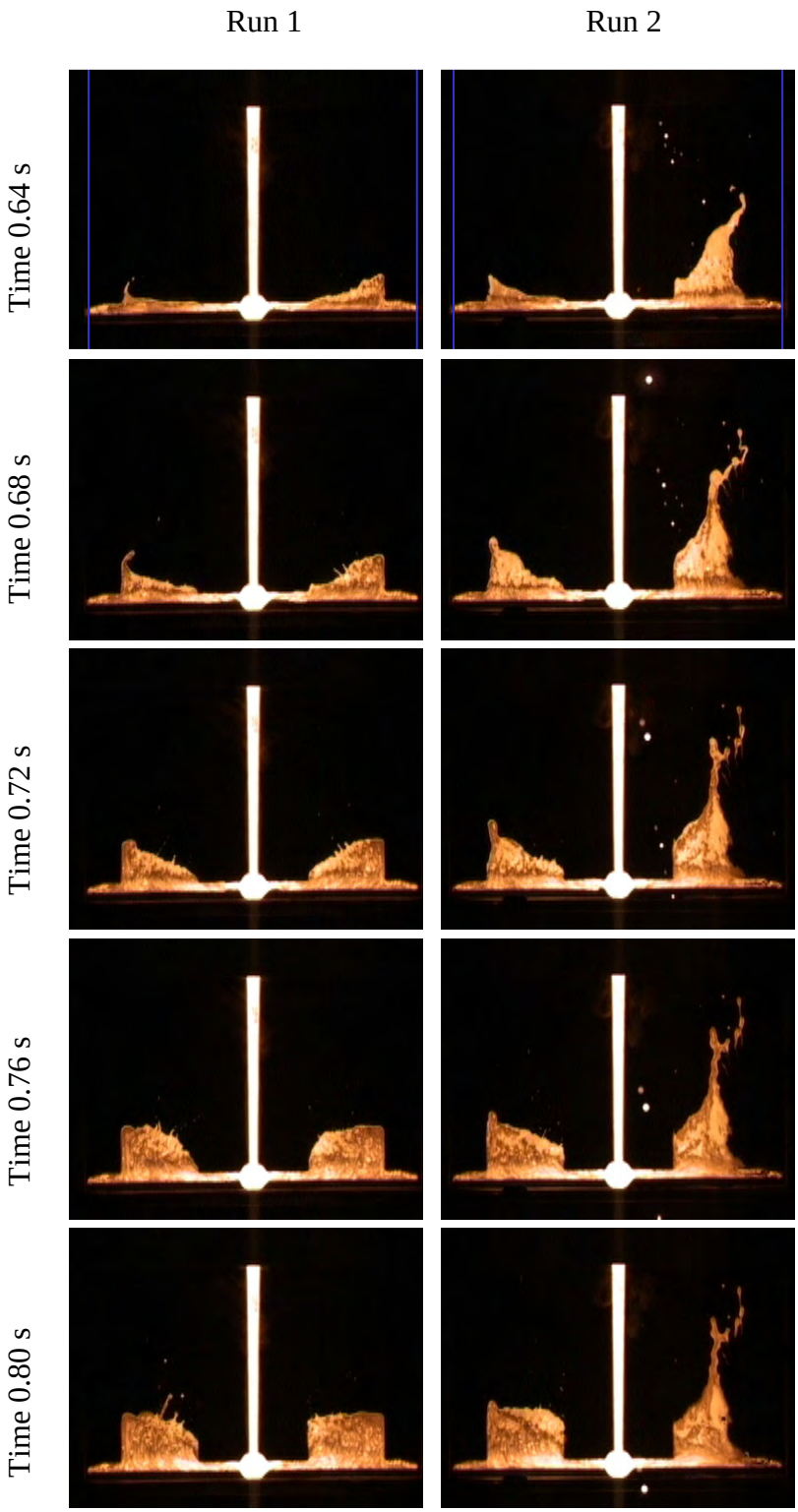

Figure 4.86 Initial filling of the 3 mm plates.

the same mould it is possible to find large differences. A symmetrical layout can give very unsymmetrical filling patterns as seen in run 2. The right cavity in run 2 would in real life probably give a scrapped casting and the left cavity would probably give a sound casting. I.e. we have the well known problem of random or “unaccountable” scrap. We think the filling of the two cavities are the same and hence we should either produce scrap or sound castings but not both from the same mould.

The very different flow patterns possible at this type of gating system are also playing an important role when talking about flow lengths before cold run occurs. If the flow takes place close to the limit where cold runs occurs such large differences in the flow patterns will influence the final flow length. For instance the melt tongue seen at the right pictures of Figure 4.86 will influence the advance of the main melt front when it moves through the plate. At such thin cross sections the melt tongue will have time to at least partly solidify before the main melt front arrives.

The above mentioned things underlines the need for gating systems first and foremost giving good control over the melt securing the melt to behave in the same way in every mould. This means designing gating systems being able to absorb minor but in real production inevitable variations in the pouring conditions from mould to mould.

4.7.3 2 mm Plates

A snapshot from the filling of the 2 mm plates can be seen on Figure 4.87. The stopper core broke in the first run. The two other runs were successful; the filling patterns were very equal.

The melt front level has been plotted in the same way as in the previous trails.

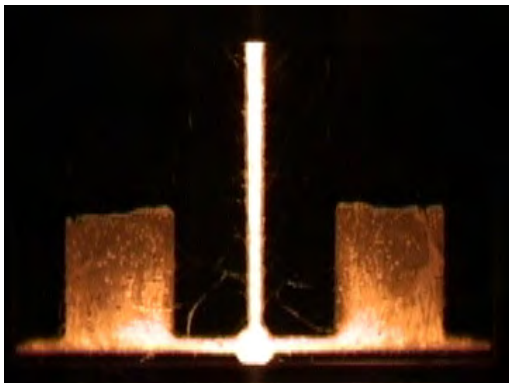

Figure 4.87 Filling of the 2 mm plates.

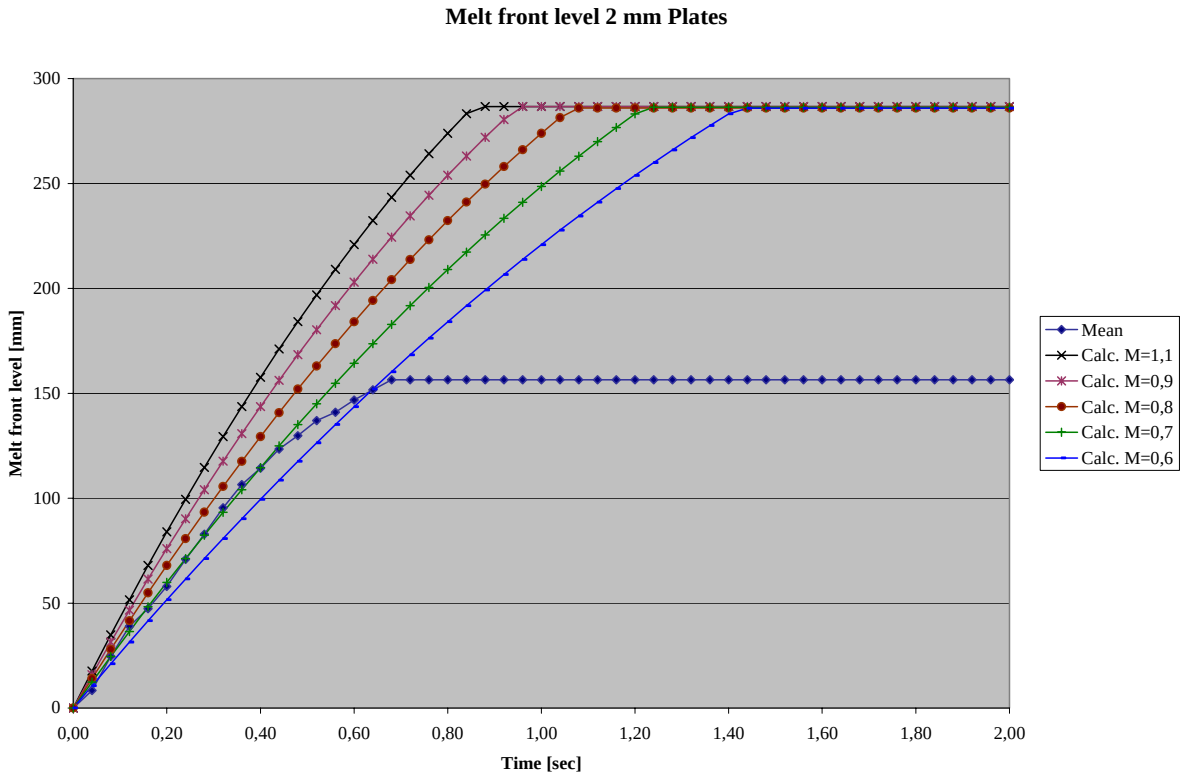

Figure 4.88 Measured and theoretical melt front levels as a function of time.

A total loss coefficient of 0.7 gives the best fit between measured and theoretical data.

4.7.3.1 Filling of the down runner

Snapshots showing the initial filling of the horizontal runner are shown below:

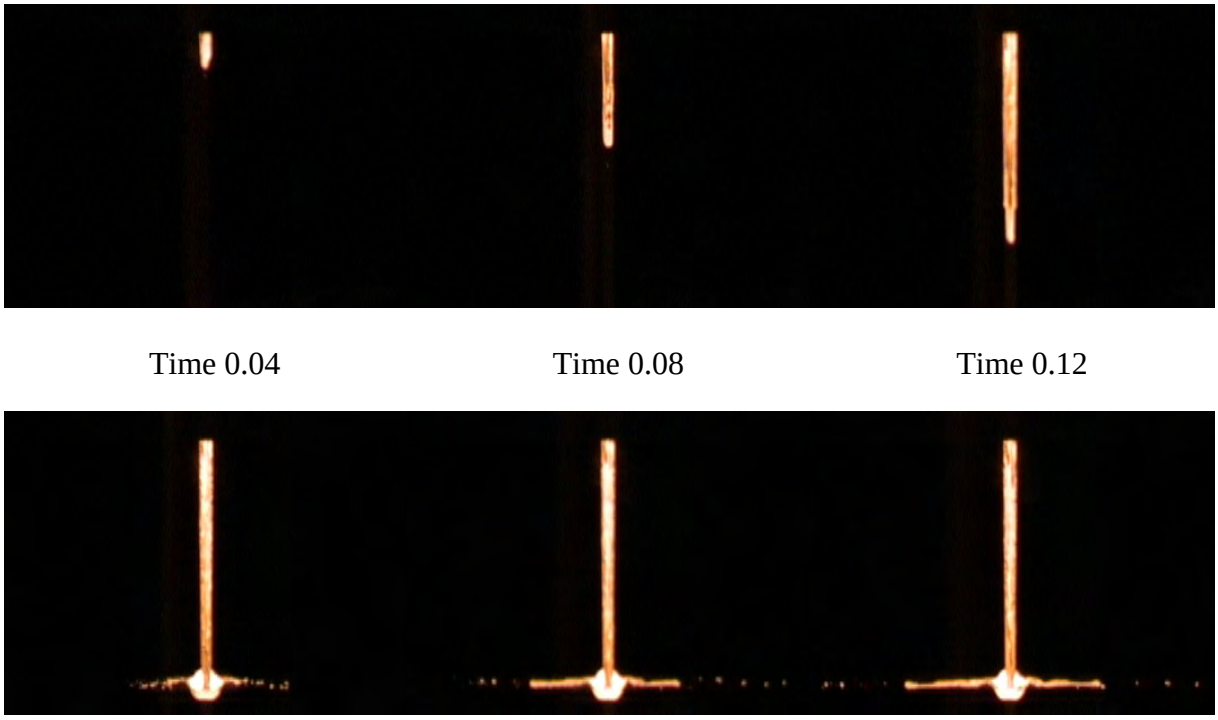

Time 0.04 Time 0.08 Time 0.12

Time 0.16 Time 0.20 Time 0.24

Figure 4.89 Filling of the down runner for the 2 mm plates.

The melt stream is almost filling the complete cross section of the down runner when it hits the bottom of the well. This can be seen at 0.12 s. The well is empty when the melt hits the bottom of it. The result is a lot of droplets shooting into the horizontal runner at 0.16 s. This is the same as discussed in the previous section with the 3 mm plates. Again an empty well is not able to handle the initial melt flow in an acceptable way. The initial melt flow rate is 125 cm^3/s when calculated without losses.

4.7.3.2 Filling of the horizontal runner

Snapshots showing the initial filling of the horizontal runner are shown below:

Time 0.28 Time 0.32 Time 0.36

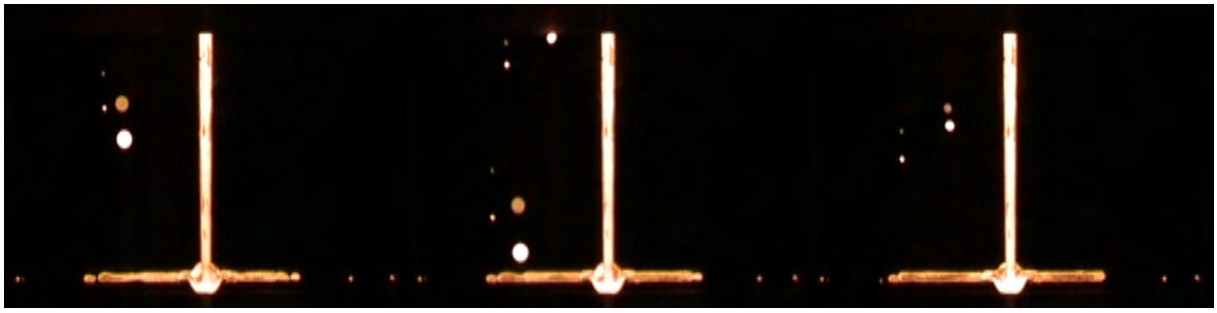

Time 0.40 Time 0.44 Time 0.48

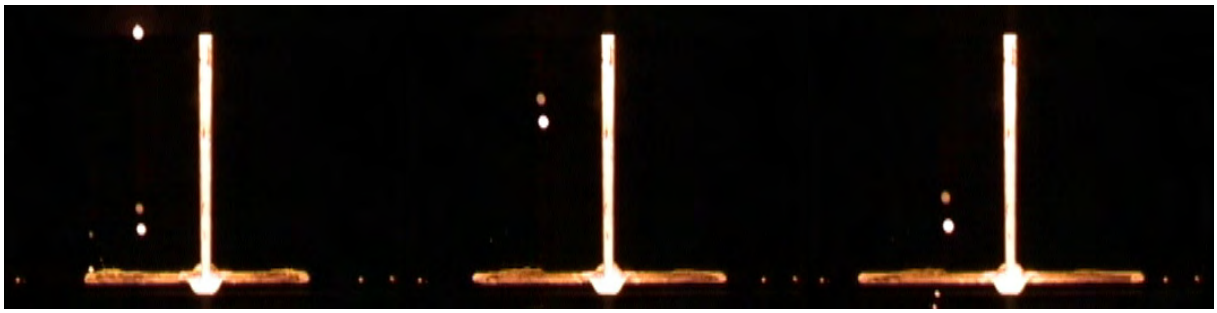

Time 0.52 Time 0.56 Time 0.60

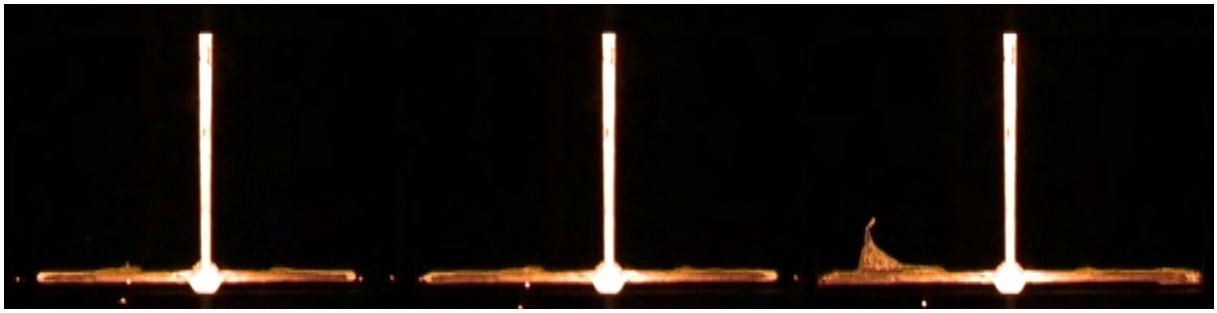

Time 0.64 Time 0.68 Time 0.72

Figure 4.90 Filling of the horizontal runner of the 2 mm plates. The big droplets to the left are from the stopper core.

A lot of droplets are seen in the horizontal runner. They are caused by a bad performing well. The main melt fronts in the horizontal runner come to an almost stand still at 0.28 s. The melt fronts start to move again at 0.56 s. The cross section of the horizontal runner is being partly filled up in the time interval from 0.28 s to 0.56 s. The melt front velocities increase from 400 mm/s to 650 mm/s from 0.56 s and until the fronts reach the ends of the horizontal runner. The increasing melt front velocity indicates that the horizontal runner is gradually being filled up behind the melt front. The velocities of the melt fronts would otherwise have been constant. Another way to look at it is to calculate the total filling time of the horizontal runner. The runner starts to fill after 0.16 s and is completely filled at 0.70 s. The length of the runner is 197 mm, i.e. the mean melt front velocity in the horizontal runner is 365 mm/s. The theoretical melt front velocity in the horizontal runner is calculated to 709 mm/s when calculated with out losses. Comparing the measured and calculated melt front velocities or filling times gives a loss coefficient of 0.5 for the filling of the horizontal runner.

This is a very high loss compared to what is found for the filling of the plates. The filling of the gating system takes place under relatively turbulent conditions, which introduces high losses. When the gating system is filled the flow takes place more smoothly and hence the losses are significant smaller. That the sizes of the losses depend on how the flow takes place is supported by the losses calculated in Table 4.6. Here the friction losses for the flow in the plates have been calculated both assuming laminar and turbulent flow. The turbulent flow results in losses approximately 3 times larger than the laminar flow.

The increasing melt front velocity in the horizontal runner shows a partly filled cross section of the runner through the complete filling of it. The cylinder shaped down runner well is hence not performing as intended. One of the main tasks of the well is to secure a completely filled cross section of the horizontal runner right from the first melt passes through.

4.7.3.3 Melt flow pattern in the plates

Snapshots from the initial filling of the 2 mm plates can be seen below:

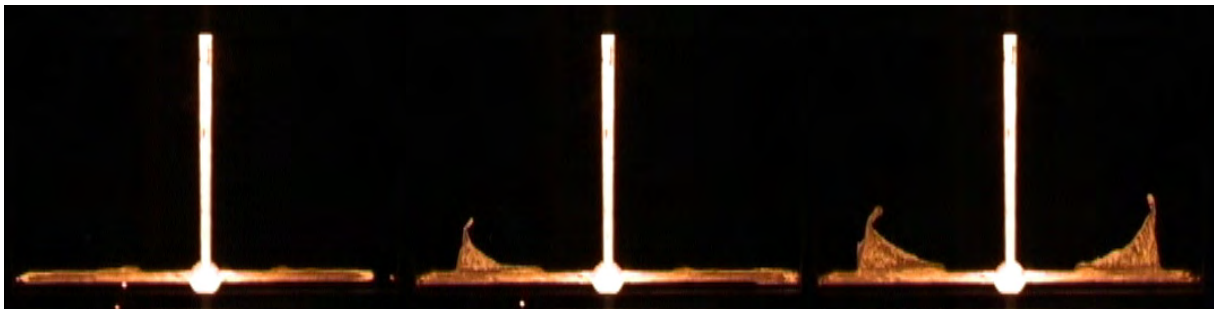

Time 0.68 Time 0.72 Time 0.76

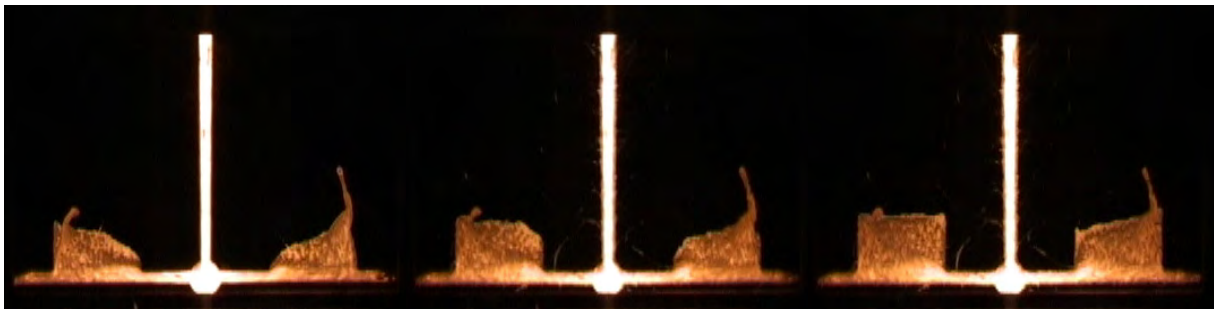

Time 0.80 Time 0.84 Time 0.88

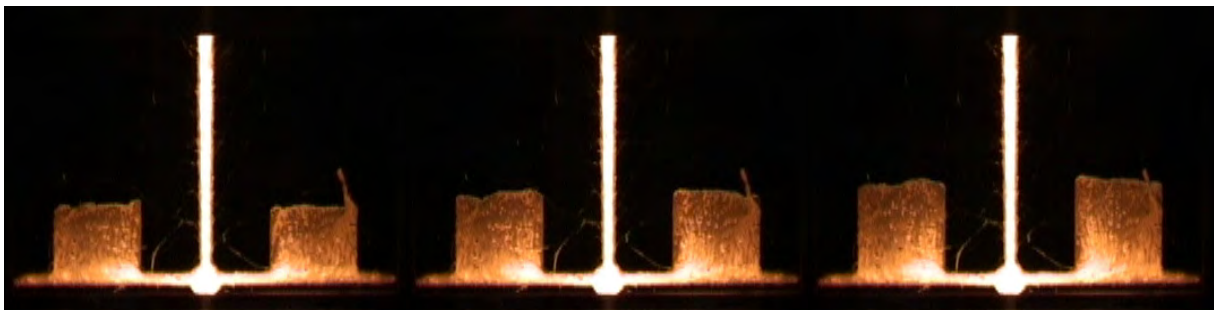

Time 0.92 Time 0.96 Time 1.00

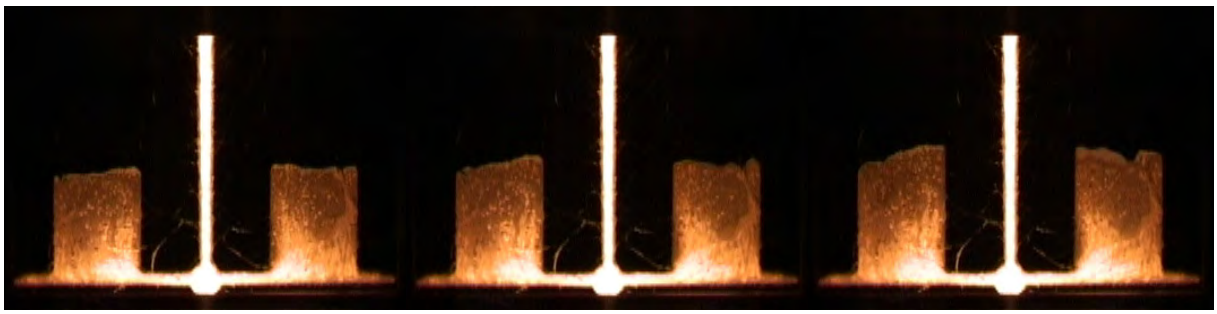

Time 1.04 Time 1.08 Time 1.12

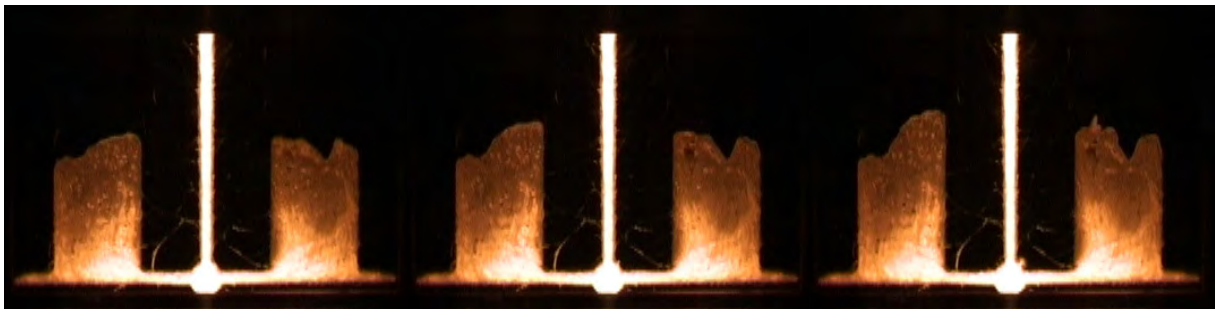

Time 1.16 Time 1.20 Time 1.24

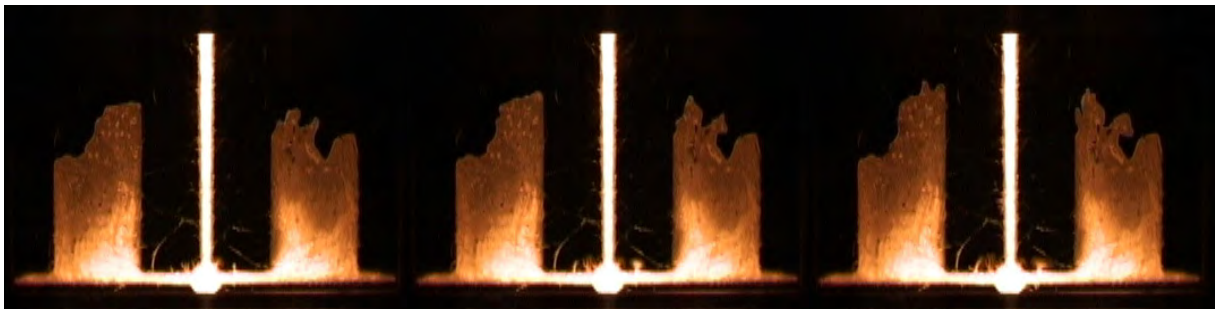

Time 1.28 Time 1.32 Time 1.36

Figure 4.91 Snapshots showing the filling of the 2 mm plates.

The velocity of the melt front is 650 mm/s when it hits the ends of the horizontal runner. The theoretical value calculated without losses is 709 mm/s. The relative small difference between the measured and the calculated figures indicates filled cross sections of the horizontal runner when the metal reaches the ends of it. The initial melt front velocity in the plates is close to the theoretical. This also indicates a filled horizontal runner. The enlargements on Figure 4.92 show the section around the well after 0.68 and 0.72 s i.e. at the same time as the melt front reaches the ends of the runner and the melt starts to flow into the plates. No voids are seen in the area of the well on Figure 4.92. This together with a completely filled cross section is the perfect starting point for at large melt tongue being blown into the plates because no buffers exist for softening the conversion of dynamic pressure to static pressure when the melt hits the end of the horizontal runner. The metal shoots into the right plate at 0.76 s. But the melt front does not break up; no droplets leave the mean melt front. Actually not a single droplet is seen in the plates at any time. The metal shoots into the plates at the outside edges in this case. The reason for this is the completely filled cross section of the horizontal runner. The last part of the horizontal runner to be filled is the ends of the runner; hence the pressure

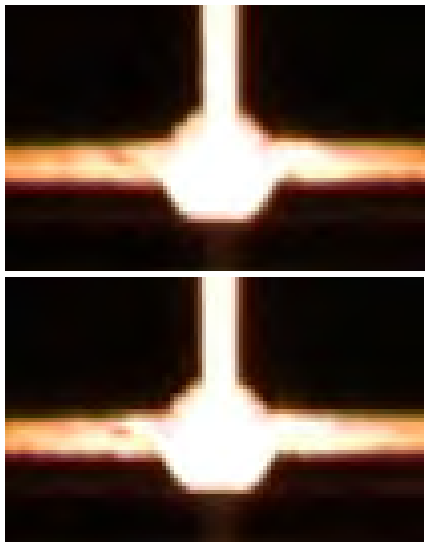

Figure 4.92 Enlargement of the area around the well at 0.68 s and 0.72 s.

shock wave is generated here. The first place the pressure shock wave can spread out is at the outside edges of the plates.

A large difference in flow pattern is revealed when comparing the flow in the 2 mm plates seen here to the fountain seen in the second run of the 3 mm plates. Even though a melt tongue also is blown into the cavity at the 2 mm plates the flow is much more controlled. The back pressure from the surface tension increases as the plate thickness decreases. The back pressure from friction generated by flow in the plate cavities is also getting larger as the thickness is decrease as showed in section 4.5.2.2. As the plate thickness gets smaller less mass has to be controlled. I.e. higher velocities can be allowed in 2 mm sections than in 3 mm sections without getting the melt front to split up into single droplets. As discussed in section 4.6.6 is it not only the velocity that decides whether the melt front breaks up or not, the appearance of pressure shock waves can also lead to breaking up of the melt front.

The effect from a gating system with dead ends and insufficient ability to gradually reduce the melt velocity is again clearly seen. When this is combined with a completely filled horizontal runner the splashes occur when the melt hits the end of the horizontal runner.

4.7.4 Summing up on the loss coefficients

The loss coefficient for the layout for the 4 and 3 mm plates is found to be 0.9. The value for the layout for the 2 mm plates is found to be 0.7. When including the effect from surface tension the loss coefficient for the layout for the 2 mm plates is changed to 0.64. The value for the layout for the 3 mm plates changes to 0.86. The value for the layout for the 4 mm plates is even less affected by surface tension than the 3 mm plates. A pouring basin has been used for the trials described in this section, resulting in a relative large final driving pressure when compared to the other test days. The influence from surface tension through the back pressure generated gets significant towards the end of the filling as the driving pressure decreases. The relatively big final driving pressure seen here due to the pouring basin reduces hence the influence from the surface tension.

The boundary conditions have been very consistent due to the use of the pouring basin. The decreasing melt level in the basin has been incorporated in the calculations of the theoretical melt front levels. Incomplete filling of the horizontal runner when the metal enters the plate cavities blurs the results some. Comparing the slopes of the measured and theoretical curves gives although a good estimate of the loss coefficients.

4.7.5 Summing up on the filling of the down runner well and the horizontal runner

The performance of the cylindrical shaped down runner well is not acceptable. The well is not able to secure a completely filled cross section of the horizontal runner from the first melt passes through the runner. It is also not able to prevent a smaller or larger amount of melt droplets being blown into the horizontal runner ahead of the main melt front. The cylindrical well is Ø30 mm, 45 mm high with 5 degrees draft. The vertical dimension of the horizontal runner is 9 mm. The well has to handle 125 cm^3/s to 298 cm^3/s during the filling of the horizontal runner when calculated without losses.

The weakness of the cylindrical well is especially seen at the 3 mm plates. Small differences in how the melt passes through the down runner results in very different performances of the well. The well performs very badly if it is empty when the main melt stream hits the bottom of it.

The flow in the horizontal runner can also be very different, partly due to differences introduced by the varying performance of the down runner well.

I.e. with this conventional type of well and runners only minor changes in the pouring conditions can lead to large changes in the filling of the gating system.

The loss coefficient for the filling of the horizontal runner at the 2 mm plates is found to 0.5. This is a high loss compared to what is found for the filling of the plates. The filling of the gating system is relatively turbulent, resulting in high losses. When the gating system is filled the flow is taking place more smoothly, and hence the losses are significant lower.

4.7.6 Summing up on the flow patterns in the plates

The closing of the last air pocket in the horizontal runner initiates a pressure shock wave. The pressure shock wave breaks up the melt surface in the plates. If there is no or only a small amount of melt in the plates when this happens no back pressure exists and a melt tongue is blown into the plate cavity. If the last air pocket is closed after a significant melt level has been reached in the plates, small “explosions” take place at the melt surface shooting small droplets ahead of the main melt front. In both cases, the melt surface breaks up as close as possible to the last air pocket, i.e. where the pressure shock wave is initiated. With this conventional type of gating system even small differences in the pouring conditions are able to change the position of the last air pocket in the gating system. I.e. small differences in the pouring conditions are able to change the filling pattern of the plates drastically.

Even in the same mould, cavities of a symmetrical layout can fill very differently with this conventional type of gating system. This can lead to random or “unaccountable” scarp. With a symmetrical layout the cavities are expected to fill in the same manner and hence they are expected both to produce either scrap or sound castings and not a sound and a scrap casting in the same mould.

The main flow patterns in the plates are the same as in the previous trial made without the pouring basing and at slightly lower velocities. The flow patterns are summarized below:

Test day	Mean velocity mm/s	Size of horizontal runner	4 mm	3 mm	2 mm
5	340	Small	Outside→Centre→Outside	Outside→Centre→Outside	Centre

Table 4.12 Main flow paths.

4.8 Discussion of the loss coefficients

The loss coefficients found in the different trial runs have been summarized in Table 4.13.

Test day	Plate thickness	Loss coefficient without surface tension	Loss coefficient including surface tension	Mean melt front velocity Design	Size of horizontal runner	Pouring basin
1	3	0.8	0.75	120	Large	No
2	4	0.7-0.8	0.7-0.8	120	Large	No
2	3	0.7	0.65	120	Large	No
3	4	0.8	0.8	300	Large	No
3	3	0.8	0.75	300	Large	No
3	2	0.7-0.8	0.6-0.7	300	Large	No
4	4	-	-	300	Small	No
4	3	0.8-0.9	0.8-0.9	300	Small	No
4	2	0.8	0.7	300	Small	No
5	4	0.9	0.9	340	Small	Yes
5	3	0.9	0.86	340	Small	Yes
5	2	0.7	0.64	340	Small	Yes

Table 4.13 Comparison of loss coefficients.

The lowest losses are seen at test day 5 where the pouring basin has been used. The driving pressures have been corrected to the actual circumstances both when pouring with and without the basin. The melt level in the pouring cup has been recorded on video at the trials made without the basin. This makes it possible to use the actual melt level in the pouring cup as the driving pressure when calculating the theoretical melt front levels. When running with the basin it is filled to a fixed level before the stopper core is removed. The continuity equation makes it possible to correct the driving pressure as the filling proceeds when completely filled runners are assumed.

The seemingly higher losses when running without the basin are due to the less stable conditions during hand pouring, i.e. for instance the direction of the pouring stream. The direction of the pouring stream is able to introduce a vena contracta at the top of the down runner as seen in section 4.6.2.3 resulting in a partly filled down runner. The partly filled down runner will mean reduced flow compared to a completely filled down runner.

The highest losses are seen for the plates cast without the pouring basin. This indicates that no momentum has been transferred from the pouring stream to the gating system. Only the 4 mm plates cast at test day 4 show reduced losses. In this case the pouring stream is seen to go directly into the down runner during the complete filling sequence. This combined with a very low melt level in the pouring cup makes it possible to transfer momentum from the pouring stream to the gating system. When the pouring cup is filled, the melt will swirl around in the cup and the momentum will be lost before the melt enters the gating system, unless very stream lined designs are used.

The influence from surface tension has been found in section 4.3.1 and section 4.7. The influence can be seen as a constant reduction in the driving pressure. The reduction is independent of flow velocity. When using bottom filling gating systems the driving pressure is getting smaller and smaller as the filling proceeds. As the effect from surface tension is equal to a constant reduction in the driving pressure, the influence from it is getting relatively larger as the filling proceeds. When increasing the final driving pressure as done in the trials with the pouring basin the influence from the surface tension is decreased as described in section 4.7.4.

When including the effect from surface tension in the calculations of the theoretical melt front levels, the curves showing the melt front levels as a function of time are getting a more realistic shape especially towards the end of the filling sequence. Hence it makes it easier to compare theoretical and measured curves.

For the complete filling of the plates the effect from surface tension will change the loss coefficient for the 2 mm plates with approximately 0.1. For the complete filling of the 3 mm plates the surface tension changes the loss coefficient with 0.05. The influence on the filling of the 4 mm plates is insignificant or as low as 0.03. The figures are valid when not running with the pouring basin. When running with the pouring basin the figures are changed to: 0.06 for the 2 mm plates, 0.04 for the 3 mm plates, and 0.03 for the 4 mm plates.

The wall friction in the plates has been estimated in section 4.5.2.2. The effect from wall friction follows the same trend as the surface tension. I.e. decreasing the wall thickness increases the resistance to flow generated by wall friction.

The wall friction in the plates is proportional to the length the metal has travelled in the section; it is also proportional to the velocity if the flow is laminar. If the flow is turbulent the wall friction is proportional to the square of the velocity. As a bottom filling gating system is used the velocity is decreasing as the filling proceeds. I.e. as the filling of the plates proceeds will the losses due to friction increase or decrease due to the balance between the increasing flow length and reduction in velocity. Whether the flow is turbulent or laminar is also influencing the development of the friction forces due to the different dependence on velocity. The estimates for the friction given in Table 4.6 and Table 4.7 indicate close to constant friction during the filling of the last half of the plates. Independent of whether the flow is turbulent or laminar. It is notable that the absolute sizes of the losses due to friction in the plates are small when comparing to the driving pressure.

The possible changing contribution to the total loss coming from friction in the plates is not included in the calculations of the theoretical melt front levels; a constant loss coefficient through the complete filling has been used. With the values given in Table 4.6 and Table 4.7 for the friction losses seems this to be a good approximation.

When comparing the curves showing the melt front levels as a function of time some of them show a tendency to higher losses towards the end of the filling. This could be due to increasing friction as the filling of the plates proceeds.

But the possible higher losses towards the end of the filling can also be caused by a starting cold shot. The mechanisms controlling cold shots described in section 2.11 will not bring the melt front to an abrupt stand still. It will instead reduce the melt velocity over some distance.

Unfortunately it is not possible to say which effect is controlling or if it is a combination of both.

The deviation between measured and theoretical data is seen not to grow constantly through the complete filling sequence, see for instance Figure 4.60. This indicates that effects from a beginning cold shot are the cause for the deviation. Because of this the slopes of the measured and the theoretical curves have been compared when determining the loss coefficients and not the total filling times or the last part of the curves.

The trials made with the pouring basin have had the best defined pouring conditions. Hence the values from these trials are the best estimates for the loss coefficients. I.e. the total loss coefficient for the layout for the 4 mm plates is estimated to 0.9, for the layout with the 3 mm plates is the estimate 0.86 and for the layout for the 2 mm plates the loss coefficient is estimated to 0.64. With the effects from surface tension and wall friction it is reasonable to get higher losses when the wall thickness decreases. The values given in Table 4.3 and Table 4.6 for the back pressure due to surface tension and friction indicate a bigger change in loss coefficient when going from 3 to 2 mm wall thickness than when going from 4 to 3 mm wall thickness. This tendency is also seen in the results from the trials.

The above mentioned losses are found for a mean melt velocities of approximately 270 mm/s in the plates. When comparing to the loss coefficients found for the other melt front velocities, higher losses are found for the lower velocities. As discussed above is this not due to the velocity but the less well defined boundary conditions. Lower losses are to be expected for lower velocities. This picture is blurred to some extend by the fact that lower velocities generally also mean higher temperature losses in the gating system, i.e. lower melt temperatures and hence higher viscosities. Higher viscosities mean higher losses as the viscous forces get larger. Still with the adverse effect from the changes in viscosity with lower melt velocity, the higher losses seen for the lower velocities are believed to be caused by the less well defined pouring conditions present at the trials with the low melt front velocities.

The loss coefficients for 2–4 mm sections given in [Ref. 4.2] indicate higher losses than observed here. The values given in [Ref. 4.2] are for flow in thin sections intended for ingates, where the velocities normally are higher than what is investigated here. It is unfortunately not possible to extract any further information about the influence of velocity from the experiments described here due to the less well defined boundary conditions at the lower velocities.

Good estimates of the loss coefficient at different wall thicknesses have been found. But investigating the loss coefficient has not been the main purpose of the trials. If this had been the main purpose better setups could have been made where the loss coefficients for different parts of the gating systems could have been directly investigated.

General expressions for loss coefficients in different geometries can be found in the literature; see for instance [Ref. 4.7] but they all assume laminar or fully developed flow, i.e. flow in sections at least 25-40 diameters down stream from the inlet to the section. This is very seldom the case in gating systems. Hence investigations comprising trials with actual gating systems have to be made when detailed studies of the losses in gating systems are made. Work has been done in this area, see for instance [Ref. 4.8], but with far from fully developed flow one has to be careful with transferring results found for one specific setup to another.

4.9 Discussion of the filling of the down runner well and the horizontal runner

A conventional bottom filling gating system has been used. The initial filling of the runners can take place in two basically different ways; with or without completely filled cross sections. The two different ways of filling the runners has large consequences for the subsequent flow patterns.

First of all the performance of the cylindrical down runner well is depending on whether the cross sections of the down runner are filled or not. In some cases a thin melt jet is ahead of the main melt front. See for instance Figure 4.83 run 1. This thin melt jet will reach the well before the main melt front and fill the bottom of it. It acts as a cushion for the main melt stream and hence it is able to reduce the amount of droplets being blown into the horizontal runner. The down runner well is not in all cases able to prevent droplets in the horizontal runner even though a melt cushion exists. One could claim that a partly filled down runner is an advantage in the sense that it reduces the amount of droplets being blown into the horizontal runner. But a partly filled down runner can lead to other problems and the advantage is only seen because the well is not performing as intended.

When the initial melt stream passing through the down runner fills the complete cross section of it, and the down runner well is empty when the main melt stream hits the bottom of it, a lot of droplets are blown into the horizontal runner, see for instance Figure 4.89. In this case the performance of the cylindrical well is very ineffective. It is not able to fulfil the main criteria for the performance of a well given in section 2.10.

In general the cylindrical well is ineffective at securing a completely filled cross section of the horizontal runner right from the first melt passes through it. The melt is in some cases reflected from the bottom of the well and blown into the horizontal runner along the top surface of the runner, see for instance Figure 4.27. The melt is able to travel quite a distance in the horizontal runner before touching the bottom surface of the it.

In some cases the melt is seen to travel half way through the horizontal runner with a partly filled cross section, then the melt front comes to an almost complete stand still and the cross section of the runner behind the melt front is filled up before any further movement of the melt front. This can for instance be seen on Figure 4.84 run 2 from 0.32 s.

I.e. the way the horizontal runner fills changes from mould to mould meaning the gating system is not able to secure stable conditions.

Pressure shock waves coming from the hammer effect when the horizontal runner is completely filled up are very difficult to avoid with this conventional type of gating system. The pressure shock waves can be initiated in two different ways, again depending on whether the cross sections of the runners are filled or not.

If the cross section of the horizontal runner is filled when the first melt passes through it, the hammer effect will occur when the melt fronts hit the ends of the horizontal runner. This means no melt or only a very low melt level is in the plates when the pressure shock wave is

initiated, hence no significant back pressure is present. The result is that melt tongues are shot into the plate cavities, see for instance Figure 4.91.

If the cross section of the horizontal runner is not completely filled when the first melt passes through it, the pressure shock wave is initiated later. Air pockets are often seen in the horizontal runner at the outlet of the well. They can exist until a significant part of the plates has been filled, see for instance Figure 4.62. When they collapse pressure shock waves are initiated. In this case the back pressure from the melt in the plate cavities is able to prevent a melt tongue being blown ahead of the main melt front. Instead small surface "explosions" are seen blowing droplets ahead of the main melt front, see for instance Figure 4.61 at 0.84 to 0.96 s. The pressure shock wave is initiated where the last air pocket in the gating system is, and hence it spreads out from here. The melt surface breaks up as close as possible to the origin of the pressure shock wave.

Whether the runner is filled from the first melt passing through it or not is controlled by very small variations in the pouring conditions with this conventional gating system. This is illustrated with the results described in section 4.7.2. Very different filling patterns of the same gating system are seen even though the pouring conditions have been kept very constant. A basin has been used for pouring the moulds, only leaving space for very little variation in the pouring conditions from mould to mould. The pouring basin gives less variation from mould to mould in the pouring conditions than seen in normal production with an automatic pouring device. I.e. minor but inevitable changes in the pouring conditions can lead to large changes in the way the initial melt flows through the gating system.

It is not only the geometry of the well that decides whether the complete cross section of the horizontal runner is filled. With large area ratios between the choke and the horizontal runner it gets more difficult to secure completely filled horizontal runners. But on the other hand too large velocities can normally not be allowed in the horizontal runner. The above discussed problems with securing a completely filled horizontal runner puts emphasis on not using larger horizontal runners than necessary, or the development of rules for maximum allowable area expansion without introducing problems with incomplete filled runner cross sections.

Different designs have been tried to gradually reduce the velocity of the melt in the horizontal runner to prevent the hammer effect giving pressure shock waves in the melt. None of the tried designs have given the wanted effect. Further work is needed to investigate other ways of gradually reducing the velocity of the melt. For instance the cross section of the horizontal runner can be reduced gradually over the complete length of the plate ingate. This has been done for a brake disc layout discussed in section 5, where the results also can be seen.

From the problems seen with partly filled runners being able to initiate pressure shock waves very late in the filling sequence emphasis must be put on the importance of securing completely filled cross section right from the first melt passes through the runners. Hence to be sure not to get pressure shock waves it is crucial both to secure completely filled runner cross sections right from the first melt passes through and to gradually reduce the melt front velocity in the horizontal runner before it hits the end.

The cylindrical down runner well used here is Ø30 mm 45 mm high with 5 degrees draft. The vertical dimension of the horizontal runner connected to it is 9 mm. The flow rate through the

well during the filling of the horizontal runner is in the range from 65 to 334 cm^3/s when calculated without losses.

From the above described problems connected to the performance of a cylindrical shaped down runner well this type of well can not be recommended. It only shows to some extent acceptable performance when the cross section of the down runner is not completely filled with the first melt passing through, and in the cases of very moderate melt flow, see section 4.5.3.1. Different designs of square shaped wells will be discussed in section 5 making it possible to compare the performance of the two types.

4.10 Discussion of the flow patterns in the plates

The flow in the plates is controlled by two different factors. The main flow pattern is controlled by the balance between the dynamic forces and the braking forces. Pressure shock waves initiated by the hammer effect when the last air pocket in the horizontal runner is closed, decide whether and when splashes occur.

The main flow paths in the plates is depending on the gating design and the thickness of the plates. The results from the trials are summarized in Table 4.14.

Test day	Mean velocity mm/s	Size of horizontal runner	4 mm	3 mm	2 mm
2	120	Large	Centre→Outside	Inside	Inside
3	300	Large	Outside→Centre→Outside	Outside→Centre→Outside	Centre
4	300	Small	Outside→Centre→Outside	Outside→Centre→Outside	Centre
5	340	Small	Outside→Centre→Outside	Outside→Centre→Outside	Centre

Table 4.14 Comparison of the main flow paths.

4 mm plates
When comparing the main flow paths in the 4 mm plates, they are seen to be very equal except for test day 2. The low flow rate and large area of the horizontal runner at test day 2 is able to change the initial balance between dynamic and braking forces to the benefit of the braking forces resulting in the initial flow going through the centre of the plates. When discussing test day 2, one has to bear in mind the design of the ends of the horizontal runner. The bends used are intended for gradually reducing the melt velocity in the horizontal runner. The bends going upwards will reduce the initial melt flow going into the plates meaning reduced dynamic forces even further than the melt velocity of 120 mm/s indicates. At all test days the final flow is taking place at the outside edge of the plates. This even though the final flow velocity in the horizontal runner varies from 107 to 381 mm/s and the velocity in the plates varies from 82 to 224 mm/s when calculated without losses. This indicates that the controlling factor for the distribution of the flow sidewise is the plate geometry and, in this range of velocities, not the velocity it self.

The influence from the hammer effect when the last air pocket in the horizontal runner is closed is resulting in a large fountain at test day 2; see Figure 4.28. At the other test days the last

air pocket in the runner is closed after a significant melt level has been reached in the plates. The result is small surface “explosions” giving droplets being blown ahead of the main melt front; see Figure 4.55 at 0.84 s and Figure 4.78 at 0.84 s. The low flow rate and large cross sectional area of the horizontal runner at test day 2 compared to the high flow rate and small area of the horizontal runner at test day 5 does not make one expect to see a fountain at test day 2 and not at test day 5. In fact the other way around would seem much more likely. This indicates a weakness in the gating design used here. Even over a vide range of flow rates and dimensions of the horizontal runner small but probably inevitable changes in the pouring conditions can change the initiation of pressure shock waves and hence result in fountains where they are not expected and suppress them where they seem to be more likely to appear.

3 mm plates
The main melt flow patterns for the 3 mm plates are similar except for the flow seen at test day 2. In test day 2 the main flow is taking place at the inside edge of the plates during the complete filling. At the other days the initial filling of the plates is taking place at the outside edges, and then the main flow is shifted towards the centre of the plates, finally the last part of the flow is taking place at the outside edges of the plates. The reason for the difference between the flow patterns at test day 2 and the other test days is the same as for the 4 mm plates.

The hammer effect causes a large fountain shooting into the plate cavity at run 2 of test day 5. I.e. in this case a fountain is seen in the trial with the highest melt velocity in the plates and with the highest melt velocity in the horizontal runner both giving the best conditions for getting a fountain. The fountain is caused by a completely filled horizontal runner and a lack of ability to gradually reduce the melt velocity. No fountain is, on the other hand, seen in run 1 of the same day. The difference in flow patterns between two runs made with very equal pouring conditions shows the variety of flow patterns obtainable with only minor changes in the pouring conditions when using this conventional type of layout.

2 mm plates
As with the 3 and 4 mm plates the flow pattern seen at test day 2 is different from the flow patterns seen at the other days. The main flow takes place at the inside edge of the plates at test day 2. At the other test days the flow is taking place at the centre of the plates. I.e. the dynamic and braking forces are balanced at the other test days.

At test day 5 the hammer effect is able to blow a significant melt tongue into the 2 mm plates, al though it is not as large as the one seen at the 3 mm plates. But it shows that even at 2 mm wall thickness where the braking forces are relatively large it is possible to get the surface to break up due to pressure shock waves. A late closing of an air pocket in the horizontal runner is also at 2 mm wall thickness able to cause small surface explosions at the melt front, see for instance Figure 4.72 at 1.04 s.

General
The flow moves towards the outside edges when the velocities in the plates are increased from 120 mm/s to 300 mm/s. This is caused by a combination of changes in the balance between dynamic and braking forces and reduced tendency to cold shot with higher velocity. The tendency to cold shot is strictly seen also a braking force. But it is most conveniently handled separately. When changing the flow velocity it is possible to change the melt distribution and also the temperature distribution in the plates. This is possible even though the wall thickness is quite low. Thin and thicker sections are often combined in real castings. The

above shows the possibility to introduce temperature profiles in very thin sections by the filling, for instance enhancing directional solidification toward the heavier section where possibly a feeder can be attached. Before changing the flow velocities in the thin walled sections to enhance the wanted temperature profiles; one of course has to secure a completely filled part. This can be difficult and in some cases demand for filling through the thin sections.

The reduction of the horizontal runner done from test day 3 to 4 does not change the flow patterns in the plates at any of the plate thicknesses. This indicates the controlling factor to be the conditions decided by the plate thickness and not the flow velocity in the horizontal runner at this melt velocity in the plates and range of velocities in the horizontal runners. I.e. the braking forces from flow in the 2 mm plates are large enough to change the balance between braking and dynamic forces when comparing to the 3 and 4 mm plates.

The balance between dynamic and braking forces is very delicate. This is shown in details in section 4.5.2.2 for flow in 3 mm plates. The balance can change during the filling sequence giving initial flow at the outside edge, intermediate flow shifted towards the centre of the plates and the last part of the flow can take place at the outside edges of the plates.

Because the balance is very delicate it is hard to predict. This means if one wants to control the distribution of melt flow through a plate shaped ingate it is not wise to rely on the balance between the dynamic and braking forces. The gating system has to be designed to control the distribution of the melt. Different ways of gradually reducing the area of the horizontal runner is used in practice to try to control the sidewise distribution in a plate shaped ingate, but it is still the balance between the dynamic and braking forces that control the distribution and this makes it hard to predict. Due to this are no effective rules existing describing how the reduction has to be done. Hence systems with wide plate shaped ingates connected to a horizontal runner can not be recommended if control over the melt distribution sidewise is needed. Examples of horizontal runners being gradually reduced over the complete length of the plate ingate and systems giving a high degree of control over the melt is shown in section 5. Gradually reducing the cross section of the horizontal runner can also be used to gradually reduce the velocity of the melt to prevent the hammer effect giving pressure shock waves as discusses previous. Even though the melt distribution is hard to predict it is consistent. The same setup gives the same main melt distribution in every mould.

The use of the pouring basin at test day 5 does not change the flow patterns in the plates compared to test day 4 where the moulds were poured by hand. This was also not expected. The better pouring conditions given by the basin were intended for securing more consistent conditions from mould to mould. Consistent pouring conditions make it possible to directly compare the initial flow from mould to mould, and hence make it possible to investigate the ability of the gating systems to secure consistent flow patterns from mould to mould.

As discussed in section 4.9 the initial filling of the gating system is taken place in different ways, initiating pressure shock waves at different stages of the filling sequence. This influences the filling of the plates. Section 4.7.2.2 shows large differences in the filling patterns of 3 mm plates caused by pressure shock waves occurring at different stages of the filling sequence. The pressure shock waves can also mean that a symmetrical layout fills very unsymmetrical. The result can be one cavity giving a sound casting and one giving a scarped casting. Hence random or “unaccountable” scarp is seen. The results show that the conventional type of gating system used here is not able to secure consistent flow patterns from mould to mould.

This means the conventional type of gating system used in this section can not be recommended for castings with high demands to the quality as the variation in the filling patterns can be very large and hence the stability of the quality will be affected.

At almost every trial the melt front in the plates is seen to break up. Either as a melt tongue shooting into the cavity or small surface “explosions”. It is not the melt velocity it self that causes the melt front to become unstable and break up. At the velocities investigated here breaking up of the melt fronts in the plates is caused by pressure shock waves initiated by a bad performing gating system. In the trials described in this section, the maximum melt front velocity is 340 mm/s. If the pressure shock waves can be avoided significantly higher melt front velocities than the 340 mm/s can probably be utilized without the melt front getting unstable. In most literature a velocity criterion is used as for instance in [Ref. 4.9] to describe when the melt fronts become unstable. The Weber number described in section 2.3 combines the velocity with the cross section thickness to give a measure for how stable the melt fronts are. But none of the today used criterions include effects from pressure shock waves. One could claim that pressure shock waves are assumed not to take place in the gating systems in question as they are very unwanted. But from the work described in this section and also the work described in section 5 is it clear that pressure shock waves are very difficult if not impossible to avoid in conventional gating systems. And hence the effect of them has to be taken into account when working with conventional gating systems.

Further work has to be done on the area to develop a criterion for the breaking up of the melt fronts, including effects from pressure shock waves. With the high tendency to get pressure shock waves in conventional gating systems it would probably be better to use the time on developing gating systems not giving pressure shock waves in stead of trying to predict them and the damage they cause. Two approaches can be taking. One is to try to build shock absorbers into the system to soften the effect from pressure shock waves. Another approach is to design the gating system without dead ends and with runners securing completely filled cross sections with the first melt passing through, hence removing the two main sources for getting pressure shock waves. Gating systems utilising such designs and hence removing the two main sources for getting pressure shock waves are shown in section 5 with one of the layouts for the brake disc and in section 6 with different gating systems for a thin walled manifold.

4.11 Conclusions

A conventional bottom filling gating system has been used for casting plates with 2, 3 and 4 mm thickness. Glass plates have been used as one mould half making is possible to record the flow patterns on video. Detailed analysis of the melt flow has been made.

The following can be concluded from the trials:

- The loss coefficients for the filling of the layouts for the plates are found to be 0.9 for the 4 mm plate layout, 0.85 for the 3 mm plate layout and 0.6 for the 2 mm plate layout. The losses are found for mean velocities of approximately 270 mm/s I the plates. For flow in such thin sections larger values are often found in the literature, but the values from the literature are often intended for ingates where the velocities normally are higher.

- A cylinder shaped down runner well cannot be recommended when moderate melt flow rates have to be handled. This type of down runner well is not able to prevent melt droplets from being blown into the horizontal runner ahead of the main melt front. The cylinder shaped well is only in seldom cases able to secure completely filled runners from the first melt passing through.

- Different designs have been tried to gradually reduce the velocity of the melt in the horizontal runner before it hits the end of it, to prevent the hammer effect, which gives pressure shock waves in the melt. None of the tried designs have lead to the wanted effect. Further work is needed to investigate other ways of preventing the pressure shock waves.

- The pressure shock waves can be initiated at two different stages in the filling sequence. If the cross section of the runners is completely filled behind the melt front when the melt reaches the end of the runner the pressure shock wave is initiated here. The result is a large melt tongue being blown into the plate cavity because no or only little melt is in the plates for giving back pressure. If the last air pocket in the horizontal runner is closed after a significant melt level has been reached in the plate cavities, the result is small surface “explosions” blowing droplets ahead of the main melt front.

- Small differences in the pouring conditions are able to change the position of the last air pocket in the gating system and hence also the flow patterns drastically. It is very important to design the gating systems in order to have good control over the melt, securing the melt to behave in the same way in every mould even though some minor but inevitable changes in the pouring conditions take place. The conventional type of bottom filling gating system used here is not able to absorb minor but inevitable changes in the pouring conditions and hence it is not able to secure consistent melt flow from mould to mould.

- Even in the same mould, cavities of a symmetrical layout are seen to be able to fill very differently with the conventional type of gating system used in this section. This can lead to random scrap which is very hard to explain. When for instance seeing inclusions in the top of the casting it is hard to figure out, that the reason may be an air pocket in the gating system closed late in the filling sequence and resulting in a pressure shock wave blowing melt ahead of the main melt front.

- Due to the fact that small differences from mould to mould in the pouring conditions can change the flow patterns drastically when using conventional gating systems, like the one used in this section, it can not be recommended to use such systems for casting thin-walled parts with high demands to the quality.

- Partly filled runners are seen to be able to initiate pressure shock waves very late in the filling resulting in melt droplets blown ahead of the main melt front in the casting cavity. Hence emphasis must be put on the importance of securing completely filled runner cross sections right from the first melt passes through. To be sure not to get pressure shock waves it is crucial both to secure completely filled runner cross sections right from the first melt passes through and to gradually reduce the melt front velocity in the runner before it hits the end of it in the case of a gating system with a dead end.

- The breaking up of the melt front in the plates is not due to the velocity of the melt front it self at the velocities investigated here but due to pressure shock waves coming from a poorly performing gating system. If the shock waves can be avoided it is probably possible to utilize significantly higher velocities than the 340 mm/s investigated here and still not getting the melt front to break up.

- The criterions used today for describing if the melt front breaks up are based on velocity and in some cases a combination of velocity and section thickness. None of them include the effects from pressure shock waves. With conventional gating systems pressure shock waves are very difficult to avoid. Hence criterions for the breaking up of the melt front including effects from pressure shock waves have to be developed. A better way to spend the time would be to develop gating systems not giving pressure shock waves.

- Another consequence of the high sensitivity to small changes in the pouring conditions for this conventional type of gating system is problems with simulating the flow patterns. With the possibility of getting very different flow patterns due to minor differences in the pouring conditions it is virtually impossible to simulate the flow patterns. The large differences in the flow patterns are mainly seen at the initial part of the filling. The main flow patterns in the subsequent flow when the gating system is completely filled are on the other hand stable and can hence be simulated with success.

- The melt flow pattern in the plates, i.e. whether the flow takes place at the outside or the inside edge of the plates, is controlled by a delicate balance between dynamic and braking forces. This makes it harder for a simulation program to predict the flow. It is of course also hard if not impossible for the foundry engineer to predict it.

- Plate shaped ingates connected to a horizontal runner cannot be recommended if a specific melt flow distribution is wanted as it is hard to predict. On the other hand the main melt flow, i.e. not the effects from the pressure shock waves, is consistent from mould to mould.

- Although the flow pattern is hard to predict it is possible to change it and hence it is also possible to change the temperature distribution in the plates. It can be done by varying the flow velocities. This is possible even though the wall thicknesses are quite small. Thin and thicker sections are often combined in real castings. It is possibility to introduce temperature profiles in very thin sections by the filling, for instance enhancing directional solidification toward the heavier sections where possibly a feeder can be attached.

The flow patterns in thin walled plates are not only interesting for casting thin walled sections. Thin walled plate shaped ingates connected to a horizontal runner are used in different very important applications. The most important is probably casting of brake discs in vertically parted green sand moulds. At least 300 million brake discs are cast every year, a major part of them are cast in vertically parted moulds utilizing plates shaped ingates.

References

Ref. 4.1 DISAMATIC 2110 Pattern Tools. 2110T1020 DISA Industries A/S, (1995)

Ref. 4.2 DISA Industries Application manual Reg. No. 9152H2111 Edition 09/95, (1995)

Ref. 4.3 Mould filling experiments on mould flow in thin wall castings. Nieswaag, H. ; Denn, H.J.J. 57th World foundry congress Exchange paper 10, (1990)

Ref. 4.4 Formfyldning af meget tyndvægget støbegods The Technical University of Denmark IPL-070-03 Søren Skov Hansen (2003)

Ref. 4.5 ASM Handbook. Volume 15 Casting. ASM International Second Printing, (1992)

Ref. 4.6 Introduction to fluid mechanics. 3rd Edition. Robert W Fox, Alan T. McDonald. John Wiley & Sons (1985)

Ref. 4.7 Handbook of Hydraulic Resistance. 3rd Edition. I.E.Idelchik. CRC Press Begell House, (1994)

Ref. 4.8 ASM Handbook. Volume 15 Casting. ASM International Second Printing, (1992)

Ref. 4.9 Castings. John Campbell. Butterworth Heinemann (2002)

Appendix 4.1

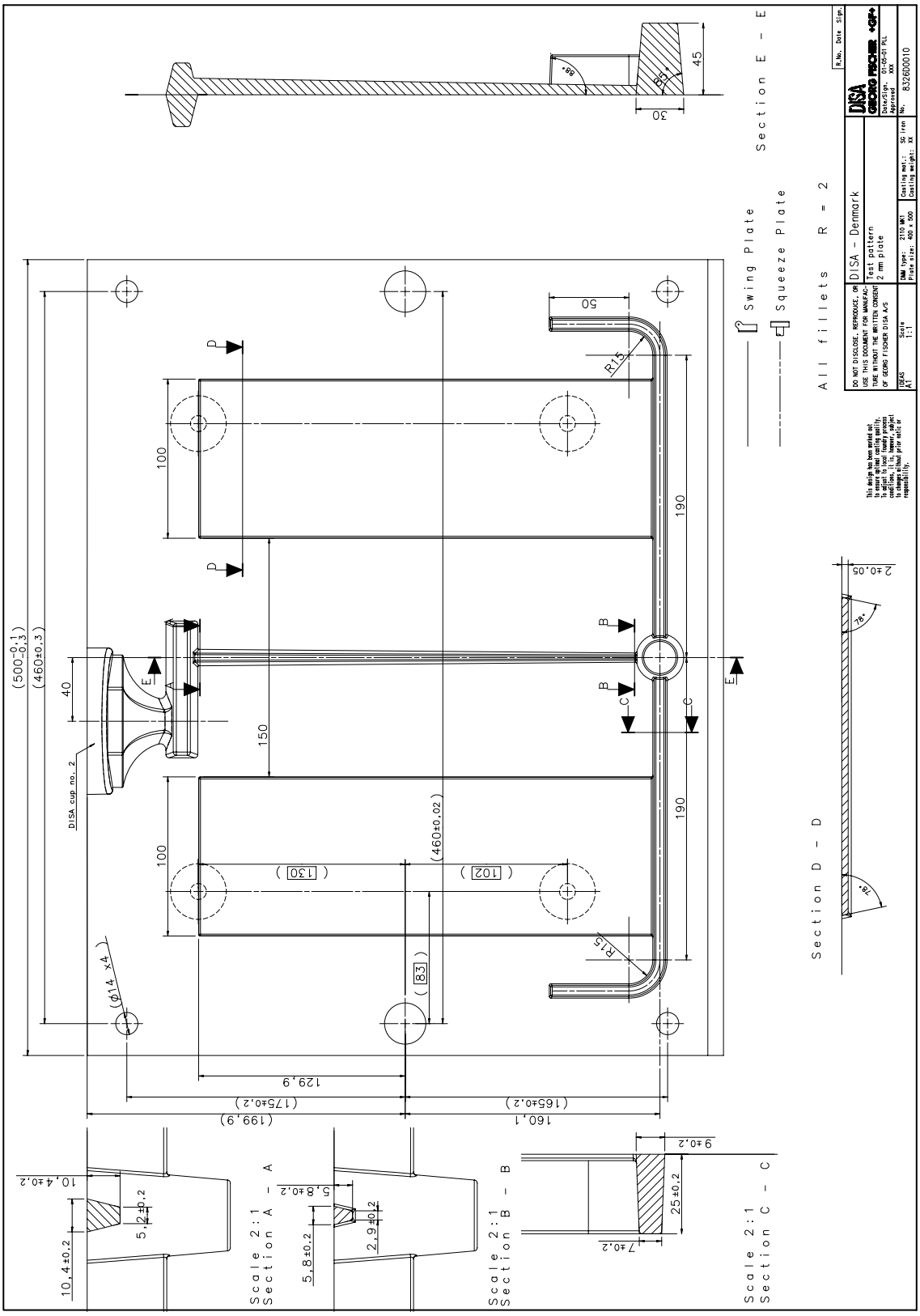
Section E - E
Swing Plate
Squeeze Plate
All fillets R = 2
DISA - Denmark
Test pattern
2 mm plate
DISA cup no. 2
Section D - D
Scale 2:1
Section A - A
Scale 2:1
Section B - B
Scale 2:1
Section C - C

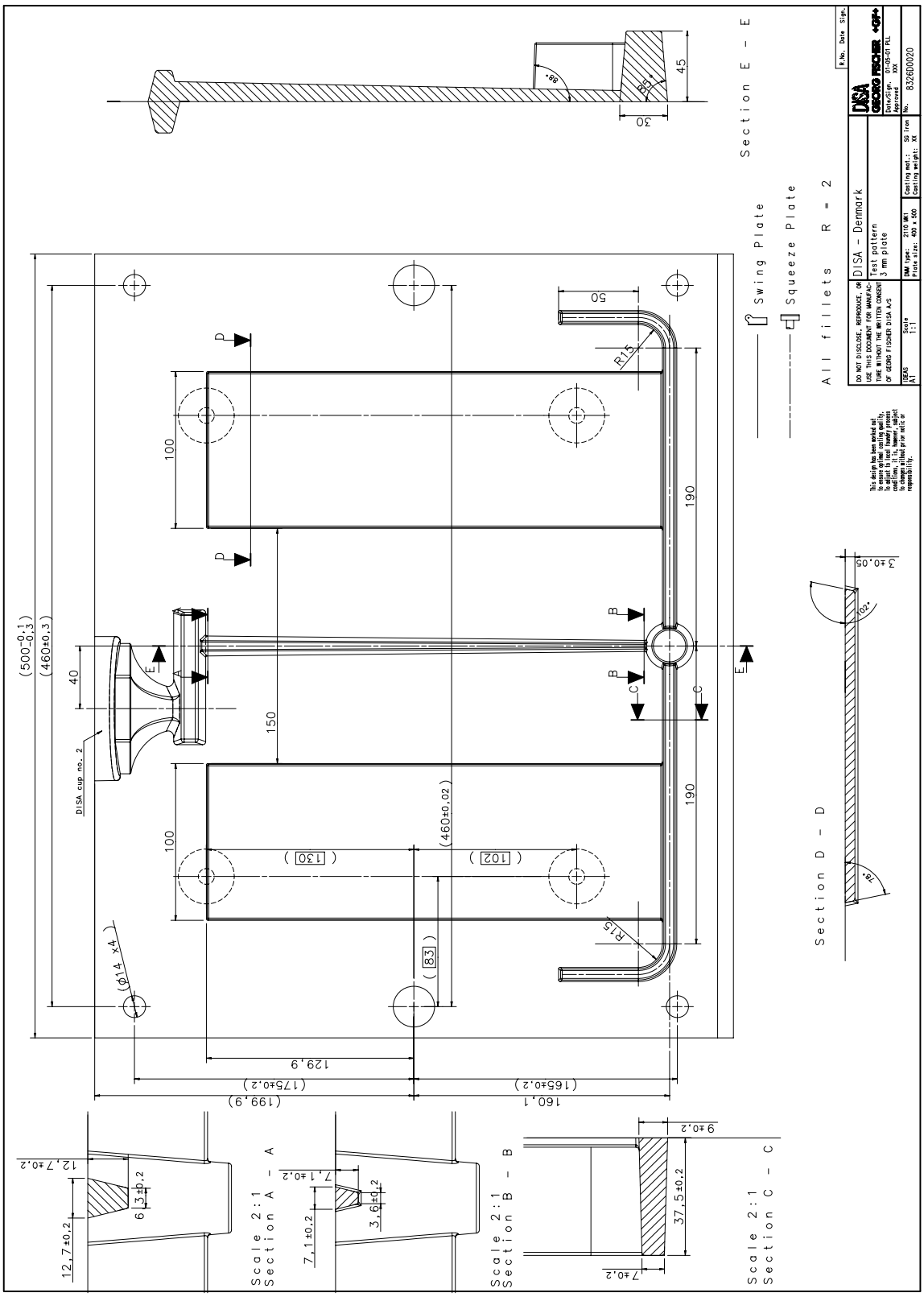
Section E - E
Swing Plate
Squeeze Plate
All fillets R = 2
DISA - Denmark
Test pattern
3 mm plate
DISA cup no. 2
Section D - D
Scale 2:1
Section A - A
Scale 2:1
Section B - B
Scale 2:1
Section C - C

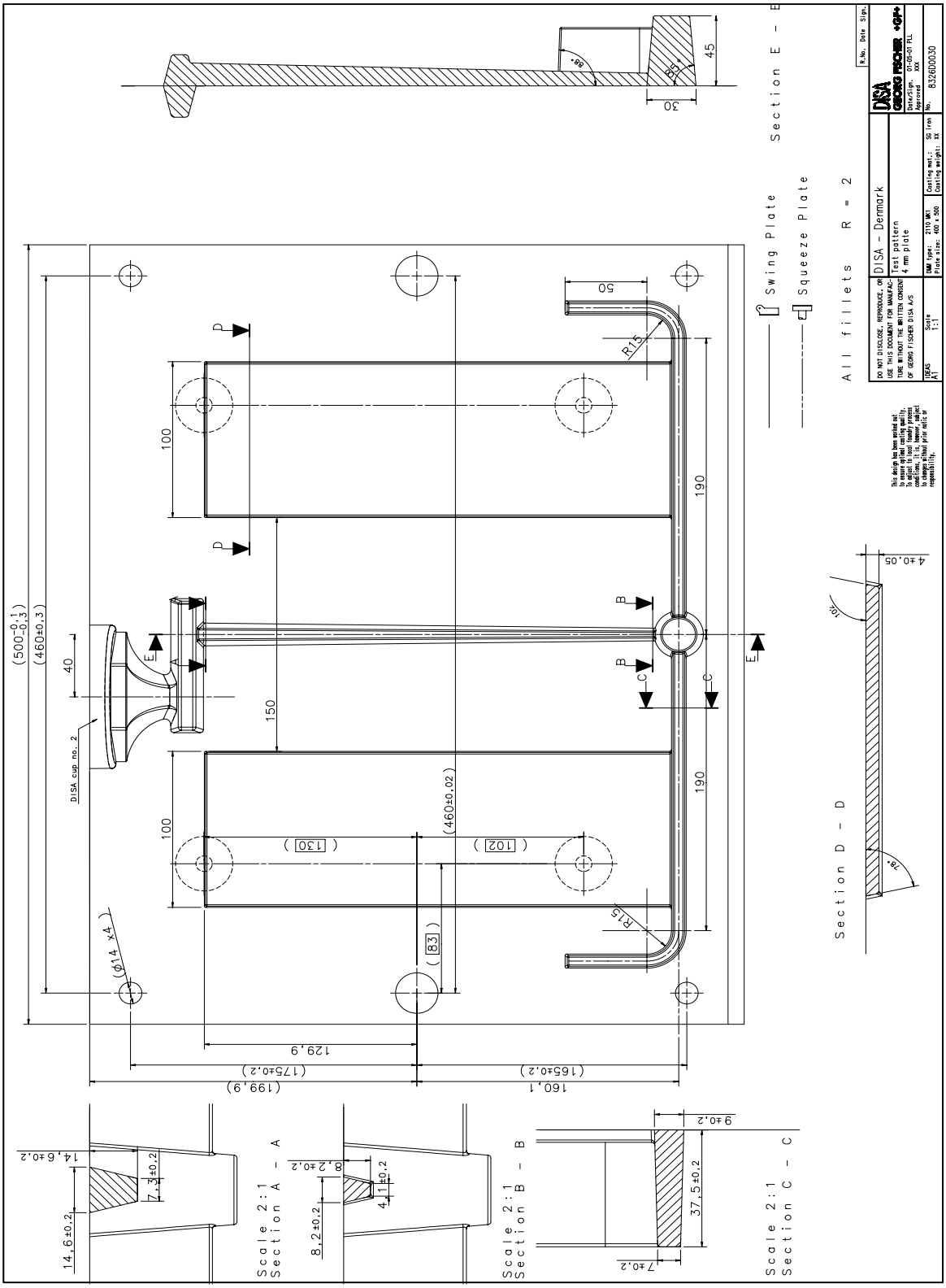
Swing Plate
Squeeze Plate
All fillets R = 2
Section E - E
Section D - D
Scale 2:1
Section A - A
Scale 2:1
Section B - B
Scale 2:1
Section C - C
DISA cup no. 2
DISA - Denmark
Test pattern
4 mm plate
DMM type: 2110 MKI
Plate size: 400 x 500
Casting mat.: SG iron
Casting weight: XX
No. 83260030
Scale 1:1
A1

Appendix 4.2

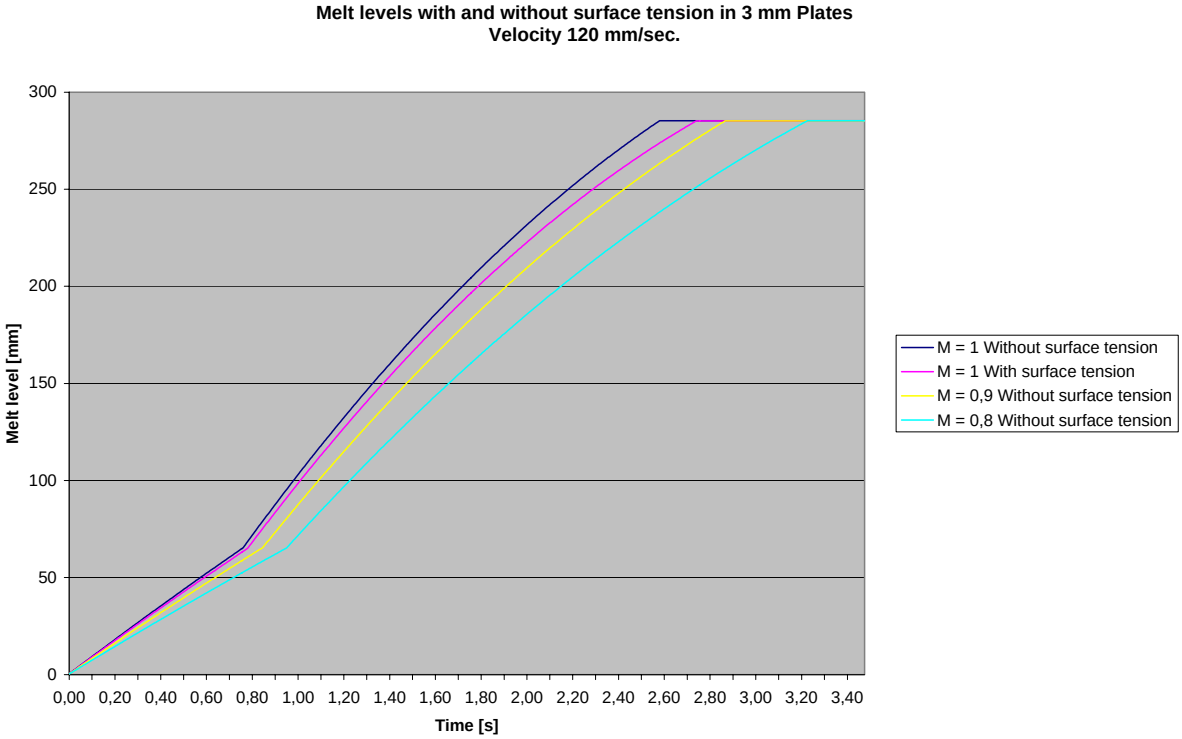
Melt levels with and without surface tension in 3 mm Plates
Velocity 120 mm/sec.
Melt level [mm]
300
250
200
150
100
50
0
0,00 0,20 0,40 0,60 0,80 1,00 1,20 1,40 1,60 1,80 2,00 2,20 2,40 2,60 2,80 3,00 3,20 3,40
Time [s]
M = 1 Without surface tension
M = 1 With surface tension
M = 0,9 Without surface tension
M = 0,8 Without surface tension

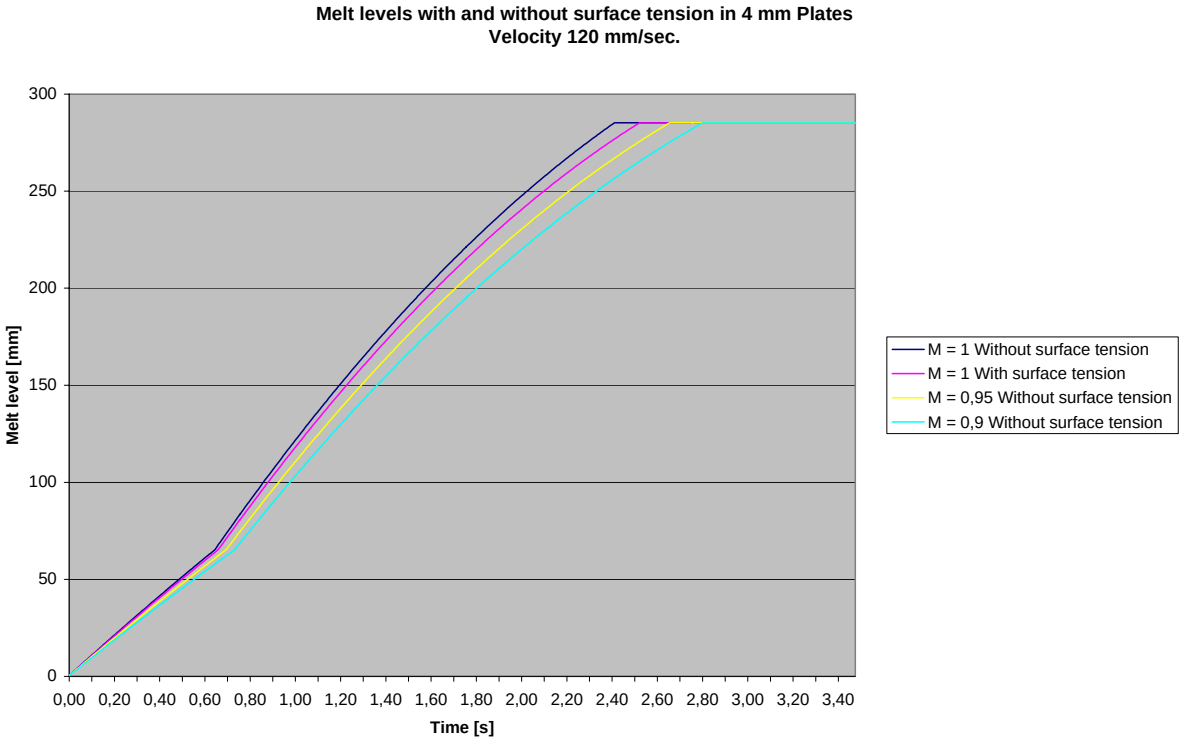
Melt levels with and without surface tension in 4 mm Plates
Velocity 120 mm/sec.
Melt level [mm]
300
250
200
150
100
50
0
0,00 0,20 0,40 0,60 0,80 1,00 1,20 1,40 1,60 1,80 2,00 2,20 2,40 2,60 2,80 3,00 3,20 3,40
Time [s]
M = 1 Without surface tension
M = 1 With surface tension
M = 0,95 Without surface tension
M = 0,9 Without surface tension

Appendix 4.3

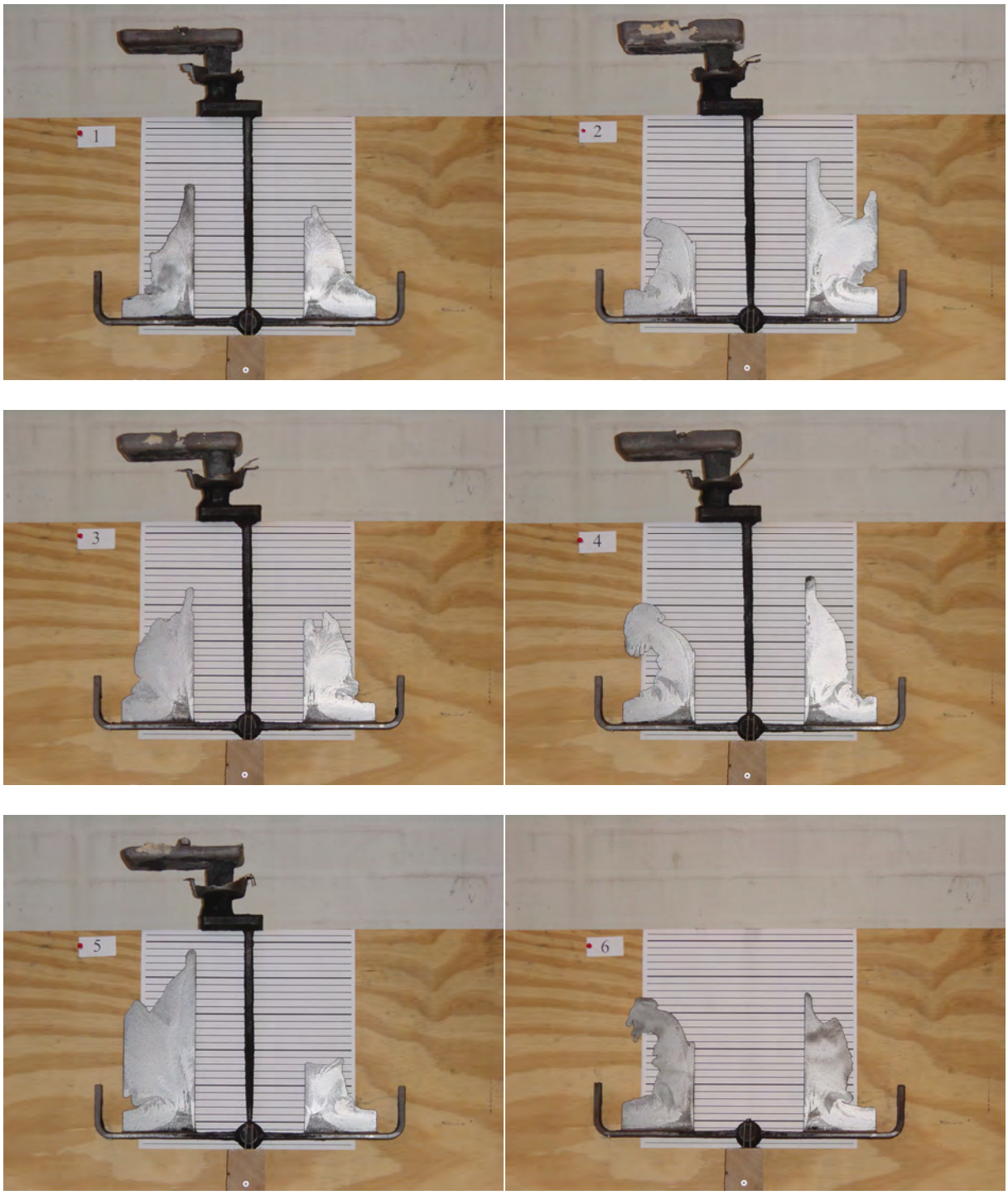

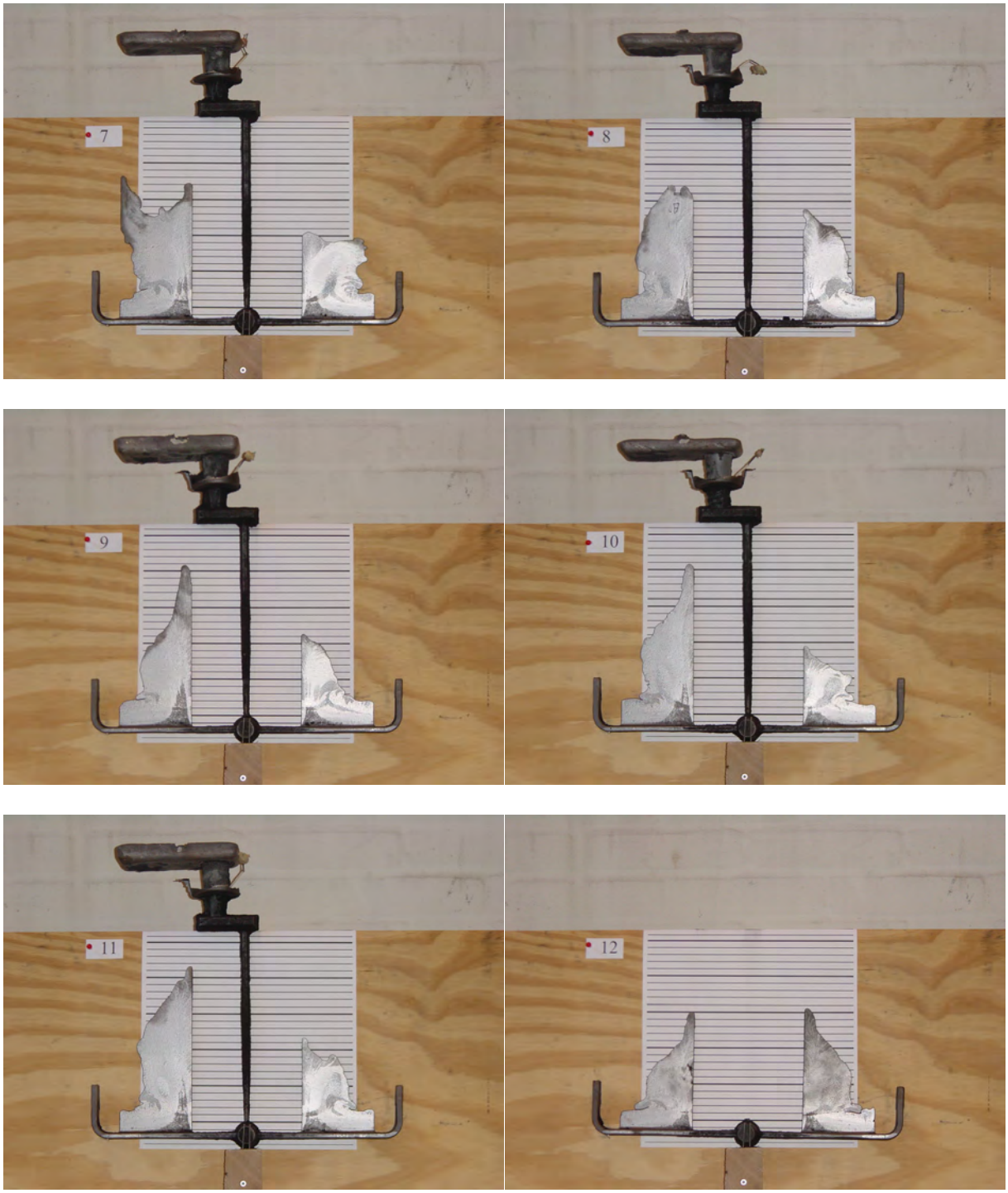
7
8
9
10
11
12

Appendix 4.4

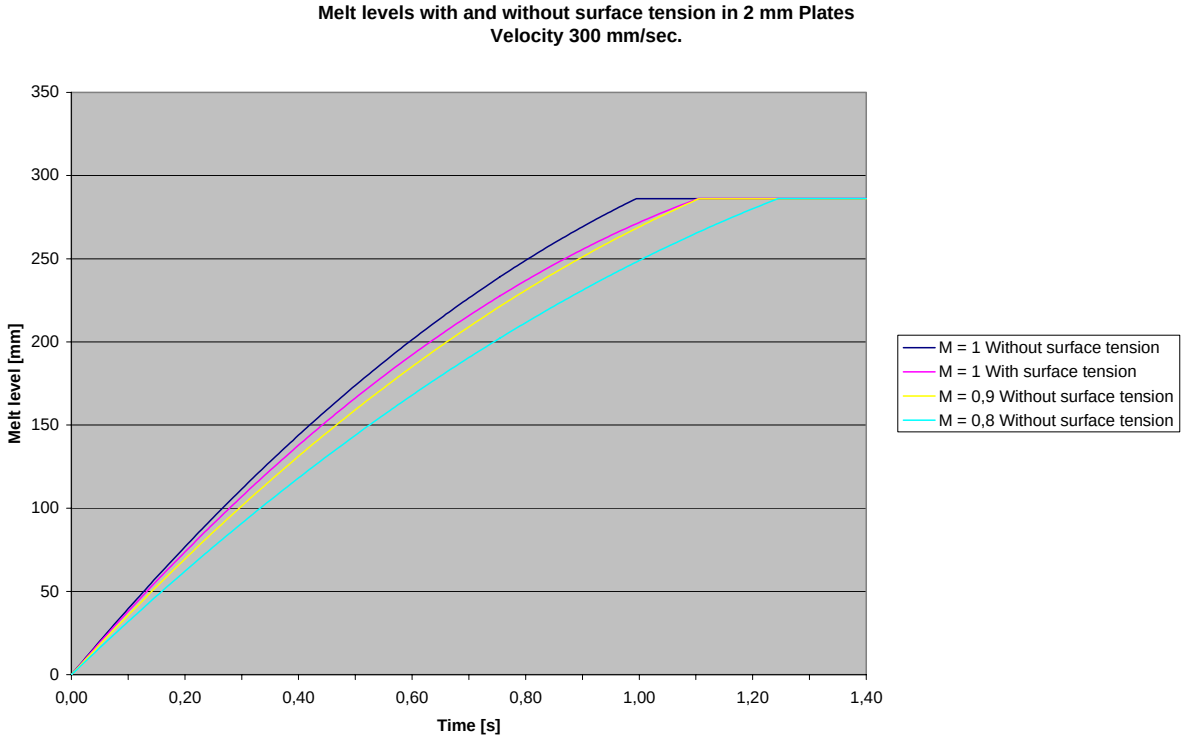
Melt levels with and without surface tension in 2 mm Plates
Velocity 300 mm/sec.
Melt level [mm]
350
300
250
200
150
100
50
0
0,00
0,20
0,40
0,60
0,80
1,00
1,20
1,40
Time [s]
M = 1 Without surface tension
M = 1 With surface tension
M = 0,9 Without surface tension
M = 0,8 Without surface tension

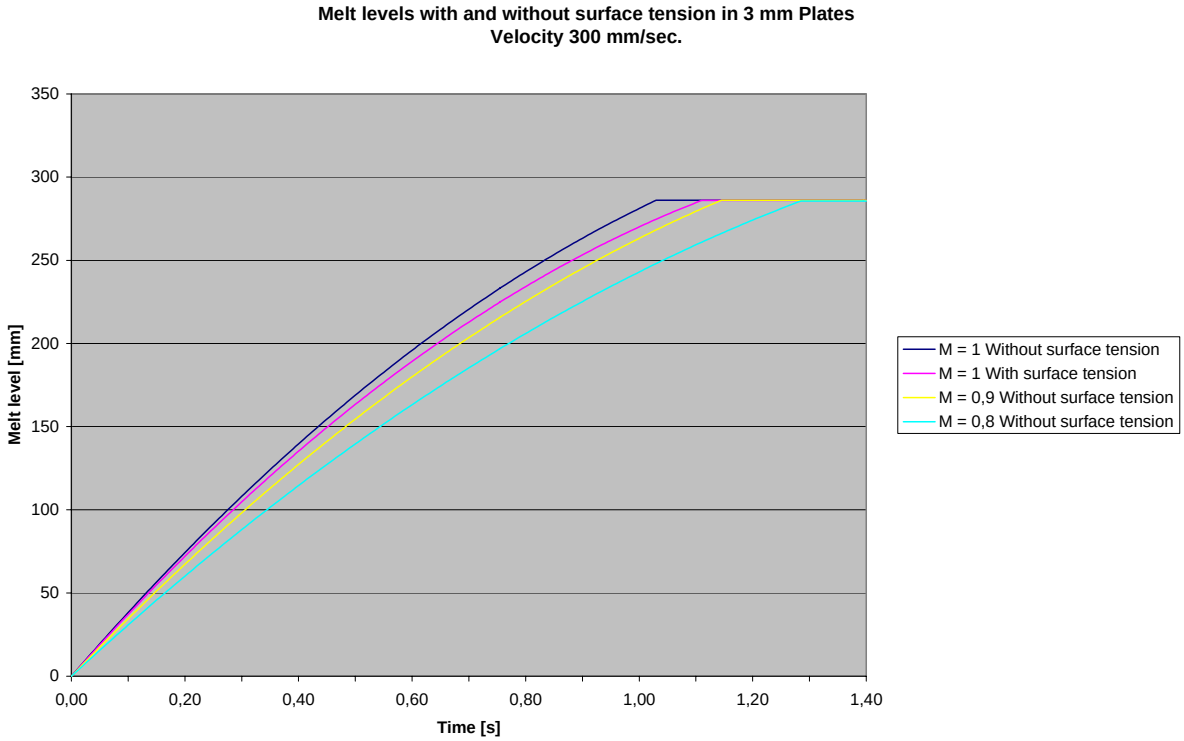
Melt levels with and without surface tension in 3 mm Plates
Velocity 300 mm/sec.
Melt level [mm]
350
300
250
200
150
100
50
0
0,00
0,20
0,40
0,60
0,80
1,00
1,20
1,40
Time [s]
M = 1 Without surface tension
M = 1 With surface tension
M = 0,9 Without surface tension
M = 0,8 Without surface tension

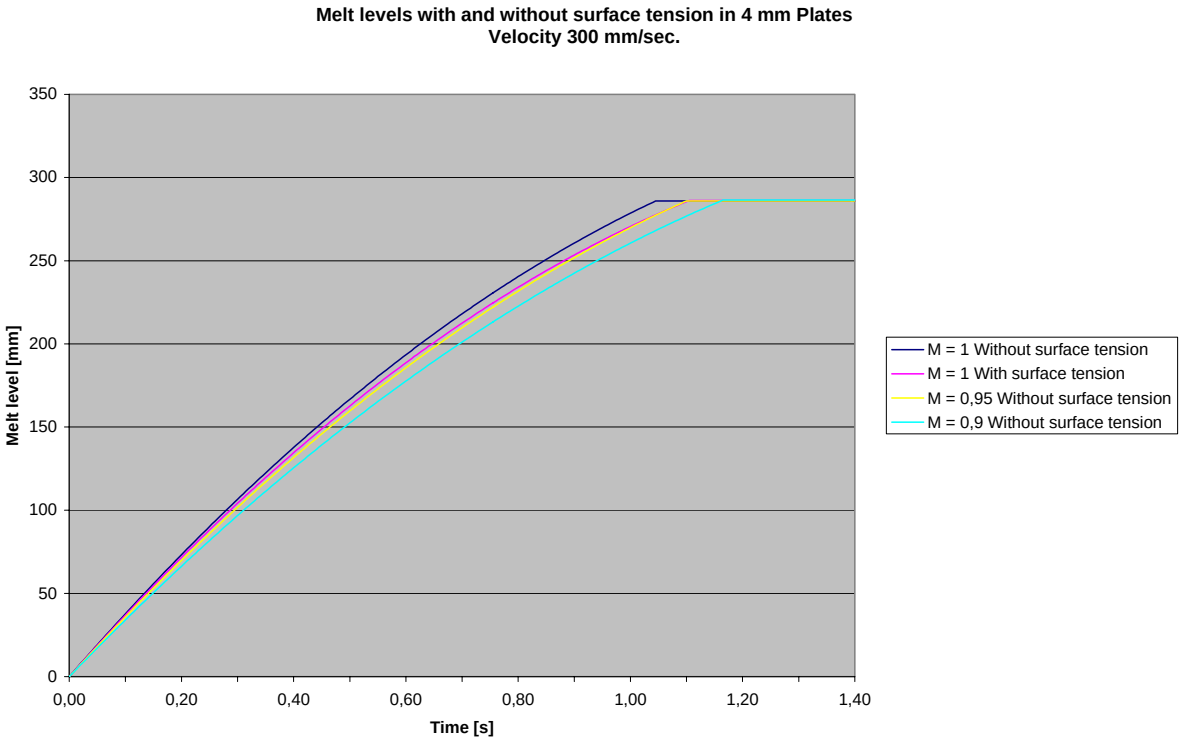
Melt levels with and without surface tension in 4 mm Plates
Velocity 300 mm/sec.
Melt level [mm]
350
300
250
200
150
100
50
0
0,00
0,20
0,40
0,60
0,80
1,00
1,20
1,40
Time [s]
M = 1 Without surface tension
M = 1 With surface tension
M = 0,95 Without surface tension
M = 0,9 Without surface tension

Appendix 4.5

When calculating the areas F_1 and F_2 shown on the figure to the right; the pouring cup is assumed to be completely filled. The areas are designed to give the same flow rate at section 1 and 2, to keep the down runner completely filled. The flow rate (kg/s) is given by [Ref. 4.2]:

$$\text{Flow rate} = F \cdot \rho \cdot \sqrt{2 \cdot g} \cdot m \cdot \sqrt{H}$$

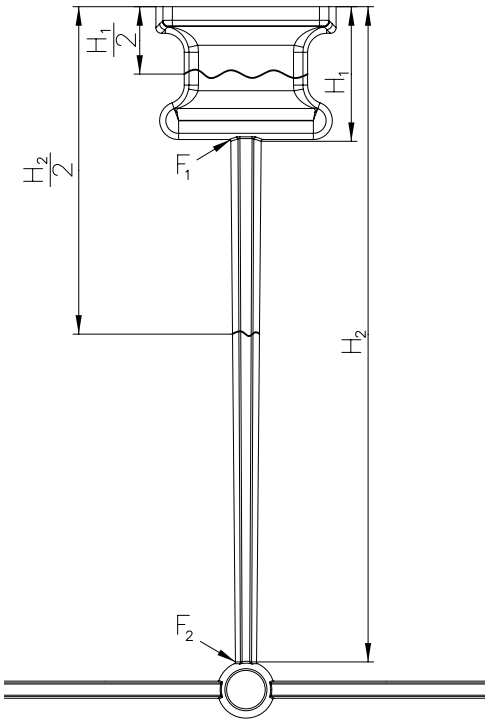

If the melt level in the pouring cup is lowered from H_1 to ½ H_1 the flow through section 1 is reduced with the square root of ½ i.e. approximately 0.71. As the area of section 2 is designed to handle the full flow rate is the down runner not kept full. A balance is established with a partly filled down runner giving a flow rate through section 2 equal to the one passing through section 1 after the reduction in driving pressure from H_1 to ½ H_1. If the flow through section 2 has to be reduced with the square root of ½ the driving pressure has to be reduced from H_2 to ½ H_2. I.e. a balance is established with a half way filled down runner when calculated on the basis of the total pressure height H_2.

This means a half way filled pouring cup results in a half way filled down runner, if the cross section of the top of the down runner is calculated with no safety margin.

Appendix 4.6

One of the many important operations in the complete casting process is getting the melt into the mould, i.e. from the ladle and to the pouring cup. Even the best gating and feeding system and metal quality will not help if this operation is done wrongly. Even though old and some times misused the saying “Keep the pouring cup full” is still valid. When the pouring cup is full the filling of the mould cavity is strictly controlled by the gating system.

It is even more important to keep the pouring cup filled when the wall thicknesses of the castings are very small. Small wall thicknesses are very sensitive to changes in melt front velocity, because small delays in the melt supply can mean a short stand still of the melt front and hence result in freezing of the melt front.

The pouring is controlled by an automatic device in modern DISAMATIC foundries securing a filled pouring cup at every mould.

For several reasons is it not possible to install an automatic pouring device in a test foundry like the one at DTU. First of all it would be very expensive to do so, and it would probably also be difficult to find equipment designed to handle such small amounts of liquid metal. And last but not least we would have to fight the problems connected to not running continuously i.e. temperature drop in the pouring device, stopper rods freezing etc.

Hand pouring will always mean partly filled pouring cups to some extend. This is very easily seen on the videos made of the filling of the thin plates.

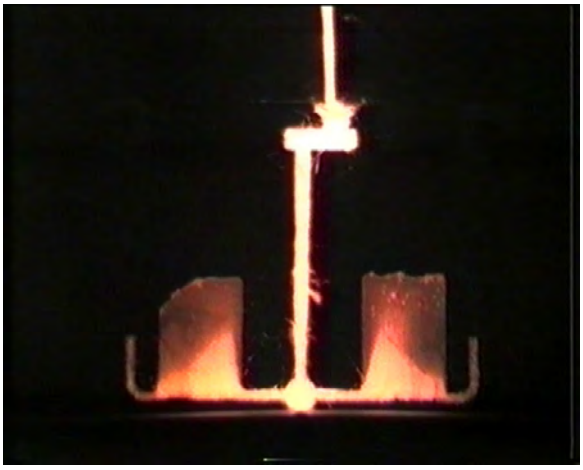

As it was not possible to install an automatic pouring device but it was necessary to have good control over the mould filling, it was decided to go for a pouring basin with a manual operated stopper rod. The pouring basin and stopper rod is most conveniently made in core sand.

An extra benefit from the pouring basin is the possibility of doing a very late melt treatment in the basin, which can be different from mould to mould. It is also possible to mount a thermo couple in the basin for recording the actual pouring temperature of each mould.

The pouring basin is not to be seen as a device used in production foundries, it is only to be seen as a substitute for an automatic pouring device.

The castings expected to be made, were all having a mass less than 7 kg including gating system. In was hence decided to design the pouring basin to be able to accommodate 8 kg iron.

To minimise the temperature loss a compact design was desired. It was decided to build in an extra wall acting as a slag trap. A section through the chosen design is seen on the picture to the right.

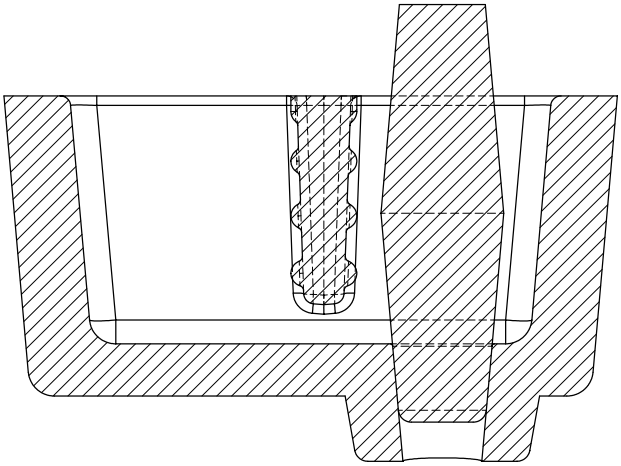

The rips on the wall core indicate the metal level at 2, 4, 6 and 8 kg iron. This makes it possible to pour a constant amount of iron into each basin without having to fill them completely.

A conical outlet nozzle was designed to secure a good connection to the green sand mould. A special pouring cup has to be mounted on the pattern plates. With this system the pouring basin is positioned very accurately on top of the moulds connecting to the gating system with a minimum of shift. The outlet nozzle fits the mould on a size to size basis except for the bottom face where an allowance of 0.5 mm has been added to give space for sand scratched of. When carefully mounted no loose sand gets into the gating system. The sand scratched of will stay in the 0.5 mm allowance and when the filling takes place the metal will try to force itself into the 0.5 mm allowance and hence not drag the loose sand into the mould.

The size of the outlet of the pouring basin was dimensioned using the standard equation for flow pr. s [Ref. 4.2]:

$$\frac{G}{T} = F \cdot m \cdot \sqrt{H} \cdot \rho \cdot \sqrt{2 \cdot g}$$

Where:

G/T	Flow [kg/s]
F	Flow area [mm^2]
m	Loss coefficient taken to be 1
H	Ferrostatic pressure height [mm]
ρ	Density [kg/m^3]

As the pressure height in the basin changes over time, the equation has been used on an incremental basis with time steps of 0.05 s. The emptying of the basin with different sizes of the outlet is seen on the next page:

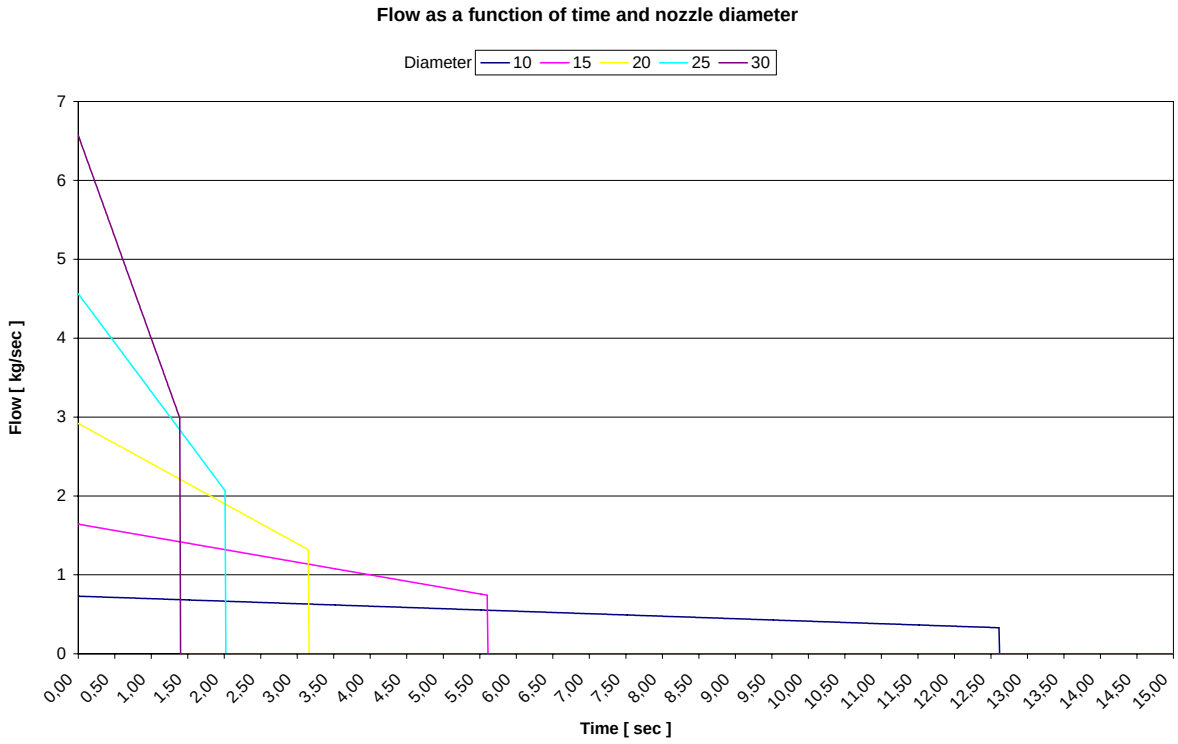

The diameter was chosen to be 30 mm to secure an adequate flow capacity and enough strength of the stopper core. This gives a flow capacity of 6.5 kg/s when the stopper rod is removed. The flow stops at 3 kg/s and not at 0 kg/s due to the pressure head given by the thickness of the bottom of the core.

The wall thickness of the basin was chosen to be 20 mm, which can seem a bit over sized, but the cores have to be made with a relatively weak binder when compared to a cold box binder. In the case of a broken stopper core the basin must also be strong enough to with stand the heat from the metal solidifying in the basin without falling apart.

The basin and the special pouring cup to be mounted on the pattern plates are shown below:

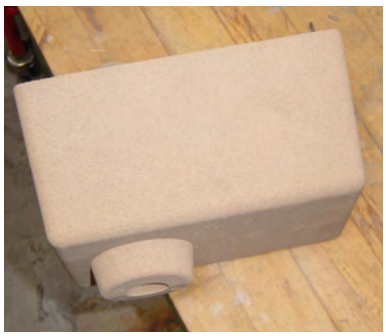

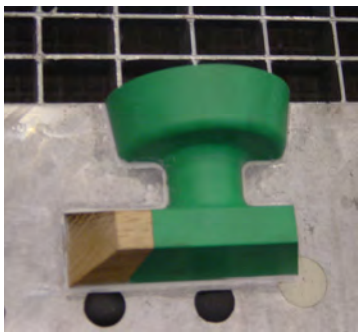

Appendix 4.7

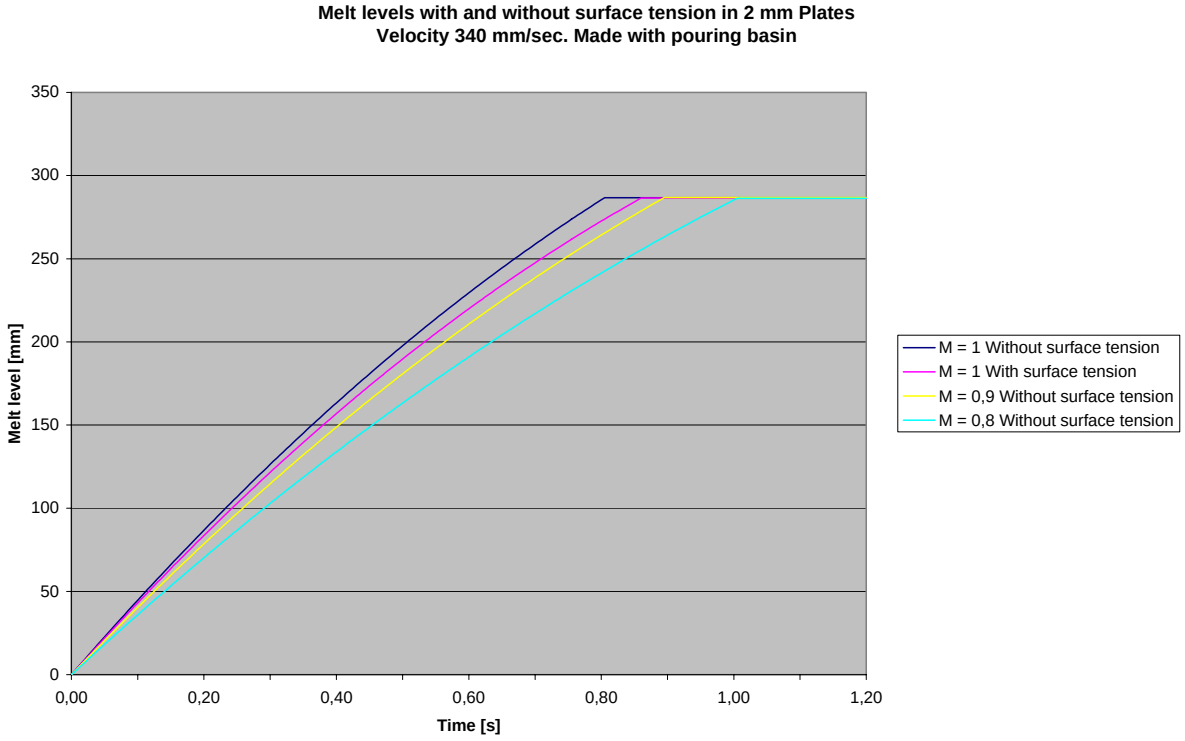
Melt levels with and without surface tension in 2 mm Plates
Velocity 340 mm/sec. Made with pouring basin
Melt level [mm]
350
300
250
200
150
100
50
0
0,00
0,20
0,40
0,60
0,80
1,00
1,20
Time [s]
M = 1 Without surface tension
M = 1 With surface tension
M = 0,9 Without surface tension
M = 0,8 Without surface tension

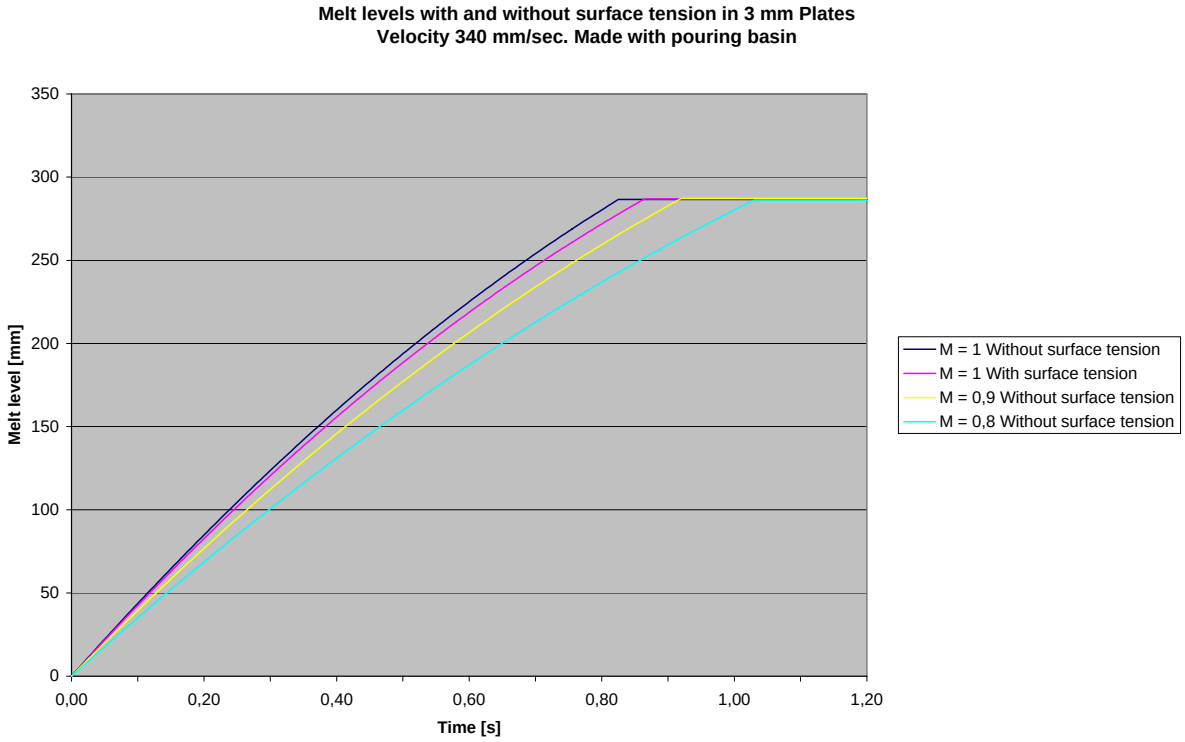
Melt levels with and without surface tension in 3 mm Plates
Velocity 340 mm/sec. Made with pouring basin
Melt level [mm]
350
300
250
200
150
100
50
0
0,00
0,20
0,40
0,60
0,80
1,00
1,20
Time [s]
M = 1 Without surface tension
M = 1 With surface tension
M = 0,9 Without surface tension
M = 0,8 Without surface tension

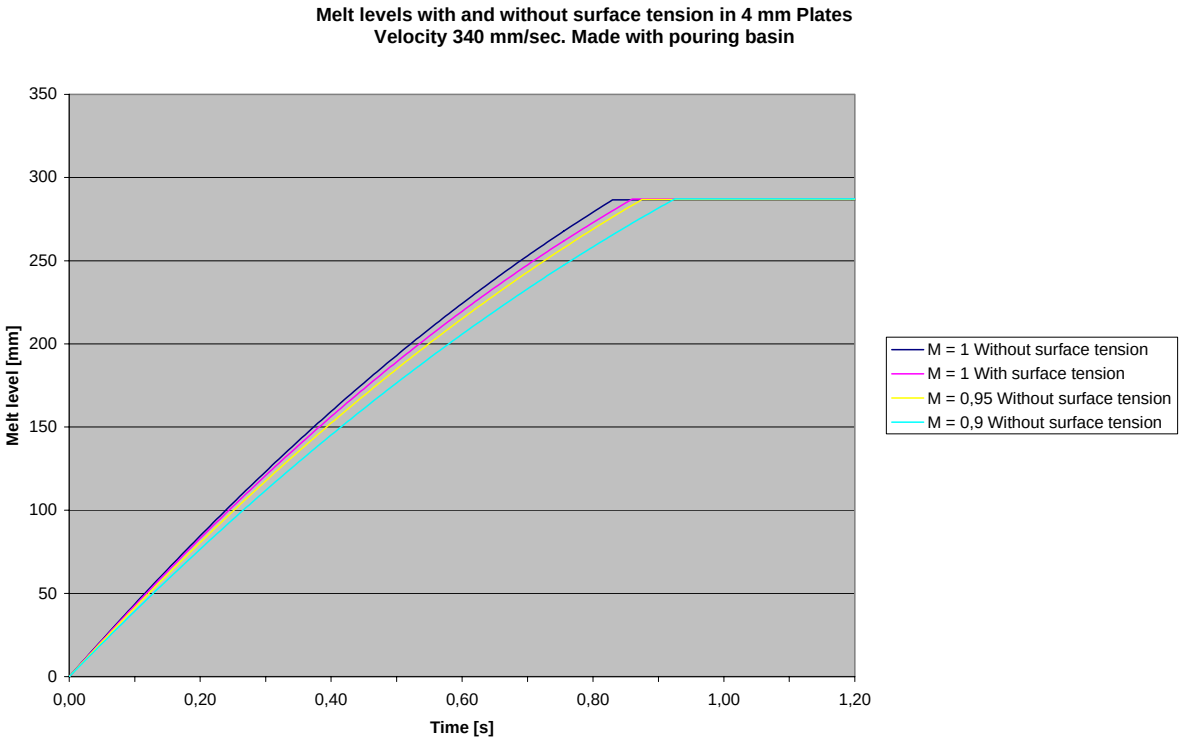
Melt levels with and without surface tension in 4 mm Plates
Velocity 340 mm/sec. Made with pouring basin
Melt level [mm]
350
300
250
200
150
100
50
0
0,00
0,20
0,40
0,60
0,80
1,00
1,20
Time [s]
M = 1 Without surface tension
M = 1 With surface tension
M = 0,95 Without surface tension
M = 0,9 Without surface tension

5 Casting of Brake Discs

Even though a brake disc is not a thin walled part is has been chosen as one of the test castings. It is a part with normal section thickness but still it has a large similarity with the plate castings analysed in section 4. The similarity comes from the way the ingate is made. When producing brake discs in vertically parted moulds a plate shaped ingate connected to a horizontal runner is very often used in practice. The thickness of the plate shaped ingate is in the same range as the plates investigated in section 4. I.e. the cross section controlling the distribution of the melt into the disc cavity is plate shaped. The cross section controlling the mass flow during the filling sequence is on the other hand normally placed somewhere else in the gating system, often at the bottom of the down runner.

Brake discs are a commercially very important casting group. World wide approximately 300 million discs are produced yearly. Around 140 million is used for new cars; the rest is for the spare part market. A large amount of the 300 million is cast in vertically parted moulds. Due to the high production numbers and very hard competition in the brake disc market the overhead in brake disc production is very small. I.e. a small improvement in effectiveness will give a relative large increase in competitiveness.

Brake discs are produced in grey cast iron. Different other materials have been proposed for the production of discs such as particle reinforced aluminium, carbon and ceramics. But these are only used in special cases such as racing cars and extremely expensive cars. Looking forward in time on a middle term basis the high volume discs will most likely continue to be produced in grey cast iron, both due to price and quality [Ref. 5.1].

Depending on what sources are used around 50 million passenger cars were produced worldwide in 2003 [Ref. 5.2]. [Ref. 5.3], [Ref. 5.4] reports slightly different numbers, but no matter what source is used the numbers are very large. Over the last 10 years the number of passenger cars produced yearly worldwide has been relatively steady growing with an average rate of approximate 2 % pr. year [Ref. 5.5]. The need for vented discs increase faster than the number of cars produced, due to the fact that cars in the lower end of the marked are changing to vented discs on the front wheels, and cars in the higher end change to vented discs on the rear wheels. The need for solid discs changes also due to the fact that brake drums on the rear wheels are changed to solid discs [Ref. 5.6]. An increasing spare part market is expected due to the growing total number of cars running world wide. At least on a middle term perspective the demand for discs will continue to be very large. As mentioned will discs most likely be produced in grey cast iron and hence a large demand for grey cast discs will exist in the future on a middle term basis. Due to the high volumes needed for the spare part market a substantial need will also exist on a longer term say at least 10 years longer than for the use in new cars.

Many different things have been done to optimize the production of discs. First of all no process has yet been found being able to compete with the casting process. A very important step in the casting process is getting the metal into the mould cavity. The aim with the trials described in this section is to gain a better understanding of what takes place inside the mould during the filling sequence when utilizing conventional and non-conventional gating systems.

6 different layouts for the same brake disc have been examined closely. Different foundry engineers all with many years of practical foundry experience designed the 6 layouts.

5.1 Trial set up

The 6 layouts for the brake disc were designed for the DISAMATIC 2110 installed in the test foundry at DTU. The mould face is 500 mm wide and 400 mm high. The disc had to have the same position on the pattern plate in all the layouts. This was decided to reduce the practical work with producing the pattern plates. The total pouring time was not allowed to exceed 5 s. This is approximately the time available for pouring when producing castings in vertically parted moulds on a modern high capacity moulding machine producing at maximum capacity [Ref. 5.7]. To simplify the needed pattern work and the running of the trials filters were not allowed.

A solid brake disc pattern was available for the trials. The dimensions can be seen on Figure 5.1. The weight of the disc is 4.9 kg. It is a rather small disc when comparing to the sizes used in modern passenger cars. But the gating techniques used are principally the same no matter the size of the disc. Limitations due to mould face size have normally larger influence on the design of the gating system.

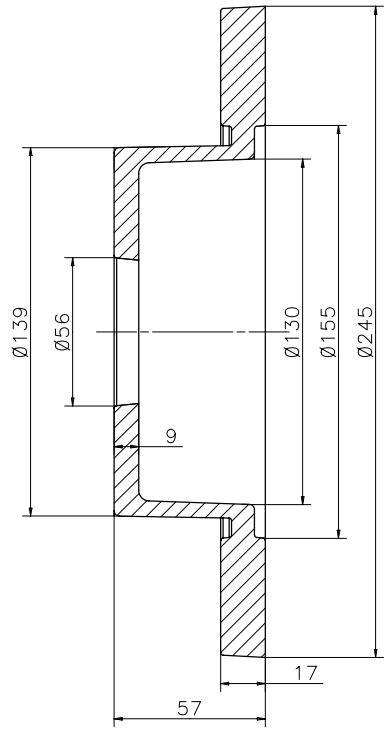

Figure 5.1 Dimensions of the disc.

The set up for making videos of the metal flow used in the section with the plates has been developed, making it possible to make videos of the filling of the brake disc layouts. The glass is now given a heat treatment to reduce residual stresses from production and cutting. A core giving the inside shape of the “hat” of the disc is made in shell core sand and glued to the inner glass plate, see Figure 5.2. As described in section 4, 3 layers of standard 4 mm window glass were used.

When the complete gating system is on the same pattern plate as the brake disc it is straightforward. In most of the layouts the gating system is on both pattern plates, making it impossible to have a glass plate replace a complete mould half. In these cases a combination of core and glass has been used for the mould half opposite the brake disc cavity. This will shortly be illustrated in the sections dedicated to each layout.

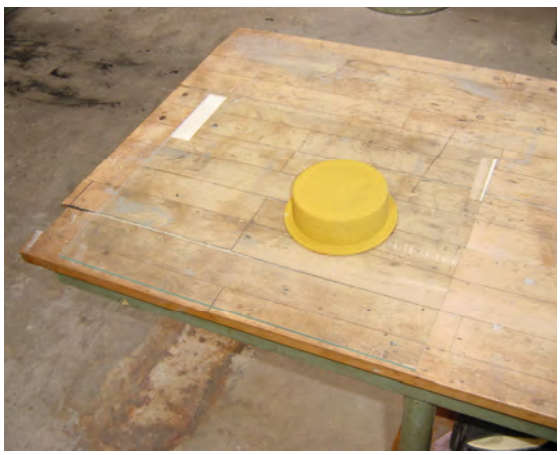

Figure 5.2 Shell core glued to glass.

To secure a good and uniform filling of the moulds from mould to mould the pouring basin described in section 4 was used. The technique with a core acting as the top of the mould of glass could directly be reused from the plate trials see Figure 5.3. A thermocouple was installed in the pouring basin to check the pouring

temperature. The core acting as the top part of the mould of glass covers the upper 15 mm of the disc. Because bottom filling gating systems are used the difficult part of the filling is expected to be the filling of the gating system and the initial filling of the disc, i.e. before back pressure has been build up. Covering the top of the disc with the core makes it impossible to record the last part of the filling. I.e. it is for instance difficult to analyse the hammer effect when the mould cavity is 100 % filled and the melt comes to a complete stand still. The hammer effect may cause penetration.

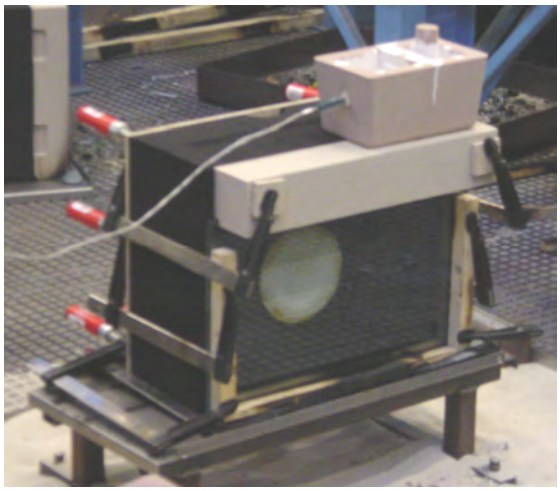

Figure 5.3 Set up for recording the flow.

The pouring basin can contain 1 litre; this is not enough for the brake disc layouts. Hence the basin was filled to the second upper rip on the slag trap. Then a break of 7 s was made in the pouring for the metal to settle and for giving the reading from the thermocouple time to stabilize. Then the stopper core was removed and manually the melt level was kept at a constant level 30 mm over the bottom of the pouring basin equal to 50 mm over the top of the green sand mould. This level could be maintained relatively precisely, as it was the initial filling of the gating system that demanded a lot of melt which was difficult to handle when pouring manually.

The pouring basin adds ferrostatic height to the gating system. When the stopper core is removed 90 mm extra ferrostatic height is acting on the metal compared to the top of the mould. This will mean higher flow rates compared to pouring without the pouring basin i.e. pouring directly into a pouring cup in the mould. When producing castings in real production a pouring automat or a pouring ladle is used. In both cases the melt enters the mould with a velocity higher then what is equal to a pressure height of 90 mm; some of this velocity can be transferred into the gating system depending on the design of the system. When using the pouring basin, only the pressure from the melt height in the basin; can be transferred to the gating system.

How big the difference in resulting pressure height is between using the pouring basin and pouring directly into a pouring cup in the mould, is difficult to calculate precisely, because it is difficult to estimate how much dynamic pressure is transferred into the gating system when pouring into a normal pouring cup in the mould. Some of the trials made with the plates described in section 4 have both been made with and without the pouring basin. Only in one case has it been possible to prove that momentum from the pouring stream is transferred into the gating system. Hence it seems that momentum only seldom is transferred into the gating system. The possible transfer of momentum from the pouring stream into the gating system is of course depending on the actual design of the pouring cup and how the gating system is connected to it.

For the calculations of the filling time of the disc cavities a constant addition of 50 mm to the ferrostatic height from the pouring basin has been used.

Brake discs are normally cast in grey iron. The melt composition used for the trials can be seen below:

	C	Si	Mn	P	S
Min %	3.3	1.8	0.4	0	0.06
Max %	3.5	2.1	0.6	0.1	0.1
Wanted %	3.4	1.9	0.5	0.1	0.06

Table 5.1 Chemical composition.

The wanted pouring temperature i.e. the temperature in the pouring basin was chosen to be 1380 °C

The filling of each layout was recorded twice on video. In most cases only minor differences between the two runs could be found. If more repetitions should have been made it would not have been possible to pour all the moulds at the same day giving possible extra contributions to the variation between the single runs.

5.2 Brake disc layouts for the trials

All layouts were first cast in sand moulds before the trials with the glass plates were made. The dimensions of the gating systems were checked on the castings.

5.2.1 Layout no. 1

The first layout tested was an existing set of pattern plates available from another project. The trial was originally only intended for testing the technique with gluing the shell core to the glass plate etc. before the other pattern plates were made. However interesting information can be extracted from the videos of the filling and hence it is taken into the report. The gating system can be seen on Figure 5.4. A detailed drawing of the layout is shown in Appendix 5.1. The gating system is depressurized [Ref. 5.8]. The flow restricting area is positioned at the bottom of the down runner.

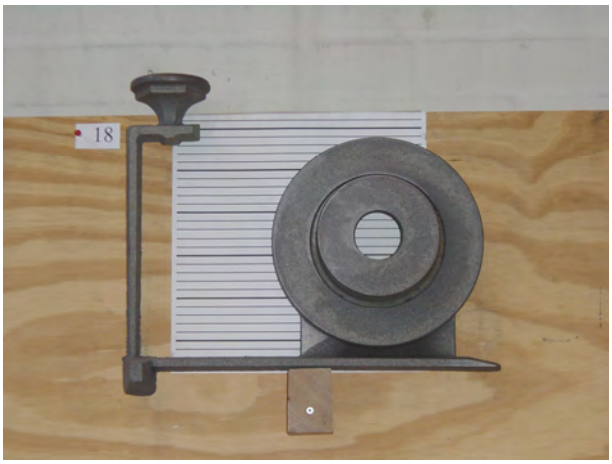

Figure 5.4 Layout no. 1.

The complete gating system is on the same pattern plate as the brake disc. This makes it possible to use the simple set up shown on Figure 5.3. Only the pouring cup was changed to the special version fitting the outlet nozzle of the pouring basin.
The total poured weight is 7.90 kg; the weight of the disc is 4.90 kg leading to a yield of 62 %.

The main data for the layout can be seen in the table on the next page:

Layout no.		1
Drawing number		8326D0120
Choke area	mm^2	108
Cross section shape of the choke	mm	6/12/12
Ferrostatic pressure height at choke inclusive the pouring basin	mm	325 + 50
Calculated initial speed at choke without losses	mm/s	2714
Calculated initial flow without losses	kg/s	2.02
Area of horizontal runner	mm^2	192
Cross section shape of horizontal runner	mm	8/16/16
Area ratio horizontal runner / choke		1.8
Calculated initial melt speed in horizontal runner without losses	mm/s	1527
Thickness of plate ingate	mm	3
Area of plate ingate	mm^2	528
Initial melt speed in the plate ingate calculated without losses	mm/s	555
Mean Ferrostatic height for the filling of the disc cavity	mm	242.5
Calculated filling time of the disc cavity found without losses	s	3.02

Table 5.2 Main data for layout no. 1.

The initial melt flow velocity in the choke has been calculated using the equation given in section 2.1:

$$V = m \cdot \sqrt{2 \cdot g \cdot H} \qquad \textbf{[Eq. 5.1]}$$

The equation has been used with m = 1, i.e. without losses. The result found is the maximum possible melt velocity in the choke.

For calculating the flow velocity in the horizontal runner this equation and the area ratio between the choke and the horizontal runner has been used. This can be done when the cross sections of the gating system are assumed to be completely filled.

The melt flow rate (kg/s) has been calculated using [Ref. 5.8]:

$$\frac{G}{t} = F \cdot \rho \cdot \sqrt{2 \cdot g} \cdot m \cdot \sqrt{H} \qquad \textbf{[Eq. 5.2]}$$

The filling time of the disc cavity has been calculated with [Ref. 5.8]:

$$t = \frac{G}{\sqrt{2 \cdot g} \cdot \rho \cdot \sqrt{H} \cdot F \cdot m} \qquad \textbf{[Eq. 5.3]}$$

Where:
H Ferrostatic pressure height [m]
g Acceleration due to gravity [9.81 m/s^2]
m Loss coefficient
t Time [s]
ρ Density [kg/m^3]
F Cross section area [m^2]

The filling time of the disc has been calculated on the basis of the mean ferrostatic height i.e. the height to the centre of the disc.

Different guide lines for the values of the loss factors can be found in the literature. But the actual values used are in all cases empirical values, very much depending on the foundry engineer's personal experience. To be able to compare the different layouts directly the above calculations have been done using a loss factor of 1. This is of course not the case with the calculations done when designing the systems. The trials make it possible to measure the filling time of the disc cavity. By comparing this to the theoretical value found without losses the loss coefficient can be calculated.

5.2.1.1 Filling of the gating system and the initial part of the disc cavity

Both runs of the trial were successful. When comparing the videos of the flow patterns from the 2 runs a little more splash is seen in run 2 than in run 1. As seen in section 4 with the plates this difference can be caused by minor differences in the way the horizontal runner is filled.

If the cross section of the horizontal runner is completely filled behind the melt front, splashes are more likely to appear when the melt front reaches the end of the horizontal runner than if the horizontal runner is only partly filled behind the melt front. In the case of a partly filled cross section of the horizontal runner the air pockets act as a buffer for the hammer effect when the melt hits the end of the runner. The possible appearance of pressure shock waves is delayed to when the last air pocket in the runner is closed.

The differences in the pouring conditions from mould to mould resulting in the two slightly different filling patterns are very small as the possible variation when using the pouring basin is very small. The possible variation in pouring conditions from mould to mould when using the pouring basin is probably smaller than what is the case when using an automatic pouring device. When using an automatic pouring device will for instance the pouring stream not hit the pouring cup at the same position at every mould as the device positioning the pouring automat is working with some tolerances. As showed in section 4.6.2.3 the direction and position of the pouring stream can change the flow. Hence the variation seen in production foundries is expected to be larger than what is the case for the pouring basin used here.

Run number 2 was chosen for the further examination of the results. In the following sections with the other layouts the run giving most splashes will be chosen for the closer examination. Snapshots from the filling of the gating system and the first part of the disc can be seen on Figure 5.5. The pictures have been trimmed to show only the part of the mould visible through the glass, i.e. not the pouring basin etc.

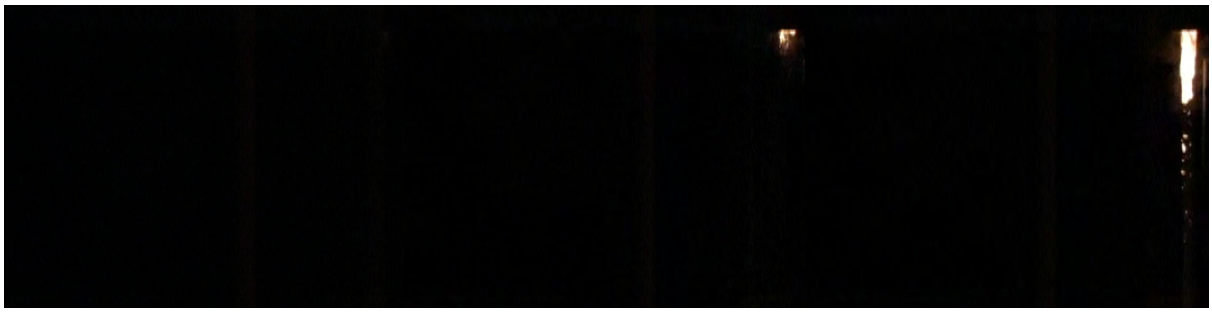

Time 0.00 Time 0.04 Time 0.08

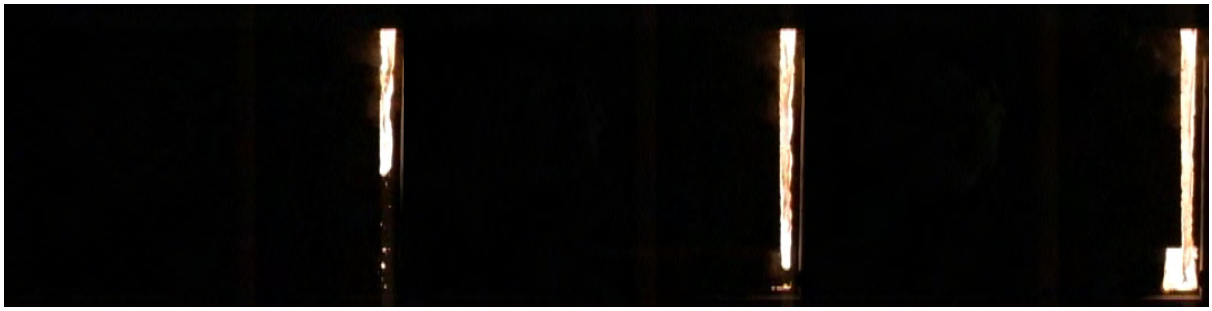

Time 0.12 Time 0.16 Time 0.20

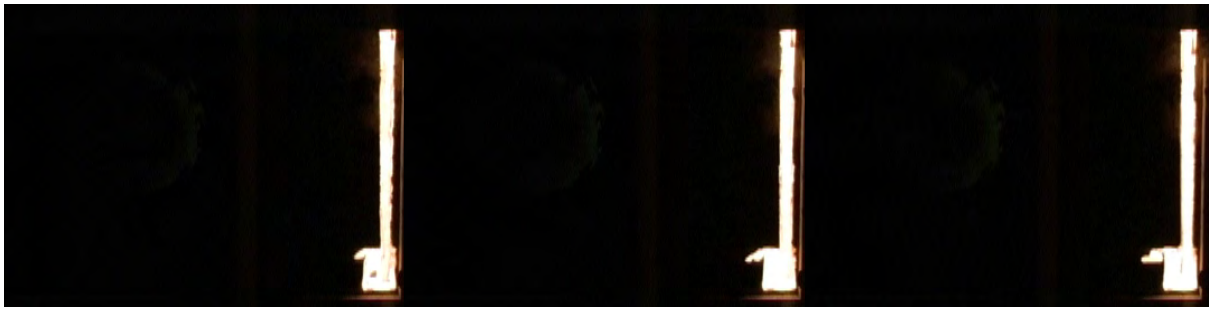

Time 0.24 Time 0.28 Time 0.32

Time 0.36 Time 0.40 Time 0.44

Time 0.48 Time 0.52 Time 0.56

Time 0.60 Time 0.64 Time 0.68

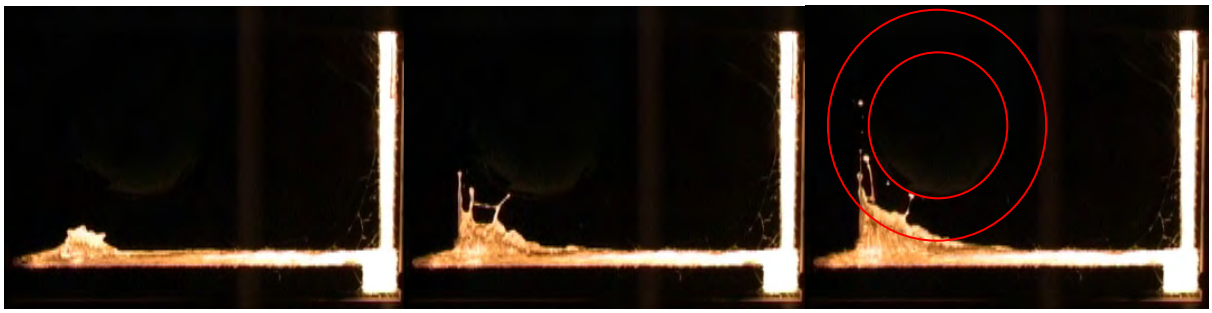

Time 0.72 Time 0.76 Time 0.80 Disc starts to fill

Time 0.84 Time 0.88 Time 0.92

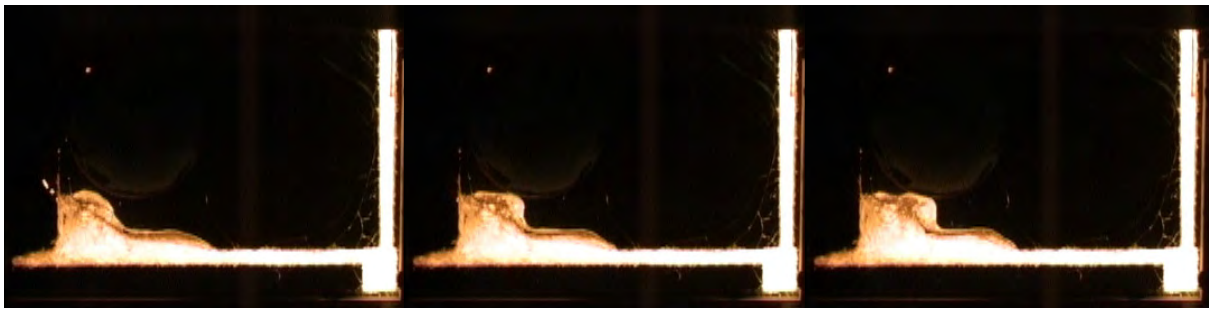

Time 0.96 Time 1.00 Time 1.04

Time 1.08 Time 1.12 Time 1.16

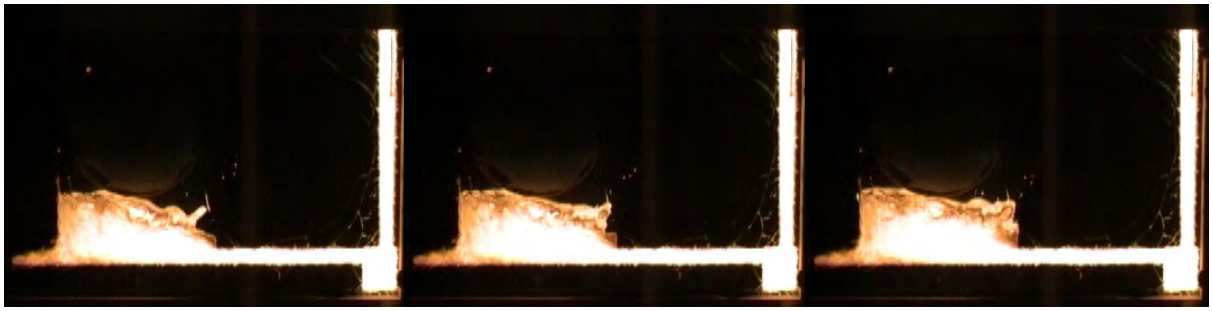

Time 1.20 Time 1.24 Time 1.28

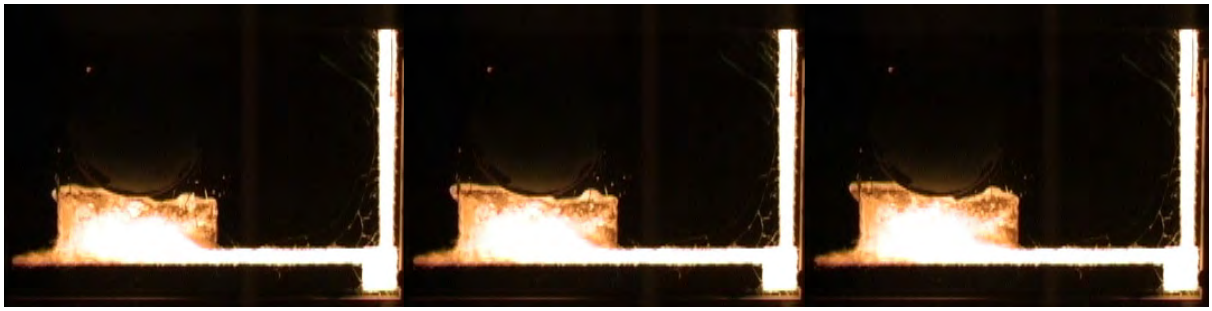

Time 1.32 Time 1.36 Time 1.40

Figure 5.5 Initial filling of layout no. 1.

The filling of the rest of the disc cavity is calm.

The outline of the disc shown after 0.80 s appears to be slightly oval. This is due to the camera angle. The camera was positioned approximately 60 cm higher than the centre of the disc cavity. This is also the case for the rest of the trials.

The filling of the down runner takes place with almost a coherent melt front; only a few droplets reach the well before the main melt stream. Furthermore the cross section of the down runner is close to completely filled right from the first melt passes through it. The cross section of the down runner is completely filled after 0.44 s.

When calculating the maximum possible flow rates through the cross sections of the down runner one gets: 2.59 kg/s for the trapezium shaped cross section (18/18/9 mm) at the top of the down runner and 2.02 kg/s. for the choke (12/12/6 mm).

The calculations are made using Eq. 5.2 with no losses, with a contribution to the metal head from the pouring basin of 50 mm, and with no back pressure from the mould cavity corresponding to the situation during the initial filling. The layout can be seen in Appendix 6.1.

From the 2.59 and 2.02 kg/s is it seen that the design has build in a safety margin of 28 % between these two cross sections.

When designing down runners normally only the top and bottom cross section areas of the runners are calculated. A straight taper is used to reduce the cross sectional area from the top to the bottom. When doing so the cross sectional area will be approximately 10 % too large on the middle of the down runner. This is valid for at setup with a pouring basin and a 350 mm long down runner as has been used here. The reason for this difference is due to the fact that the cross sectional area has to follow $1/\sqrt{h}$. When using a straight taper it follows 1/h. This will be shown in details in section 6.2 with the thin walled manifold. I.e. unless the cross sectional area at the top of the down runner has been designed large enough to account for the too large area at the middle of down runners with a straight taper, a partly filled down runner will be the result. In this case is the safety margin for the cross sectional area of the top of the down runner found to 28 %. This is enough to compensate for the too large area on the middle.

The square shaped well performs significantly better than the cylinder shaped wells used in section 4 with the plates. Even though the well is almost empty when the main melt stream hits the bottom of it, and the cross section of the down runner is completely filled, the well performs good. Not a single droplet is blown into the horizontal runner before the main melt stream enters it. The well is also able to hold the melt back from 0.16 to 0.32 s until the well has been completely filled. The cross section of the horizontal runner behind the melt front is almost completely filled right from the first melt enters the runner. The only visible problem with the well is the vena contracta at the bottom of the horizontal runner at the exit from the well. An enlargement of the well at 0.64 s can be seen on Figure 5.6. When the melt hits the end of the horizontal runner at 0.72 s resulting in the hammer effect the vena contracta is temporarily closed. It

Figure 5.6 Vena contracta at the exit of the well.

opens up again afterwards. The low pressure area at the exit of the well can be identified until 0.92 s when examining enlargements of the area around the well. The well has been designed according to the recommendations given in [Ref. 5.9] and [Ref. 5.10].

When the melt front hits the end of the horizontal runner between 0.68-0.72 s the dynamic pressure is converted into static pressure. Melt droplets are blown into the disc cavity through the 3 mm thick plate shaped ingate. The droplets end up in the upper part of the disc cavity, some of them lying on top of the core giving the inside hat shape of the disc. If these melt droplets are not completely remelted when the main melt stream arrives defects will be the result. I.e. in this case inclusions in the top of the disc can be caused by an ineffective design of the horizontal runner. Without investigations as the one done here it is very hard to find the exact reason for such inclusions. The end of the horizontal runner is designed according to the recommendations in [Ref. 5.8]. The direction of the flow in the horizontal runner will also try to drive the metal into the disc cavity at the far end of the horizontal runner. Due to the explosive entrance of the melt into the disc cavity it is most likely controlled by a pressure shock wave as the conversion of the dynamic pressure to static pressure takes place almost instantaneously.

To prevent the problem with melt droplets being blown into the disc cavity when the melt hits the end of the horizontal runner, the melt velocity has to be taken out of the flow in a more gentle way, than the brake at the end of the runner is able to do. Different things can be tried to gradually reduce the melt velocity. The horizontal runner can be gradually tapered down from the start of the plate ingate to a point say 30 mm after the end of the ingate. This design is seen in many layouts where a plate shaped ingate is utilized in connection with a horizontal runner. It is also used in the brake disc layout no. 4 and 5 described in section 5.2.4 and 5.2.5. A gradually reduction of the horizontal runner will introduce larger braking forces by the surface tension and wall friction. On the other hand as the cross section gets smaller the flow velocity will increase, resulting in larger dynamic forces. Under all circumstances, it would be very interesting to see how the flow patterns change if the horizontal runner was gradually reduced.

Another way to reduce the problem could be to enlarge the horizontal runner and hence reduce the average melt velocity. But it is difficult to design a transition from the down runner to the horizontal runner securing a completely filled cross section of the horizontal runner when the area ratio between the down runner and the horizontal runner is large. Even if the horizontal runner is completely filled, the flow will follow a preferred flow path which can lead to relative high local velocities even though the cross sectional area of the runner should result in relative low velocities.

The thickness of the plate ingate could also be reduced. The wall friction and the back pressure from surface tension would get larger as described in section 4. But again this will result in larger velocities. The plate ingates used for casting iron discs are often thinner than the 3 mm used here or tapered down close to the disc.

5.2.1.2 Flow pattern in the disc cavity

The temperature distribution in the disc during the filling sequence shows indirectly the flow pattern in the disc cavity. Snapshots from the filling of the disc are shown below:

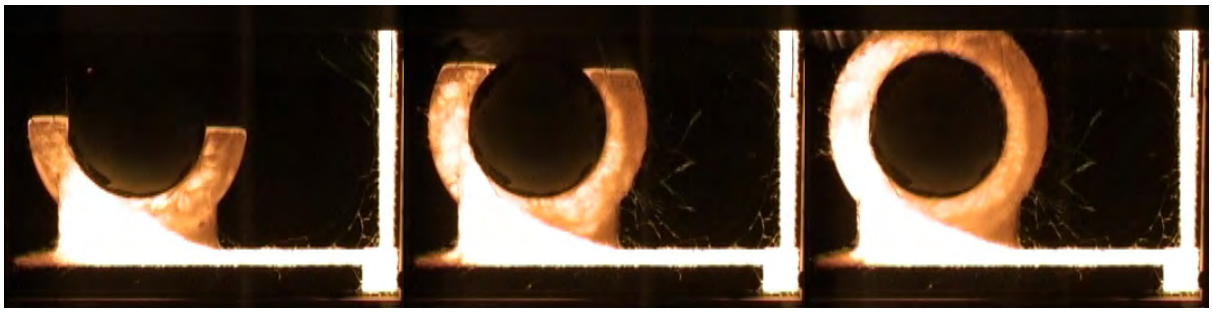

Time 2.88 Time 4.36 Time 5.88

Figure 5.7 Filling of the disc cavity in layout no. 1.

The temperature distribution sidewise in the disc is seen to be very unsymmetrical. This reflects an unbalanced flow pattern, where the flow predominately takes place in the left side of the ingate. When using the terminology with braking and dynamic forces introduced in section 4 means the unbalance in the filling towards the left side that the dynamic forces are much larger than the braking forces. The flow patterns in the discs will be compared in section 5.6.

The unbalanced filling, results in a difference in the melt levels in the left and right side of the disc. The melt level in the left side is 10-15 mm ahead in the first part of the filling. The bottom part of the disc and part of the left side is getting extra heated compared to the rest of the disc.

The possible tapering down of the horizontal runner discussed in section 5.2.1.1 will also reduce the tendency of the melt to enter into the disc cavity at the far end of the plate ingate as is seen on the final temperature distribution shown to the right on Figure 5.7. As discussed in section 4 it is hard to predict the melt distribution in designs utilising a wide plate shaped ingate connected to a horizontal runner, as the melt distribution relies heavily on the balance between dynamic and braking forces.

5.2.1.3 Comparison of flow patterns with and without glass

For parts cast with glass as one mould half the hot areas seen on the videos are the areas where the main flow takes place. For parts cast in sand moulds without glass the areas with excessive sand burn on are the areas where the main flow takes place. Hence comparing these two patterns give a good indication of how equal the flow patterns are when the parts are cast with and without glass as one mould half.

On the snapshots shown on Figure 5.7 the right side of the plate ingate is seen not to be active or at least almost not active. The same layout cast in sand can be seen on Figure 5.8 with an enlargement of the plate ingate. The absence of sand burn on, on the triangle to the right on

the plate ingate reveals a flow pattern with an inactive right side much like the one seen on Figure 5.7 for the trials with a glass plate.

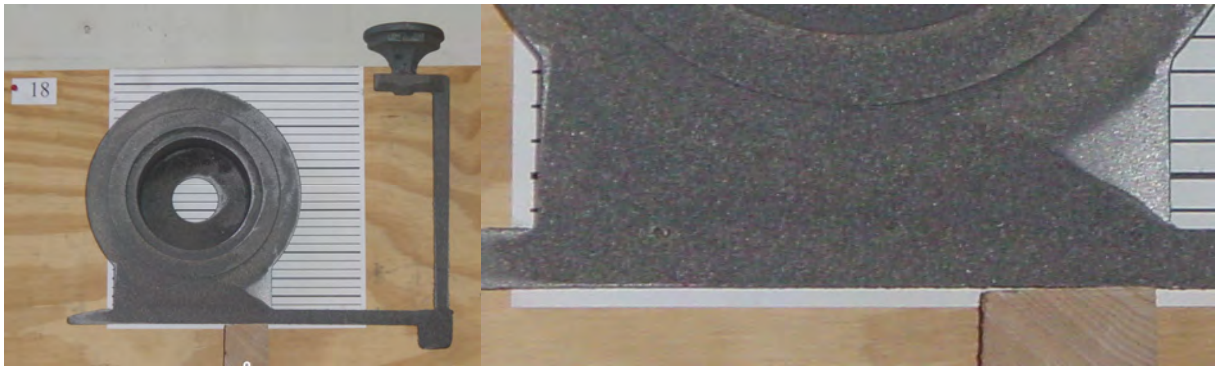

Figure 5.8 Sand burn on of layout no. 1 showing inactive part of plate ingate.

Enlargements of the inactive triangles when the layout is cast with and without glass as one mould half can be seen on Figure 5.9. The angel between horizontal and the line indicating to where the flow takes place is measured to be 33 degrees in both cases.

This angle is a measure for the balance between the dynamic forces and the braking forces. If for instance the braking forces are significantly larger in the case without glass the angle would be larger. Hence equal angles are a good indication of similar flow conditions in the two cases.

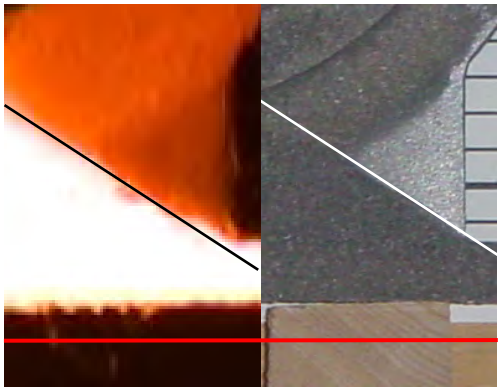

Figure 5.9 Flow patterns with and with out glass.

This indicates that it is possible to use glass as one mould half and still get flow patterns very close to what is the case for a mould with both halves made out of sand.

5.2.1.4 Generation of core gasses

The well-known problem with generation of gas from cores was clearly seen on some of the videos. This is illustrated on Figure 5.10, where a snapshot from one of the preliminary trials is shown. When the core is completely submerged, the gas has to escape through the metal as seen on the picture. During the filling until the core is submerged the melt front is planar. The shell core is solid and no venting of the core has been used, this makes the gas problem even larger.

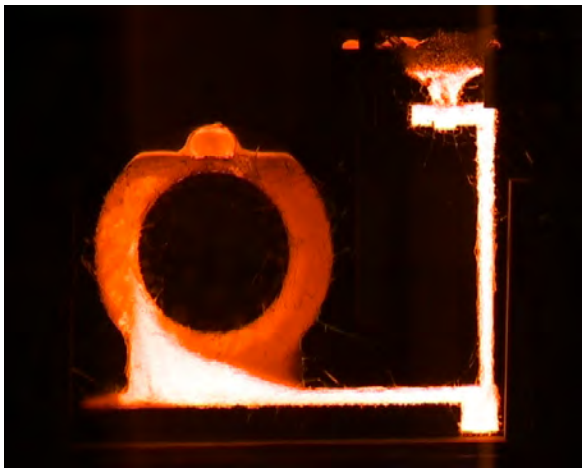

Figure 5.10 Bubble from core gas.

5.2.1.5 Filling time

The total filling time of layout no. 1 is approximately 6.18 s. Due to the core, seen on Figure 5.3, covering the top of the disc; the ending of the filling can not be seen on the videos. The time from the melt front disappears behind the core to the complete filling of the layout has been calculated from the melt front velocity measured for the filling of the last 15 mm of the disc cavity before the melt front disappears behind the core. 0.3 s have been added for the filling of the pouring cup and the horizontal runner connected to it. This part of the filling sequence is hidden in the top core. The 0.3 s have been found from layout no. 3 where the filling of the pouring cup and the runner connected to it is visible. The filling of the disc starts after 0.84 s, i.e. the filling time for the disc cavity is 5.04 s. The calculated filling time for the disc cavity without losses is 3.02 s. This yields an overall loss coefficient for the filling of the disc cavity of 0.60. The total loss coefficient for the filling of the disc cavity is found by dividing the measured filling time for the disc cavity with the theoretical filling time found without losses with Eq. 5.3.

5.2.2 Layout no. 2

The second layout can be seen on Figure 5.11. A detailed drawing of the layout is shown in Appendix 5.2. The flow restricting area in this gating system is positioned at the transition between the top of the down runner and the horizontal extension of the pouring cup. I.e. the gating system is non-pressurized [Ref. 5.8].

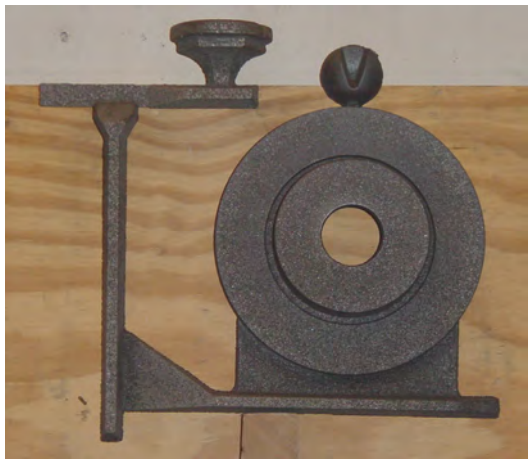

Figure 5.11 Layout no. 2.

A feeder has been used in this layout. The need for at feeder depends on the capability of the gating system to feed the liquid shrinkage and the metallurgical composition.

If the gating system is designed correct it will be able to feed the liquid shrinkage of the disc before the ingate solidifies. If the metallurgical composition and the temperature distribution in the disc are right and the precipitation of graphite can be controlled through the inoculation to take place over a suitable range of the solidification, the graphite expansion will compensate for the solidification shrinkage in the disc. Generally speaking, if inexpensive raw materials are used like for instance chips from machining it is difficult to get the inoculation to control the graphite precipitation to take place over a suitable range of the solidification and hence often feeders are needed in such cases. On the other hand if high quality and expansive raw materials are used the graphite expansion can be controlled through proper inoculation and feeders can be avoided. Both strategies are used with success, local conditions like scrap and melting costs decide what strategy is the most feasible.

The complete gating system is on the same pattern plate as the brake disc, except for the pouring cup and the horizontal runner connected to it. This makes it possible to use the same set up as for layout no. 1. Only the pouring cup had to be changed to the special version fitting the outlet nozzle of the pouring basin.

The total poured weight is 10.00 kg; the weight of the disc is 4.90 kg leading to a yield of 49 %.

The main data for the layout can be seen in the table below:

Layout no.		2
Drawing number		8326D0130
Choke area	mm^2	168
Cross section shape of the choke	mm	4.2/40
Ferrostatic pressure height at choke inclusive the pouring basin	mm	67 + 50
Calculated initial speed at choke without losses	mm/s	1516
Calculated initial flow without losses	kg/s	1.75
Area of horizontal runner	mm^2	486
Cross section shape of horizontal runner	mm	9/18/36
Area ratio horizontal runner / choke		2.9
Calculated initial melt speed in horizontal runner without losses	mm/s	524
Thickness of plate ingate	mm	2.5
Area of plate ingate	mm^2	500
Initial melt speed in the plate ingate calculated without losses	mm/s	509
Mean Ferrostatic height for the filling of the disc cavity	mm	242.5
Calculated filling time of the disc cavity found without losses	s	2.79

Table 5.3 Main data for layout no. 2.

For the calculations of the filling time of the disc cavity and the different velocities the same equations have been used as at layout no. 1.

5.2.2.1 Filling of the gating system and the initial part of the disc cavity

Both runs of the trial were successful. When comparing the videos of the flow patterns from the 2 runs no significant differences could be found. Run number 2 was chosen for the further examination. Snapshots from the filling of the gating system and the first part of the disc cavity can be seen on Figure 5.12 on the following pages.

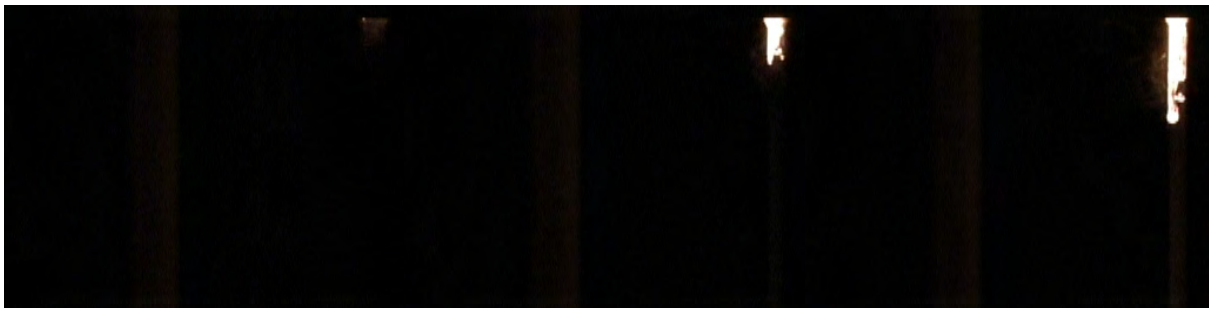

Time 0.00 Time 0.04 Time 0.08

Time 0.12 Time 0.16 Time 0.20

Time 0.24 Time 0.28 Time 0.32

Time 0.36 Time 0.40 Time 0.44

Time 0.48 Time 0.52 Time 0.56

Time 0.60 Time 0.64 Time 0.68

Time 0.72 Time 0.76 Time 0.80

Time 0.84 Time 0.88 Time 0.92

Time 0.96 Time 1.00 Time 1.04

Time 1.08 Time 1.12 Disc starts to fill Time 1.16

Time 1.20 Time 1.24 Time 1.28

Time 1.32 Time 1.36 Time 1.40

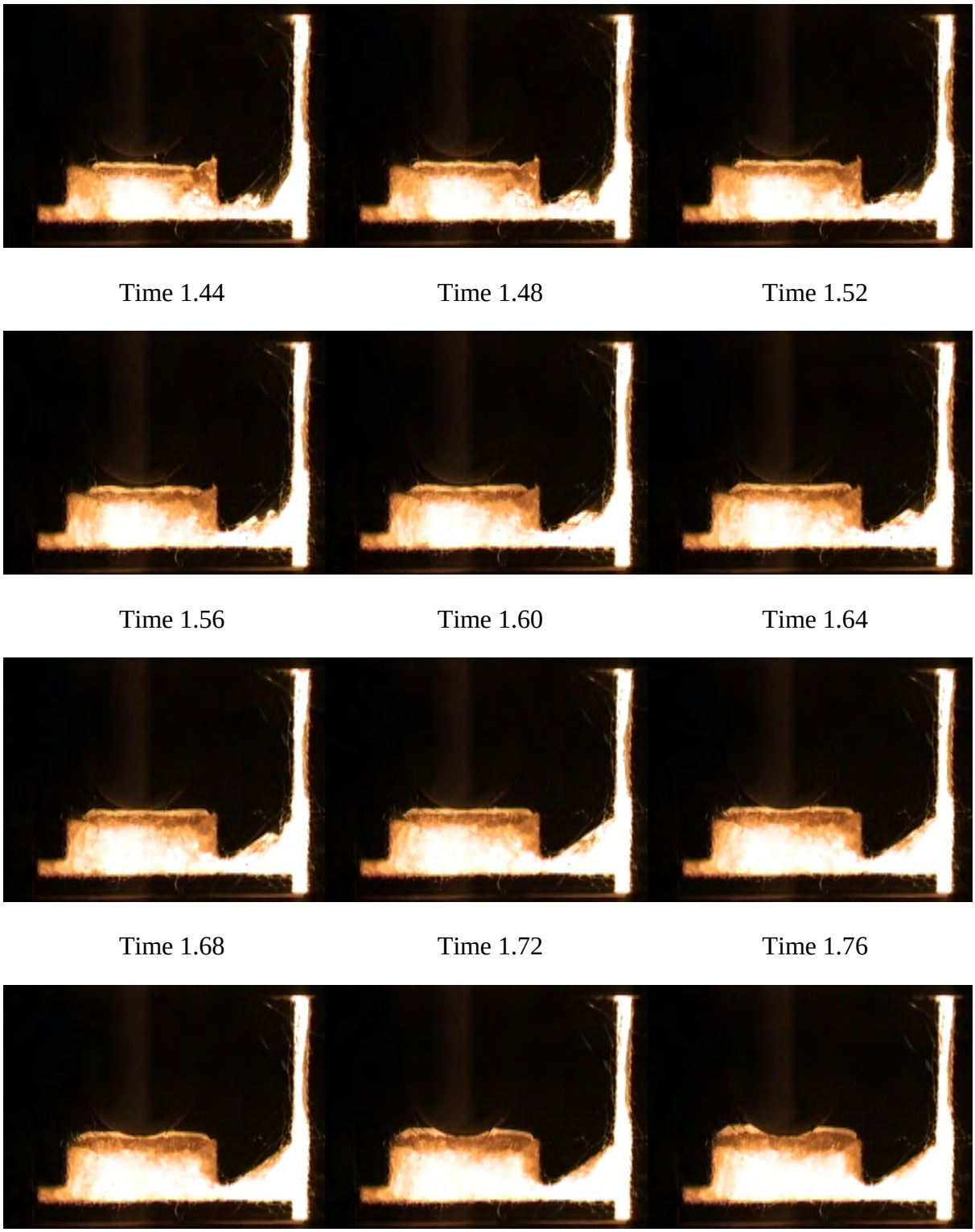

Figure 5.12 Initial filling of layout no. 2.

The filling of the rest of the disc cavity is calm.

The filling of the down runner takes place with one coherent melt front, not a single melt droplet reaches the bottom of the down runner before the main melt front. This is the case even though the section size of the down runner is quite heavy compared to the down runners seen at the other layouts. It is 20/30/10 at the top and 18/27/9 at the bottom; the layout can be seen in Appendix 5.2.

The down runner is filled completely at the same time as the disc cavity is completely filled. This is due to the depressurized design where the flow restricting cross sectional area is at the top of the down runner where it laps over the horizontal extension of the pouring cup. The free falling metal in the down runner contracts as it accelerates during the passage through the runner. This means the air pockets are not low pressure areas in the same sense as air pockets caused by vena contractas. The aspiration will hence not be as powerful as at air pockets caused by vena contractas. The non constrained metal flow will although drag some air into the system. This takes place during most of the filling sequence. The triangle connecting the down runner and the horizontal runner is filled after 1.72 s, i.e. when a significant back pressure from the metal in the disc cavity has been build up.

When the melt hits the bottom of the down runner after 0.24 s some melt is blown into the horizontal runner in front of the main melt stream. Hence the triangle shaped transition from down runner to horizontal runner can not be recommended.

After 0.64 s one coherent melt front exists in the horizontal runner, the cross section of the horizontal runner is almost completely filled behind the melt front. This is a little surprising having the heavy cross section of the horizontal runner (18/36/9 mm) and the depressurized design in mind. But the explanation is the relatively low velocities seen in the horizontal runner making easier for the melt front to stay coherent. From 0.64 s the rest of the filling is calm. No melt droplets are blown into the disc cavity when the horizontal runner is completely filled up, i.e. no pressure shock wave can be identified. This is the advantage of a depressurized gating system. When the disc starts to fill at 1.12 s a large air pocket is seen in the down runner, meaning the effective driving pressure is relative small resulting in a calm filling. Furthermore the initial melt velocity in the horizontal runner found in Table 5.3 to 0.52 m/s is relative low. This also helps to obtain a calm filling. A small surface protrusion is seen at 1.32 s at the right side of the plate shaped ingate. If this is due to a small pressure shock wave or a melt wave rolling from left to right due to initial melt flow predominantly taken place in the left side of the ingate is difficult to say.

5.2.2.2 Flow pattern in the disc cavity

The temperature distribution in the disc during the filling sequence shows indirectly the flow pattern in the disc cavity. Snapshots from the filling of the disc are showed below:

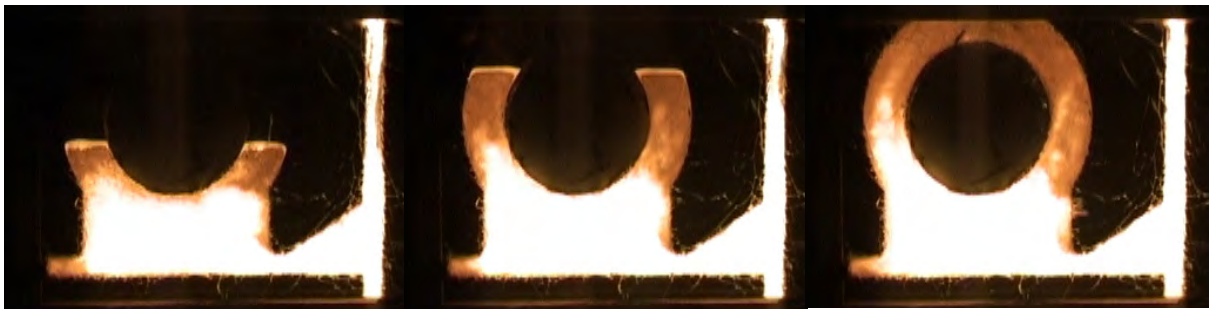

Time 2.64 Time 3.88 Time 5.16

Figure 5.13 Filling of the disc cavity in layout no. 2.

The temperature distribution in the disc after the filling is close to symmetrical sidewise; this means a close to sidewise balanced flow into the disc. During the first part of the filling sequence i.e. until 1.28 s the flow is shifting a little to the left side, due to the momentum in the melt when it fills the horizontal runner. As soon as a little backpressure is build up from the disc cavity the flow is balanced. The flow pattern in the disc will be discussed and compared to the other layouts in section 5.6.

5.2.2.3 Filling time

The total filling time of layout no. 2 is approximately 5.46 s. As with layout no. 1 the top of the disc is hidden behind the top core. The ending of the filling has been calculated in the same way as with layout no. 1. 0.3 s have been added to the filling time for the filling of the pouring cup and the runner connected to it in the same way as with layout no. 1. The filling of the disc starts after 1.12 s, i.e. the filling time for the disc is 4.04 s. The calculated filling time for the disc cavity without any losses is 2.79 s. This yields a total loss coefficient for the filling of the disc of 0.69.

5.2.3 Layout no. 3

The third layout can be seen in Figure 5.14. A detailed drawing of the layout is shown in Appendix 5.3. The flow restricting area is at the bottom of the down runner, i.e. it is a depressurized system [Ref. 5.8].

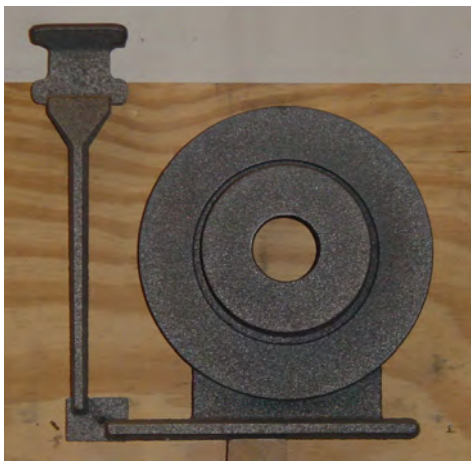

Figure 5.14 Layout no. 3.

The gating system is not on the same pattern plate as the brake disc, furthermore has a special pouring cup with an overlap at the bottom been used. These things make it impossible to use the simple set up shown on Figure 5.3.

A special set up was made with a V shaped core making it possible to capture some of the flow in the down runner, a large portion of the flow in the horizontal runner and the complete filling of the disc cavity on the videos. The set up and the tooling can be seen on Figure 5.15 and Figure 5.16. The shape of the outlet nozzle of the pouring basin was fitted to go into the special pouring cup used, making it possible to keep the overlapping at the bottom of the pouring cup.

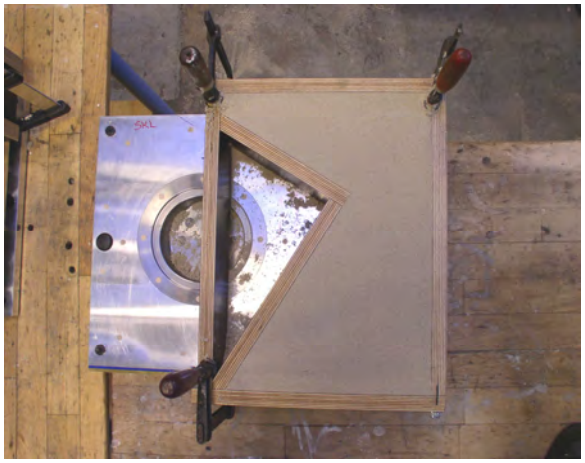

Figure 5.15 Core for layout no. 3 made over the swing plate pattern.

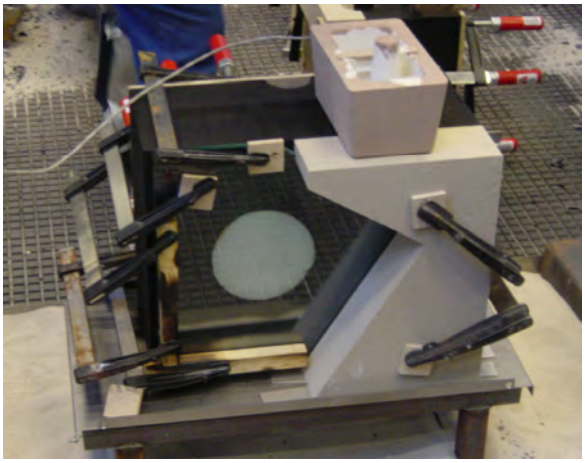

Figure 5.16 Set up for layout no. 3.

The V shaped core seen on Figure 5.16 is made over the swing plate as seen on Figure 5.15 with the aid of a wooden frame. A recess is moulded into the core for fixing the glass. The core is rammed by hand in sodium silicate bounded sand. The hand ramming makes it possible to mould very thin fins reducing the needed safety distance between the glass and the runners to around 3 mm.

The total poured weight is 7.78 kg; the weight of the disc is 4.90 kg leading to a yield of 63 %.

The main data for the layout can be seen in Table 5.4.

Layout no.		3
Drawing number		8326D0090
Choke area	mm^2	126.5
Cross section shape of the choke	mm	6.5/13/13
Ferrostatic pressure height at choke inclusive the pouring basin	mm	311 + 50
Calculated initial speed at choke without losses	mm/s	2663
Calculated initial flow without losses	kg/s	2.32
Area of horizontal runner	mm^2	384
Cross section shape of horizontal runner	mm	8/16/32
Area ratio horizontal runner / choke		3.0
Calculated initial melt speed in horizontal runner without losses	mm/s	877
Thickness of plate ingate	mm	2.5
Area of plate ingate	mm^2	388
Initial melt speed in the plate ingate calculated without losses	mm/s	869
Mean Ferrostatic height for the filling of the disc cavity	mm	242.5
Calculated filling time of the disc cavity found without losses	s	2.58

Table 5.4 Main data for layout no. 3.

For the calculations of the filling time of the disc cavity and the different velocities the same equations have been used as at layout no. 1.

5.2.3.1 Filling of the gating system and the initial part of the disc cavity

Both runs of the trial were successful. When comparing the videos of the flow patterns from the 2 runs no significant differences could be found. Run number 2 was chosen for the further examination. Snapshots from the filling of the gating system and the first part of the disc cavity can be seen on Figure 5.17 on the following pages.

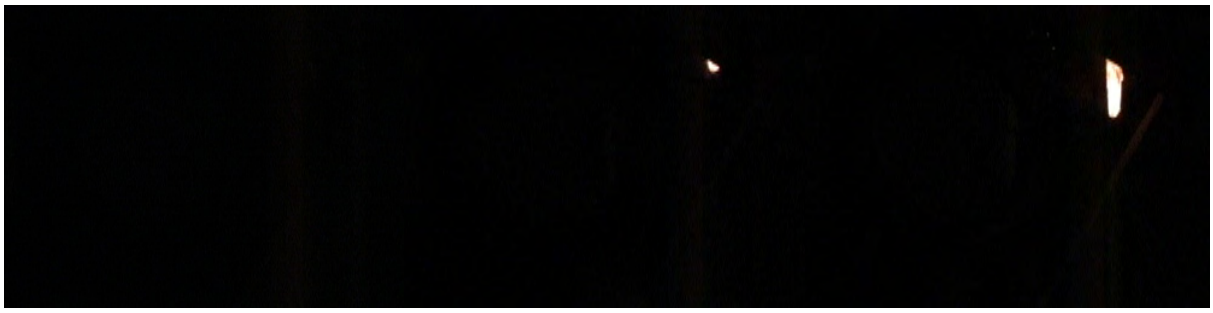

Time 0.00 Time 0.04 Time 0.08

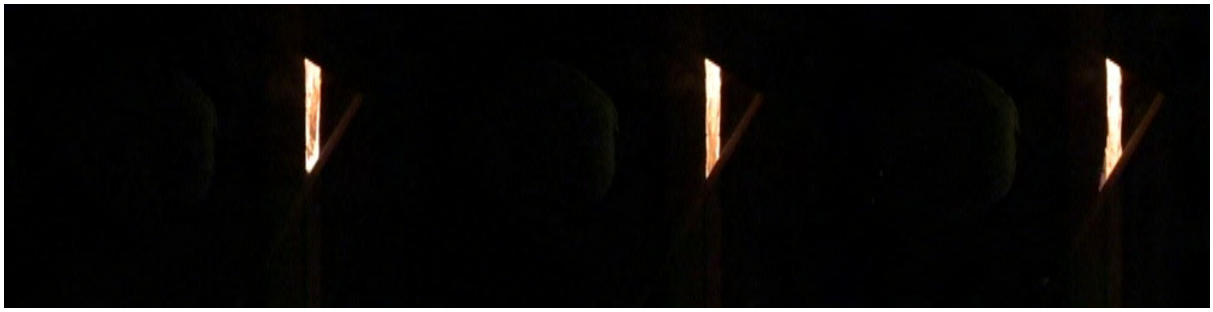

Time 0.12 Time 0.16 Time 0.20

Time 0.24 Time 0.28 Time 0.32

Time 0.36 Time 0.40 Time 0.44

Time 0.48 Time 0.52 Time 0.56

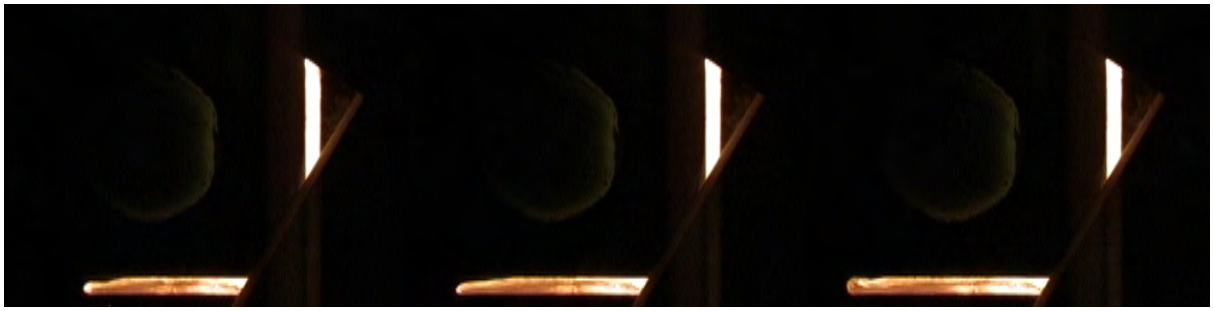

Time 0.60 Time 0.64 Time 0.68

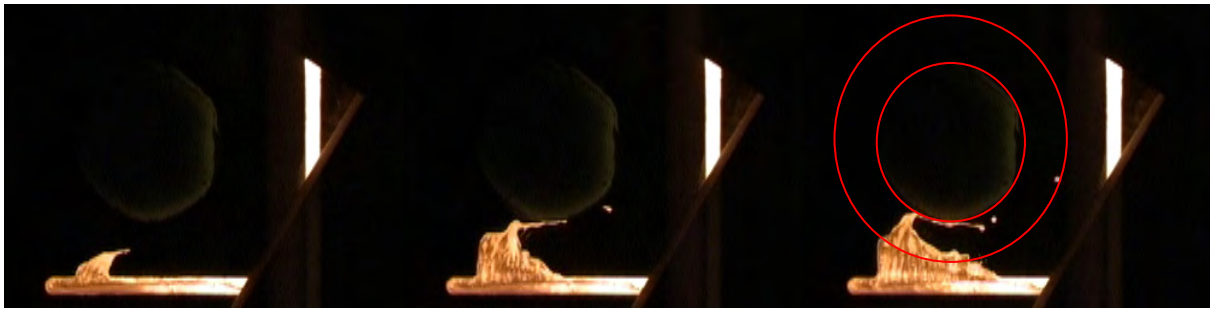

Time 0.72 Time 0.76 Time 0.80 Disc starts to fill

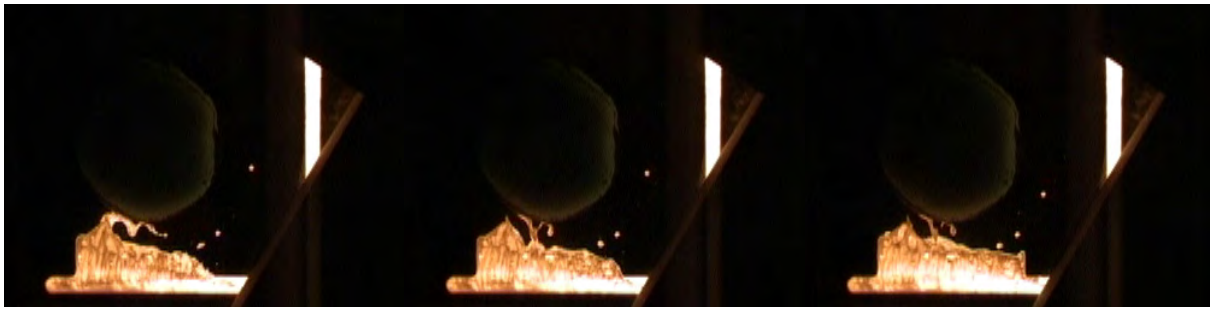

Time 0.84 Time 0.88 Time 0.92

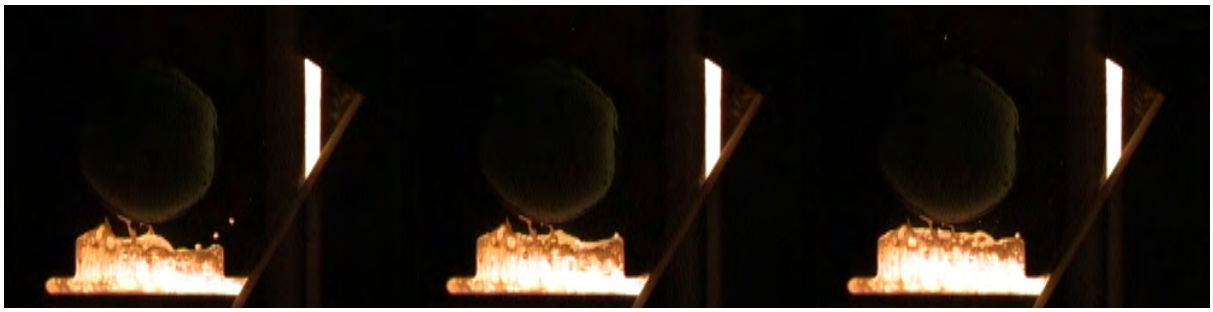

Time 0.96 Time 1.00 Time 1.04

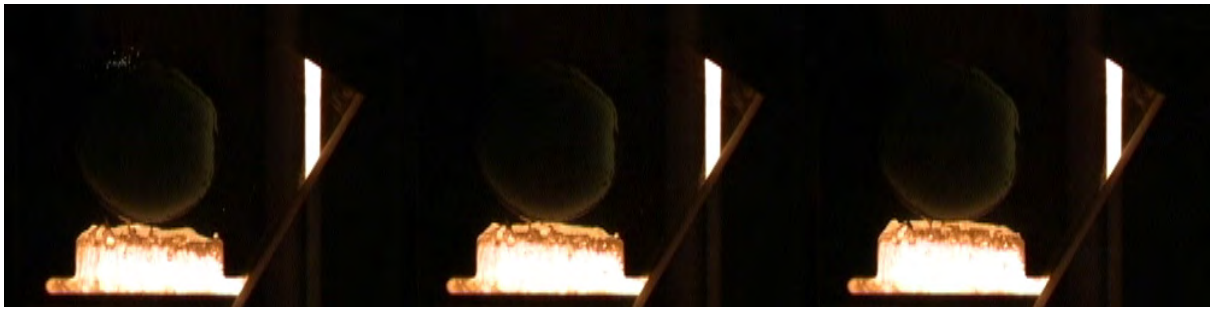

Time 1.08 Time 1.12 Time 1.16

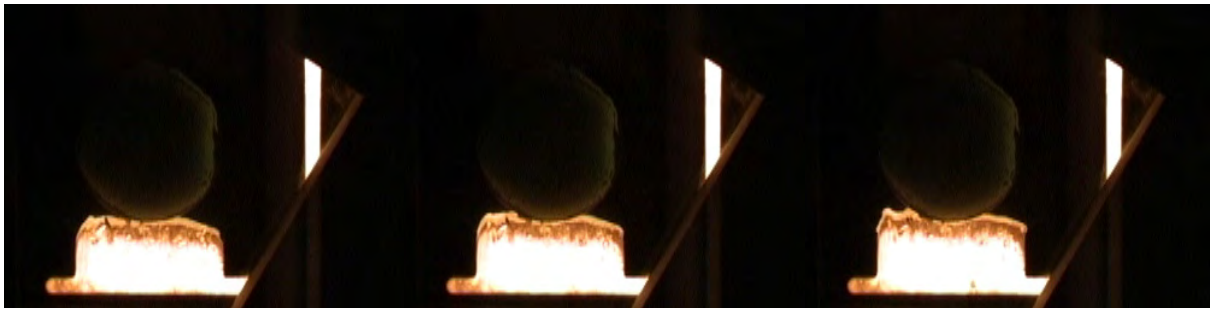

Time 1.20 Time 1.24 Time 1.28

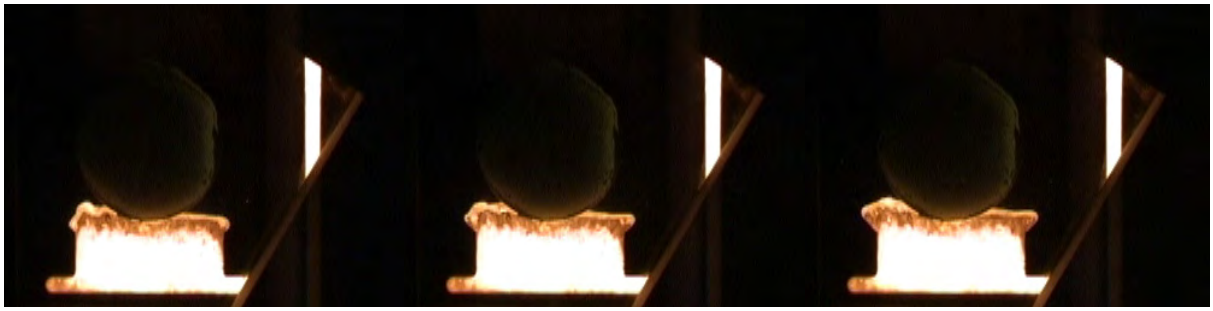

Time 1.32 Time 1.36 Time 1.40

Figure 5.17 Initial filling of layout no. 3.

The filling of the rest of the disc cavity is calm.

The cloud of small droplets seen at 0.36 and 0.40 s at the bottom of the pictures are coming from the stopper core. They are outside the mould cavity.

The cross section of the visible part of the down runner fills almost completely with the first melt passing through it. But it is first completely filled after 0.60 s. This means aspiration can take place in the down runner during this initial part of the filling. The partly filled down runner can be caused by different things. As described in section 5.2.1.1 will the cross sectional area of the down runner be approximately 10 % to large on the middle of a 350 mm long down runner if a straight taper is used for reducing the cross section area from the top to the bottom section.

When calculating the possible maximum flow rates through the cross sections of the down runner one gets: 2.39 kg/s for the overlap between the top of the down runner and the pouring cup, 2.25 kg/s for the trapezium shaped cross section (16/16/8 mm) at the upper part of the down runner and 2.15 kg/s for the choke (13/13/6.5 mm).

The calculations are made using Eq. 5.2 without losses, with a contribution to the metal head from the pouring basin of 50 mm and with no back pressure from the mould cavity corresponding to the situation during the initial filling. The layout can be seen in Appendix 5.3.

From the 2.39 and 2.25 kg/s is it seen that the design only has build in a safety margin of 6 % between these two cross sections. From 2.25 to 2.15 kg/s a safety margin of 5 % is seen. Hence the cross sections are designed very close to the limit. The safety margin used when designing the top cross section area is not able to compensate for the 10 % mentioned above.

Apart from the very tightly designed gating system another factor can also promote the partly filled down runner. At the overlap from the pouring cup to the top of the down runner the metal has to make a relatively sharp bend, this can lead to the appearance of a vena contracta, as illustrated on Figure 5.18. The vena contracta reduces the effective cross section the metal flow takes place in and hence acts as an artificial choke. The appearance of a vena contracta can not be verified as this part of the gating system can not be captured on the videos. From the results described in the following sections a vena contracta can be expected at this position.

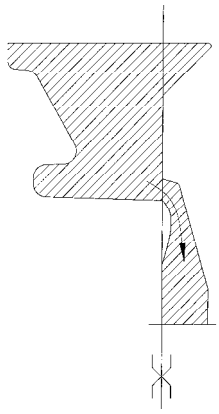

Figure 5.18 Vena contracta at pouring cup.

The down runner will be partly filled until a significant back pressure has been build up and hence reduces the flow rate. Even though the loss in the system will grow as the melt passes through the down runner towards the bottom of it the increasing back pressure from the losses is not large enough to compensate for the too large area, as the losses in the down runner will be relatively small.

The initial filling of the horizontal runner takes place in a very controlled way. Only a single droplet is in front of the main melt stream in the horizontal runner, it can be seen after 0.28 s. Unfortunately it is not possible to capture the function of the well on the videos due to the overlapping of the parting line at the well. But the appearance of only a single droplet indicates a good functioning well. This also sounds reasonable because the melt has to cross over the parting line twice when it passes through the well. The overlapping of the parting line puts

extra hindrances into the flow. The good performance of the well is seen even though the horizontal runner connects to the bottom of the well instead of the top. Connecting the horizontal runner to the top of the well will force the well to be filled up before the melt can enter the horizontal runner i.e. it means extra hindrances for the flow. Putting the outlet of the well at the top of the well has been done with good results in layout no. 1.

The cross section of the horizontal runner is almost completely filled behind the advancing melt front. This together with no tapering of the horizontal runner or other means to try to gradually reduce the melt velocity in the horizontal runner is an effective basis for getting splashes shooting into the casting due to the pressure shock wave caused by the hammer effect when the melt hits the end of the horizontal runner. After 0.72 s a melt fountain is blown into the disc cavity. If the melt droplets end up at the top of the core that shapes the inside of the disc they may not be remelted and the result will be inclusions in the disc.

The fountain going into the disc cavity is having its origin at the left end of the horizontal runner i.e. where the metal comes to an abrupt stand still. This indicates a completely filled cross section of the horizontal runner with no air pockets acting as buffers for the pressure shock wave. The fountain is hence a direct result of the hammer effect when the melt hits the end of the horizontal runner. The different appearances of pressure shock waves are more closely discussed in section 4. When comparing the data for layout no. 2 given in Table 5.3 and the data for layout no. 3 given in Table 5.4 is the initial melt front velocity in the horizontal runner calculated without losses seen to be significantly higher at layout no. 3 compared to no. 2. This increases the tendency to splashes shooting into the disc cavity. The difference in velocity is mainly due to the depressurized design of layout no. 2. What also increases the likelihood of splashes shooting into the disc cavity is the pressure behind the melt. Layout no. 2 is a non-pressurized system. As shown in section 5.2.2.1 is the effective metallostatic head when the metal enters the disc cavity relative small at layout no. 2. On the other hand when the metal enters the disc cavity at layout no. 3 described in this section the runners are completely filled resulting in maximum metallostatic head behind the melt. The metal shooting into the disc cavity at the far end of the horizontal runner is furthermore promoted by the direction of the melt flow in the horizontal runner. As at layout no. 1 is the entrance of the melt into the disc cavity rather explosive. This indicates the controlling parameter to be a pressure shock wave instead of only the direction of the melt.

5.2.3.2 Flow pattern in the disc cavity

The temperature distribution in the disc in the rest of the filling sequence shows indirectly the filling pattern in the disc. Snapshots from the filling of the disc are showed below:

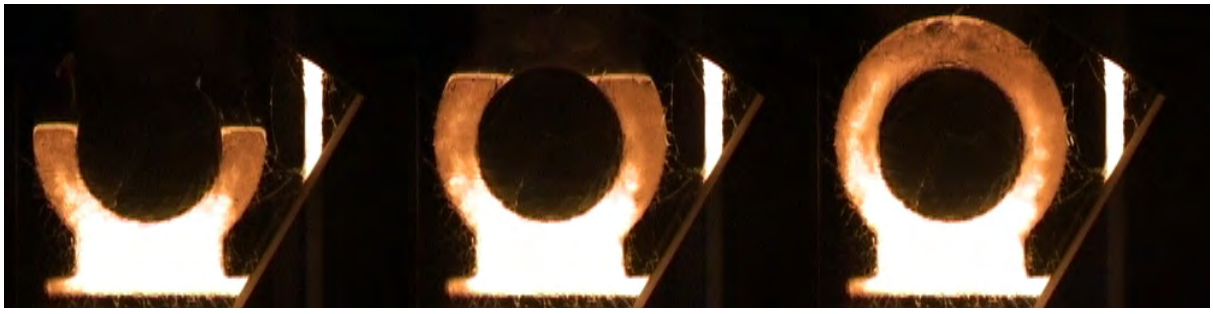

Time 2.92 Time 4.44 Time 5.96

Figure 5.19 Filling of the disc cavity in layout no. 3.

Even though heavy splashes shooting into the disc cavity at the left side is seen when the melt enters the disc, the temperature distribution in the disc after the initial filling is close to symmetrical around the vertical centreline. Only a small tendency for the flow to take plate at the left side is seen. This shows a sidewise balanced flow once a limited melt level in the disc has been reached. This balanced filling will be discussed more closely in chapter 5.6. The disc is significantly hotter in the bottom than in the top, this can only be so when working with bottom filling systems.

The temperature differences seen after the filling on Figure 5.13 are equalized after the filling has ended. This is seen on the left side of Figure 5.20 showing the mould shortly after the filling is ended. Later in the cooling sequence is the plate shaped ingate acting as a cooling fin. This is seen on the right side of Figure 5.20.

Figure 5.20 Temperature distribution shortly after the filling and 2 minutes later.

5.2.3.3 Filling time

The total filling time of layout no. 3 is 6.26 s. 0.3 s have been added for the filling of the pouring cup as in the other layouts. The filling of the disc is seen to start after 0.80 s, i.e. the filling time for the disc is 5.16 s. The calculated filling time for the disc without losses is 2.58 s. This yields a total loss coefficient for the filling of the disc of 0.50.

5.2.3.4 Simulation of the mould filling

The mould filling has been simulated with MAGMAsoft. The boundary conditions used for the filling simulation are the outlet area of the pouring basin and a pressure equal to 50 mm metal head from the basin. I.e. conditions equal to what is the case in the trials have been transferred to the simulation. Snapshots from the simulated filling sequence are shown on Figure 5.21 on the following pages. It has been chosen to use the same time scale as used on Figure 5.17 to make it easier to compare how the melt fronts proceed in the trials and in the simulation. Friction between the mould walls and the melt has been incorporated into the simulation.

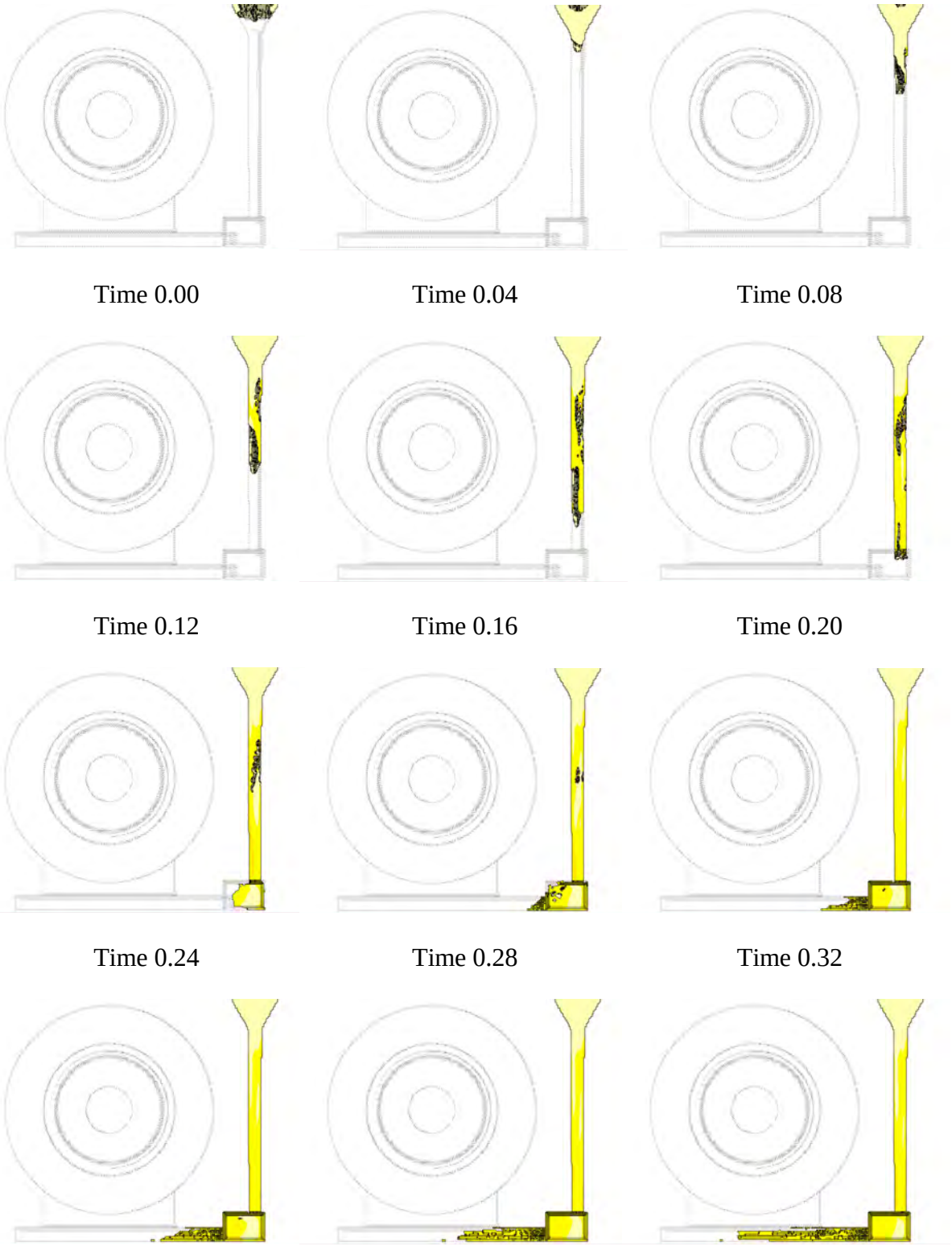

Time 0.00 Time 0.04 Time 0.08

Time 0.12 Time 0.16 Time 0.20

Time 0.24 Time 0.28 Time 0.32

Time 0.36 Time 0.40 Time 0.44

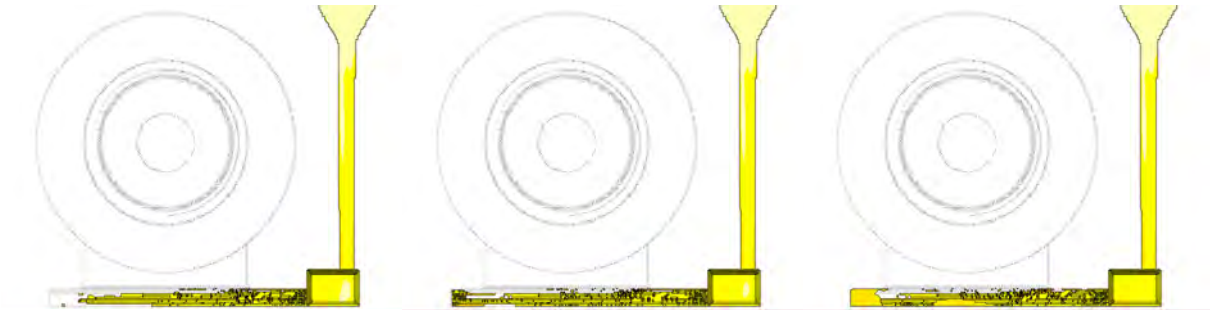

Time 0.48 Time 0.52 Time 0.56

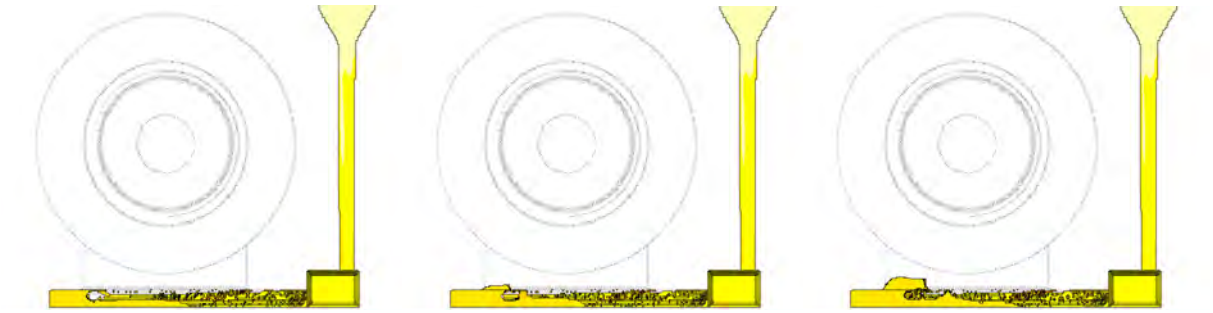

Time 0.60 Time 0.64 Time 0.68

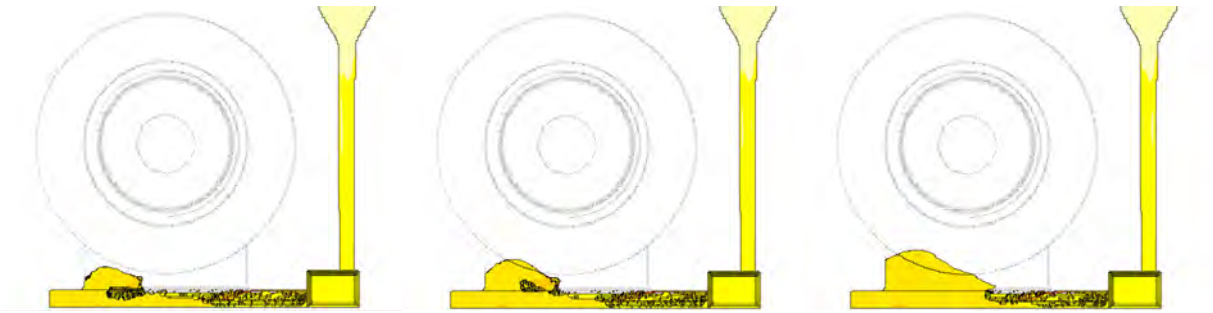

Time 0.72 Time 0.76 Time 0.80

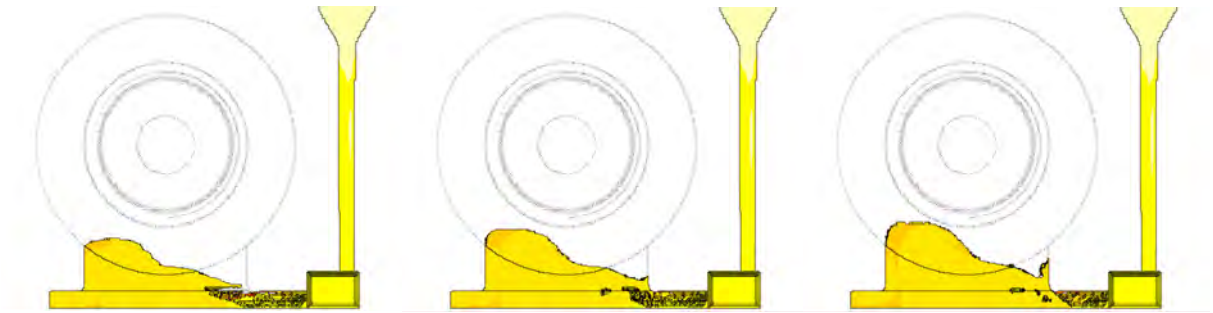

Time 0.84 Time 0.88 Time 0.92

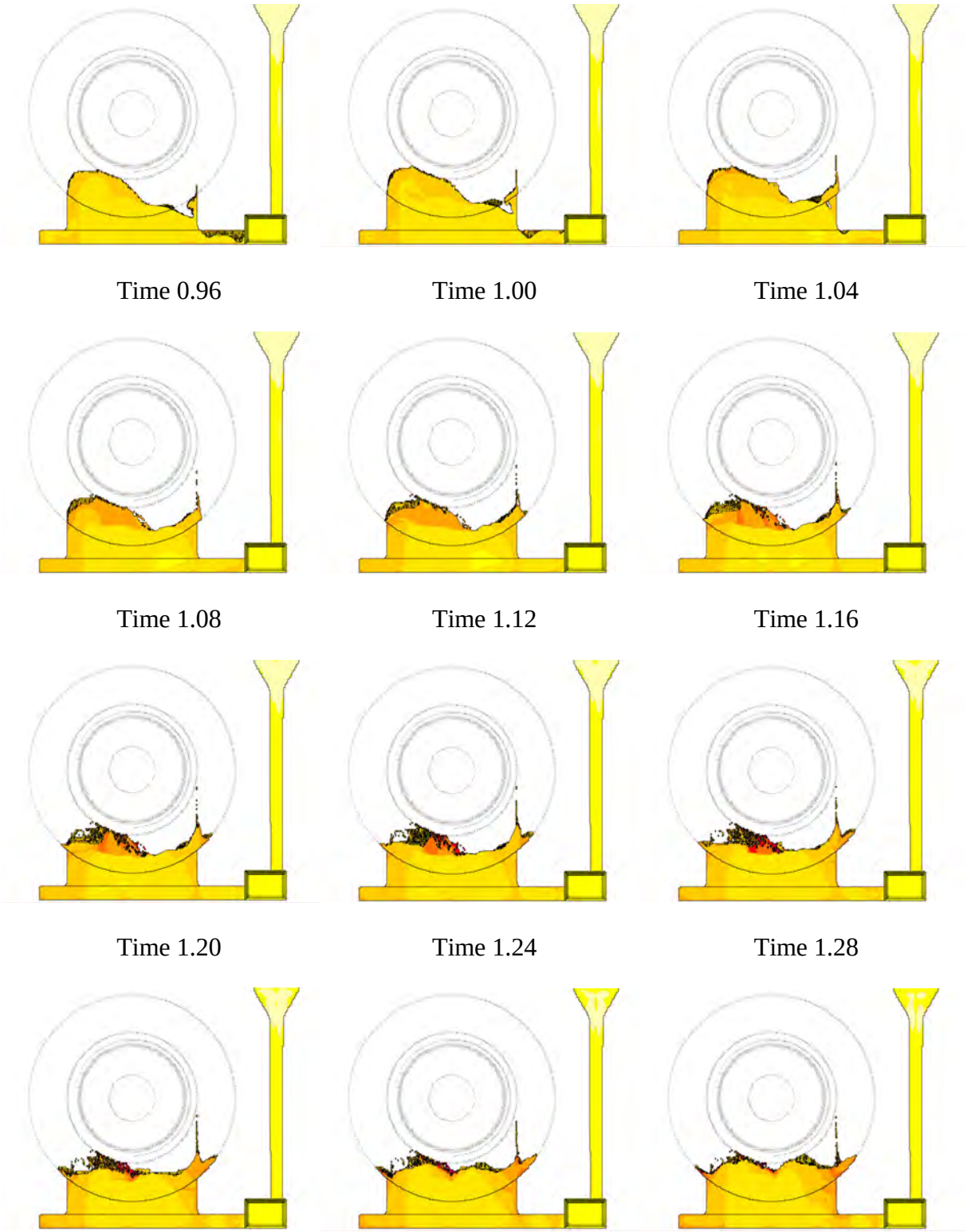

Figure 5.21 Initial filling of layout no. 3 simulated.

The filling of the rest of the disc cavity is calm.

When comparing the simulated filling sequence seen on Figure 5.21 and the real filling sequence seen on Figure 5.17 some differences can be seen:

The filling of the horizontal runner in the experiments takes place with one coherent melt front almost filling the complete cross section of the horizontal runner with the first melt passing through. At the simulation the melt flows over the bottom surface of the horizontal runner in a relatively thin layer. This simulated flow pattern results in the melt front reaching the end of the horizontal runner after 0.52 s and then the melt starts to back fill the horizontal runner from the far end. As the horizontal runner is only partly filled when the melt hits the end of the runner no pressure shock wave is initiated. Only the back rolling wave is observed. This simulated filling sequence of the horizontal runner results in some melt entering into the disc cavity at the far end of the runner after 0.72 s but due to the back filling of the horizontal runner an air pocket still exits in the right part of the horizontal runner. When the air pocket starts to get closed at around 0.96 s a melt jet is blown into the disc cavity just above the closing pocket. This is in good agreement with what is seen in the trials. The good agreement with the trial results has to be understood in the way that it has several times been observed that the closing of an air pocket can lead to a pressure shock wave making the melt front break up. Hence this phenomenon is well described in the simulation.

In the trials the filling of the horizontal runner takes place with an almost completely filled cross section behind the melt front. This results in a pressure shock wave when the melt hits the end of the horizontal runner. The shock wave drives the metal into the disc cavity at the left side i.e. as close as possible to the place where the shock wave has been initiated.

Hence the filling sequence of the horizontal runner is very important to be able to get the initial filling of the disc cavity right. When the melt flows over a horizontal surface, surface tension and friction keeps the melt stream together and hence results in given thickness of the advancing melt front. In the simulations the surface tension is not included. This makes it very difficult to simulate the flow over a horizontal surface. Hence the differences between the simulated results and the results from the trials are seen.

The simulated temperature distribution in the rest of the filling sequence can be seen on Figure 5.22 below.

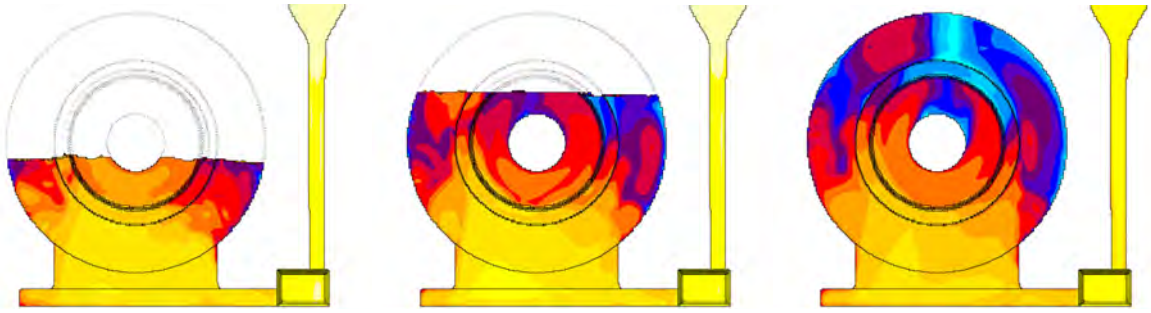

Time 2.92 Time 4.44 Time 5.96

Figure 5.22 Simulated filling of the disc cavity in layout no. 3.

The corresponding snapshots from the trials can be seen on Figure 5.19. Both the trials and the simulation show a relatively symmetrical heat distribution sidewise. As discussed pre-

viously, in this kind of gating system the sidewise balance of the flow is controlled by the balance between the dynamic and the braking forces. Hence it is quite difficult to predict for the casting engineer. The simulation is seen to give a good picture of the balance.

The total filling time in real life is found to 6.3 s. The simulation results in 6.26 s. This agreement is very good and probably a little better than normally can be expected. On the other hand have the boundary conditions applied in the trials been very well defined and they have been easy to transfer to the boundary conditions needed in the simulations.

The flow patterns inside the down runner well can not be examined with the videos made of this gating system. Even in the cases where the well is visible on the videos it can only be observed whether droplets are blown into the horizontal runner etc. The flow patterns in the well can be visualized in the simulation. The simulated flow patterns in the well of the layout discussed in this section can be seen on Figure 5.23. The flow is seen not to be smooth. A significant part of the flow is reflected from the bottom of the well into the top of the well and then it exits the well after another sharp bend.

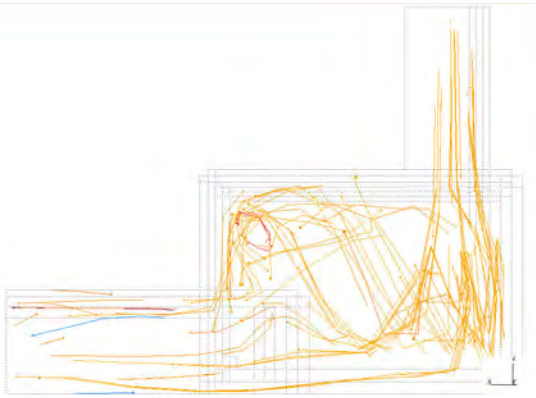

Figure 5.23 Flow pattern in the down runner well.

Hence this type of well introduces a lot of turbulence into the melt. Seen from a velocity reduction point of view it is good as turbulence takes energy out of the melt and the direction is changed not pointing directly into the horizontal runner. But the turbulence can also mean problems like sand erosion resulting in inclusions.

5.2.4 Layout no. 4

The fourth layout can be seen in Figure 5.24. A detailed drawing of the layout is shown in Appendix 5.4. The flow restricting area is positioned at the bottom of the down runner, i.e. it is a depressurized system [Ref. 5.8]. The cross section of the horizontal runner is gradually tapered down over the width of the plate shaped ingate. This design is intended for gradually reducing the melt velocity in the horizontal runner and to give a sidewise more balanced filling of the disc. No well established rules exist for designing the gradually reduction of the horizontal runner. The actual design depends on the personal experience of the foundry engineer.

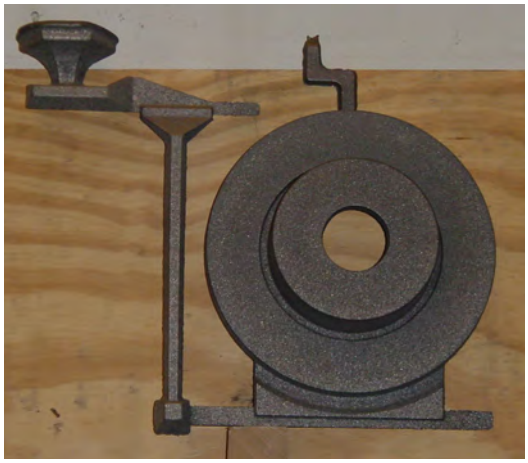

Figure 5.24 Layout no. 4.

The layout is designed with lapping over the parting line at the top of the down runner, at the exit of the well and from the horizontal runner to the plate shaped ingate. This makes it impossible to use the simple set up shown on Figure 5.3.

A special set up was made with a core shaped as a frame around the disc making it possible to capture the metal flow in most of the down runner, most of the plate shaped ingate and the disc except for the upper 15 mm. The set up and the tooling can be seen on Figure 5.25 to Figure 5.27.

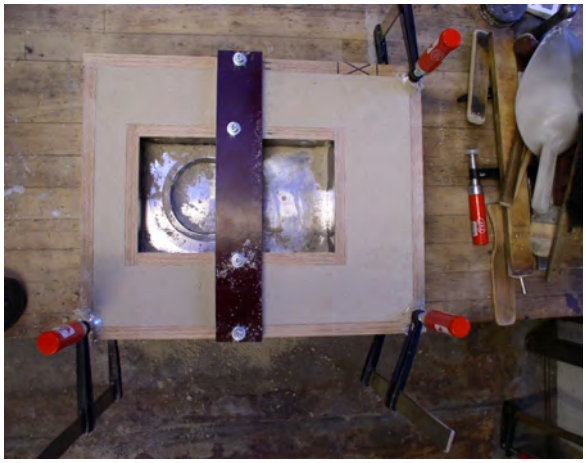

Figure 5.25 Frame core for layout no. 4 made over the swing plate pattern.

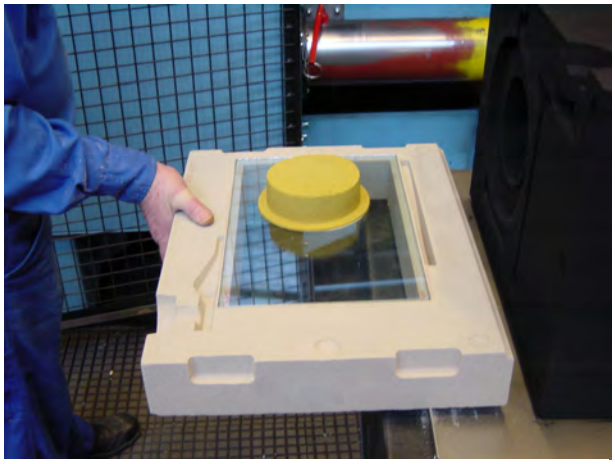

Figure 5.26 Frame core mounted with glass for layout no. 4.

The total poured weight is 7.66 kg; the weight of the disc is 4.90 kg leading to a yield of 64 %

The main data for the layout can be seen in Table 5.5 below:

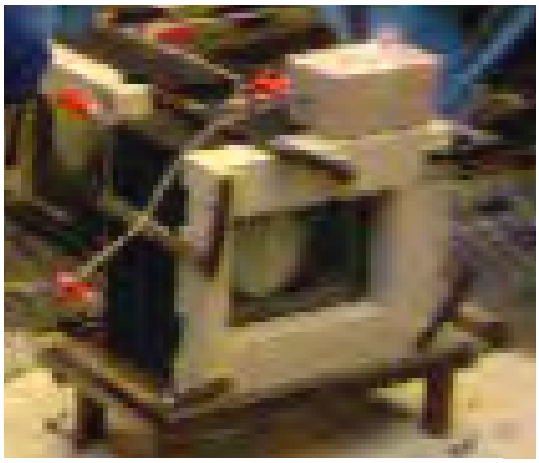

Figure 5.27 Set up for layout no. 4.

Layout no.		4
Drawing number		8326D0110
Choke area	mm^2	147
Cross section shape of the choke	mm	7/14/14
Ferrostatic pressure height at choke inclusive the pouring basin	mm	318 + 50
Calculated initial speed at choke without losses	mm/s	2688
Calculated initial flow without losses	kg/s	2.72
Area of horizontal runner	mm^2	294
Cross section shape of horizontal runner	mm	7/14/28
Area ratio horizontal runner / choke		2.0
Calculated initial melt speed in horizontal runner without losses	mm/s	1344*
Thickness of plate ingate	mm	2
Area of plate ingate	mm^2	316
Initial melt speed in the plate ingate calculated without losses	mm/s	1251
Mean Ferrostatic height for the filling of the disc cavity	mm	242.5
Calculated filling time of the disc cavity found without losses	s	2.22

Table 5.5 Main data for layout no. 4.

For the calculations of the filling time of the disc cavity and the different velocities the same equations have been used as at layout no. 1.

* Calculated on the basis of the area of the horizontal runner before it is gradually reduced.

5.2.4.1 Filling of the gating system and the initial part of the disc cavity

Both runs of the trial were successful. When comparing the videos of the flow patterns from the 2 runs, run no. 2 gave a few extra melt droplets in the disc cavity compared to run no. 1. Run number 2 was chosen for the further examination. Snapshots from the filling of the gating system and the first part of the disc cavity can be seen on Figure 5.28 on the following pages:

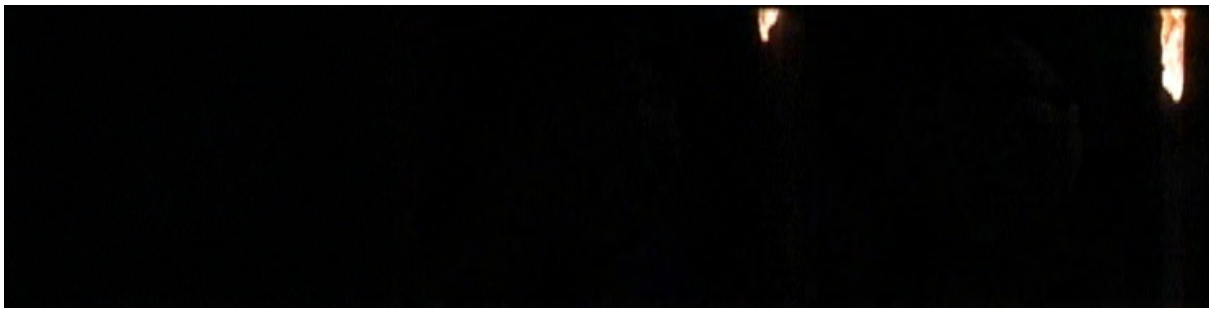

Time 0.00 Time 0.04 Time 0.08

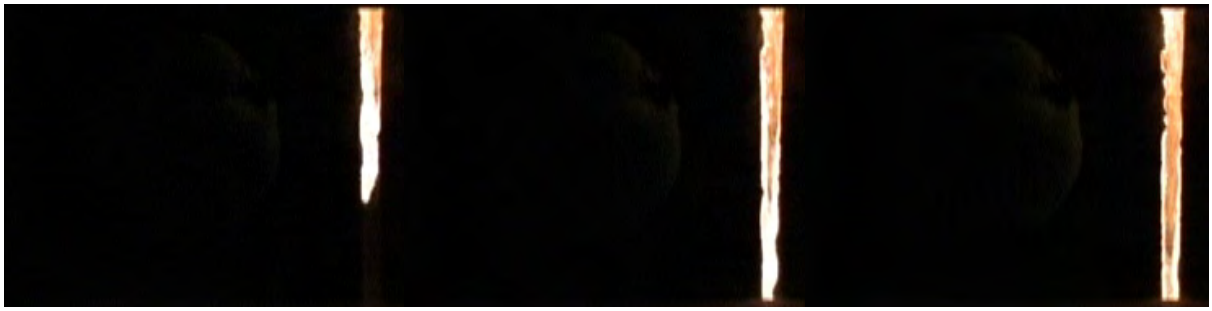

Time 0.12 Time 0.16 Time 0.20

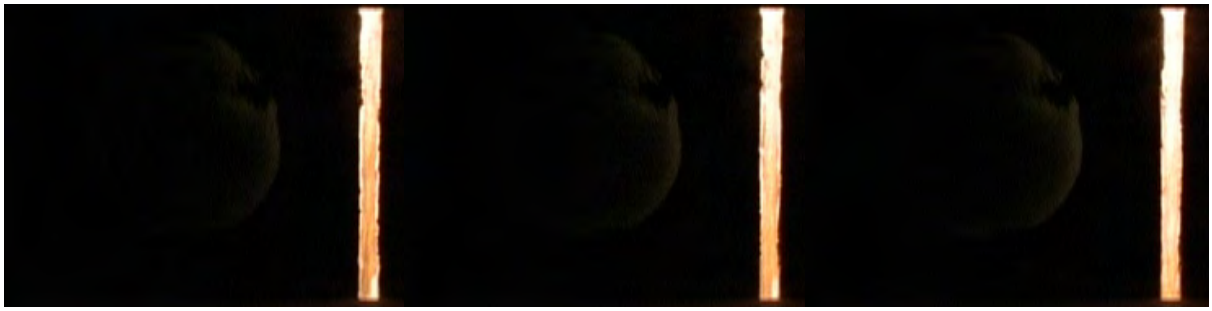

Time 0.24 Time 0.28 Time 0.32

Time 0.36 Time 0.40 Time 0.44

Time 0.48 Time 0.52 Time 0.56

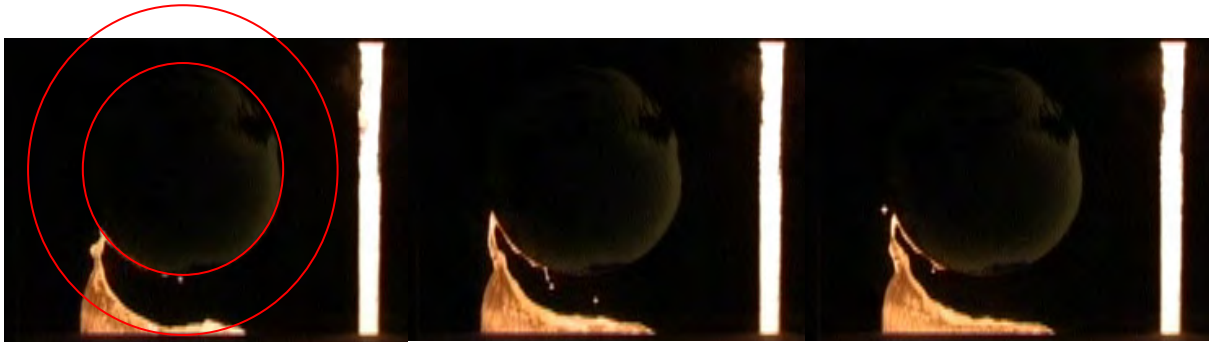

Time 0.60 Disc starts to fill Time 0.64 Time 0.68

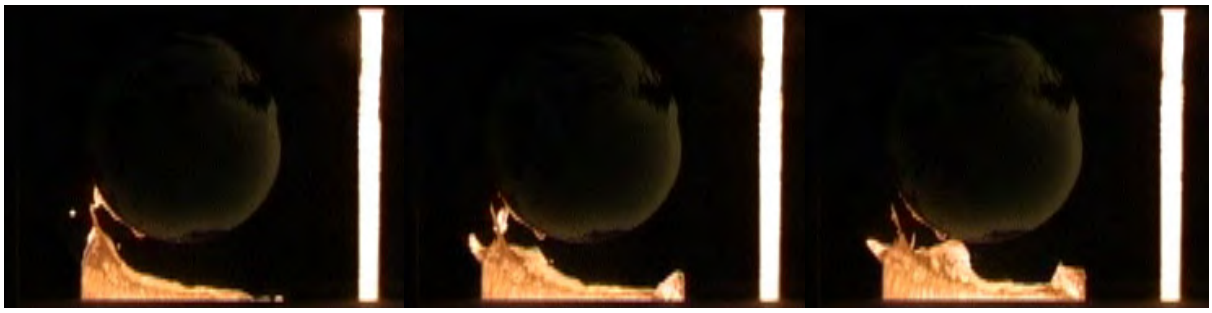

Time 0.72 Time 0.76 Time 0.80

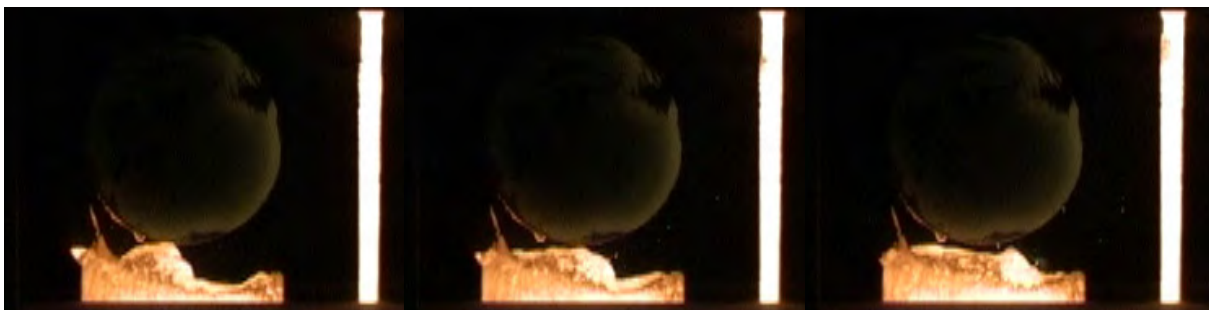

Time 0.84 Time 0.88 Time 0.92

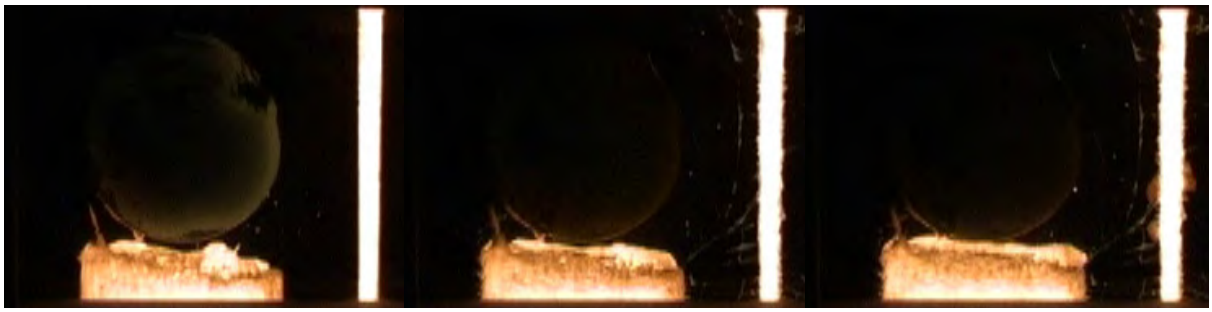

Time 0.96 Time 1.00 Time 1.04

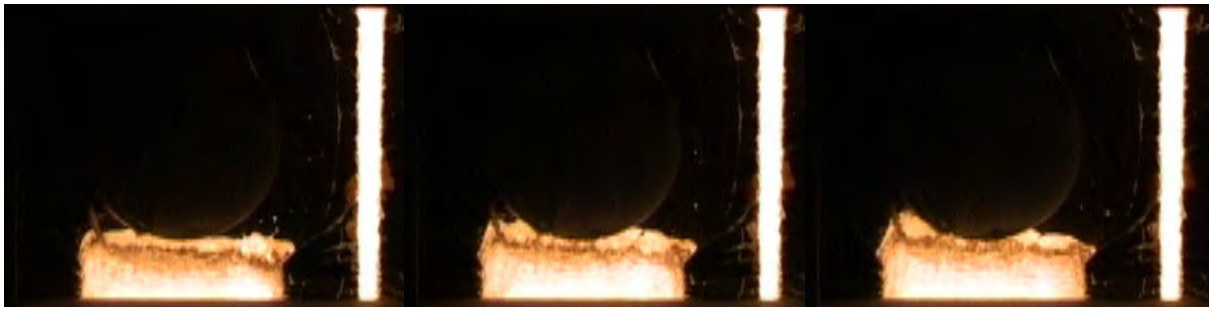

Time 1.08 Time 1.12 Time 1.16

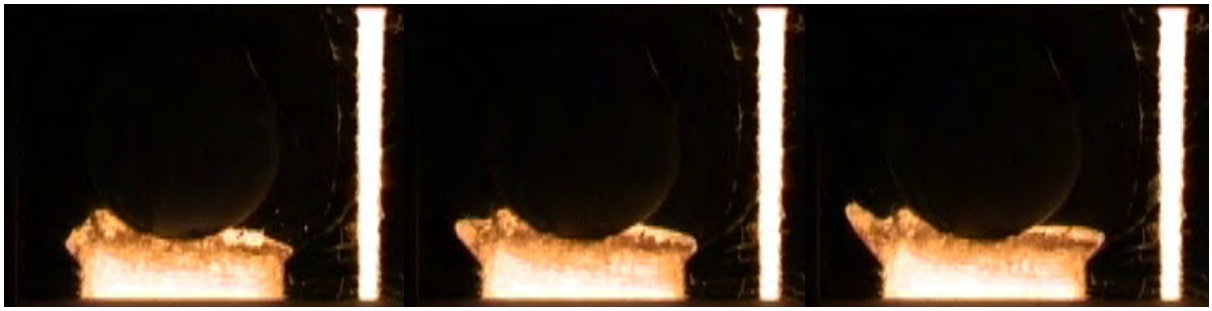

Time 1.20 Time 1.24 Time 1.28

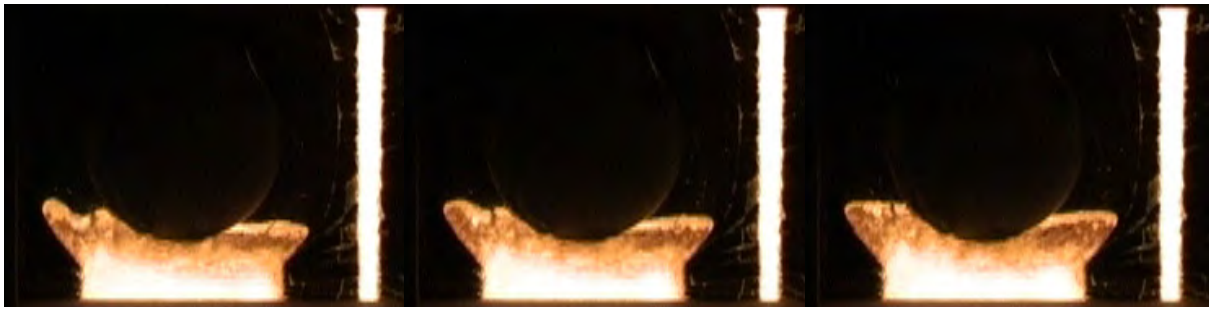

Time 1.32 Time 1.36 Time 1.40

Figure 5.28 Initial filling of layout no. 4.

The filling of the rest of the disc cavity is calm.

The filling of the visible part of the down runner takes place with a coherent melt front. No droplets leave the main melt front. Even though the cross section of the down runner is almost completely filled with the first melt passing through it, it is first completely filled after 0.96 s.

A possible explanation for the partly filled down runner in the initial phase could be too small cross sectional areas at the top of the down runner. When calculating the maximum flow rates through the cross sections of the down runner one gets: 3.22 kg/s for the overlap between the top of the down runner and the horizontal extension of the pouring cup, 2.84 kg/s for the trapezium shaped cross section (18/18/9 mm) and 2.72 kg/s for the choke (14/14/7 mm).

The calculations are made using Eq. 5.2 without losses, with a contribution to the metal head from the pouring basin of 50 mm, and no back pressure from the mould cavity corresponding to the situation during the initial filling. The layout can be seen in Appendix 5.4.

When comparing 2.72 and 2.84 kg/s around 5 % safety margin is added for the trapezium shaped cross section (18/18/9 mm) in the upper part of the down runner. The safety margin for the lapping over at the horizontal extension of the pouring cup is found by comparing 2.84 and 3.22 kg/s it is 13 %.

Another explanation for the partly filled down runner in the initial phase of the filling is the design of the transition from the horizontal extension of the pouring cup to the top of the down runner. The metal has to make a relatively sharp bend when passing through the transition. When the melt has to make a sharp bend, a vena contracta is likely to appear. This is especially the case when no back pressure exists and hence the maximum velocities are present. Unfortunately the transition is hidden in the frame core seen on Figure 5.26. In the trials described in section 6.5, a very stream lined version of this type of transition has been used. In this case it was possible to capture part of the flow through the transition on video. The video shows a vena contracta even with the very stream lined design. This supports the likelihood of the presence of a vena contracta at the top of the down runner in the design described in this section. The vena contracta will reduce the effective area for metal flow and hence act as an artificial choke. The 13 % safety margin can very easily be consumed by the size of the vena contracta. The appearance and size of a vena contracta is depending on the geometry, the velocity of the metal and the properties of the metal. Going into more detailed flow analysis makes it possible to estimate the appearance and size of vena contractas; though this is out of the scope of this work. The appearances of vena contractas very clearly illustrate the issue about effective cross sectional area for the flow. The effective cross sectional area it not just the physical area of the channel the flow takes place in. A reduction in the effective cross sectional area for the flow compared to the physical area of the channel does not necessarily come from an air pocket. As seen at layout no. 1 are inactive areas also likely to appear, if non stream lined designs are used. This is illustrated on Figure 5.8, showing an area filled with melt, but the melt is not flowing in the area.

The metal flow in the horizontal runner and the well cannot be seen as it takes place in the frame core seen on Figure 5.26. At 0.56-0.64 s a melt fountain is blown into the disc cavity. This happens even though the cross section of the horizontal runner has been gradually reduced over the width of the plate shaped ingate to try to gradually reduce the melt velocity before the melt hits the end of the horizontal runner. I.e. the gradual reduction in area is not (at least under the conditions seen here) able to gradually reduce the velocity of the melt and hence prevent a pressure shock wave shooting metal into the casting cavity. The direction of the

melt flow in the horizontal runner also enhances the tendency for the first melt to enter into the brake disc cavity at the far end of the runner. Like in layout no. 1 and no. 3 is the entrance of the melt into the disc cavity explosive, indicating that the entrance is controlled by a pressure shock wave.

Actually the adverse effect from a gradual reduction of the horizontal runner can be imagined. When the horizontal runner is gradually reduced, the velocity of the melt will grow unless the increasing friction is able to keep it down. Hence whether the velocity grows or not is a balance between the reduction in cross sectional area and increasing resistance to flow. Unfortunately it is not possible to capture the advancing metal front because the flow takes place in the frame core. The initial melt front velocity in the horizontal runner before the gradual reduction in the cross sectional area calculated without losses is given in Table 5.5 to 1344 mm/s. This is a relatively high velocity when for instance compared to the velocity found for layout no. 3. The area of the horizontal runner is reduced from 294 to 128 mm^2. Hence in theory the velocity of the initial melt in the horizontal runner can be accelerated to 3094 mm/s when the melt hits the end of the horizontal runner. The dynamic pressure is given by [Ref. 5.11]:

$$P_{Dynamic} = 1/2 \cdot \rho \cdot v^2 \qquad \text{[Eq. 5.4]}$$

The dynamic pressure is seen to follow the square of the velocity. This pressure is converted to static pressure when the melt comes to a stand still. Because of the square relation to the velocity small increases in velocity will give significant increases in dynamic pressure.

The gradual reduction in the horizontal runner also assists in securing a completely filled cross section behind the melt front. The lack of possible air pockets behind the melt front acting as buffers for the pressure shock wave combined with a possible increase in velocity increases the likelihood of getting a melt fountain blown into the casting cavity.

The metal is blown into the disc cavity at the far end of the horizontal runner. As discussed in section 5.2.3.1 the melt fountain at this position indicates a completely filled cross section of the horizontal runner when the melt front hits the end of the runner.

The lapping over at the transition from the horizontal runner to the plate shaped ingate together with a 2 mm thick plate ingate is not able to prevent the pressure shock wave blowing metal into the disc cavity.

The same gradually reduced horizontal runner is used in layout no. 5 described in the next section. In this case it has been possible to capture the metal flow in the horizontal runner on video. Hence the function of the gradually reduced horizontal runner will be discussed more closely in this section.

5.2.4.2 Flow pattern in the disc cavity

The temperature distribution in the disc during the filling sequence shows indirectly the flow pattern in the disc cavity. Snapshots from the filling of the disc are showed below:

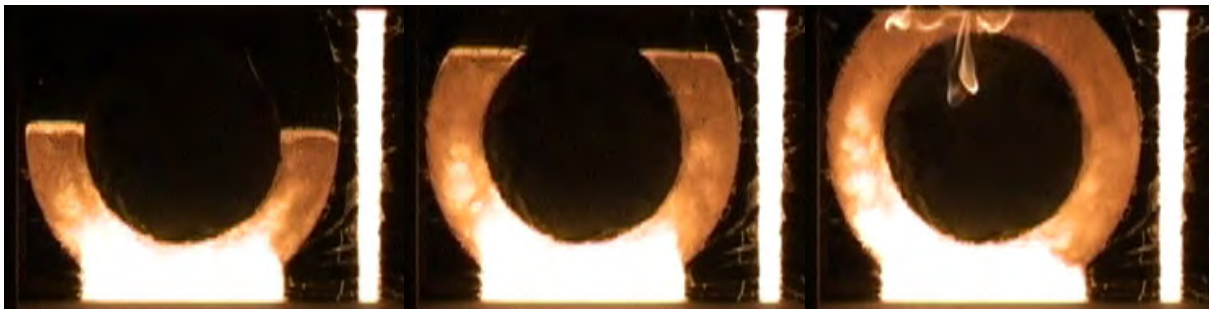

Time 2.60 Time 3.80 Time 4.96

Figure 5.29 Filling of the disc cavity in layout no. 4.

The temperature distribution in the disc after 2.60 s is close to symmetrical sidewise. This indicates a balanced filling at this point. During the rest of the filling sequence the temperature distribution gets slightly unsymmetrical indicating a non balanced flow, with the preferred flow path at the left side of the plate ingate. I.e. the dynamic forces are larger than the braking forces and hence they are able to shift the flow to the left side of the disc. This unbalance towards the left side is seen even though the cross sectional area of the horizontal runner (hidden in the frame core) is gradually reduced over the width of the plate shaped ingate as can be seen in Appendix 5.4. The change in flow pattern from a symmetrical one at 2.60 s to one shifted towards the left side in the last part of the filling sequence can be caused by a reheating of the left part of the horizontal runner as is seen in section 4.5.2.2 with the thin plates. Again the flow in the horizontal runner is not visible and hence this mechanism can not be verified. The flow pattern seen here will be compared to the flow patterns seen at the other layouts section 5.6.

5.2.4.3 Filling time

The total filling time of layout no. 4 is 5.26 s. As with layout no. 1 the top of the disc is hidden behind the top core. The end of the filling has been calculated in the same way as at layout no. 1. 0.3 s have been added for the filling of the pouring cup and the runner connected to it in the same way as with layout no. 1. The filling of the disc starts after 0.60 s, i.e. the filling time for the disc is 4.36 s. The calculated filling time for the disc without losses is 2.22 s. This yields a total loss coefficient for the filling of the disc of 0.51.

5.2.5 Layout no. 5

The fifth layout can be seen in Figure 5.30. A detailed drawing of the layout is shown in Appendix 5.5. This layout is a variant of layout no. 4, i.e. it is also depressurized. Compared to layout no. 4 is layout no. 5 adjusted to have the complete gating system inclusive the pouring cup on the same pattern plate. This is done to make it possible to capture the metal flow in the complete gating system on video. This means that the overlaps at the top of the down runner, at the exit of the down runner well and at the transition from the horizontal runner to the plate shaped ingate have been removed. Otherwise are the parts of the gating system the same as for layout no. 4. The dimensions are also the same. Having the complete gating system on the same pattern plate as the disc makes it possible to use a glass plate covering the complete mould face.

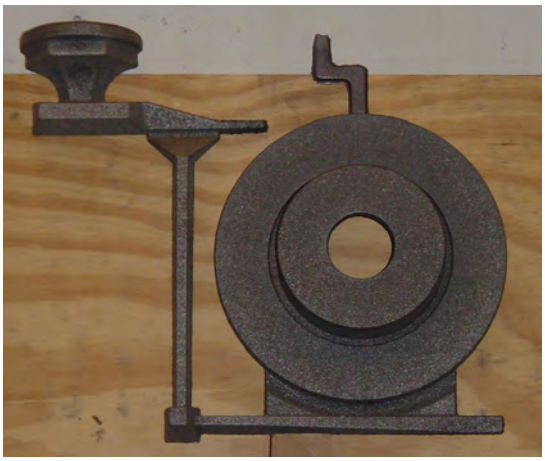

Figure 5.30 Layout no. 5.

The shape of the outlet nozzle of the pouring basin was fitted to go into the standard pouring cup used on this layout.

The total poured weight is 7.39 kg; the weight of the disc is 4.90 kg leading to a yield of 66 %.

The main data for the layout can be seen in the table below:

Layout no.		5
Drawing number		8326D0100
Choke area	mm^2	147
Cross section shape of the choke	mm	7/14/14
Ferrostatic pressure height at choke inclusive the pouring basin	mm	318 + 50
Calculated initial speed at choke without losses	mm/s	2688
Calculated initial flow without losses	kg/s	2.72
Area of horizontal runner	mm^2	294
Cross section shape of horizontal runner	mm	7/14/28
Area ratio horizontal runner / choke		2.0
Calculated initial melt speed in horizontal runner without losses	mm/s	1344
Thickness of plate ingate	mm	2
Area of plate ingate	mm^2	316
Initial melt speed in the plate ingate calculated without losses	mm/s	1251
Mean Ferrostatic height for the filling of the disc cavity	mm	242.5
Calculated filling time of the disc cavity found without losses	s	2.22

Table 5.6 Main data for layout no. 5.

For the calculations of the filling time of the disc cavity and the different velocities the same equations have been used as at layout no. 1.

5.2.5.1 Filling of the gating system and the initial part of the disc cavity

When comparing the videos of the flow patterns from the 2 runs no significant differences could be seen in the filling of the gating system and the initial filling of the disc cavity. The glass breaks in run number 2 when the disc is approximately 75 % filled. Run number 1 was chosen for the further examination. Snapshots from the filling of the gating system and the first part of the disc can be seen on Figure 5.31 on the following pages:

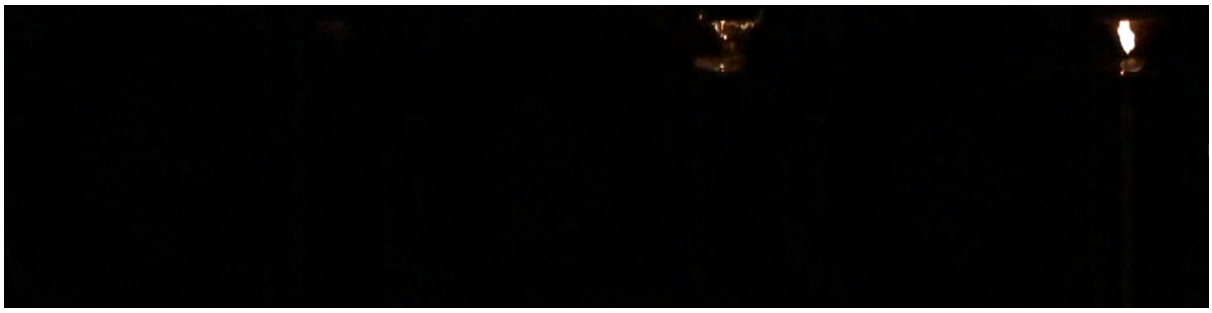

Time 0.00 Time 0.04 Time 0.08

Time 0.12 Time 0.16 Time 0.20

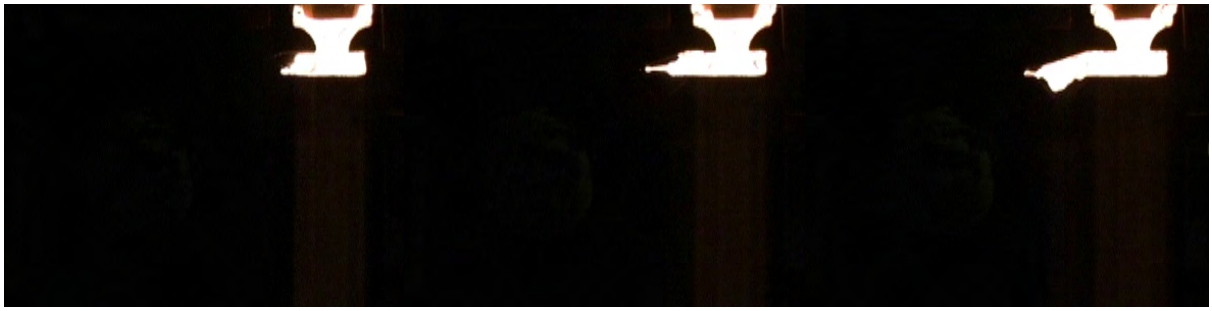

Time 0.24 Time 0.28 Time 0.32

Time 0.36 Time 0.40 Time 0.44

Time 0.48 Time 0.52 Time 0.56

Time 0.60 Time 0.64 Time 0.68

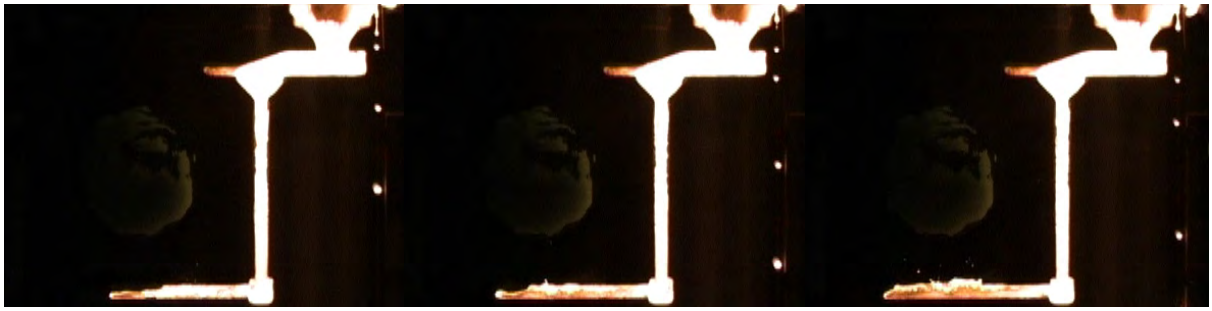

Time 0.72 Time 0.76 Time 0.80

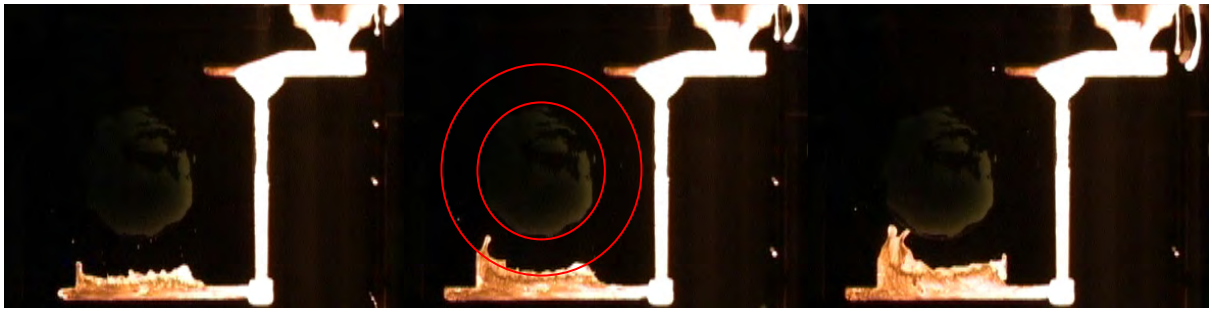

Time 0.84 Time 0.88 Disc starts to fill Time 0.92

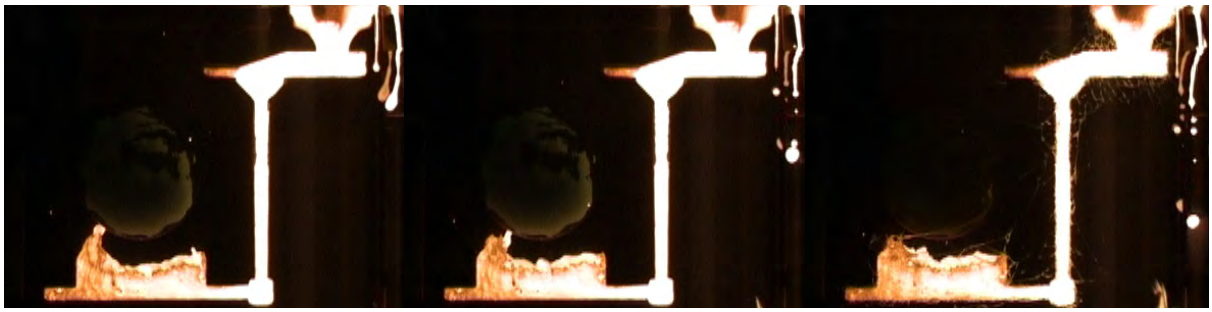

Time 0.96 Time 1.00 Time 1.04

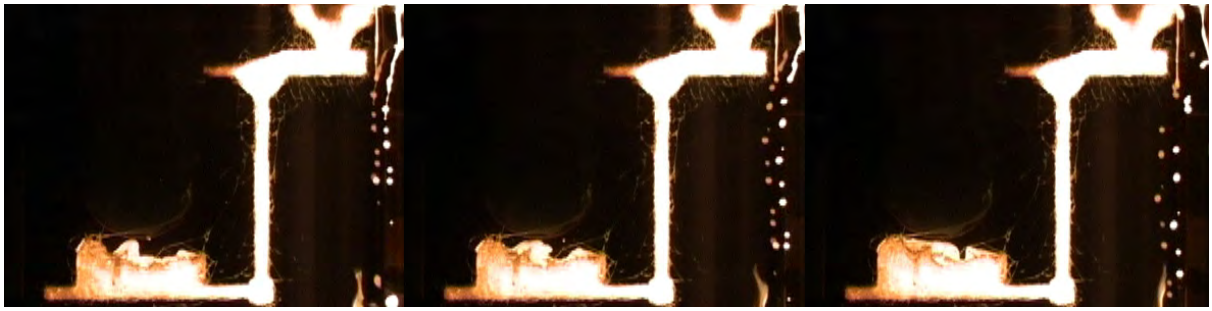

Time 1.08 Time 1.12 Time 1.16

Time 1.20 Time 1.24 Time 1.28

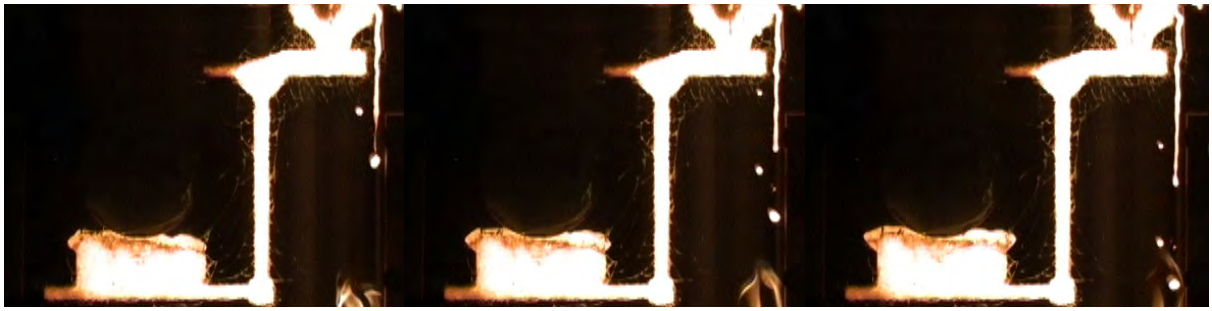

Time 1.32 Time 1.36 Time 1.40

Figure 5.31 Initial filling of layout no. 5.

The filling of the rest of the disc cavity is calm.

After 0.60 s droplets are seen to the right on the snapshots. The pouring basin was not sealed properly against the top of the mould making it possible for a small amount of the melt to escape here. A melt level of 50 mm could be maintained in the basin during the filling sequence as with the other layouts, meaning the leak did not affect the filling of the mould.

The pouring cup and the small horizontal runner connected to it are filled after 0.30 s. The filling of the down runner takes place with one coherent melt front filling almost the complete cross section of the down runner, with the first melt passing through it.

At this layout as with layout no. 4 the top of the down runner is not filled during the initial stages of the filling, this can be seen on the enlargement of the top of the down runner shown on Figure 5.32. The section where the trapeze shaped down runner is connected to the spout shaped part is further enlarged on Figure 5.33. Both snapshots are after 1.00 s. A vena contracta is seen at the inside corner of the transition from the spout to the trapezium shaped part. The vena contracta reduces the effective cross sectional area of the metal flow and hence works as an artificial choke. The resistance of the melt to run around sharp corners is clearly seen on Figure 5.33. If the corner had been a 90 degree bend the vena contracta would have been even larger.

Figure 5.32 Air pockets at the top of the down runner at 1.00 s.

At layout no. 4 which is the same as this layout except for the lapping over the parting line used at no. 4 a partly filled down runner was also seen. Due to the top core it was not possible to see the upper part of the down runner at layout no. 4. On the basis of the results seen here it is very likely to be a vena contracta that also causes the partly filled down runner at layout no. 4. At layout no. 4 the metal flow also has to lap over the parting line at the transition from the horizontal extension of the pouring cup to the top of the down runner. I.e. the metal has to make another relatively sharp bend also making it possible for a vena contracta to appear at this point.

Figure 5.33 Vena contracta at 1.00 s.

Unfortunately after 1.00 s the glass layers crack making it impossible to judge when the vena contracta at the top of the down runner disappears and the cross section at the top of the down runner is completely filled.

No melt droplets reach the well under the down runner before the main melt front. Even though one coherent melt stream hits the bottom of the empty well, the well performs acceptable. Only a single droplet is seen in front of the main melt front in the horizontal runner, this happens at 0.52 s. The good performance of the well is surprising taken the size of the well into consideration. The design could maybe be improved a little by moving the outlet to the top of the well instead of having it positioned at the middle of the side of the well. The design used at layout no. 4 with an overlap at the exit of the well is probably performing even better.

When the metal starts to enter the plate ingate only 1 droplet leaves the main melt front after 0.80 s and enters the disc cavity on its own. The melt starts to enter the plate ingate before the horizontal runner is completely filled. This happens at 0.80 to 0.84 s while the melt reaches the end of the horizontal runner after 0.88 s. A melt tongue is being pushed into the left side of the disc cavity after 0.92 s. It is not possible to say whether the reason is the melt front hitting the end of the horizontal runner or whether the reason is the reduction in the cross sectional area of the horizontal runner. Reducing the cross sectional area of the horizontal runner will at some point make it more feasible for the melt to flow into the disc cavity instead of continue in the horizontal runner due to the growing resistance to flow when the area is reduced.

A little less splashing when the melt enters the disc is seen on this layout compared to layout no. 4. This is surprising, since the layouts are the same except for the lapping over used at layout no. 4 at the top of the down runner, at the exit of the well and from the horizontal runner to the plate shaped ingate. The lapping over is normally seen as a way to prevent splashes as the overlaps are expected to catch the possible flying droplets. Due to the directional changes connected to overlaps, overlaps also introduces extra losses into the system. The absence of any clear evidence of the positive function of the overlaps used at layout no. 4 could lead to the conclusion that they have a limited effect on the flow. More trials have to be conducted before this can be concluded. Effects as for instance the ability to catch slag have also to be investigated before the final conclusion on the value of overlaps can be made. In section 2.6 were the contributions from the different parts of the gating system to the total loss in the system estimated. In was shown that the major part of the loss was coming from the down runner including the choke. Directional changes etc. have relatively little influence on the total loss in the system when the flow is established. This has been found for a conventional gating system.

The reason for the smaller amount of metal shooting into the disc cavity at the initial part of the filling at layout no. 5 compared to what is seen at layout no. 4 is hard to identify. It could be due to the possible variations in the pouring conditions. Even though the pouring basin is used some limited variations in the pouring conditions will exist. If the gating system is not able to absorb these variations, differences will be seen in the flow patterns in the same way as seen in section 4.7.2.2 for instance. I.e. the explanation could be natural variations. Another explanation could be the absence of the lapping over between the horizontal runner and the plate ingate compared to layout no. 4. Without the lapping over, the metal will more easily enter the plate shaped ingate and continue into the disc cavity. At layout no. 5 the metal enters the plate shaped ingate before the metal has reached the end of the horizontal runner, hence some of the pressure has been relieved and some metal is in the plate ingate when the metal hits the end of the horizontal runner. Both will soften the result of the hammer effect when the melt hits the end of the horizontal runner. Hence although the lapping over has only limited influence on the losses when the flow is established the overlap can act as a physical barrier for the first melt passing through the system and hence have some influence on the initial flow patterns.

5.2.5.2 Flow pattern in the disc cavity

The temperature distribution in the disc during the filling sequence shows indirectly the flow pattern in the disc cavity. Snapshots from the filling of the disc are showed below:

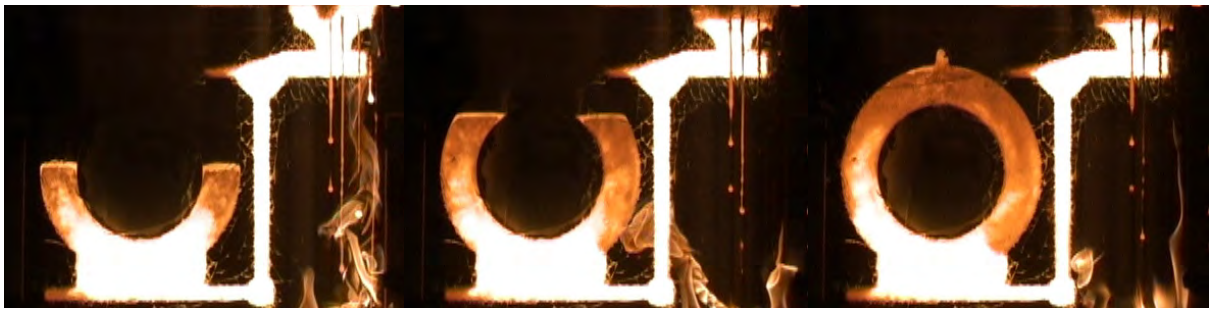

Time 2.76 Time 4.12 Time 5.48

Figure 5.34 Filling of the disc cavity in layout no. 5.

The final temperature distribution in the disc is a little unsymmetrical sidewise; indicating a not completely balanced flow sidewise. The final temperature distribution is very similar to the one seen in layout no. 4. This indicates that the lapping over at the transition from the horizontal runner to the plate shaped ingate not significantly changes the flow patterns. The flow pattern seen here will be compared to the flow patterns seen at the other layouts in section 5.6.

5.2.5.3 Filling time

The total filling time of layout no. 5 is 5.48 s. The filling of the disc starts after 0.88 s, i.e. the filling time for the disc is 4.60 s. The calculated filling time for the disc without losses is 2.22 s. This gives a total loss coefficient for the filling of the disc of 0.48.

The filling of the pouring cup and the small horizontal runner connected to it takes around 0.3 s. Some of the layouts have been cast with a top core covering the pouring cup and if present the small horizontal runner connected to it. The 0.3 s seen here, has been used to estimate the time for the hidden flow in the other cases.

5.2.6 Layout no. 6

The sixth layout can be seen on Figure 5.35. A detailed drawing of the layout is shown in Appendix 5.6. This gating system has been designed with gating techniques developed for aluminium. The layout has only a dead end at the horizontal extension of the pouring cup, and not at the end of the horizontal runner under the disc cavity. This is the case for the other layouts. The runners used are very narrow to secure a coherent melt stream and completely filled runners from the first melt passing through. The fan shaped transition from the runner to the plate ingate is designed to spread out the melt to secure a sidewise symmetrical filling. The flow restricting area is at the bottom of the down runner, i.e. the system is depressurized [Ref. 5.8].

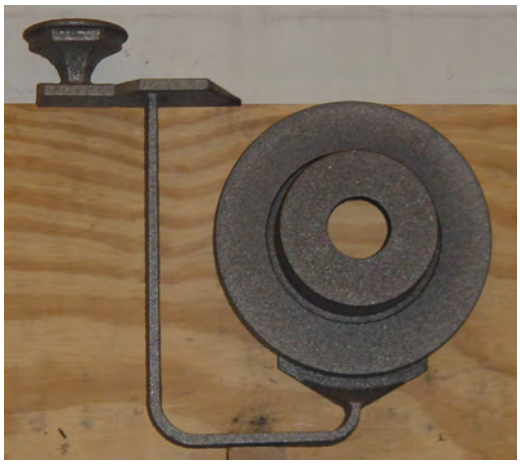

Figure 5.35 Layout no. 6

The complete gating system is on the same pattern plate as the brake disc, except for the pouring cup. This makes it possible to use the same set up as for layout no. 1 shown on Figure 5.3. Only the pouring cup had to be changed to the special version fitting the outlet nozzle of the pouring basin.

The total poured weight is 7.76 kg; the weight of the disc is 4.90 kg leading to a yield of 63 %.

The main data for the layout can be seen in the table below:

Layout no.		6
Drawing number		8326D0140
Choke area	mm^2	133
Cross section shape of the choke	mm	9/10/14
Ferrostatic pressure height at choke inclusive the pouring basin	mm	341 + 50
Calculated initial speed at choke without losses	mm/s	2771
Calculated initial flow without losses	kg/s	2.54
Area of horizontal runner	mm^2	239
Cross section shape of horizontal runner	mm	7/10/28
Area ratio horizontal runner / choke		1.8*
Calculated initial melt speed in horizontal runner without losses	mm/s	1542
Thickness of plate ingate	mm	1.5
Area of plate ingate	mm^2	195
Initial melt speed in the plate ingate calculated without losses	mm/s	1890
Mean Ferrostatic height for the filling of the disc cavity	mm	242.5
Calculated filling time of the disc cavity found without losses	s	2.45

Table 5.7 Main data for layout no. 6.

For the calculations of the filling time of the disc cavity and the different velocities the same equations have been used as at layout no. 1.

* Based on the area of the horizontal runner when it connects to the fan shaped transition to the ingate.

5.2.6.1 Filling of the gating system and the initial part of the disc cavity

Both runs of the trial were successful. When comparing the videos of the flow patterns from the 2 runs a little more splash is seen in run 2 compared to run 1. Run number 2 was chosen for the further examination. Snapshots from the filling of the gating system and the first part of the disc cavity can be seen on Figure 5.36 on the following pages.

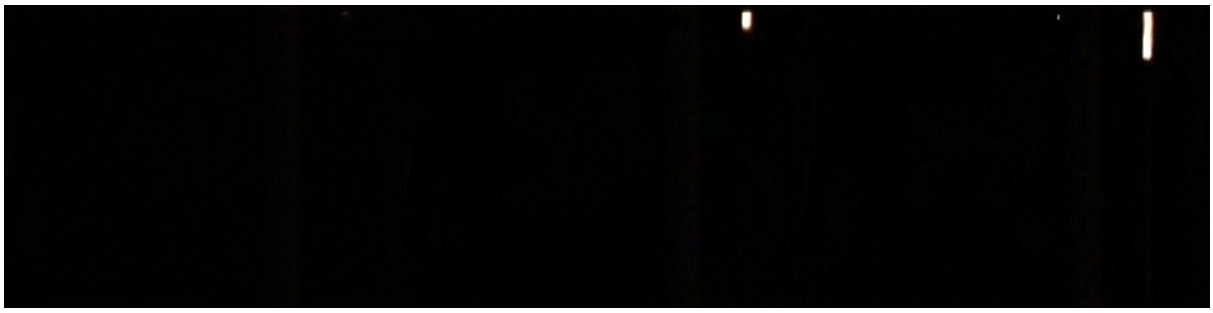

Time 0.00 Time 0.04 Time 0.08

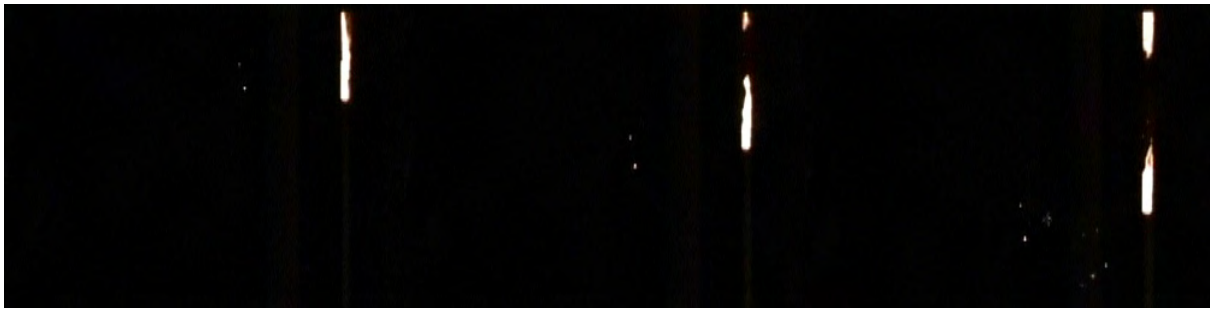

Time 0.12 Time 0.16 Time 0.20

Time 0.24 Time 0.28 Time 0.32

Time 0.36 Time 0.40 Time 0.44

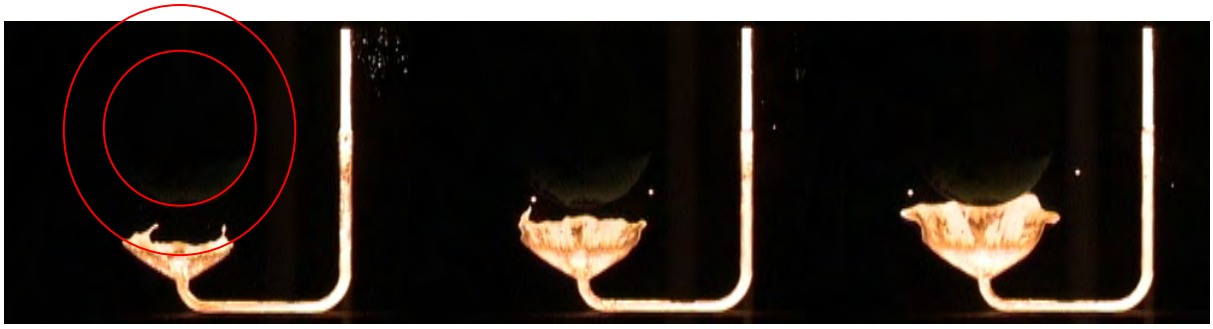

Time 0.48 Disc starts to fill Time 0.52 Time 0.56

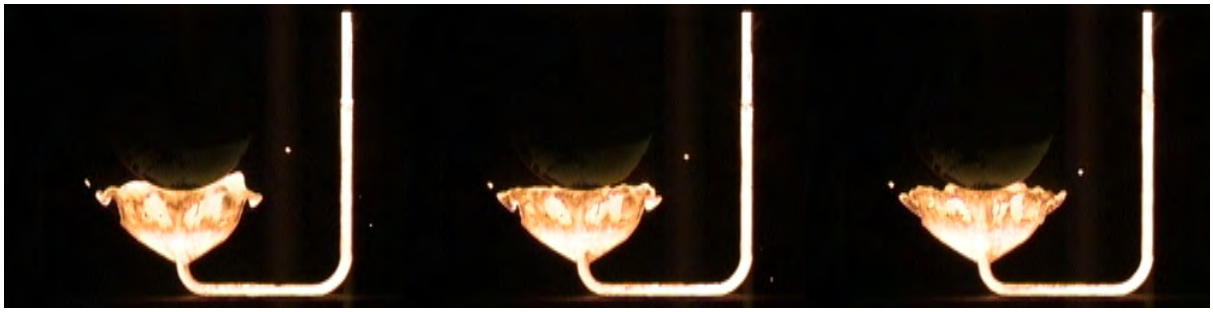

Time 0.60 Time 0.64 Time 0.68

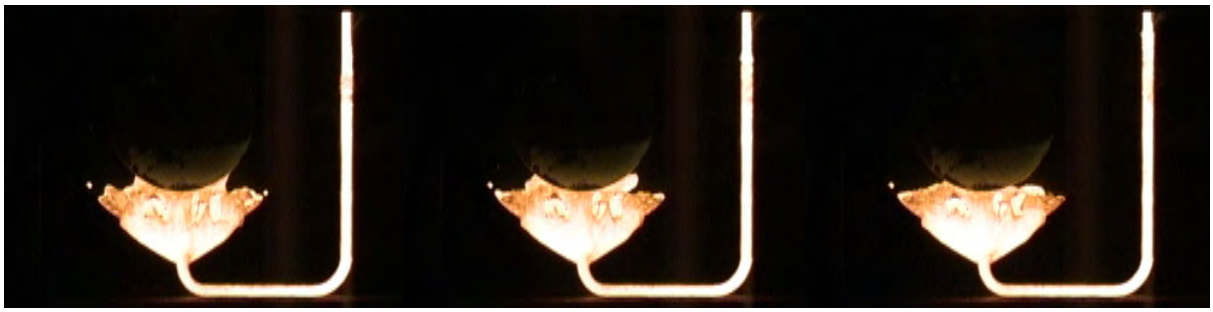

Time 0.72 Time 0.76 Time 0.80

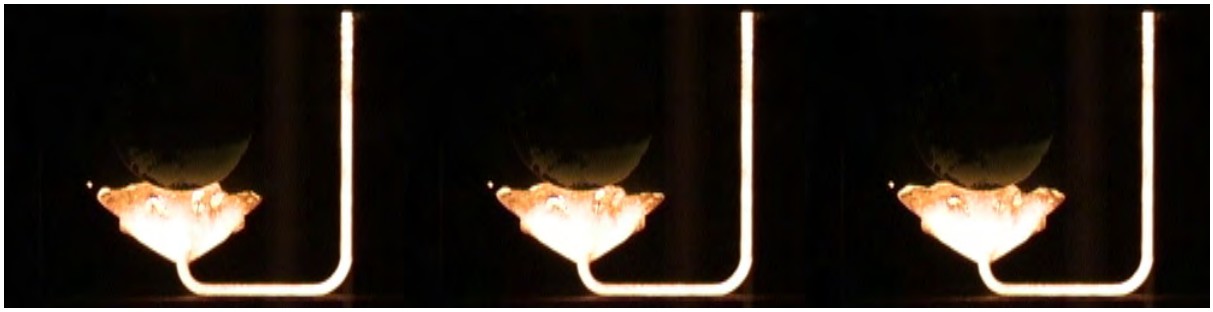

Time 0.84 Time 0.88 Time 0.92

Time 0.96 Time 1.00 Time 1.04

Time 1.08 Time 1.12 Time 1.16

Time 1.20 Time 1.24 Time 1.28

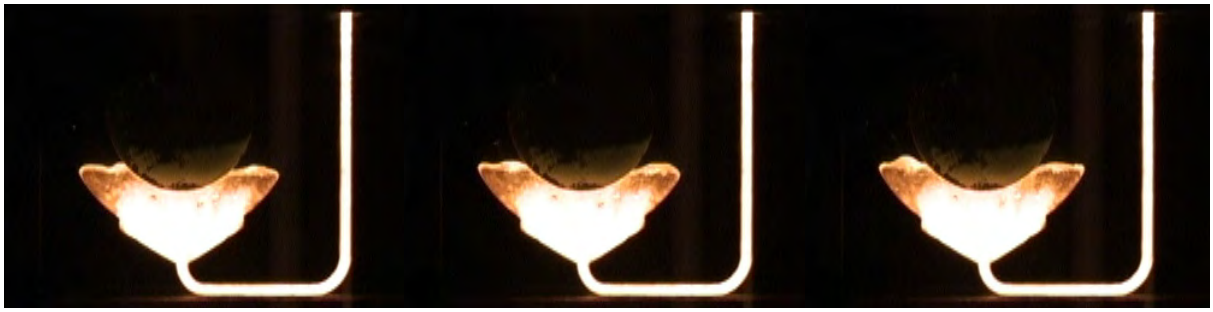

Time 1.32 Time 1.36 Time 1.40

Figure 5.36 Initial filling of layout no. 6.

The filling of the rest of the disc cavity is calm.

The runners are designed 10 mm wide at the pattern plate and with 3 degree draft. The cross sectional area is changed by changing the height of the runners. This design is used to secure a coherent melt front and completely filled runner cross sections as the first melt passes through the runners. When metal is falling free, the surface tension will result in a curvature of the melt front. The idea with runners with narrow cross sections is to have narrow sections with the smallest dimension in the same size as the curvature of the melt front and through this to secure a completely filled cross section of the runner together with the first melt passing through. Even though narrow sections have been used, the melt stream splits up after 0.16 s. This is also the case in run no. 1 only a little less pronounced. With the other down runners in mind with chunkier cross sections it is surprising to see the melt stream spilt up here.

The reason for the melt stream splitting up is difficult to identify because the flow in the horizontal runner connected to the pouring cup and the top of the down runner is hidden in the top core.

When comparing the way the transition from the horizontal extension of the pouring cup to the top of the down runner is made at the 6 layouts, they are seen to be made quite different. In layout no. 2, 3, 4 and 5 is the transition made with a spout shaped top of the down runner. This type of transition is in practice very often used.

Layout no. 1 and 6 is basically seen designed in the same way, i.e. with a 90 degree bend. But at layout no. 6 an extension of the horizontal runner connected to the pouring cup has been utilized. When the metal hits the end of the horizontal runner the hammer effect will result in a pressure shock wave. This shock wave may be relieved through the down runner resulting in the separation of the melt stream. This could cause the splitting up seen after 0.16 s. No hard evidence can be identified to support this explanation due to the hidden flow. But it is striking that the melt stream in the down runner splits up at both runs of layout no. 6 and at none of the others. Hence some explanation must exist. In section 6 gating systems also with cross sections 10 mm wide has been used without the melt stream splitting up.

The upper part of the down runner is seen not to be filled completely during the first 0.88 s of the filling sequence, see Figure 5.37.

Too little area at the top of the down runner can give the problem. Until back pressure is build up the top cross section of the down runner can give a flow rate of 2.79 kg/s and the choke 2.54 kg/s. Calculated with Eq. 5.2 with no loses and with 50 mm metal head from the pouring basin. I.e. a safety margin of around 10 % is build into the system. This should be adequate to secure a completely filled cross section of the down runner especially when working with a pouring basin preventing a partly filled pouring cup.

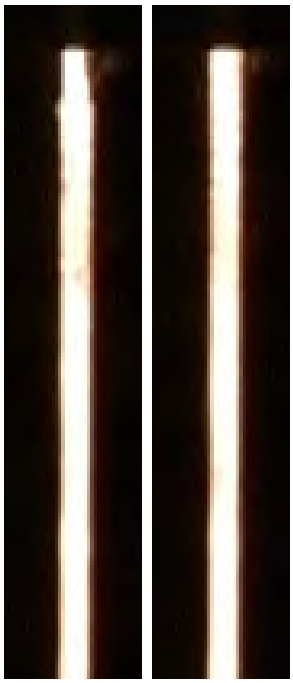

Figure 5.37 Upper part of the down runner at 0.80 and 0.88 s.

The reason for the partly filled cross section at the down runner during the first 0.88 s is more likely to be the transition from the horizontal extension of the pouring cup to the down runner. The transition is made as a 90 degree bend with fillets. I.e. the design is far from

stream lined. In section 5.2.5.1 a vena contracta at the top of the down runner was identified. The bend the melt had to pass through in section 5.2.5.1 was not as sharp as the one the melt has to pass through at this layout. Hence a vena contracta is most likely to be present at the top of the down runner. The vena contracta reduces the effective cross sectional area of the melt flow and hence acts as an artificial choke. Unfortunately the transition from the horizontal extension of the pouring cup to the down runner can not be captured on the video due to the top core. The results of the vena contracta a little down stream in the down runner can although be seen on Figure 5.37 as air pockets at the top of the down runner. To more strictly follow the basic idea of the layout with very stream lined runners, a redesign of the transition is needed. Going to the extreme a 90 degree bend made as a curve as done at the bottom of the down runner could be utilized. This has been done in section 6, where the results of it are discussed also.

When the melt passes through the ingate into the disc cavity at 0.48 s 2 droplets leaves the main melt front, 1 in each side of the ingate. This is seen at 0.52 and 0.56 s. The same was seen at run 1 just a little less pronounced.

The limited amount of splash shows the possibilities in this type of design. Adjustments to the geometry of the fan shaped transition from the runner to the plate shaped ingate are likely to be able to secure an initial filling of the disc cavity without braking up of the melt front.

The design used here must be seen as a first attempt. Further development of the transition is needed. Incorporating the design rules for dimensioning the fan shaped ingates used in high pressure die casting like done in [Ref. 5.12] would for sure be helpful.

The disadvantage of such transitions seems to be the relatively large distance below the disc cavity needed for the fan shaped transition compared to a standard plate shaped ingate connected to a horizontal runner. This results in lower mould face utilization, which of course also is an important parameter when securing the competitiveness of a foundry.

No dead ends exist in the gating system except for the horizontal extension of the pouring cup. This means that when the extension is filled up, the melt does not come to an abrupt stand still any where else in the gating system, and hence the main reason for getting a pressure shock wave does not exist. As described in section 4 the closing of air pockets in the gating system can also result in quite powerful pressure shock waves. Hence to be sure to avoid pressure shock waves it is also necessary to secure completely filled cross sections of the runners right from the first melt passing through. Systems with narrow runners like the one used here are well suitable for securing completely filled runners right from the first melt passing through. The problems seen here with the melt stream splitting up after 0.16 s are caused by a non stream lined design introducing a vena contracta at the top of the down runner.

The glass crack very late in the filling sequence at both runs, compared to what is seen at the other brake disc layouts, and compared to what is seen at the layouts for the plates discussed in section 4. This could be a coincidence but it could also indicate a filling sequence without pressure shock waves making the glass able to withstand the pressure and temperature for a longer time.

The fan shaped transition is giving a uniform melt distribution, and the friction in the 1.5 mm thick plate shaped ingate brake down the melt velocity. Together the two features are almost

able to prevent splashing when the melt enters the disc cavity. The initial melt velocity in the plate shaped ingate is 1890 mm/s when calculated without losses. This is more than 3 times what is found for layout no. 1 where heavy splashes shot into the disc cavity. The comparison to the other layouts will be done more closely in section 5.5.

5.2.6.2 Flow pattern in the disc cavity

The temperature distribution in the disc during the filling sequence shows indirectly the flow pattern in the disc cavity. Snapshots from the filling of the disc are showed below:

Time 2.72 Time 4.04 Time 5.40

Figure 5.38 Filling of the disc cavity in layout no. 6.

The temperature distribution in the disc during and after the filling is very symmetrical sidewise. It reflects a sidewise balanced flow pattern. This is also to be expected from the design of the gating system. In this layout the balance between the dynamic and braking forces is not controlling the sidewise distribution of the flow. For instance raising the velocity of the melt i.e. the dynamic forces and lowering the viscosity i.e. the braking forces would still result in a symmetrical filling of the disc cavity.

The geometry of the gating system described here is in that sense very restrictive compared to the other gating systems investigated in this section. The balance between the braking and dynamic forces plays an important rule at the other gating systems in controlling the melt distribution sidewise.

Going to extreme velocities in the gating system investigated here, a small vertical section has probably to be added before the fan shaped part, to prevent the melt from shooting through the bend and fan shaped section into the left side of the disc.

With restrictive gating systems one can also expect a larger ability to absorb minor variations in the pouring conditions, resulting in more uniform flow patterns from mould to mould. This will be more closely discussed in section 6.

5.2.6.3 Filling time

The total filling time of layout no. 6 is 5.70 s. As with layout no. 1 the top of the disc is hidden behind the top core. The end of the filling has been calculated in the same way as at layout no. 1. 0.3 s have been added for the filling of the pouring cup and the runner connected to

it in the same way as with layout no. 1. The filling of the disc starts after 0.48 s, i.e. the filling time for the disc is 4.92 s. The calculated filling time for the disc without losses is 2.45 s. This gives a total loss coefficient for the filling of the disc of 0.50.

5.3 Quality of the discs

First of all, the trials have been conducted in a test foundry; hence it has only been possible to produce a very limited number of discs with each layout. If a fair judgement of the quality supplied by the single layouts has to be made, longer series of say 100 discs with each layout has to be run.

The 6 layouts were poured in random order. The pattern plates were changed for each mould to make it possible to pour the mould string from one end.

The discs were inspected visually after they were shot blasted. No differences could be found between the 6 layouts at this stage.

The discs were machined on the brake faces to investigate whether inclusions were just below the surface. At one disc from 3 of the layouts an inclusion was revealed after the machining.

2 of the discs cast with each layout were x-rayed after machining. The errors found on the x-rays corresponded to the inclusions found in the surface after machining. The x-rays furthermore revealed some internal errors. But the errors revealed by x-ray were all found in the 5 first discs cast.

This could indicate slag in the melt during the pouring of the first moulds. As it is a small furnace and it is used for trials and not continuous production slag builds up at the lining. From time to time some of the slag on the lining starts to dissolve and is hence rejected into the melt. As the different layouts were poured in random order, the result showing only internal errors in the 5 first discs cast, indicates that the reason for the internal errors it not due to differences in the layouts but due to a unclean melt during the pouring of the first moulds.

From the data available it has not been possible to rank the quality of the discs from the different layouts, and hence it is not possible to give hard facts on the scrap levels generated by each layout.

5.4 Discussion of the initial filling of the gating systems

In practice only bottom filling gating systems are used for casting brake discs in vertically parted moulds. The initial filling of the gating system and disc cavity is the most difficult part of the filling sequence in bottom gated systems. This is due to the lack of back pressure at this part of the filling sequence. Hence the maximum amount of splashes and splitting up of the melt stream will be seen here. To avoid aspiration and hence the formation of excessive oxides completely filled runners are also wanted as early as possible in the filling sequence.

Different parameters can be used to judge the quality of the initial filling of the gating system. One way to do it is to compare when the down runner is completely filled. Ideally the cross

section of the down runner should be filled completely with the first melt passing through it. The down runners of the 6 gating systems are completely filled at the times given in Table 5.8 below:

Layout no.	1	2	3	4	5	6
Time until the down runner is 100 % filled [s]	0.44	5.16	0.60	0.96	>1.00	0.88

Table 5.8 Time until the cross section of the down runner is completely filled.

The times given are taken from the snapshots of the initial filling showed in the sections dedicated to each layout. Layout no. 2 gives an extremely high value due to the fact that it is a non pressurized system, designed to work with a partly filled down runner. The glass crackles at layout no. 5 making it impossible to give the exact time for the down runner to be completely filled.

The down runner of layout no. 1 is completely filled after 0.44 s. This is the shortest time seen for the 6 layouts. The transition from the pouring cup to the down runner at this layout is made very direct. No extension of the horizontal runner connected to the pouring cup past the top of the down runner has been used. Furthermore the cross sectional area of the top of the down runner is designed with a safety margin of 28 % calculated on the basis of the maximum flow rates through the cross sections at the top and bottom of the down runner. When only calculating the cross sectional areas at the top and at the bottom of the down runner and using a straight taper to reduce the area from the top to the bottom the cross sectional area in a 350 mm long down runner will be approximately 10 % too large on the middle as described in section 5.2.1.1.

Rapid filling of the down runner is furthermore often hampered by the appearance of a vena contracta at the top of the down runner. The vena contracta is reducing the effective cross sectional area of the melt flow and hence introducing an artificial choke. This is positively seen at layout no. 5 illustrated on Figure 5.32 and Figure 5.33. The result is seen to be a partly filled down runner for a large part of the filling sequence of this layout. Due to the top cores used at the other layouts only the result i.e. partly filled down runners can be seen. It is hence difficult positively to say whether the reason for the partly filled down runners is a vena contracta or a too small cross sectional area at the top not being able to compensate for the 10 % described above. When calculating the maximum flow rates through the top and bottom cross sections of the down runner at least part of the reason for the incompletely filled down runners turns out to be too small cross sectional areas at the top of the down runner. This means the partly filled down runners are probably caused by a combination of a vena contracta at the top of the down runner and generally too small cross sectional areas at the top of the down runner.

Very narrow runners are used at layout no. 6. The cross section of the runners is only 10 mm wide at the bottom of the runner at the pattern plate. The narrow runners promote obtaining completely filled cross sections from the first melt passing through. Unfortunately is the effect of the narrow runners used at layout no. 6 not seen clearly due to a less efficient design of the transition from the horizontal extension of the pouring cup to the top of the down runner. In section 6 different gating systems are shown where the effect of using narrow runners clearly can be seen.

Another way to judge the quality of the initial filling of the gating system is to judge the performance of the directional change made at the bottom at the down runner. The directional change is normally made with a down runner well. The directional change is one of the most difficult parts of a gating system if splashes are to be avoided, and a completely filled cross section of the horizontal runner is to be secured from the first melt passing through it.

At layout no. 3 and 4 is the directional change at the bottom of the down runner taken place in the core fixing the glass and hence it is not visible on the videos. The triangle shaped transition used in layout 2 in connection with a non pressurized system is not performing acceptable. A lot of melt is seen in the horizontal runner in front of the main melt front.

At layout no. 1 and 5 is a square shaped transition used. In both cases the performance is acceptable. Only a single droplet is seen in the horizontal runner in front of the main melt front at layout no. 5. No droplets enter the horizontal runner in front of the main melt front at layout no. 1. In both cases the cross section of the horizontal runner is close to be complete filled with the first melt passing through it.

The function of the well used at layout no. 3 can not be seen due to the core. But the cross section of the horizontal runner is seen to be filled almost completely with the first melt passing through it. Only a single droplet disengages from the main melt front. The well is made with lapping over the parting line both at the entrance and the exit of the well. The well is able to secure a almost completely filled cross section of the horizontal runner even though the area ratio between the horizontal runner and the choke is 3 which is the largest seen at the 6 layouts tested here.

The drawback of a square shaped well is the internal melt flow in the square block. The simulations shown in section 5.2.3.4 show the very chaotic flow in the well with a lot of turbulence. Furthermore a vena contracta can be expected at underside of the horizontal runner where it connects to the well as shown on Figure 5.6. Even though good at securing a completely filled cross section of the horizontal runner, for instance when comparing to a cylinder shaped down runner well it is not perfect at doing so.

At layout no. 6 the directional change is made with a curved section instead of a sharp directional change as is used at the other layouts. Unfortunately the performance of the curved directional change is not clearly seen due to splitting up of the melt stream early in the filling sequence. Similar directional changes are used in section 6 with good success. The disadvantage with this type of directional change is the lack of ability to significantly reduce the velocity of the metal. At layout no. 3 for instance is the area ratio between the horizontal runner and the choke around 3 resulting in a corresponding reduction in velocity. On the other hand is the curved shaped directional change superior in securing a smooth flow through the directional change when compared to what takes place in a square shaped well.

Summing up on the directional change from the down runner to the horizontal runner it can be said that the square shaped down runner wells are good at preventing melt from entering the horizontal runner before the main melt stream and they are able to give an almost completely filled cross section of the horizontal runner with the first melt passing through. Even though an area ratio of up to 3 between the horizontal runner and the choke is used a square shaped well is able to secure an almost completely filled cross section of the horizontal runner from the first melt passing through. Hence it is a good at reducing the melt velocity also. The draw-

back of a square shaped well is the internal flow in the block shaped geometry. The performance of the curved transition can not be fairly judged here but it has proven its qualities in section 6. It is although not able to reduce the velocity of the melt as the square shaped transition is.

5.5 Discussion of the initial filling of the disc cavities

When looking at the initial filling of the disc cavities at the layouts investigated here, the critical part of the filling sequence is the initial part. This is due to the fact that no back pressure exists during the initial part of the filling. When a little back pressure from melt in the disc cavity has been build up, the flow is calm in all the investigated cases. The way the gating system fills is of course also essential, this part of the filling sequence has been discussed in the previous section. Snapshots from the initial filling of the disc cavities showing the maximum amount of splash generated at each layout can be seen on Figure 5.39.

Layout no. 1 Time 0.80 s Layout no. 2 Time 0.96 s Layout no. 3 Time 0.84 s

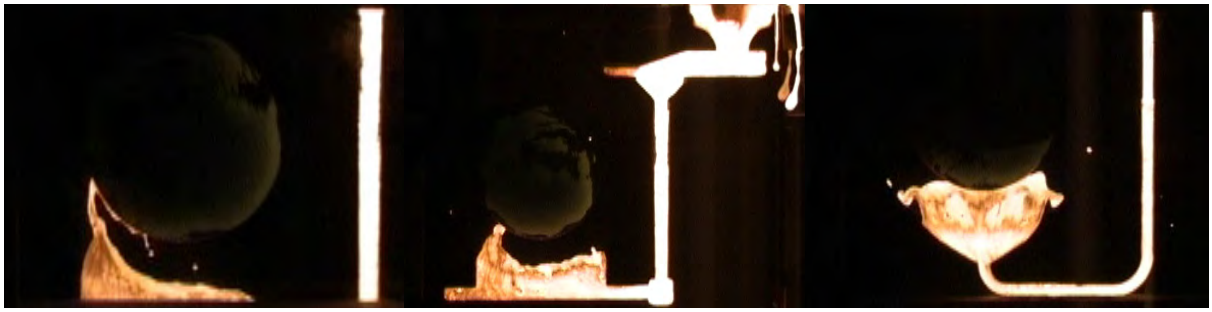

Layout no. 4 Time 0.64 s Layout no. 5 Time 0.96 s Layout no. 6 Time 0.60 s

Figure 5.39 Maximum splashes during filling of the 6 layouts.

Droplets leaving the main melt front are seen at layout no. 1, 3, 4, and 6. In layout no. 5 only a single melt droplet leaves the main melt front and enters the disc cavity on its own. The melt front in layout no. 5 is though very close to break up into several droplets.

All systems except layout no. 2 are depressurized systems [Ref. 5.8] having the flow rate controlling area at the bottom of the down runner. Layout no. 2 is having the flow rate controlling area at the top of the down runner; hence it is a non pressurized system [Ref. 5.8]. This can first of all be seen if the maximum flow rates through the different cross sections of the gating system are calculated and secondly be seen from the snapshots of the filling showing a partly filled down runner until very late in the filling sequence. The non pressurized system leads to

a relatively calm initial filling of the disc cavity when compared to the other layouts. The non pressurized layout is the only gating system not giving splashes during the initial filling of the disc. The drawbacks of a non pressurized system are the partly filled runners giving the basis for aspiration, and the large runners resulting in a low yield.

The total filling times of the different layouts and key velocities are showed in Table 5.9.

Layout no.	1	2	3	4	5	6
Total measured filling time of the layout [s]	6.18	5.46	6.26	5.56	5.48	5.70
Measured filling time for the disc cavity [s]	5.04	4.04	5.16	4.36	4.60	4.92
Initial velocity in horizontal runner [mm/s] *	1527	524	877	1344	1344	1542
Initial velocity in the ingate [mm/s] *	555	509	869	1251	1251	1890
Mean velocity in horizontal runner [mm/s]+	735	362	359	555	526	605
Mean velocity in the ingate [mm/s]+	267	352	356	516	489	741

Table 5.9 Total filling times and key velocities.

Values marked with * in Table 5.9 are theoretical values calculated without losses. This is done because the horizontal runners are not visible on all the layouts hence it is not possible to get measured values from all layouts for comparing the different designs. As later is shown in section 5.8 the loss coefficients for all the gating systems are comparable. This indicates that the relative sizes between the velocities calculated without losses and the relative sizes between the real velocities are close to the same. I.e. if the velocity calculated without losses is large compared to the other layouts, the real velocity can be expected to be large compared to the other layouts also.

Values marked with + in Table 5.9 are calculated from the measured filling times of the disc cavity and the areas of the corresponding gating system.

When comparing the flow velocities and the corresponding splashes for the different layouts several things need to be commented:

Except for layout no. 6 are all layouts designed with a plate shaped ingate connected to a horizontal runner. I.e. they are conventional layouts. In the 5 cases with a plate shaped ingate connected to at horizontal runner the first melt entering into the disc cavity enters at the far end of the horizontal runner, this means in the direction of the flow. Several designs have been used which normally are seen to be helpful in giving a sidewise balanced filling. The designs include tings like gradually reduction of the cross section area of the horizontal runner towards the end, an overlap between the horizontal runner and the plate shaped ingate, quite large area ratios between the horizontal runner and the choke and finally a depressurized gating system has also been utilized. None of the used designs can prevent the first melt entering into the disc cavity from entering at the far end of the horizontal runner due to the direction of the melt flow. From the conventional layouts only the non pressurized system results in flow not giving droplets disengaging from the main melt front. Still a clear effect from the direction of the flow in the horizontal runner is seen at this layout also to.

The reason for the initial melt entering at the far end of the horizontal runner into the disc cavity is not only the direction of the melt flow in the horizontal runner. Both the conventional depressurized systems and the conventional non pressurized system have a dead end in the ga-

ting system at the end of the horizontal runner. In the case of pressure shock waves occurring when the melt hits the end of the horizontal runner, the first melt entering the disc is also promoted to enter the disc at the far end of the horizontal runner as the pressure is relieved as close a possible to the place where the pressure shock wave is initiated. The effect from a pressure shock wave is explosive, as the dynamic pressure almost instantaneously is converted into static pressure. The dynamic pressure is given by [Ref. 5.11]:

$$P_{Dynamic} = 1/2 \cdot \rho \cdot v^2 \qquad \text{[Eq. 5.5]}$$

Hence it is strongly depending on the velocity. The melt hitting the end of the runners is not the only source for getting pressure shock waves. As shown in section 4 with the thin walled plates, the closing of air pockets in the runners are also able to generate pressure shock waves. The generation of pressure shock waves from the closing of air pockets in the runners has not been observed in the trials described in this section. The explanation for this difference could be the better performing down runner wells used here compared to the well used at section 4. The better performing wells reduce the appearance of air pockets in the runners and hence also reduce the risk of getting pressure shock waves from the closing of them.

From the amount of droplets blown into the disc cavity at the different layouts seen at Figure 5.39 it looks like pressure shock waves exist at layout no. 1, 3 and 4.

At layout no. 1 the highest velocities in the horizontal runner are seen. This combined with a completely filled cross section of the horizontal runner is a good basis for getting a powerful pressure shock wave. Droplets are seen to be blown very vigorously into the disc cavity clearly indicating a pressure shock wave.

The velocity in the horizontal runner of layout no. 3 is 0.36 m/s i.e. only around half the velocity seen at layout no. 1. The down runner well used at layout no. 3 is able to secure a completely filled cross section of the horizontal runner behind the melt front before the melt hits the end of the runner. This combined with no attempts to reduce the velocity gradually results in a somewhat explosive entrance of the first melt into the disc cavity much in the same way as seen at layout no. 1. The result is droplets being blown around in the disc cavity. This indicates the appearance of a pressure shock wave even at relatively low velocities in the horizontal runner.

The velocity in the horizontal runner at layout no. 4 when the melt hits the end of the runner is hard to judge as the runner cross section is tapered down over the width of the plate shaped ingate. As discussed in section 5.2.4.1 two effects from the reduced cross sectional area can be identified. The reduced cross sectional area will mean extra friction and hence reduce the velocity. On the other hand reducing the cross sectional area will mean higher velocities due to the smaller cross section. The balance between the two effects controls whether the velocity increases or decreases. Rather powerful splashes shooting into the disc cavity are seen in Figure 5.39 indicating that they are caused by a pressure shock wave. The lapping over the parting line between the horizontal runner and the plate shaped ingate is probably able to prevent the melt from entering into the plate shaped ingate before the melt hits the end of the horizontal runner. Hence the velocity in the horizontal runner has not been reduced when the melt reaches the end of the runner and the hammer effect takes place.

At layout no. 5 which is the same as layout no. 4 except for the overlaps, is the initial flow into the disc cavity much calmer. The initial flow at layout no. 5 does not split up as seen at layout no. 4. From the snapshots of the filling of layout no. 5 is the melt seen to enter into the plate shaped ingate before it reaches the end of the horizontal runner. Hence some of the velocity is taken out of the melt before it reaches the end of the horizontal runner resulting in less splashes. The reason for the melt entering into the plate shaped ingate at layout no. 5 and not at layout no. 4 is discussed in section 5.2.5.1. The overlap is believed to act as a physical barrier for the initial melt. When the flow is established the overlap has only minor influence on the flow.

As described above, the cross section of the horizontal runner at layout no. 4 and 5 has been reduced gradually over the width of the plate shaped ingate. The design is intended to gradually reduce the melt velocity before it hits the end of the horizontal runner and for giving a sidewise more balanced flow into the casting cavity. At layout no. 4 is the gradually reduced horizontal runner combined with lapping over the parting line from the horizontal runner to the plate shaped ingate. Even though this is done is the initial filling far from under control. The results are a little better when the gradually reduced horizontal runner is connected to the plate shaped ingate without lapping over the parting line. From the trials made here it is difficult to give a final conclusion on the effect from a gradually reduced horizontal runner. As it is a design feature used very often in practice and as the effects are questionable as showed here closer examination is needed. Interesting trials can be made if the same layout is cast with and without a gradual reduction of the cross section of the horizontal runner. This will directly show the influence of gradually reducing the horizontal runner on the flow patterns.

The highest velocities in the ingate both calculated without losses and measured are found at the non conventional layout no. 6. But when looking at Figure 5.39 and comparing the maximum amount of splashes seen at the different layouts, layout no. 6 does not give the largest amount of splashes. If the layouts have to be ranked according to the amount of splashes generated, layout no. 6 would be somewhere in the better half behind no. 2 and maybe behind no. 5. The filling time of layout no. 6 is close to the filling times found for the other layouts. Hence no effect from this aspect can be expected. When comparing layout no.1 and no. 6 is the velocity in the ingate around 3 times larger at layout no. 6 than at layout no. 1, both when comparing initial and mean velocities. The velocities in the horizontal runners are very similar for the two layouts. The velocity in the ingate in layout no. 1 is very low compared to layout no. 6. In spite of that layout no. 1 generates a lot of splashes shooting into the disc cavity while the initial filling of the disc cavity at layout no. 6 is done almost without splashes. This can be seen on Figure 5.39. The main reason for the melt being blown into the disc cavity at layout no. 1 and not at layout no. 6 is the presence of a dead end at the end of the horizontal runner at layout no. 1 resulting in a very powerful shock wave.

This shows very clearly that it is not enough to (try to) keep the velocities down to obtain a calm filling with coherent melt fronts. It is very important also to avoid pressure shock waves as they are the reason for the splashes for instance seen at layout no. 1. This is in contrast to normal practice when designing gating systems for calm flow. Normally only velocity criterions are used to secure a calm flow, as for instance is seen in [Ref. 5.8] and [Ref. 5.9]. The results described here show the importance of also avoiding pressure shock waves. Pressure shock waves are first and foremost initiated by dead ends in the gating system. Hence they have to be avoided if pressure shock waves are to be avoided. As seen in section 4 can the closing of air pockets in the runners also result in pressure shock waves, hence completely fil-

led runners are also needed. Furthermore is it important to secure as uniform velocities over the cross section as possible to avoid local high velocities. If this is done, relatively high velocities can be allowed while still getting an acceptable coherent melt flow as seen with layout no. 6.

Layout no. 6 is designed without dead ends in the gating system below the pouring cup. This means if the runners are completely filled from the first melt passing through there is no basis for getting pressure shock waves. Two droplets are seen to have disengaged from the main melt front otherwise is the melt front coherent. As mentioned in section 5.2.6.1 the design of the fan shaped transition from the runner to the plate shaped ingate is to be seen as a first attempt. If the design rules used for designing fan shaped ingates normally used in high pressure die casting are used for optimizing the fan used here, the droplets disengaging from the main melt front can probably be avoided [Ref. 5.12]. Further development has to be done in this direction.

The quality demands for brake discs vary from end user to end user. But generally seen has the quality demands increased significantly over the last 10 years. After the disc has been machined the smallest pinpoint mark on the brake face can nowadays mean a scrapped disc. Hence it is very important to control the amount of inclusions. This means first of all reducing the slag particles in the poured melt. Secondly the generation of slag and other non solvable particles during the metal flow through the gating system has to be minimized. This can only be done by securing coherent melt fronts and completely filled cross sections of the runners with the first melt passing through. Especially splashes shooting droplets in front of the main melt front have to be avoided. The turbulence of the flow has to be reduced also as it can result in inclusion, for instance due to sand erosion. Hence it is important to have good control over the flow in the gating system, or at least be well aware of how the flow takes place in the gating system.

For instance, at layout no. 1 inclusions at the top of the disc can be a problem due to the droplets being blown into the disc cavity. The droplets can end up at the top of the core giving the inside shape of the hat geometry. If the droplets are not remelted when the main melt front arrives or if they stick to the mould wall shaping the brake face they will result in inclusions. But getting problems at the brake face at the upper part of the disc and realising that they are caused by the design of the horizontal runner is hard if not impossible without information of the same type as generated by the trials described in this section.

When producing castings on a modern moulding machine for vertically parted moulds the available time for pouring in the machine cycle is as low as 5.5 s when producing with maximum capacity [Ref. 5.7]. I.e. the filling times seen here are on the high side of what is permissible if the moulding machine is not going to be slowed down. This means the splashes seen on the snapshots on Figure 5.39 are not due to unrealistically low pouring times. The competition on the market for discs is very hard meaning very low prizes. To be able to earn money on production of discs a very high production rate is hence normally needed.

Summing up on the initial filling of the gating system it can be said that it is very difficult to avoid splashes shooting into the disc cavity with a conventional gating system. From the conventional gating systems a non pressurized system leads to the calmest initial filling of the disc cavity. A non conventional gating system designed with gating techniques developed for aluminium shows some very promising results, but further development is needed.

5.6 Discussion of the flow patterns in the disc cavity

The final heat distributions in the discs can be seen below:

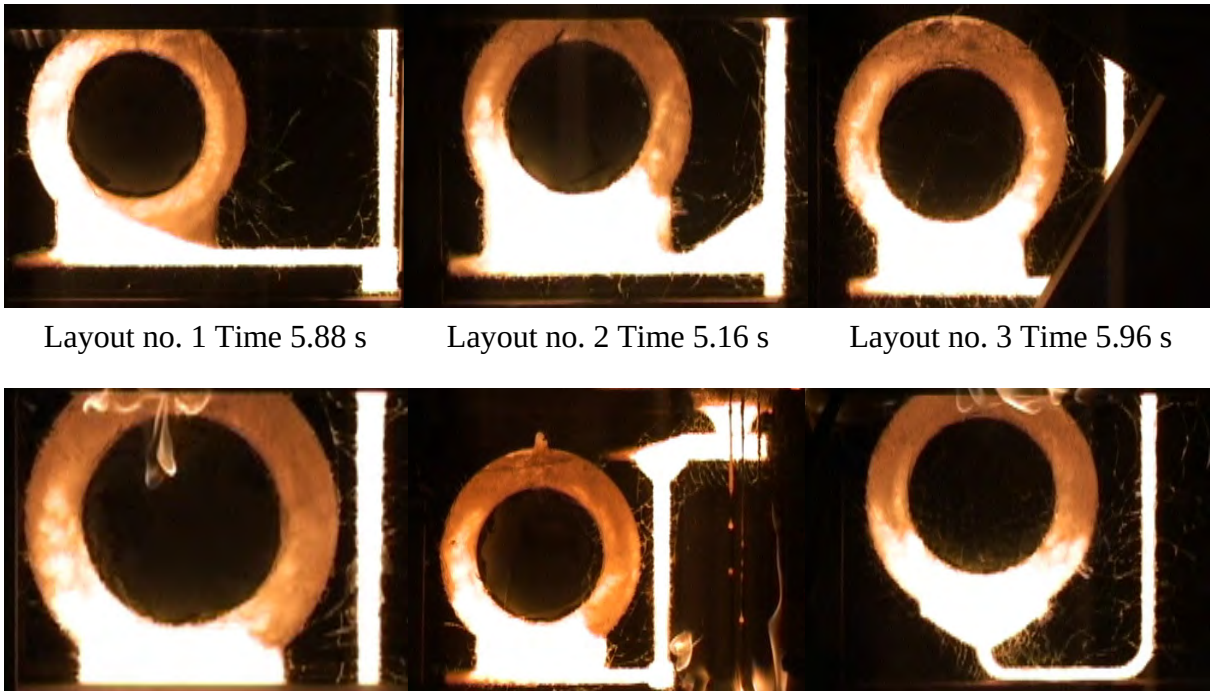

Layout no. 1 Time 5.88 s Layout no. 2 Time 5.16 s Layout no. 3 Time 5.96 s

Layout no. 4 Time 4.96 s Layout no. 5 Time 5.48 s Layout no. 6 Time 5.40 s

Figure 5.40 Final heat distributions in the 6 layouts.

The heat distributions in the discs at the end of the filling are seen to be very different. The heat distributions indirectly show the preferred flow paths during the filling of the disc cavity.

Due to the velocity of the melt it contains dynamic forces. The dynamic forces are counter acted by friction forces etc. acting as braking forces in the system. The designs of layout no. 1 to 5 are seen to be very similar, they all use a plate shaped ingate connected to a horizontal runner. This design of the gating system puts relatively few restrictions on the flow in the sense that the relative sizes of the dynamic and braking forces in the system plays an important role in deciding where the main flow takes place. I.e. whether the filling of the disc is balanced sidewise or for instance the main flow into the disc takes place at the far end of the horizontal runner as is the case for layout no. 1. It is of course not randomly determined whether the flow is balanced sidewise or not, the balance between the dynamic and braking forces strictly controls the flow. As showed in section 4, is the reproducibility of the main flow patterns very good. The problem is, that the balance between the dynamic and braking forces is very hard to predict for the casting engineer. No well documented rules exist for manually calculating the sidewise flow distribution as a function of velocity and geometry. On the other hand simulation can determine the sidewise distribution of the main melt flow as shown in section 5.2.3.4.

Compared to the other layouts, layout no. 6 has a fan shaped transition from the runner to the plate shaped ingate. This geometry restricts the flow much more than the design used at the other layouts. The design forces the flow to be very symmetrical. The result is very predictable flow patterns, putting the casting engineer in control of the flow patterns.

The expected symmetrical heat distribution of layout no. 6 and the more or less unsymmetrical and difficult to predict heat distributions of the other layouts are clearly seen on Figure 5.40.

The mean melt flow velocities in the horizontal runner during the filling of the discs are showed in Table 5.10 below:

Layout no.	1	2	3	4	5	6
Measured filling time of disc [s]	5.04	4.04	5.16	4.36	4.60	4.92
Area horizontal of runner [mm^2]	192	486	384	294	294	**
Shape of horizontal runner [mm]	8/16/16	9/18/36	8/16/32	7/14/28	7/14/28	**
Mean melt velocity [mm/s]*	735	362	359	555***	526***	**

Table 5.10 Mean melt velocities in the horizontal runners during filling of the disc.

* The velocity has been calculated from the measured filling time of the disc, the cross sectional area of the horizontal runner and the volume of the disc.

** No values have been given for layout no. 6 as this layout is basically designed differently than the others. The mean melt velocity after the choke is 1087 mm/s. After the increase of the cross section of the horizontal runner is the mean melt velocity 605 mm/s at the entrance to the fan shaped transition assuming completely filled runner cross sections.

*** Based on the area of the horizontal runner before it is gradually reduced.

The highest velocity in the horizontal runner is seen at layout no. 1. This is reflected in the most unbalanced temperature distribution sidewise in the disc cavity seen at the 6 layouts. And hence it indirectly means the most unbalanced flow sidewise at the 6 layouts.

The lowest flow velocities in the horizontal runner are seen in layout no. 2 and 3, both having mean flow velocities around 360 mm/s. The temperature profiles in the discs and hence also the flow patters are sidewise balanced to almost the same degree in the 2 layouts. It is the sidewise most balanced patterns seen when not taken the non conventional layout no. 6 into account.

The flow velocities in the horizontal runner, of layout no. 4 and 5 are close to each other. The flow velocities in the horizontal runners before they are gradually reduced are somewhere between the velocities for layout no. 1 and layout no. 2 / 3. The resulting flow is balanced to a degree between layout no. 1 and layout no. 2 / 3. In layout no. 4 and 5 it has been tried to balance the flow by gradually reducing the cross sectional area of the horizontal runner, drawings of the layouts can be seen in Appendix 5.4 and Appendix 5.5. But from the degree to which the flow is balanced compared to the velocities before the reduction it does not seem to have the wanted effect on the flow. The cross sectional area is reduced from 294 mm^2 to 80 mm^2 over the width of the plate shaped ingate, i.e. a 73 % reduction in cross sectional area. If the flow is going to be balanced the cross section has to be reduced even more. Unfortunately time did not allow it, but it would have been very interesting to see the impact on the flow if the trials were repeated without the reduction of the horizontal runner and with an even larger reduction of the runner.

Different ways have been used to balance the flow sidewise at the conventional layouts. And good results have been obtained. One has although to remember that when using bottom filling gating systems a significant temperature difference between top and bottom will exist, as also clearly is seen on Figure 5.40. Hence no matter how balanced the sidewise temperature distribution is; the difference between top and bottom will still exist. This means it is not crucial to create a completely sidewise balanced temperature distribution as the top to bottom distribution will still be there. It is more important to have the focus on securing a calm initial filling of the gating system and the disc cavity without breaking up of the melt surface. In the cases where a feeder is needed is it often placed at the top of the disc, in such cases it is helpful to have a reasonable sidewise balanced temperature distribution for obtaining symmetry.

On the other hand in the cases where the feeder is placed at the side of the disc, an asymmetrical heat distribution introduced by the filling, as the one seen at layout no. 1, can promote the feeding capability of the casting. If the feeder is attached to the hot side of the disc an initial directional temperature distribution towards the feeder is secured through the filling. I.e. good starting conditions for the feeding of the casting have been established. This way of designing a feeder for a disc is probably more relevant for the casting of aluminium discs where a feeder under all circumstances is needed.

Summing up on the degree to which the flow is balanced sidewise it can be said that the degree to which the flow is balanced is directly connected to the flow velocity in the horizontal runner for the conventional layouts investigated here. The distribution of the melt sidewise is hence in the conventional gating systems to a large degree controlled by the difficult to predict balance between dynamic and braking forces in the gating system. In the non conventional layout no. 6, the distribution of the melt sidewise is on the contrary strictly controlled by the geometry of the runners and not relying on the balance between dynamic and braking forces. This makes the flow patterns predictable for the casting engineer. The gradual reduction of the cross sectional area of the horizontal runner used at layout no. 4 and 5 seems not to influence the flow patterns in the wanted direction. More trials have though to be made to investigate the impact on the flow from gradually reduced horizontal runners before final conclusions can be made about the effects on the flow patterns.

5.7 Discussion of the loss coefficients and filling times

The loss coefficient for the filling of the disc cavity for the 6 different layouts can be seen in Table 5.11 together with different key figures describing the gating systems.

Layout no.	1	2	3	4	5	6
Loss coefficients for filling of the disc cavity	0.60	0.69	0.50	0.51	0.48	0.50
Thickness of the ingate [mm]	3.0	2.5	2.5	2.0	2.0	1.5
Cross section area of the ingate [mm^2]	528	500	388	316	316	195
Perimeter of the ingate [mm]	358	405	315	320	320	263
Filling time of the disc cavity [s]*	5.04	4.04	5.16	4.36	4.60	4.92
Total filling time of the layout [s]*	6.2	5.5	6.3	5.6	5.5	5.7
Mean velocity in the ingate [mm/s]**	267	352	356	516	489	741
Mean velocity in horizontal runner [mm/s]**	735	362	359	555	526	605
Mean melt flow in the ingate [kg/s]**	0.97	1.21	0.95	1.12	1.07	1.00

Table 5.11 Comparison of loss coefficients.

* Measured values
** Based on the measured filling time of the disc cavity, cross sectional areas of the runners and the volume of the disc.

The loss coefficients are calculated from the ratio between the calculated filling time for the disc cavity found without losses with Eq. 5.3 and the measured filling time for the disc cavity. I.e. it is a total loss coefficient containing all contributions to the losses in the complete gating system like wall friction, flow resistance at directional changes, back pressure due to surface tension etc. The loss coefficient is based on the cross sectional area of the choke. At depressurized systems where the cross sectional area is opened up after the choke the loss in the system after the choke will be relatively small.

The loss coefficients are seen to be similar for all the layouts except for layout no. 1 and no. 2. Layout no. 2 is a non pressurized gating system while the others are depressurized systems. In a non pressurized system a significant part of the gating system is only partly filled during a large part of the filling sequence. Due to the partly filled runners at the non pressurized system the wall friction will not have the same significant influence on the losses as at the other systems. Hence lower losses can be expected at non pressurized systems resulting in a larger numerical value of the loss coefficient.

Looking at the loss coefficients of the depressurized layouts only the loss coefficient for layout no. 1 is different from the others. The 4 other layouts have loss coefficients of 0.5 or very close to 0.5. The loss coefficients of the 4 layouts are very similar even though the thicknesses of the plate shaped ingates vary from 1.5 to 2.5 mm, and the mean melt velocities in the plate shaped ingates vary from 356 to 741 mm/s for the filling of the disc cavities.

The parameters like cross sectional area of the ingate, thickness of the ingate, perimeter of the gate and mean velocity in the ingate vary quite a lot and do not reflect the uniformity of the total loss coefficients for the 4 above mentioned depressurized layouts.

Larger differences between the 4 loss coefficients were expected having the quite different designs in mind resulting in quite different velocities in the ingates and the horizontal runners. But at all layouts a straight down runner with gradually reduced cross sectional area is used. The cross sectional area at the bottom of the down runner is in all cases controlling the flow

rate. Apart from being the flow rate controlling cross section, the bottom cross section of the down runner is also the cross section where the maximum velocities are found.

A gating system similar to the depressurized gating systems used here is investigated in section 2.6. In section 2.6 expressions describing the losses coming from the different parts of the gating system have been showed. With the aid of these expressions it has been possible to identify the significant contributions to the total loss in the gating system. Both the gating system described in section 2.6 and the depressurized gating systems described in this section include a vertical down runner, the flow rate in the layout is controlled by the cross section at the bottom of the down runner, a directional change at the bottom of the down runner, a straight horizontal runner and a transition to a plate shaped geometry. Hence the gating system investigated in section 2.6 is very similar to the depressurized gating systems described in this section. The loss coming from the down runner at the layout investigated in section 2.6 is found to be approximately 70 % of the total losses. With the similarities between the layout the 70 % is found for, and the layouts investigated in this section, it is reasonable to expect also around 70 % of the total losses to come from the down runners at the layouts described in this section.

Approximately 70 % of the total loss in this conventional type of gating system investigated here is coming from the down runner. Hence making changes to the rest of the gating system will have a relatively low influence on the total loss. Due to this the loss coefficients can be very similar even though the rest of the gating system as for instance the thicknesses of the ingate and velocity in the ingates differ quite a lot.

Layout no. 1 has a little higher loss coefficient than the 4 other depressurized layouts, i.e. the loss in this gating system is lower than in the others. This is likely to be due to the relatively large safety margin used for calculating the top cross section of the down runner helping in obtaining a completely filled down runner very fast. The fastest filling time of the down runner is seen at layout no. 1. The full metal head will only act on the system when the down runner is completely filled. This means if for some reason the upper part of the down runner is only partly filled, the filling time will be prolonged resulting in a seemingly higher loss coefficient for the system. The loss coefficient is found by comparing the theoretical filling time calculated on the basis of the full metal head without losses with the measured filling time.

At layout no. 1 a relatively thick plate ingate (3 mm) has been used. This combined with a relatively low mean velocity in the plate ingate during the filling of the disc will also decrease the losses in the system. This can for instance be seen by comparing to layout no. 6 where a very thin ingate with a high mean velocity has been used. Assuming turbulent flow in the plate shaped ingates at both layouts, Eq. 2.30 and Eq. 2.31 can be used estimate the losses in the ingates. For layout no. 1 the pressure loss in the plate shaped ingate is found to 57 Pa, for layout no. 6 it is found to 549 Pa. Both are calculated on the basis of the mean velocities through the ingate during the filling of the disc cavity. Almost a factor of 10 differ the two figures. Eq. 2.48 can be used to calculate the total pressure loss in the system at different stages of the filling if the corresponding velocities and areas are known. When the disc cavity is 50 % full the total loss is found to be around 19.7 kPa for all layouts. The velocity of the melt when the disc is 50 % full is found on the basis of the measured filling time of the disc cavity, the volume of the disc and the cross sectional area at the middle of the disc. Even though the 549 Pa found for layout no. 6 is around 10 times the value for layout no. 1, it is still insignificant when comparing to the total loss in the system.

The filling times for the 6 layouts are seen to be in the range 5.5 to 6.3 s i.e. they are quite similar. The relatively small variation in filling times does not lead to any conclusions about the differences between the layouts based on a difference in the filling time. As mentioned in section 5.5 is the time available for pouring in the machine cycle as low as 5.5 s when running with maximum speed on modern moulding machines producing vertically parted moulds. I.e. the filling times found here are a little on the high side. On the other hand the filling times are only exceeding 5.5 s marginally. If all the layouts have to be adjusted to give a filling time of 5.5 s no significant changes to the flow patterns can be expected due to the small deviations from the 5.5 s. Actually no changes have been made on any of the layouts to adjust the total pouring time. In that sense the filling times must be said to be calculated precisely during the design of the layouts.

5.8 Discussion of the yield at the different layouts

When designing gating systems, getting the melt into the casting cavity in the best possible way seen from a flow point of view is not the only ruling factor. Another very important factor is the yield, i.e. how much metal is used for the gating system and the feeders as this has to be handled in the foundry, remelted, reconditioned with alloying elements, inoculated etc. before it can be poured into another mould. The competition on the casting market is very hard. One way to increase the competitiveness of a foundry is to increase the yield. With the increasing focus on the use of resources, and the increasing world market prizes on raw materials the yield aspect is getting even more important in the future.

The yields of the different layouts have been listed in Table 5.12 below.

Layout no.	1	2	3	4	5	6
Total mass [kg]	7.90	9.40*	7.78	7.66	7.39	7.76
Mass of the gating system [kg]	3.00	4.50*	2.88	2.76	2.49	2.86
Yield [%]	62	52*	63	64	66	63

Table 5.12 Comparison of yields.

* In layout no. 2 a feeder has been used. The need for at feeder is depending on the metallurgical quality and the ability of the gating system to feed the liquid shrinkages. The layouts have all been cast from the same melt, assuming the metal quality is sufficient to produce sound discs without feeders. Hence it is fair to remove the feeder from layout no. 2 when calculating the yield for comparison with the other layouts. This has been done in Table 5.12.

From Table 5.12 the yield is seen to be rather constant. It is between 62 % and 66 % for all the layouts except for layout no. 2 having a yield of 52 %. The gating system in layout no. 2 is a non pressurized system while the others are depressurized systems. The impact on the yield is clearly seen, the yield is around 10 % points lower for the non pressurized system when compared to the depressurized systems. From section 5.5, the initial filling of the disc is seen to be very calm at the non pressurized system compared to the depressurized systems. On the other hand the runners are not kept full in the non pressurized system for instance giving the basis for aspiration during the filling sequence. I.e. pro’s and con’s exist for both types of systems. In practice variations of the depressurized system are the most used at the moment.

Even though the yields are relatively equal for the depressurized layouts the differences in the yields are important. Due to the very hard competition on the brake disc market, will raising the yield only a few % points result in a relatively large increase in the total overhead. When producing discs very long series are normally made. This also makes it extra feasible to optimize the layouts.

When producing discs in vertically parted moulds the yield can be higher than the 62 - 66 % seen here. Normally brake discs are produced on moulding machines giving larger mould faces than the 500 mm x 400 mm used for the trials described here. A popular moulding machine for producing brake discs is the DISA 230 X with a mould face size of 750 mm x 535 mm. At least two discs can be produced in each mould even when going to the largest discs used for passenger cars. This means for instance only one pouring cup is needed for the pouring of 2 or more discs, this optimizes the yield making it possible to reach values of around 75 %.

When describing the yield of a gating system and hence the amount of iron going to be remelted, it is not fair only to look at the yield directly coming from the gating system. When optimizing the yield of a gating system i.e. reducing the size of the gating system and the feeders, the scrap rate will start to go up at some point. Meaning the sum of runners, feeders and the scrap all going to be remelted is the parameter to be optimized and not only the yield. The value of scraped castings is higher than the value of runners due to the fettling cost, machining costs etc. spent before the casting is scrapped.

The trials have been made in a test foundry without the possibility to run longer series, hence very limited numbers of discs have been produced with each layout. This makes it impossible to give a figure for the scrap levels for the different layouts. But from the videos of the filling sequences some idea about the relative sizes of the 6 scrap levels can be estimated. For instance, at layout no. 1 is a powerful fountain at the initial filling of the disc seen. This means probably a relatively large scrap level for this layout due to inclusions.

5.9 Conclusions

Approximately 300 million brake discs are cast worldwide every year. A large part of them are cast in vertically parted moulds. Even though such high production numbers world wide are encountered many different ways to gate brake discs cast in vertically parted moulds are used. An important step in obtaining good quality of the discs is to secure good mould filling. The mould filling of brake discs cast in vertically parted moulds has been investigated in this section.

6 different layouts for the same brake disc have been tested. 5 of them are conventional layouts and 1 is a non conventional layout designed with gating techniques developed for aluminium. The technique with replacing a part of or a complete mould half with glass plates has been used to investigate the mould filling at the 6 layouts. In this way videos of the real filling sequences have been made. The technique has proven to give very useful information about the metal flow in the mould cavities.

From the experiments the following can be concluded:

- Due to the velocity of the melt, it contains dynamic forces. Forces from wall friction etc. tries to counter act the dynamic forces; i.e. they act as braking forces. In conventional gating systems, as for instance seen in layout no. 1 to 5 investigated here the balance between the dynamic forces and the counter acting braking forces have a large influence on the flow patterns. I.e. the geometry of the gating system is not restrictive enough to solely control the flow patterns.

- When the balance between dynamic and braking forces plays an important role in controlling the flow patterns, the patterns are difficult to predict for the casting engineer. This is typically seen at designs with a wide plate shaped ingate connected to a horizontal runner.

- Systems giving better control over the melt flow not letting the relative sizes of the dynamic and braking forces have large influence on the flow patterns can be made. This is demonstrated with layout no. 6. This type of gating system is very restrictive in the sense that the balance between the dynamic and braking forces only has very limited influence on the flow patterns. The flow patterns are to a very large degree controlled by the geometry of the gating system. Hence the casting engineer can easily predict them.

- In practice only bottom filling gating systems are used for casting discs in vertically parted moulds. I.e. the initial filling of the disc cavity is the difficult part as no back pressure exists. Once a few centimetres of melt are in the disc cavity the melt flow becomes calm almost no matter how the gating system is designed. In conventional depressurized gating systems it is very difficult to avoid some splashes shooting into the disc cavity during the initial part of the filling. I.e. before back pressure has been build up.

- Using a non pressurized gating system results in a calmer initial filling of the disc cavity when comparing to depressurized systems. Unfortunately non pressurized gating systems have several drawbacks. The drawbacks are things such as partly filled runners during most of the filling sequence giving the basis for aspiration and low yields when compared to depressurized systems.

- Both the conventional depressurized systems and the non pressurized system have a dead end in the gating system at the end of the horizontal runner. When the melt hits the end of the horizontal runner, the hammer effect results in a pressure shock wave. Depending of the velocity of the melt the shock wave is able to blow metal droplets far into the disc cavity as for instance is seen at layout no. 1.

- The non conventional depressurized layout no. 6 does not have dead ends in the gating system below the pouring cup. I.e. the basis for getting pressure shock waves does not exist as long as the runners are completely filled. When comparing to the other layouts the flow is seen to be relatively calm especially when having the high velocities seen in the ingate in mind.

- The fan shaped transition from the runner to the plate shaped ingate used at layout no. 6 leads to a very uniform velocity distribution sidewise in the plate shaped ingate. The fan shaped transition also helps to reduce splashes shooting into the disc cavity at the

initial filling. If the design rules used for designing fan shaped ingates normally used for high pressure die castings are used for optimizing the fan used here, the droplets seen disengaging from the main melt front can probably be avoided. Due to the promising results it is reasonable to do further development in this direction.

- When calm flow without splashes is wanted normally the gating system is designed to give low velocities. But to secure calm flow without splashes pressure shock waves also have to be avoided, as they can cause the melt to be shot into the casting cavity as a fountain. This is most clearly seen at layout no. 1. This means the velocity criterions normally used for securing calm flow is not enough. Criterions also taken the effect from pressure shock waves into account are also needed. Layout no. 6 is designed to avoid pressure shock waves and to give a uniform melt distribution in the ingate. Very high velocities when compared to the other layouts are used in the ingate of this layout, and still a very calm filling is obtained when compared to the other layouts.

- Pressure shock waves are first and foremost generated by dead ends in the gating system. Hence they have to be avoided if pressure shock waves are to be avoided. Furthermore the closing of air pockets in the gating system can lead to pressure shock waves. Completely filled runners from the first melt passing through are hence also needed to be sure not to get pressure shock waves in the gating system.

- Different things can be done to gradually reduce the melt velocity before it hits the end of the horizontal runner to try to minimize the pressure shock wave from the hammer effect. An often used design feature is to gradually reduce the cross section of the horizontal runner over the width of the plate shaped ingate. This design is also seen as helpful in securing a sidewise balanced flow through the plate shaped ingate. No clear effects on reducing the splashes during the initial filling of the disc due to the gradually reduction of the horizontal runner can be seen. The effect on securing a balanced melt flow is also not clear. More trials are needed to finally conclude on the effects from gradually reducing the horizontal runner.

- The square shaped type of down runner well used in 4 of the 6 layouts all perform acceptable when comparing to the performance of the cylinder shaped type of well used in section 4. Generally seen are the square shaped wells good at preventing melt from entering into the horizontal runner in front of the main melt front, and they are able to secure an almost completely filled cross section of the horizontal runner with the first melt passing through it. The main problems of square shaped down runner wells are the internal flow in the well as it is very turbulent and a possible vena contracta at the exit of the well.

- At layout no. 6 is a curved transition from the down runner to the horizontal runner used. This type of transition does not have the problematic turbulent internal flow as the conventional square shaped down runner well has. The curved transition gives a very smooth directional change. The disadvantage of the curved transition is the lack of ability to significantly reduce the velocity of the melt. At the square shaped transitions area ratios between the horizontal runner and the choke of around 3, resulting in a corresponding reduction in velocity, have been used with relatively good success.

- The degree to which the flow into the disc cavity is balanced sidewise in the conventional gating systems is very different and hard to predict. Although it is hard to predict it is possible to obtain a relatively balanced filling sidewise with conventional systems. The non conventional system showed at layout no. 6 results in a very balanced filling, which furthermore is easy to predict. With bottom filling systems a temperature difference between top and bottom of the disc can not be avoided.

- The loss coefficients for the filling of the disc cavities have been found for the 6 layouts. The loss coefficients for 4 of the 5 depressurized layouts are seen to be very similar. They are all close to 0.5. The reason for this similarity is due to the fact that the major part of the loss is in the down runner. As the down runner is designed similar in all layouts the total loss coefficient will also be quite similar. The loss in the fifth depressurized layout is a little lower. At this layout the full metal head is obtained faster than at the other depressurized layouts and hence the full driving pressure is available for at larger part of the filling sequence. The loss coefficient in the non pressurized system is found to be 0.69, i.e. the losses are smaller than in the depressurized systems. This is also expected as the runners in the non pressurized system is only partly filled resulting in lower friction against the mould walls.

- The yields in the depressurized systems are all in the range 62 - 66 %. I.e. quite similar. Even though the yields are similar the differences are important as the competition on the brake disc marked is very hard. This means if the yield is raised only a few % points the result will be a relative largely increase in the total overhead. The yield for the non pressurized system is 52 % i.e. significantly lower than the yields from the depressurized systems.

- The mould filling of layout no. 3 has been simulated. The simulated sidewise melt distribution during the filling of the disc cavity is very close to the distribution seen in the trials. This is the case even though the sidewise distribution is controlled by the balance between dynamic and braking forces which is hard to predict for the casting engineer. Possible splashes shooting into the disc cavity at the initial phase of the filling are significantly influenced by the filling sequence of the horizontal runner. As surface tension is not taking into the simulation it is hard to get the filling of the horizontal runner right and hence also the initial filling of the disc. The simulated and measured filling times are very equal. The simulation supplies useful information about the internal flow paths in the melt stream, which is not possible to capture on the videos. This is illustrated with the flow paths through the well at layout no. 3.

Many different types of gating systems other than the types investigated in this section can be examined with the same technique as used here. For instance would it be interesting to closely examine the effect on the flow patterns from gradually reduced horizontal runners. It would also be interesting to test other variations of the 6 gating systems investigate in this section. Many small design features are believed to have important influence on the flow. Unfortunately very seldom is hard evidence present to support the theories used for explaining the effects of such design features. Furthermore would it be very interesting to see how the non conventional layout no. 6 performs under real production conditions. Further development of the very stream lined design is also needed. Hence a lot of further work on the area of gating systems for brake discs is needed.

Even though the layouts investigated in this section all are for brake discs the knowledge gained here can be used for many other types of castings as the conventional type of gating system used for layout no. 1-5 is used for many other parts than brake discs.

References

Ref. 5.1 Buderus erweitert Bremsscheiben Produktion in Breidenbach, Giesserei 90 6/2003 p. 188 -189

Ref. 5.2 Marktbereicht / Marktstudien 30.01.04-6.02.04 (KW 6) VDMA

Ref. 5.3 The worldwide demand for passenger cars, Foundry trade journal March 2003 p. 8-10

Ref. 5.4 Production and Operation. The global car manufacturing market. Stephen Ison Anglia Polytechnic University, Cambridge. http://www.ac777.dial. pipex.com/bes/bes_spring 2001/sec11.htm

Ref. 5.5 Auto Jahresbericht 2003 Verband der Automobilindustrie e.V. (VDA) Frankfurt am Main

Ref. 5.6 "Total Methoding" Ein neuer Weg zur Beherrschung der Gussstruktur

Ref. 5.7 DISA 230 versus DISAMATIC 2013 Reg. No. 9155H0510 Edition 01-02

Ref. 5.8 DISA Industries Application manual Reg. No. 9152H2111 Edition 09/95 p. 3.5

Ref. 5.9 Castings. John Campbell. Butterworth Heinemann 2002

Ref. 5.10 A study of the principles of gating as applied to sprue base design. K. Grube, J.G. Kura and J.H. Jackson. AFS transactions 60 p. 125-136 (1952)

Ref. 5.11 Introduction to fluid mechanics. 3rd Edition. Robert W Fox, Alan T. McDonald. John Wiley & Sons (1985)

Ref. 5.12 Formfyldning af meget tyndvægget støbegods The Technical University of Denmark IPL-070-03 Søren Skov Hansen (2003)

Appendix 5.1

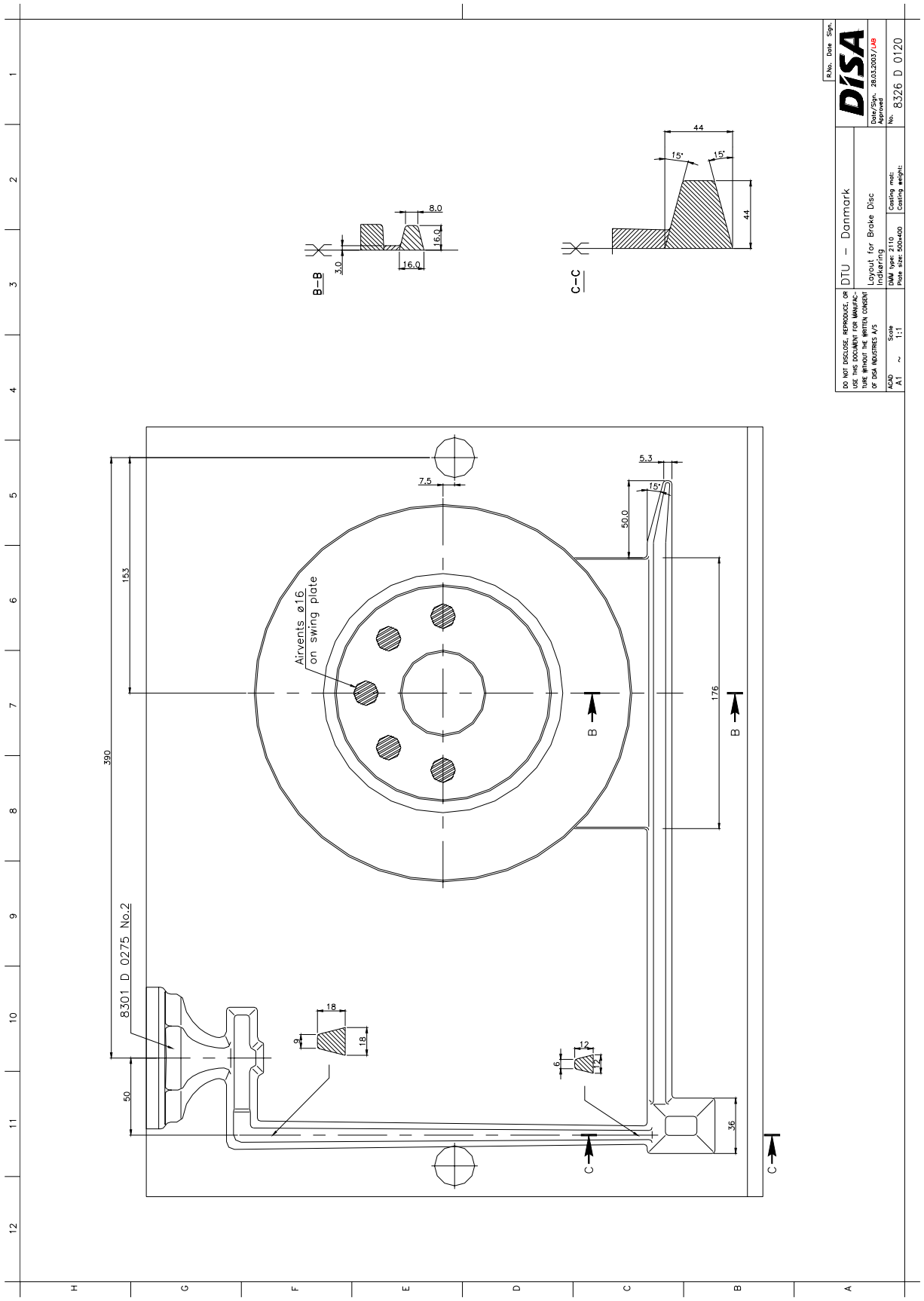
B–B
C–C
Airvents ø16
on swing plate
8301 D 0275 No.2
DTU – Danmark
Layout for Brake Disc
Indkøring
DISA
8326 D 0120

Appendix 5.2

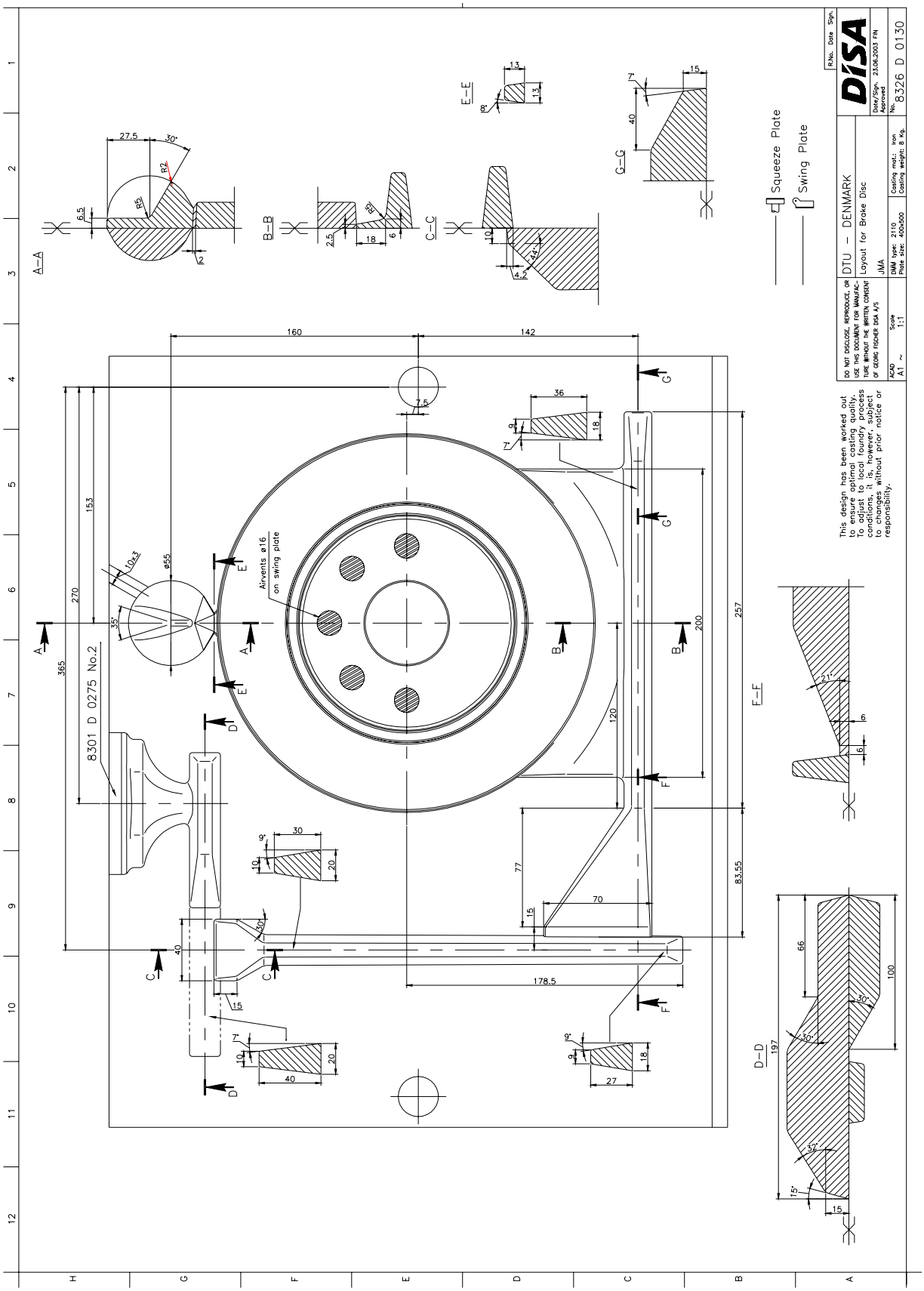
Squeeze Plate
Swing Plate
DTU – DENMARK
Layout for Brake Disc
JMA
8326 D 0130
8301 D 0275 No.2
Airvents ø16 on swing plate
This design has been worked out to ensure optimal casting quality. To adjust to local foundry process conditions it is however subject to changes without prior notice or responsibility.
A–A
B–B
C–C
D–D
E–E
F–F
G–G

Appendix 5.3

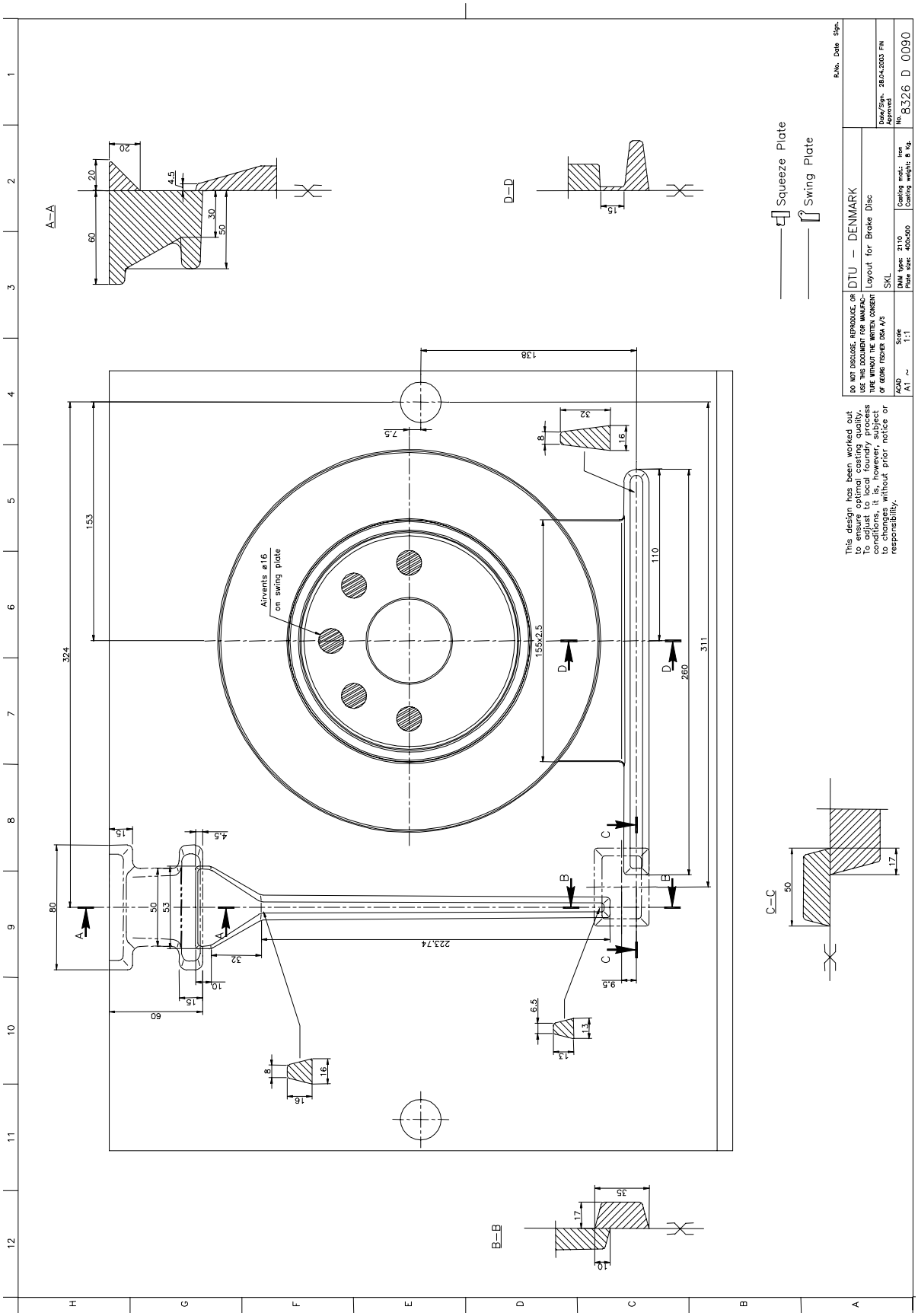
A–A
D–D
B–B
C–C
Squeeze Plate
Swing Plate
Airvents ø16
on swing plate
155x2.5
223,74
DTU – DENMARK
Layout for Brake Disc
SKL
8326 D 0090
This design has been worked out to ensure optimal casting quality. To adjust to local foundry process conditions, it is, however, subject to changes without prior notice or responsibility.

Appendix 5.4

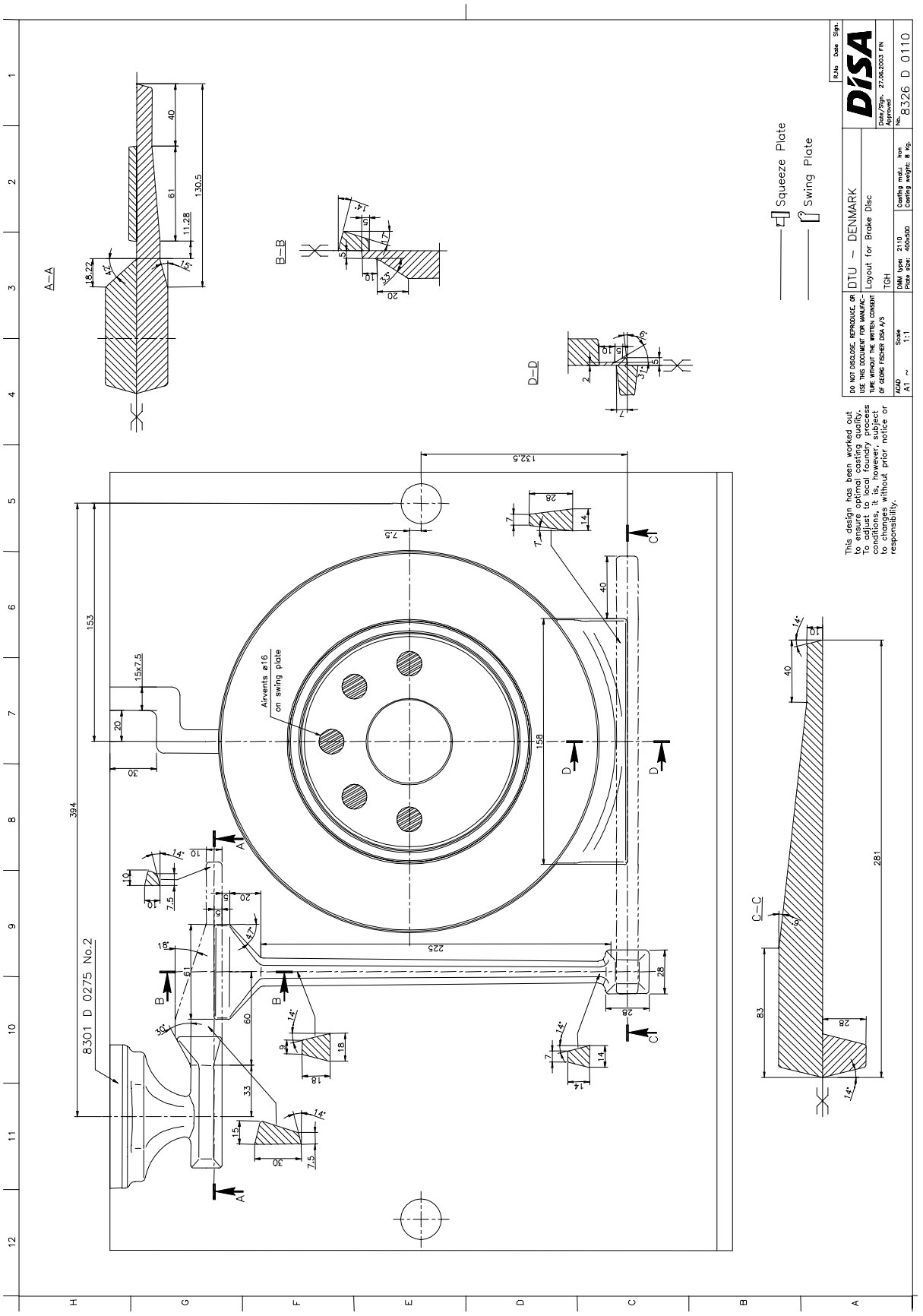
A–A
B–B
D–D
C–C
Squeeze Plate
Swing Plate
Airvents ø16
on swing plate
8301 D 0275 No.2
DISA
DTU – DENMARK
Layout for Brake Disc
8326 D 0110
This design has been worked out to ensure optimal casting quality. To obtain best casting results under conditions, it is, however, subject to changes without prior notice or responsibility.

Appendix 5.5

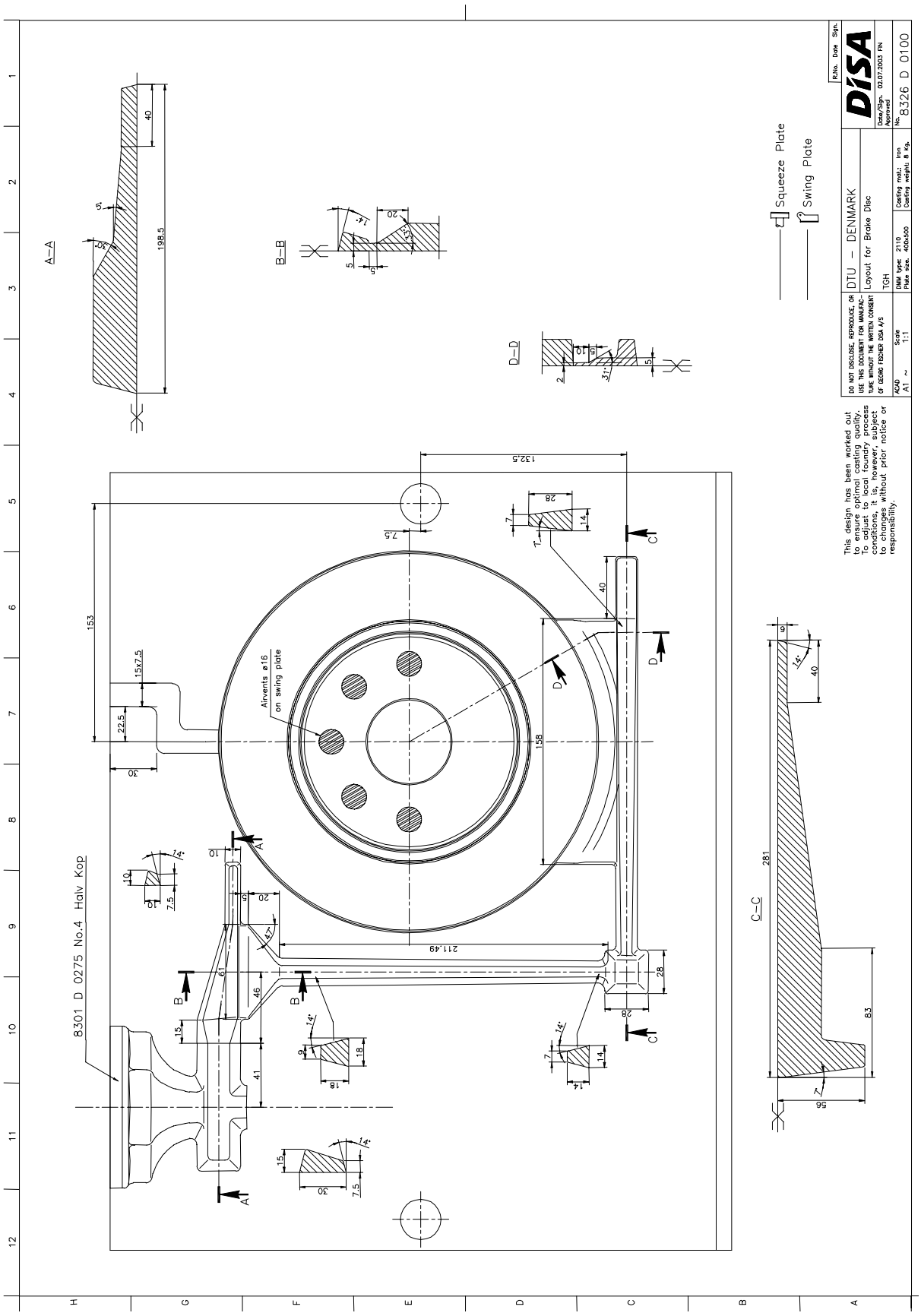
A–A
B–B
D–D
C–C
Squeeze Plate
Swing Plate
Airvents ø16
on swing plate
8301 D 0275 No.4 Halv Kop
DTU – DENMARK
Layout for Brake Disc
DISA
8326 D 0100
DO NOT DISCLOSE, REPRODUCE, OR USE THIS DOCUMENT FOR MANUFACTURE WITHOUT THE WRITTEN CONSENT OF GEORG FISCHER DISA A/S
This design has been worked out to ensure optimal casting quality. To adjust to local foundry process conditions, it is, however, subject to changes without prior notice or responsibility.

Appendix 5.6

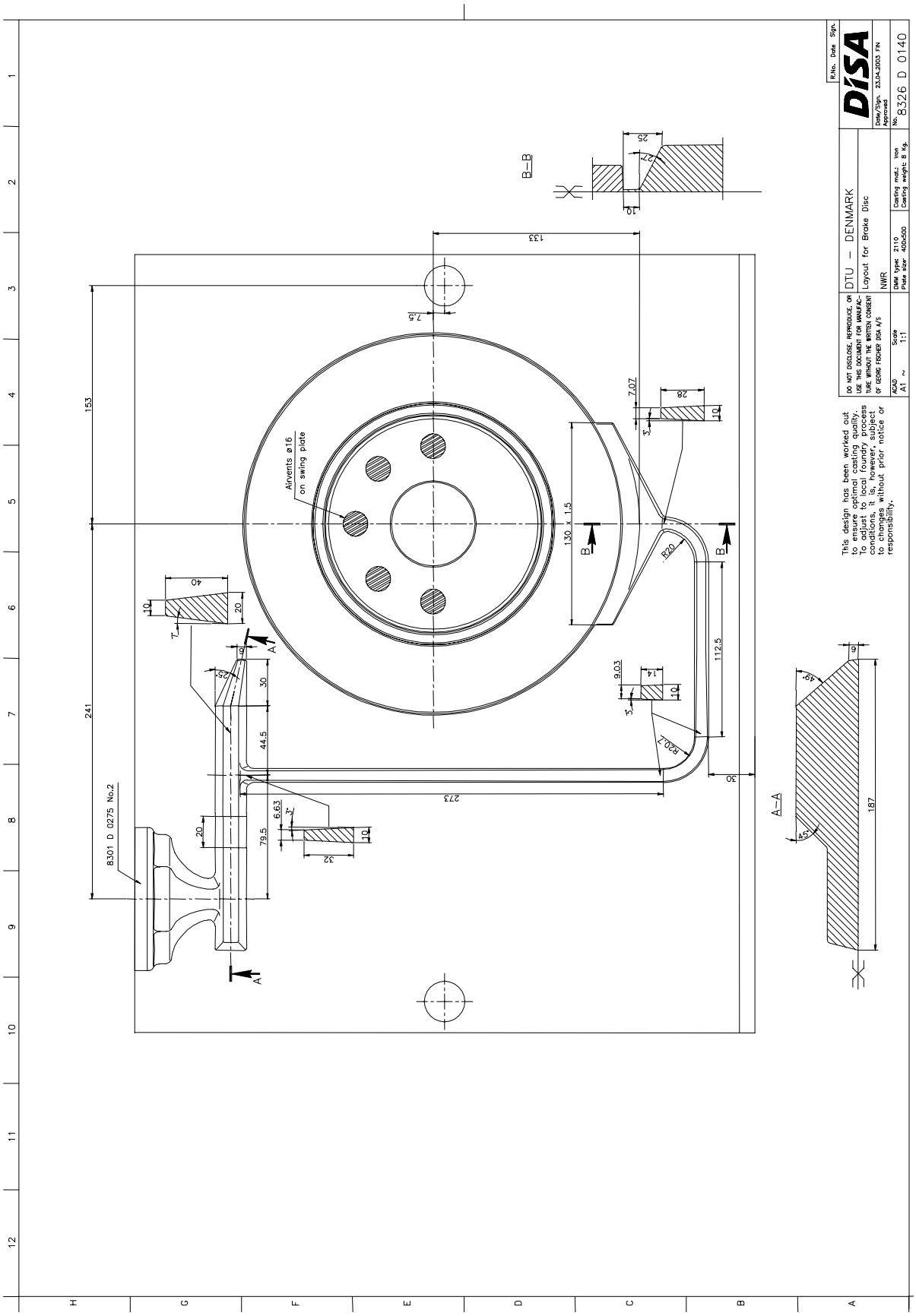
B–B
A–A
Airvents ø16
on swing plate
8301 D 0275 No.2
DTU – DENMARK
Layout for Brake Disc
DISA
8326 D 0140
This design has been worked out to ensure optimal casting quality. To adjust to local foundry process conditions, it is, however, subject to changes without prior notice or responsibility.

6 Casting of Manifolds

An exhaust manifold was chosen as the second test casting. A large market exists for exhaust manifolds as at least one is needed for every car built. 50 million passenger cars were built in 2003 [Ref. 6.1]. Some of them even needing two manifolds if equipped with V engines. Adding the relatively small but still existing need for the spare part marked is the total production number well over 50 millions per year world wide.

Exhaust manifolds are produced in iron based materials. Optimizing the efficiency and the specific power of combustion engines result in increasing working temperatures. This means the working temperature of the exhaust manifold is also increasing [Ref. 6.2], [Ref. 6.3]. The working temperature of exhaust manifolds has been increasing from the range 400 to 500 °C to almost 1100 °C for modern high performance engines. Due to the high and constant increasing working temperatures of the manifolds it is impossible to substitute iron with aluminium or another light weight material, at least with the materials available to day. The result is that exhaust manifolds most likely will continue to be produced in iron based materials. Furthermore as the working temperature of the manifolds is constantly increasing new high temperature resistant alloys have to be developed [Ref. 6.2].

Even though iron is going to be used as the base material it does not necessarily mean cast iron. Work is constantly going on to try to make it feasible to produce manifolds from tubes welded to the flanges. Stampings giving half the tubes and then welded together and to the flanges is another possibility also competing with the cast manifolds. The processes based on tubes or plate stampings as the raw materials have the advantage of being able to go down to very small wall thicknesses and hence saving both weight and material used. Furthermore the low weight of the manifolds produced with the alternative processes mean low heat capacity. A low heat capacity is wanted to ensure rapid heating at cold starts of the exhaust system including the catalytic converter. When the exhaust system is running below the working temperature the catalytic converter does not work optimal hence resulting in excessive pollution. Fast heating of the exhaust system to minimize the pollution is needed to fulfil the most restrictive pollution regulations. Trials have shown that it is possible to obtain the same low pollutions rates with cast manifolds if the flow properties and weight of the cast manifolds are optimized [Ref. 6.2]. Due to the higher geometrical freedom when producing cast manifolds compared to producing manifolds with the alternative processes it is possible to obtain significantly better flow properties in cast manifolds, this even though the surface roughness of cast manifolds is higher than for manifolds produced with the alternative processes. Apart from resulting in reduced pollution the better flow properties also results in higher performance [Ref. 6.2].

Due to the needed high temperature resistance, the increasing focus on the resources being used and the pollution aspect, is the critical issue for production of manifolds in the future not whether they are going to be produced in iron or another material. The critical issue is whether cast parts can compete with the above mentioned alternative processes in the ongoing development to save resources both during production and during the life in service of the part. As described, the pollution aspect is closely connected to the weight of the part as lower weight results in less pollution at cold starts.

This means that the main criteria for maintaining exhaust manifolds as a cast part is the ability to reduce the wall thickness of the part and still obtain the needed functionality.

Apart from the weight and heat capacity issues different other aspects influence the relative feasibility of the casting process and the alternative processes. The engines have to deliver higher and higher specific effects and at the same time pollute less. This leads to a more and more widespread use of super charging the engines with turbochargers. This is valid for both diesel and petrol engines [Ref. 6.2]. When a turbocharger is needed the trend goes towards building the manifold and the turbine housing as one part. This shortens the distance from the engines to the turbocharger and hence reduces the response time. Combining the manifold and the turbocharger makes the geometry even more complicated. The trend with building the manifold and the turbine housing together can change the balance of the feasibility between the different processes as it seems to be more complicated to produce the combined parts of tubes or plate stampings compared to casting them in one piece. When casting them in one piece it is on the other hand not possible to use different materials for the manifold and the turbo housing.

Contrary to the exhaust manifolds it is possible to produce intake manifolds in aluminium and in some cases even in temperature resistant plastic. Hence iron can not be expected to be used for intake manifolds.

The purpose of this section is to demonstrate the casting of an exhaust manifold with very small wall thickness and through this to show the still existing potential in the casting process. The manifold chosen for the tests can be seen on Figure 6.1. Two different sets of core boxes have been made making it possible to cast the manifold with 2 mm and 2.5 mm wall thickness. The approximate outer dimensions of the manifold are 335 mm x 145 mm x 95 mm. This makes it suitable for running on the DISAMATIC 2110 in the test foundry at DTU. The geometry of the manifold has kindly been put at the disposal for the project by Valdemar Birns Iron Foundries.

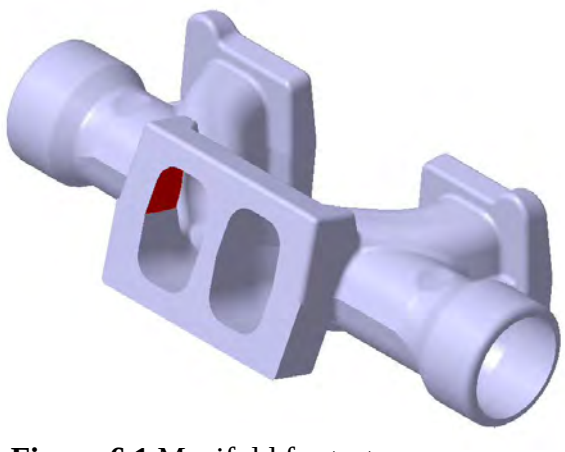

Figure 6.1 Manifold for tests.

Furthermore the purpose of this section is to demonstrate the function of very stream lined gating systems with narrow runners. This will as in the previous sections be done with videos of the real metal flow in the gating systems.

6.1 Design of the basic layout

The trials were made on a DISAMATIC 2110 which has a mould size of 500x400 mm. It was chosen to position the manifold on the pattern plate as shown on Figure 6.2 below.

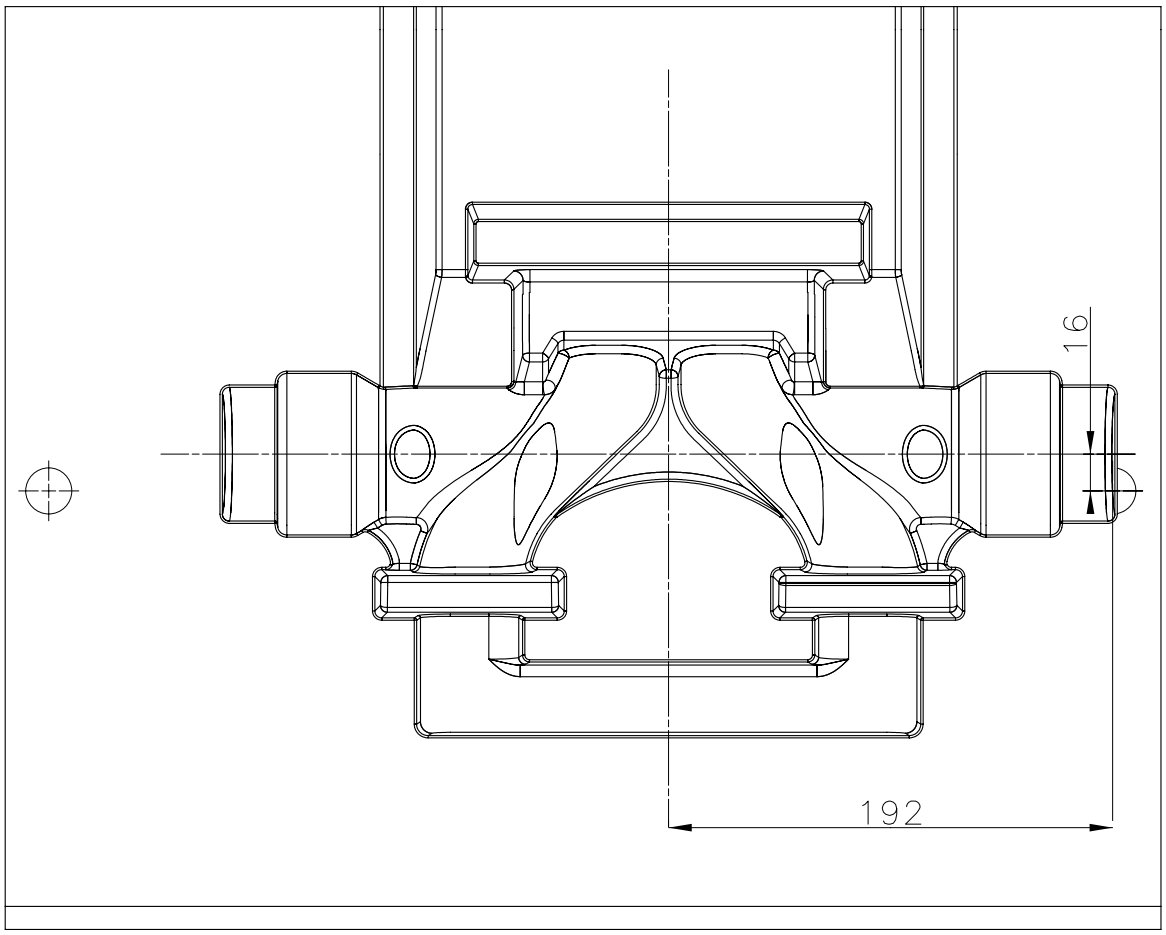

Figure 6.2 Basic layout for the manifold. Pressure plate pattern.

The swing plate pattern can be seen in Appendix 6.1.

The position and orientation of the manifold on the pattern plate was chosen for several reasons. The heavy flange where the tubes join is turned upward in the mould to make it easier to position feeders for the flange. The pattern was shifted to one side to get more space for different designs of down runners. Standard core locators have been used [Ref. 6.4]. The parts of the core coming out of the two flanges at the bottom of the pattern have been connected to build extra strength into the core and make it dimensionally more stabile.

The layouts shown here are all without feeders. This is done well knowing that feeders are necessary when casting ductile iron. The primary goal has been to fill the thin sections; hence the focus has been on the gating system and not the feeders. Normally is feeding the flanges of a manifold a solvable problem. Furthermore if the first parts are cast without feeders a very good picture of where feeders are needed is established. If feeders are put on the layout when the first parts are cast they are often not removed or reduced if the parts are sound. Hence pos-

sible unnecessary feeders or too large feeders are likely to stay on the layout harming the yield.

6.2 Design of the gating systems

First of all it was wanted to design a gating system with bottom filling to secure calm metal flow with a minimum of splashing. A depressurized design has been chosen with the choke at the bottom of the down runner. Due to the extremely small wall thicknesses of 2 and 2.5 mm it could be claimed that filling from the top would not lead to splashes as the wall thickness is so small that surface tension and wall friction will keep the melt fronts together. This is probably also true to some extend. But the flow paths will be less controlled when there is free flow from the top of the part to the bottom of it. Hence relatively large variations in the flow patterns in the casting from mould to mould can be expected. More uniform flow patterns from mould to mould can be expected when the flow is directional from the bottom to the top of the part.

Secondly, it was wanted to fill in through the relatively heavy flanges at the bottom of the part. The intension is that the flange is filled first, and then the metal starts to enter the tube shaped cavity over the complete cross section of the tube resulting in more uniform flow velocities in the different areas of the tube.

Casting very small wall thicknesses can sometimes demand for filling through the sections with the small wall thickness to be able to fill the part. Unless filling through the flanges the flow direction will be perpendicular to the tube wall and hence the flow will be directly on the core increasing the tendency to erosion of the core. Flow perpendicular to the tube wall will also mean that the melt has to make a sharp directional change when it hits the core resulting in heavy splashes etc. which can reduce the quality of the part.

When casting thin parts several ingates are often used. But this means the flow fronts have to meet in many different places. When pouring very thin parts it is difficult to get meeting melt fronts to fuse perfectly together [Ref. 6.5]. This was also seen in the trials made in section 4. Hence it was chosen to have only two inlets to minimize the number of places where the metal fronts meet. On the other hand the metal has to flow a longer distance before it meets another melt front or reaches the end of the cavity. To minimize the number of places where the melt fronts have to meet the inlets were positioned at the two flanges. In this way advantage of the stream lined design of the manifold is taken.

A basic design of the gating system as shown on Figure 6.3 was chosen.

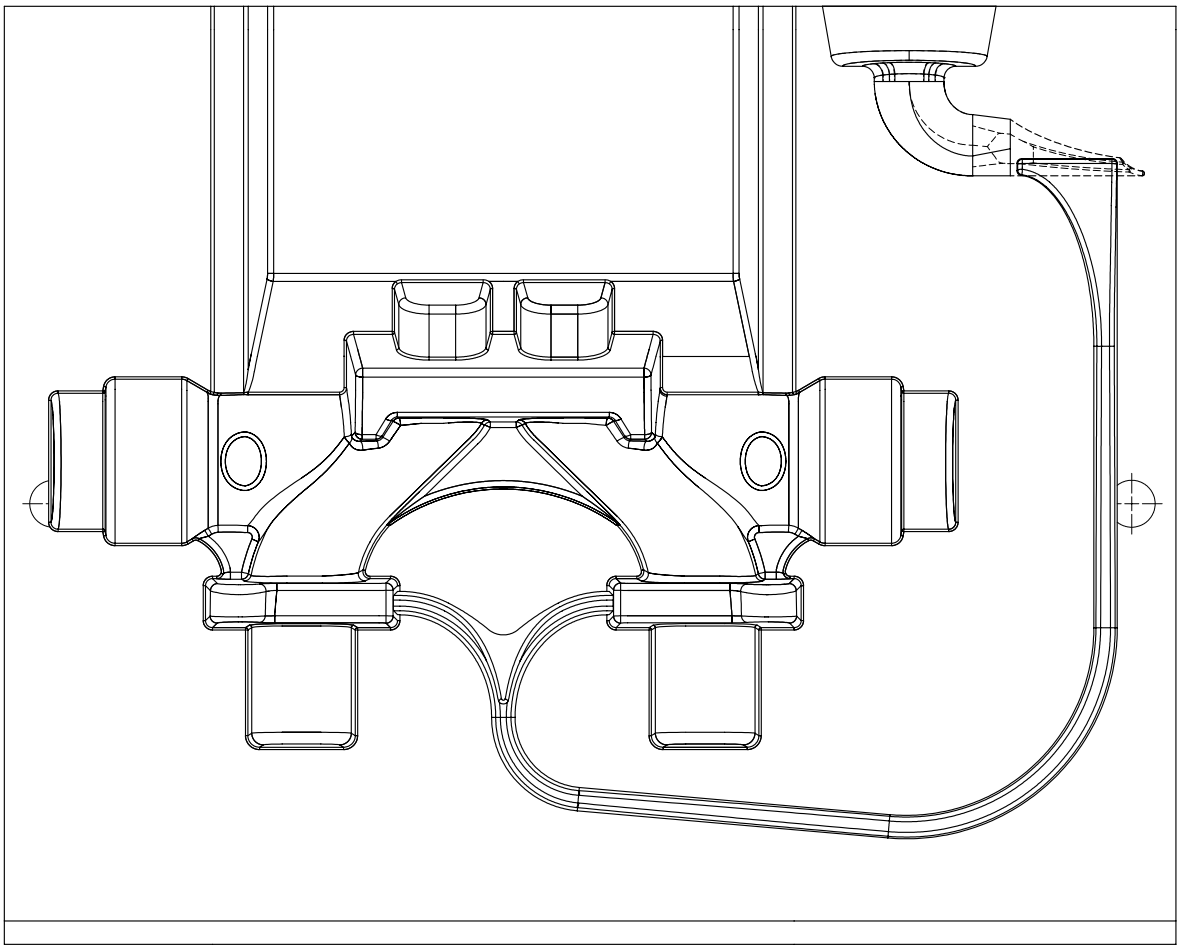

Figure 6.3 First design of the gating system.

The pouring cup is designed to attach to the pouring basin used in the previous trials. The dotted lines indicate parts of the gating system being on the opposite pattern plate. The part of the gating system below the pouring cup is only on one pattern plate.

The idea behind the design is to make the gating system very stream lined with no dead ends and to use narrow runners.

The stream lined design is chosen to secure as smooth flow as possible for instance avoiding the very turbulent flow in a conventional square shaped down runner well. Furthermore a stream lined design will also decrease the likelihood of getting vena contractas in the system as seen several times in the previous sections. A vena contracta can act as an artificial choke and as it is a low pressure area it will lead to aspiration. The closing of a vena contracta can also initiate a pressure shock wave.

Dead ends below the pouring cup are avoided as they are the main reason for getting pressure shock waves as seen in the trials described in section 4 and 5. The small horizontal runner connected to the pouring cup is a relic from the conventional designs. The lapping over at the horizontal extension of the pouring cup is working as a slag trap. But it is also encountering a dead end. The dead at the horizontal runner is in the upper part of the gating system and will thus not be able to introduce shock waves affecting the initial filling of the casting cavity. The design of the horizontal extension has been made very stream lined with a gradual reduction

of the cross sectional area to prevent a whirl at the end of it being able to drag slag and sand particles into the system. The gradual reduction in the cross sectional area also helps in promoting a sidewise more uniform flow into the top of the down runner. The spout shaped top of the down runner has also been designed in a very stream lined way to decrease the likelihood of getting a vena contracta at the upper left corner of it where the metal has to make a relatively sharp bend for entering the down runner.

The narrow runners have been used to promote coherent melt fronts and completely filled runner cross sections with the first melt passing through. The narrow runners will help in obtaining coherent melt fronts and completely filled runner cross sections due to the surface tension and friction. When metal is free falling, the surface tension will result in a curvature of the melt front. If the smallest dimension of a narrow runner is approximately the same as the thickness of the free falling melt stream the melt will touch the mould walls and friction will be introduced also helping to keep the melt front together. Hence the complete filling of the runner cross section from the first melt passing through is promoted. Due to the constant acceleration of free falling melt, the melt stream will continue to get thinner and thinner and eventually break up into droplets the size of which is controlled by the surface tension. But the constant reduction in cross sectional area of the down runner has to compensate for this effect. The width of the runners at the pattern plate is chosen to be 10 mm. 3 degrees draft has been used. The cross sectional area has been changed by changing the height of the runners.

Enhancing coherent melt fronts and completely filled runner cross sections both reduces aspiration and possible pressure shock waves coming from air pockets being closed. The design of the gating system has furthermore been inspired by [Ref. 6.6]. The narrow runners have the large dimension perpendicular to the pattern plate. This makes it easier to make a directional change while still maintain completely filled runner cross sections [Ref. 6.6] and [Ref. 6.7].

For calculating the cross sectional areas of the gating system the basic equation has been used [Ref. 6.4]:

$$F = \frac{G}{t \cdot \rho \cdot m \cdot \sqrt{2 \cdot g \cdot H}} \qquad \textbf{[Eq. 6.1]}$$

This equation or variations of it is used for calculating the cross sectional areas of a large part of all gating systems made world wide for gravity driven pouring.

When designing down runners it is normal practice to calculate the cross section areas at the top and the bottom of the runners. The cross sectional area of the down runner is then reduced linearly from the top to the bottom. This means making a straight taper from the top to the bottom.

On the graph shown on Figure 6.4 is the cross sectional area plotted of the down runner shown on Figure 6.3 when it strictly follows Eq. 6.1. The curve is labelled nominal area. If the cross sections at the top and bottom are calculated and the width and height of the runner are linearly reduced from the top to the bottom, the cross sectional area will not follow Eq. 6.1. The cross sectional area resulting from linearly reducing both width and height of the runner is also plotted. The curve is labelled 2D taper. This way to reduce the cross sectional area of the down runner is normal practice.

The curve labelled 1D taper on Figure 6.4 is the cross section area of a down runner where the width has been held constant and only the height of the runner has been reduced linearly to reduce the cross sectional area from the top to the bottom of the down runner. This would be normal practice for the narrow runners. The difference in cross sectional area in percent between the runner where only the height has been reduced and the runner strictly following Eq. 6.1 is also plotted. The curve is labelled % difference.

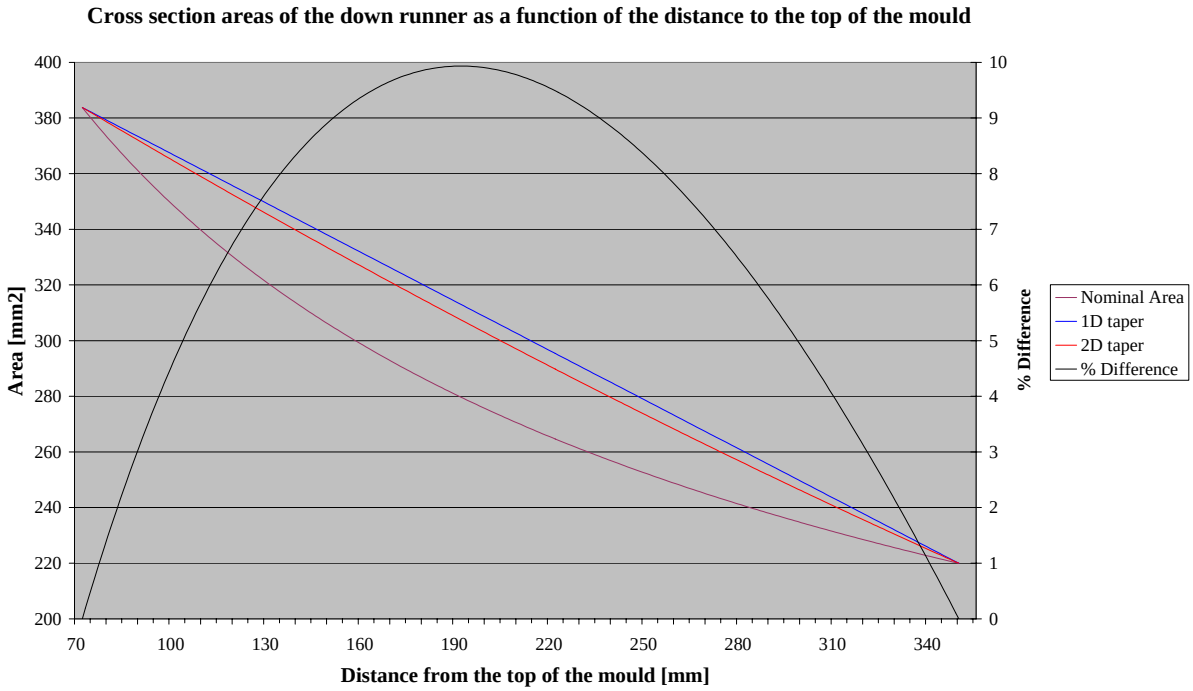

Figure 6.4 Cross sectional area of the down runner as a function of the distance to the top of the mould with different reductions in the cross sectional area.

The calculations are made under the follow conditions: As the pouring basin is going to be used an extra metal head of 64 mm has been added. Furthermore is the top of the down runner positioned 72 mm below the top of the mould as this is equal to using a standard pouring cup no. 2 from [Ref. 6.4].

Figure 6.4 shows that when using straight tapers is the cross sectional area of the down runner almost 10 % to large around the middle of the runner. This makes it impossible to keep the down runner completely filled in the initial part of the filling sequence.

Furthermore, it is important to remember to dimension the top cross sectional area of the down runner on the basis of the maximum flow rate through the gating system. For depressurized gating systems with the choke at the bottom of the down runner is the maximum flow rate (kg/s) the flow rate seen when no backpressure exist from the mould cavity. If Eq. 6.1 is rearranged the maximum flow rate through the choke can be calculated with:

$$\frac{G}{t} = F \cdot \rho \cdot m \cdot \sqrt{2 \cdot g \cdot H} \qquad \textbf{[Eq. 6.2]}$$

H is the metal head for the choke; F is the cross sectional area of the choke and m is the loss coefficient.

The needed cross sectional area at the top of the down runner can then be calculated from Eq. 6.3 where the flow rate G/t is obtained from Eq. 6.2:

$$F = \frac{G}{t} \cdot \frac{1}{\rho \cdot m \cdot \sqrt{2 \cdot g \cdot H}} \qquad \textbf{[Eq. 6.3]}$$

H is the metal head for the top cross section of the down runner.

This approach has been used when making the calculations for Figure 6.4. If the maximum flow rate seen at the initial part of the filling sequence is not used for dimensioning the top cross sectional area of the down runner the cross section will be too small and hence restrict the flow during the initial part of the filling. The result will be a partly filled down runner. In such cases the down runner will first be completely filled when enough backpressure from the mould cavity has been build up to reduce the flow through the choke adequate to balance the flow rates through the choke and the top of the down runner.

Close to the top of the mould the needed cross sectional area of the down runner given by Eq. 6.1 increases relatively fast as the metal head decreases. This is due to the square root of H seen in the denominator. This means if the top cross section of the down runner is closer to the top of the mould than the 72 mm used here will the maximum difference between the area given by Eq. 6.1 and the runners with a straight taper may it be in 1 or 2 dimensions increase fast. As mentioned earlier 64 mm metal head is added to the calculations due to the use of the pouring basin. This equals to have the top of the down runner 64 mm lower in the mould. If the pouring had to be made without the pouring basin, the 64 mm had to be taken out of the calculations for dimensioning the down runner. If this is done the graph shown on Figure 6.4 changes to the graph shown in Appendix 6.2. Due to the lower metal head the cross sectional areas increase. But what is more important, the maximum difference between the nominal cross sectional area of the down runner and the runners made with straight tapers for connecting top and bottom cross sections increases to more than 20 %. Hence significant air pockets can not be avoided. The setup giving 20 % difference in the cross sectional area is equal to what is seen under normal production. Hence the 20 % in difference is what is to be expected in moulds 400 mm high.

Apart from designing the cross sectional areas of the down runner strictly according to Eq. 6.1, the flow has furthermore been constrained by adding a safety margin of 20 % to promote obtaining completely filled cross sections of the down runner with the first melt passing through. This has been done by adding 20 % to the cross sectional areas starting with 0 % at the choke and increasing the addition linearly to 20 % at the top of the down runner. In this way the flow is constantly being constrained on the way through the down runner.

This way of dimensioning the down runner can seem a lot more time consuming than just dimensioning the top and bottom cross sections and then connect them with a straight taper. But with the use of a computer and a spread sheet, the nominal cross sectional areas can easily be calculated for points say at every 10 mm of the down runner. The addition of the linear increasing safety margin starting with 0 % at the choke and ending with 20 % at the top of the

down runner is also done easily in the spread sheet. Using the narrow runners with a fixed width at the pattern plate and a fixed taper the height of the runner at the points where the area is calculated can also easily be calculated in the spread sheet. The height of a narrow runner with width W at the pattern plate, taper α and cross sectional area A can be calculated from:

$$H = \frac{W - \sqrt{(W^2 - A \cdot 4 \cdot \tan(\alpha))}}{2 \cdot \tan(\alpha)} \qquad \textbf{[Eq. 6.4]}$$

The data points giving the height of the runner can be plotted into a CAD system. If the data points are connected with a spline the result is a smooth curve very close to the theoretical one. In some CAD programs the mathematical expression for the height of the runner can even be giving in, leading to the CAD programme calculating the exact shape of the runner.

When the spread sheet once is established it is very easy to change the parameters i.e. the distance from the top of the mould to the choke and to the top of the down runner, and the maximum flow rate needed. Hence the following gating systems are dimensioned automatically if the 3 parameters are given in.

The design and manufacturing of the gating systems have been done with 3D CAD/CAM, but it can as well be done by hand as long as the heights of the cross sections of the down runner are available at suitable intervals. A skilled pattern maker will without problems be able to connect the points giving the height of the down runner with a smooth line very close to the theoretical one.

The directional change at the bottom of the down runner is made with a curved bend instead of a conventional down runner well. This is done to promote a smooth flow and to maintain completely filled cross sections of the runner. The radius of the curved bend is relatively large. It can be made smaller but as long as there is free space on the pattern plate there is no need to make the bend sharper than necessary.

The horizontal runner is inclined 15 degrees to promote the melt front to stay coherent. The cross section of the runner is gradually increased from the curved bend at the bottom of the down runner to the inlet into the casting to gradually reduce the velocity. This is against the idea of having runners 100 % constraining the flow. But if this is not done the velocity will be around 2.6 m/s in the horizontal runner, even though it is inclined 15 degrees. The narrow runners and the uphill flow are expected to result in a close to completely filled cross section of the horizontal runner with the first melt passing through even though the flow is not 100 % constrained. This is due to the fact that the narrow runner and uphill flow result in a backpressure promoting a completely filled runner.

The connection to the manifold is made with a very stream lined design splitting the flow into two and at the same time making a directional change. The design can be seen on Figure 6.5.

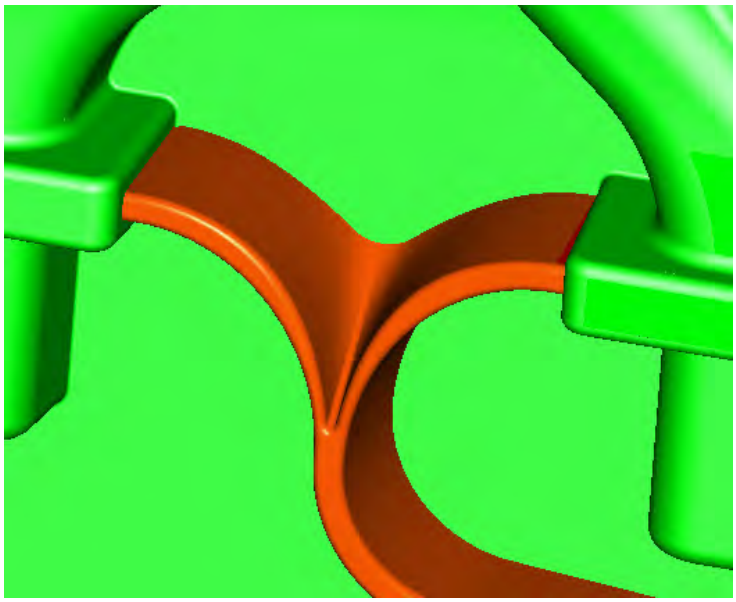

Figure 6.5 Transition from runner to mould cavity.

The design shown on Figure 6.5 and in general the design of the complete gating system is made to have good control over the melt. Hence the flow patterns in the gating system are easy to predict for the casting engineer. In the conventional gating systems described in section 4 and 5, the balance between the dynamic and the braking forces plays a significant rule in deciding the flow patterns. Hence the flow patterns are not solely controlled by the geometry of the gating system. The dynamic forces are due the velocity of the melt. The braking forces are for instance due to wall friction in the gating system. In gating systems where the balance between the dynamic and the breaking forces play a significant rule, a change for instance in the braking forces by a lower viscosity will be able to change the flow patterns significantly. The influence from the balance between dynamic and braking forces has been minimized in this layout due to the restrictive geometry used.

When using very stream lined runners sand erosion will be minimized. Sand erosion is especially seen where the metal makes a sharp bend and as sharp bends are eliminated in the stream lined runners sand erosion is minimized. The stream lined runners with good control over the melt will also result in more uniform velocities over the cross sections, especially if fan shaped ingates are used. Uniform velocities remove areas with high local. Areas with high local velocities mean excessive heating resulting in sand burn on etc. at these areas.

6.3 Tooling

The tooling needed i.e. patterns and core boxes were machined out from polyurethane block material. The material type chosen has very good wear resistance and low heat distortion values. The patterns were mounted on aluminium pattern plates to give extra stability. The tooling can be seen on Figure 6.6.

Figure 6.6 Swing plate pattern and core box.

When using polyurethane patterns is it not possible to use pattern heating. Due to the smooth surfaces possible to obtain when machining polyurethane and the low heat transfer coefficient of the material sand sticking to the patterns is not a problem.

Apart from being relative easy to machine compared to metal, another important advantage of the polyurethane material is the weight. As the cores were made on a manual core shooter the light polyurethane boxes were advantageous.

For producing the runners it was chosen to machine out negatives and then cast the runners in polyurethane.

All parts needed for the patterns, core boxes and the gating system were machined out directly from the original CAD files made when designing the tools.

6.4 Experimental set up

The manifolds were cast with the same alloy as used for the plates described in section 4. The composition can be seen in Table 4.1. The pouring basin was used to secure uniform filling from mould to mould. The setup can be seen on Figure 6.7. The pouring basin was completely filled with iron before the stopper core was removed. The temperature in the pouring basin before removal of the stopper core was recorded with a thermocouple of the S-type. The furnace temperature was adjusted to result in a temperature in the basin of 1420 °C.

Figure 6.7 Casting the manifolds using the pouring basin.

As the gating system is placed on the plane section of the parting line it was possible to record the flow in the gating system on video as done in the previous section. A special pattern was made with the gating system. Blocks having the same volume and mass centre as the manifold were mounted on the pattern plate. The pattern plate can be seen on Figure 6.8. When the metal is filling the blocks the flow resistance will be smaller than at the filling of the real manifolds due to the very thin wall thickness of the manifold. Until a significant melt level has been reached in the blocks the flow rate will be close to the flow rate at the real manifolds.

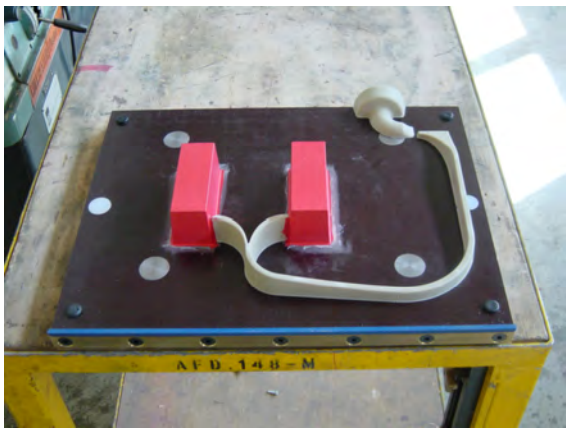

Figure 6.8 Pattern plate for recording the metal flow on video.

The setup for capturing the melt flow in the gating system on video can be seen on Figure 6.9. Again a top core acting as the upper part of the mould of glass plates had to be made. The top core was made by hand over the opposite pattern plate as with the other trials. The top core covers the upper part of the down runner. Three layers of plain window glass were used. The 2 blocks give a quite heavy thermal and mechanical impact on the 3 layers of glass. Surprisingly the glass was able to withstand the impacts and only a few cracks were seen hence the metal did not run out in any of the runs.

Figure 6.9 Setup for making videos. Snapshot after the stopper core has been removed and half way through the mould filling.

6.5 1. Series of Trials

6.5.1 Gating system

The first gating system was designed as shown on Figure 6.3. The gating system is designed to give an initial melt front velocity in the tubes of the manifold with 2 mm wall thickness of 400 mm/s. The 400 mm/s has been chosen from the flow lengths seen in the trials described in section 4. Furthermore the pouring temperature has been raised which also increases the maximum flow length. Higher velocities or extremely high velocities could have been chosen to increase the likelihood of getting the manifold completely filled. But generally, keeping the velocities as low as possible is preferable as raising the velocities means increasing the likelihood of getting quality problems such as sand erosion, inclusions and sand burn on.

The initial velocity in the inlets is 0.63 m/s when assuming completely filled cross sections of the inlets and no losses in the system.

The gating system is designed to be very restrictive using narrow runners for promoting coherent melt fronts and completely filled runner cross sections with the first melt passing through. Furthermore, the gating system is designed to give good control over the melt not letting the balance between dynamic and braking forces have significant control over the flow patterns.

6.5.2 Initial melt flow in the gating system

As mentioned in section 6.4 was a special pattern made, making it possible to record the metal flow in the gating system on video. The filling sequences of 4 moulds were recorded on video. The flow patterns were very similar from mould to mould. At run no. 1 a single droplet disengaged from the main melt front shortly as the melt enters the casting cavity (the block). This filling sequence has been used for the further examinations to be sure not to over estimate the capability of the gating system. The uniformity of the 4 filling sequences will be shown in section 6.5.3.

Snapshots showing the first melt passing through the system can be seen on Figure 6.10 on the following pages.

Time 0.00 Time 0.04 Time 0.08

Time 0.12 Time 0.16 Time 0.20

Time 0.24 Time 0.28 Time 0.32

Time 0.36 Time 0.40 Time 0.44

Time 0.48 Time 0.52 Time 0.56

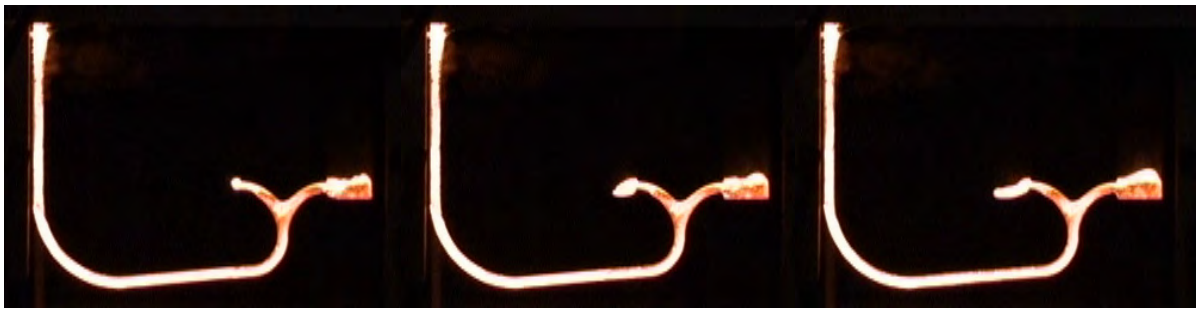

Time 0.60 Time 0.64 Time 0.68

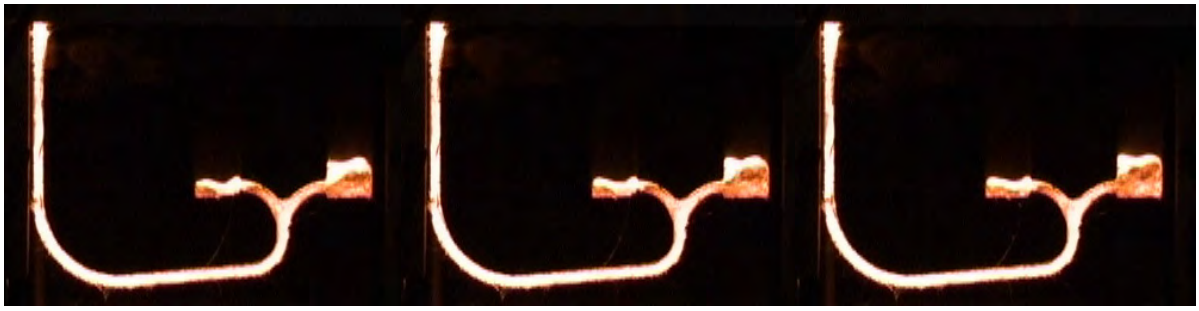

Time 0.84 Time 0.88 Time 0.92

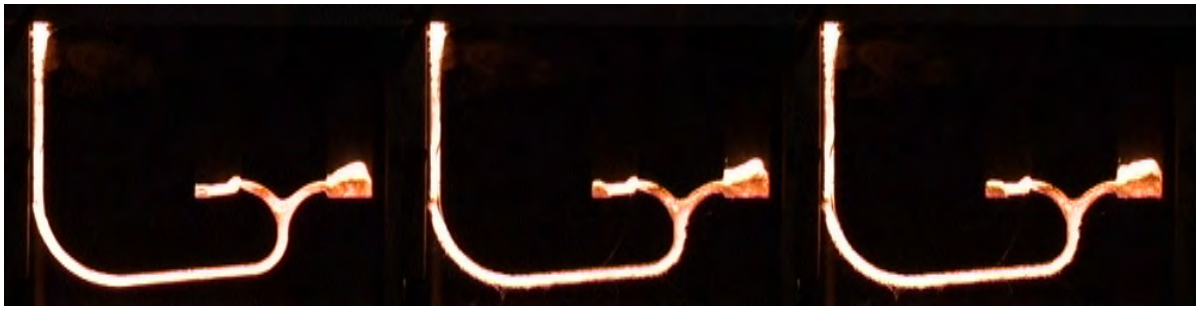

Time 0.72 Time 0.76 Time 0.80

Time 0.96 Time 1.00 Time 1.04

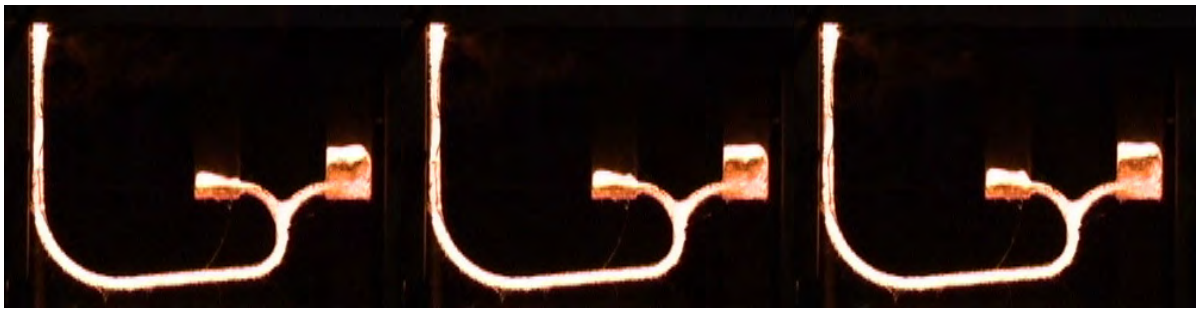

Time 1.08 Time 1.12 Time 1.16

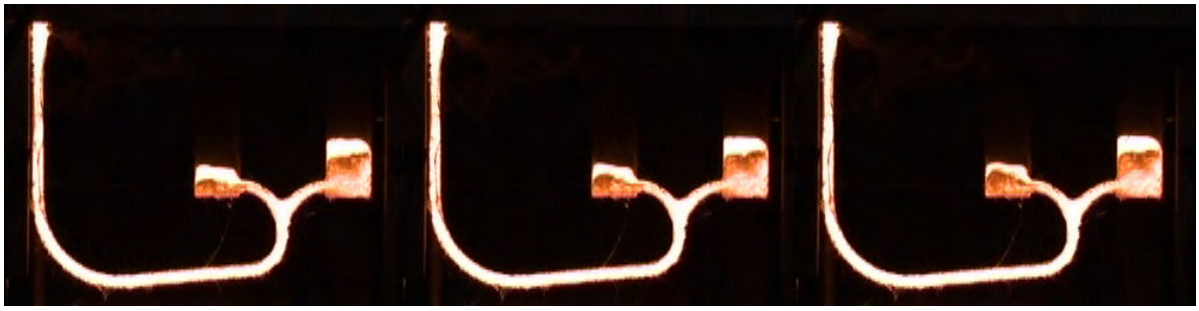

Time 1.20 Time 1.24 Time 1.28

Time 1.32 Time 1.36 Time 1.40

Figure 6.10 Snapshots showing the initial melt passing through the gating system.

The times given are from the melt front appears under the top core.

The initial melt is seen to pass through the gating system with one coherent melt front. When the melt enters the casting cavity at 0.32 s a single droplet is seen in the right cavity, 0.04 s later is the droplet incorporated into the main melt stream again. Otherwise no droplets disengage from the main melt front during the filling sequence.

A similar gating system also with very narrow runners was made in section 5 (Layout no. 6). With the similar layout investigated in section 5 problems were seen with the initial melt front splitting up during the flow through the down runner. This problem is not seen here indicating that the problems can be solved.

The melt front is coherent when it travels through the gating system, but the complete cross section of the down runner is not filled with the first melt passing through. Enlargements of the down runner can be seen on Figure 6.11. The enlargement after 1.60 s shows a completely filled down runner for comparison. The enlargements are from run no. 4 as the focus is better at this run. The filling sequences of the down runner in the 4 runs are very similar. The upper left corner of the down runner at run no. 4 has been hidden behind a falsely placed clamp.

The partly filled down runner is seen even though the gating system has been shaped strictly according to Eq. 6.1 and a safety margin of 20 % has been added as described in section 6.2. The reason for the partly filled down runner has to be found at the transition from the horizontal extension of the pouring cup to the top of the down runner.

Figure 6.11 Initial flow through the down runner after 0.16, 0.68 and 1.60 s.

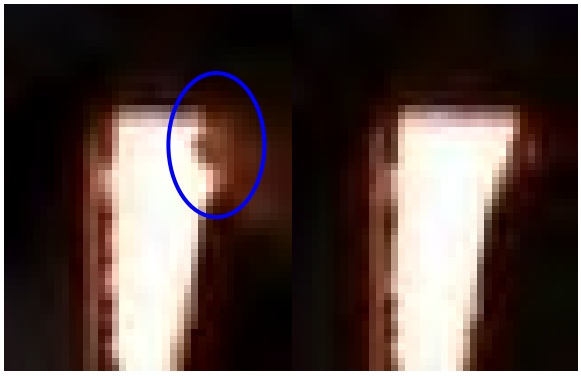

Figure 6.12 Top of down runner after 1.40 s with a vena contracta and at the end of the filling.

Although the transition from the horizontal extension of the pouring cup to the top of the down runner has been designed very stream lined a vena contracta is seen in this area. The enlargements on Figure 6.12 show the upper part of the down runner after 1.40 s and at the end of the filling sequence. The snapshots are from run no. 1. When comparing the two enlargements an air pocket is clearly seen at the upper right corner of the down runner after 1.40 s. The air pocket is caused by a vena contracta appearing where the melt has to make a relatively sharp bend for entering the down runner. The vena contracta restricts the cross sectional area the flow takes place in and hence acts as an artificial choke. The air pocket is very clearly seen at all 4 runs of the trial. When examining the snapshots shown on Figure 6.12 one has to remember that the top of the down runner is hidden behind the top core seen on Figure 6.9. The upper 15 mm of the down runner below the pouring cup can due to this not been seen. The air pocket seen on Figure 6.12 is hence only a part of the total air pocket. Because the upper part of the air pocket is hidden, it is difficult to estimate the size of it. But the influence can be judged from the filling time of the mould. Rearranging Eq. 6.1 gives the following equation for the filling time:

$$t = \frac{G}{F \cdot \rho \cdot m \cdot \sqrt{2 \cdot g \cdot H}} \qquad \textbf{[Eq. 6.5]}$$

The filling time of the two blocks is calculated to 1.76 s when found without losses, i.e. with m = 1. The measured filling time for the blocks is 3.1 s. The loss coefficient for the filling of the block cavities can be found by dividing the measured and the calculated filling times with each other. The result is a loss coefficient of 0.57 for the filling of the blocks. With the very stream lined gating design and relatively thick sections the flow takes place in, a loss coefficient of 0.57 seems to be relatively small, reflecting higher losses in the system than would be expected. The seemingly high losses are caused by the vena contracta at the top of the down runner resulting in an artificial choke prolonging the pouring time.

The initial melt front velocity in the inlets was found to be 0.63 m/s when calculated without losses. Multiplying the velocity with the found loss coefficient gives a good estimate for the real initial melt front velocity in the ingates. The result is 0.36 m/s, when assuming completely filled cross sections of the runner.

The design of the transition from the horizontal extension of the pouring cup to the down runner is quite conventional with an overlap and a spout shaped geometry of the upper part of the down runner. Even though the transition is made very stream lined both when looking at the horizontal extension of the pouring cup and the spout it has not been possible to avoid the vena contracta.

The vena contracta was to some extend expected as simulations of the mould filling had shown problems here during the initial part of the filling. Two reasons made it interesting to test the design anyway. It is a design used very often in practice hence it is interesting to see how the flow takes place in such a popular design feature. Furthermore was the version used here very stream lined. Meaning if this version of the design can not avoid a vena contracta problems have to be expected at most other designs.

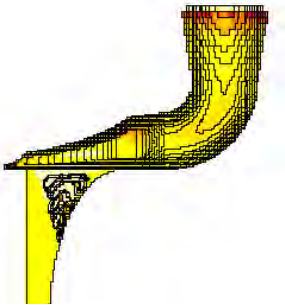

Figure 6.13 Snapshot from the initial part of the mould filling simulation.

The flow through the curved bend at the bottom of the down runner is seen to take place without any splashes. The cross section of the bend is not filled with the first melt passes through. This can only be so with the partly filled down runner caused by the artificial choke at the top of the down runner.

The complete cross section of the horizontal runner is filled very fast. But again the real performance of the design is hard to judge due to the artificial choke at the top of the down runner. Generally, the design looks promising. At 0.24 s where the flow is going upwards into the fan shaped transition for splitting the melt flow into two the melt front is close to brake up. This means not much higher velocities can be allowed with this design without getting the melt front to break up. If higher velocities are wanted thinner sections have to be used. Thinner sections will be able to introducing more back pressure from friction and surface tension and hence keep the melt front together at higher velocities.

The filling of the right cavity is seen to be a little in front of the left cavity. This is due the direction of the flow in the horizontal runner pointing towards the right cavity. If a vertical section had been build into the gating system below the fan shaped part splitting the flow into two the problem could have been reduced or maybe even completely avoided.

6.5.3 Uniformity of the filling sequences

The gating system is designed to be very restrictive not letting the balance between the dynamic and braking forces have significant influence on the flow patterns. The restrictive design is also intended for securing as uniform flow patterns from mould to mould as possible. In section 4.7.2.2 the flow patterns in conventional gating systems have been shown to be able to vary some from mould to mould.

The mould filling sequence of the gating system described in this section has been recorded 4 times on video. Statistically seen is 4 repetitions not a large material to build conclusions on when investigating new areas. But as the 4 repetitions give very equal results a good indication of the uniformity of the flow patterns from mould to mould is obtained. The melt distribution at the 4 runs after 0.32 s can be seen on Figure 6.14

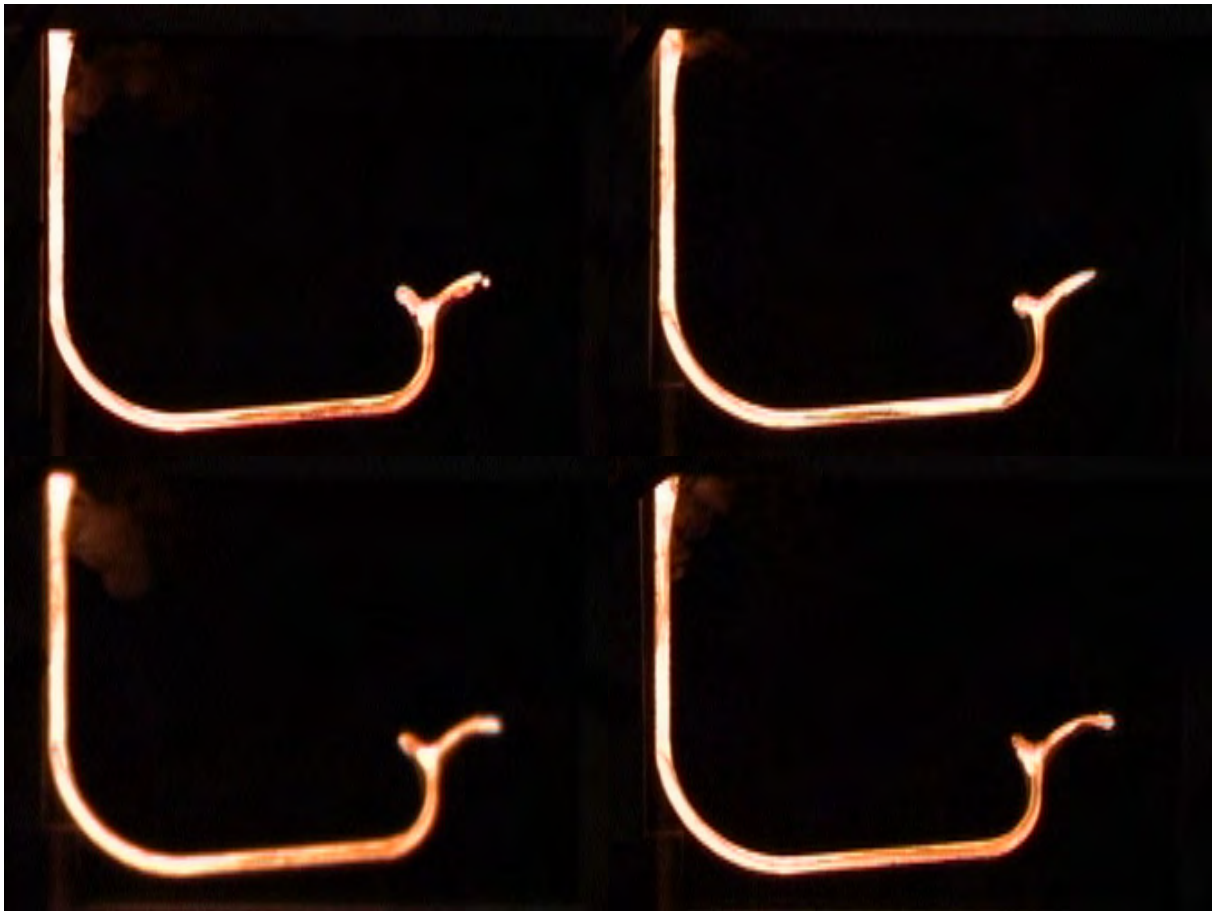

Figure 6.14 Melt distribution in the 4 runs after 0.32 s.

Further sets of snapshots showing the uniformity of the flow in the 4 runs can be seen in Appendix 6.3. The largest difference between the 4 runs is the droplet seen going into the right cavity at the upper left picture on Figure 6.14. During the rest of the filling sequence no other significant differences can be seen. At the two snapshots shown to the right on Figure 6.14 and in Appendix 6.3 is the upper left corner of the down runners hidden behind an incorrectly positioned clamp.

The air pocket at the upper right corner of the down runner is clearly seen on Figure 6.14 and in Appendix 6.3 for all 4 runs. This means the vena contracta is present at all runs, and it can be seen as a stable phenomenon.

Even though only 4 repetitions have been made, the large degree of similarity between the 4 repetitions shows the stability of the gating system very clearly. The probability of making 4 very equal runs is very small unless the process is stable. Hence the gating system is able to absorb the minor but inevitable changes in the pouring conditions; this is in contrary to what is the case for the conventional type of gating system investigated in section 4.

6.5.4 Filling of the manifolds

With the layout shown on Figure 6.3 it was not possible to fill the manifold with 2 mm wall thickness completely. The result can be seen on Figure 6.15.

Figure 6.15 Manifold with 2 mm wall thickness cast with the first gating system.

It was very close to completely filled. The problems are limited to some of the melt fronts not fusing completely together. This is marked on the left side of the enlargement shown on Figure 6.16.

Furthermore errors on the core for the manifold with 2 mm wall thickness were discovered resulting in only 1 mm of wall thickness at the areas where the geometry makes a depression. One of the areas is marked on Figure 6.16 to the right.

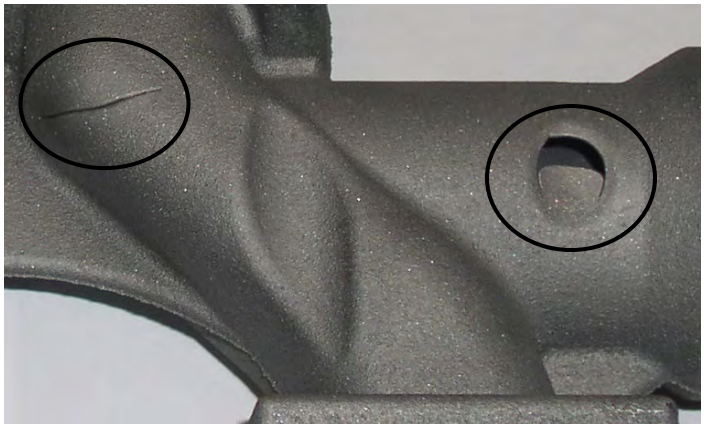

Figure 6.16 Section marked to the right is with 1 mm wall thickness. Section marked to the left is showing meeting melt fronts only partly fused together.

The gating system is designed for an initial melt front velocity in the tubes of 400 mm/s at the manifold with 2 mm wall thickness. The 400 mm/s is when calculating without losses in the gating system.

The loss coefficient for the gating system when connected to the blocks used in the trials for making videos of the flow is in section 6.5.2 found to be 0.57. The total loss will be larger when the metal enters the 2 mm thick sections of the manifold. For the initial part of the filling of the manifold 0.57 will although be a reasonable estimate for the loss. Hence the initial melt velocity in the 2 mm section of the manifold is estimated to 228 mm/s.

The manifold was also cast with 2.5 mm wall thickness. The result can be seen on Figure 6.17. The wall thickness was changed by using a core with a reduced size at the sections shaping the part of the manifold with the thin wall thickness. The same gating system as used for the manifold with 2 mm wall thickness was also used for the one with 2.5 mm wall thickness. The increase in wall thickness means larger cross sectional area of the tubes and hence is the nominal initial velocity lower compare to the manifold with 2 mm wall thickness.

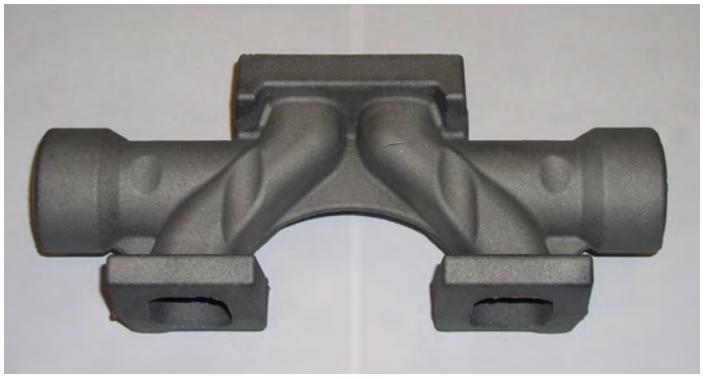

Figure 6.17 Manifold with 2.5 mm wall thickness cast with the first gating system.

The initial velocity in the tubes for the manifold with 2.5 mm wall thickness is 332 mm/s when calculated without losses. The filling of the manifold with 2.5 mm wall thickness was a little more complete than the filling of the manifold with 2 mm wall thickness. The manifold with 2.5 mm wall thickness can be seen on Figure 6.17. As with the manifold with 2 mm wall thickness did the meeting melt fronts not completely fuse together. This can be seen on the enlargement shown on Figure 6.18. The problems are seen to be at the same position on the manifold as at the one with 2 mm wall thickness. I.e. the flow patterns at the two wall thicknesses seems to be the same, as the coldest melt fronts meet at the same position at both cases. An estimate for the real initial melt velocity in the tubes can be found by multiplying the 332 mm/s with the loss coefficient found in section 6.5.2 to 0.57. This yields an initial melt front velocity in the tubes of 190 mm/s at the manifold with 2.5 mm wall thickness.

Figure 6.18 Sections marked to the left is showing meeting melt fronts only partly fused together.

6.6 2. Series of Trials

Due to the misruns seen at the 1. series of trials, adjustments had to be made. Changes on the gating system have been made to increase the melt front velocity in the manifold. Furthermore has the cores for the manifolds with 2 mm wall thickness been corrected to give 2 mm wall thickness on the areas where the wall thickness falsely was 1 mm. Extra mould cavity venting has been added to reduce the possible back pressure from the air in the mould cavity.

6.6.1 Gating system

At the trials with the first gating system the problems were limited to melt fronts not fusing together. Hence it was chosen to keep the basic layout of the gating system and increase the filling rate. The second gating system is designed to fill 50 % faster than the first gating system. I.e. the initial melt velocity in the tubes has been raised to 600 mm/s from 400 mm/s in the manifold with 2 mm wall thickness. Both values are calculated without losses. Furthermore the design around the pouring cup has been changed to avoid the vena contracta at the top of the down runner seen at the first gating system. The vena contracta was able to limit the flow at the first gating system. Hence the real increase in flow velocity is probably more than 50 %. The new gating system can be seen on Figure 6.19 below:

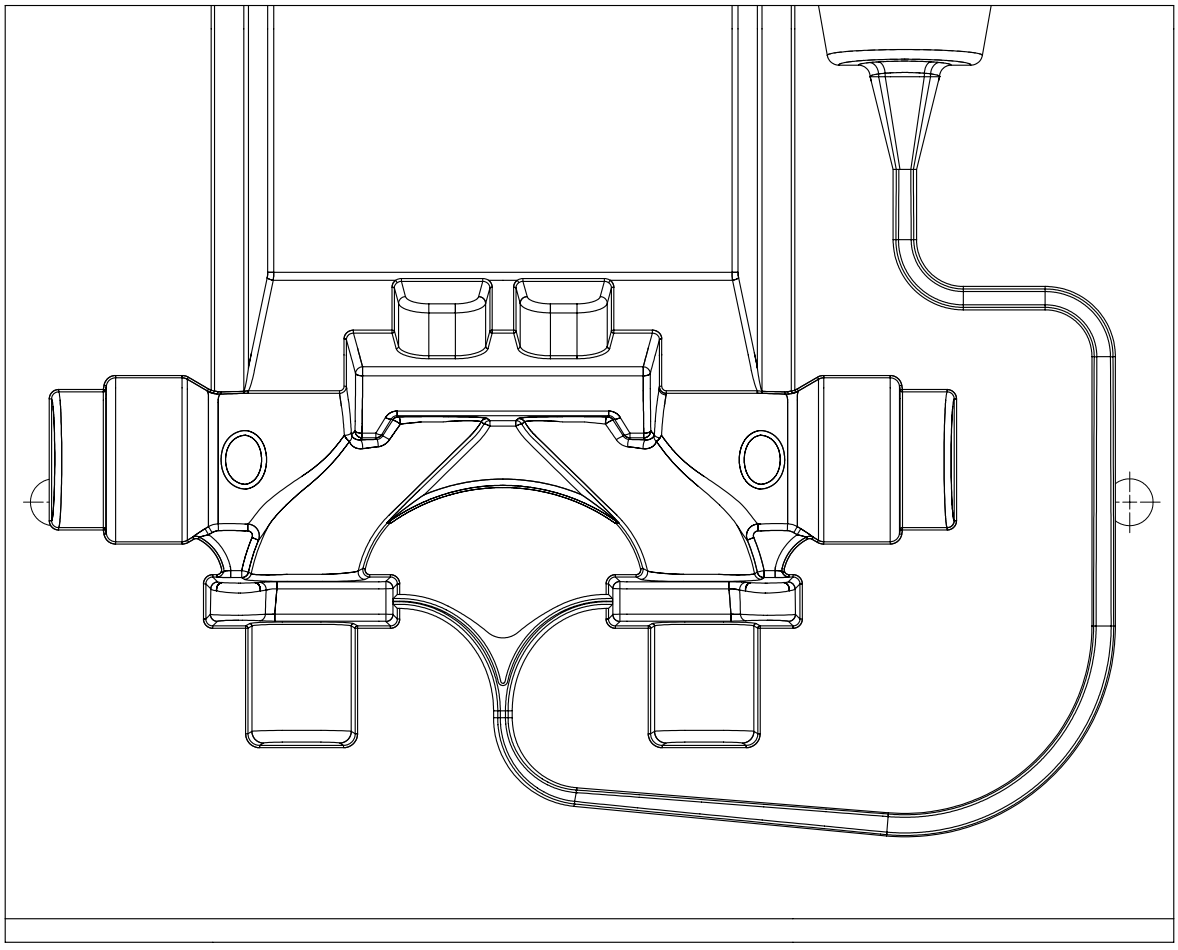

Figure 6.19 Second design of the gating system.

Instead of using the conventional transition from the pouring cup to the down runner it was decided to pour directly into the down runner. This design does not contain abrupt directional changes and hence does the main basis for getting vena contractas no exist.

125 mm below the top of the mould is a horizontal section build into the system. This is done to prevent the melt from having direct access from the pouring cup to the bottom of the mould. Even though the initial melt flow through the down runner of the first gating system took place with a coherent melt front showing no tendency to split up this extra security was build into the system. The 90 degree bend before the horizontal section of the runner and the horizontal section it self will act as a physical barrier for the melt and hence decrease the likelihood of the melt front splitting up. Due to the direct pouring into the down runner higher velocities than seen at the first gating system can also be expected enhancing the tendency for the melt front to split up as for instance is seen at layout no. 6 in section 5. Furthermore the two directional changes also introduce extra losses in spite of the stream lined design and hence they will reduce the maximum velocity at the bottom of the down runner.

A secondary advantage of the horizontal runner in the upper part of the gating system is the possibility to study the efficiency of making directional changes with curved sections as done here.

Narrow runners with 10 mm width at the pattern plate has at the first gating system proven to be an efficient design to secure coherent melt fronts. Hence runners with 10 mm width are also used for the second gating system. When it is wanted to increase the flow rate with 50 %, the cross sectional area of the runners have to be increased by 50 % also. To prevent the runners from getting extremely high due to the far larger cross sectional areas the runners have been placed symmetrically on both pattern plates, this also includes the ingate into the casting. To do so the part of the core seen on Figure 6.2 connecting the two tubes at the bottom of the pattern had to be removed.

The width of the horizontal runner at the bottom of the mould is gradually decreased from 10 mm to 8 mm. This is done to change the section the flow takes place in to a thinner and higher geometry. Thinner and higher inlets are wanted to have them to freeze as early as possible to minimize feeding of the gating system from the casting. Reducing the width of the horizontal runner from 10 to 8 mm and making the runner correspondingly higher means the change in section geometry can take place over a longer distance. In the fan shaped transition which splits the flow up into two the width of the runner is further reduced ending up with 6 mm at the inlet to the manifold.

6.6.2 Initial melt flow in the gating system

As with the first gating system a special pattern plate has been made, making it possible to record the melt flow in the gating system on video. At the second gating system the runners are positioned symmetrical on both pattern plates, hence it is not possible to capture the melt flow in a complete gating system if one mould half has to be changed to glass plates. To make it possible to record the melt flow on video only half a gating system has been used. I.e. the glass plates are in the symmetry plane of the gating system. This has also been done in [Ref. 6.8]. The influence on the filling times from the glass plates is in [Ref. 6.8] found to be insignificant. Furthermore the runners used here are very high and narrow. This means that the part of the circumference of the runner consistent of glass in stead of being a symmetry plane in the flow is relative low.

Two variants of the gating system shown on Figure 6.19 have been made for the trials with making videos of the metal flow.

One variant is made with a gradually increasing cross sectional area after the choke when compared to the needed area given by Eq. 6.1. The gradually increasing cross sectional area is intended for reducing the melt velocity before it enters the casting. The gating system can be seen on Figure 6.20.

Figure 6.20 Gating system with increasing cross sectional area after the choke.

Another variant is made where the cross sectional area of the runner after the choke strictly followings Eq. 6.1 plus a linearly increase in the cross sectional area of 0 - 10 % from the choke to the ingates. The linearly addition has been made to compensate for the losses in the system after the choke, to be sure that the melt flow is not choked further after it has passed the intended choke at the bottom of the layout. The gating system can be seen on Figure 6.21

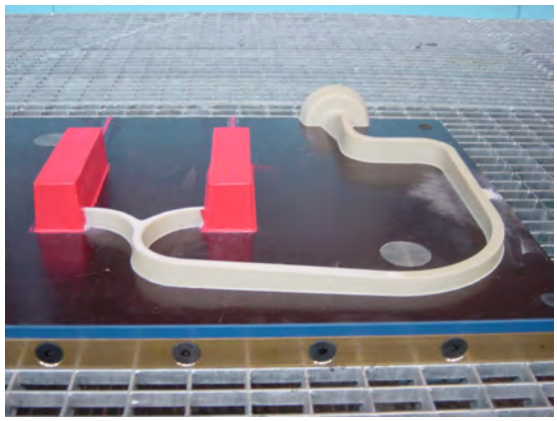

Figure 6.21 Gating system without increasing cross sectional area after the choke.

The cross sectional area of the part where the flow is split up into two is unfortunately not strictly following Eq. 6.1. The same negative for casting the two sets of gating systems had to be used and hence the reduction of the cross sectional area after the choke had to be made by milling the top of the runner away. This can be done rather precisely at the sections before and after the part where the runner splits up into two with a manually controlled milling machine. But the reduction of the height at the part where the runner splits up into two is a rather complicated geometry if the cross sectional area has to follow Eq. 6.1 strictly. It is not possible to pro-

duce it with a manually controlled machine precisely. After the flow has been split up into two the cross sectional area again strictly follows Eq. 6.1 plus the added safety margin.

When calculated without losses is the initial melt front velocity in the ingates of the layout with increasing cross sectional area 1.0 m/s. Without the increase in the cross sectional area is the initial melt front velocity in the ingate 2.0 mm/s. Both figures assume completely filled cross sections of the runners.

The difference in the heights of the ingates shown on Figure 6.20 and Figure 6.21 could indicate a larger difference in cross sectional area and hence also ingate velocity. But due to the 3 degree draft and the narrow section is the cross sectional area in the top of the runner relative small.

This idea with the two trials is to investigate whether an increase in the cross sectional area after the choke has an influence on the initial flow before back pressure is built up, or whether the melt continues as a jet, not influenced by the increasing cross sectional area like water coming out of a hose.

6.6.2.1 Gating system with increasing cross sectional area after the choke

The filling sequences of 4 moulds with each variation of the gating system were recorded on video. At each gating system were the flow patterns very similar from mould to mould.

Snapshots showing the first melt passing through the gating system with the increasing cross sectional area after the choke can be seen on Figure 6.22 shown on the following pages.

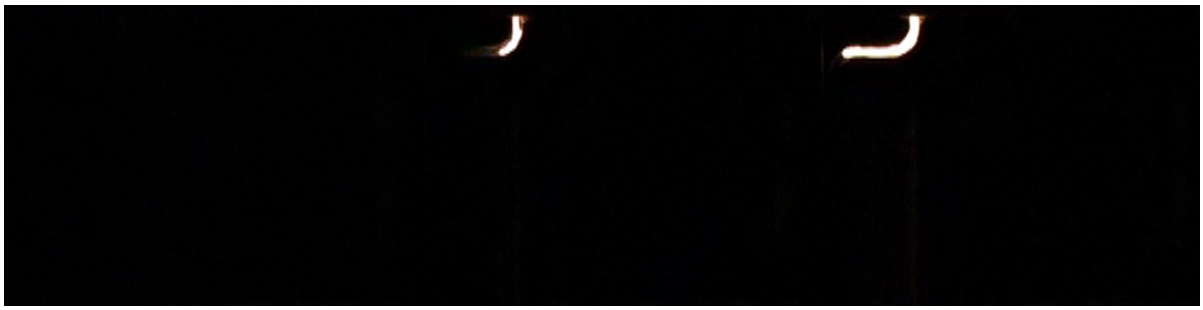

Time 0.00 Time 0.04 Time 0.08

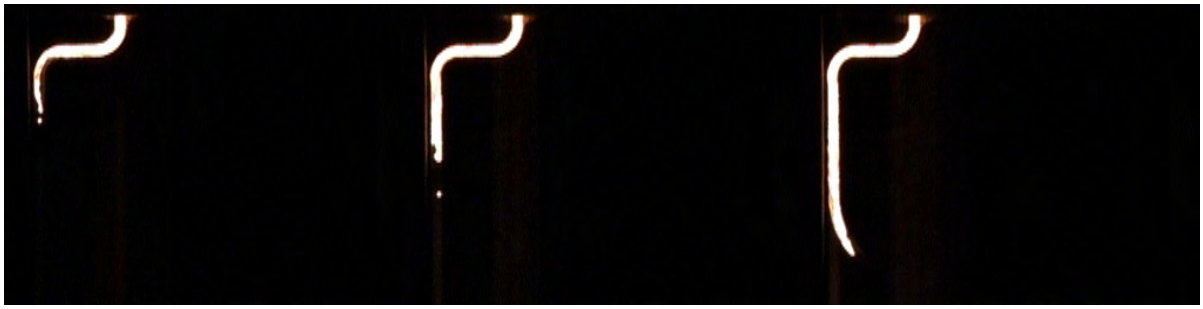

Time 0.12 Time 0.16 Time 0.20

Time 0.24 Time 0.28 Time 0.32

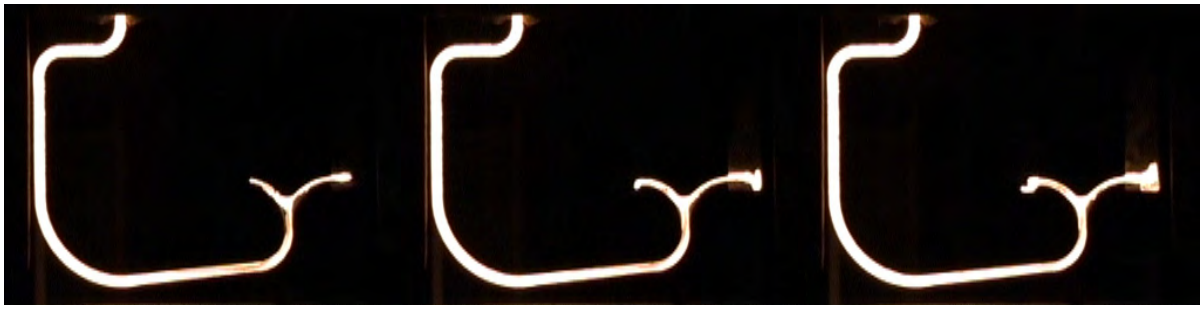

Time 0.36 Time 0.40 Time 0.44

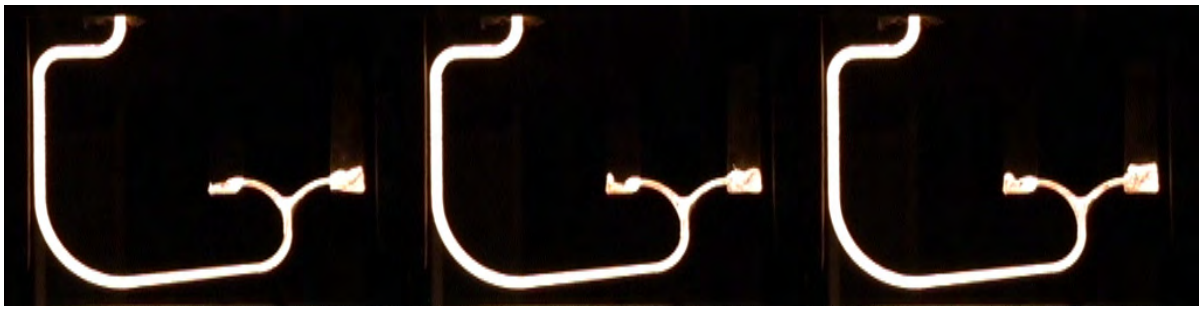

Time 0.48 Time 0.52 Time 0.56

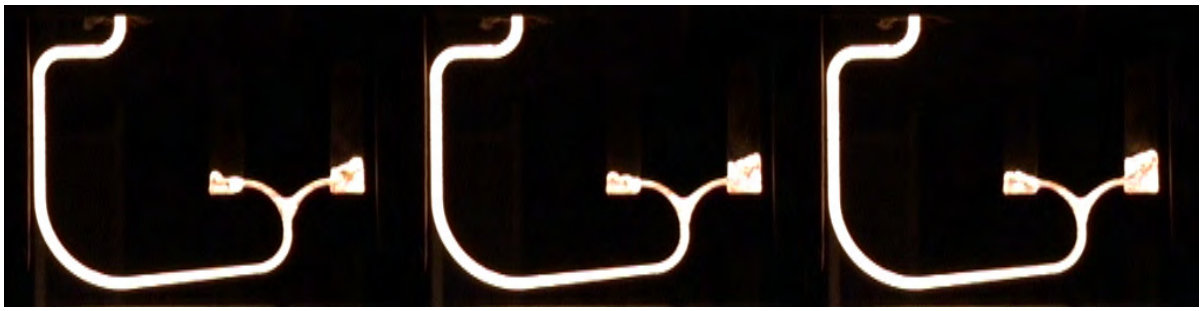

Time 0.60 Time 0.64 Time 0.68

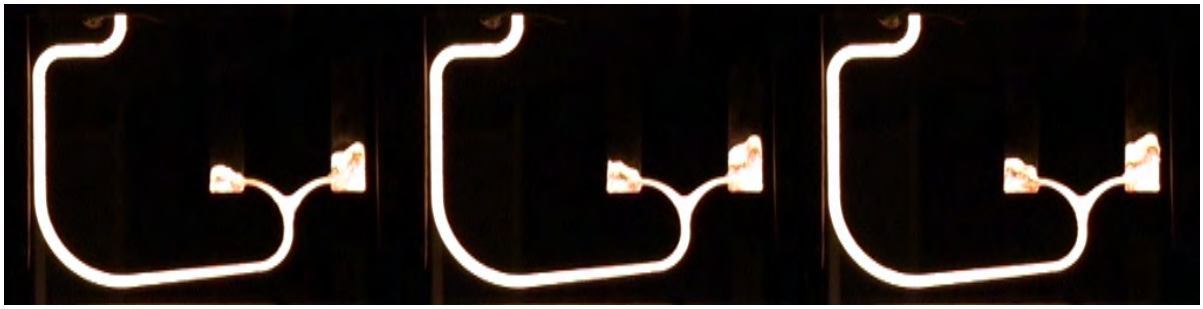

Time 0.72 Time 0.76 Time 0.80

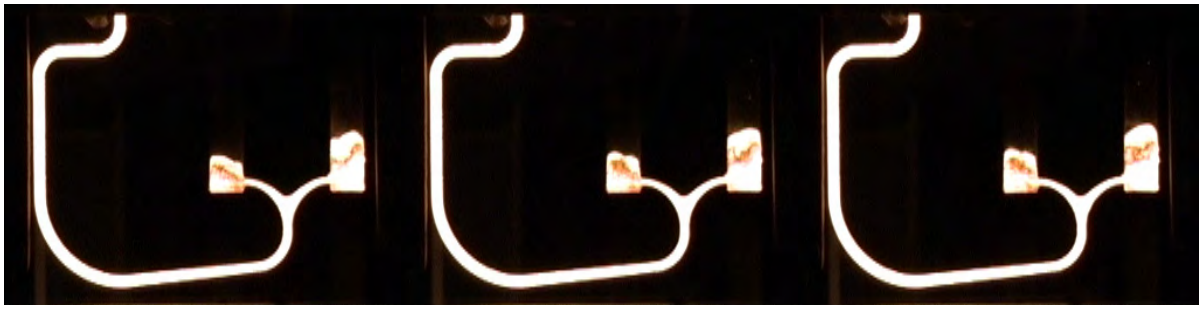

Time 0.84 Time 0.88 Time 0.92

Time 0.96 Time 1.00 Time 1.04

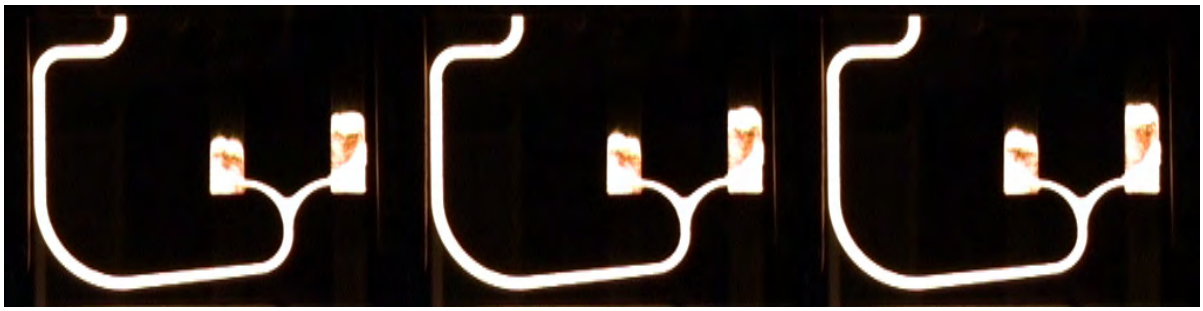

Time 1.08 Time 1.12 Time 1.16

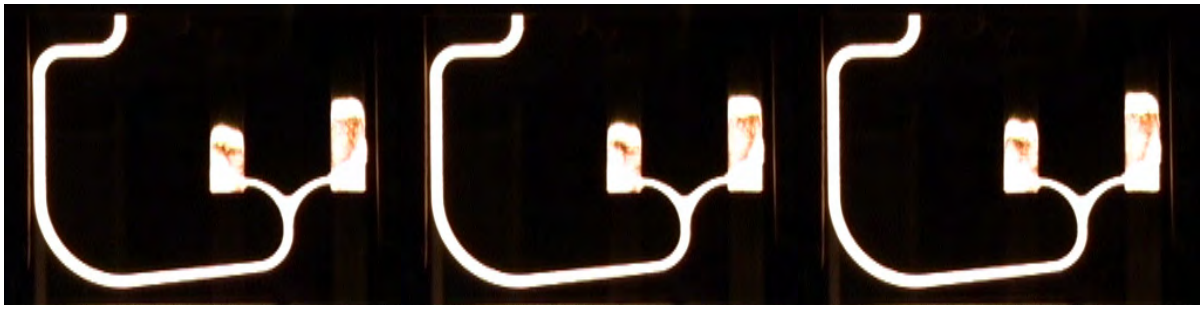

Time 1.20 Time 1.24 Time 1.28

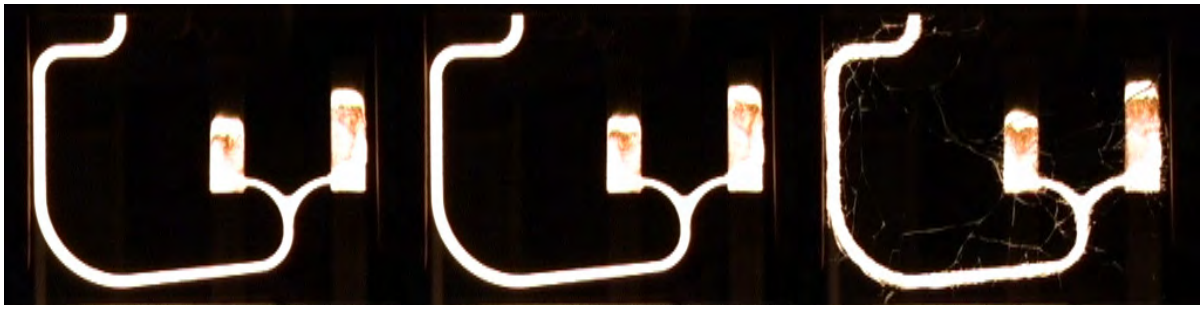

Time 1.32 Time 1.36 Time 1.40

Figure 6.22 Snapshots showing the initial melt passing through the gating system. The cross sectional area of the runner is increased linearly from the choke to the inlets. The glass starts to crack after 1.40 s.

The times given are from the melt front appears under the top core.

At 0.12 and 0.16 a single melt droplet disintegrates from the main melt front. Otherwise takes the filling of the gating system and the blocks place with coherent melt fronts. At the 3 other runs of the trial no droplets disintegrated from the main melt front. Hence the worst case has been chosen to be sure not to overestimate the performance of the gating system.

The cross sections of the runner are very close to be completely filled with the first melt passing through the system. At the snapshot at 0.12 s where the melt enters the down runner a melt tongue is approximately 50 mm ahead of the main melt front. At the next snapshot at 0.16 s the cross section of the runner is again filled completely behind the melt front. Apart from this incomplete filled runner cross section during 0.04 s are the two directional changes in connection with the horizontal section just below the pouring cup seen to perform as intended. It is possible to make directional changes with the radius used here without getting air pockets at the inside edges of the bend. The mean radius of the bend is 25 mm. The allowable minimum radius is depending on the velocity of the melt, i.e. on the vertical position in the mould.

The area just below the section where the runner is split into two is seen not to be completely filled with the first melt passing through at 0.32 s. Unfortunately it has not been possible to design the cross sectional area of this part to strictly follow Eq. 6.1. After 0.40 s the area is completely filled with melt.

The filling times for the blocks for run no. 2, 3 and 4 are respectively 1.68, 1.56 and 1.56 s. The mean value of the filling time is hence 1.60 s. The filling time for run no. 1 has been prolonged 0.8 s due to a leak between the glass plates and the mould caused by a falsely placed clamp. Using Eq. 6.5 to calculate the filling time of the blocks without losses results in a theoretical filling time of 1.16 s. Dividing the calculated filling time with the measured mean filling time of the blocks gives the loss coefficient. The loss coefficient is found to 0.72.

At the first gating system the loss coefficient was found to be 0.57. I.e. the losses in the system described in this section are significantly lower. The difference is found even though the two systems are similar except from the increased flow rate. The difference in the loss coefficients supports the theory of an artificial choke coming from the vena contracta at the transition from the horizontal extension of the pouring cup to the top of the down runner at the first gating system. The artificial choke results in a prolonged filling time.

The metal enters the blocks after 0.40 s. The initial flow into the blocks is relative calm; no splashed are seen.

In the gating system described in this section no abrupt directional changes are made and hence the main basis for getting vena contractas has been removed.

6.6.2.2 Gating system without increasing cross sectional area after the choke

Snapshots showing the first melt passing through the system with the cross sectional area after the choke following Eq. 6.1 strictly as described in section 6.6.2 can be seen on Figure 6.23 on the following pages.

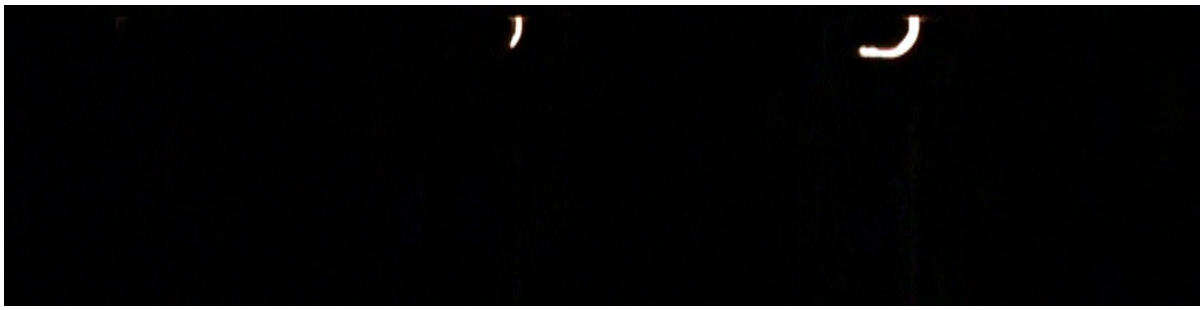

Time 0.00 Time 0.04 Time 0.08

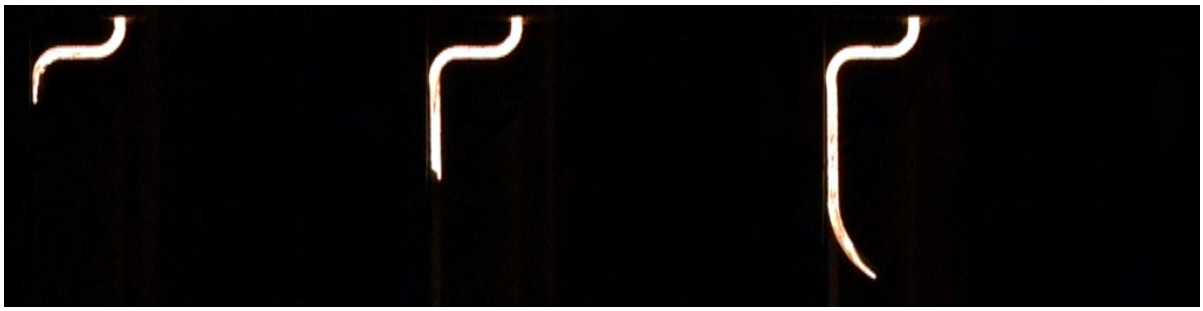

Time 0.12 Time 0.16 Time 0.20

Time 0.24 Time 0.28 Time 0.32

Time 0.36 Time 0.40 Time 0.44

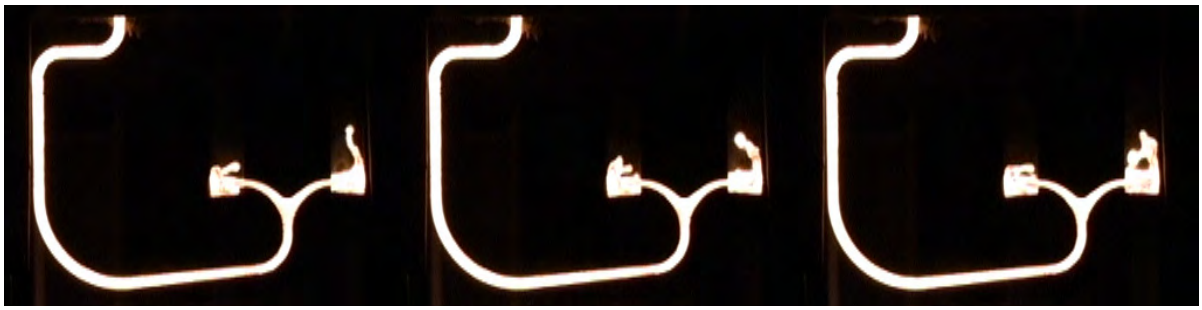

Time 0.48 Time 0.52 Time 0.56

Time 0.60 Time 0.64 Time 0.68

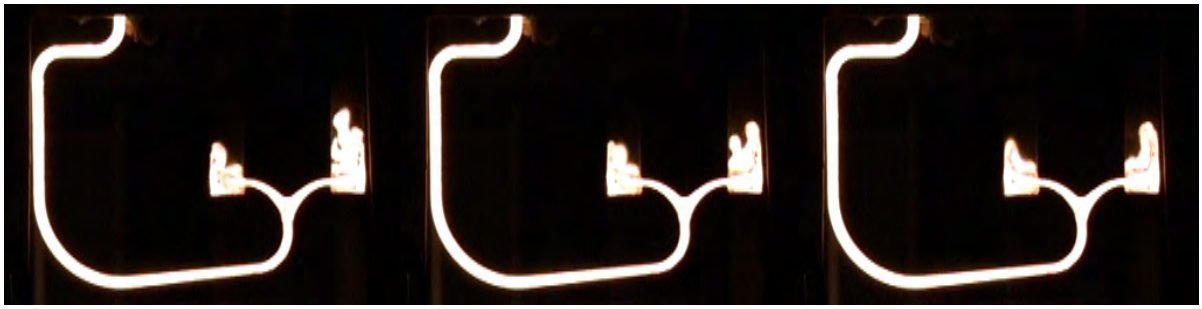

Time 0.72 Time 0.76 Time 0.80

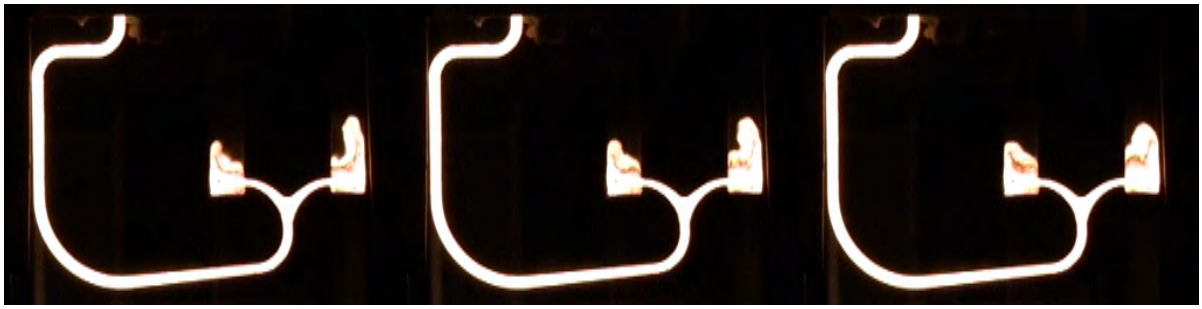

Time 0.84 Time 0.88 Time 0.92

Time 0.96 Time 1.00 Time 1.04

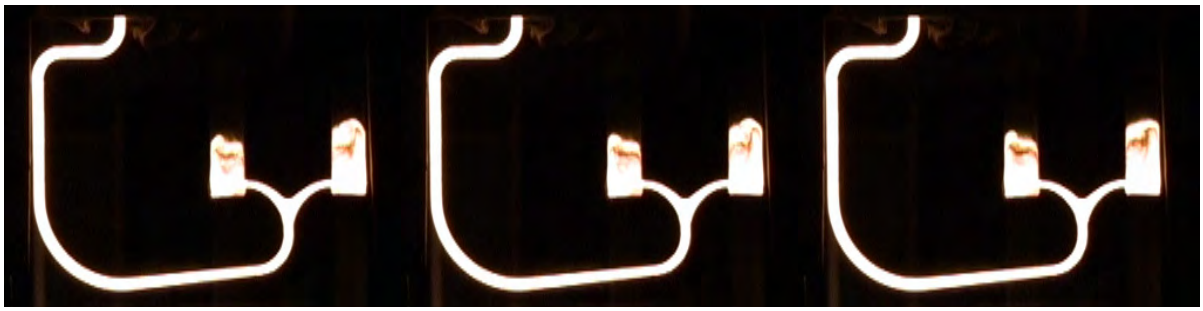

Time 1.08 Time 1.12 Time 1.16

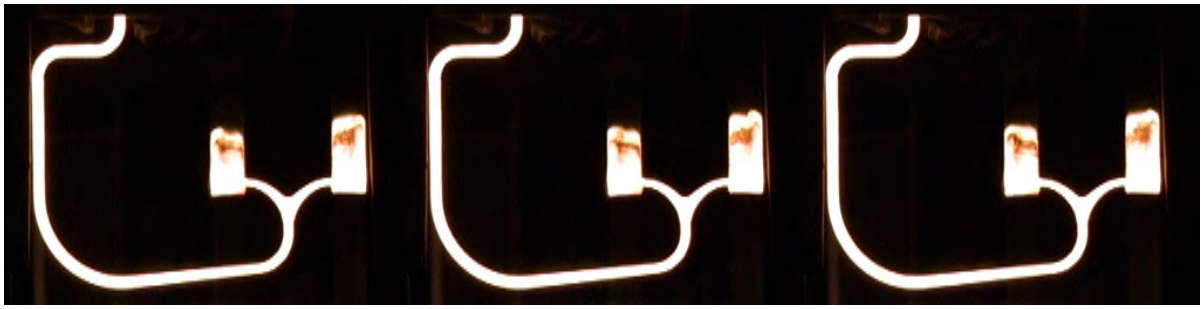

Time 1.20 Time 1.24 Time 1.28

Time 1.32 Time 1.36 Time 1.40

Figure 6.23 Snapshots showing the initial melt passing through the gating system. The cross sectional area of the runner is strictly following Eq. 6.1.

The times given are from the melt front appears under the top core.

The filling of the gating system is seen to take place with coherent melt fronts. This is the case for all 4 runs of the trial.

As with the gating system with the increasing cross sectional area after the choke, is the cross sections of the runner close to completely filled with the first melt passing through. The area just below the section where the runner is split into two is seen not to be completely filled with the first melt passing through at 0.32 s. Unfortunately it has not been possible to design the cross sectional area of this part to strictly follow Eq. 6.1. After 0.36 s the area is completely filled with melt. This design of this section has to be developed further to have the cross sectional area to follow Eq. 6.1 strictly. The cross sectional area after the section where the runner is split into two again follows Eq. 6.1 strictly plus a linearly addition of 10 % to compensate for losses in the runners after the choke as described in section 6.6.2.

The metal enters the two blocks after 0.40 s. The initial flow in the blocks is rather turbulent with a melt fountain almost going to the top of the block shaped cavity.

The mean filling time for the blocks is 1.99 s for the 4 runs. As with the gating system with an increasing cross sectional area after the choke is the theoretical filling time of the blocks 1.16 s when calculated without losses. This results in a loss coefficient of 0.58.

6.6.3 Comparison of the initial flow in the two gating systems

The 4 moulds with each gating system have been poured alternately. Hence no effects from possible changes in the melt etc. with time can have caused significant differences between the filling patterns of the two gating systems, and between the filling patterns seen for each of the two gating systems.

The initial flow into the blocks for the two variants of the gating system can be seen on Figure 6.22 and Figure 6.23. In both cases is the flow entering the blocks after 0.40 s. When comparing the initial flow into the blocks the gating system without an increasing cross sectional area is seen to result in a very turbulent flow.

This means the velocity of the melt is reduced in the gating system with a gradually increasing cross sectional area after the choke, the melt is not continuing as a jet. I.e. is possible to reduce the velocity of the melt by increasing the cross sectional area gradually when narrow runners are used. In this case the cross sectional area is increased with a factor of 2.

The loss coefficient for the gating system with an increasing cross sectional area is found to 0.72, for the gating system without an increasing cross sectional area is the coefficient found to 0.58. I.e. a significant difference can be seen even though the gating systems are very similar from a geometrical point of view.

The difference comes from the melt velocities after the choke. The initial melt velocity in the inlets of the gating system with an increasing cross sectional area after the choke is 1 m/s when calculated without losses. The same value for the gating system without an increasing cross sectional area after the choke is 2 m/s. The higher velocities result in higher losses.

When multiplying the theoretical initial velocities in the inlets with the corresponding loss coefficients are estimates for the real initial velocities in the inlets found. They are found to be 0.72 m/s for the runner with the increasing cross sectional area after the choke, and 1.16 m/s for the gating system without an increase in the cross sectional area after the choke. I.e. the ratio between the real initial velocities in the inlets is 1.6. When calculated without losses is the ratio found to be 2. Hence the real difference between the velocities in the two variants of the layout is significantly smaller than what is the case when calculated without losses.

6.6.4 Uniformity of the filling sequences

The filling of the gating systems with and without an increasing cross sectional area after the choke has been recorded 4 times each on video. This makes it possible to examine the uniformity of the flow patterns from mould to mould.

6.6.4.1 Gating system with increasing cross sectional area after the choke

The melt distribution at the 4 runs after 0.32 s in the gating system with an increasing cross sectional area after the choke can be seen on Figure 6.24 below:

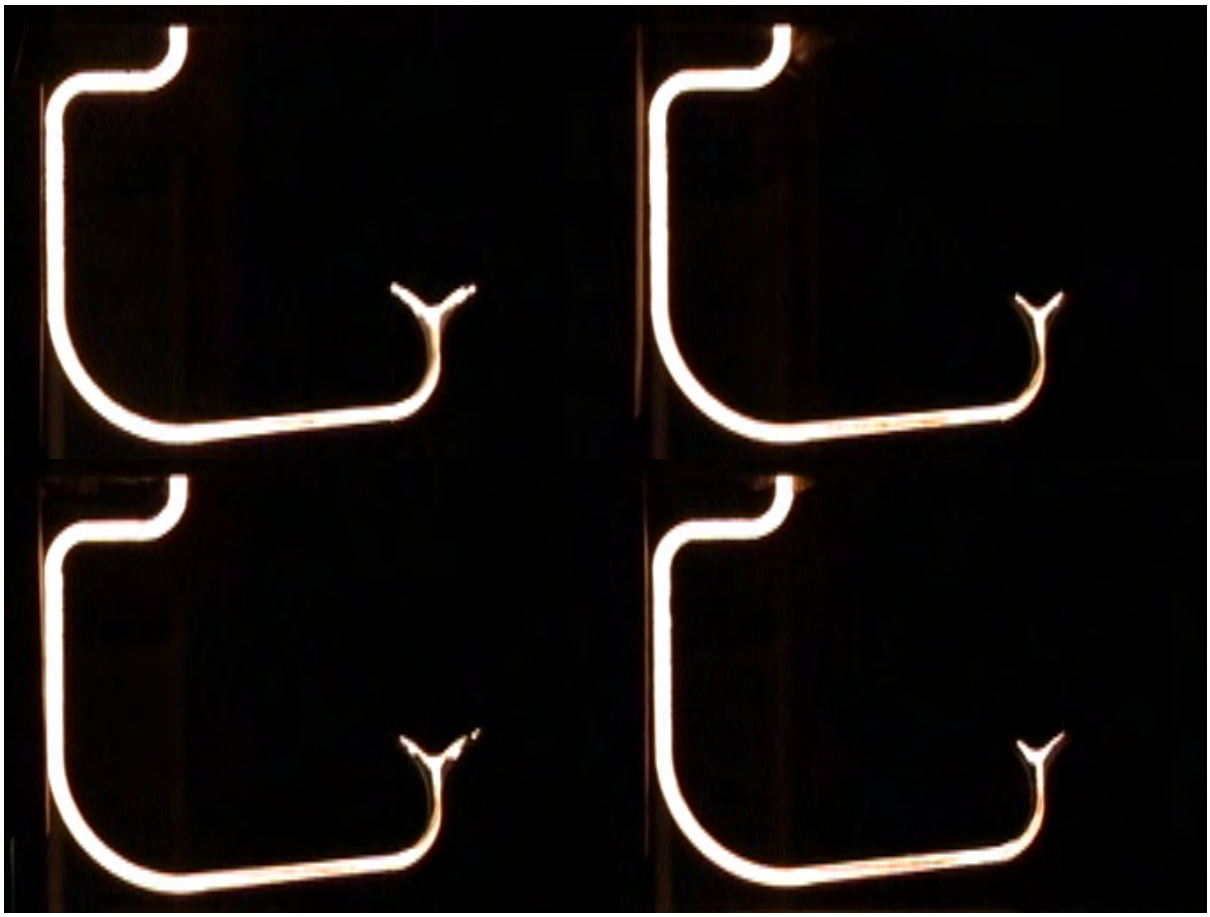

Figure 6.24 Melt distribution in the 4 runs after 0.32 s. The cross sectional area of the runner is increased linearly from the choke to the inlets.

Further sets of snapshots showing the uniformity of the flow in the 4 runs can be seen in Appendix 6.4. The largest difference between the 4 runs is the droplet seen on the lower right picture after 0.16 s in Appendix 6.4. Otherwise are the flow patterns very similar at the 4 runs.

After 1.44 s is a leak appearing between the glass and the mould at run no. 1. This prolongs the pouring time of the mould compared to the 3 others.

6.6.4.2 Gating system without increasing cross sectional area after the choke

The melt distribution at the 4 runs after 0.32 s in the gating system without an increasing cross sectional area after the choke can be seen on Figure 6.24 below:

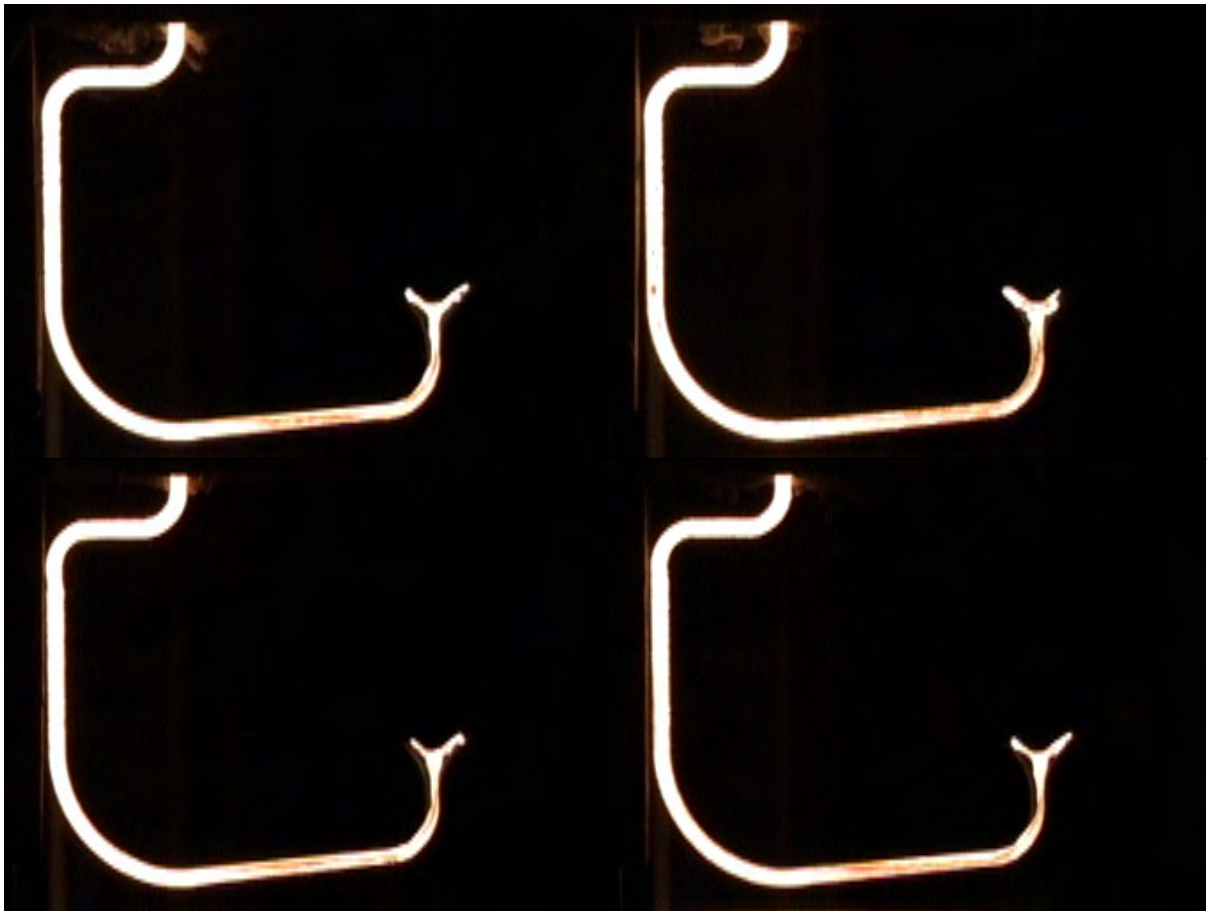

Figure 6.25 Melt distribution in the 4 runs after 0.32 s. The cross sectional area after the choke follows Eq. 6.1 strictly.

Further sets of snapshots showing the uniformity of the flow in the 4 runs can be seen in Appendix 6.5. The largest difference between the 4 runs is the only partly filled down runner seen on the upper right picture after 0.16 s in Appendix 6.5. At the snapshots before and after this picture i.e. 0.04 s before and after is the cross section of the down runner completely filled. Otherwise are the flow patterns very similar at the 4 runs.

6.6.5 Filling of the manifolds

With the layout shown on Figure 6.19 it was possible to fill the manifolds with 2 and 2.5 mm wall thickness. The result for the manifold with 2 mm wall thickness can be seen on Figure 6.26.

Figure 6.26 Manifold with 2 mm wall thickness cast with the second gating system.

The gating system is designed for an initial melt front velocity in the tubes of 600 mm/s at the manifold with 2 mm wall thickness. The 600 mm/s is when calculating without losses in the gating system. The gating system used for casting the manifolds is with the increasing cross sectional area after the choke. The loss coefficient for this gating system when connected to the blocks used in the trials for making videos of the flow is in section 6.6.2.1 found to be 0.72. The total loss will be larger when the metal enters the 2 mm thick sections of the manifold. For the initial part of the filling, 0.72 will although be a reasonable estimate for the loss. Hence the initial melt velocity in the 2 mm section of the manifold is estimated to 432 mm/s.

The manifold with 2.5 mm wall thickness was also cast using this gating system. As at the 2 mm wall thickness it was possible to fill the manifold with 2.5 mm wall thickness. Due to the larger wall thickness the initial velocity in the tubes is lower than at the manifold with 2 mm wall thickness. The initial velocity in the tubes when calculated without losses is 498 mm/s at the manifold with 2.5 mm wall thickness. When multiplying with the loss coefficient found for the filling of the blocks an estimate for the real initial velocity in the tubes is found. This yields 359 mm/s.

6.7 Discussion of the results

No pressure shock waves have been observed in the 12 runs where the filling sequences have been captured on video. Furthermore, the glass plates did not break completely in any of the trials only cracks were seen. At the trials made with the plate castings described in section 4 both the thermal and mechanical impacts on the glass were significantly lower apart from possible pressure shock waves. The glass plates broke from time to time in the plate trials, but it did not break in the trials described in this section. This also indicates that no pressure shock waves have been initiated here.

No dead ends below the pouring cup exists in the gating systems investigated in this section. The runners have been close to completely filled from the first melt passing through. The two things together means no basis exists for initiating pressure shock waves.

3 different gating systems have been investigated in this section. The melt flow patterns at each gating system are shown to be very uniform form mould to mould. In section 4.7.2.2 flow patterns are also compared from mould to mould. In that section a conventional gating

system was used. At the conventional gating system significant differences in the flow patterns from mould to mould could be identified. Compared to this the flow pattern seen here varies very little from mould to mould.

The pouring basin has been used for all the tests. This means the difference in the uniformity of the flow patterns from mould to mould between the gating systems described in section 4.7.2.2 and the gating systems described in this section can not be due to differences in the pouring conditions. Hence it can be concluded that the gating systems used in this section give a higher degree of stability from mould to mould. They are able to absorb minor but inevitable changes from mould to mould in the pouring conditions.

Securing uniform mould filling from mould to mould is very important as it means getting a more stable process. Things like “unexplainable” casting defects appearing from time to time are reduced when the process is getting more stable. Having a more stable process means lower scrap levels and also the possibility to run with smaller safety margins. Both factors increase the efficiency of the foundry.

The initial velocity in the ingates has been varied from 0.36 m/s over 0.72 m/s to 1.16 m/s. At the two lower velocities is the initial filling of the blocks relatively calm. At 1.16 m/s the initial filling of the blocks is very turbulent with fountains approximately 100 mm high. Hence when passing through an abrupt increase in the cross sectional area and hitting a wall after approximately 40 mm, as is the case when the melt leaves the narrow runner and enters the blocks, a maximum velocity somewhere between 0.72 and 1.16 m/s, can be allowed if calm flow is wanted. At the trials with the initial melt front velocity in the inlets of 0.72 m/s and 1.16 m/s the cross section of the inlet was 6 mm wide at the pattern plate. At the trials with 0.63 m/s initial melt front velocity in the inlets, the inlet was 10 mm wide at the pattern plate.

The found loss coefficients for the 3 gating systems investigated in this section vary some. The first gating system was designed to result in an initial melt velocity in the 2 mm section of the manifold of 400 mm/s. For this gating system the loss coefficient was found to be 0.57. A vena contracta was identified at the transition from the horizontal extension of the pouring cup to the top of the down runner. The vena contracta introduces an artificial choke into the system prolonging the pouring time compared to the one calculated on the basis of the intended choke at the bottom of the down runner. In the case of the gating system with the artificial choke the real velocity in the inlet is approximately 0.36 m/s for the initial flow when assuming completely filled runner cross sections. I.e. relative low velocities are seen. The cross section used for the runners is 10 mm wide at the pattern plate with 3 degree draft, which is a relative large cross section when talking losses. The combination of relative low velocities and relative wide runners would normally mean low losses reflected in a larger loss coefficient than the 0.57 found here. But as described above an artificial choke due to a vena contracta reduces the melt flow.

The second and the third gating system is the same except for the size of the runner after the choke. In the second gating system the cross sectional area after the choke has been increased. The real melt velocity in the inlets is 0.72 m/s for the initial flow. The loss coefficient for this system is found to be 0.72. In the third gating system the cross sectional area after the choke has only been increased slightly to compensate for the losses in the system after the choke. With this tight design of the cross sectional area after the choke is the real melt velocity in the inlets 1.16 m/s for the initial flow. The loss coefficient for this system is found to be 0.58 re-

flecting higher losses in the system compared the previous. Hence when increasing the melt velocities the losses also increase.

No vena contractas are seen in the second and third gating system. Hence the loss coefficients found for these two systems can be seen as real loss coefficients as no artificial chokes are present in the systems.

In general relative low melt velocities are seen in the gating systems used in this section. This is partly due to the designs aimed at reducing the velocity after the choke, and partly due to the relative low mould height limiting the maximum melt velocity at the bottom of the mould. When going to larger moulds giving higher maximum velocities at the bottom of the mould, higher loss coefficients can be expected, as the losses depend on the velocity. At higher moulds it will also be more difficult to obtain the same low velocities in the ingates as seen here since a larger reduction of the velocity than seen here will be necessary.

It has been possible to cast the manifold with 2 mm wall thickness without any visible defects coming from the filling. The initial melt front velocity in the 2 mm section is approximately 430 mm/s. Figure 6.22 show snapshots of the initial melt passing through the gating system. When the melt enters the blocks after 0.40 s, the melt flow in the blocks is relatively calm. The blocks simulate the flanges on the manifold where the inlets are attached to. The calm flow means the flanges can be expected to be completely filled before the melt enters the tubes with the 2 mm wall thickness. When the flanges are completely filled before the melt enters the tubes the full metallostatic pressure is present when the metal enters the tubes giving a very steady filling. Furthermore the gating system is shown to result in very consistent flow patterns from mould to mould. This also promotes the filling of the very thin sections. This is due to the fact, that in gating system giving different flow patterns from mould to mould melt tongues are often seen to be blown ahead of the main melt front. These melt tongues will have time to cool before the main melt front arrives and hence the filling of the thin sections is disturbed.

The performance of gating systems giving very equal flow patterns from mould to mould can a little simplistic be describes as either does the gating system work or not.

6.8 Conclusions

From the trials the following can be concluded:

- If the transition from the pouring cup to the down runner is made in the conventional way with an overlap and a spout shaped geometry of the top of the down runner it is very difficult to avoid a vena contracta at the top of the down runner where the metal has to make a relatively sharp bend. This can be seen on Figure 6.12. The vena contracta acts as an artificial choke, if the top cross sectional area of the down runner is not designed with a sufficiently large safety margin. The vena contracta is seen even though a very stream lined design has been utilized.

- The appearance of a vena contracta will act as an artificial choke if the gating system has not been designed with a sufficiently large safety margin. The vena contracta can hence prolong the pouring time compared to the theoretical pouring time found without losses.

The result is seemingly higher losses in the system, but the explanation is an artificial choke.

- When using narrow runners 10 mm wide at the pattern plate as done here coherent melt fronts can be obtained. Hence droplets in front of the main melt front are efficiently prevented with the narrow runners.

- The gating systems investigated in this section have been designed without dead ends below the pouring cup. Furthermore has a design been utilized promoting completely filled runner cross sections right from the first melt passing through the system. The two things together have been able to prevent pressure shock waves. Hence relatively calm flows without splashes have been obtained.

- The geometries of the gating systems designed in this section are very restrictive compared to conventional gating systems. The result is very uniform flow patterns from mould to mould when comparing to what is seen for conventional gating systems. A more stable process results in a reduction of “unexplainable” casting defects appearing from time to time. Having a more stable process means it is easier to reduce the scrap levels and also make it possible to run with smaller safety margins. Both factors increase the effectiveness of the foundry.

- It is possible to reduce the melt velocity of the initial melt passing through the gating system by a gradual increase in the cross sectional area after the choke. In this case the cross sectional area has gradually been increased 100 %.

- With the narrow runners used here an abrupt increase in the cross sectional area and the melt hitting a wall after approximately 40 mm, will mean turbulent flow with a fountain like appearance if the velocity is exceeding a value somewhere between 0.72 and 1.16 m/s.

- Increasing the velocities in the narrow runners increases the losses in the system. For a gating system with an initial melt velocity in the inlets of 0.72 m/s the loss coefficient is found to be 0.72. For a similar gating system with an initial melt velocity in the inlets of 1.16 m/s the loss coefficient is found to be 0.58. The runners in the two gating systems have a narrow geometry with the same width at the pattern plate only the height has been chanced to change cross sectional area and hence the velocities.

- With the very stream lined gating system it has been possible to cast an exhaust manifold with 2 mm wall thickness with no visible defects coming from the filling. The initial melt velocity in the 2 mm sections is approximately 430 mm/s.

References

Ref. 6.1 Marktberichte / Marktstudien 30.01.04-6.02.04 (KW 6) VDMA (2004)

Ref. 6.2 Hochleistungsfähige Gußwerkstoffe für Abgaskrümmer und Turbolader-Turbinengehäuse. Wilhelm Kallen, Klaus Röhrig. Konstruieren + gießen 26 (2001) Nr. 4

Ref. 6.3 High performance cast materials for exhaust manifolds and turbocharger housings. W. Kallen, J.C. Morrison, K. Röhrig. Paper on 40th Foundry Conference in Portoroz 18th – 16th of May 2000

Ref. 6.4 DISA Industries Application manual Reg. No. 9152H2111 Edition 09/95 (1995)

Ref. 6.5 Castings. John Campbell. Butterworth Heinemann (2002)

Ref. 6.6 Aluminium Castings made in Vertically Parted Green Sand Moulds. Ph.D. Thesis by Niels Winther Rasmussen. The Technical University of Denmark (1998)

Ref. 6.7 Flow through bends in gating systems. Final report for EDP 005MUP2 Niels Tiedje (1997)

Ref. 6.8 Flow Analysis of mould filling using high speed motion pictures of the metal. Water modeling and numerical calculations. Preben Ingerslev and Svend Thorhauge Andersen Technical University of Denmark Institute of Manufacturing Materials 1987

Appendix 6.1

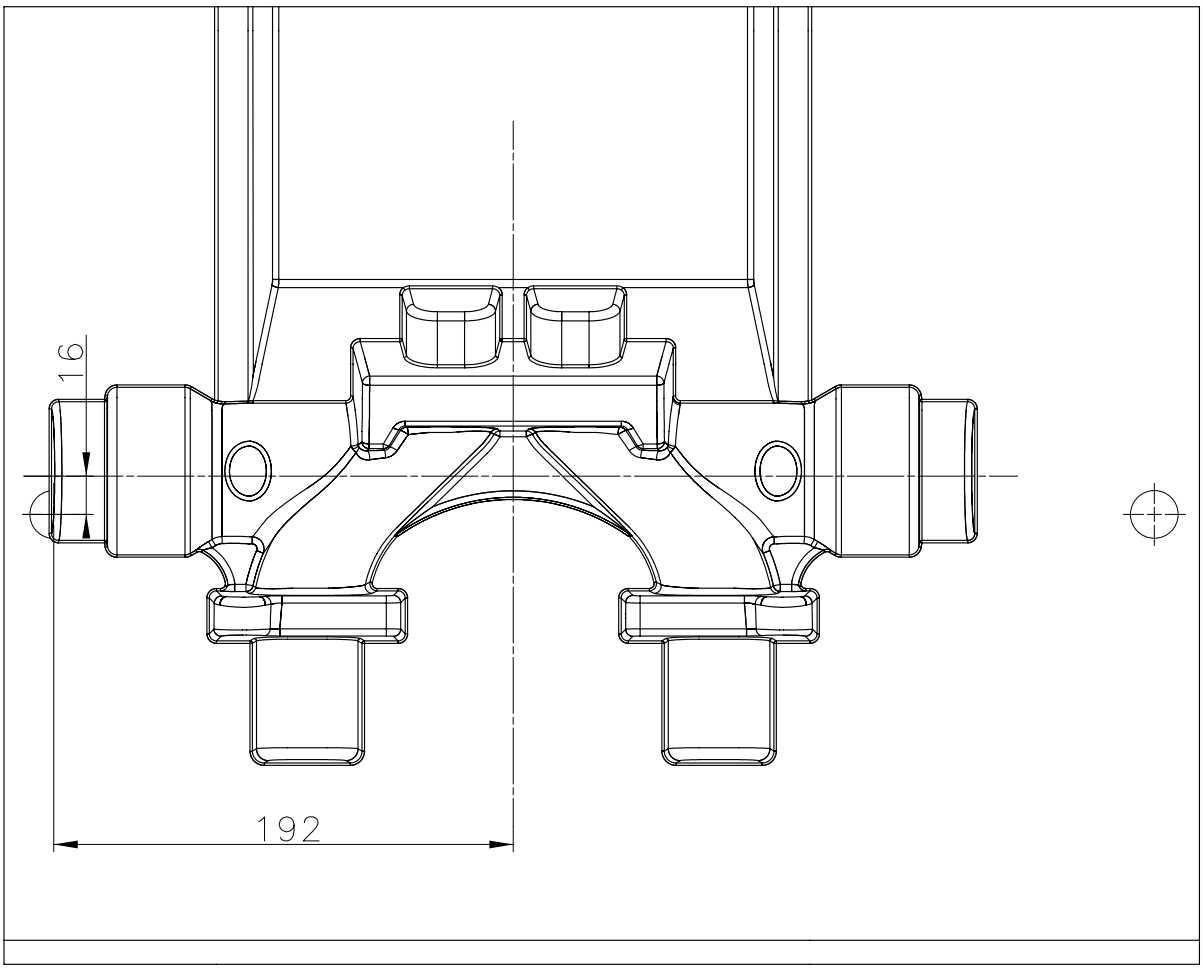

Appendix 6.2


Cross section areas of the down runner as a function of the distance to the top of the mould
Area [mm2]
% Difference
Distance from the top of the mould [mm]
700
650
600
550
500
450
400
350
300
250
200
25
20
15
10
5
0
70
100
130
160
190
220
250
280
310
340
Nominal Area
1D taper
2D taper
% Difference

Appendix 6.3

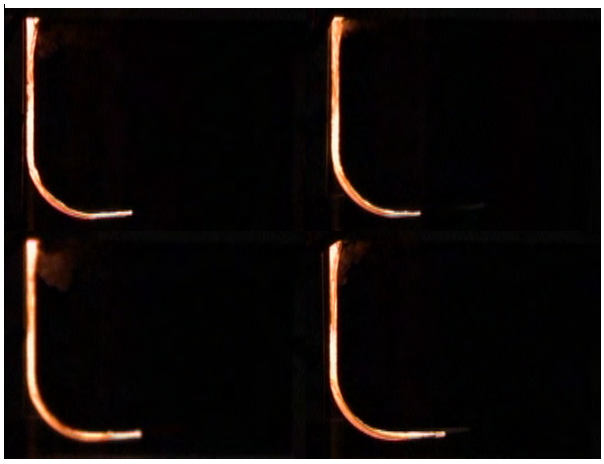

Time 0.16 s

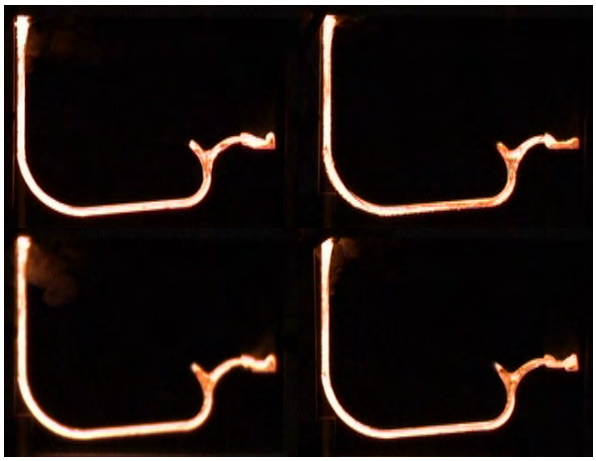

Time 0.48 s

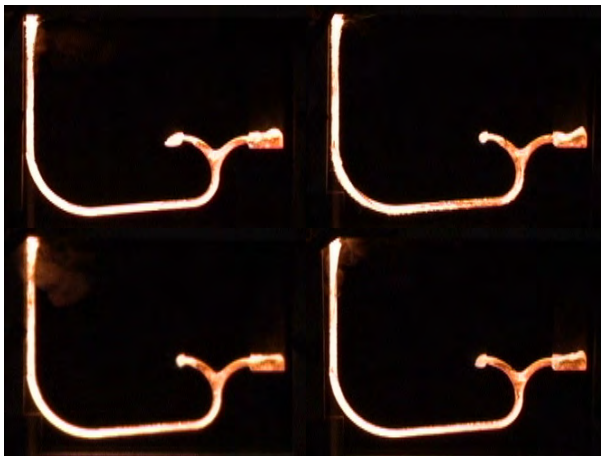

Time 0.64 s

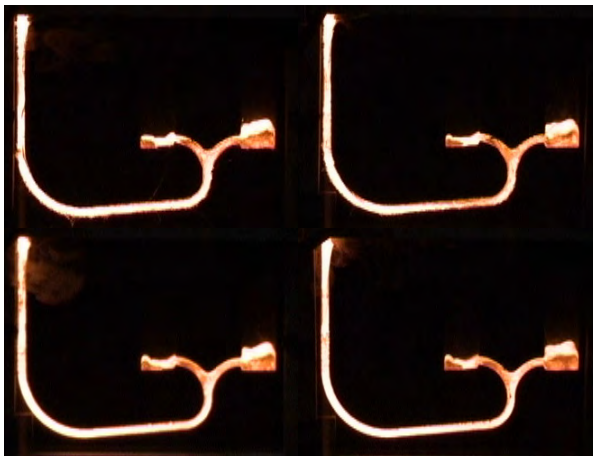

Time 0.80 s

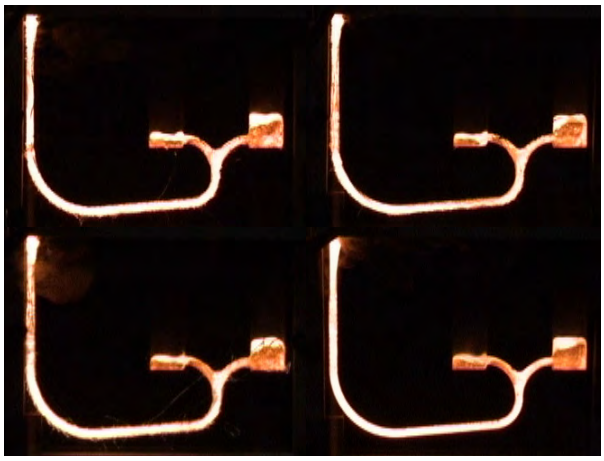

Time 0.96 s

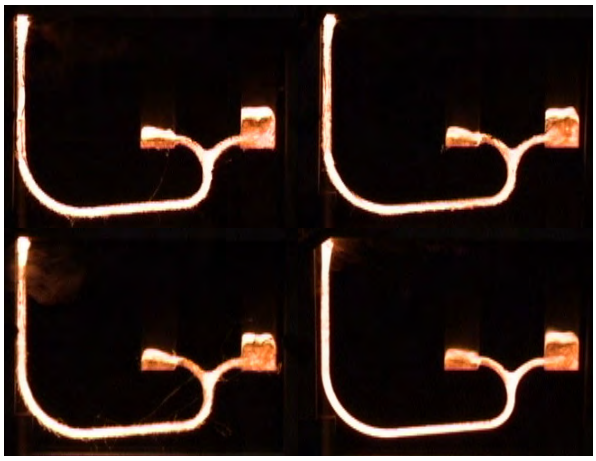

Time 1.12 s

Appendix 6.4

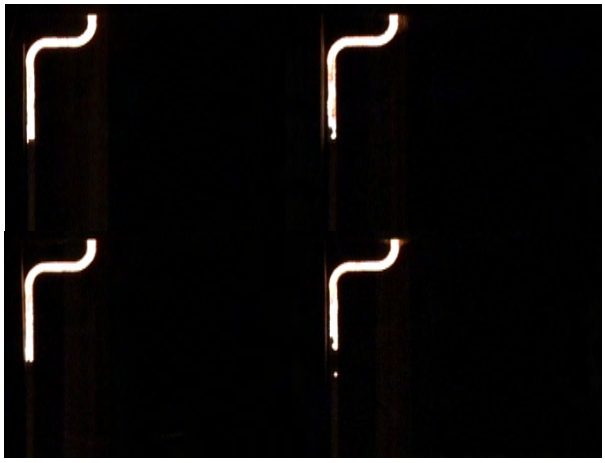

Time 0.16 s

Time 0.24 s

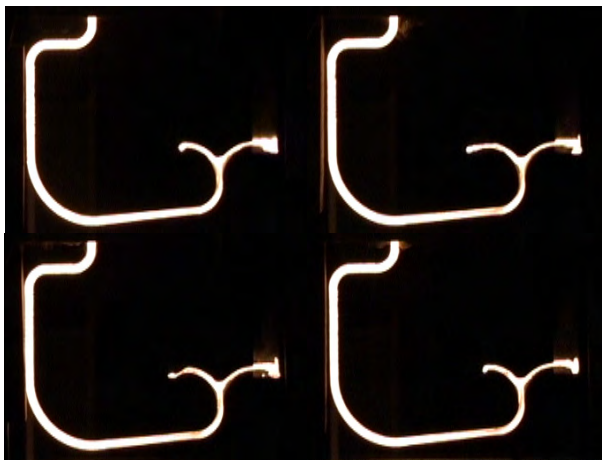

Time 0.40 s

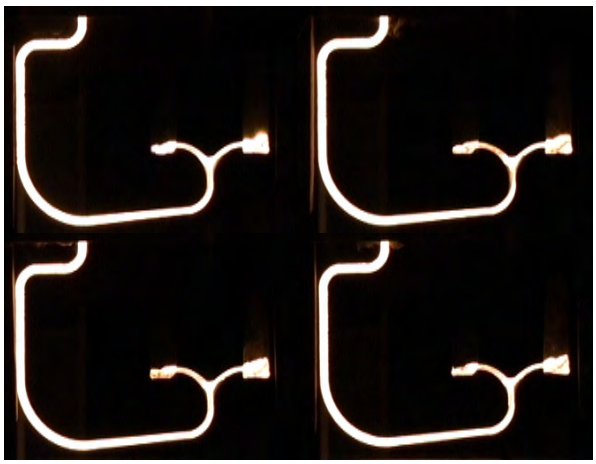

Time 0.48 s

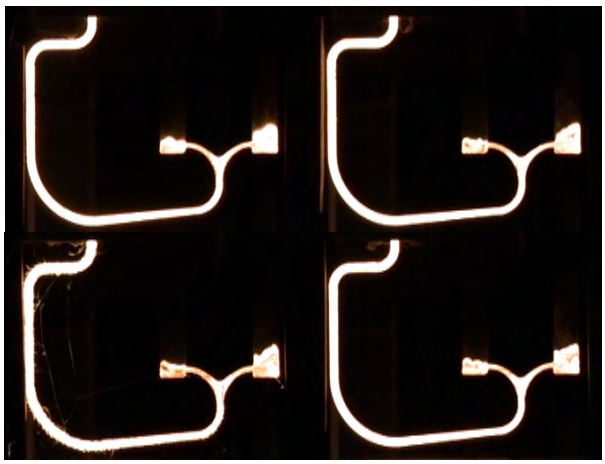

Time 0.64 s

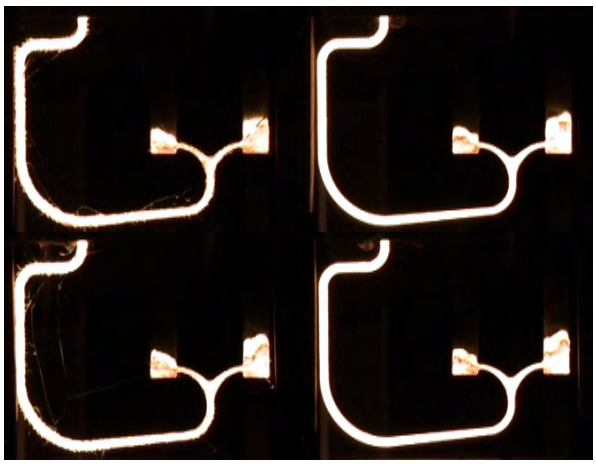

Time 0.80 s

Appendix 6.5

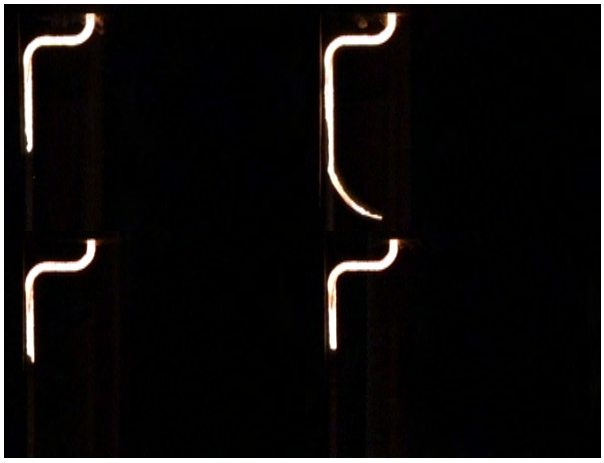

Time 0.16 s

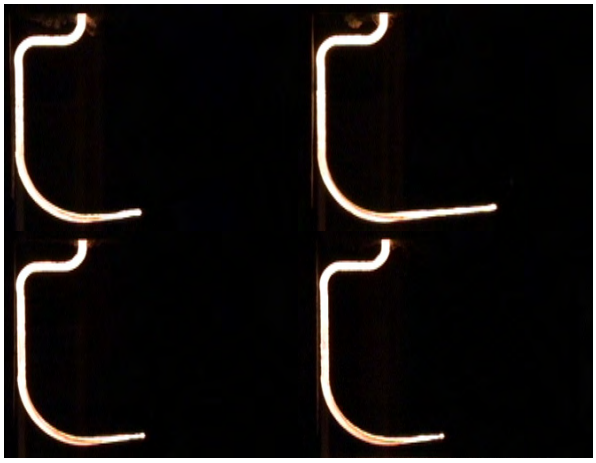

Time 0.24 s

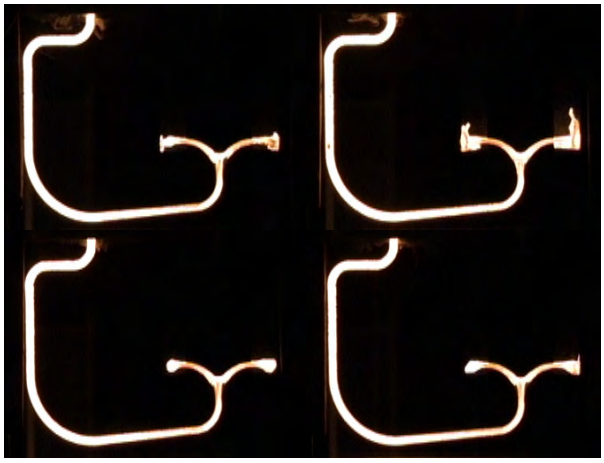

Time 0.40 s

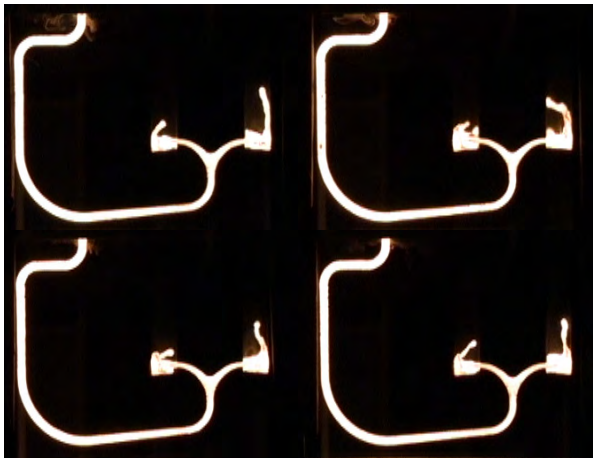

Time 0.48 s

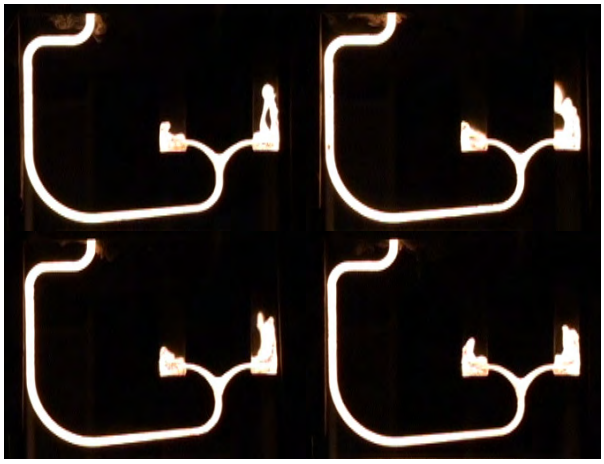

Time 0.64 s

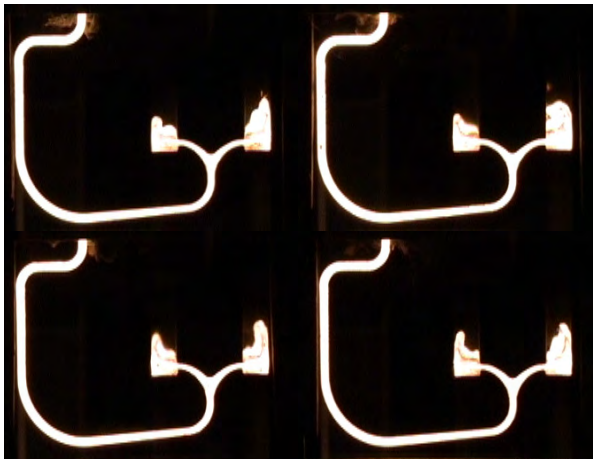

Time 0.80 s

7 Conclusions

Melt flow in thin sections have been investigated. Both conventional and non-conventional gating systems have been examined. Trials including video recordings of the real metal flow in the mould cavities have been conducted.

The following have been shown through the trials:

In gating systems containing dead ends, pressure shock waves are likely to appear due to the melt coming to an abrupt standstill at the dead end. This is the case when the cross section of the runner is completely filled behind the melt front. The pressure shock waves are able to make the melt front disintegrate and drive melt droplets far ahead of the main melt front.

In the case of partly filled runners, the closing of the last air pocket in the runner can also result in a pressure shock wave being able to break the melt front up into droplets.

When designing for calm flow normally only velocity criterions are used, but transient phenomena such as pressure shock waves may affect the melt flow to a much larger degree than the velocity itself. These will have to be avoided to be sure to obtain calm flow without disintegrations of the melt front.

In gating systems containing a wide plate-shaped ingate connected to a horizontal runner the balance between the dynamic and braking forces has a significant influence on the flow patterns. The dynamic forces are due to the velocity of the melt; the braking forces are due to wall friction etc. The balance between the dynamic and the braking forces is difficult for the casting engineer to predict.

Stream-lined gating systems have been designed to be very restrictive. The gating systems are restrictive in the sense that the balance between the dynamic and the braking forces in the system only have minor influence on the flow patterns. This means the flow patterns are solely controlled by the geometry of the gating system and hence the flow patterns can by predicted by the casting engineer.

The flow patterns in gating systems containing several abrupt directional changes, dead ends and incompletely filled runner cross sections can vary significantly from mould to mould. This means the gating system cannot absorb minor but inevitable changes in the pouring conditions from mould to mould. The result is low process stability. In the stream-lined gating systems are the flow patterns shown to be very uniform from mould to mould.

The stream-lined gating systems developed are utilising very narrow runners promoting completely filled runner cross sections from the first melt passing through.

The gating systems with and without dead ends have been tested on thin plates, a brake disc and an exhaust manifold with 2 mm wall thickness. The trials with the thin plates show the possibility of controlling the flow patterns in very thin sections. The trials with the brake discs show the performance of 6 different gating systems for the same disc. The developed stream-lined gating systems have been tested on the exhaust manifold with 2 mm wall thickness. With the stream-lined gating system it has been possible to cast the manifold.

7.1 Recommendations on future work

A new type of stream-lined gating systems for iron has been developed and the performance of it has been documented in laboratory trials. The laboratory trials have been conducted in relatively small moulds resulting in a low pressure height. The effect from larger moulds giving larger pressure heights and hence also higher velocities has to be investigated. The next step in the process is to test the performance of the gating systems under production conditions. The optimum would be to run the same part with a conventional gating system and a stream lined system. The combination of yield and scrap generated at the two systems has to be compared.

When going down to very small wall thicknesses, other aspects of the casting process apart from getting the metal into the mould cavity become more difficult. The other main aspects are getting the correct metallurgical structure and the dimensional capabilities of the process.

From trials not included in this report the largest problem seems to be to get the correct metallurgical structure in parts containing both thin and thick sections. I.e. to obtain the same structure independent of section thickness.